American Journal of Engineering Research (AJER)

CONTENTS

Volume-4 Issue-7

CONTENTS

CONTENTS

Research Paper	Open Access

Numerical solution of MHD flow in presence of induced Magnetic field and hall current Effect Over an Infinite Rotating vertical Porous plate through porous medium

P. Biswas[1], A. Biswas[2], M. K. Das[3] & S. F. Ahmmed[4]

1,2,3,4 Mathematics Discipline, Khulna University, Khulna-9208
pronabbiswas16@gmail.com[1], abku07@gmail.com [2], mahadeb.ku@gmail.com [3] and sfahmmed@yahoo.com[4]

ABSTRACT: *The one dimensional MHD unsteady magneto-hydrodynamics fluid flow past an infinite rotating vertical porous plate through porous medium with heat transfer considering hall current has been investigated numerically under the action of induced magnetic field. The numerical solution for the primary velocity field, secondary velocity field and temperature distributions are obtained by using the implicit finite difference method. The obtained results have been represented graphically for different values of parameters. Finally, the important findings of the investigation are concluded.*

***Keywords*:** *MHD, rotating porous plate, porous medium, heat transfer, hall current, finite difference method.*

I.   INTRODUCTION

In astrophysical and geophysical studies, the MHD boundary layer flows of an electrically conducting fluid have also vast applications. Many researchers studied the laminar flow past a vertical porous plate for the application in the branch of science and technology such as in the field of mechanical engineering, plasma studies, petroleum industries Magneto hydrodynamics power generator cooling of clear reactors, boundary layer control in aerodynamics and chemical engineering. Many authors have studied the effects of magnetic field on mixed, natural and force convection heat and mass transfer problems which have many modern applications like missile technology used in army, nuclear power plant, parts of aircraft and ceramic tiles. Indeed, MHD laminar boundary layer behavior over a stretching surface is a significant type of flow having considerable practical applications in chemical engineering, electrochemistry and polymer processing. This problem has also an important bearing on metallurgy where magneto hydrodynamic (MHD) techniques have recently been used.

H. L. Agarwal and P. C. Ram [1] have studied the effects of Hall Current on the hydro-magnetic free convection with mass transfer in a rotating fluid. H. S. Takhar and P. C. Ram [2] have studied the effects of Hall current on hydro-magnetic free convective flow through a porous medium. B. K. Sharma and A. K. Jha [3] have analyzed analytically the steady combined heat and mass transfer flow with induced magnetic field. B. P. Garg [4] has studied combined effects of thermal radiations and hall current on moving vertical porous plate in a rotating system with variable temperature. Dufour and Soret Effects on Steady MHD Free Convection and Mass Transfer Fluid Flow through a Porous Medium in A Rotating System have been investigated by Nazmul Islam and M. M. Alam [5]. Hall Current Effects on Magneto hydrodynamics Fluid over an Infinite Rotating Vertical Porous Plate Embedded in Unsteady Laminar Flow have been studied by Anika et al [6]. S. F. Ahmmed and M. K. Das [7] have investigated Analytical Study on Unsteady MHD Free Convection and Mass Transfer Flow Past a Vertical Porous Plate.

Abo-Eldahab and Elbarbary [8] have studied the Hall current effects on MHD free-convection flow past a semi-infinite vertical plate with mass transfer. The effect of Hall current on the steady magneto hydrodynamics flow of an electrically conducting, incompressible Burger's fluid between two parallel electrically insulating infinite planes have been studied by M. A. Rana and A. M. Siddiqui [9].

Hence our aim is of this paper is to extend the work of Anika.et al [6] to solve the problem by implicit finite difference method. The proposed model has been transformed into non-similar coupled partial differential equation by usual transformations. Finally the comparison results have been shown graphically as well as tabular form.

II.　MATHEMATICAL MODEL OF THE FLOW

Let us consider an unsteady electrically conducting viscous incompressible, laminar fluid flow through a vertical porous plate. The fluid is assumed to be in the x-direction which is taken along the porous plate in upward direction and y-axis is normal to it. Let the unsteady fluid flow starts at t=0 afterward the whole frame is allowed to rotate about y-axis with t>0,the plate started to move in its own plate　with constant velocity U and temperature of the plate is raised to T_w to T_∞ A strong uniform magnetic field B_o is applied normal to the plate that induced another magnetic field on electrically conducting fluid. In the presence of magnetic field. Then the fluid is affected by hall current, which gives rise t a force in z-direction. The physical configuration of the problem is furnished in Figure- a. Thus according to above assumptions the governing boundary layer equations with Bounssineq's approximation are:
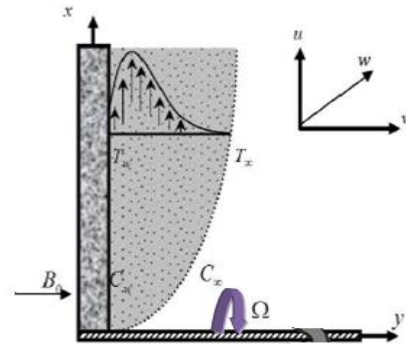
Figure- a. Physical configuration and co-ordinate system

$$\frac{\partial u}{\partial t} - v_0 \frac{\partial u}{\partial y} = \upsilon \left(\frac{\partial^2 u}{\partial y^2} \right) + g\beta(T - T_\infty) - \frac{\sigma' B_0^2}{\rho(1+m^2)}(u+mw) + 2Rw - \frac{\mu}{\rho k}u \tag{1}$$

$$\frac{\partial w}{\partial t} - v_0 \frac{\partial w}{\partial y} = \upsilon \left(\frac{\partial^2 w}{\partial y^2} \right) - \frac{\sigma' B_0^2}{\rho(1+m^2)}(mu-w) - 2Ru \tag{2}$$

$$\frac{\partial T}{\partial t} - v_0 \frac{\partial T}{\partial y} = \left(\frac{K}{\rho c_p} \frac{\partial^2 T}{\partial y^2} \right) + \frac{1}{c_p}\upsilon[(\frac{\partial u}{\partial y})^2 + (\frac{\partial w}{\partial y})^2] \tag{3}$$

With corresponding boundary conditions

$$t > 0 ;\begin{cases} u = U_0 , w = 0, T = T_w \ at\ y = 0 \\ u = 0, w = 0, T \to T_\infty \ \ as\ y = \infty \end{cases} \tag{4}$$

where u, v and w are the x, y and z components of velocity vector, m_e is the Hall parameter, where e is the electron frequency, is the kinematic coefficient viscosity, is the fluid viscosity, is the density of the fluid, is the thermal conductivity, C_p is the specific heat at the constant pressure, K is the thermal diffusion ratio, respectively. The rotation is described by the R .

III.　MATHEMATICAL FORMULATION

To obtain the governing equations and the boundary condition in dimension-less form, the following non-dimensional quantities are introduced as;

$$Y = y\frac{U_0}{u} , U = \frac{u}{U_0}, W = \frac{w}{U_0} , \tau = t\frac{U_0^2}{\upsilon}, \overline{T} = \frac{T-T_\infty}{T_w-T_\infty}$$

Using the above non-dimensional parameters, we get the governing equation with boundary conditions in the following form,

$$\frac{\partial U}{\partial \tau} - S\frac{\partial U}{\partial Y} = \frac{\partial^2 U}{\partial Y^2} + G_r T - \frac{M}{(1+m^2)}(u+mw) + 2RW - KU \tag{5}$$

$$\frac{\partial W}{\partial \tau} - S\frac{\partial W}{\partial Y} = \frac{\partial^2 W}{\partial Y^2} + \frac{M}{(1+m^2)}(u+mw) - 2RU \tag{6}$$

$$\frac{\partial T}{\partial t} - S\frac{\partial T}{\partial y} = \frac{1}{P_r}\frac{\partial^2 T}{\partial Y^2} + E_c[(\frac{\partial U}{\partial Y})^2 + (\frac{\partial W}{\partial Y})^2] \tag{7}$$

With corresponding boundary conditions

$$t > 0 ; \begin{cases} U = 1, W = 0, T = 1 \ at \ Y = 0 \\ U = 0, W = 0, T = 0 \quad as \ Y = \infty \end{cases} \tag{8}$$

Where t represents the dimensionless time, Y is the dimensionless Cartesian coordinate, U and W are the dimensionless velocity component in X and Z direction, T is the dimensionless temperature

$S = \dfrac{\upsilon_0}{U_0}$ (Suction parameter), $G_r = \dfrac{g B_T (T_w - T_\infty) \upsilon}{U_0^3}$ (Grashoff Number), $M = \dfrac{\sigma B_0^2 \upsilon}{\rho U_0^2}$ (Magnetic

parameter), $P_r = \dfrac{\rho C_p \upsilon}{K}$ (Prandlt Number), $R = \dfrac{L \upsilon}{U_0^2}$ (Rotation parameter), $m = \dfrac{\sigma_e B_0}{e n}$ (hall parameter),

$E_c = \dfrac{U_0^2}{C_p (T_w - T_\infty)}$ (Eckert Number)

IV.   NUMERICAL SOLUTIONS

In order to solve the non-dimensional system by the implicit finite difference technique, it is required a set of finite difference equations. In this case, the region within the boundary layer is divided by some perpendicular lines of Y-axis, where Y-axis is normal to the medium as shown in Figure- b. It is assumed that the maximum length of boundary layer is $Y_{max} = 25$ as corresponds to Y i.e. Y varies from 0 to 25 and the number of grid spacing in Y-directions is $P = 400$, hence the constant mesh size along Y axis becomes $\Delta Y = 0.0625 (0 \le Y \le 25)$ with a smaller time-step $\Delta t = 0.001$ Let U', W' and C' denotes the values of U, W and C at the end of time-step respectively.
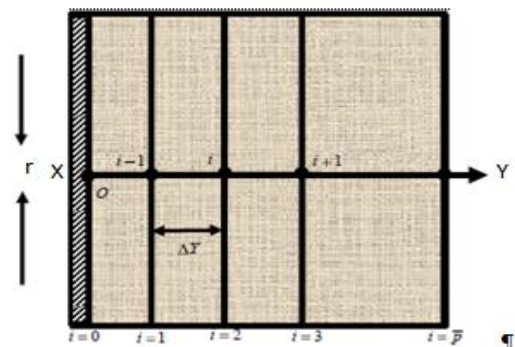
Figure-(b): Implicit finite differece space grid

Using the implicit finite difference approximation, the following appropriate set of finite difference equations are obtained as;

$$\frac{U_i^{n+1} - U_i^n}{\Delta \tau} - S \frac{U_{i+1}^n - U_i^n}{\Delta Y} = \frac{U_{i+1}^n - 2 U_i^n + U_{i-1}^n}{(\Delta Y)^2} + G_r \overline{T} - \frac{M}{(1 + m^2)} (U_i^n + m W_i^n) \tag{9}$$

$$+ 2 R W_i^n - K U_i^n$$

$$\frac{W_i^{n+1} - W_i^n}{\Delta \tau} - S \frac{W_{i+1}^n - W_i^n}{\Delta Y} = \frac{W_{i+1}^n - 2 W_i^n + W_{i-1}^n}{(\Delta Y)^2} + \frac{M}{(1 + m^2)} (m U_i^n - W_i^n) - 2 R U_i^n \tag{10}$$

$$\frac{T_i^{n+1} - T_i^n}{\Delta \tau} - S \frac{T_{i+1}^n - T_i^n}{\Delta Y} = \frac{1}{P_r} \frac{T_{i+1}^n - 2 T_i^n + T_{i-1}^n}{(\Delta Y)^2} + E_c \left[\left(\frac{U_{i+1}^n + - U_i^n}{\Delta Y} \right)^2 - \left(\frac{W_{i+1}^n + - W_i^n}{\Delta Y} \right)^2 \right] \tag{11}$$

with the finite difference boundary conditions,

$$U_{0,j}^n = 0 ; V_{0,j}^n = 0 ; \overline{T}_{0,j}^n = 0$$

$$t > 0 ; \begin{cases} U_{i,0}^n = 1 ; W_{i,0}^n = 0 ; \overline{T}_{i,0}^n = 1 \\ U_{i,L}^n = 0 ; V_{i,L}^n = 0 ; \overline{T}_{i,L}^n = 0 \end{cases} \tag{12}$$

Here the subscript i designates the grid points with Y coordinate and the superscript n represents a value of time, $t = n \Delta t$, where $n = 0, 1, 2 \ldots\ldots$. The primary velocity U secondary velocity W, temperature T distributions at all interior nodal points may be computed by successive applications of the above finite difference equations. The numerical values of the shear stresses, Nusselt number are evaluated by Five-point approximate formula.

V. RESULTS AND DISCUSSION

For observing the physical situation of the unsteady state situations have been illustrated in Figure–1 to Figure-27 up to dimensionless time t=80.00, but at the present case the changes appear till t=60.Therefore t=60 represents the steady state solution of the problem. The primary velocity, secondary velocity and temperature distributions are displayed for various values of m, M, G_r, P_r, R, S in Figure–1 to Figure-18 to the time step t= 1,10,60 and Share stress and Nusselt Number are shown in Figure-19 to Figure-27 at the same time step. These results shows that the primary velocity and secondary velocity are increase with the increase of R, G_r and E_c, and decrease with the increase of M, P_r, S so it follows the boundary conditions both for primary and secondary velocities. It is noted that the temperature distribution is increased with the increase of G_r and decrease with the increase of M, P_r, and S. The velocities are shown in Figure -1 to Figure -14.for different values of the parameter m, M, G_r, P_r, S. $P_r=0.71$ has been used for air at 20^0C, $P_r=1.00$ has been used for electrically solution like saline water at 20^0C, $P_r=7.00$ has been used to water at 20^0C. The other parameters are used arbitrarily. The effect of P_r causes fall of temperature at the same values of Prandlt number P_r. Therefore Heat is able to diffuse away more rapidly and for large suction S. The velocity profile decrease drastically where as the secondary velocity decrease severally with the increase of S. This is because sucking decelerates fluid particles through the wall reducing the growth of the boundary layer as well as thermal boundary layer, Shown in Figure -13 to Figure -14. The share stress t_x increase for the values of $G_r \geq 1$. The Nusselt Number $(-Nu)$ has increased with the increase of P_r and S in Figure -25 and Figure -27. The dimensionless Parameter R, G_r, and E_c resists the time development of Nusselt-Number(-Nu) in X-direction shown in Figure -23, Figure -24 and figure-26.respectively The share stress t_x is increased with the increase of R, G_r and E_c, shown in Figure -19, Figure -(20) and Figure -22 .The suction parameter S caused effects for different values on share-stress. The share-stress falls drastically for large suction and $(-Nu)$ rises severally with the increase of suction S, shown in Figure -21 and in Figure -27 respectively.
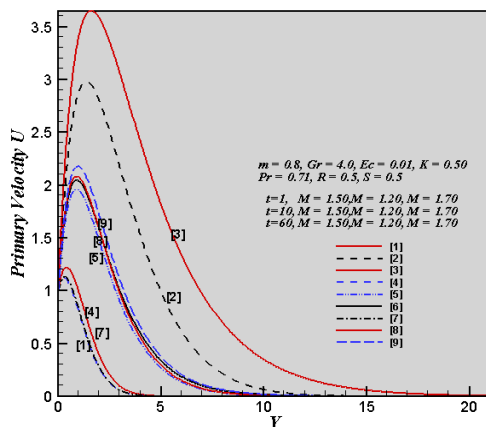
Figure- 1. Primary velocity profiles for the parameter *M*
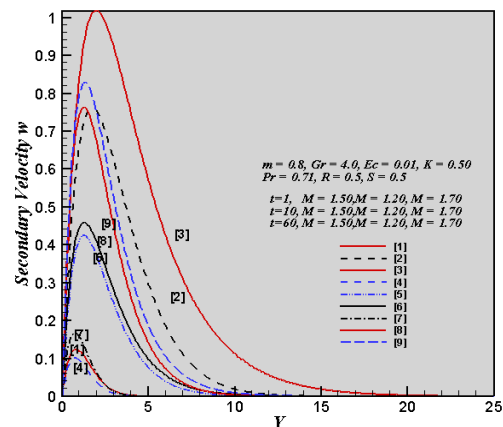
Figure- 2. Secondary velocity profiles for the parameter *M*
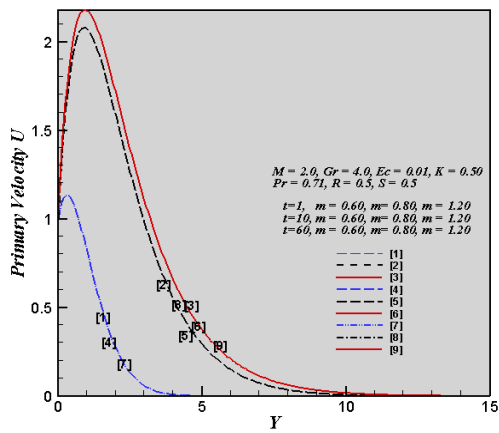
Figure- 3 Primary velocity profiles for the parameter *m*
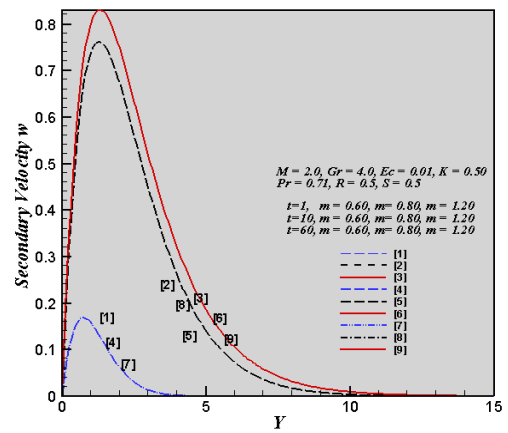
Figure- 4 Secondary velocity profiles for the parameter *m*
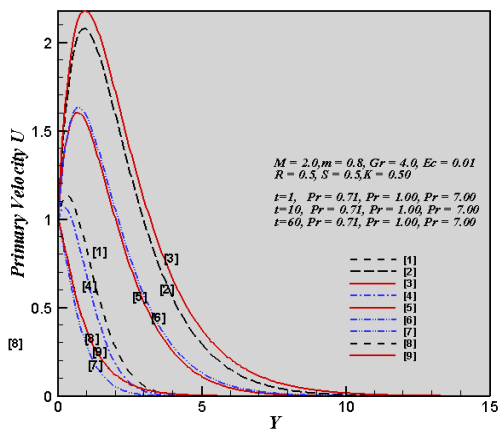
Figure- 5 Primary velocity profiles for the parameter P_r
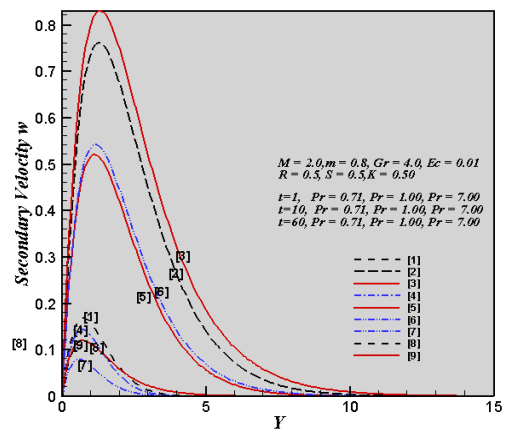
Figure- 6 Secondary velocity profiles for the parameter P_r
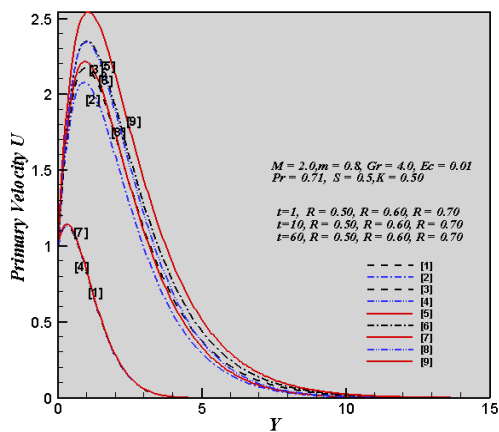
Figure- 7 Primary velocity profiles for the parameter *R*
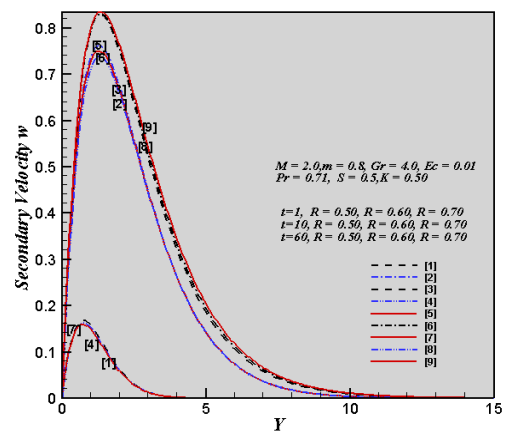
Figure- 8 Secondary velocity profiles for the parameter *R*
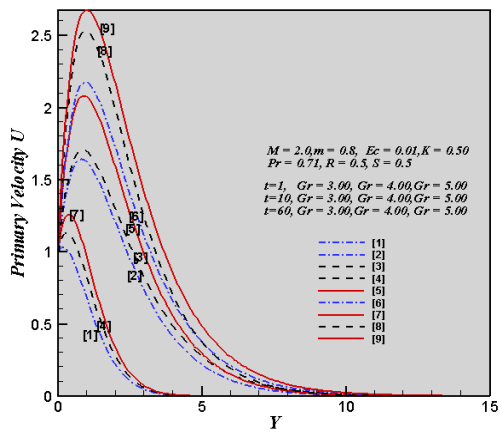
Figure- 9 Primary velocity profiles for the parameter G_r
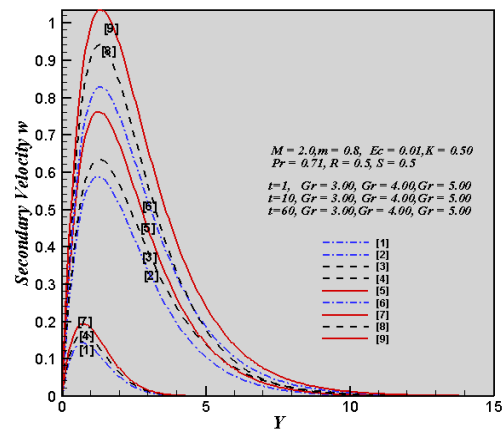
Figure- 10 Secondary velocity profiles for the parameter G_r
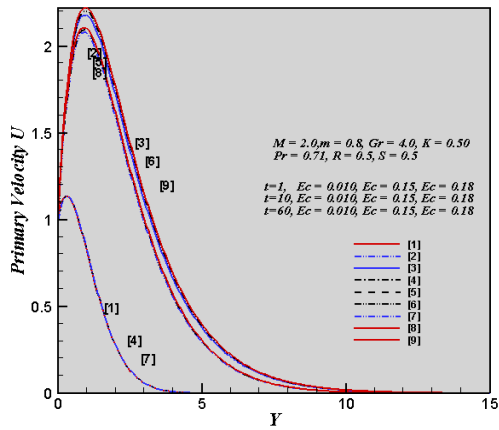
Figure- 11 Primary velocity profiles for the parameter E_c
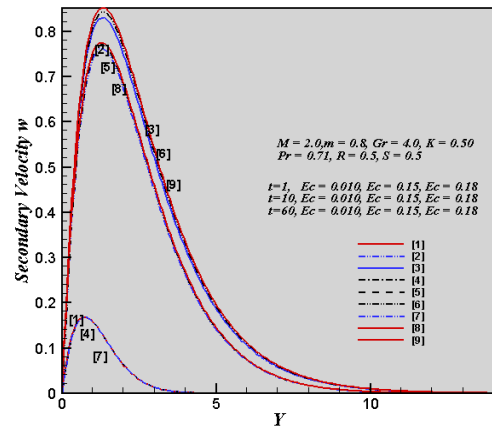
Figure- 12 Secondary velocity profiles for E_c
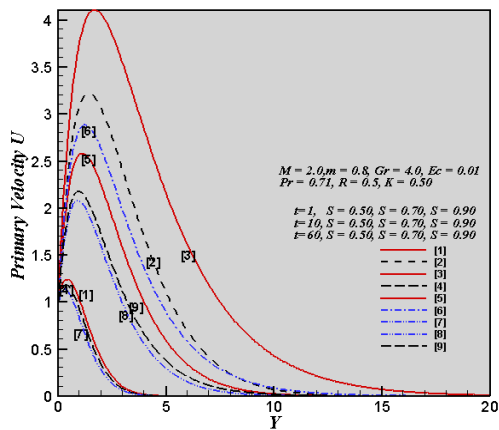
Figure- 13 Primary velocity profiles for the parameter S
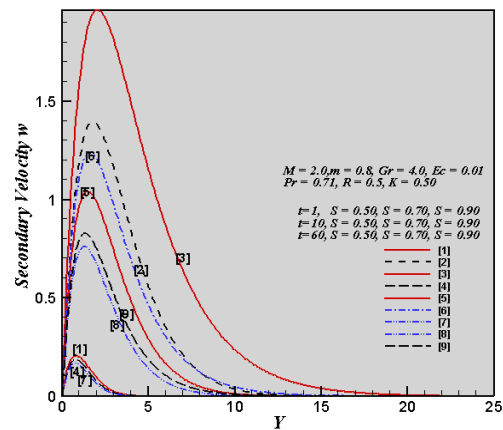
Figure- 14 Secondary velocity profiles for the parameter S
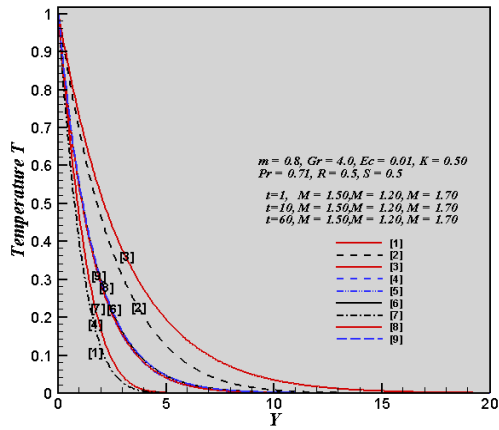
Figure- 15 Temperature profiles for the parameter *M*
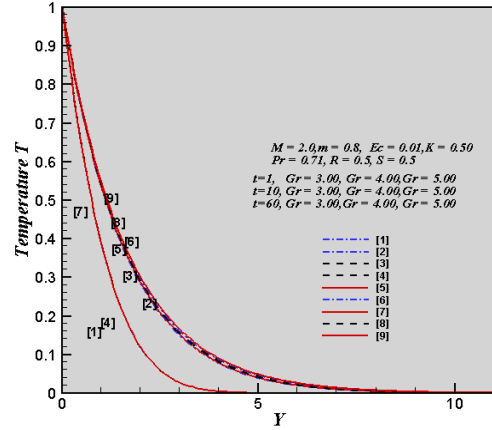
Figure- 16 Temperature profiles for the parameter G_r
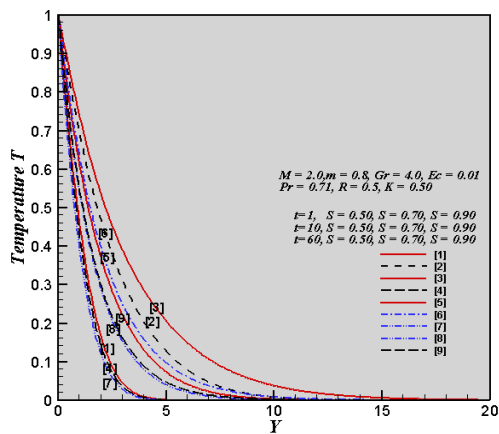
Figure- 17 Temperature profiles for the parameter *S*
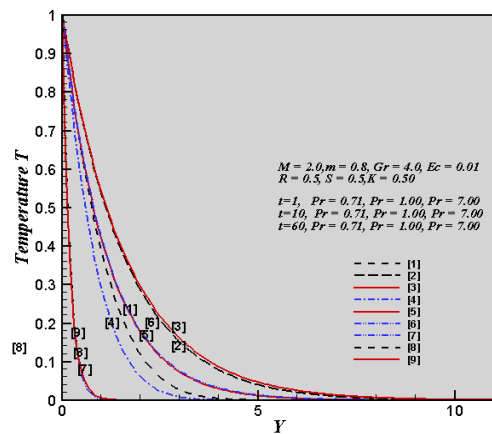
Figure- 18 Temperature profiles for the parameter P_r
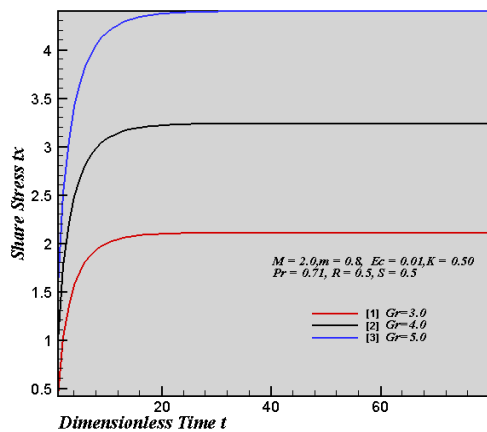
Figure- 19 Share Stress t_x for the parameter G_r
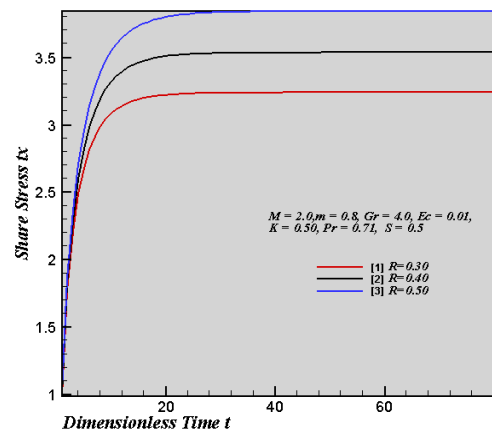
Figure- 20 Share Stress t_x for the parameter *R*
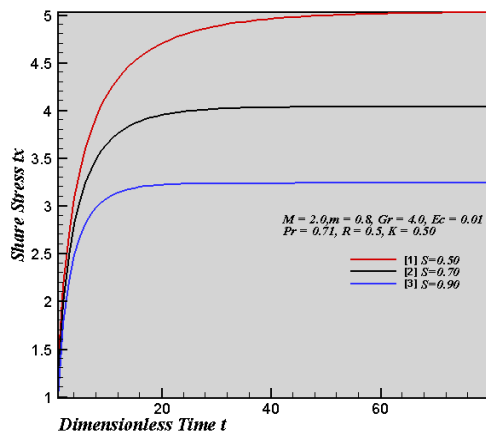
Figure- 21 Share Stress t_x for the parameter S
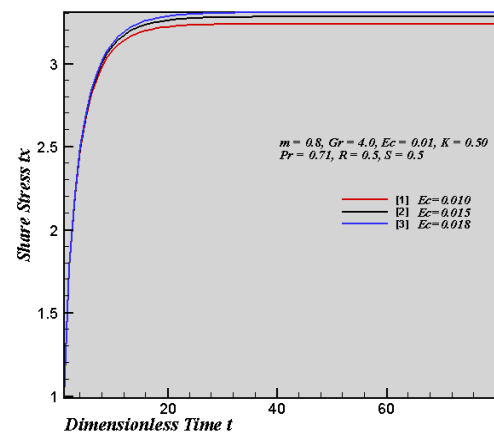
Figure-22 Share Stress t_x for the parameter E_c
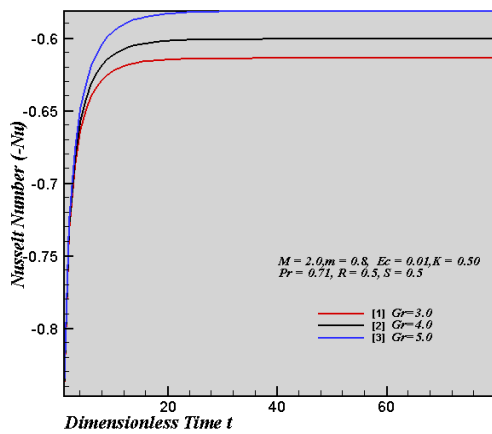
Figure- 23 Nusselt Number($-N_u$) for the parameter G_r
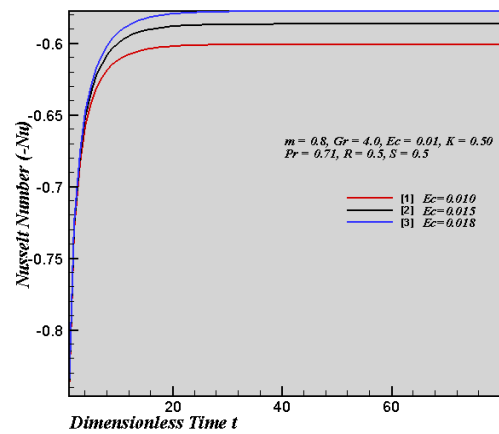
Figure- 24 Nusselt Number($-N_u$) for the parameter E_c
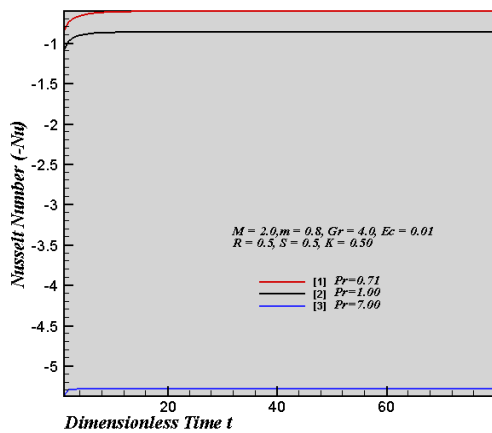
Figure- 25 Nusselt Number($-N_u$) for the parameter P_r
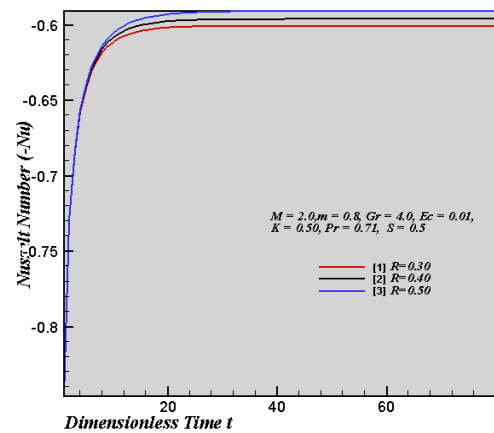
Figure- 26 Nusselt Number($-N_u$) for the parameter R
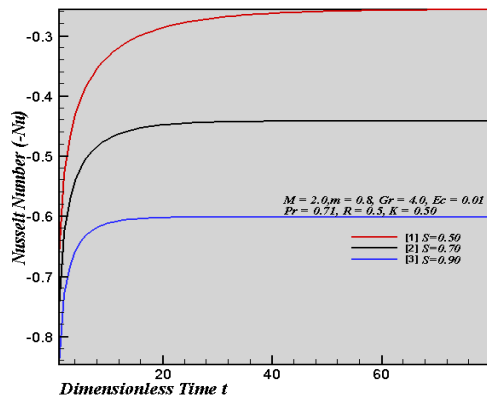
Figure- 27 Nusselt Number($-N_u$) for the parameter S

Qualitative comparison of the result with the previous result

Increased parameter	Previous result given by Anika and Nazmul					Present result				
	U	W	T	t_x	$-Nu$	U	W	T	t_x	$-Nu$
M	Dec	Inc	Dec	Dec	Inc	Dec	Dec	Dec	A bit impact	
P_r	Dec	Inc	Dec	Dec	Inc	Dec	Dec	Dec	A bit impact	Inc
R	Dec	Inc	Inc	Dec	Dec	Inc	Inc	A bit impact	Inc	Dec
G_r	Inc	Dec	Inc	Inc	Dec	Inc	Inc	Inc	Inc	Dec
E_c	Inc	Dec	Inc	Inc	Dec	Inc	Inc	A bit impact	Inc	Dec
S	Dec	Inc	Dec	Dec	Inc	Dec	Dec	Dec	Dec	Inc

Here, Dec= Decreasing, Inc= Increasing.

VI.   CONCLUSIONS

In this study, the finite-difference solution on unsteady MHD fluid flow past a vertical porous plate has been considered in the presence of strong magnetic field, hall current m, rotating parameter R is investigated. In the present investigation, the Primary velocity, Secondary velocity increase with the increase of R, G_r, and E_c and decrease with the increase of M, P_r and suction S. The temperature distribution increases with the increase of G_r and decreases when M, P_r, and S are increase. The Nusselt-Number ($-Nu$) decreases with the increase of R, G_r, and E_c and increase when P_r and S are increase. The share stress t_x follow the trend of Primary velocity, Secondary velocity. The accuracy of present work is qualitatively good in case of all the flow parameters.

REFERENCES

[1]   H. L. Agarwal, "P.C.Ram and V.Singh, Effects of Hall currents on the hydro-magnetic free convection with mass transfer in a rotating fluid." *Astrophysics and Space Science,* 100 (1984) 277-283.
[2]   H. S. Takhar and P. C. Ram, "Effects of Hall current on hydro-magnetic free convection flow through a porous medium." *Astrophysics and Space Science*, 192(1992) 45-51.
[3]   B. K. Sharma, A. K. Jha and R. C. Chaudhary, "Hall effect on MHD mixed convective flow of a viscous incompressible fluid past a vertical porous plate immersed in porous medium with heat source/sink." *Journal of Physics,* 52(5) (2007) 487-503.
[4]   B. P. Garg, "Combined effects of thermal radiations and hall current on moving vertical porous plate in a rotating system with variable temperature." *International Journal of Pure and Applied Mathematics*, 81(2) (2012) 335-345.
[5]   N. Islam and M. M. Alam, "Dufour and soret effects on steady MHD free convection and mass transfer fluid flow through a porous medium in a rotating system." *Journal of Naval Architecture and Marine Engineering,* 4 (2007) 43-55.
[6]   Nisat Nowroz Anika, Md. Mainul Hoque and Nazmul Islam, Hall Current Effects on Magneto hydrodynamics Fluid over an Infinite Rotating Vertical Porous Plate Embedded in Unsteady Laminar Flow." *Annals of Pure and Applied Mathematics Vol. 3, No.2, 2013, 189-200.*
[7]   S. F. Ahmmed, M. K. Das, L. E. Ali. Analytical Study on Unsteady MHD Free Convection and Mass Transfer Flow Past a Vertical Porous Plate. *American Journal of Applied Mathematics.* Vol. 3, No. 2, 2015, pp. 64-74. doi: 10.11648/j.ajam.20150302.16.
[8]   E. M. Abo-Eldahaband, E. M. E. Elbarbary, "Hall current effect on magneto hydrodynamic free convection flow past a semi-infinite vertical plate with mass transfer." *Int. J. Engg*. Sci., 39 (2001) 1641-1652.
[9]   M. A. Rana, A. M. Siddiqui and N. Ahmed, "Hall effect on Hartmann flow and heat transfer of a Burger's fluid." *Phys. Letters A,* 372 (2008) 562-568.

Research Paper   Open Access

Effect of a Magneto-hydrodynamic Natural Convection in a Square Cavity with Elliptic Shape Adiabatic Block

M. Jahirul Haque Munshi[1,*], M. A. Alim[2], A. H. Bhuiyan[2], G. Mostafa[1]

[1]*Department of Mathematics, Faculty of Science, Engineering & Technology*
Hamdard University Bangladesh (HUB), Newtown, Sonargaon, Narayngonj-1440, Bangladesh
[2]*Department of Mathematics, Bangladesh University of Engineering and Technology*
(BUET), Dhaka- 1000, Bangladesh

ABSTRACT: *In this paper, the effect of magneto-hydrodynamic natural convection fluid flow and heat transfer in a square cavity filled with an electric conductive fluid with elliptic shape adiabatic block are studied numerically. The governing differential equations are solved by using finite element method (weighted-residual method). The horizontal and top wall assumed to be adiabatic. The left wall is kept heated T_h and right wall is kept at cold T_c. Also all the walls are assumed to be no-slip condition. Numerical predictions are obtained for a wide range of Rayleigh number (Ra) and different Hartmann number (Ha) at the Prandtl number 0.733. The numerical results show that the effect of the magnetic field is to decrease the rate of convective heat transfer and the average Nusselt number decreases as Hartmann number increases. The results are presented for Rayleigh number from 10^4 up to 10^6 in form of streamlines, isotherms and Nusselt number for various Rayleigh and Hartmann numbers.*

KEYWORDS: *Natural convection, numerical study, square enclosure, magnetic field, elliptic shape adiabatic block.*

Nomenclatures:

B_0	Strength of the magnetic field	Greek symbols	
g	gravitational acceleration	α	Thermal diffusivity
L	length of the cavity	β	Volumetric coefficient of thermal expansion
Nu	Nusselt number		
P	dimensional pressure	v	Kinematic viscosity of the fluid
p	pressure	θ	non-dimensional temperature
Pr	Prandtl number	ρ	density of the fluid
Ra	Rayleigh number	ψ	non-dimensional stream function
T	dimensional temperature		
u, v	velocity components	Subscripts	
U, V	non-dimensional velocity components	c	cold wall
x, y	Cartesian coordinates	h	hot wall
X, Y	non-dimensional Cartesian coordinates		

I. INTRODUCTION

Natural convection is a subject of central importance in the present technology development and all kinds of engineering applications. Historically, some of the major discoveries in natural convection have helped shape the course of development and important fields for the application of the cooling of power electronics, solar collectors, solar stills, attic spaces, etc. Now a days, natural convection have industrial applications in which the heat and mass transfer occur concurrently as a result of combined buoyancy effects of thermal and species diffusion.

A number of studies have been conducted to investigate the flow and heat transfer characteristics in closed cavities in the past. Kuhen et al. (1976) an experimental and theoretical study of natural convection in the annulus between horizontal concentric cylinders. Patankar et al. (1980) Numerical methods for heat transfer and fluid flow, New York, Hemisphere. Acharya (1985) studied natural convection in an inclined enclosure containing internal energy sources and cooled from below. Fusegi et al. (1992) performed a numerical study on natural convection in a square cavity by using a high-resolution finite difference method. The authors considered differentially heated vertical walls and uniform internal heat generation in the cavity. Natural convection heat transfer in rectangular cavities heated from the bottom had been investigated by Hasaaoui et al. (1995). Ganzarolli et al. (1995) investigated the natural convection in rectangular enclosures heated from below and cooled from the sides. Turkoglu et al. (1995) made a numerical study using control volume approach for the effect of heater and cooler locations on natural convection on cavities. The authors indicated that for a given cooler position, average Nusselt number increases as the heater is moved closer to the bottom horizontal wall. Asan et al.(2000) studied the steady-state, laminar, two-dimensional natural convection in an annulus between two isothermal concentric square ducts. Roychowdhury et al. (2002) analyzed natural convective flow and heat transfer features for a heated cylinder kept in a square enclosure with different thermal boundary conditions. Dong et al. (2004) studied the conjugate of natural convection and conduction in a complicated enclosure. Their investigations showed the influences of material character, geometrical shape and Rayleigh number (Ra) on the heat transfer in the overall concerned region and concluded that the flow and heat transfer increase with the increase of thermal conductivity in the solid region; the overall flow and heat transfer were greatly affected by both geometric shape and Rayleigh number. Braga et al. (2005) numerically studied steady laminar natural convection within a square cavity filled with a fixed amount of conducting solid material consisting of either circular or square obstacles. It was found that the average Nusselt number for cylindrical rods was slightly lower than those for square rods. De et al. (2006) performed a simulation of natural convection around a tilted heated square cylinder kept in an enclosure within the range of $10^3 \leq Ra \leq 10^6$. They reported detailed flow and heat transfer features for two different thermal boundary conditions and obtained that the uniform wall temperature heating was quantitatively different form the uniform wall heat flux heating. Kahveci et al.(2007) studied natural convection in a partitioned vertical enclosure heated with a uniform heat flux. Basak et al.(2008) studied and solved the finite element analysis of natural convection flow in a isosceles triangular enclosure due to uniform and non-uniform heating at the side walls. Pirmohammadi et al. (2009) shows that the effect of a magnetic field on Buoyancy- Driven convection in differentially heated square cavity.

Rahman et al.(2011) offered a numerical model for the simulation of double-diffusive natural convection in a right-angled triangular solar collector. Mahmoodi et al. (2011) studied numerically magneto-hydrodynamic free convection heat transfer in a square enclosure heated from side and cooled from the ceiling. Jani et. al. (2013) numerically investigated magneto-hydrodynamic free convection in a square cavity heated from below and cooled from other walls. Bhuiyan et al. (2014) numerically investigated magneto hydrodynamic free convection in a square cavity with semicircular heated block.

On the basis of the literature review, it appears that no work was reported on the natural convection flow in a square cavity with elliptic shape adiabatic block. The obtained numerical results are presented graphically in terms of streamlines, isotherms, local Nusselt number and average Nusselt number for different Hartmann numbers and Rayleigh numbers.

II.   PHYSICAL CONFIGURATION

The physical model considered in the present study of natural convection in a square enclosure with elliptic shape adiabatic block is shown in Fig. 1.

The height and the width of the cavity are denoted by *L* and inside the cavity with elliptic shape adiabatic block. The left wall is kept heated T_h and right wall is kept at cold T_c. The magnetic field of strength B_0 is applied parallel to *x*- axis. The square cavity is filled with an electric conductive fluid with Pr = 0.733 that is considered Newtonian and incompressible.
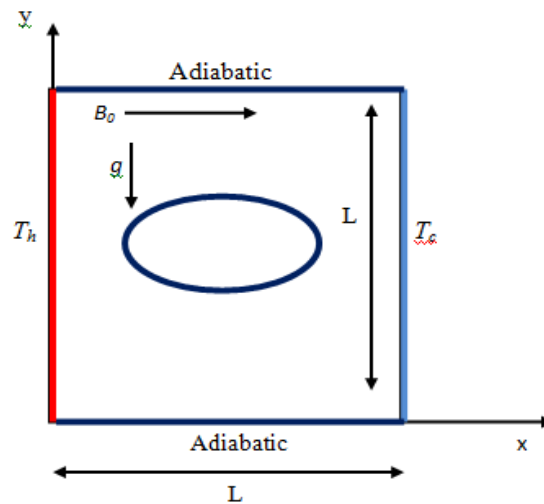
Fig. 1

Fig. 1. Schematic view of the cavity with boundary conditions considered in the present paper

III.   MATHEMATICAL FORMULATION

The flow is considered to be two dimensional, steady, laminar and incompressible fluids. The governing equations for mass, momentum and energy equation and natural convection flow in a cavity are as follows:

$$\frac{\partial u}{\partial x} + \frac{\partial v}{\partial y} = 0 \qquad \text{-------------------- (1)}$$

$$\rho\left(\frac{\partial u}{\partial x} + \frac{\partial u}{\partial y}\right) = -\frac{\partial p}{\partial x} + \mu\left(\frac{\partial^2 u}{\partial x^2} + \frac{\partial^2 u}{\partial y^2}\right) \qquad \text{-------------------- (2)}$$

$$\rho\left(\frac{\partial v}{\partial x} + \frac{\partial v}{\partial y}\right) = -\frac{\partial p}{\partial y} + \mu\left(\frac{\partial^2 v}{\partial x^2} + \frac{\partial^2 v}{\partial y^2}\right) + \rho g\beta(T - T_c) - \sigma B_0^2 v \qquad \text{------------------- (3)}$$

$$u\frac{\partial T}{\partial x} + v\frac{\partial T}{\partial y} = \alpha\left(\frac{\partial^2 T}{\partial x^2} + \frac{\partial^2 T}{\partial y^2}\right)$$

where x and y are the distances measured along the horizontal and vertical directions respectively, u and v are the velocity components in the x and y directions respectively, T denotes the fluid temperature, p is the pressure and ρ is the fluid density.

Boundary conditions:

On the left wall of the square cavity: u = 0, v = 0, T = T_h
On the right wall of the square cavity: u = 0, v = 0, T = T_c
The above equations are non-dimensionalized by using the following dimensionless quantities

$$X = \frac{x}{L}, Y = \frac{y}{L}, U = \frac{uL}{\alpha}, V = \frac{vL}{\alpha}, P = \frac{pL^2}{\rho\alpha^2}, \theta = \frac{(T - T_c)}{(T_h - T_c)} \qquad \text{-------------------- (5)}$$

where $\upsilon = \frac{\mu}{\rho}$ is the reference kinematic viscosity and θ is the non-dimensional temperature. After substitution of dimensionless variable we get the non- dimensional governing equations which are:

$$\frac{\partial U}{\partial X} + \frac{\partial V}{\partial Y} = 0 \qquad \text{-------------------(6)}$$

$$U\frac{\partial U}{\partial X} + V\frac{\partial U}{\partial Y} = -\frac{\partial P}{\partial X} + \Pr\left(\frac{\partial^2 U}{\partial X^2} + \frac{\partial^2 U}{\partial Y^2}\right)$$ ----------------(7)

$$\rho\left(\frac{\partial v}{\partial x} + \frac{\partial v}{\partial y}\right) = -\frac{\partial p}{\partial y} + \mu\left(\frac{\partial^2 v}{\partial x^2} + \frac{\partial^2 v}{\partial y^2}\right) + \rho g\beta(T - T_c) - \sigma B_0^2 v$$ ---------------- (8)

$$U\frac{\partial \theta}{\partial X} + V\frac{\partial \theta}{\partial Y} = \left(\frac{\partial^2 \theta}{\partial X^2} + \frac{\partial^2 \theta}{\partial Y^2}\right)$$ ----------------(9)

where *Ra, Pr* and *Ha* are the Rayleigh, Prandtl and Hartman numbers are defined as follows:

$$Ra = \frac{g\beta(T_h - T_c)L^3}{\alpha v}\ , \Pr = \frac{v}{\alpha}\ , Ha = B_0 L\sqrt{\frac{\sigma}{\rho v}}$$ ---------------- (10)

where *g* is the gravitational acceleration, v is the dynamic viscosity, β is the volumetric coefficient of thermal expansion, B_0 is the magnitude of magnetic field, α is the thermal diffusivity.

The effect of magnetic field into the momentum equation is introduced through the Lorentz force term $\vec{J} \times \vec{B}$ that is reduced to $-\sigma B_0 v^2$ as shown by Pirmohammadi et al. (2009).
To computation of the rate of heat transfer, Nusselt number along the hot wall of the enclosure is used as follows:

$$Nu_y = \frac{\frac{\partial \theta}{\partial X}\big|X=0}{(\theta_h - \theta_c)}\quad N_u = \int_0^1 Nu_y dY$$ ---------------- (11)

Boundary conditions:
On the left wall of the square cavity: U = 0, V = 0, $\theta = 1$
On the right wall of the square cavity: U = 0, V = 0, $\theta = 0$

The non-dimensional stream function is defined as $U = \frac{\partial \psi}{\partial Y}, V = -\frac{\partial \psi}{\partial X}$ ---------------- (12)

IV.   NUMERICAL TECHNIQUE
The nonlinear governing partial differential equations, i.e., mass, momentum and energy equations are transferred into a system of integral equations by using the Galerkin weighted residual finite-element method. The integration involved in each term of these equations is performed with the aid Gauss quadrature method. The nonlinear algebraic equations so obtained are modified by imposition of boundary conditions. These modified nonlinear equations are transferred into linear algebraic equations with the aid of Newton's method. Lastly, Triangular factorization method is applied for solving those linear equations.

4.1. Program Validation and Comparison with Previous Work
In order to check on the accuracy of the numerical technique employed for the solution of the problem considered in the present study, the code is validated with Pirmohammadi et al. (2009). The left wall is kept heated T_h and right wall is kept at cold T_c. By performing simulation for natural convection in the upper and lower wall are adiabatic. Streamlines and isotherms are plotted in Fig. 2. showing good agreement.
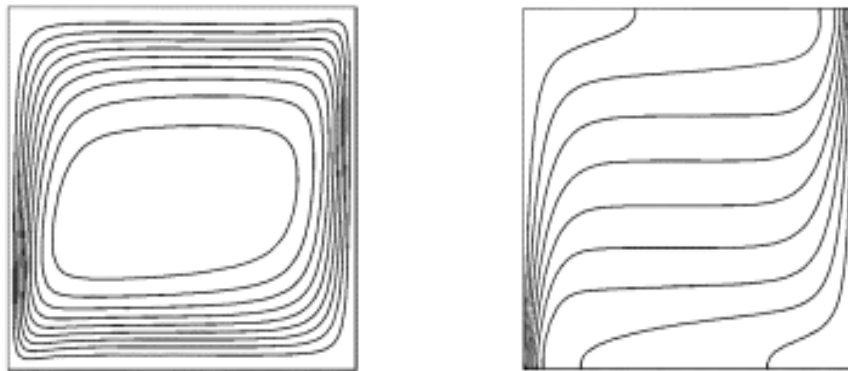
Fig. 2(a). Pirmohammadi et al. [15] Obtained streamlines and Isotherms for Ra = 10^6, Pr = 0.7 33 and Ha=50.
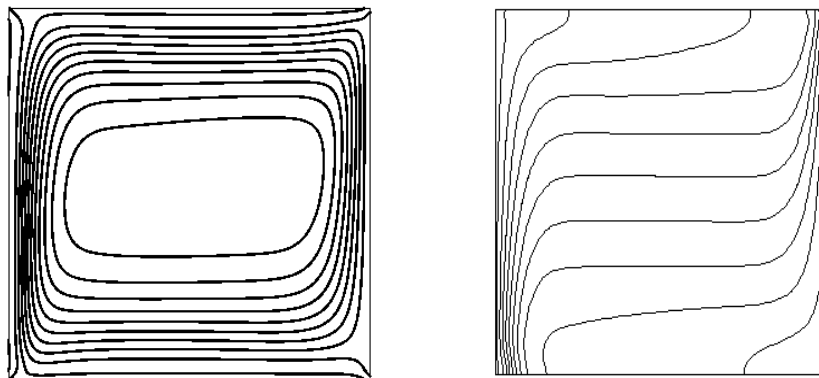
Fig. 2(b). Present: Obtained streamlines and Isotherms for Ra = 10^6, Pr = 0.733 and Ha = 50

V.   RESULT AND DISCUSSION

A numerical work was performed by using finite element method to natural convection in a square enclosure with elliptic shape adiabatic block. In this section, some representative results are presented to illustrate the effects of various controlling parameters on the fluid flow and heat transfer processes inside the cavity. These controlling parameters include Rayleigh number ranging from 10^4 to 10^6 and the Hartmann number varying from 0 to 150 with fixed Prandtl number Pr = 0.733. The results are presented in terms of streamlines and isotherms inside the cavity at various Hartmann numbers and Rayleigh numbers is shown in Figs. 3, 4, 5 and 6, 7, 8. The maximum absolute value of stream function can be viewed as a measure of the intensity of natural convection in the cavity. It is evident from the Figs. 3 to 8 that because of the absent of magnetic field, the maximum value of the stream function increases due to the increase of the Hartmann number.

We observed from the figures with existence centerline of the cavity, the flow and temperature fields are symmetrical about this line. As can be seen from the streamlines in the Fig. 3, 4, 5 a pair of counter-rotating eddies are formed in the left and right half of the cavity for all Rayleigh numbers considered. Each cell ascend through the symmetry axis, then faces the right wall and moves horizontally and finally descends along the corresponding cold side wall. Since upper, lower walls adiabatic and elliptic shape adiabatic block, so the curve moves to left wall to right wall.

From this figure we see that, as the Hartmann number increases 100 to 150, the central stream line is elongated. The isotherms are shown almost parallel to the vertical walls, indicating that most of the heat transfer is by heat conduction. The main effect of the introduction of the magnetic field is to decrease the overall heat transfer rate between the hot and cold walls. For moderate and high Rayleigh numbers 10^5 to10^6 and for a weak magnetic field strength there is a temperature stratification in the vertical direction and the thermal boundary layer is wall established along the side walls. This is because at high Rayleigh number and low Hartmann number, convection is dominant heat transfer mechanism. Heat transfer by convection alters the temperature distribution to such an extent that temperature gradients in the centre is closed to zero. From the stream line pattern we see that there is a strong upward flow near the heated side wall and downward flow at the cold wall. With increases in Rayleigh number and buoyancy force, the elliptic shape of the eddies move upward in so far as at Ra= 10^6, locate in the upper half of the cavity. At Ra= 10^6 the elliptic shape are elongated along the height of the cavity.
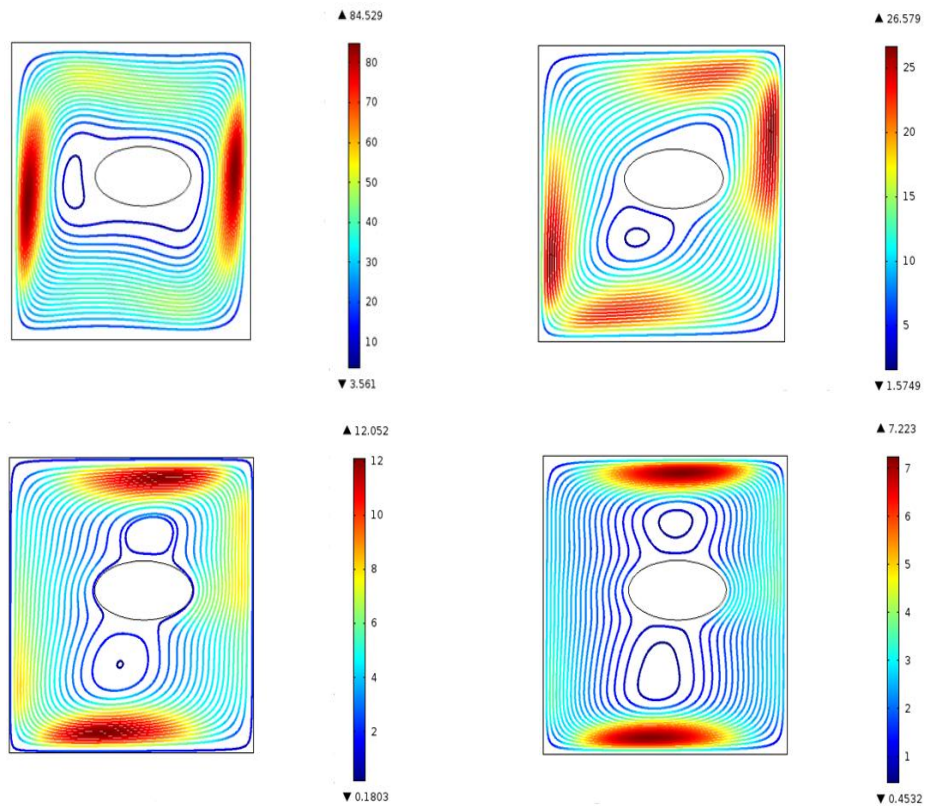
Fig. 3. Streamlines for (a) Ha = 0 ; (b) Ha = 50; (c) Ha = 100; (d) Ha = 150 while
Ra = 10000 and Pr = 0.733
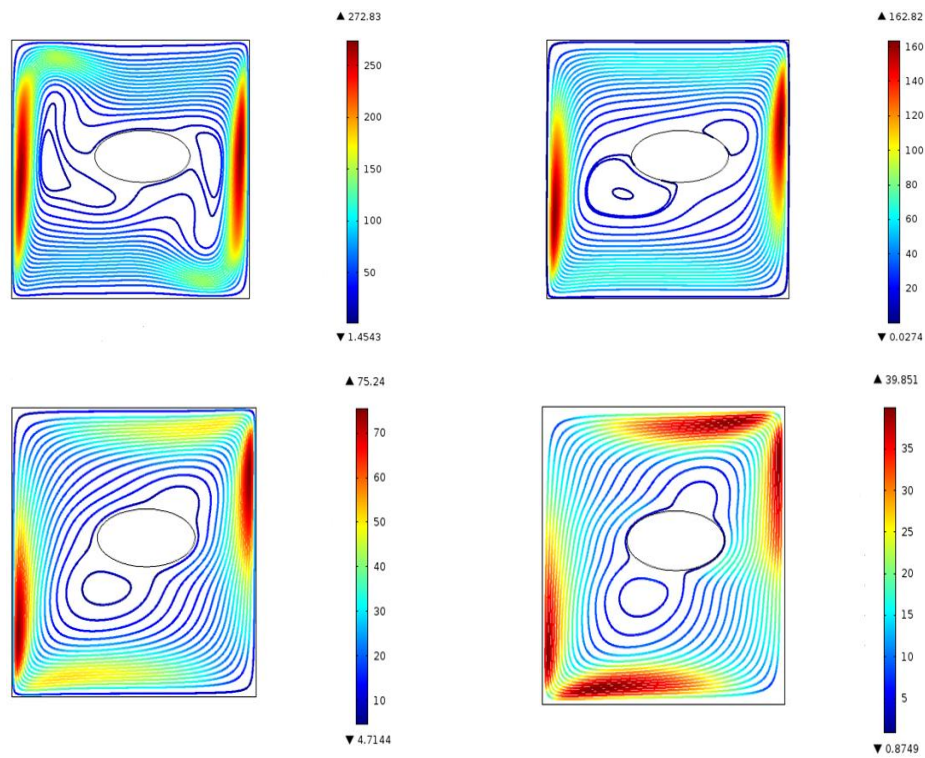
Fig. 4. Streamlines for (a) Ha = 0; (b) Ha = 50; (c) Ha = 100; (d) Ha = 150 while
Ra = 100000 and Pr = 0.733
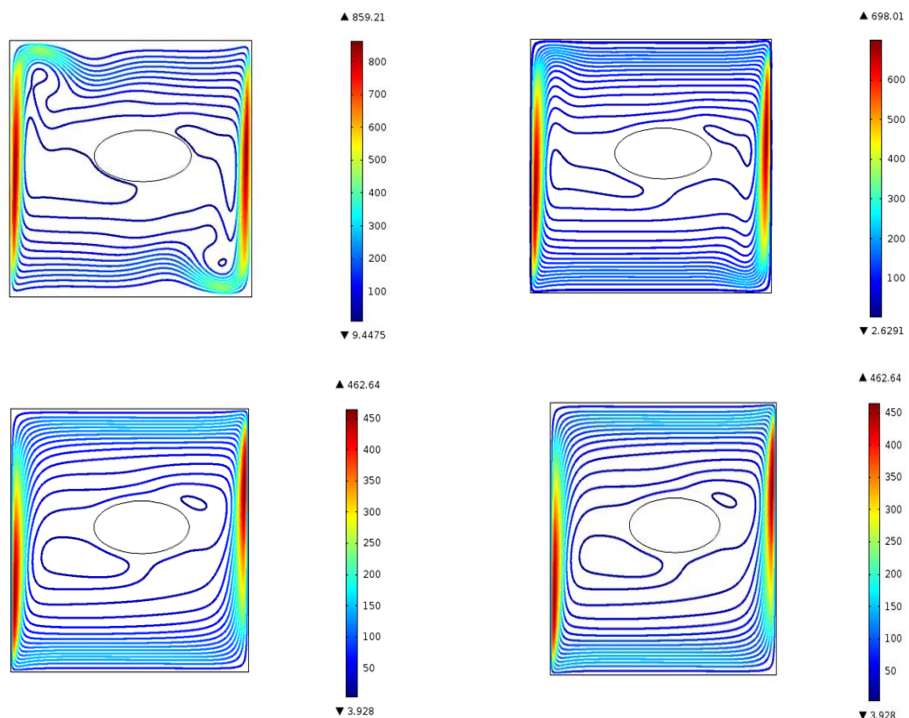
Fig. 5. Streamlines for (a) Ha = 0 ; (b) Ha = 50; (c) Ha = 100; (d) Ha = 150 while
　　Ra = 1000000 and Pr = 0.733

Conduction dominant heat transfer is observed form the isotherms in Fig. 6, 7, 8 at Ra= 10^4 to 10^6. With increasing the Rayleigh number, the isotherms are condensed next to the side wall which means increasing heat transfer through convection. Formation of thermal boundary layers can be found from the isotherms at Ra= 10^4 and 10^6. The cavity was heated at the left and right wall are cooled while the rest of the boundaries were insulated.
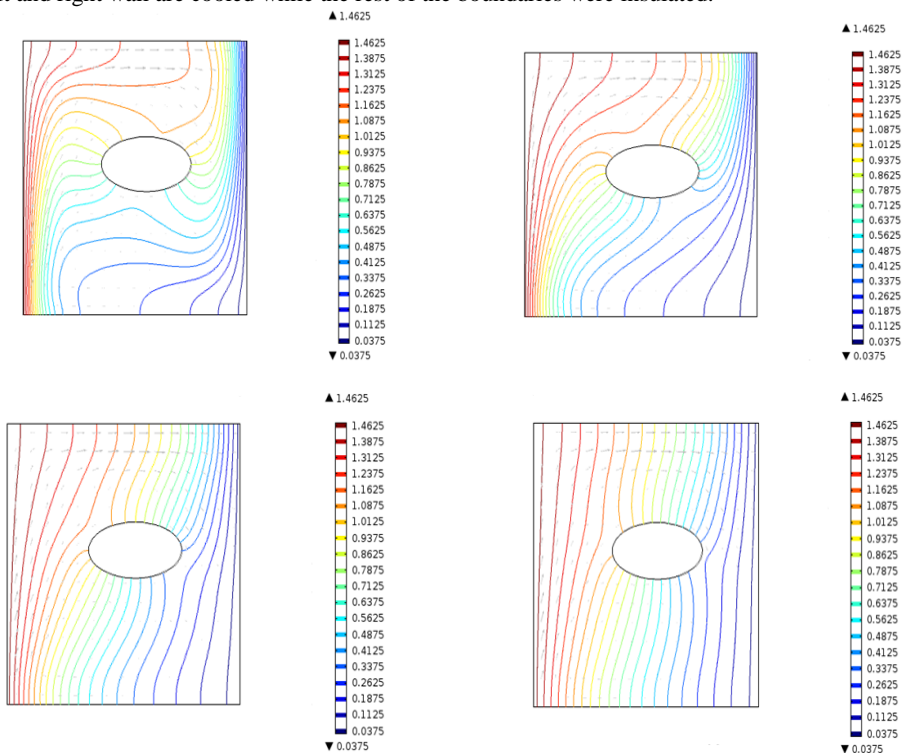
Fig. 6. Isotherms for (a) Ha = 0 ; (b) Ha = 50; (c) Ha = 100; (d) Ha = 150 while
Ra = 10000 and Pr = 0.733
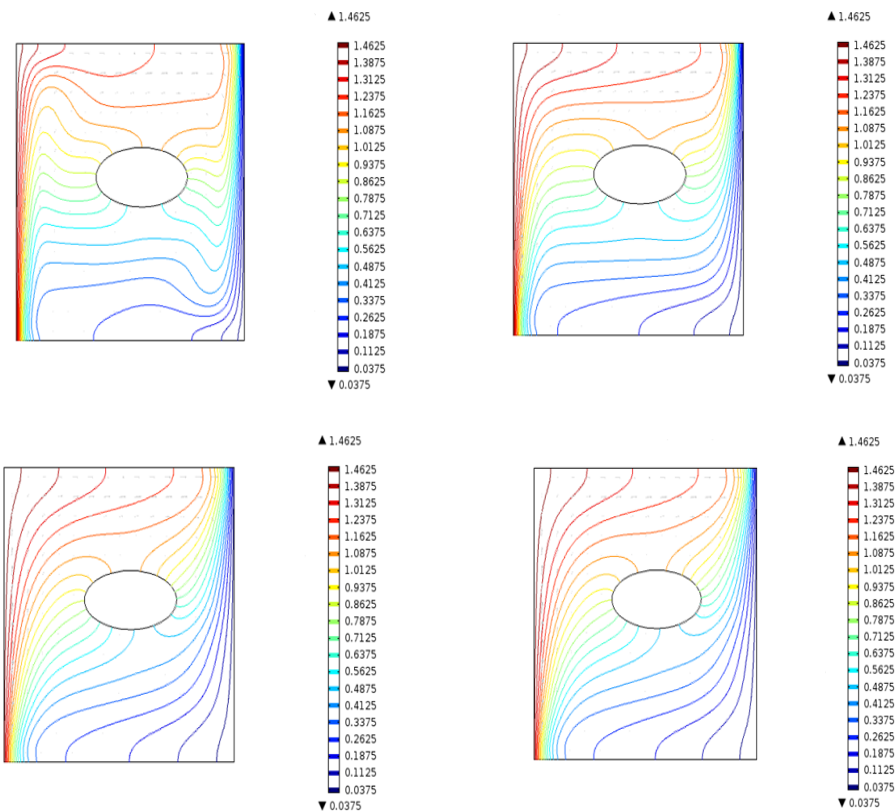
Fig. 7. Isotherms for (a) Ha = 0 ; (b) Ha = 50; (c) Ha = 100; (d) Ha = 150 while
Ra = 100000 and Pr = 0.733.
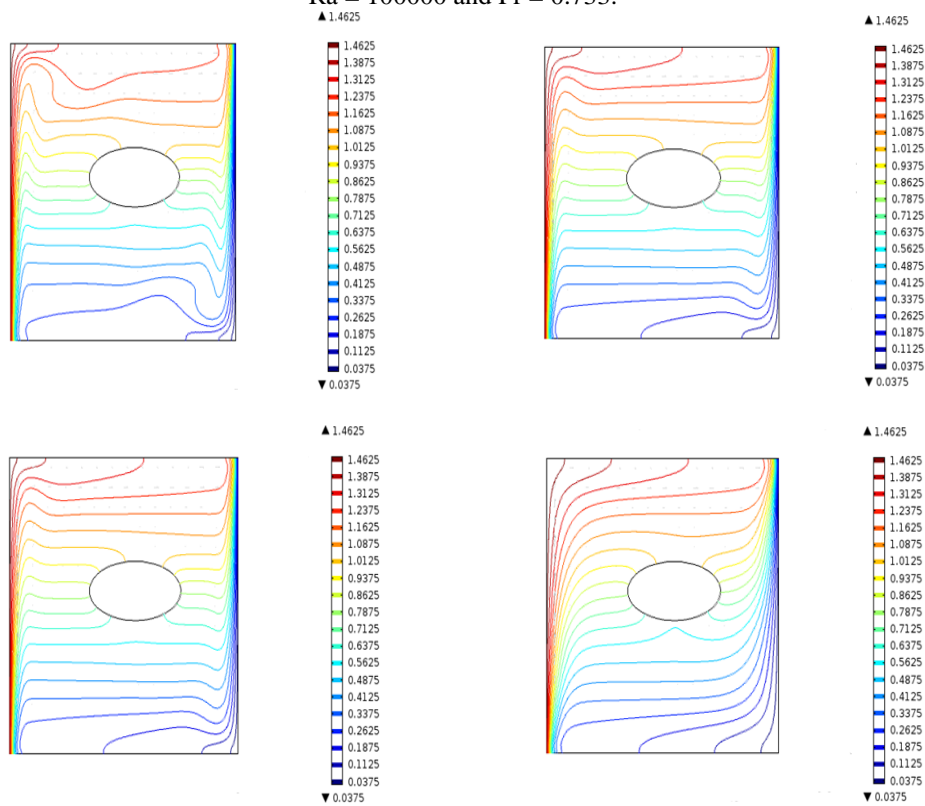
Fig. 8. Isotherms for (a) Ha = 0 ; (b) Ha = 50; (c) Ha = 100; (d) Ha = 150 while
Ra = 1000000 and Pr = 0.733

Variations of the local Nusselt number along the bottom wall of the square cavity with the Rayleigh number at different Hartmann number shown in Fig. 9. Owing to the symmetry in thermal boundary conditions, the local Nusselt number is symmetrical with respect to the vertical midline of the cavity. We see from the figure that the local Nusselt number increases with the Rayleigh number in major portion of the hot wall. In the middle of the bottom wall the local Nusselt number equals to zero and does not change significantly with increase in the Rayleigh number. It can be seen from the figure that the local Nusselt number increases with the Rayleigh number in major portion of the hot wall. In the middle of the left wall the local Nusselt number equals to zero and does not change significantly with increase in the Hartmann number.
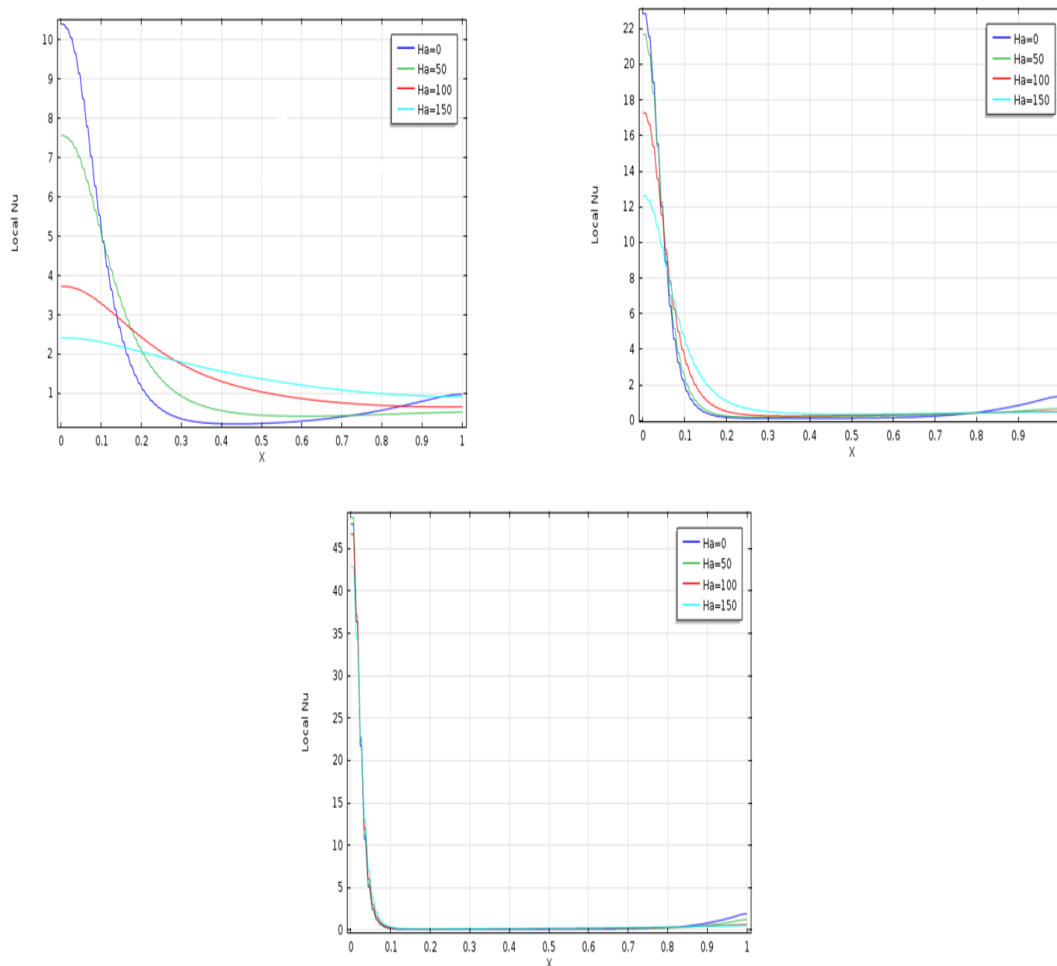
Fig. 9. Variation of local Nusselt number along the bottom wall for different Hartmann number
with Pr = 0.733 and Ra = Ra = 10000, 100000, 1000000.
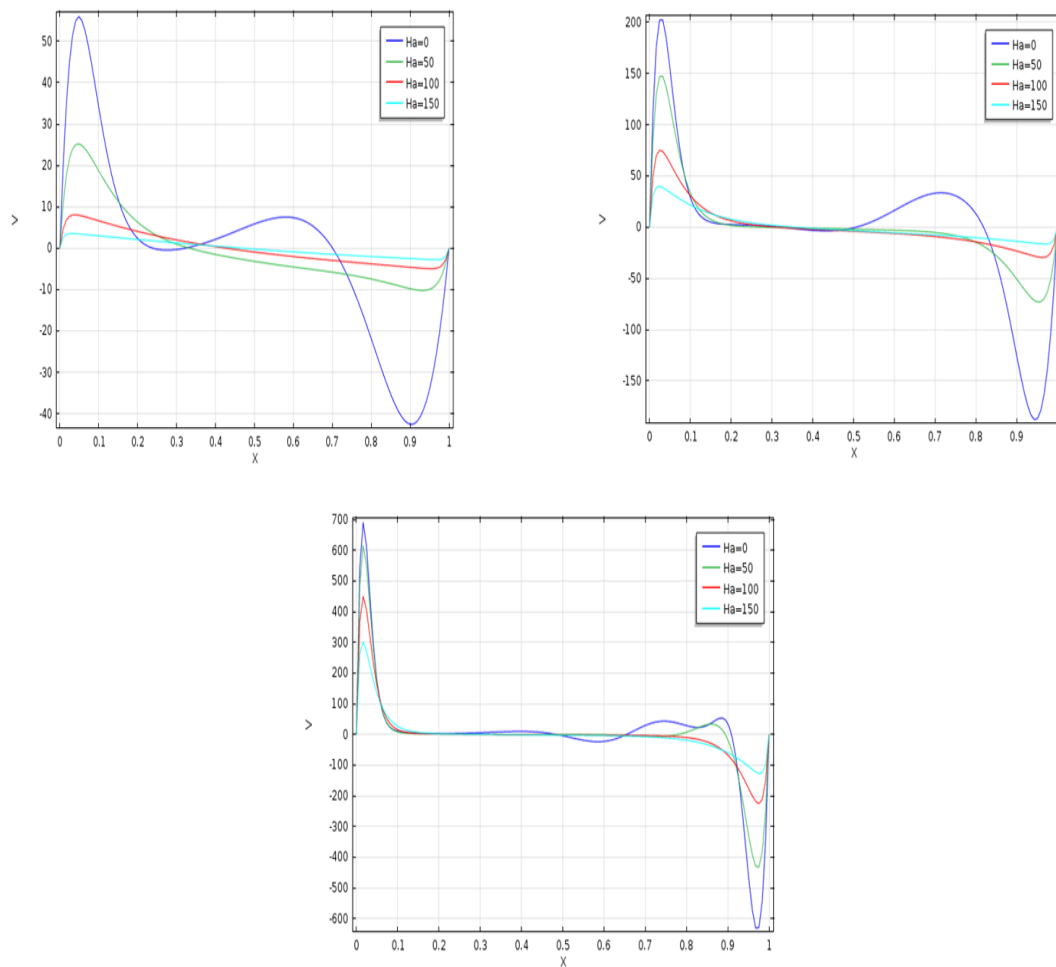
Fig. 10. Variation of velocity profile along the bottom wall at different Hartmann number
with Pr = 1.733 and Ra = 10000, 100000, 1000000

Variations of the velocity components along the bottom wall for different Rayleigh number with Pr = 0.733 of the cavity are shown in Fig. 10. From the figure it can be observed that the curves are symmetrical x-axis because of symmetrical adiabatic ellipse block. The velocity increasing and decreasing for various types of Rayleigh number when Ha = 0.

Variation of the dimensionless temperature along the bottom wall of the square cavity with Rayleigh number at different Hartmann number are shown in Fig. 11. For moderate and high Rayleigh number (Ra= 10^4 ,10^5 and 10^6) and for a weak magnetic field strength there is a temperature of the absolute value of maximum and minimum value of temperature increases with increasing the Rayleigh number (increasing the buoyant force). Convection is dominant heat transfer mechanism because of high Ra and low Ha. Heat transfer by convection alters the temperature distribution to such an extent that temperature gradients in the centre are close to zero. From the stream line pattern we see that there is a strong upward flow near the cold wall and downward flow at the hot wall.
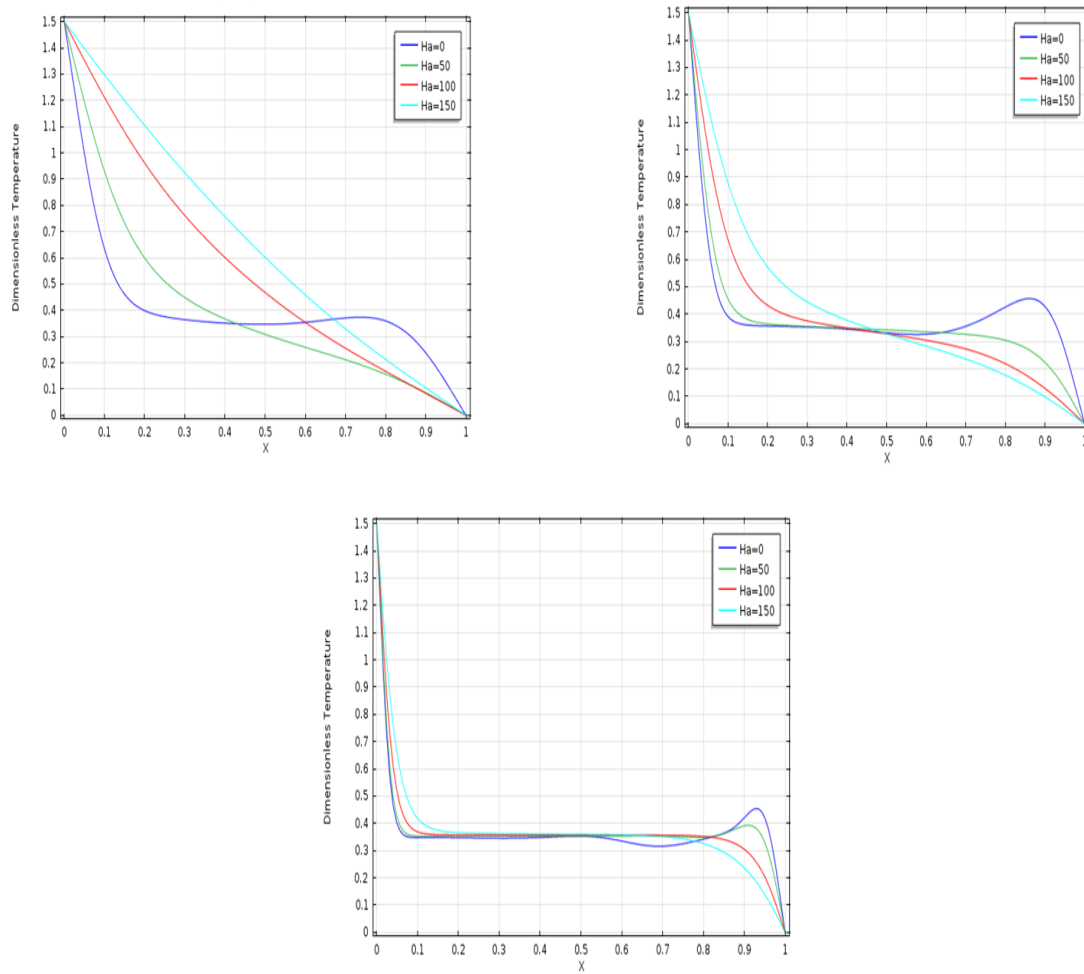
Fig. 11. Variation of temperature profiles along the bottom wall at different Hartmann number
with Pr = 1.733 and Ra = 10000, 100000, 1000000.

Also effect of different Rayleigh numbers on the flow field while Ha = 0 and Pr = 0. 733 are shown in figure below. Variation of local Nusselt number, Variation of velocity profiles, Variation of dimensionless temperature profiles, and Variation of the average Nusselt number are shown below in Fig. 12.
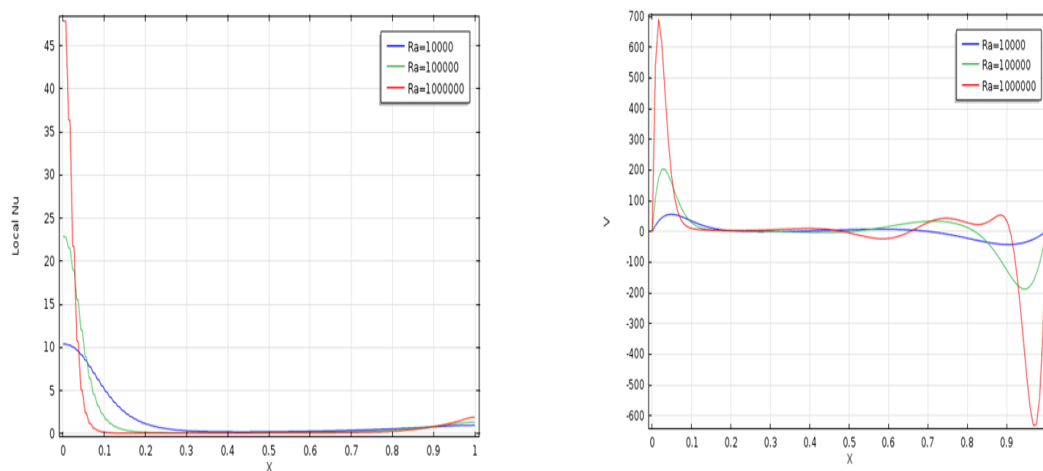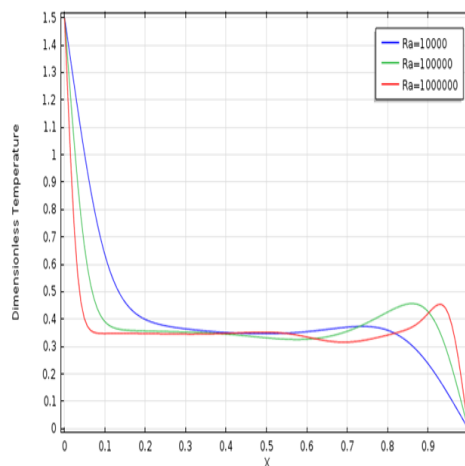
Fig. 12. Variation of local Nusselt number, velocity profile, temperature profiles along the bottom wall at different Rayleigh number with Pr = 0.733 and Ha = 0.
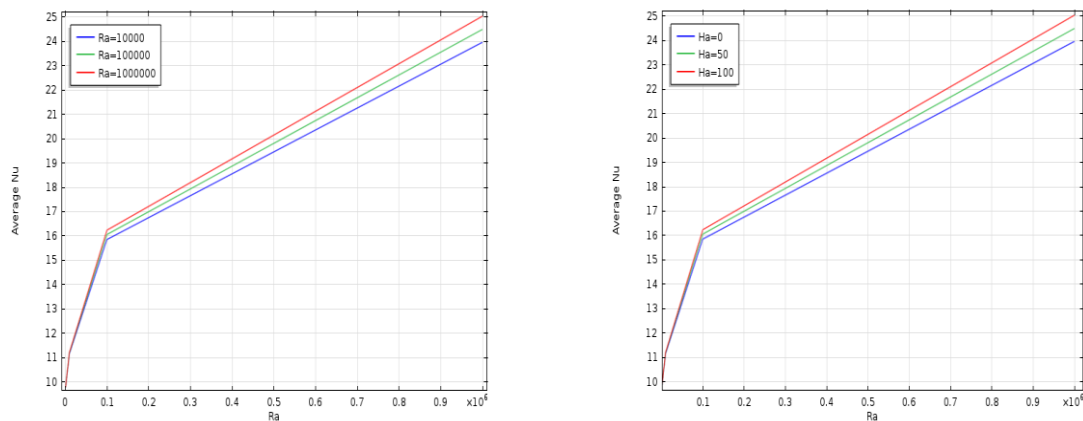
Fig. 13. Variation of the average Nusselt number along the bottom wall of the square cavity with different Rayleigh numbers & different Hartmann numbers at Prandtl number 0.733.

Plot of the average Nusselt number of the adiabatic bottom wall as a function of Rayleigh number at different Hartmann number is shown in Fig. 13. For a fixed Hartmann number, with increases in the Prandtl number the flow velocity decreases, the free convection is suppressed and finally the rate of heat transfer decreases. When Ra increases then we see that the flow strength is also increases in cold & adiabatic walls at fixed Ha & Pr. At a constant Prandtl number, with increase in Rayleigh number the buoyancy force increases and the heat transfer is enhanced. Therefore at high Rayleigh numbers, a relatively stronger magnetic field is needed to decrease the rate of heat transfer.

VI. CONCLUSION

Effect of magneto-hydrodynamic natural convection fluid flow and heat transfer in a square cavity filled with an electric conductive fluid with elliptic shape adiabatic block are studied numerically. Finite element method was used to solve governing equations for a heat generation parameters, Rayleigh numbers and Hartmann numbers. We observed that there were very good agreements between Ra & Ha in different cases. For all cases considered, two counter rotating eddies were formed inside the cavity regardless the Rayleigh and the Hartmann numbers. The obtained results showed that the heat transfer mechanisms, temperature distribution and the flow characteristics inside the cavity depended strongly upon both the strength of the magnetic field and the Rayleigh numbers. From the present investigation the following conclusions may be drawn as: with increase in the buoyancy force via increase in Rayleigh number, to decrease natural convection, a stronger magnetic field is needed compared to the lower Rayleigh numbers.

REFERENCES

[1]   T.H. Kuhen, R.J. Goldstein (1976): an experimental and theoretical study of natural convection in the annulus between horizontal concentric cylinders, J. of Fluid Mechanics, vol. 74, pp. 695- 719.

[2]   S. V. Patankar (1980): Numerical methods for heat transfer and fluid flow, New York, Hemisphere.

[3]   Acharya, S. (1985): Natural convection in an inclined enclosure containing internal energy sources and cooled from below, Int. J. Heat & Fluid flow, vol. 6, No. 2, pp. 113-121. doi:10.1016/0142-727X(85)90045-1.

[4]   Fusegi, T., Hyun, J. M., Kuwahara, K. (1992): Natural convection in a differentially Heated square cavity with internal heat generation, Num. Heat Transfer Part A, vol. 21, pp. 215-229. doi:10.1080/10407789108944873.

[5]   Hasnaoui, M., Bilgen, E., Vasseure, P. (1995): Natural convection heat transfer in rectangular cavities heated from below, J. Thermophysics Heat Transfer, vol.6, pp. 225-264.

[6]   Ganzarolli, M., M., Milanez, L., F. (1995): Natural convection in rectangular enclosures heated from below and symmetrical cooled from the sides, Int. J. of Heat and Mass Transfer, vol. 38,pp.1063-1073. doi:10.1016/0017-9310(94)00217-J.

[7]   Turkoglu, H., Yucel, N. (1995): Effect of heater and cooler locations on ural convection in square cavities,Num. Heat Transfer Part A, vol. 27, pp. 351-358. doi:10.1080/10407789508913705

[8]   H. Asan (2000): Natural convection in an annulus between two isothermal concentric square ducts, Int. Comm. Heat Mass Transfer, vol. 27, pp. 367-376.

[9]   D. G. Roychowdhury, S. K. Das, and T. S. Sundararajan.(2002): Numerical Simulation of Natural Convection Heat Transfer and Fluid Flow Around a Heated Cylinder Inside an Enclosure, Heat Mass Transfer, vol. 38, pp. 565- 576.

[10]   S. F. Dong and Y. T. Li.(2004): Conjugate of Natural Convection and Conduction in a Complicated Enclosure, Int. J. Heat Mass Transfer, vol. 47, pp. 2233- 2239.

[11]   E. J. Braga and M. J. S. de Lemos.(2005): Laminar Natural Convection in Cavities Filed with Circular and Square Rods, Int. Comm. Heat Mass Transfer, vol. 32, pp. 1289- 1297.

[12]   A. K. De and A. Dalal.(2006): A Numerical Study of Natural Convection Around a Square Horizontal, Heated Cylinder Placed in an Enclosure, Int. J. Heat Mass Transfer, vol. 49,   pp. 4608- 4623.

[13]   K. Kahveci, (2007): Natural convection in a partitioned vertical enclosure heated with a uniform heat flux, J. Heat Transfer, vol. 129, pp. 717-726.

[14]   T. Basak, S. Roy, S.K. Babu, A.R. Balakrishnan, (2008): Finite element analysis of natural convection flow in a isosceles triangular enclosure due to uniform and non- uniform heating at the side walls, Int. J. Heat Mass Transfer, vol. 51, pp. 4496- 4505.

[15]   Mohsen Pirmohammadi, Majid Ghassemi, and Ghanbar Ali Sheikhzadeh, (2009): Effect of a magnetic field on Buoyancy-Driven convection in differentially heated square cavity, IEEE transactions on magnetic, Vol. 45, No. 1.

[16]   M.M. Rahman, M.M. Billah, N. A. Rahim, N. Amin, R. Saidur and M. Hasanuzzaman,(2011): A numerical model for the simulation of double-diffusive natural convection in a right-angled triangular solar collector, International Journal of Renewable Energy Research 1(50-54).

[17]   M. Mahmoodi, Z. Talea'pour, (2011): 'Magnetohydrodynamic Free Convection Heat Transfer in a Square Enclosure heated from side and cooled from the ceiling' Computational Thermal Science, vol. 3, 219- 226.

[18]   S. Jani, M. Mahmoodi, M. Amini, (2013): Magnetohydrodynamic free convection in a square cavity heated from below and cooled from other walls, International Journal of Mechanical, Industrial Science and Engineering Vol. 7 No. 4.

[19]   A. H. Bhuiyan, R. Islam, M. A. Alim, (2014): Magnetohydrodynamic free convection in a square cavity with semicircular heated block, International Journal of Engineering Research & Technology (IJERT), Vol. 3 Issue 11.

Research Paper   Open Access

"J & K" SAFFRON?... *(RAMANUJAM "PLANT")*
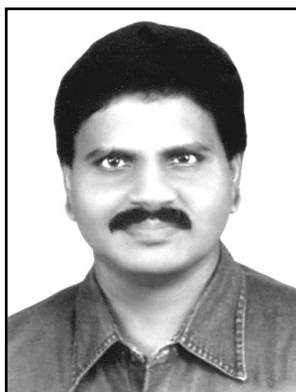
M.Arulmani,
B.E. (Engineer)

V.R.Hema Latha,
M.A., M.Sc., M.Phil. (Biologist)

I.   FOREWORD:

This scientific research focus about the Ancestral origin of **J & K Saffron** based on global level importance on saffron flower during author's tour to the land of **Kashmir** from **10-6-2015 to 14-6-2015**.

II.   EXPERIENCING KASHMIR:

The land of J & K also alternatively known as "**PARADISE ON THE EARTH**" is a secular soil where people belong to various religions like Hindu, Buddhism, Christian, Islam, Sikh are living together. The existence of very old Sankaracharya temple at Zambavar mountain, Sun temple at Martland, ancient Church, Mosque are some of the example of flourishing of various religions on this land.

The **Kashmir valley** is flourished by river "**JHELUM**" (**J-EZHEM**) passing through Srinagar and enriching the land of **PAKISTAN** also without any discrimination. Further the "**DAL LAKE**" surrounded by four garden like Mughal garden, Shalimar garden gives additional beauty to Kashmir. Further the experience of Boat house, Shicharya ride on the Dal Lake, Gondola rope car leading to top range of Himalaya of snow glaciers (about 18000 feet above MSL) is marvelous.

From prehistoric geological evolution it is focused by the author that "**J & K**" shall be considered as the "**Single large continent**" consider exists with different genetic value (i.e.) state of continent **before sunshine** and **after sunshine**. "**K**" shall be considered as the "**BLUE CONTINENT**" (K-Nadu) before sunshine and "**J**" shall be considered as the "**GREEN CONTINENT**" (J-Nadu) after

sunshine derived from "**DARK CONTINENT**" (Kandy) and "**WHITE CONTINENT**" mass from "**MARS PLANET**". Hence the **J & K** land shall be called as "**PARADISE ON THE EARTH**". All other global nations shall be considered as the **J & K diversity** during "**TRIASSIC PERIOD**" and **three nuclear age**.

It is further focused by the author that the **J-CONTINENT** shall be considered as the land of "**FIRST SUNSHINE**" on the "**EARTH PLANET**" and the J-population might have birth of first sunshine and birth of "**SAFFRON FLOWER**" on the land of "**J-CONTINENT**" (**J-NADU**). The author call these J-population as origin of **DRAVIDIAN**. **DRAVIDIAN** shall mean the human race born of "**SUNSHINE**" and having "**BROWN SKIN COLOUR COMPLEXION**". The population lived in "**K-CONTIENENT**" (**K-NADU**) shall be called as "**Proto Indos**" who shall be considered as "**BLUISH BLACK POPULATIONS**". The Dark population shall be considered as belong to "**PLASMA CONTINENT**" (**KANDY**) descended from "**WHITE CONTINENT**" (Mars Planet). The three stigma of saffron flower might lead to **Sivaism** and worship of lord Shiva in Dravidian culture.

**Ancient Sankaracharya Temple,
Srinagar, Kashmir**
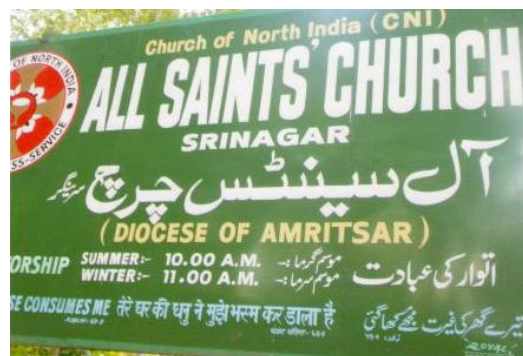
**Ancient Tamil Alphabet in
Kashmir Language**

**Am I Pakistan Arab (Red Dravidian)?...
No... No... No... I am Kashmir Arab (Black
Dravidian)... Dark Glass is symbol of
Dravidian culture**
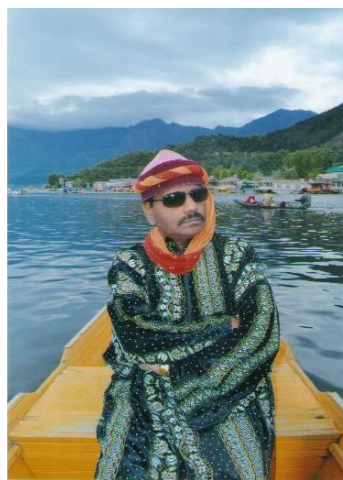
**What a wonderful J&K
Himalaya!... God has created
life time energy in the form of
snow glaciers and slowly melts
according the need during
entire cosmological life cycle!...**

**Gondola cable car, Gulmarg,
Kashmir**

III.   ABSTRACT

It is focused that the plant "SAFFRON" also called in Proto Indo Europe root as "KUNGUMA POO" is especially cultivated only in the land of "J & K" and in some places in "IRAN" and nowhere cultivated in other parts of global nations. **What is the Specially of Saffron in the land of J & K?...** It is globally believed that if "SAFFRON" is consumed in the beginning of "Trimester of Pregnancy" the baby born of will be **colourful and beautiful**. **What is the Specially of J & K Saffron flower?...**

**J&K Saffron Flower
(Crocus sativus)**

It is further focused that in Taxonomy of Biological Science the "**Plant Kingdom**" is basically divided into two categories as (i) Flowering plants (ii) Non – Flowering plants.

> *i) "SAFFRON" is a "FLOWER"?...*
>
> *ii) "SAFFRON" is a "PLANT"?....*
>
> *iii) "SAFFRON" is a "FLOWERING   PLANT"?...*
>
> *- Author*

This scientific research focus that "**FLOWER**" and "**PLANT**" shall be considered as distinguished classification. As such "**SAFFRON**" shall be considered as "**FLOWER**" rather than "**PLANT**" in the plant kingdom Further "**SAFFRON**" shall be considered as new species to "**JAFFRON**" evolved in the land of "**J-CONTINENT**" due to impact of "**FIRST SUNSHINE**" on the earth planet (Say 1,00,000 years ago). The "**SAFFRON**" shall also be called as "**DRAVIDIAN FLOWER**". **SAFFRON** shall be considered as **SOUL** of 2nd generation flowers. The philosophy of Jaffron shall be described as below. **JAFFRON** (**JAMMU**) shall mean "**MOTHER OF FLOWER**" and ancestral to "**SAFFRON**" (three stigma).

(i)

J

ௗ
(JAFFRON)

(ii)
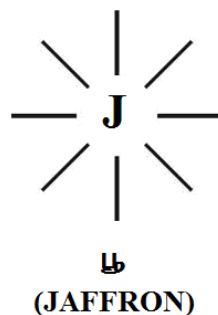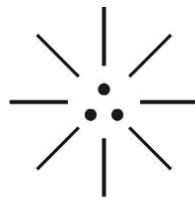
பூஜை

(LAW OF CULTURE)

i)   **Right dot PROTON – "LOVE" (DHARMAM)**
ii)   **Left dot ELECTRON –"MERCY" (KARMAM)**
iii) **Center dot PHOTON –"HOPE" (BRAHMAM)**

This scientific research further focus that the entire universe shall be considered created by "**Supernatural Person**" called by name by another as "**RAMANUJAM**" who considered created everything through his "**MOTHER JANAKI**" (**SOUL**). **RAMANUJAM** shall be considered as a "**Supernatural Plant**" and **JANAKI** shall be considered as "**DIVINE FLOWER**" (**JAFFRON**) and considered integral part of "**PLANT**". The philosophy of "**PLANT**" (**RAMANUJAM**) and "**FLOWER**" (**JANAKI**) shall be distinguished as below. Various flowers of Tree, Herb, Shrub, Climber shall be considered as species to **JAFFRON.**

(i)
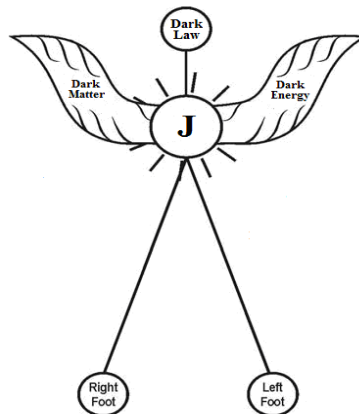
பூமகன்
(Virgin Father)
(DARK PLANT)

(ii)

கலைமகள்
(Virgin Mother)
(WHITE LOTUS)

The philosophy of "JAFFRON" and "JAMMU" shall be defined within the following scope.

i)   **JAFFRON** shall mean "**WHITE LOTUS**" (**BUD**)
ii)   **JAFFRON** shall mean exist under "**ENDOTHERMIC ENVIRONMENT**"
iii)   **JAFFRON** shall mean "**MOTHER OF FLOWERS**" (**SOUL**).
iv)   **JAMMU** shall mean "**WHITE LOTUS PETAL**"
v)   **JAMMU** shall mean exist under "**EXOTHERMIC ENVIRONMENT**"
vi)   **JAMMU** shall mean "**Three-in-one**" petal

(i.e.) THREE-IN-ONE petal which consists of Billions of "**TRISUL**" (**Gynoecium**) having distinguished genetic value (**Allele**)

> *"JAFFRON" (Bud) shall mean exist due to impact of "J-RADIATION" "JAMMU" (petal) shall mean the state of flower exist due to impact of "SUN SHINE". "JAFFRON" shall mean belong to "FLOWER FAMILY" rather than "PLANT FAMILY". "SAFFRON" shall mean species to "JAFFRON". No JAFFRON shall mean NO FLOWERS. NO JAFFRON shall mean no fruits. No JAFFRON shall mean no vegetables. "KEVA TEA" shall mean energetic Dravidian drink "KASAYAM" derived from "K" (K-NADU).*
>
> *- Author*

Philosophy of "PLANT" AND "FLOWER"?...

It is hypothesized that "**PLANT**" shall be considered like a pre existing "**MEGA STAR**" whose "**SOUL**" shall be considered like a source of "**Creative Radiation**" emanating billions of rays composed of **three-in-one** fundamental particles **PHOTON, ELECTRON, PROTON** responsible for varied genetic characteristics of Billions of "**Flower species**" from a single ancestral source say "**ALLELE FAMILY**". Plant is like "**SPIRIT**". Flower is like **SOUL**.
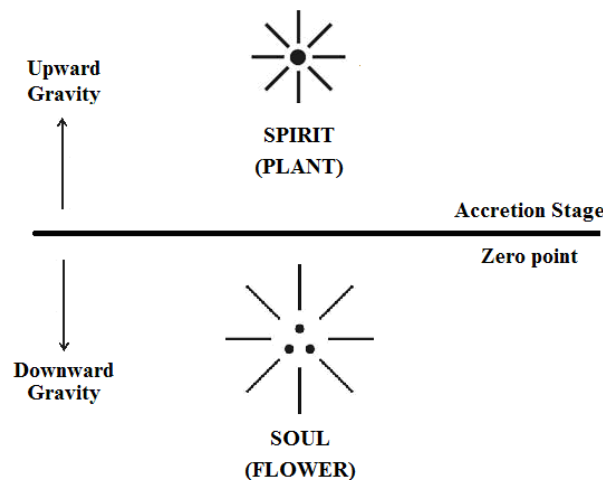
It is further focused that "**JAFFRON**" shall be considered as the mother of flowers composed of billions of **Gynoecium** (**Trisul**) having distinguished genetic value (**Allele**) as described.

(i)
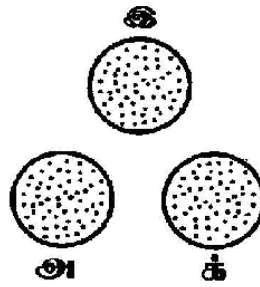
JAFFRON
(Alle-e Family)

(ii)

WHITE LOTUS
(Natural Flower)

i)　　*RAMANUJAM is like "PLANT"*
ii)　　*JANAKI is like "FLOWER"*
iii)　*RAMANUJAM is like "ACCEA FAMILY"*
iv)　*JANAKI is like "ALLE-e FAMILY"*

Author.

1.0　Philosophy of "DARK LOTUS"?...

It is focused that thousands of mushrooms are spontaneously evolved during rainy season due to impact of "**LIGHTNING**" in darkness even without "**Sun-light**".

DARK LOTUS
(Mushroom)

> *i)*   ***Mushroom is a Plant?...***
> *ii)*   ***Mushroom is a Flower?...***
> *iii)*   ***Mushroom is a Flowering plant?...***
>
> *- Author*

It is hypothesized that Mushroom (agaricus bisporous) shall be considered as species to "**JAFFRON**" (Alle-e) shall also be called by author as "**DARK LOTUS**" or "**DIVINE FLOWER OF EARTH**". It is hypothesized that during "**Plasma age**" of expanding universe (say 3,00,000 years ago), the **white lotus** considered become **Dark lotus**. The dark lotus shall also be called by author as "**KAFFRON**" (**KALAN**). **SAFFRON** shall alternatively be called as "**BROWN LOTUS**".

IV.   CONCLUSION:

In Hindu mythology the Philosophy of Brahma, Rama, Krishna, Shiva shall be considered as the god of flowers of different generations in the expanding Universe as described below.

i)   Brahma – God of White Lotus
ii)   Rama – God of Dark Lotus
iii)   Krishna – God of Blue Lotus (Kaffron)
iv)   Shiva - God of Brown Lotus (Saffron)
v)

(J & K SAFFRON DIVERSITY)

" இந்தியநாடு என் தாய்;

தமிழ்நாடு என்தாயின் பாதஅடி.

என் தாயின் பாத அடியில் இப்புத்தக அஞ்சலி "
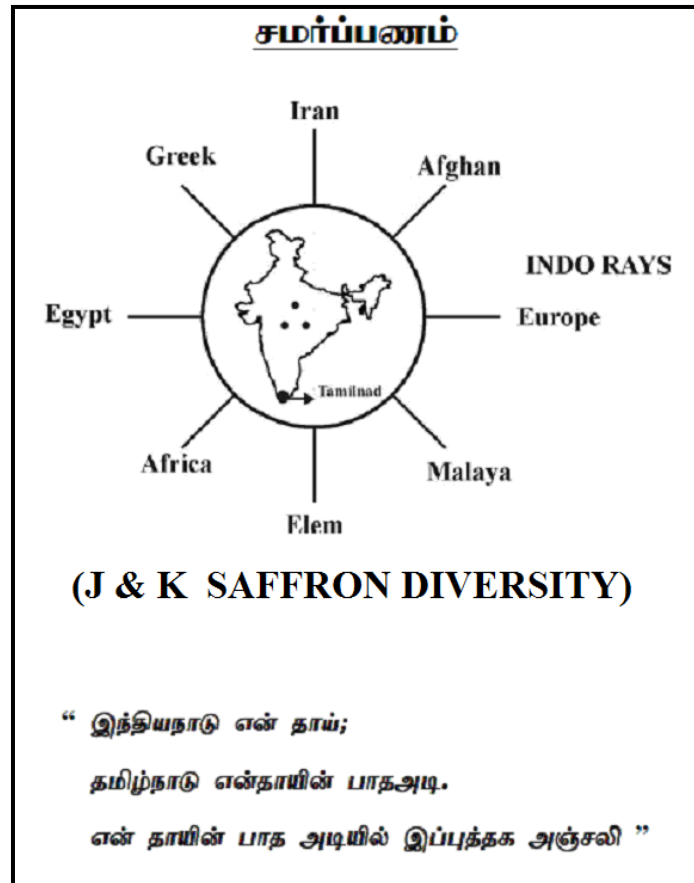
புதுக்கவிதை
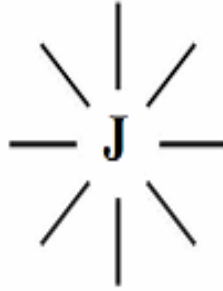
ஜானகி
(Jaffron)
(WHITE LOTUS)

அன்னையே... ஆரோக்கிய அன்னையே...

பூ வடிவிலான புவியாளும் பூங்கோதையே...

பூலோகத்தின் பூர்வீகமே... பூக்களின் சங்கமே...

கன்னித்தாயே... கலைமகளே... (White Lotus)

சேற்றில் பிறந்த வெண்தாமரையா நீ...

இல்லை... இல்லை... இல்லை...

பூமகனின் (Ramanujam) இதயத்தில்...

பூத்த வெண்தாமரை நீ (Soul)...

பூமிக்கு வந்த ஆகாயத்தாமரை நீ... (Divine flower)

நீ கருமை வடிவிலான "புரட்சித்தாய்" (Dark Lotus)

நீ செந்நிற வடிவிலான "திராவிடத்தாய்" (Brown Lotus)

நீ பொன்னிற வடிவிலான "செந்தமிழ்த்தாய்" (Red Lotus)

பூமகன்
(Ramanujam)
(PLANT)
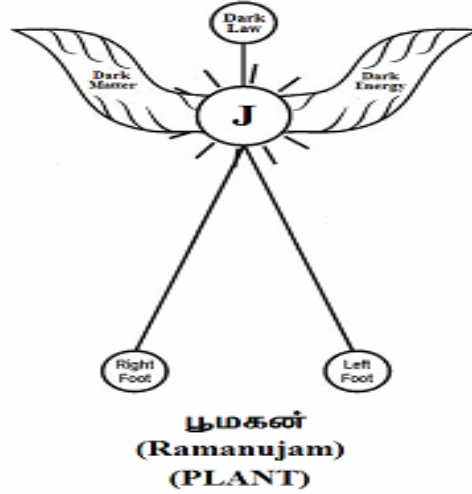
— M அருள்மணி
தமிழ்ப்பேசம் இந்தியன்

PREVIOUS PUBLICATIONS:

[1]. YUGADI WISHES (IARA, March 2015)
[2]. TAMIL PUTHANDU!... (AJER, April 2015)
[3]. THEN MADURAI?... (IJERD, April 2015)
[4]. TAMIL NEW YEAR COOL DRINK?... (AJER, April 2015)
[5]. SCIENTIFIC RAMANUJAM?... (IJERD, April 2015)
[6]. ARENKA NAYAKI IS MOTHER OF RAMA?... (AJER, April 2015)
[7]. TRIVIDAITE?... (IJERD, April 2015)
[8]. THALI CULTURE OF ANGELS?... (AJER, April 2015)
[9]. UNIVERSAL POET?... (IJERD, April 2015)
[10]. "JANGLISH" IS CHEMMOZHI?... (AJER, April 2015)
[11]. RAMANUJAM PARLIAMENT?... (IJERD, May 2015)
[12]. CAN LORD JUDGE GOD?... (AJER, May 2015)
[13]. MAY DAY?... (IJERD, May 2015)
[14]. DEEMED UNIVERSITY?... (AJER, May 2015)
[15]. CAR FESTIVAL?... (IJERD, May 2015)
[16]. MISSING HEART?... (AJER, May 2015)
[17]. Morning Star!... (AJER, May 2015)
[18]. JAYAM (J-AUM)!... (IJSER, June 2015)
[19]. RAMANUJAM CONSCIENCE (IJERD, June 2015)
[20]. "J & K" (IJSER, June 2015)

Research Paper	Open Access

The boundary layer flow of nanofluids over an isothermal stretching sheet influenced by magnetic field.

Preeti Agarwala [1], R. Khare [2]

[1] *Department of Mathematics & Statistics, SHIATS, Allahabad, INDIA*
[2] *Department of Mathematics & Statistics, SHIATS, Allahabad, INDIA*

ABSTRACT :   *An analysis is carried out to study the effect of the magnetic field on the boundary layer flow of the nanofluids over an isothermal stretching surface. Two types of nanofluids namely Ag–water and Cu–water are considered. Similarity transformation is used to convert the governing nonlinear equations into coupled higher order nonlinear ordinary differential equations. Fourth-order Runge–Kutta method with shooting technique is employed for the numerical solution of the obtained equations. Numerical results are obtained for distribution of velocity, temperature and concentration, for both cases .The numerical results indicate that an increase in the nanoparticle volume fraction will decrease the velocity boundary layer thickness. Meanwhile, the presence of nanoparticles results in an increase in the magnitude of the skin friction along the surface. Such effects are found to be more evident in the Ag–water solution than in the Cu–water solution. The obtained numerical results have been presented graphically and discussed in details.*

KEYWORDS – *MHD Flow, Magnetic field , Nanofluids, Runge-Kutta Method .*

I.   INTRODUCTION

A large number of theoretical investigations dealing with magnetohydrodynamic (MHD) flows of nanofluids have been performed during the last decades due to their swiftly increasing applications in many fields of technology and engineering, such as MHD power generation, . Recently, the application of magnetohydrodynamics in the polymer industry and metallurgy has attracted the attention of many researchers. Heat and mass transfer processes by means of external force effects is one of the most important problems in modern applied physics. The study of the magnetic field effect on heat and mass transfer is of substantial significance in various industries. Sattar and Alam [1] studied the thermal diffusion as well as transportation effects on MHD free convection and mass transfer flow past an accelerated vertical porous plate. Choi [2] who coined the term nanofluid proposed that the thermal conductivity of the base fluid can be increased by adding low concentration of nanoparticles of materials having higher thermal conductivity than the base fluid.Putra et,al [3]studied about the temperature dependence of thermal conductivity enhancement for nanofluids. Raptis and Perdikis [4] studied the viscous flow over a non-linearly stretching sheet in the presence of a chemical reaction and magnetic field. Singh et al. [5] studied the effects of thermal radiation and magnetic field on unsteady stretching permeable sheet in presence of free stream velocity. Khan and Pop [6] examined the boundary-layer flow of a nanofluid past a stretching sheet. Momentum and energy equations for a nanofluid over a linearly impermeable stretching surface in the absence of slip and magnetic field were studied by Noghrehabadi et al [7] they also studied the theoretical investigations of SiO_2-water nanofluid heat transfer enhancement over an isothermal stretching sheet. Makinde and Aziz [8] analyzed the boundary layer flow of nano fluids over a stretching sheet with convective heat transfer boundary condition. Rana and Bhargava [9] numerically studied the flow and heat transfer of a nanofluid over a nonlinearly stretching sheet. Yacob et al.[10] analyzed enhancement of two types of nanofluids, namely, Cu-water and Ag-water nanofluids over an stretching sheet with convective boundary condition. Khare and Rai [11] examined the MHD flow of non-Newtonian fluid through a rectangular channel. Khare and Srivastava [12] studied the effect of Hall current on MHD flow of a dusty viscoelastic liquid through porous medium past an Infinite Plane. Several researches investigated the MHD boundary layer flow [13,14,15] in various situations.

In this paper, an analysis is carried out numerically to study the effect of the magnetic field on the boundary layer flow of the nanofluids over an isothermal stretching surface. Two types of nanofluids namely Ag–water and Cu–water are considered. . The effects of the governing parameters on the velocity and temperature have been discussed and presented in tables and graphs.

II.   FORMULATION OF MATHEMATICAL MODEL FLOW

Consider an incompressible steady two-dimensional boundary layer flow past an isothermal stretching sheet in a water-based nanofluid which can contains different volume fraction of Cu (copper) and Ag (silver) nanoparticles and uniform magnetic field is applied on it. It is assumed that the induced flow of nanofluid is laminar, and the base fluid (i.e. water) and the nanoparticles are in thermal equilibrium and no slip occurs between them. The thermophysical properties of the fluid and nanoparticles are given in Table 1. It is assumed that the sheet surface has constant temperature of T_w, and the temperature of ambient fluid is T_∞. The fluid outside the boundary layer is quiescent, and the stretching sheet velocity is $U(x) = cx$ where c is a constant. Under the usual boundary layer approximations, the continuity, momentum and energy equations for the nanofluid, in the Cartesian coordinates can be represent as.

The continuity equation;

$$\frac{\partial u}{\partial x} + \frac{\partial v}{\partial y} = 0 \tag{1}$$

The momentum equation

$$u\frac{\partial u}{\partial x} + v\frac{\partial u}{\partial y} = \frac{\mu_{nf}}{\rho_{nf}}\frac{\partial^2 u}{\partial^2 y} \tag{2}$$

The energy equation

$$u\frac{\partial T}{\partial x} + v\frac{\partial T}{\partial y} = \alpha_{nf}\frac{\partial^2 T}{\partial y^2} \tag{3}$$

The initial and boundary conditions are;

$$at \quad y = 0; \quad v = 0, \quad u = U_w(x), \quad T = T_w$$

$$at \quad y = \infty; \quad u = 0, \quad v = 0, \quad T = T_\infty \tag{4}$$

where, u and v are the velocity components in the x and y directions respectively. T is temperature of the nanofluid, T_∞ temperature of the ambient nanofluid, B_0 the uniform magnetic field strength, σ electrical conductivity of base fluid, ρ_{nf} effective density of the nanofluid, α_{nf} thermal diffusivity of the nanofluid, μ_{nf} dynamic viscosity of the nanofluid are respectively given as:

$$\rho_{nf} = (1-\varphi)\rho_f + \varphi\rho_s \tag{5}$$
$$\alpha_{nf} = \frac{K_{nf}}{(\rho C_p)_{nf}} \tag{6}$$
$$\mu_{nf} = \frac{\mu_f}{(1-\varphi)^{2.5}} \tag{7}$$

The effective density of the nanofluid is given by
$$(\rho C_p)_{nf} = (1-\varphi)(\rho C_p)_f + \varphi(\rho C_p)_s \tag{8}$$

$$\frac{K_{nf}}{K_f} = \frac{(K_s + 2K_f) - 2\emptyset(K_f - K_s)}{(K_s + 2K_f) + \emptyset(K_f - K_s)} \tag{9}$$

Here $\vartheta_f, \mu_f, \rho_f, K_f$ are the Kinematic viscosity, dynamic viscosity, density and thermal conductivity of the base fluid respectively $\rho_s, K_s, (\rho C_P)_s$ are the density, thermal conductivity and heat capacitance of the nanoparticles respectively; φ is the solid volume fraction of nanoparticles and K_{nf} is thermal conductivity of the nanofluid. Subscripts f and s are used for base fluid and nanoparticles respectively. In this case, water as base fluid with nonoparticles of copper and silver are studied.

Table1: Thermophysical Properties For Pure Water And Various Types Of Nanoparticles.

Physical properties	water (H2O)	copper (Cu)	silver (Ag)
$\rho(kg/m^3)$	997.1	8933	10500
$C_p(J/kg\,K)$	4179	386	234
$k(W/mK)$	0.613	400	429

III.   SOLUTION OF THE PROBLEM

To simplify the mathematical analysis of our study we introduce the following similarity transformations

$$\psi(x,y) = f(\eta)x(v_f c)^{1/2} \qquad u = cxf'(\eta)$$

$$v = -f(\eta)(v_f c)^{1/2} \qquad \eta = y(c/v_f)^{1/2}$$

$$\theta(\eta) = \frac{T - T_\infty}{T_w - T_\infty} \tag{10}$$

Where $\psi(x,y)$ is the stream function with $\quad u = \frac{\partial \psi}{\partial y}, v = -\frac{\partial \psi}{\partial x}$

$\theta(\eta)$ = dimensionless temperature.

$f(\eta)$ = dimensionless velocity

where primes denote differentiation with respect to the similarity variable η. By applying the introduced similarity transforms (10) on the governing equations (1-3), the equations are reduces as follows,

$$\frac{\mu_{nf}}{\mu_f} f''' + \left[(1-\phi) + \phi \frac{\rho_s}{\rho_f}\right](f f'' - f'^2) - M f' = 0 \tag{11}$$

$$\frac{k_{nf}}{k_f}\theta'' + \Pr\left((1-\phi)+\phi\frac{(\rho c_p)_s}{(\rho c_p)_f}\right)f\theta' = 0 \tag{12}$$

Subject to the following boundary conditions:

$$\eta = 0, \quad y = 0, \quad f = 0, \quad f' = 1, \quad \theta = 1$$

$$\eta \to \infty, \quad y \to \infty, \quad f' = 0, \quad \theta = 0 \tag{13}$$

$$\Pr = \frac{\mu_f}{k_f} \qquad \Pr = \text{Prandtl number.}$$

The physical quantities of interest in this problem are the local skin friction coefficient C_f and the Nusselt number Nu_x, which are defined as

$$C_f = \frac{\tau_w}{\rho_f u_w^2} \qquad\qquad Nu = \frac{q_w}{k_f(T_w - T_\infty)} \tag{14}$$

Where ,

τ_w is the surface shear stress and q_w is the surface heat flux ,which are given by

$$\tau_w = \mu_{nf}\left(\frac{\partial u}{\partial y}\right)_{y=0} \qquad\qquad q_w = -k_{nf}\left(\frac{\partial T}{\partial y}\right)_{y=0} \tag{15}$$

Using the similarity variable (10), we obtain

$$\text{Re}_x^{1/2}C_f = \frac{1}{(1-\phi)^{2.5}}f''(0) \qquad\qquad \text{Re}_x^{-1/2}Nu = -\frac{k_{nf}}{k_f}\theta'(0) \tag{16}$$

$$\text{Re}_x = u_w x/v_f \qquad \text{is the local Reynolds number.}$$

IV.   RESULTS AND DISCUSSIONS

In the present paper an analysis is carried out numerically to study the effect of the magnetic field on the boundary layer flow of the nanofluids over an isothermal stretching surface. Two types of nanofluids namely Ag–water and Cu–water are considered. It is found that the behavior of the fluid flow changes with the change of nanoparticle type.As the governing boundary layer equations (11) and (12) are non linear, it is not possible to get the closed form solutions. As a result, the equations with the boundary conditions (13) are solved numerically using Runge - Kutta forth order method with a systematic guessing of $f''(0)$ and $\theta'(0)$ by the shooting technique until the boundary conditions at infinity are satisfied. The step size $\Delta\eta = 0.001$ is used while obtaining the numerical solution. The numerical computations are carried out for velocity, temperature at different values of magnetic parameter M and are presented in figures 1- 6.

Table2: Thermophysical Properties of Ag- water Nanofluid.

Φ	ρ_{nf}	Cp_{nf}	μ_{nf}	k_{nf}	Pr_{nf}
0.00	997.10	4179.00	0.001002	0.613	6.830927
0.01	1092.129	4139.55	0.001027	0.631496	6.735387
0.02	1187.158	4100.10	0.001054	0.650367	6.644136
0.03	1282.187	4060.65	0.001081	0.669626	6.55695
0.04	1377.216	4021.20	0.00111	0.689284	6.47362
0.05	1472.245	3981.75	0.001139	0.709354	6.393956
0.06	1567.274	3942.30	0.00117	0.729849	6.317781
0.07	1662.303	3902.85	0.001201	0.750783	6.24493
0.08	1757.332	3863.40	0.001234	0.77217	6.175252
0.09	1852.361	3823.95	0.001268	0.794025	6.108607
0.10	1947.39	3784.50	0.001304	0.816363	6.044863

Table3: Thermophysical Properties of Cu- water Nanofluid**.**

Φ	ρ_{nf}	Cp_{nf}	μ_{nf}	k_{nf}	Pr_{nf}
0.00	997.100	4179	0.001002	0.61300	6.830927
0.01	1076.459	4141.07	0.001027	0.63149	6.737917
0.02	1155.818	4103.14	0.001054	0.650356	6.649174
0.03	1235.177	4065.21	0.001081	0.669609	6.564476
0.04	1314.536	4027.28	0.00111	0.689261	6.483621
0.05	1393.895	3989.35	0.001139	0.709325	6.406421
0.06	1473.254	3951.42	0.00117	0.729814	6.332704
0.07	1552.613	3913.49	0.001201	0.750741	6.262308
0.08	1631.972	3875.56	0.001234	0.772121	6.195085
0.09	1711.331	3837.63	0.001268	0.793968	6.130898
0.10	1790.69	3799.7	0.001304	0.816299	6.069621

Fig1. It shows the dimensionless velocity f '(η) for various values of magnetic parameter M. As the value of magnetic parameter M increases,the retarding force increases because of interaction of electric and magnetic fields   and consequently the velocity decreases. Fig2. Exhibits the effect of shear stress distribution for various values of M. It is observed that the magnitude of the wall of shear stress given by $(1/(1-\Phi)^{2.5})f''(0)$ decreases when the value of magnetic parameter M increases. Fig 3: Dipicts the dimensionless velocity profiles for selected values of volume fraction Φ. it shows that increase of nanoparticle volume fraction have not significant effect on the velocity profile. Fig 4: Shows effect of Prandtl number Pr on volume fraction for Cu-water and Ag-water nanofluids. It is obvious that as prandtl number Pr decreases volume fraction increases in both   the cases and the decrease of Pr is slightly more for Ag- water nanofluid than Cu- water   nanofluid. Fig 5: Reveals the effect of volume fraction on density of the Cu-water and Ag-water nanofluids.It is observed that when volume fraction increases, density of all nanofluids increases and the increase is more for Ag –water nanofluid than other nanofluid. Fig. 6. It exhibits the temperature profile for selected values of volume fraction Φ. It is very much evident from the fig that temperature of nanofluids increases as the value of volume fraction increases.
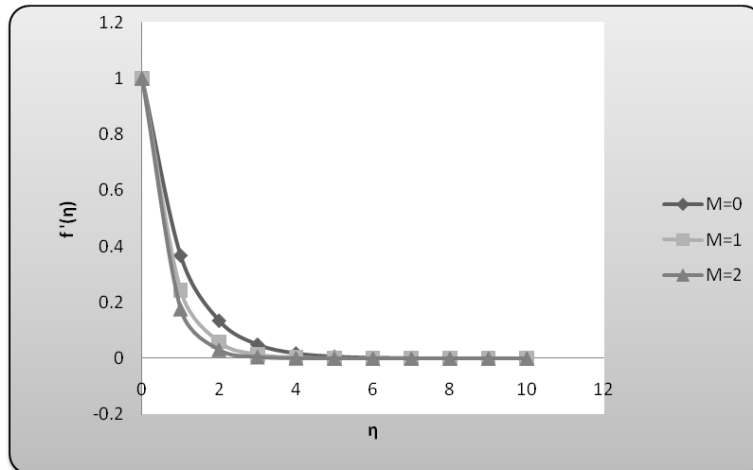
Figure1.Effect of magnetic parameter M on dimensionless velocity profiles f '(η)
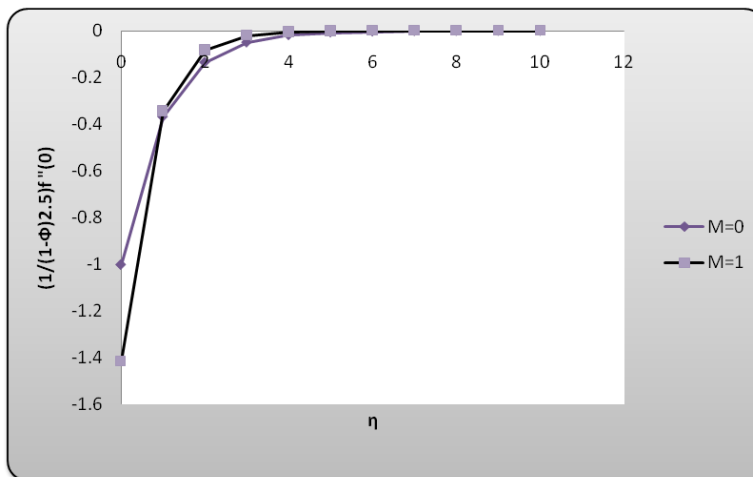
Figure2: Shear stress distribution for various values of M
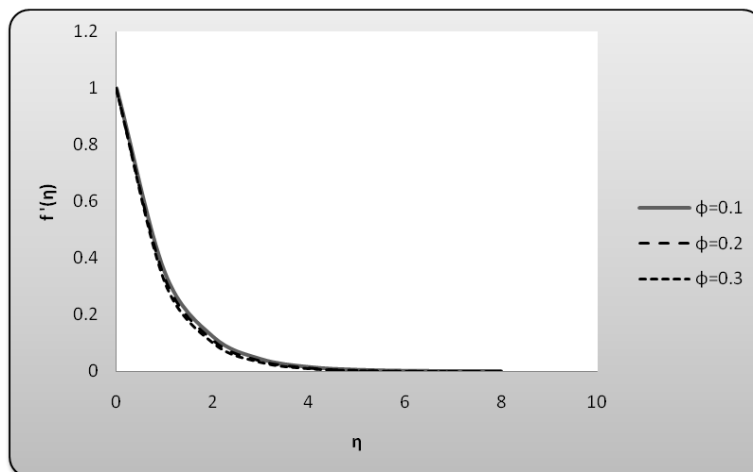
Figure3: Dimensionless velocity profiles for selected values of volume fraction Φ
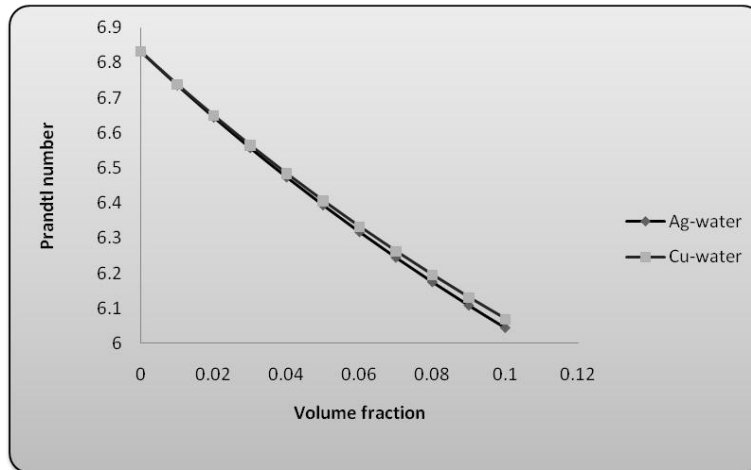
Figure 4: Effect of Prandtl number Pr on volume fraction for Cu-water and Ag-water nanofluids
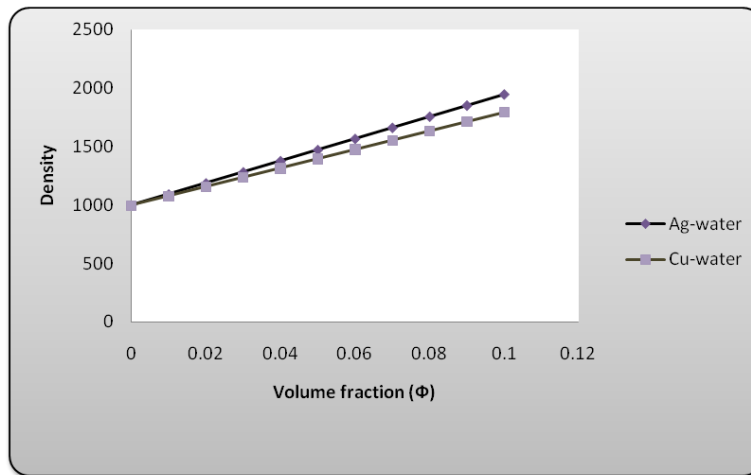
Figure 5: Effect of volume fraction on density of the Cu-water and Ag-water nanofluids
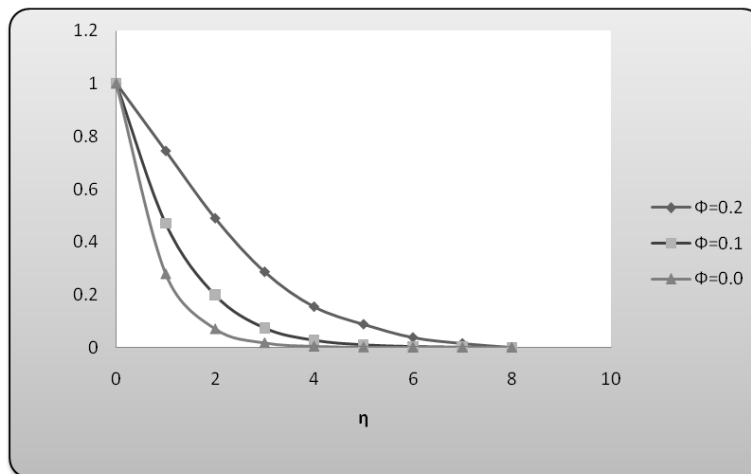
Figure 6: Temperature profile for selected values of volume fraction Φ

V.   CONCLUSION

In this paper the effect of the magnetic field on the boundary layer flow of the nanofluids over an isothermal stretching surface was presented. Velocity and temperature distribution in the flow and thermal boundary layers studied. Numerical results prove that nanofluids under the influence of magnetic field lead to drop of dimensionless velocity and magnitude of the wall of shear stress at the surface. However, it was also observed that when volume fraction increases, density and temperature of all nanofluids increases. Such effects were found to be more evident in the Ag–water solution than in the Cu–water solution

REFERENCES

[1]   Sattar. M.A.,Alam.M.M, Thermal Diffusion as well as transportation effects on MHD free convection and mass transfer flow past an accelerated vertical porous plate, *Indian Journal of pure applied Mathematics, Vol25(6)*, pp.679-688,1994.

[2]   Choi,S.U.S. Enhancing thermal conductivity of fluids with nanoparticales, in:The proceedings of the 1995 *ASME International Mechanical Engineering Congress and Exposition,San Fransisco,USA*, 66 ,pp.99-105. 1995.

[3]   Putra N,Thiesen P, and Roetzel W.,Temperature dependence of thermal conductivity enhancement for nanofluids , *Journal of Heat Transfer .125*(2003),pp.567-574.

[4]   Raptis, A. and Perdikis, C. Viscous flow over a non-linearly stretching sheet in the presence of a chemical reaction and magnetic field. *International Journal of Non-Linear Mechanics, Vol41*, pp. 527–529.2006

[5]   Singh, P., Jangid, A., Tomer, N.S. and Sinha, D.: Effects of thermal radiation and magnetic field on unsteady stretching permeable sheet in presence of free stream velocity. *International Journal of Information and Mathematical Sciences. 6(3),* pp160-166, (2010).

[6]   Khan, W.A.and Pop,I. Boundary-layer flow of a nanofluid past a stretching sheet, *International Journal of Heat and Mass Transfer., Vol 53*,pp.2477-2483,2010.

[7]   Noghrehabadi, A, Ghalambaz,M and Ghalambaz,M,"Theoretical Investigations of Sio2-water Nanofluid Heat Transfer Enhancement over an Isothermal Stretching Sheet,"International journal Of Multidisciplinary Science and Engineering. vol. 9, May 2011.

[8]   Makinde, O.D. and Aziz, A., "Boundary layer flow of a nanofluid past a stretching sheet with a convective boundary condition," International Journal of Thermal Sciences, vol. 50, pp. 1326-1332, 2011.

[9]   Rana.P and Bhargava.R , "Flow and heat transfer of a nanofluid over a nonlinearly stretching sheet: A numerical study," *Communications in Nonlinear Science and Numerical Simulation,* 2011.

[10]   Yacob, N. A. Ishak,A Pop. I and Vajravelu.K, "Boundary layer flow past a stretching/shrinking surface beneath an external uniform shear flow with a convective surface boundary condition in a nanofluid," *Nanoscale research letters, vol. 6*, article no. 314, 2011.

[11]   Khare R. and Rai A. MHD flow of non-Newtonian fluid through a rectangular channel. *Journal of International Academy of Physical Science. vol. 17(1)* pp. 39-52. 2013

[12]   Khare, R. and Srivastava, S. Effect of Hall Current on MHD flow of a dusty viscoelastic liquid through porous medium past an Infinite Plane. *Research Journal of Mathematical and Statistical Sciences , vol 2 (10)* pp. 8-13.2014.

[13]   Nandy.S.K,Sumanta Sidui.S,Mahapatra.T.R: "Unsteady MHD boundary layer flow and heat transfer of nanofluid over a permeable shrinking sheet in the presence of thermal radiation*." Alxendria eng.journal*, 53,929-937,2014.

[14]   Hunegnaw .D, Naikoti .K," Unsteady MHD Flow of Heat and Mass Transfer of Nanofluids over Stretching Sheet with a Non-Uniform Heat/Source/Sink Considering Viscous Dissipation and Chemical Reaction" , *International Journal of Engineering Research in Africa, Vol.14*,pp. 1-12. 2015

[15]   Na T.Y.and pop I., "Unsteady flow past a stretching sheet",*Mechanics Research Communications*, vol.23 pp.413-422 1996.

Research Paper	Open Access

Small Scale Performance Evaluation Of A Multi-Effect Humidification-Dehumidification System In Makurdi

[1]Edeoja, A. O., [2]Aliyu, S. J., [1]Ameh, J. A.

[1]*Department of Mechanical Engineering, University of Agriculture, Makurdi, Nigeria*
[2]*Department of Mechanical Engineering, Landmark University, Omuaran, Nigeria*

ABSTRACT: *A multi-effect humidification (MEH) -dehumidification solar desalination system utilizing a solar collector was designed and evaluated. A blackened aluminium storage tank was used for the feed water and was positioned so that water enters the collector by gravity for the passive test and through the pump for the active case with slight preheating. The heated water exits the collector into the desalination chamber made up of a humidifier and a dehumidifier. The ambient, collector inlet and outlet water, evaporator and condenser temperatures were measured hourly as well as the volume of water produced 10.00 to 16.00 hours. The collector was able to achieve a mean elevation above the inlet condition of about 20.8^0C and 29^0C respectively for the active and passive cases. The mean collector, water production and the overall efficiencies were computed as 0.51, 0.50 and 0.256 respectively for the active case while the corresponding values for the passive case were 0.69, 0.55 and 0.37. The respective mean daily yields of the active and passive options were 0.298 cm^3 and 2.39 cm^3 per unit volume of evaporator, 0.098 cm^3 and 0.785 cm^3 per unit volume of condenser or 0.0035 cm^3 and 0.028 cm^3 per cm^2 of collector aperture. A good potential for the system to contribute significantly to the production of safe drinking water in relatively larger quantities especially with passive option exists.*

KEYWORDS: Multi-effect Humidification-dehumidification, solar collector, performance evaluation, active test, passive test, desalination, drinking water

I. INTRODUCTION

Drinking water of acceptable quality has become a scarce commodity. In many places of the world only brackish or polluted water is available [1]. This leads to an increasing interest in new desalination technologies. In many arid regions of the world, and especially in the Middle East, where conventional sources of fresh water (e. g., rivers, lakes and ground water) are not readily available, seawater desalination will continue to supply drinking water [2]. Apart from drinking, cooking and general domestic uses, pure water is needed to meet requirement of pharmacology, medical, chemical and industrial applications such as food processing industries. Thus, provision of portable water is one of the basic infrastructural facilities for upliftment of the standard of living of people, as well as rapid industrialization of any nation [3]. In Makurdi, the Benue state capital, residents face acute shortage of drinking water despite the prolonged greater Makurdi water works [4].

Sources of raw water (ground water, upland lakes, rivers, canals and lowland reservoirs, rain etc.) are usually contaminated either by the presence of dissolved solid, salts or pathogens in the water. However, water meant for human consumption must be free from chemical substances and micro organisms in amounts which constitute health hazards. Potable water must not only be safe and free from dangers to health, it must be of good chemical and physical quality so as to be acceptable to the people. The water must not be turbid, (i.e. cloudy), it must also be colourless, tasteless and odourless [3, 5].

Water infested with pathogens or which contain unacceptable levels of dissolved contaminants or solids in suspension when consumed leads to widespread acute and chronic illness and is a major cause of death in many developing countries. In 2006, water borne diseases were estimated to cause 1.3 million deaths each year while about 1.1 billion people lacked proper drinking water. It is also reported that, every year, over 200,000 South African children drink themselves to death. Diseases caused by contaminated water kill thousands of South African children every year. More tragic is the fact that, these deaths could have been prevented if all children had access to safe drinking water [1, 3, 5].

Over the decades, many technologies/techniques have been developed in different parts of the globe to treat water and make it suitable for required demands. In general, the methods used in a water treatment plant include physical processes like filtration and sedimentation, biological process such as slow sand filters or activated sludge chemical process such as flocculation and chlorination and use of electromagnetic radiation such as ultra violet light [6, 7]. Desalination of sea water could also be carried out by distillation or reverse osmosis, Reverse osmosis is a pressure – driven process that forces the separation of fresh water from other constituents through a semi permeable membrane. This is usually the preferred method in large-scale desalination implementations where electricity is cheaply available [8-10]. Distillation can be achieved by the relatively cheaper use of solar thermal systems. Here, solar energy is collected and converted into electrical or mechanical energy to initiate the process. Solar desalination systems are simple and easy to operate and maintain since they have no moving parts. They are also environmentally friendly because they do not require the use of fossil fuel [11-13].

Desalination is a water treatment process that converts brackish or saline water to freshwater by removing dissolved minerals from the water. A proven technology that has been used for many years, desalination is increasingly common in areas with scarce water supplies. However, because of its relatively high cost, it is generally used only if fresh water supplies are limited. Water desalination technologies can be categorized on the basis of the energy used to run them, usually thermal or electric. The technologies utilizing thermal energy are known as the multi-stage flash, multiple-effect distillation and vapour compression [13-15]. The desalination technologies that use electric energy rely on a membrane system, such as reverse osmosis and electro dialysis. There are also other technologies that rely on solar energy or combined electric and thermal energy. Each of these technologies has advantages and disadvantages, based on the quantity and quality of the required water and the location. Desalination processes require large amounts of thermal or electric energy; however, advances in desalination technology continue to make these processes more efficient [15-17].

Recent investigations have focused on the use of renewable energy to provide the required power for the desalination processes. The most popular renewable energy source is solar energy [18-21]. An emerging technology for smaller scale desalination systems is solar multi-effect humidification-dehumidification. This process uses solar energy to evaporate fresh water, which is condensed on a cool surface and collected. Solar desalination systems are simply and easy to operate and maintained. The main idea of the multi-effect humidification-dehumidification solar desalination system is based on the evaporation of water and the condensation of steam to and from humid air. The humid air circulation driven by natural convection between evaporator tower (humidifier) and condenser tower (dehumidifier). Evaporator and condenser are located in the same insulated box. The heated seawater from central receiver is distributed onto the evaporator tower through a vertically hanging sprayer and is slowly trickling downwards. The condenser unit is located opposite to the evaporator. Here the saturated air condenses on a single tube copper coil. Water with ambient temperature was used as a coolant for the condenser. The distillate runs down to a collecting tank. Two modifications were introduced on the desalination chamber to enhance the desalination system productivity. The first modification was using water jacket at one side of the dehumidifier tower to increase the condensation surface. The second modification was to use seven flat mirrors to concentrate solar radiation on one side of the humidifier tower (0.003 m ordinary window glass) to heat the humid air to increase the system productivity [22, 23].

They are also environmentally friendly because they do not require fossil fuels. In locations with abundant sunshine, such as Makurdi the state capital of Benue state, Nigeria, solar desalination is a potentially viable option, especially for small-scale plants in remote locations. Multi-effect humidification-dehumidification solar system was suggested as an efficient method for the production of desalinated water, initially for small quantity in remote arid areas. The desalination chamber consists of humidifier and dehumidifier towers. The circulation of air in the two towers was obtained by natural convection [23].

Drinking water is a major problem within Makurdi despite the on-going greater Makurdi water works. Providing sufficient quality water by relatively cheap and environmentally clean methods has been a major research focus and solar desalination has been prominent with new methods such as the multi-effect humidification and dehumidification system being attempted in order to increase water yield [4, 12].

Nigeria, like other countries in the sub-Saharan region is blessed with abundant sunshine all year round. Nigeria is located within the Sun Belt (between 20^0 - 30^0 N and 20^0 - 30^0 S) and receives as much radiation as 490 W/m^2 each day [24]. Makurdi, the location of this study, is on latitude 7.7^0 and longitude 8.73^0 and receive an average insulation of 35430 kJ/m^2/day from an average 6.13 hours of sunshine with the highest and lowest in August and December respectively [25]. It has an altitude of 104 meters above sea level.

The abundant solar radiation and water resource in River Benue Makurdi, could be harnessed for the production of drinking water as for remote areas in town. Several efforts have been made recently by the Energy Research Group in this Department in the past but most of them have been limited to the simple basin water still and some modifications made to it. Since the viability of solar distillation as a major player in the drinking water provision mix depends largely on the yield, focus. In this paper, the performance evaluation of a multi-effect humidification and dehumidification system for water desalination

II.   MATERIALS AND METHODS

The solar collector used for the study was a flat plate collector, similar in design and configuration to the flat plate collector used in study carried out by [12]. The materials selected for the construction were based on the recommendations of [26, 27] and include aluminium sheet, Plain widow glass sheet, Copper tubes (evaporator coils), Wood (soft wood), ½" ply wood sheets, Black oil paint, Saw Dust, PVC plumbing valve and pipes, Water pump and hose, PVC gum, Silicone sealant, Wood adhesive (Top gum). The materials selected for the storage tank include, Thick aluminium sheet, Putty, Plumbing PVC pipes, Black paint. The materials selected for the desalination chamber include, Sprayer, Light gauge aluminium sheet, PVC rubber, Putty, Copper tube, Black oil paint, Epoxy glue, Water pump, Water hose

The flat plate solar collector was designed to have a length of 200 cm and a width of 100 cm with fourteen parallel copper tubes 188 cm each running along the length of the panel with 6 cm gap between the tubes. The fourteen parallel tubes were formed by bending and attached to the plate using rivets. The collector has a glass cover at the top and the rice chaff as insulator beneath the plate. The collector box was made of wood with ½ inch plywood sheet as the base of the box. The design specifications for the solar panel are given in Table 1 below.

Table 1: Design Specifications for the Solar Collector

Parameter	Dimensions
Width of glass	100 cm
Length of glass	200 cm
Area of glass cover	20000 cm^2
Thickness of glass	0.4 cm
Width of aluminium sheet	100 cm
Length of aluminium sheet	200 cm
Area of aluminium sheet	20000 cm^2
Diameter of tube	1 cm
Tube spacing	6 cm
Plate to cover spacing	3 cm
Collector box	100 x 200 cm
Height of box	9 cm

The box, housing which provides the strength needed, was constructed with fasteners according to the design specifications from Table 1. Appropriate holes were drilled in the box to allow for the inlet and outlet copper tubes. The wooden box was designed with a height of 9 cm. Glass of thickness 4 mm with length and width according to the specifications given in Table 1 was used as cover plate. The function of the glass is to prevent heat lost by the plate by radiation. The glass was pasted on top of the wooden box using silicone sealant. The gap between the cover glass and the plate was 3 cm. The space underneath the plate (between the plate and the base of the box) was packed with rice husk as insulation to prevent heat loss through the plate by conduction. The plate was constructed using 3 mm thick aluminium sheet. The sheet was cut to size using cutting scissors according to the design specifications in Table 1. The 10 mm diameters (O.D) copper tube was

bend to form a continuous loop on the top surface of the aluminium plate, with ten parallel copper runs along the length of the plate. The copper tubes were attached to the upper surface of the plate by using screw fasteners. The upper surface of the plate together with the copper tubes were painted black to enhance absorption of heat to heat up the water flowing through the copper tubes. The orthographic representation of the flat plate collector is shown in fig. 1.
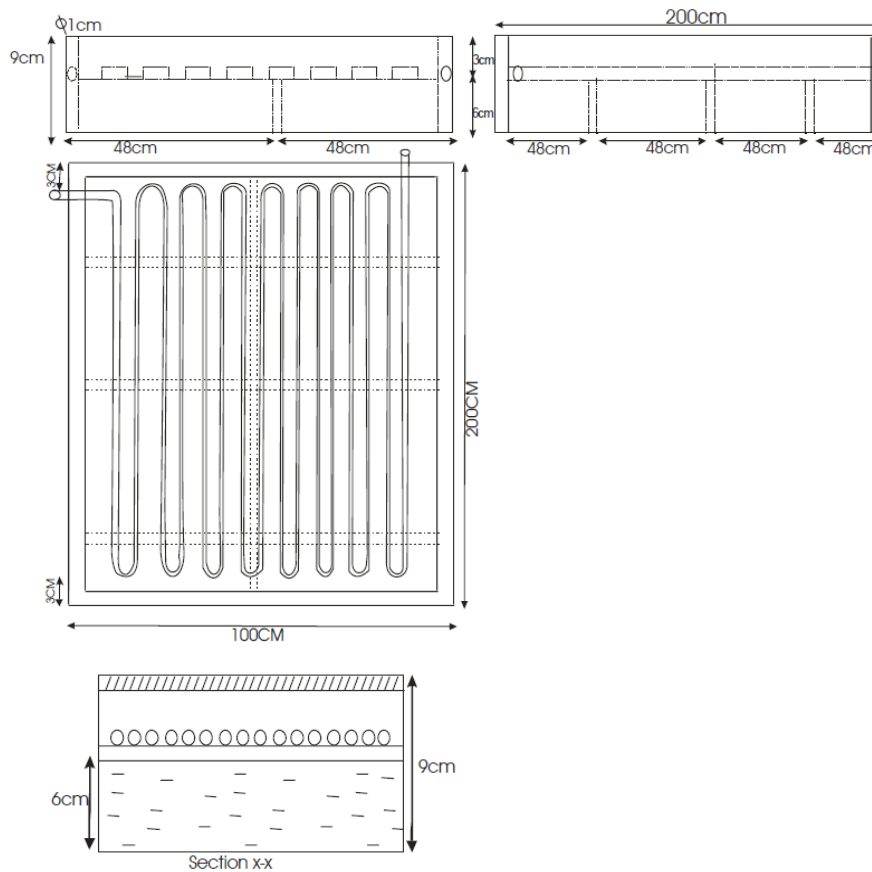
Fig. 2: The Flat Plate Collector in 1st Angle Projection

A storage tank was designed to serve the solar collector. It was designed to have a capacity of 0.032 m^3 (32 l) of water. The equation for the volume of a cylinder was used to design the tank. The tank has a height of 45cm and a diameter of 30 cm. The equation was used to calculate for the perimeter of the tank, which was found to be 88 cm. Thick plain aluminium sheet was cut to size, and bend to form a cylinder. This was joined by brazing. The top and bottom covers for the tank were also cut to size and brazed. A mixture of putty and a hardening substance was applied on the brazed joints to provide a water tight seal. The design specifications for the storage tank are shown in Table 2 below.

Table 2: Design Specifications for the Storage Tank

Parameter	Dimensions
Height of tank	45 cm
Diameter of tank	30 cm
Perimeter of tank	94 cm
Volume of tank	32000 cm^3

The desalination chamber is divided into two parts, evaporator and condenser towers. The evaporator was designed to have a capacity of 235 cm^3 of water. The equation for the volume of the cone was used to designed the cone, it has a height (h) of 14 cm, radius (r) of 4 cm and slant height (l) of 15 cm. light aluminium sheet was cut to size, and bend to form a cone. A paste of putty and epoxy glue was applied on the welded edges to prevent leakages.

The condenser was designed to have a capacity of 716 cm^3 of vapour. The equation for the volume of the cone was used to design the cone; it has a height (h) of 19 cm, radius (r) of 6 cm and slant height of 20 cm. Light aluminium sheet was cut to size, and bend to form a cone. The joint was fabricated; a mixture of putty and a hardening substance (epoxy glue) was applied on the fabricated joint to provide a air tight seal. The design specifications for the desalination chamber are shown in Table 3 below. Plate 1 shows a photo of the components of the desalination chamber.

Table 3: Design Specifications for the Desalination Chamber

Parameter	Dimensions
Height of evaporator	14 cm
Radius of evaporator	4 cm
Slant height of evaporator	15 cm
Volume of evaporator	235 cm^3
Height of condenser	19 cm
Radius of condenser	6 cm
Slant height of condenser	20 cm
Volume of condenser	716 cm^3
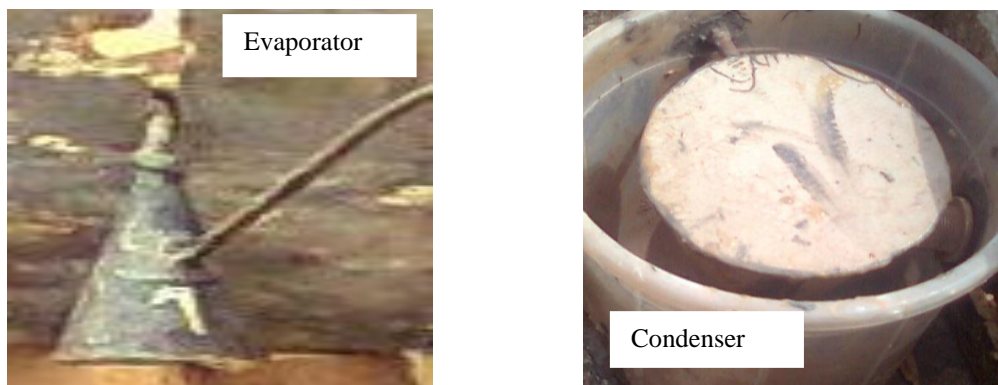
Plate 1: Photo of the Evaporator and the Condenser

The test rig consists of the storage tank, flat plate solar collector, desalination chamber, 0.5 Hp water pump (for the active test) and a thermometer. The storage tank is installed 99 cm above the ground level. The collector is inclined at an angle of 29.7^0 as the angle of tilt. A flexible hose connects the tank mouth piece to the collector inlet with the aid of a PVC gum and hose clip. The outlet of the flat plate collector is connected with the aid of epoxy and super glue to a sprayer which is located half way inside the evaporator. Heated water leaves the collector and is distributed into the evaporator tower through the hanging sprayer and slowly trickles downwards. Unvaporised water in the evaporator tower is collected downward to the storage tank while by natural convection water vapour is circulated into the condenser unit via a copper tube where the saturated air condenses inside the coned shape condenser layer. Cold water circulated by means of a small pump as a coolant for the condenser to transfer heat from it to the environment. The condenser chamber is located inside a water jacket. The distillate runs down to a collecting tank.

A thermometer was installed on the outlet port of the storage tank to measure the initial temperature of the water. Another thermometer was installed on the outlet pipe of the collector to measure the temperature of the water exiting from it. The volume and temperature of the distilled water from the condenser were also measured. Plate 2 shows a photo of the set up.

The storage tank was first filled with water to full capacity. Then, the valve on the mouth piece of the tank was opened so that water is drawn into the inlet pipe of the collector by the pump for the active test and by gravity for the passive test. A type K thermometer was used to measure the ambient and initial temperatures of the water before it enters the collector. The position of the tank permitted a water flow of about 0.00054 l/s for the passive option and the pump was regulated for the active option such that water flows through the collector at about 0.002 l/s in order to maintain a reasonable resident time within the black-coated copper tubes of the collector thereby absorbing more heat by conduction.

The final temperatures of water from the solar collector, the evaporator and the condenser as well as the temperature of the outer surface of the collector glazing were measured hourly from 10:00 am to 4:00pm. The hourly solar radiation values were determined using the estimation provided by [28]. Plate 2 shows the active experimental set up.

Plate 2: Photo of the active System

The vaporization ratio which is a measure of the efficiency of the evaporator in producing water at steady state as well as the collector efficiency was computed. This was computed as a ratio of the water produced to the feed water. The collector efficiency was computed using equation 1 according to [26, 27].

$$\eta = \frac{Q_U}{I_t \times A_c} = F_R \times \tau \times \alpha - F_R \times U_L \left(\frac{t_i - t_a}{I_t} \right) \qquad (1)$$

Where Q_U = useful energy delivered by collector (W), A_c = total collector area, (m^2), I_t = solar energy received on the upper surface of the sloping collector structure, (W/m^2), τ = fraction of incoming solar radiation that reaches the absorbing surface, transmissivity, α = absorptivity, U_L = over all heat loss coefficient, W/ m^2 ^{0}C, t_i = temperature of fluid entering the collector, °C, t_a = atmospheric temperature, °C and F_R = heat removing factor. An estimate of the overall system efficiency was computed by multiplying the collector efficiency and that of the evaporator in producing water. Some of the measured and computed parameters were then plotted.

Results and Discussion

The results obtained from the tests are presented in the graphs below. The order adopted for each presentation is the results for the active system first and then the results for the passive system.

The mean ambient hourly and daily temperatures for the period of the active test were both 26^{0}C while the corresponding values for the passive test were 30^{0}C. This is untypical of Makurdi towards the end of the year [25]. However, this further stresses the fact that weather conditions no longer adhere strictly to the usual patterns as a result of climate change issues. It is therefore a reasonable justification for exploring ways of utilizing the potentially available energy for useful purposes such the provision of scarce quality potable water. The use of a black-painted reservoir for the feed water in the system produced a pre-heating []29 above ambient temperature by mean value about 4.4^{0}C and 2^{0}C for the active and passive options respectively. The slight pre-heating of the feed water enhances a more effective operation of the collector.

The mean hourly and daily temperatures at the outlet of the collector were about 51^{0}C and 61^{0}C for the respective options. The hourly mean values exhibited parabolic trends and peaked with 70.4^{0}C and 81.4^{0}C between 12.00 and 13.00 hours. These peak values expectedly corresponded to mean ambient temperatures of 29.4^{0}C and 34.6^{0}C respectively, translating to an elevation of the water temperature between collector inlet and outlet of about 35.3^{0}C and 44^{0}C. The daily mean values exhibited a more linear tendency than the hourly values which indicates that the conditions for the period of the study were reasonably similar from day to day for both options. The respective mean values of the available radiation also exhibited similar trends.

Fig. 2 shows the variation of the various measured system temperatures with time of the day. The evaporator temperature (T_v) was expectedly the highest and the figure shows that additional heating was achieved between the collector outlet and the evaporator. This resulted from the use of blackened aluminium sheet for the construction of the evaporator. The additional heating was necessary to compensate for the inability of the collector to achieve an outlet temperature of water close to 100^0C. The water outlet temperature (T_f) was the next followed by the water temperature at the collector inlet (T_i) and then the ambient temperature (T_a). The least of the system temperatures was that of the condenser (T_c) especially in the morning and in the evening. Generally, these temperatures exhibited the expected trends with the time of the day. However, this tendency was more clearly shown by T_v, T_f, T_i and T_a. A clustering of T_a, T_i and T_c for both options shows a good performance since the initial water and condenser temperatures were in the region of the ambient temperature.
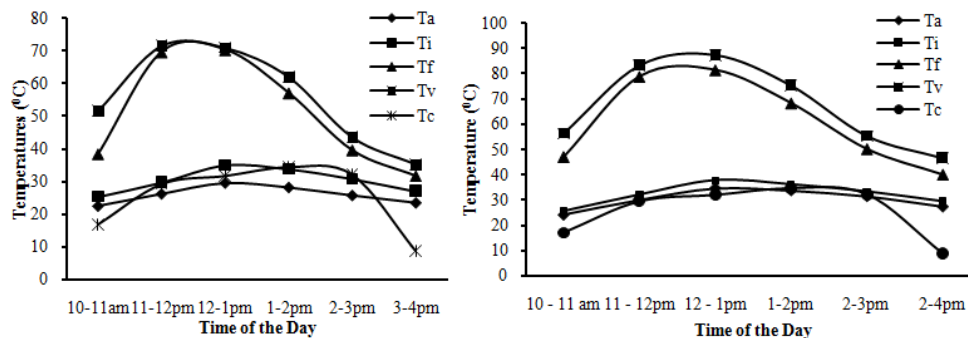
Fig. 2: Variation of the Mean Temperatures with Time of the Day

Fig. 3 shows the differences between some of the system measured temperatures. The highest difference was $T_v - T_c$ followed by $T_f - T_i$ and then $T_i - T_a$ in that order. This is expected and indicative of good performance because the driving force for water production is $T_v - T_c$ while $T_f - T_i$ shows that the collector produced the required significant temperature rise in the water. The patterns of these differences were similar for the two options though there was a slight difference for the passive option in terms of $T_v - T_c$ as shown in the figure. This was as a result weather fluctuation during the course of the passive test.
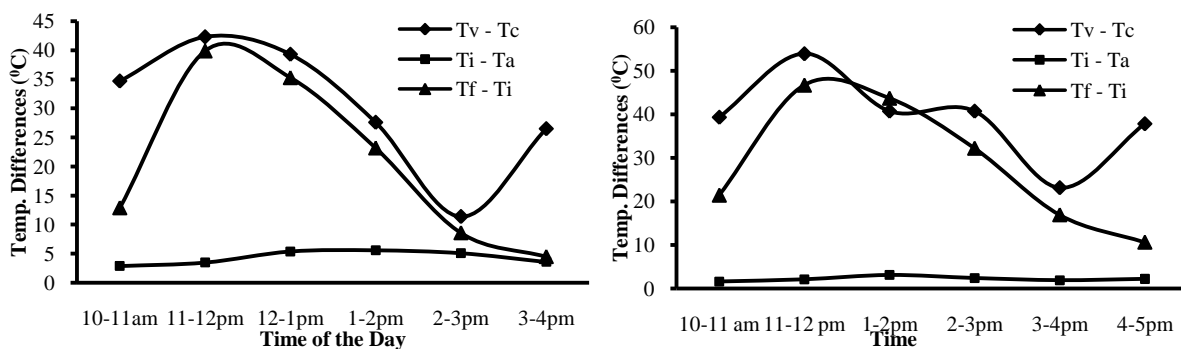
Fig. 3: Variation of Mean Temperature Differences with Time of the Day

Fig. 4 shows the variations of these temperature differences with days for the periods of the study. A similar pattern was observed except that on the 4th day for the active option, $T_f - T_i$ was the highest. This was not expected and could be traced to the departure in the condenser temperature resulting slightly different daily weather conditions and probably because mean values were used. The passive option had more distinct trends for these temperature differences with the indication of better weather conditions in terms of solar radiation on the 4th day.
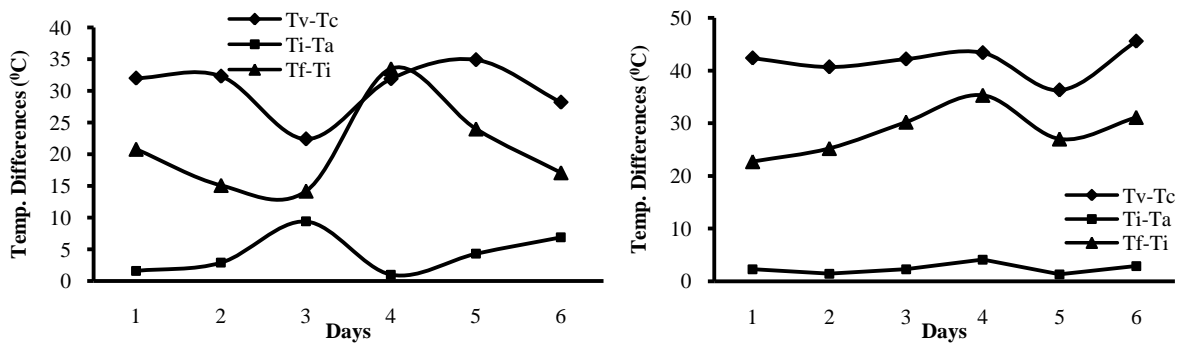
Fig. 4: Variation of Mean Temperature Differences with Days

The mean computed collector efficiencies on an hourly and daily basis for the active option were both 0.51. The respective values for the passive option were 0.65 and 0.69. These values compare favourably with values reported for the same location [12]. This indicates primarily that some attention was given to good construction and probably due to the time of the year that the study was carried out. For the present work, the efficiency of the collector therefore gives credibility to be overall system performance. Fig. 5 shows a variation of the collector efficiency with days for the period of the study. It shows that the peak efficiency for the period occurred on the 4th day of the study when the mean radiation available was the highest (190.1 W/m^2). This agrees with the general provisions for collector operation [27, 30]. Fig. 6 shows the variation of the water production efficiency with days. It is essentially the same as fig. 5 especially for the passive option. The variations of these efficiencies for the active system expectedly had some differences due to additional issues such as the fluctuation of power supply for pumping the water. However, the relationship between the daily values was smoother in fig. 5 probably because collector efficiency largely depends mostly of the available radiation while other factors such as relative humidity affect water production.

The mean water production efficiency for the active system was determined as 0.50 while that of passive system was 0.55. These were reasonably higher than values obtained by using some other systems like the simple basin water still in the same location. With efficiency in this range and better design, the prospects for the production of very significant quantities of drinking water by this method exist for this location. It can be theoretically assumed that the system is capable of producing safe drinking water half the volume of the feed water. Estimates of the overall system efficiencies were obtained as 0.256 and 0.37 for the active and passive options respectively which are acceptable for systems of this nature.
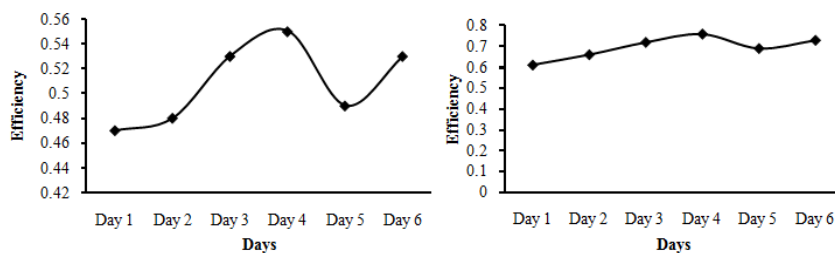
Fig. 5: Variation of Collector Efficiency with Days
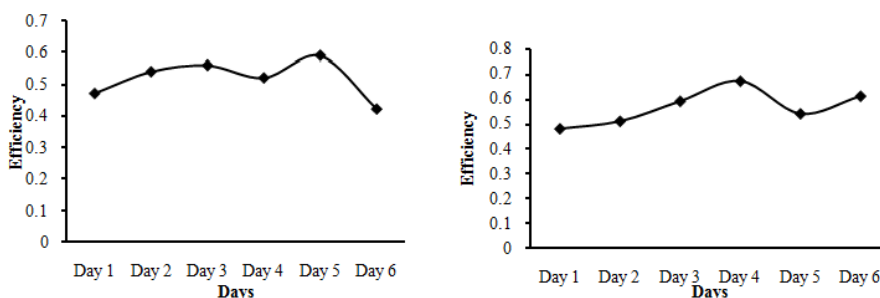
Fig. 6: Variation of Water Production Efficiency with Days

Fig. 7 shows the variation of the total volume of water produced with time for the period of the study. For the two options, very linear correlations were indicated with R^2 values of about 0.99 and 0.95 respectively. This is to be expected as the momentum for water production is cumulatively carried on during the course of the day. The relationships between the two quantities for this system are given by the trend equations in the respective graphs.

The hourly volumes of water varied strongly with a parabolic trend as expected with R^2 value of 0.94 and 0.98 for the respective options. This indicates that the water production rate increases to the peak value and then decreases to a minimum towards evening. This is shown in fig. 8. The relationships between the two quantities are given by the trend equations shown.
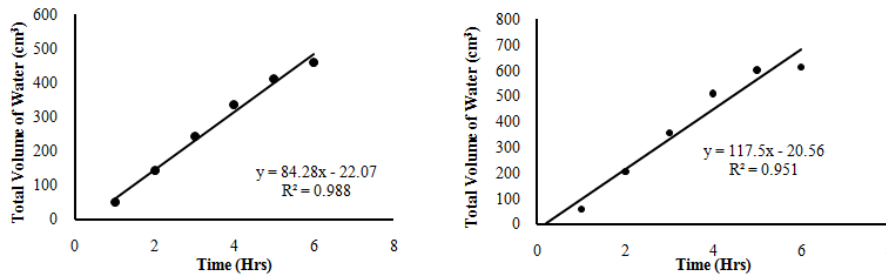
Fig. 7: Variation of total Water Volume Produced with Time

The total volume of water produced for the period of the study was 420.2 cm^3 for the active set up and 3,373 cm^3 for the passive option. This represents respective daily means of about 70 cm^3 and 562 cm^3. In terms of unit volume of evaporator, the yield for the active system was 0.298 cm^3 while that for the passive option was 2.39 cm^3. The respective values in terms of condenser volume were 0.098 cm^3 and 0.785 cm^3. Furthermore, based on unit square centimetre of collector aperture, the yields were respectively 0.0035 cm^3 and 0.028 cm^3. The foregoing indicate that the potentials for the system can be more effectively tapped by utilizing a larger collector aperture with more passes of tubing as well larger dimensions of evaporator and condenser than the ones utilized for this study. On an hourly basis, the mean volumes of water produced were about 272.9 cm^3 and 391 cm^3.
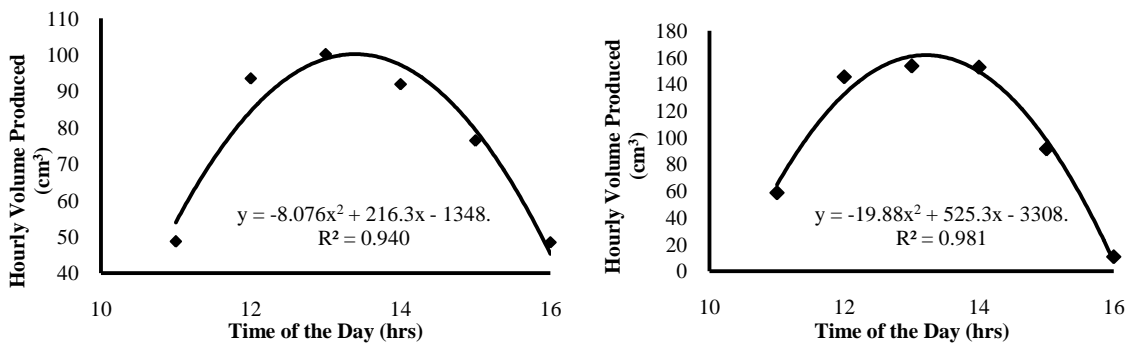
Fig. 8: Variation of Mean Hourly Volume of Water Produced with Time

Fig. 9 shows that a parabolic relationship exists between hourly overall system efficiency and volume of water produced. This further strengthen the fact already established that water production increases to a peak and then decreases in the evening. It can be conveniently assumed therefore that a plot of these values on a daily basis will also give a good linear relationship. The relationship for the hourly quantities had an R^2 value of about 0.89 and 0.78 with the trend equations are shown in the respective graphs for the two options.
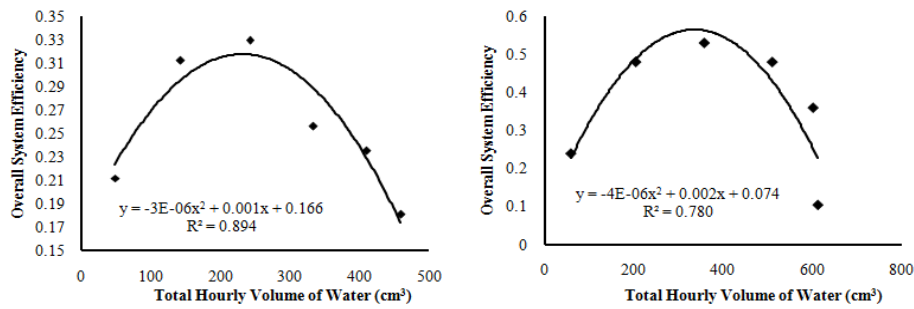
Fig. 9: Variation of Overall System Efficiency with Total Hourly Water Produced

Figs. 10 and 11 show the relationship between the volume of water produced and the available radiation on daily and hourly basis respectively for the period of the study. In fig. 10, the R^2 value for the active system indicates very poor correlation while that for the passive option was much better. A factor which could feature as a reason for this could be irregular power supply leading the flow fluctuation earlier mentioned from day to day. Another factor could be as a result unstable weather pattern from day to day during the study period. The R^2 values for the hourly data show polynomial patterns as expected. Again the passive option correlated better as shown in fig. 11. The respective trend equations are given in the figures. They can be used to estimate these values for systems of similar configuration and sizes.
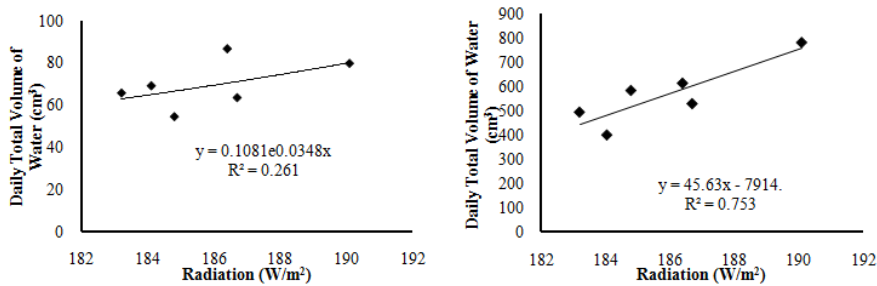
Fig. 10: Variation of Mean Total Daily Volume of Water with Mean available Radiation
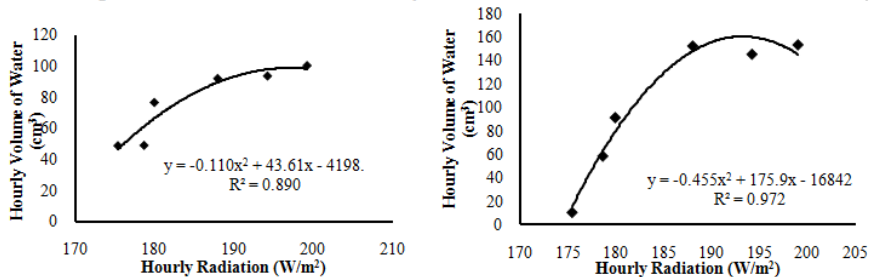
Fig. 11: Variation of Mean Hourly Volume of Water produced with Hourly Radiation available

CONCLUSION AND RECOMMENDATIONS

Having observed the practical operating conditions of the multi–effect humidification–dehumidification systems coupled with an active and a passive flat plate collector, it can be said, that, the optimum performance of a the multi–effect humidification–dehumidification systems depends on the insolation available to it. The system was found to show potentials and suitability for contributing to the provision drinking water for Makurdi and other areas with similar availability of radiation coupled with unavailability of drinking water. However, for the active system, power supply needs to be steady for greater effectiveness and the heat transfer surface areas need to be adequately large. This will translate to prohibitively larger costs that can negate the potentials of the system. Hence, the passive option has shown considerable potentials for utilisation especially with the virtually insufficient power supply. Apart from lower costs, it can be utilised in the many rural locations in Benue State.

Further work will be carried out with copper tubes of diameter less than 10 mm in order to increase the surface area of water flow through the copper tubes. Also, in order to ensure a longer resident time resulting in a higher collector output temperature, more passes of the copper tubes be considered for further work. Larger volumes of the components of the desalination chamber will also be investigated in order to increase the system productivity. However, this should be done bearing in mind the final cost of the system.

REFERENCES

[1].   **Centre for Affordable Water and Sanitation Technology (CAWST),** "Household water Treatment Guide," March 2008.

[2].   **Shiklomanov, I. A., (2000),** Appraisal and Assessment of world water resources, Water International, 25(1): 11-32.

[3].   **World Health Organization and UNICEF (2005)**, Water for life: Making it happen.

[4].   **Ibrahim, J. S., Kuhe, A. and Edeoja, A. O. (2008),** Performance Test of the Effect of Coupling a Preheat Tank and Relector to a Basin Still under Makurdi Humid climate, Journal of Research in Engineering, International Research and Development Journals, Uyo, Nigeria.

[5].   **World Health Organization (2007),** combating waterborne Diseases at the household level, part1

[6].   **Wangnick, K. (2001).**   A Global overview of water Desalination Technology and the perspectives. In: Proceedings of the International conference Spanish Hydrologic plan and sustainable water management: Environmental aspects, water reuse and desalination, Zaragoza, Spain.

[7].   **Wade, N.M. (2001),** Distillation plant Development and cost update. Desalination, 136: 3 -12.

[8].   **Velmurugan, V., Kumar, K. J. N., Haq, T. N. and Srithar, K. (2009).** Performance analysis in stepped solar still for effluent desalination, Energy, 34, 1179 –1186

[9].   **Medugu, D. W. and Ndatuwong, L. G. (2009).** Theoretical analysis of water distillation using solar still, International Journal of Physical Sciences, Vol. 4 (11), 705-712

[10]. **Garcia-Rodriguez, l. (2003),** "Renewable Energy Applications in Desalination: State of the Art", Solar Energy 75, 381-393.

[11]. **Adnan S., Ali M. A., Omari I. A. (2001).** Optimizing the tilt angle of solar collectors, Department of Applied Physics, Jordan University of Science and Technology, PO Box 3030, Irbid, Jordan.

[12]. **Edeoja, A. O., Bam, S. A. and Edeoja, J. A. (2009).** Comparison of a Flat Plate Collector and a Manually – Tracking Concentrating Collector for Air Heating in Makurdi, Global Journal of Mechanical Engineering, Paper No. GJMENG-2009-05

[13]. **Foster, R. E., Amos, W. and Eby, S. (2005)**, Ten years of Solar Distillation Applications along the US – Mexica Boarder, Solar World Congress, International Solar Energy Society, Orlando, Florida.

[14]. **Ismail, B. I. (2009).** Design and performance of a transportable hemispherical solar still, Renewable Energy, 34, 145–150

[15]. **Arunkumar, T., Denkenberger, D., Ahsan, A. and Jayaprakash, R. (2013)**. The augmentation of distillate yield by using concentrator coupled solar still with phase change material, Desalination, 314, 189 – 192, Elsevier Ltd.

[16]. **Dev, R. and Tiwari, G. N. (2009).** Characteristic equation of a passive solar still, Desalination, 245, 246–265

[17]. **Tanaka, H. and Nakatake, Y. (2009).** Increase in distillate productivity by inclining the flat plate external reflector of a tilted-wick solar still in winter, Solar Energy, 83, 785–789

[18]. **Kumar, K. V. and Bai, R. K. (2008).** Performance study on solar still with enhanced condensation, Desalination, 230, 51– 61

[19]. **Badran, O. O. and Al-Tahaineh, H.A. (2005).** The effect of coupling a flat-plate collector on the solar still productivity, Desalination, 183, 137–142

[20]. **Tanaka, H. (2010).** Monthly optimum inclination of glass cover and external reflector of a basin type solar still with internal and external reflector, Solar Energy, 84, 1959 –1966

[21]. **Murugavel, K. K. and Srithar, K.. (2011).** Performance study on basin type double slope solar still with different wick materials and minimum mass of water, Renewable Energy, 36, 612 – 620

[22]. **Al-Shammiri M. and Safar M. (1999)**, Multi-effect Distillation plants: state of the Art, Desalination, 126:45-65.

[23]. **Abdelkader, M. (2006).** Investigation of Multi-Effect Humidification-   Dehumidification   Solar Desalination System Coupled With Solar Central Receiver Fac. of Eng., Port Said, Suez Canal Univ., Egypt.

[24]. **Okwonkwo, W. I., Akubuo, C. O. and Mageswaran, P. (1999)**. Development and Evaluation of a concentrating solar cooker under Nsukka climate, Journal of Agricultural Engineering and Technology, 7: 29-35

[25]. **Itodo I. N. and Fulani A. U. (2004)**,Development of a passive solar crop dryer with an air Pre- heater unit, proceeding of the 5th International Conference and 26th AGM of the Nigerian institution of Agricultural Engineers, (26): 406-411

[26]. **George, O. G. (1980). "**Flat plate and Non-concentrating Collectors", In Solar Energy Technology Handbook (part B), pp. 239.

[27]. **Whillier,** A., Prediction of performance of solar collectors", In applications of solar Energy for the Heating and Cooling of building, ASHRAE GRP – 170, 1977.

[28]. **Yohanna, J. K., Itodo, I. N. and Umogbai, V. I. (2011).** A model for determining the global solar radiation for Makurdi, Nigeria, Renewable Energy, 36, pp. 1989 – 1992, Elsevier Limited.

[29]. **Conor, D. W. (1980).** Solar Energy Technology Handbook part A, "Low Temperature Sensible Heat Storage", pp. 721, Marcel Dekker Incorporated.

Research Paper   Open Access

Effects of fertilizers on soil's microbial growth and populations: a review

[1]Ojo OI, [2]Olajire-Ajayi BL, [2]Dada OV, and [2]Wahab OM

[1]*Dept of Agricultural Engineering, Ladoke Akintola University of Technology, Nigeria*
[2]*Dept of Forestry Technology, Federal College Of Forestry, Ibadan, Nigeria*

ABSTRACT: *Soil nutrients availability and decomposition of organic matter depends on microorganism but there are little available literatures on the possible effects of nutrients fixing chemicals and substances on the survival and population distribution of various microbes. Also, because of importance of organic and inorganic fertilizers to increase the soil microorganisms needed for the growth of plants there is need for comprehensive review of existing literature on the subject. This paper reviewed the effects of fertilizers on soil's microbial growth and populations in available literatures. Various studies agreed that low microbe population due to lack of organic matter can be easily rectified by amending the soil with fertilizers and organic matter and allowing time for microbial growth therefore jump-starting the reproduction of microbes by adding beneficial microbes along with organic matter. Microbe improves soil structure by the humus they create while digesting organic matter and also help in nitrogen fixing.*

I.   INTRODUCTION

The real deal is that without soil microbe, we would all die. The work they do in our soil is incredibly complex but it all boils down to this: microbes eat, thus we eat. Plants are unable to take from the soil the nutrition they need without microbes working in the soil. Microbes are alive, and must have nutrition to survive, and that nutrition comes from organic matter. As they consume the nutrients they need, microbe creates foods like nitrogen, carbon, oxygen, hydrogen, phosphorus, potassium and trace minerals for our plants. It is the microbes that convert the NPK and minerals in the soil into a form our plants can use to grow and produce food flowers for us (Parr *et al. 1994*). Microbes are everywhere. They are in the air, in the rivers and oceans, in our drinking water, in the soil and our skin. Of course we know some microbes are bad, like salmonella and *Eumeria coli,* but more are considered beneficial and out-compete pathogens for survival in the soil (Higa, 1995). There are all kinds of microbes like algae, protozoa, bacteria and fungi with many others waiting to be discovered. Their population in soil are numerous as many as one billion of up to 13,000 species can preside gram of soil (1 gram = 0.0022 pounds, so maybe a teaspoon) (Dundas *et al*, 2002). Most microbes need organic carbon to live; they get this from eating wood chips, leaves, manures and other organic matter, they creates humus which increases soil structure, good for root penetration and development (compaction can nullify much of this action) (Parr *et al*., 1994). Microbes also get some carbon from the rhizosphere (the area immediately around plant roots) because roots gives off substances the microbes can use, like sugars and amino acids and then the microbes convert some of it back forms the plants can use, as minerals, vitamins, nitrogen's and smino acids. (Amino acids are building blocks of protein (Schulz and Jorgensen, 2001). Humans need 20 amino acids to make muscle, hair, skin, and connective tissues, and human bodies' only make use of 10 of them. While the other must be supplied by food from plants and animals (Cornis, 2002) some microbes (like some bacteria and blue-green algae) are able to fix nitrogen from air and make it available to plants. Some plants and trees cannot grow if deprived of specific microbes (mycorrhizal fungi) around their roots. That's why some plants need a good shovelful of additional soil from around their roots for company when transplanting (Horneck, 1981). There are microbes and touelene from gasoline leaks. The word for that action is bioremediation and research is ongoing to select microbes that digest other toxins our soil (Landford, 2004). There are many garden products available containing beneficial microbes for the soil. Some are fast-action form of foliar sprays, and some are home-brewed compost teas used to spray or drench. In all cases, foliar sprays are not enough; there most also organic matter you added last summer need continual replenishment. Microbes multiply, and if your microbes population is low due to lack of organic matter, it can easily rectified by mending the soil with soil organic and

allowing time for microbial growth (Kuruvilla *et al.,* 2009). The uniqueness of microorganism and their often unpredictable nature and biosynthetic capabilities, has given a specific set of environment and cultural conditions, and it also make them likely candidates for solving particularly difficult problems in the life sciences and other sciences as well. The various ways in which microorganisms have been used over the past 50 years to advance medical technology, human and animal health, food processing, food safety and quality genetic engineering, environment protection, agricultural and municipal waste provide a most impressive record of achievement (Higa,1991). Many of these technology advances would not have possible using straightforward chemical and physical engineering methods, if they were, they would not have been practically or economically feasible (Parr *et al.*, 1994). While microbial technologies have been applied to various agricultural and environment problems with considerable success in recent years. They are been widely accepted by scientific community because it is often difficult to consistently reproduce their beneficial effects (Parr and Hornick, 1992). Microorganisms are useful in eliminating problems associated with the use of the chemical fertilizers and pesticides. They are widely applied in nature farming and organic agriculture (Higa, 1991; Par *et al.*, 1994).

Organic fertilizers are composed of natural ingredient from plant parts such as leaves and peanut hulls, and poultry droppings. Compost, a blend of plant debris broken down by natural processes is also considered a natural or organic fertilizer. Inorganic fertilizers on the other hand are manufactured from minerals or synthetic chemicals. Both organic and inorganic supplement the soil and feed plants with nutrients. Macronutrients-those nutrients that plants require in large amounts which include nitrogen, phosphorus and listed as percentage on the fertilizer bag (Reganold *et l.,* 1990). Inorganic fertilizers nearly are readily dissolved and unless added have few other macro and micro plant nutrient). Inorganic fertilizer nitrogen, phosphorus and potassium compounds are released from the complex organic compounds as the animal or plant matter decays. In commercial fertilizer, the same required compounds are available in easily dissolved compounds when water is applied. Inorganic fertilizer are usually much more concentrated with up to 64 % (18-46-0) of their weight being a given plant nutrient, compared to organic fertilizers that only provide nutrient (Stewart *et al.,* 2005). The need to boost food production is on the increase everywhere in the world today as world's population is geometrically increasing day by day while the supply of land fixed, thus farmers regularly use forms of fertilizers and other organic manures to enhance productivity without considering the probable effects toxic or non- toxic on soil microbes. This review therefore considers it reasonable to identify some effects on soil's microbial growth and populations.

II.   HISTORY OF SOIL BIOLOGY

Soil biology is the study of microbial and faunal activities and ecology in soil. Soil like, soil biota, or edaphon is a collective term for the organism within the soil. This organisms living include earthworm, nematodes, protozoa, fungi, bacterial and different arthropods, soil biology play a vital role in determine many soil characteristics yet, been a relatively new science, much remains unknown about soil biology and about the nature of soil is affected (Whitman *et al.,* 1998). The soil is home to large proportion of world's bio-diversity. The links between soil function are observed to be incredibly complex. The interconnectedness and complexity of this soil 'food web' means any appraisal of soil function must necessarily take into account interaction with the communities that exist within the soil (Higa, 1995). We know that soil organism prevent nutrient loss by leaching. Microbial exudates act to maintain soil structure, and earthworms are important in bioturdation. However, we find that we don't understand critical aspects about how these functions interact. The discovery of globalin in 1995 indicates that we lack the knowledge to correctly answer some of the most basic question about the biogeochemical cycle in soils. We have much work ahead to gain a better understanding of how soil biological components. We have much work ahead to gain a better understanding of soil biological components affect us and the biosphere (Comis, 2002). In balanced soil, plants grow in an active and steady environment. The mineral content of the soil and its healthful structure are important for their well being, but it is the life in the earth that powers its cycles and provides its fertility without the activities of soil organisms, organic materials would accumulate and litter the soil surface, and there would be no food for plants (Parr et al., 19994).

The soil biota includes:
i.   Megafauna: Size range - 20mm upward, e.g moles rabbits, and rodents,
ii.   Macrofauna: size range -2 to 20mm e.g. woodlice, beetles, centipedes, slugs, snails, ant and harvestmen,
iii.   Mesofauna: size range -100 micrometres to 2mm e.g. Tardigrade, mites and springtails,
iv.   Microfauna and microflora: size range -1 to 100 micrometres, e.g. yeast bacteria (commonly actinobacteria), fungi, protozoa, roundworms, and rotifers.

Of these, bacteria and fungi play key roles in maintaining soil. They act as decomposers that break down organic materials to produce detritus and break down products. Soil detrivores like earthworms, ingest detritus and decompose it. Saprotophs (macrofauna) help by breaking down the same way but they also provide motion part as they move in their armies. Also the rodents, wood-eaters help the soil to be more absorbent (Parr and Hornick, 1992).

2.1 Characteristics and functions soil microbes in the soil
Soil biology involves work in the following areas:

i.   Modelling of biological processes and population dynamics.
ii.   Soil biology, physics and chemistry: occurrence of physicochemical parameters and surface properties on biological processes and population behavior.
iii. Population biology and molecular ecology: methodological development and contribution to study microbial and faunal population; diversity and population dynamics; genetic transfers, influences of environmental factors.
iv.   Community ecology and functioning processes; interactions between organisms and minerals or organic compounds; involvement of such interactions in soil pathogenesis; transformation of minerals and organic compound compounds; cycling of elements; soil structuration.

Complementary disciplinary approaches are necessarily utilized which involve molecular biology, genetics, ecophysiology, biogeography, ecology, soil processes, organic matter, nutrient dynamics and landscape ecology (Comis, 2002).

2.2   Bacteria
Bacteria are single-cell organisms and most denizens of agriculture, with populations ranging from 100 million to 3 billion in a grain. They are capable of very rapid reproduction by binary fission (dividing into two) in favourable conditions. One bacterium is capable of producing 16 million more in 24 hours. Most soil bacteria live close to plat roots and are often referred to as rhizobacteria (Higa, 1991). Bacteria live in soil water, including the film moisture surrounding soil particles, and some are able to swim by means of flagella. The majority of the beneficial soil-dwelling bacteria need oxygen (and are thus termed aerobic bacteria), whilst those that do not require air are referred to as anaerobic, and tend to cause putrefaction of dead organic matter (Higa, 1991). Aerobic bacteria are most active in a soil that is moist (but not saturated, as this will deprive aerobic bacteria of the air that they required), and neutral soil pH, and where there is plenty food (carbohydrates and micronutrients from organic matter) available. Hostile conditions will not completely kill bacteria; rather, the bacteria will stop growing and get into a dormant stage, and those individuals with pro-adaptive mutations may compete better in new conditions. Some gram-positive bacteria produce spores in order to wait for more favourable circumstances, and gram-negative bacteria get into a "nonculturable" stage. Bacteria are colonized by persistent viral agents (bacteriophages) that determine gene word order in bacteria host (Higa, 1991; Parr *et al,* 1994).

2.2.1 Importance of bacteria: the nitrogen cycle
Nitrification: is a vital part of the nitrogen cycle, wherein certain bacteria 9which manufacture their own carbohydrates supply without using the process of photosynthesis) are able to transform nitrogen in the form of ammonium, which is produced by the decomposition of proteins, into nitrates, which are available to growing plants, and once again converted to proteins (Pimental, 2007).
Denitrification: while nitrogen fixation converts nitrogen from the atmosphere into organic compounds, a series of processes called denitrificationreturs an approximately equal amount of nitrogen to the atmosphere. Denitrifying bacteria tend to anaerobes, or facultative anaerobes (can alter between the oxygen dependent and oxygen independent types of metabolism), including Achromobacter and Pseudomonas. The purification process caused by oxygen-free conditions converts nitrate and nitrite in soil into nitrogen gas or into gaseous compounds such as nitrous oxide or nitric oxide. In excess, denitrification can lead to overall losses of soil fertility. However denitrification returns it to the atmosphere (Comis, 2002).

2.3   Fungi
A gram of garden soil can contain around one million fungi, such as yeasts and moulds. Fungi have no chlorophyll, and are not able to photosynthesis; besides, they cannot use atmospheric carbon dioxide as a source of carbon, therefore they are chemoheterophic, meaning that like animal, they require a chemical source of energy rather than being able to use light as an energy source, as well as a organic substrates to get carbon for growth and development (Higa, 1991). Many fungi are parasitic, often causing disease to their living host plant,

although some have beneficial relationships with living plants. In terms of soil and humus creation, the most important fungi tend to saprotrophic; that is, they live on dead or decaying organic matter, thus breaking it down and converting it to forms that are available to the higher plants. A succession of fungi species will colonise the dead matter, beginning with those that sugars and starches, which are succeeded by those that are able to break down cellulose and lignins (Whitman *et al,* 1998). Fungi spread underground by sending long thin threads known as mycelium throughout the soil; these threads can be observed throughout many soils and compost heaps. From the mycelia the fungi is able to throw up its fruiting bodies, the visible part above the soil (e.g. mushrooms, toadstools and puffballs), which may contain millions of spores. When the fruiting body bursts, these spores are dispersed through the air to settle fresh environments, and are able to lie dormant for up to year until the right condition for their activation arise or the right food is made available. (Whitman *et al,* 1998).

Mycorrhizae: Those fungi that are to live symbiotically with living plants, creating a relationship that is beneficial to both, are known as mycorrhizae (from myco meaning fungal and rhiza meaning root). Plant root hairs are invaded by the mycelia of the mycorrhiza, which lives partly in the soil and partly in the root root, and may either cover the length of the root hair as a sheath or be concentrated around its tip. The mycorrhiza obtain the carbohydrates that it require from the root, In return providing the plant with living plants, creating a relationship that is beneficial to both, are known as mycorrhizae (from myco meaning fungal and rhiza meaning root). Plant root hairs are invaded by the mycelia of the mycorrhiza, which lives partly in the soil and partly in the root, and may either cover the length of the root hair as a sheath or be concentrated around its tip. The mycorrhiza obtains the carbohydrates that it requires from the root, in return providing the plant with nutrient including nitrogen and moisture. Later the plant roots will also absorb the mycelium into its own tissues (Parr and Hornick, 1992). Beneficial mycorrhizal association are to be found in many of our edible and flowering crops. Shewell cooper suggests that these include at least 80% of the brassica and solanum families (including tomatoes and potatoes), as well as the majority of tree species, especially in forest and woodlands. Here the limits of the tree's roots, greatly increasing their feeding range and actual causing neighbouring tree to become physically interconnected. The benefits of mycorrhizal relations to their plant partners are not limited to nutrients, but can be essential for plant reproduction; in situation where little light is able to reach the forest floor, such as the north American pine forest, a young seedlings cannot obtain suffient light to photosynthesis for itself and will not grow properly in a sterile soil, but if the ground is underlain by a mycorrhizal mat, then the developing seedling will throw down roots that can link with the fungal threads and through them obtained from its parents or neighbouring trees (Burges *et al*., 1967). David (1995) points out the plants, fungi, animal relationship that creates a "three way harmonious trio" to be found in forest ecosystems, wherein the plant/fungi symbiosis is enhanced by animal such as the wild boar, deer, mice, or flying squirrel, which feed upon the fungi's fruiting bodies, including truffles, and cause their further spread (David, 1995). A greater understanding of the complex relationships that pervade natural systems is one of the major justifications of the organic gardener, in refraining from the use of artificial chemicals and the damage these might cause. Recent research has shown that arbuscular mycorrhizal fungi produce globalin, a protein that binds soil particles are important part of soil organic matter (Comis, 2002).

2.4 Types of microorganism in soil

Living organisms both plants and animals constitute an important component of soil. The pioneering investigations of a number of early microbiologists showed for the first time that the soil was not an inert static material but a medium pulsating with life. The soil is now believed to be a dynamic or rather a living system, containing a dynamic population of microorganism than the fallow land, and the soil rich in organic matter contains much more population than sandy and eroded soils. Microbes in the soil are important to us in maintaining soil fertility/productivity, cycling of nutrient elements in the biosphere and sources of industrial products such as enzymes, antibiotics, vitamin, hormones, organic acids e.t.c. at the same time certain soil microbes are the causal agents of human and plant diseases. The soil organisms are broadly classified into two groups: which are soil flora and soil fauna, the detailed classification of which is as follows (Higa, 1991).

2.5 Habits and ecology

Microorganism is found in almost every habitat present in nature. Even in hostile environments such as the poles, deserts, geysers, rocks and the deep sea. Some types of microorganism have as extremophiles. Extremophiles have been isolated from rocks as much as 7 kilometres below the earth's surface, (Szcwzyku *et al*., 1994). It has been suggested that the amount of living organisms below the earth's surface may be comparable with the amount of life on or above the surface. (Gold, 1902). Extremophiles have been known to survive for a prolonged time in a vacuum, and can be highly resistant to radiation, which may even allow them to survive in space. (Horneck, 1981). Many types of microorganism have intimate symbiotic relationships with other larger organisms; some of which are mutually microorganism can use disease in host they are known as pathogens.

2.5.1　Extremophiles

Extremophiles are microorganisms that have adapted so that can survive and even thrive in conditions that are normally fatal to most life-forms. For example, some species have been found in the following extreme environments; Temperature: as high as 130^0c (266^0F), (Madigan and Martinko, 2006), as low as -17^0c (1^0F) (Rybicki, 1990). Acidity/alkalinity: Less than pH 0, (Max, 2012). Up to pH 11.5 (Christner *et al.*, 2008). Pressure: up to 1,000-2,000 atm, down to 0 atm (e.g. vacuum of space) (Schopf, 2006).

2.6　Soil microbes

The nitrogen cycle in soils depends on the fixation of atmospheric nitrogen, one way this can occur is in the nodules in the root of legumes that contain symbiotic bacteria of the genera rhizobium, bradyrhizobium and azorhizobium (Barae *et al.*, 2005).

2.6.1　Symbiotic microbes

Symbiotic microbes such as fungi and algae from association in lichen, certain fungi form mycorrhizal symbioses with trees that increase the supply of nutrients to the trees (Tickell *et al.*, 2000).

2.6.2　Importance of soil microbes

Microorganisms are vital to human and the environment, as they participate in the earth's element cycles such as the carbon cycle and nitrogen cycle, as well as fulfilling other vita roles in virtually all ecosystems, such as recycling other organisms' dead remains and waste products through decomposition. Microbes also have an importance place in most higher-order multicellular organisms are symbionts. Many blame the failure of biosphere 2 on an improper animal; stomach help in their digestion. For example, cows have a variety of different microbes in their stomachs that aid them in their digestion of grass and hay (Kitani *et al.*, 1989).

2.6.3　Uses of microbes
2.6.3.1　Use in food

Food Fermentation: Microorganisms are used in brewing, winemaking, baking, pickling and other food-making processes. They are also used in the control of fermentation process in the production of cultured diary such as yogurt and cheese. The cultures also provide flavour and aroma, and inhibit undesirable organism.

2.6.3.2　Use in water treatment

Sewage treatment: Specially-cultured microbes are used in the biological treatment of sewage and industrial waste effluent. A process known as bio augmentation (Gray, 2004).

2.6.3.3 Use in energy

Algae fuel, cellulosic ethanol and ethanol fermentation: Microbes are in fermentation to produce ethanol, And in biogas reactors to produce methane (Piimental, 2007). Scientists are researching the use of algae fuels. And bacteria to converts various forms of agricultural and urban waste into usable fuels (Inslee *et al.,* 2008).

2.6.3.4　Use in production of chemicals and enzymes

Many microbes are used for commercial and industrial production of chemicals, enzymes and other bioactive molecules. Examples of organic acid produced include:
i.　Acetic acid: produces by the bacterium acetobacter acetic and other acetic bacteria (AAB);
ii.　Butyric acid Ibutanoic acid): Produced by the bacterium clostridium butyricum.
iii.　Citric acid: produced by the fungus aspergillus niger, microbes are used for preparation of bioactive molecules and enzymes. Strepkinase produced by the bacterium strtoccus and modified by genetic engineering is used as a clot buster for removing clots from blood vessels of patients who have undergone myocardial infections leading to heart attack. Cyclosporine A is a bioactive molecules infarctions leading to heart attack. Cylosporin A is a bioactive molecule used as an immunosuppressive agent in organ transplantation. Stains produced by the yeast monascus purpureus is commercialized as blood cholesterol lowering agent which acts by competitively inhibiting the enzymes responsible for synthesis of cholesterol (Tickell, *et al*; 2000).

2.6.3.5　Use in science

Microbes are also essential tools in biotechnology, biochemistry, genetics and molecular biology. The yeasts (Saccharmyces cerevixiae) and fission yeast (Schizosaaharomyces pombe) are important model organism in sciences, since they are simple eukaryotes that can be grown rapidly in large numbers and are easily manipulated (Castrillo and Oliver, 2004). They are particularly valuable in genetics. Genomics and pproteonomics (Sunnerhagen, 2002). Microbes can be harnessed for uses such as creating steroids and treating skin diseases. Scientists are also considering using microbes for living fuel cells (Soni, 2007) and as a solution for pollution (Moses *et al*., 1999).

2.6.3.6　Use in warfare

Biological warfare: In the middle ages, diseases coepses were thrown into castles during sieges using catapults or other siege engines. Individuals near the corpses were exposed to the deadly pathogens and were likely to spread that pathogen to others (Langford, 2004).

2.6.4　Diseases caused by microbes

Pathogenic microbes: Microorganisms are the cause of many infectious diseases. The organisms involved include pathogenic bacteria, causing diseases such as plague, tuberculosis and anthrax; protozoa, causing diseases such as malaria, sleeping sickness and toxoplasmosis; and fungi causing diseases such as ringworm, candidiasis or histoplamsmosis. However, other diseases such as influenza, yellow fever or AIDS are caused by pathogenis viruses, which usually classified as living organisms and are not, therefore, microorganisms by the strict definition. As of 2007, no clear examples of archaean pathogen are known, (Eckburg *et al*., 2003). Although a relationship has been proposed between the presence of somemethanogens and human periodontal diseases (Lepp *et al*., 2004)

2.6.5　Ecology

Microbes are critical to the processes of decomposition required to cycle nitrogen and other element back to the natural world.

2.6.6　HYGIENE

Hygiene is the avoidance of infection or food spoiling by eliminating microorganisms from the surroundings. As microorganisms, in particular bacteria, are found virtually everywhere, the levels of harmful microorganisms can be reduced to acceptable levels. However, in some cases, it is required that an object or substance be completely sterile, i.e. devoid of all living entities and viruses. A good example of this is a hypodermic needle (Burges *et al*., 1967). In food preparation microorganisms are reduced by preservation methods (such as the addition of vinegar), clean utensils used in preparation, short storage periods, or by cool temperatures. If complete sterility is needed, the two most common methods are irradiation and the use of an autoclave, which resembles a pressure cooker. There are several methods for investigating the level of hygiene in a sample of food, drinking water, equipment, e.t.c. water samples can be filtrated through an extremely fine filter. This filter is then placed in a nutrient medium. Microorganisms on the filter then grow by replacing a sample in a nutrient both designed to enrich the organism in question. Various methods such as selective media or PCR can then be used for detection. The hygiene of hard surfaces, such as cooking pots, can be tested by touching them with a solid piece of nutrient medium and allowing the microorganism to grow on it. There are no conditions where all microorganisms would grow and therefore often several different methods are needed. For example, a food sample might be analysed on three different nutrient mediums designed to indicate the presence of total bacteria 9condition where many but all, bacteria grow), molds (conditions where the growth of bacteria is prevented by, e, g, antibiotics) and coliform bacteria (these indicates sewage contamination) (Burges *et al*., 1967).

2.7　Factors affecting distribution, activity and population of soil microorganisms

Soil microorganism (flora and fauna), just higher plants depends entirely on soil their nutrition, growth and activity. The major soil factor which influences the microbial population, distributions like soil are: soil fertility, cultural practices, soil moisture, soil temperature and soil aeration. Others include light, soil pH (h-ion concentration), organism matter, food and energy supply, nature of soil and microbial association. All these factors play a great role in determining not only the number and type of organisms but also their activities. Variations in any one or more of these factors may lead to the changes in the activity of the organisms which affect the soil fertility (Schilz and Jorgensen, 2001). Brief account of all these factors influencing soil micro flora/ organisms are their activities are discussed below:

i.   Cultural practices (Tillage): Cultural practices viz, cultivation, crop rotation, application of manures and fertilizers. Liming and gypsum application, pesticide/fungicide and weedicide application have their effect on soil organism. Ploughing and tillage operations facilitate aeration in soil and exposure of soil to sunshine and thereby increase the biological activity of organisms, particularly of bacteria. Crop rotation with legume maintains the favourable microbial population balance, particularly of N2 fixing bacteria and thereby improve soil fertility. Liming of acid soils increases activity of bacteria and actinomycetes and lowers the fungal population. Fertilizers and manure applied to the soil for increased crop production, supply and nutrition not only to the crops but also to microorganisms in soil and thereby proliferate the activity of microbes (Eckburg *et al.*, 2003). Foliar or doil application of different chemical (pesticides, fungicides, nematicides e.t.c) in agriculture are either degraded by the soil organism or are liable to leave toxic residues in soil which are hazardours to cause profound reduction in the normal microbial activity in the soil (Stewart *et al.*, 2005).

ii. Soil fertility: Fertility level of the soil has a great influence on the microbial population and their activity in soil. The availability of N, P and K require for plant as well as microbes in soil determines the fertility level of soil. On the other hand soil micro flora has greater influence on the soil fertility level (Reganold *et al.,* 1990).

iii. Soil moisture: It is one of the important factors influencing the microbial population and their activity in soil. Water 9 soil moisture is useful to the microorganisms in two ways i.e. it serve as a source of nutrient and supplies hydrogen/oxygen to the organism and it serve as solvent and carrier of other food nutrient to the microorganisms. Microbial activity and population proliferate best moisture range of 20% to 60%. Under excess moisture condition/water logged conditions due to lack of soil aeration (oxygen) anaerobic micro flora become active and the aerobes get die out due to tissue dehydration and some of them change their forms into resting stages spore or cysts and tide over adverse conditions. Therefore optimum soil moisture (range 20 to 60%) must be there for better population and activity of microbes in soil (Burges *et al.*, 1967).

iv. Soil temperature: Next to moisture, temperature is the most important environmental factor influencing the biological physical and chemical processes and of microbes, microbial activity and population is soil. Though microorganisms can tolerate extreme temperature (such as -60 or +60 u) condition, but the optimum temperature range at which soil microorganisms can grow and function actively is rather narrow. Depending upon the temperature range at which microorganisms can grow and function, are divided into three groups i.e. psychrophiles (growing at low temperature below 10^0c) and mesophiles (growing well in temperature range between 20^0c to 45^0c) and thermopiles (can tolerate temperature above above 45^0c and optimum 45- 60^0c). Most of the soil microorganisms are mesospheric (25 to 40^0) and optimum temperature for most mesophiles is 37^0c. True psychripiles are almost absent in soil, and thermopiles though present in soil behaves like mesophiles. True thermopiles are more abundant in decaying manure and compost heaps where high temperature prevails. Seasonal changes in soil temperature affect microbial population and their activity especially in temperature regions. By winter, when temperature is low (below 50^0c) the number and activity of microorganisms fall down, and as the soil warms up in spring, they increase in number as well as activity. In general. Population and activities of soil microorganism are the highest in spring and lowest in winter season (Burges *et al.*, 1967).

v.   Soil air (aeration): For growth of microorganisms better aeration (oxygen and sometimes co_2) in the soil is essential. Microbes consume oxygen from soil air and gives out carbon dioxide. Activities of soil microbes is often measured in terms of the amount of oxygen absorbed or amount of co_2 evolved by the organisms in the soil environment. Under high soil moisture level/water logged conditions, gaseous exchange is hindered and the accumulation of co_4 occurs in soil air which is toxic to microbes. Depending upon oxygen requirement, soil microorganisms are grouped into categories viz aerobic (require oxygen for like processes), anaerobic (do not require oxygen) and microaerophilic (require oxygen concentration/level of oxygen) (Lepp *et al.,* 2004).

vi. Light: Direct sunlight is highly injurious to most of the microorganism except algae. Therefore upper portion of the surface soil a centimetre or less is usually sterile or devoid of microorganisms. Effect of sunlight is due to heating and increase in temperature (more than 45^0) (Burges et al., 1967).

vii. Soil reaction / soil pH: Soil reaction has definite influence/ effect on qualitative composite on of soil microbes. Most of the soil bacteria, blue-green algae, diatoms and protozoa prefer a neutral or slightly alkaline reaction between pH 4.5 and 8.0 and fungi in acidic reaction between pH 4.5 and 6.5 while actinomyvetes prefer slightly alkaline soil reaction also influence the type of the bacteria present in soil. For example nitrifying bacteria (*Nitrosomonas* and *Nitrobacter*) and diazotrophs like *Azobacter* are absent totally or inactive in acid soils while diazotrophs like Beijerickia, Derxia, and sulphur oxidizing bacteria like thiobaccillus thiooxidans are active in acidic soils (Langford, 2004).

viii. Soil organic matter: The organic matter in soil being the chief source of energy and food for most of the soil organisms, it has great influence on the microbial population. Organic matter influence directly or indirectly on the population and activity of the microorganisms (Arthur and Lars, 1997).

ix. Food and energy supply: Almost all microorganisms obtain their food and energy from the plant residues or organic matter/ substance added to the soil. The heterotrophy utilizes the energy liberated during the oxidation of complex organic simple inorganic compounds (chemoautotroph) or from solar radiation (photoautotroph). Thus, the source of food and energy rich material is essential for microbial activity in soil. The organic matter, there serves both as a source of food nutrients as well as energy required by the soil organisms (Langford, 2004).

x. Nature of soil: The physical, chemical physiochemical nature of soil and its nutrient status influence the microbial population both quantitatively and qualitatively. The chemical nature of soil has considerable effect on microbial population in soil. The essential for optimum microbial activity. Similarly nutrient (macro and micro) and organic consistent of humus are responsible for absence or presence of certain type of microorganisms and their activity. For example activity and presence of nitrogen fixing bacteria is greatly influenced by the availability of molybdenum absence of available phosphate restrict the growth of *Azobacter* (Higa, 1995).

xi. Microbial association / interactions: Microorganism interacts with each other giving to antagonistic or symbiotic interaction. The association existing between one organism and other whether of symbiotic or antagonistic influences the population and activity of soil microbes to a great extent. The habit protozoa and more mycobacter which feed in bacteria may suppress or eliminate certain bacteria. On the other hand, the activities of some of the microorganisms are beneficial to each other. For instance organic acids liberated by fungi, increase in oxygen by the activity of algae, change in soil reaction e.t.c. favours the activity of bacteria and other organism in soil (Higa, 1995).

2.8   Fertilizer
All fertilizer supply plant with the nutrients your garden needs to be in tip-top shape. However, organic and inorganic fertilizer supplies nutrients to soil in different ways. Organic fertilizers create a healthy environment for the soil over a long period of time, while inorganic fertilizers work much quickly, but fail to create a sustainable environment (Stewart *et al.*, 2005). These will help the people in choosing the one that best fits your needs, or consider combining them to get the best of both options.

2.8.1 Organic and inorganic fertilizer
Organic fertilizers are composed of natural ingredient from plant or animals. Example includes manure and a blend parts such as leaves and peanut hulls. Compost: a blend of plant debris broken down of natural processes is also considered a natural or organic fertilizer (Stewart *et al.*, 2005). Inorganic fertilizer, on the other hand, is manufactures from minerals or synthetic chemicals. Both organic and inorganic fertilizers supplement the soil and feed plants with nutrients. Macronutrients: -those nutrients that plant requires in large amounts include nitrogen, phosphorus and potassium and are listed as percentage on the fertilizer bag (Reganold *et al.*, 1990).

2.8.2 Pros and cons of organic and inorganic fertilizer
There are benefits and what some may consider disadvantages of organic and inorganic fertilizer, deciding which kind to use may depend on your horticultural situation. According to North Caroline state university, organic matter in natural fertilizers promotes and environment conducive for earthworms and increase the capacity for holding water and nutrients. Organic fertilizer release nutrient slowly, relying on soil organisms to break down organic matter. A slow-release scenario decreases the risk of nutrient leaching but takes time to supply nutrient to plant. Inorganic fertilizer contains a higher percentage of nutrients and provides them more quickly than organic fertilizer. This is a benefit for plants with a short life span, such as bedding plants, but the concentrated form increase the risk of burning the plant if applied incorrectly, and the quick-release of nutrients may result in soil leaching (Artur and Lars, 1997).

2.8.3 Long-term effectiveness or organic and inorganic fertilizer
Research comparing organic and inorganic fertilizer provides compelling evidence that organic fertilizer bolster soil health over the long term. In a study conducted in Sweden over32 years, scientists Arthur Granstedt and Lars Kjellenburg reported on the difference in soil structure crop quality between an organic and inorganic system. They found that soil in the organic system had higher fertilizer, and organic crops had higher starch content than the inorganic system. In contrast, long-term use of synthetic fertilizer depletes soil organisms of the organic matter they need, state the main organic farmers and gardeners association. Eventually, these organisms disappear in soil dependent on inorganic fertilizer (Artur and Lar, 1997).

2.8.4 Integrated approach

It does not have to be either organic or inorganic fertilizer. An integrated approach blends the use of both. A study published in 2009 describes the benefits of an integrated system on rice fields in India. The authors found that a combination of organic and synthetics fertilizers resulted in yield that increased over five years. They concluded that an integrated approach improved the capacity of soil to supply nutrients. A blend of both organic and inorganic fertilizers may suit your landscape (Kuruvilla *et al*., 2009).

III.   RECOMMENDATION

Microbes multiply and if your microbe population in low due to lack of organic matter, it can be easily rectified by amending the soil with organic matter and allowing time for microbial growth jump-starting the reproduction of microbes by adding beneficial microbes along with organic matter is an option depending on how soon you want to see result, and the cost. It can be said that microbes are the workhorse of our gardens. Microbes make nutrient in the soil available to plants in a form the plants can use. Microbes create some of those nutrient; they resist disease better and tolerate environmental stress better. Microbe improves soil structure by the humus they create while digesting organic matter. Microbes help in nitrogen fixing.

REFERENCES

[1]. Artur, G. and Lars, K. (1997): Effects of organic and inorganic fertilizers on soil fertility and crop quality". "Proceedings of an International Conference Boston, Tufts University, *Agricultural Production and Nutrition,* Massachusetts; Long term filed experiment IN Sweden.

[2]. Barea, J., Pozo, M., Azon, R. and Azon-Aguilar, C. (2005): "Microbial co-operation in the rhizosphere"   *Journal of Soil biology and Biochemistry.* 56 (417): 1761-71.

[3]. Burges, A. and Raw, F. (1967): Soil biology*: Journal of Soil Fertility and Biodiversity in Organic Farming,* 296 (5573: 1694-1697.

[4]. Carstrillo, J. and Oliver, S. (2004): "Yeast as a touchstone in post-genomic research strategies for integrative analysis in functional genomics. *"Journal of Biochemistry and Molecular Biology, 37(1): 93-106.*

[5]. Christner, B. (2008): "Ubiquity of biological ice nucleators in snowfall". *Journal of Biological Science, 319(5867): 1214.*

[6]. *Comis, D. (2002): "*Glomalin: hiding place for a third of the world's stored soil carbon" Agricultural Research (United States Department of Agriculture Agricultural Research Service): 4-7.

[7]. Dundas, E., Paul, O. and John H. (2002): Mahavira is dated 599-527 BCE. The jains London: Routledge ISBN 0-415-26606-8 PAGE 24.

[8]. Dyall-Smith, M. Mike, O. and Haloarchea, K. (2002): University of Melbourne. *Journal of WHO mortality data assessed* 20, January 2007. 69(1): 21-25

[9]. Eckburg, P., Lepp, P. and Roland D. (2003): "Archaea and their potential roles in human disease". *Infect immune 71 (2): 6176-81.*

[10]. *(*French) Domin: que soltner, les bases de la production vegetal, tome: Le sol et son amelioration, collection sciences et Techniques Agricoles, (2003).

[11]. FRIN, (2008): Agro metrological station report, Forestry Research Institute of Nigeria, pg 96-120.

[12]. Gillen, B. and Alan, L. (2007): The genesis of germs: the origin of diseases and the plagues. *Journal, new leaf publishing group.* 47: Pp 4495-4499.

[13]. Gold, T. (1992): "The deep, hot biosphere". Applied and environmental microbiology 71 (10) 5779-5786.

[14]. Gray, N. (2004): Biology of waste treatment. *Journal of Imperial College press 7:5-11.*

[15]. HIga, T. (1991): Effective microorganisms: A biotechnology for mankind. Page 8-14 in J. F. Parr, S. B. Hormick and C. E. Whitman edition proceedings of the first international Conference on kyusei Nature farming U.S. Department of Agriculture, Washington, D.C., U.S.A.

[16]. Higa, T. (1995): Effective microorganisms: their role in kyusei nature farming and sustainable edition: proceedings of the third international conference on kyusei nature farming U.S. Department of Agriculture, Washington, D.C., U.S.A.

[17]. Higa, T. and Wididana, G. (1991): The concept and theories of effective microorganisms. Pp. 118-124 In pair, S.B Hormick, and C.E. Whitman edition; proceedings of the first international conference on kyusei nature farming U.S. Department of Agriculture, Washington, D.C., U.S.A.

[18]. Horneck, G. (1981): Survival of microorganisms in space". A review advance space resource 1 (14): 39-48.

[19]. Hormick, S. (1992): Whitman edition. Proceedings of the first international conference on kyusei nature farming U.S Department of agriculture. Washington D.C., U.S.A. Pp 8-14.

[20]. Hormick, S. (1995): Effective microorganisms: their role in kyusei nature farming and sustainable edition: Proceedings of the third International Conference on kyuse nature farming U.S. Department of Agriculture, Washington D. C., U.S.A. Pp.65.

[21]. Islee, R., Jay, I. and Payne, A. (2008): Apollo's fire igniting America's clean energy economy. Journal of island press, Page 157.

[22]. Kitani, A., Osumu, E. and Carl, W. (1989): Biomass handbook. Taylor and Francis U. S. page 236.

[23]. Kuruvilla, V., Delong, E. and Pace, N. (2009): the proceedings of the international plant nutrition collopuim xvi.

[24]. Langford, R. (2004): Introduction to weapons f mass destruction: Radiological, chemicals, and Biological, Wiley – IEEE. Page 140.

[25]. Lepp, P., Brinig, M., Osuverney, C., Palm, K., Armitage, G. and Relman, D. (2004): "methanaogenic archaea and human periodontal disease". Proc national academic science U.S.A. 101(16): 6176-81.

[26]. Mader, P., Andreas, D., Dubois, L., Gunst, P., Fried N. and Niggli, U. (2002): "Soil Fertilizer, and Biodiversity in Organic Farming" Pp. 1694-1697.

[27]. Madigan, M. and Martinko, J (2006): Brook biology of microorganisms' 13th edition, Pearson education, *Journal of Agricultural and Biological Science,* Pp 1096.

[28]. Max, P. (2012): "Horizontal DNA transfer between bacteria in the environment" Journal of health physics 67 (30): 280-282.

[29]. Moses, A., Vivian, O. and Cavalier-Smith, T. (1999): Biotechnology: the Science and the business. CRC press page 563.

[30]. Parr, J. and Hornick, S. (1992): Agricultural use of organic amendments. *A historical perspective American journal alternative agric.* 7:181-189.

[31]. Parr, J., Hornick, S. and Kaufmman, D. (1994): Use of microbial inoculants and organic fertilizers in agricultural production. Proceedings of the International Seminar on the use of Microbial and Organic Fertilizers in Agricultural Production, Published by the food and fertilizer technology center, Taipei, Taiwan.91

[32]. Pismental, D. (2007): Food, energy and society CRC press. Page 289.

[33]. Pinmentol, D., Hepperly, P., Hanson, J., Douds, D. and Seidel J. (2005): Environment, Energetic, and Economic Comparisons of Organic and Conventional Farming System", *Journal of Biological Science. Vol. 55 No. 7 Pp. 573-582.*

[34]. Reganold, J., Papendick, R. and Parr, J. (1990): Sustainable Agriculture, *Journal of Scientific America. 262(6): 112-120.*

[35]. Rybicki, E. (1990): "the classification of organisms at the edge of life, or problems with virus systematic. Page. 861: 182-6.

[36]. Schoopf, J. (2006): "Fossil Evidence of Archaean Life" Phios trans R. soc lond B Biology Science 361 (1470): 869-85.

[37]. Schulz, H. NS Jorgensen, B. (2001): "Big bacteria". *Annual revision microbiology 55:105-37.*

[38]. Soni, S. (2007): Microbes, A source of energy for 21st century, New India (Mumbai Publishing page 14-6.

[39]. Stewart, W., Dibb, D., Johnson, A. and Smyth, T. (2005): "The contribution of commercial fertilizer nutrients to food production". *Journal of agronomy. 97: 1-6.*

[40]. Sunnerhagen, P. (2002): "Prospects for functional genomics in schizosaccharomysces pombe" Current genetics. 42(2): 73-84.

[41]. Szewzyk, U., Szewzyk, R. and Stenstorm, T. (1994). Themophilic, anaerobic bacteria isolated from a deep borehole in granite in Sweden. *Journal of Agricultural and biological science. 5: 1810-3.*

[42]. Tickell, N., Joshua, E. and Suter. B. (2000): From the Fryer to the fuel tank: The complete guide to suing   vegetable oil as an alternative fuel. Biodiesel America. Page 53.

[43]. Whitman, W., Coleman, D. and Wiebe, W. (1998): "Prokaryotes: the unseen majority. "Applied and environmental Microbiology 71(10): 5779-5786.

[44]. Zublena, J., Baird. And Lilly, J. (2009): "Soilfacts-Nutrient Content of Fertilizer and Organic Materials". North Carolina Cooperative Extension Services, Pg. 115.

Research Paper   Open Access

Investigation of Electrical and Optical Transport Properties of N-type Indium Oxide Thin Film

M. A. Islam[1], M. Nuruzzaman[1], R. C. Roy[2], J. Hossain[2], K.A. Khan[2]

([1]Department of Physics, Rajshahi University of Engineering & Technology, Rajshahi-6204, Bangladesh)
([2]Department of Applied Physics & Electronic Engineering, University of Rajshahi, Rajshahi-6205, Bangladesh)

ABSTRACT : *Indium Oxide (In_2O_3) thin films were prepared on glass substrate by electron beam technique. The films were characterized by Scanning Electron Microscopy (SEM), electrical, optical and Hall measurement studies. SEM study revealed that the surfaces of the as-deposited films are distributed through the uniform small grains. The electrical resistivity decrease with the increase of temperature indicating that In_2O_3 thin films are semiconducting in nature. The reduction in the resistivity is associated with thermally activated conduction mechanism. The effect of the magnetic field on Hall coefficient (R_H), carrier concentration (n) and Hall mobility (μ_n) were also studied. From Hall study It is observed that the films exhibit n-type electrical conductivity with carrier concentration of about $10^{19}(cm^{-3})$. The optical properties such as transmittance (T), absorption coefficient (α), were determined. The absorption coefficient is found to be the order of 10^4 (cm^{-1}). The study of absorption coefficient of the In_2O_3 thin films shows a direct type of transition. The optical band gap for In_2O_3 thin film ranges 3.34 -3.69 eV.*

KEYWORDS - *Thin films, e-beam, as-deposited, Electrical conductivity, Hall coefficient, Optical band gap*

I.   INTRODUCTION

Indium oxide (In_2O_3) is a prominent material for microelectronic applications [1]. Indium oxide belongs to transparent conducting oxide (TCO) are widely used in engineering and electronic industry. It has variety of applications including transparent conductive electrodes in flat-panel displays and solar cells, coating for architectural glasses [2], and optoelectronic devices [3] because of its good electrical conductivity, high optical transparency in the visible region, and high reflectivity in the IR region. Indium oxide is a wide-band-gap semiconductor with energy gap of E_g ~3.70 eV as found in literature. As a wide-band-gap semiconductor, Indium oxide exhibits an isolating behaviour in its stoichiometric form (In_2O_3) [4]. It is also used as antireflection coating in solar cells owing to its less optical reflectivity. In_2O_3 thin films have been deposited by several techniques in order to improve the structural, optical and electrical properties of the material such as dc magnetron sputtering [5], evaporation [6-8], thermal oxidation of indium films [9], atomic-layer epitaxial growth [10], pulsed laser deposition [11-12], sol-gel process [13], and chemical pyrolysis to metal organic chemical vapour deposition [14]. Although there have been several studies on the growth and characterization of In_2O_3 thin films, there is still a lack of understanding of the structural, electrical and optical properties. These properties of Indium oxide thin films are strongly affected on the preparation techniques and experiment conditions [4-5].

In this work, electron beam (e-beam) evaporation technique was used to deposit indium oxide thin films on to glass substrate. E-beam evaporation technique yields high quality epitaxial thin films with smooth surfaces. Here we report the surface morphological, electrical and optical properties of indium oxide (In_2O_3) thin films.

II.   EXPERIMENTAL DETAILS

In_2O_3 thin films were deposited on to glass substrate by e-beam evaporation technique at a pressure of 3×10^{-3} Pa from In_2O_3 powder (99.999% pure) obtained from Aldrich Chemical Company, USA.

When the chamber pressure reduced to $\sim 3\times10^{-3}$ Pa, the deposition was then started with 30 mA current by turning on the low-tension control switch. All the films were deposited at room temperature. The deposition rate was about 5 nms^{-1}. The film thickness was measured by the Tolanasky interference method with an accuracy of $\pm$ 5nm [15]. The thickness of the In$_2$O$_3$ films ranges from 50 to 150 nm, respectively.

Electrical conductivity and Hall effect measurement investigated by the Van-der-Pauw technique [15]. The optical transmittance spectra of In$_2$O$_3$ films was recorded from 400 nm to 1100 nm wavelength using a SHIMADZUUV- double beam spectrophotometer.

III.   RESULTS AND DISCUSSION

3.1 Morphological Study

Scanning Electron Microscope (SEM) has been used to study the surface morphology of In$_2$O$_3$ thin films. SEM micrographs of the as-deposited In$_2$O$_3$ thin film of different magnifications are shown in Fig. 1. It shows a uniform surface morphology with a more dense homogeneous distribution of grains. The average grain sizes observed from SEM images are approximately equal.
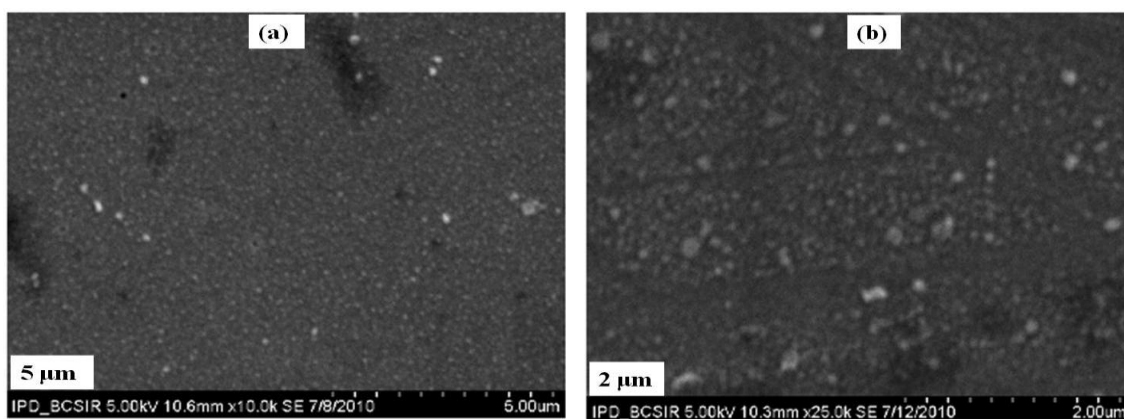
Fig. 1: SEM micrograph of the as-deposited In$_2$O$_3$ thin films of thickness 200 nm at two different magnifications.

3.2. Temperature Dependence of Electrical Resistivity and Activation Energy

Figure 2 shows the temperature dependence of electrical resistivity of In$_2$O$_3$ films of different thicknesses in the temperature range 300-475K.The resistivity decrease with increase in temperature confirms the semiconductor nature of the as-deposited In$_2$O$_3$ films. It is seen from Fig.2 that the resistivity of the films depends upon thickness, and the resistivity of the thicker films is found to be comparatively less than that for thinner films. At room temperature, resistivity reduced from 10^{-1} to 10^{-2} (Ω-cm) as the thickness varies from 50 to 150nm. This decrease in resistivity with thickness can be attributed on the basis of grain boundary scattering as explained by Wu and Chiou [16]. As the grain size increases with thickness (not shown in Figure), the size of grain boundaries become relatively reduced; which in turn reduces the grain boundary scattering, consequently reducing the resistivity. The gradual decrease in resistivity up to around 435 K for all films is associated with thermal activation process which leads to an increase in carrier concentration. At higher temperature regions, the behaviour of resistivity becomes almost independent of temperature.

The activation energy is calculated by the following relation:

$$\sigma = \sigma_0 \exp(-\Delta E/2K_BT) \qquad\qquad\qquad (1)$$

where ΔE is the activation energy, σ_0 is the conductivity at 0 K, K_B is the Boltzmann constant, and T is the absolute temperature. The logarithmic variation of electrical conductivity as a function of inverse temperature at several thicknesses is shown in Fig. 3.The activation energies calculated from linear least square fit of Arrhenius relation are tabulated in Table-1. From Table-1 it is observed that the activation energy of In$_2$O$_3$ films decreases with increasing film thickness which is associated with the reduction of scattering at grain boundaries as mentioned earlier. This behaviour of activation energy with thickness also implies semiconducting behaviour of the films [17]. It is also observed from the Table-1 that activation energy is found to increase with increasing temperature. It can be assumed that, at higher temperature, the carriers activated to the localized states moves towards the Fermi level.
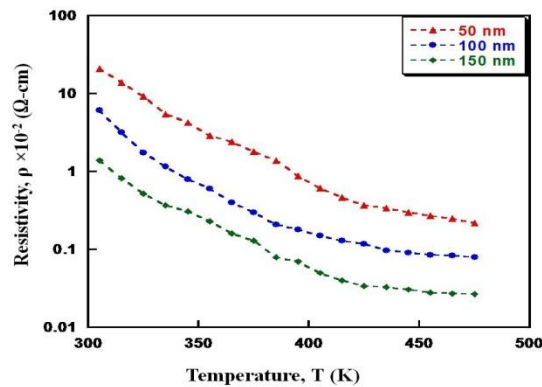
Fig. 2: Variation of resistivity of In_2O_3 thin films of different thicknesses with temperature.

3.3 Hall Effect Study

The Hall coefficient (R_H) was calculated by the following relation [15]:

$$R_H = \pm\, V_B\, t/IB \quad (m^3/coulomb) \tag{2}$$

where V_B is the generated Hall voltage, t is the film thickness, and B is the applied magnetic field. It is well known that the negative value of R_H indicates the n-type semiconducting behaviour of the materials. The negative value of R_H, as seen in the Fig.4 (a), indicates that In_2O_3 samples are n-type conductivity with electrons as majority charge carriers which is well agreed with the reported value [18]. The following relation was used to calculate the value of carrier concentration:

$$R_H = \pm\, 1/ne \tag{3}$$

where e is the electronic charge. Figure 4(b) shows the plot of the carrier concentration versus the applied magnetic field. The carrier concentration is found to be the order of 10^{19} cm^{-3} [19]. Figure 4(c) shows the variation of Hall mobility with magnetic field. It is seen that Hall mobility decreases with increasing magnetic field.
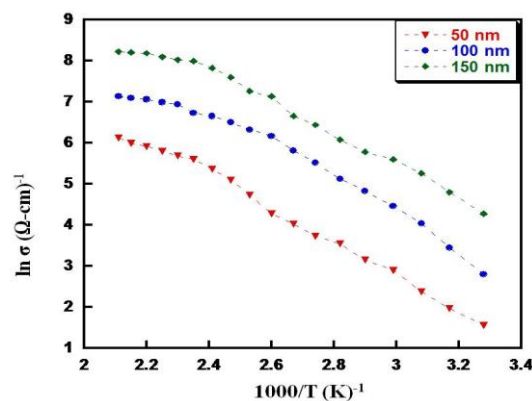
Fig. 3: Plot of In(σ) versus 1000/T of as-deposited In_2O_3 thin films of different thicknesses.

Table-1: The Activation Energies of In_2O_3 Thin Films of Different Thicknesses

Thickness (nm)	Activation energies, ΔE in (eV)	
	Temperature ranges	
	305-435K	435-475K
	ΔE (eV)	ΔE (eV)
50	0.52	0.85
100	0.11	0.78
150	0.09	0.66
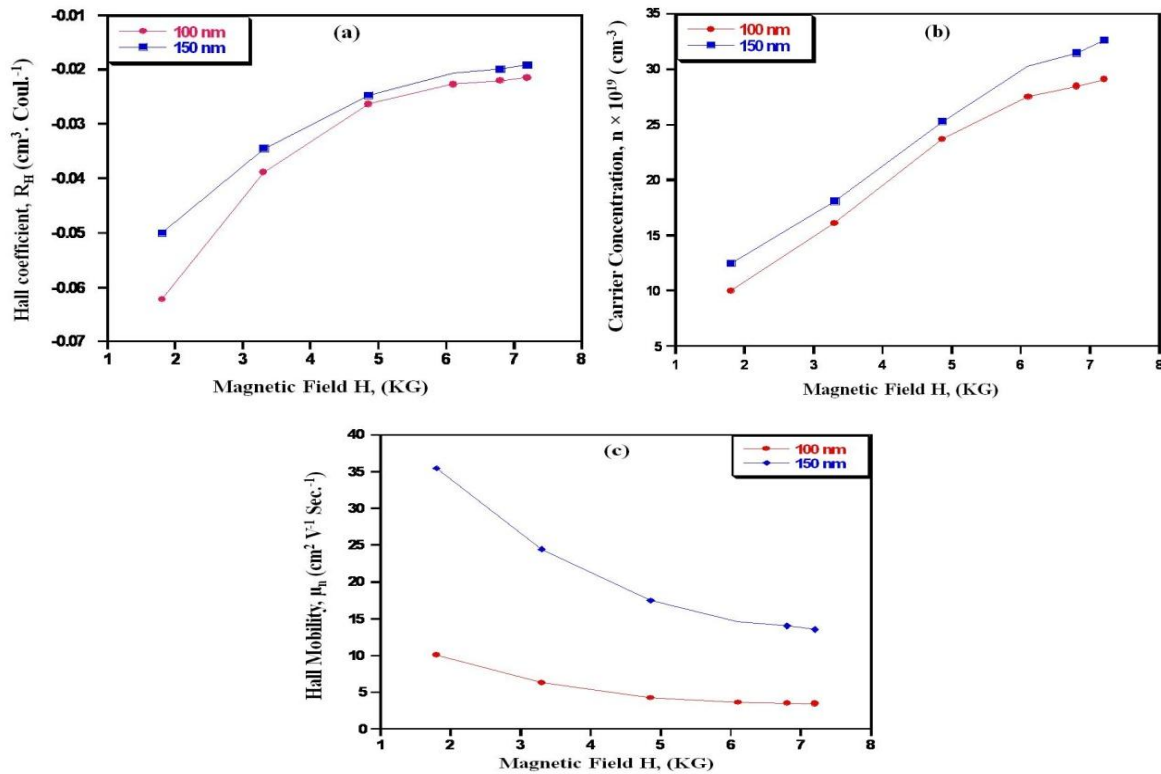
Fig. 4: Variation of (a) Hall coefficient (R_H), (b) carrier concentration (n), and (c) Hall mobility (μ_n) with magnetic field (H) of In_2O_3 thin films.

3.4 Optical Transmittance and Band Gap Studies

Optical transmittance T (%) were measured at wavelength (λ) range $400 \leq \lambda \leq 1100$ nm using a "UV-Visible SHIMADZU double beam spectrophotometer" at room temperature. The variation of transmittance T (%) with wavelength (λ) for the as-deposited films of different thicknesses is shown in Fig. 5. A high optical transparency of about 85% for films with thickness 50 - 100 nm was observed in the visible and near infrared region, and it decreases with decreasing wavelength towards UV region. The transmittance decreases appreciably when the thickness of the film increase to 150 nm.

The absorption coefficient α was calculated from the transmittance (T) measurement, using the following relation:

$$\alpha = \frac{1}{t} \ln\left(\frac{1}{T}\right) \qquad\qquad (4)$$

where t is film thickness in nm and T is the transmittance. Figure 6 shows the variation of absorption coefficient with photon energy of the as-deposited In_2O_3 thin films of two different thicknesses of 50nm and100nm, respectively. The absorption coefficient is found to be the order of 10^4 cm^{-1}.
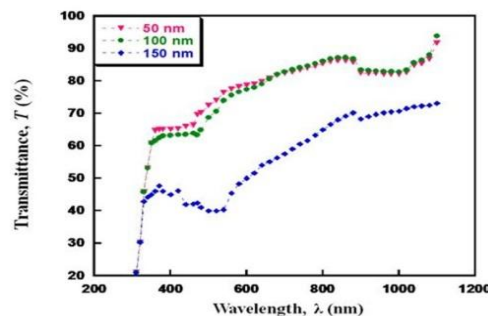
Fig. 5: Spectral variation of transmittance of as-deposited In_2O_3 thin film.

Since the reflectance of the film with thickness 150 nm is relatively high (not shown here), the absorption coefficient of that film is not shown in Fig.6. The absorption coefficient of In_2O_3 thin films was used to calculate the energy band gap. In order to determine the value of optical band gap, $(\alpha h\nu)^n$ versus photon energy ($h\nu$) curves have been plotted. The values of the tangents, evaluated by least mean square method, intercepting the energy axis give the values of optical band gap (E_g). From these curves it is observed that best fit is obtained for $(\alpha h\nu)^2$ vs. $h\nu$ which indicates direct allowed transition. The plot of $(\alpha h\nu)^2$ vs. photon energy ($h\nu$) of the as-deposited In_2O_3 thin films for the different thicknesses is shown in Fig.7. The direct optical band gap is varies between 3.34 and 3.69eV [20].It is also seen that band gap increases with increases of film thickness.
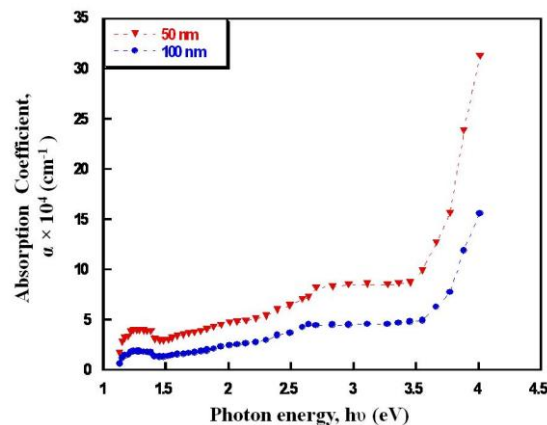
Fig. 6: Absorption coefficient (α) vs. photon energy ($h\nu$) of as-deposited In_2O_3 thin films.
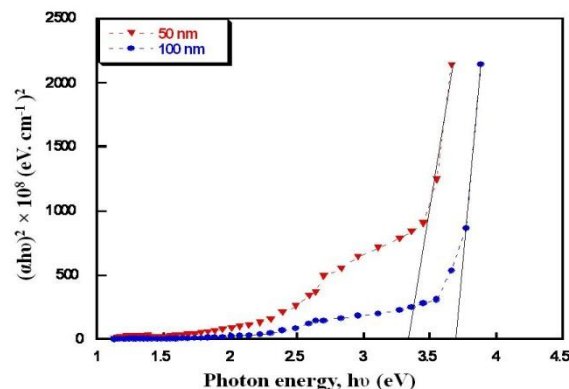
Fig. 7: Plots of $(\alpha h\nu)^2$ vs. $h\nu$ of as-deposited In_2O_3 thin films of two different thicknesses.

IV.   CONCLUSIONS

In_2O_3 thin films of different thicknesses have been successfully deposited on well cleaned glass substrates by e-beam evaporation technique. SEM micrograph shows a uniform surface morphology with a relatively small grain structure. The electrical conductivity variation with temperature indicating semiconducting nature of the as-deposited In_2O_3 films. In the studied temperature range, the conduction is due to a thermally activated process. From the Hall measurement, it is found that In_2O_3 films are n-type electrical conductivity with carrier concentration of order of 10^{19} cm^{-3}. High optical transparency is obtained in visible and infrared regions. Optical band gap of these thin films was calculated and found 3.34 eV, 3.69 eV, respectively for the two films. These characteristics of In_2O_3 films of low resistivity, high transparency, high absorption coefficient and wide band gap make them suitable candidate for technological applications such as antireflection coating for solar cells and opto-electronic devices as mentioned in previous section.

REFERENCES

[1]　C. Xirouchaki, G. Kiriakidis, and T. F. Pedersen, Photo reduction and oxidation of as-deposited microcrystalline indium oxide, *Journal of Applied Physics, 79(12)*, 1996, 9349-9352.

[2]　C. G. Granqvist, Transparent conductive electrode for electrochromic devices: A review, *Applied Physics A: Solids and Surfaces, 57(1)*, 1993, 19-24.

[3]　S. Pissadakis, S. Mailis, L. Reekie, J. S. Wilkinson, R. W. Eason, N. A. Vainos, K. Moschovis, and G. Kiriakidis, Permanent holographic recording in indium oxide thin films using 193nm excimer laser radiation, *Applied Physics A: Materials Science & Processing, 69(3),* 1999, 333-336.

[4]　C. Jimenez, A. Mendez, S. Paez, E. Ramierz, and H. Rodriquoz, Production and characterization of indium oxide and indium nitride, *Barzilian Journal of Physics, 36 (3b)*, 2006, 1017-1020,

[5]　M. Bender, N. Katsarakis, E. Gagaoudakis, E. Hourdakis, E. Douloufakis, V. Cimalla, and G. Kiriakidis, Dependence of the photoreduction and oxidation behavior of indium oxide films on substrate temperature and film thickness, *Journal of Applied Physics, 90(10)*, 2001, 5382-5387.

[6]　S. Naseem, M. Iqbal, and K. Hussain, Optoelectrical and structural properties of evaporated indium oxide thin film, *Solar Energy Materials and Solar Cells, 31(2),* 1993, 155-162.

[7]　S. Agilan, D. Mangalaraj, Sa.K. Narayandass, G. Mohan Rao, S. Velumani, Structure and temperature dependence of conduction mechanisms in hot wall deposited CuInSe2 thin films and effect of back contact layer in CuInSe2 based solar cells, *Vacuum, 84,* 2010, 1220-1225.

[8]　S. Muranaka, Y. Bando, and T. Takada, Influence of substrate temperature and film thickness on the structure of reactively evaporated In_2O_3 films, *Thin Solid Films, 151(3)*, 1987, 355-364.

[9]　V. D. Das, S. Kirupavathy, L. Damodare, and N. Lakshminarayan, Optical and electrical investigations of indium oxide thin films prepared by thermal oxidation of indium thin films, *Journal of Applied Physics, 79(11)*, 1996, 8521-8530.

[10]　T. Asikainen, M. Ritala, W.M. Li, R. Lappalainen, and M. Leskela, Modifying ALE grown In_2O_3 films by benzoyl fluoride pulses, *Applied Surface Science, 112,* 1997, 231-235.

[11]　Y. Yamada, N. Suzuki, T. Makino, and T. Yoshida, Stoichiometric indium oxide thin films prepared by pulsed laser deposition in pure inert background gas, *Journal of Vacuum Science & Technology A, 18(1),* 2000, 83-86 .

[12]　F. O. Adurodija, H. Izumi, T. Ishihara, H. Yoshioka, M. Motoyama, and K. Murai, Influence of substrate temperature on the properties of indium oxide thin films, *Journal of Vacuum Science & Technology A, 18(3),* 2000, 814-818.

[13]　S. Naseem, I. A. Rauf, and K. Hussain, Effects of oxygen partial pressure on the properties of reactively evaporated thin films of indium oxide, *Thin Solid Films, 156 (1),* 1988, 161-171.

[14]　S. K. Poznyak, A. I. Kulak, Characterization and photo electrochemical properties of nano-crystalline In_2O_3 film electrodes, *Electrochimica Acta, 45(10),* 2000, 1595-1605.

[15]　S. Tolansky*, Multiple beam interferometry of surface and films*, (London: Oxford University Press, 1948).

[16]　W. Wen-Fa, C. Bi-Shiou, Effect of annealing on electrical and optical properties of RF magnetron sputtered indium tin oxide films, *Applied Surface Science, 68(4)*, 1993, 497-504.

[17]　Y. Zi-Jian, Z. Xia-Ming, W. Xiong, Z. Ying-Ying, W. Zheng-Fen, Q. Dong-Jiang, W. Hui-Zhen, D. Bin-Yang , 'Preparation and Characteristics of Indium Oxide Thin Films, *Journal of Inorganic Materials, 15(2)*, 2010, 141-144.

[18]　S. Noguchi and H.Sakata, Electrical properties of undoped In_2O_3 films prepared by reactive evaporation, *Journal of Physics D: Applied Physics, 13(6)*, 1980, 1129-1134.

[19]　K. L. Chopra, S. Major and D. K. Pandya, "Transparent Conductors—A Status Review, *Thin Solid Films, 102(1),* 1983, 1-46

[20]　R. L. Weiher, and R. P. Ley, Optical Properties of Indium Oxide, *Journal of Applied Physics, 37(1),* 1966, 299-302.

Research Paper   Open Access

3D Design & Simulation of a Z Shape Antenna with a CPW Tx Line

Protap Mollick[1], Amitabh Halder[2], Mohammad Forhad Hossain[3],
A S M Wasif[4]

[1](CSE, American International University-Bangladesh, Bangladesh)
[2](EEE, American International University-Bangladesh, Bangladesh)
[3](EEE, American International University-Bangladesh, Bangladesh)
[4](MSc in IT, Central Queensland University, Australia*)*

ABSTRACT : *This paper presents design of à new Z shaped antenna with a cpw (coplanar waveguide) transmission line. In this proposed research paper, the impedance increases with a pair of Z shape combined design on the FR-4 substrate and ground plane. The main features of the Z antenna are the compact dimensions and band-operating characteristics that are obtained without modifying the radiator or the ground plane. The antenna consists of a linear patch as radiator, a partial CPW-ground plane, and a slotted conductor-backed plane. Impedance matching for dual-band operations is achieved by a pair of mirror square-shaped slots at the conductor-backed plane. This antenna size is very compact with 28.8 mm × 37.2 mm × 1.6 mm and covers 1.696 GHz to 2.646 GHz and can be used for GSM and WLAN applications. Our designing aim is to describe radiation pattern both 3D and normal and discuss obtained gain.*

KEYWORDS – *Microstrip, Coplanar waveguide, Impedance, HFSS, Bandwidth.*

I.   INTRODUCTION

In recent years demand for small antennas on wireless communication has increased the interest of research work on compact microstrip various kind of shaped antenna design among microwaves and wireless technology. To support the high mobility necessity for a wireless telecommunication device, a small and light weight Z shape antenna is likely to be preferred. For this purpose compact Z shaped antenna is one of the most suitable applications. The development of Z shaped antenna for wireless communication also requires an antenna with more than one operating frequencies. This is due to many reasons, mainly because there are various wireless communication systems and many telecommunication operators using various frequencies. However, the general Z shaped patch antennas have some disadvantages such as narrow bandwidth etc. Enhancement of the performance to cover the demanding bandwidth is necessary [1]. But overhead those drawbacks Z shaped antenna is now most popular antenna. In the design of a Z shape antenna with a coplanar waveguide, the shape of the Z antenna patch, the ground plane, and the geometry of the ground plane slots are of great importance. Proposed Z shaped have included rectangular ones. Different methods, such as the truncated slot on the antenna patch, have been pro-posed for increasing impedance bandwidth .Recently, some coplanar waveguide (CPW) Z antennas have been reported. In most reported antennas, up to now, the slots have been used for improving the lower frequency of the band and enhancing the upper frequency of the band. In this paper, a novel CPW-fed Z antenna without slot on the patch or ground plane is proposed with a Z-shaped form. In this antenna, using a pair of Z-shape combined (ESC) design on the patch, a proper control on the upper and lower frequencies of the band can be achieved. In addition, on the ground plane, a pair of ESC form is located for improving impedance matching and optimizing gain [2]. Coplanar waveguide is a type of electrical transmission line which can be fabricated using printed circuit board technology, and is used to convey microwave-frequency signals. On a smaller scale, coplanar waveguide transmission lines are also built into monolithic microwave integrated circuits. Conventional coplanar waveguide (CPW) consists of a single conducting track printed onto a dielectric substrate, together with a pair of return conductors, one to either side of the track. All three conductors are on the same side of the substrate, and hence are coplanar. The return conductors are separated from the central track by a small gap, which has an unvarying width along the length of the line. Away from the central conductor, the return conductors usually extend to an indefinite but large distance, so that each is notionally a semi-infinite plane.

The advantages of coplanar waveguide are that active devices can be mounted on top of the circuit, like on microstrip. More importantly, it can provide extremely high frequency response since connecting to coplanar waveguide does not entail any parasitic discontinuities in the ground plane. One disadvantage is potentially lousy heat dissipation. However, the main reason that coplanar waveguide is not used is that there is a general lack of understanding of how to employ it within the microwave design community.

II. DESIGN AND EQUATIONS

The dielectric constant of the substrate is closely related to the size and the bandwidth of the Z shape antenna. Low dielectric constant of the substrate produces larger bandwidth. The resonant frequency of Z shape antenna and the size of the radiation patch can be similar to the following formulas while the high dielectric constant of the substrate results in smaller size of antenna [3].
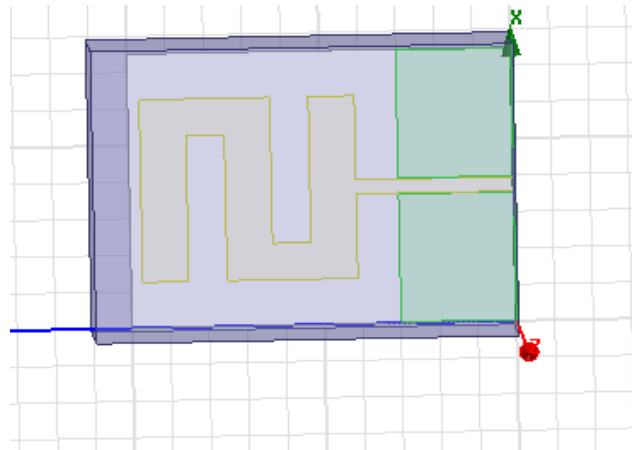
Figure 1: Z shape antenna

Figure 1 shows the geometry of the design of Z shape with a coplanar waveguide transmission line in which the Length of ground plane of Antenna is 38.4 mm and Width is 46.8 mm, L & W of the patch is 28.8 mm & 37.2 mm.

The patch width, effective dielectric constant, the length extension and also patch length are given by

$$w = \frac{C}{2f\sqrt{\varepsilon r}}$$

where *c* is the velocity of light, e is the dielectric content of substrate, *f* is the antenna working frequency, W is the patch non resonant width, and the effective dielectric constant is e given as,

$$\varepsilon_{eff} = \frac{(\varepsilon_r + 1)}{2} + \frac{(\varepsilon_r - 1)}{2}\left[1 + 10\frac{H}{W}\right]^{-\frac{1}{2}}$$

The extension length Δ is calculates as,

$$\frac{\Delta L}{H} = 0.412 \frac{(\varepsilon_{eff} + 0.300)\left(\frac{W}{H} + 0.262\right)}{(\varepsilon_{eff} - 0.258)\left(\frac{W}{H} + 0.813\right)}$$

By using above equation we can find the value of actual length of the patch as,

$$L = \frac{c}{2f\sqrt{\varepsilon_{eff}}} - 2\Delta L$$

III. SIMULATION RESULTS AND TABLE

The antenna simulation pattern is a measure of its power or radiation distribution with respect to a particular type of coordinates. We generally consider spherical coordinates as the ideal antenna is supposed to radiate in a spherically symmetrical pattern [4]. However antennae in practice are not Omni directional but have a radiation maximum along one particular direction. Z shape antenna is a broadside antenna wherein the maximum radiation occurs along the axis of the antenna [5].
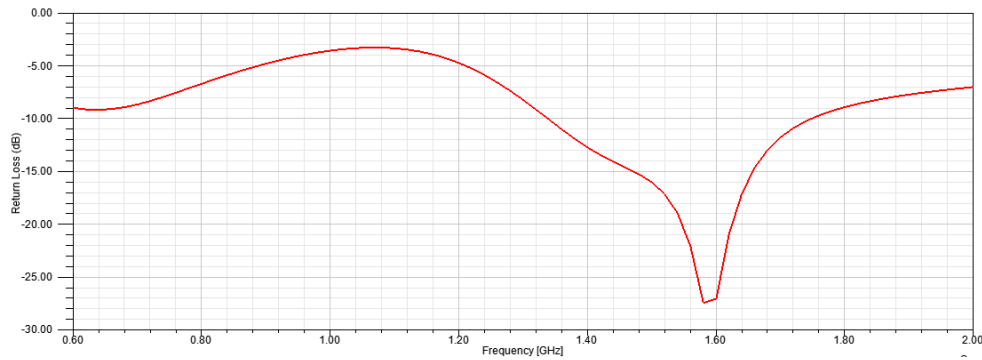
Figure 2: Graph of Return loss.

In Figure 2 presents the graph of the return loss. It is clearly shown that lowest return loss is found at 1.60 GHz. And highest return loss found at 1 GHz frequency. Overall average return loss is not very effective.
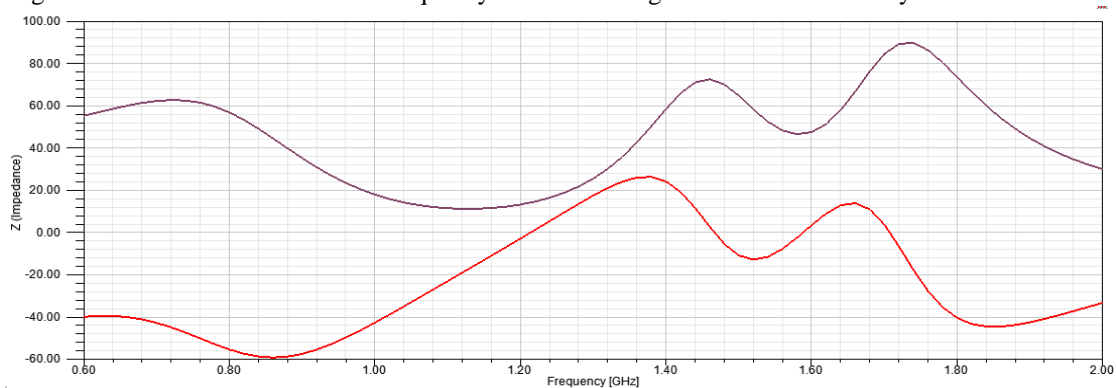
Figure 3: Frequency Vs Imaginary Impedance Graph.

In figure 3 describe the Impedance graph. There are two lines. One of them the upper one represents Imaginary Impedance graph and other one presents Real Impedance graph. We got Imaginary values are the highest in every frequency rather than real impedance graph. When frequency is 1.70 GHz found the highest impedance values for both graph.
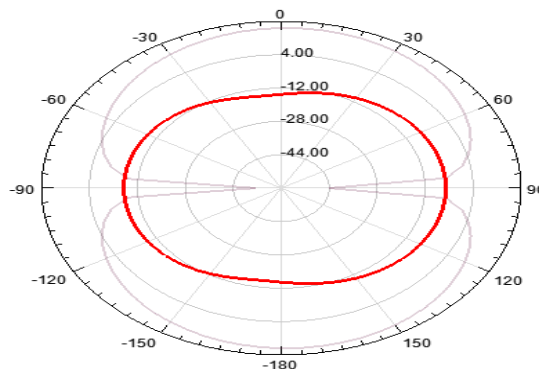
Figure 4: Radiation pattern of Z shape coplanar waveguide antenna.

In figure 4 describe the radiation graph. There are two lines. One of them the upper one light color graph represents Z shape antenna with coplanar waveguide and other one presents dark red graph represents with using coplanar waveguide. We got without coplanar values are the highest in every angel rather than other graph.
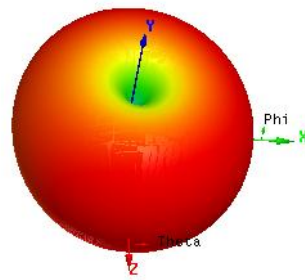
Figure 5: 3D pattern of Z shape antenna.

Figure 5 presents basic 3d pattern of Z shape antenna with using coplanar waveguide transmission line.

	Theta [deg]	rETotal [V] Setup : LastAdaptive Freq='0.9GHz' Phi='0deg'
1	-180.000000	447.377879
2	-175.000000	440.121530
3	-170.000000	431.593863
4	-165.000000	421.963485
5	-160.000000	411.437042
6	-155.000000	400.249550
7	-150.000000	388.653887
8	-145.000000	376.910252
9	-140.000000	365.276345
10	-135.000000	353.998841
11	-130.000000	343.306583
12	-125.000000	333.405660
13	-120.000000	324.476369
14	-115.000000	316.671854

We found at least 73 values from our simulation here we submit 14 values as a sample.it is clearly shown that it follow per 90 degree cycle that means per 90 degree its values at the nadir point and after that complete 90 degree it is in crest point.

IV. CONCLUSION

This thesis detailed the various aspects associated with the modelling of Z shape antenna with coplanar guide transmission line. One of the goal was introduction of HFSS as a simulation tool for electromagnetic analysis. An effort was understanding of the design process in HFSS, which aid the reader in building any simulation in HFSS [6]. In this paper a compact size Z shaped antenna has been designed having good impedance matching as well as high antenna; efficiency of about 95% is achieved. The proposed antenna has larger impedance bandwidth of 43.578% covering the frequency range from 1.696 GHz to 2.646 GHz which is suitable for PCS-1900, GSM and WLAN (802.11b) applications. Obviously there are some limitations of Z shape antenna some of them are listed below:

- Its effective dielectric constant is lower.
- Layout is very compact.
- Shunt element is quite low.

V. ACKNOWLEDGEMENTS

REFERENCES

[1] X. F. Shi, Z. H. Wang, H. Su and Y. Zhao, "A H-Type CPW Slot Antenna in Ku-band Using LTCC Technology with Multiple Layer Substrates," *Second International Conference on Mechanic Automation and Control Engineering* (*MACE*), Hohhot, 15-17 July 2011, pp.7104-7106.

[2] U. Chakraborty, S. Chatterjee, S. K. Chowdhury and P. Sarkar, "A Compact Z shape Patch Antenna for Wireless Communication, "*Progress in Electromagnetics Research C*, Vol.18, 2011, pp.211-220.

[3] H. Sabri and Z. Atlasbaf, "Two Novel Compact Triple Band CPW Annular-Ring Slot Antenna for PCS-1900 and WLAN Applications," *Progress in Electromagnetics Research Letters*, Vol. 5, 2008, pp. 87-98. http://dx.doi.org/10.2528/PIERL08110301

[4] K. Kumar and N. Gunasekaran, "A Novel Wideband Slotted mm Wave Micro strip Patch Antenna," *International Conference on Signal Processing, Communication, Computing and Networking Technologies* (*ICSCCN*), Thackeray, 21-22 July 2011, pp. 10-14.

[5] D. Xi, L. H. Wen, Y. Z. Yin, Z. Zhang and Y. N. Mo, "A Compact Dual Inverted C Shaped Slots Antenna for WLAN Application," *Progress in Electromagnetics Research Letters*,Vol.17,2010,pp.115-123.

[6] G. M. Zhang, J. S. Hong and B. Z. Wang, "Two Novel Band-Notched UWB Slot Antennas Fed by Z shape Line," *Progress in Electromagnetics Research*, Vol. 78, 2008, pp. 209-218. http://dx.doi.org/10.2528/PIER07091201

Research Paper

Comparative Study for Improving the Thermal and Fluid Flow Performance of Micro Channel Fin Geometries Using Numerical Simulation

S.Subramanian[1],   K.S.Sridhar[2],   C.K.Umesh[3]

[1]*Microwavetube Research & Development center, Jalahalli, Bangalore, 560 013, India*
[2]*PES Institute of Technology, 100 feet Ring Road, BSK III Stage, Bangalore, 560 085,India*
[3]*University Visvesvaraya College of Engineering, KR Circle, Bangalore, 560 001, India*

ABSTRACT : *There is a continuous quest for improving the performance of micro channels for handling the increased dissipation of heat from electronics circuits. The Oblique fin micro channels are attractive as they perform better than plate fin & pin fin configurations. There are scopes for further improvements in oblique fin micro channels. Hence this work is about the investigation for the performance enhancement by modifying the oblique fin geometry. Seven variants of micro channel geometries have been explored using three dimensional numerical simulations. The variants are plate fin, in-line pin fin, staggered pin fin, oblique fin, oblique fin with two slit angles, oblique with nozzle type slit and improved oblique fin. The simulation results are validated using the published data. To ensure a common reference for comparison, hydraulic diameter, inlet flow conditions, heat loads and the boundary conditions are kept identical across all the geometries. The results of simulation are compared for the thermal & fluid flow performances. Heat transfer correlations have been developed using the simulation data. The proposed modification is found to enhance the performance significantly.*

Keywords - Micro channels, heat sinks, Electronics cooling, Single phase cooling, Forced convection cooling, CFD simulation

I.   INTRODUCTION

The operational effectiveness of electronic circuits depends mainly on the thermal handling capability of their cooling system. Most often, it is required to achieve higher heat transfer coefficient in compact volume. Hence micro channel heat sinks are prospective options which can handle enhanced levels of heat flux due to its higher surface area to volume ratio. Micro channel research has been under active consideration since the work of Tuckerman and Pease [1]. Li and Peterson [2] have optimized the plate fin micro channel geometries for the constant pumping power criterion. They achieved 20% lower thermal resistance than Tuckerman & Pease. Lee and Garimella [3] studied the plate fin micro channels by varying the aspect ratios. They proposed a generalized correlation for predicting Nusselt number. There was uncertainty over the applicability of conventional heat transfer theory for micro channel system. Hence the liquid flow in the micro channels were investigated both experimentally & numerically [4]. They concluded that the conventional theory is applicable for predicting the flow behavior.

Lee P S et al. [5] proved that it is possible to increase the local heat transfer coefficient by creating a small recess at the cover lid near the hot spot region. They found that the small recess caused the breakage and re-initialization of boundary layer resulting in the increased heat transfer coefficient. This concept was pursued further by many researchers. As an extension of this Lee, Y. J. et al., [6] have experimentally studied the heat transfer from silicon chips using oblique fins. They have proposed to vary the oblique fin pitch for the mitigating local hot spots in silicon chips. Xu et al. [7-8] have carried out experimental and numerical studies to enhance heat transfer rate by using the concept of boundary layer redevelopment. They found that the interruption in the fins leads to boundary layer redevelopment thus increasing the heat transfer coefficient. These interruptions induced pressure recovery at the exit & pressure loss at the entrance. Qu [9] has reported that the pin fin heat sinks are thermally efficient than the conventional plate fin micro channels of the same hydraulic diameter but with a penalty of higher pressure drop. The performance of the Pin fin heat sink was reported to degrade at lower flow rates [10]. Liu et al. [11] have conducted experiments on square pin fins

keeping the diagonal of the fin aligned to the flow direction. They have developed heat transfer correlations from the experimental data. However it is observed that the numerical simulations have been extensively used by many researchers to predict the performance of micro channel heat sinks. Rubio-Jimenez et al. [12] used numerical analysis to propose the concept of variable fin density for maintaining more uniform temperature of the IC chip junction. They reported to have achieved an overall temperature gradient lesser than 2^oC/mm by varying the pitch. Fan et al. [13] have numerically simulated the performance of oblique fins on the cylindrical surfaces. The results of simulation were compared using a performance index. Lee Y J et al. [14-16] have studied the performance of oblique fin micro channels both experimentally & numerically. They were able to study the thermal & flow behavior inside the channel by carrying out detailed numerically simulations which are not otherwise possible by experimentation. Danish et al. [17] have carried out a comparative study using numerical simulation for optimizing the parameters of rectangular & oblique fin micro channel heat sinks. The Oblique fin micro channel is reported to enhance the thermal performance with a reasonable pressure drop when compared with pin fin & plate fin micro channels. This shows that there are scopes for the improvement of performance of the oblique fin micro channel geometry using the numerical simulation.

The present study consists of two parts. In the first part, the laminar flow through plate fin and oblique finned micro channel heat sinks are simulated. The results are validated using the published experimental data. In the second part, seven different micro channel fin geometries are investigated for performance enhancement using numerical simulation while imposing certain common criteria. Theoretical heat transfer correlations are developed using simulation data. The results are compared on the basis of performance index.

II.   MICRO CHANNEL HEAT SINK DETAILS

The micro channel geometry consists of inlet, repetitive fluid passages & outlet. Seven micro channel fin geometries have been considered for simulation studies. To ensure a reasonable basis for comparison, some of the dimensional parameters such as the hydraulic diameter, inlet flow conditions, heat load and boundary conditions are held common across all the geometries. The details of the common parameters are shown in Table1. The specific dimensional details pertaining to six of seven geometries are presented in Table 2. The rectangular plate fin micro channel is considered as the seventh geometry. Other than the pin fins & staggered pin fins, three different modifications are proposed for the oblique fin micro channels. In the first type the angle of the secondary flow passage is modified to have two angles for the smooth injection fluid in the main channel. This modification is termed as the oblique fin with two angles. In the second type the secondary flow passage is modified like a convergent nozzle. This is termed as nozzle type micro channels. In the third type fluid entering the secondary flow passage is given an entry and exit angle for smoother diversion & injection of secondary flow with the main flow. This modification is termed as the improved oblique fin micro channels.

III.   COMPUTATIONAL DOMAIN & BOUNDARY CONDITIONS

The micro channel heat sinks have periodically repeating fin and channel pairs. This periodic nature is exploited in order to reduce the computational load. Hence only one pair of a fin and a channel has been chosen as the computational domain. The typical computational domains for the plate fin and the oblique fin micro channels are indicated as the dashed line in Fig 1 and Fig 2. The governing equations relevant to the present computational domain are continuity equations, Navier-Stroke equations and the energy equations in their incompressible form. These equations are not reproduced here as they are well known. A commercially available computational fluid dynamics software ANSYS CFX v.14.5 [19] has been employed for the numerical simulation which has the capability to solve the above equations using finite volume techniques.

Table 1 Common parameters of the micro channels heat sinks

Feature	Details
Width of main channel in micrometers	500
Depth of channel in micrometers	1500
Width of fin in micrometers	500
Size of heat sink in mm X mm	25 X 12.5
Aspect ratio	3
Single fin length in mm	25
Heat sink material	Copper
Coolant fluid	Water
Heat flux in W/cm^2	65

Table 2 Micro channel fin geometries with specific dimensional details

Plan view of the micro channels fin geometries. All dimensions are in mm

1.In Line Pin fin
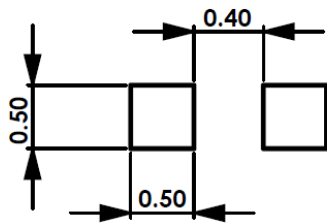
2.Staggered Pin fin
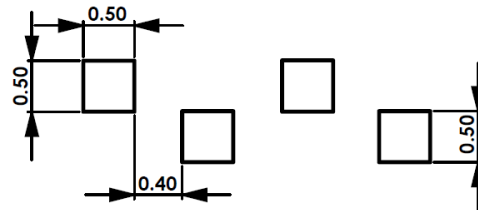
3.Oblique with Two Angle
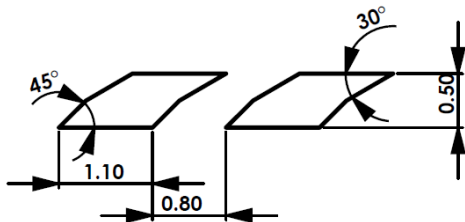
4.Nozzle type
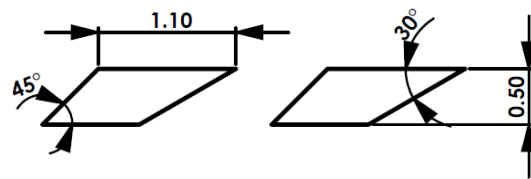
5.Oblique fin
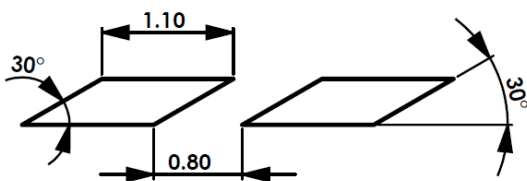
6.Improved Oblique fin
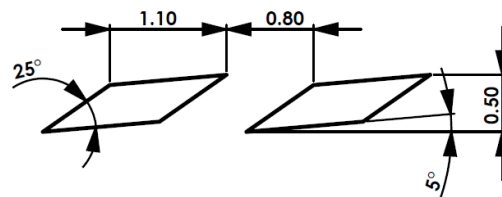
Fully developed velocity profile is assigned to the inlet. Periodic boundary condition is assigned to the sides. A uniform heat flux of 65 W/cm^2 is applied to the heat sink surface at the bottom. The top of the micro channel heat sink is considered to be bonded with adiabatic cover. Pressure boundary condition is assigned to the outlet, where the flow reaches atmospheric pressure. The approach velocity of the fluid is varied from 0.4 m/s to 1.2 m/s. The Reynolds number ranged from 391 to 1130. The temperature dependent materials properties of water [16] have been used for the simulation with the help of CEL expressions in the ANSYS CFX[19].
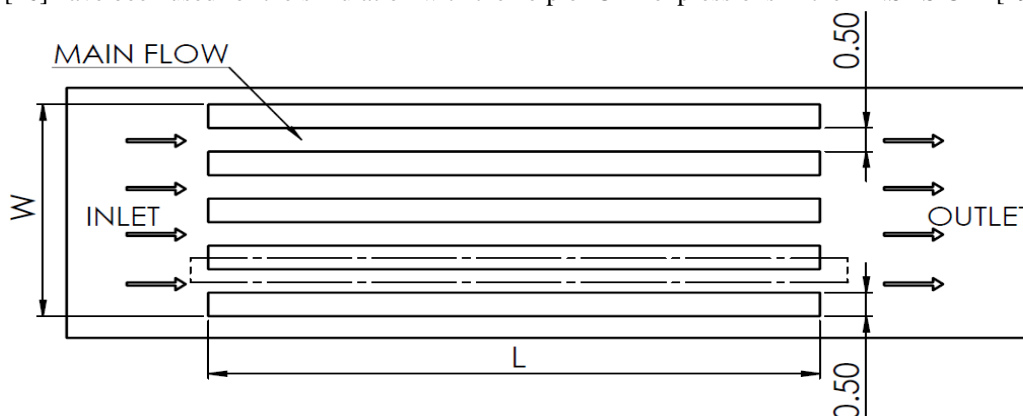
Fig. 1 Plan View of Plate fin Micro channels with dimensions in mm
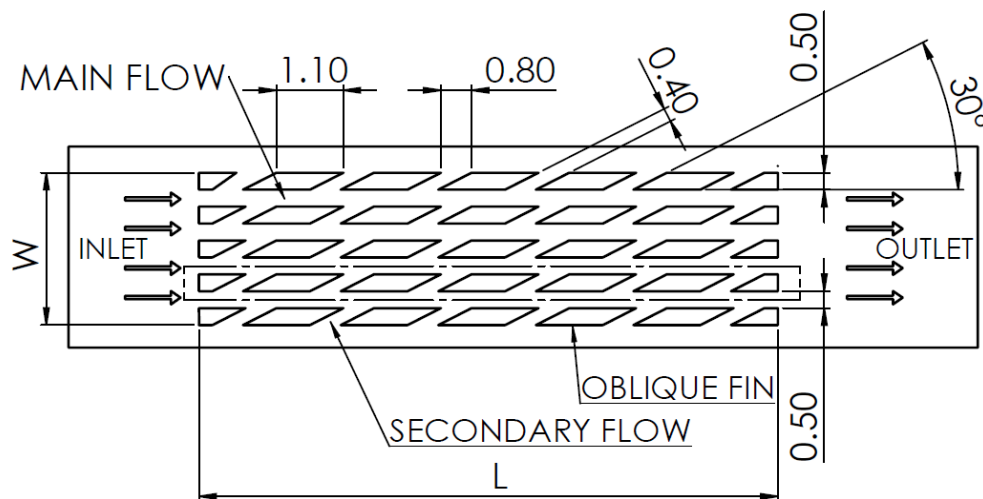
Fig. 2 Plan view of Oblique fin Micro Channels with dimensions in mm

IV.　GRID INDEPENDENCY CHECKING

To ensure grid independent results the model has been meshed at four different grid levels consisting of 676982, 1599592, 23277930 and 4257452 elements. All solid to fluid interfaces have been inflated to a thickness of 100 micrometers with 8 layers. The Face spacing of 50 micrometers to 20 micrometers has been applied to fluid region for better resolution. High resolution scheme is selected as solver option. Double precision has been activated for improving the accuracy. The convergence criterion of 10^{-6} is set for residues. Nusselt numbers are found to be in close proximity of to each other except the mesh of 676982. The average Nusslets number varied by 1.3 % from the first to second mesh level and only by 0.8 % for the second to third meshes level. The fourth mesh level varied by 0.15% from the third level. Hence the mesh level of 2327790 has been used. In the similar manner grid dependency check was carried out for each type of simulation.

V.　VALIDATION

The plate fin micro channel and the oblique fin micro channel have been selected for the validation purpose. The geometric details are chosen in the similar lines of the work carried out by Y.J.Lee et al [16] which is considered as the reference data for validation. The dimensional details are shown in Table 3. The computational fluid dynamic analysis was carried out using ANSYS CFX by varying the inlet velocity. The heat load of 65 W/cm^2 was applied. Figure 3 presents the variation of Nusselt number with Reynold number. It is observed that the Nusselt number calculated using ANSYS CFX matches closely with that of published experimental as well as Fluent data for both plate fin and oblique fin micro channels.. The simulated results of the present study matched closely with that of Fluent results[16] and the experimental data [16]. Hence the simulation procedure is validated and the same is adopted for the rest of the analysis.

Table 3 Dimensional details used for validation

Parameter	Plate fin	Oblique fin
Size of heat sink	25mm X25 mm	25mm X 25mm
Main channel width (micrometers)	547 micron	539
Fin width (micrometers)	458	465
Channel depth (micrometers)	1482 micron	1487
Oblique channel width (micrometers)	-	298
Oblique angle (degrees)	-	27
Oblique fin pitch (micrometers)	-	1995
Oblique fin length (micrometers)	-	1331
Hydraulic diameter (micrometers)	799	792
Heat sink material	Copper	Copper
Coolant fluid	Water	Water
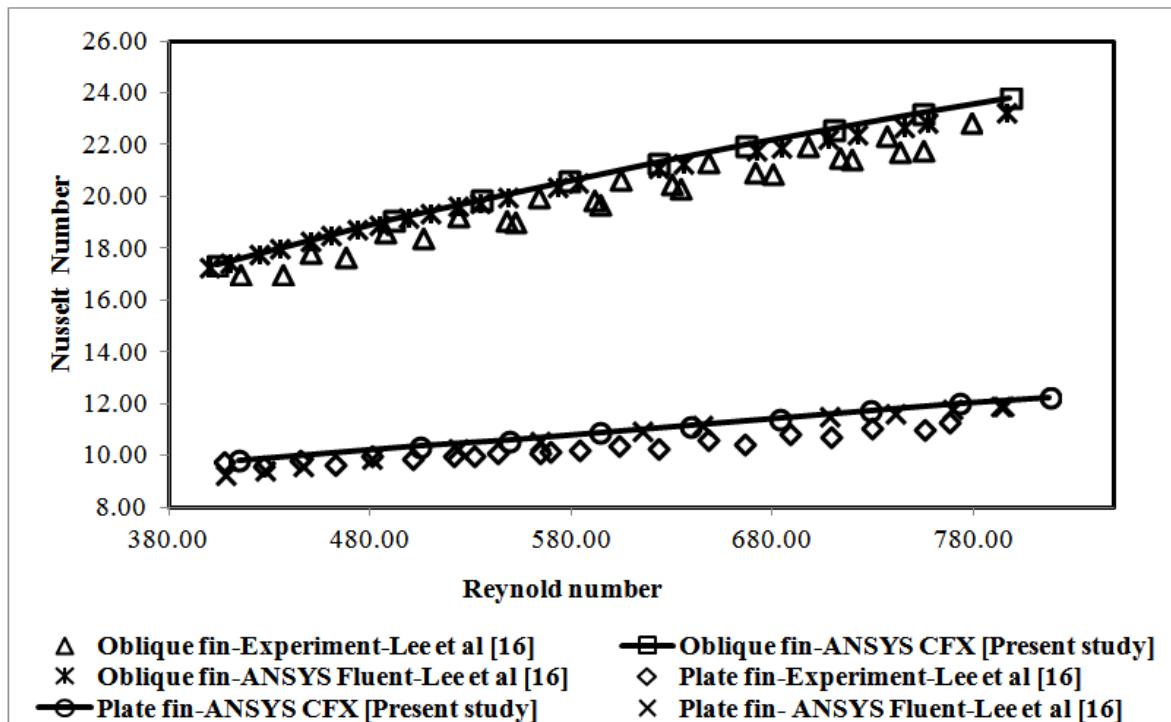
Fig. 3 Validation of Simulation

VI.   RESULTS AND DISCUSSIONS

The effect of inlet flow velocity over the pressure drop is presented in two different plots for the sake clarity which are shown as Fig 4 & Fig 5. The effect of velocity on the pressure drop incurred by all the micro channel geometries under consideration excluding staggered pin fin configuration is presented as Fig 5. It is seen that the pressure drop increases with respect to the inlet flow velocities for all the micro channel geometries. The pressure drop of the plate fin micro channel is the least of all. The pressure drop of the nozzle type micro channel is the highest as the main channel flow is interrupted by accelerated fluid from the secondary channel. Whereas the pressure drop of the improved micro channel is the second lowest and is lower than the oblique micro channel due to the presence of entry exit angles in the secondary flow passage. The pressure drop of in line pin fin & Oblique with two angles is intermediate between oblique & improved oblique fin. The comparison of fluid flow performance of all the micro channel geometries with respect to staggered pin fin is presented in Fig 5. The pressure drop of staggered pin fin is found to be around 4 to 8 folds higher that of the other types.
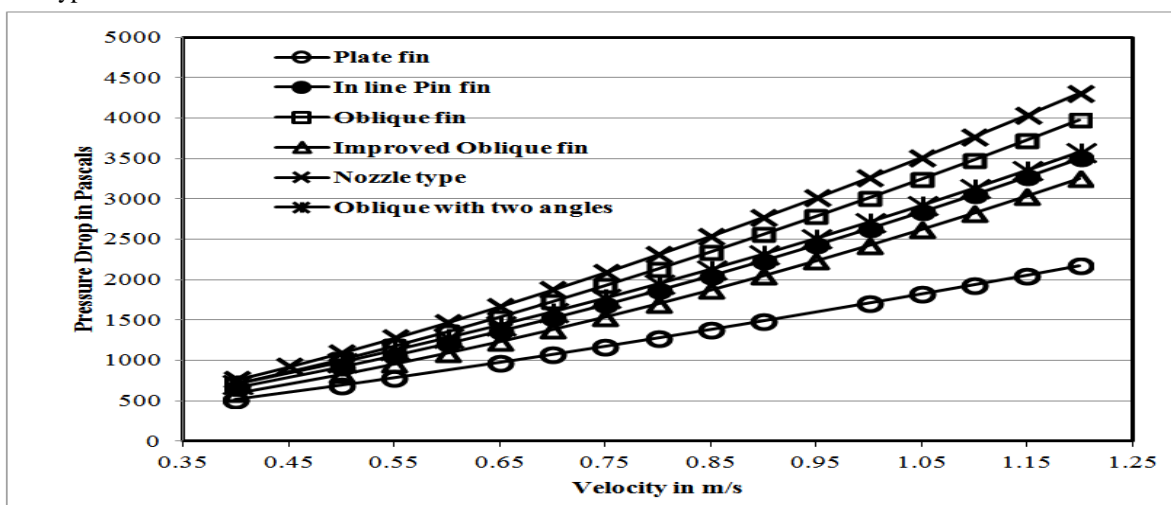
Fig. 4 Comparison of Pressure drop

The effect of inlet flow velocity over the heat transfer coefficient is presented in two graphs which are illustrated as Fig 6 & Fig 7 for the sake of clarity. Figure 7 depicts thermal performance of all the micro channels except staggered pin fin micro channel. The boundary layer breakage & redevelopment concept is used by all types of micro channels except the plate fin. Since the boundary layer grows steadily, the heat transfer coefficient of plate fin is the lowest for the same sets of boundary conditions. The nozzle type micro channel is found to have higher heat transfer coefficient for the entire range of inlet velocities. The performance of inline pin fin & improved oblique fin is found to be nearly equal. The performance of the oblique fin & oblique fin with two angles are found to be lesser than that of the improved oblique fin. Figure 8 compares the performance of staggered pin fin with that of all other geometries. It is observed that the staggered pin performs better.
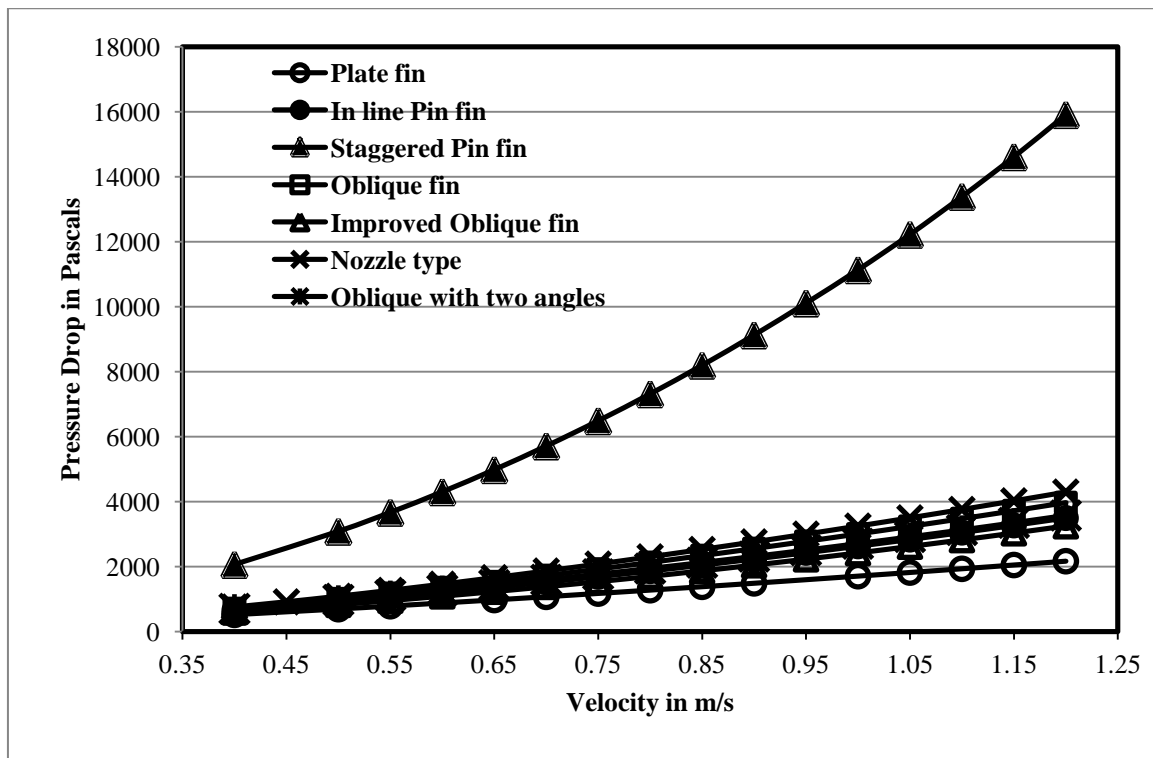
Fig. 5 Pressure drop Compared with Staggered Pin fin

It is important to verify the thermal performance considering the available the wetted surface of the micro channel fin geometries. The heat transfer coefficient is directly proportional to the available heat transfer area & velocity of flow. The comparison of the wetted surface area is presented in Fig 8. The plate fin geometry has the lowest wetted surface resulting in the lower thermal performance. The pin fin geometries and the oblique fin geometry found to have higher wetted surface area leading to higher thermal performance than the plate fin geometry.

4.1 Discussion on the Performance improved Oblique fin micro channel
The wetted surface area of the improved oblique fin is lesser than inline pin fin & oblique fin geometries. But the thermal performance of improved oblique fin is found to be closer to that of inline pin fin and oblique fin geometries. The wetted surface area of the improved oblique fin and nozzle type micro channel is lesser than oblique fins but the thermal performance is better than oblique fins due to the accelerated secondary flow.

The flow impinges the corner of the oblique fin encountering a shock which will results in early separation from the fin surface . The wetted surface will not be effectively utilized in the oblique channel. The performance improvement of improved oblique fin can be attributed to smoother branching of secondary flow. The flow gets modulated without encountering any shock. This delays the flow separation on the trailing end of the oblique fin leading to the effective utilization of the wetted surface.
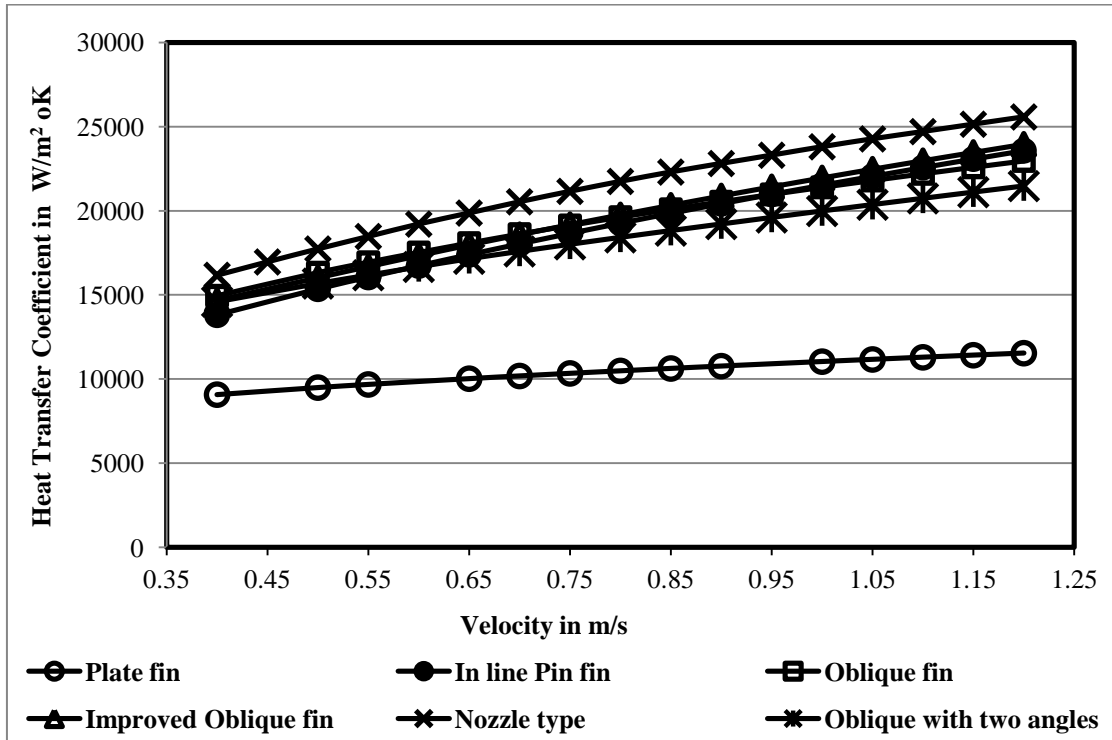
Fig. 6 Comparison of Heat Transfer Performance
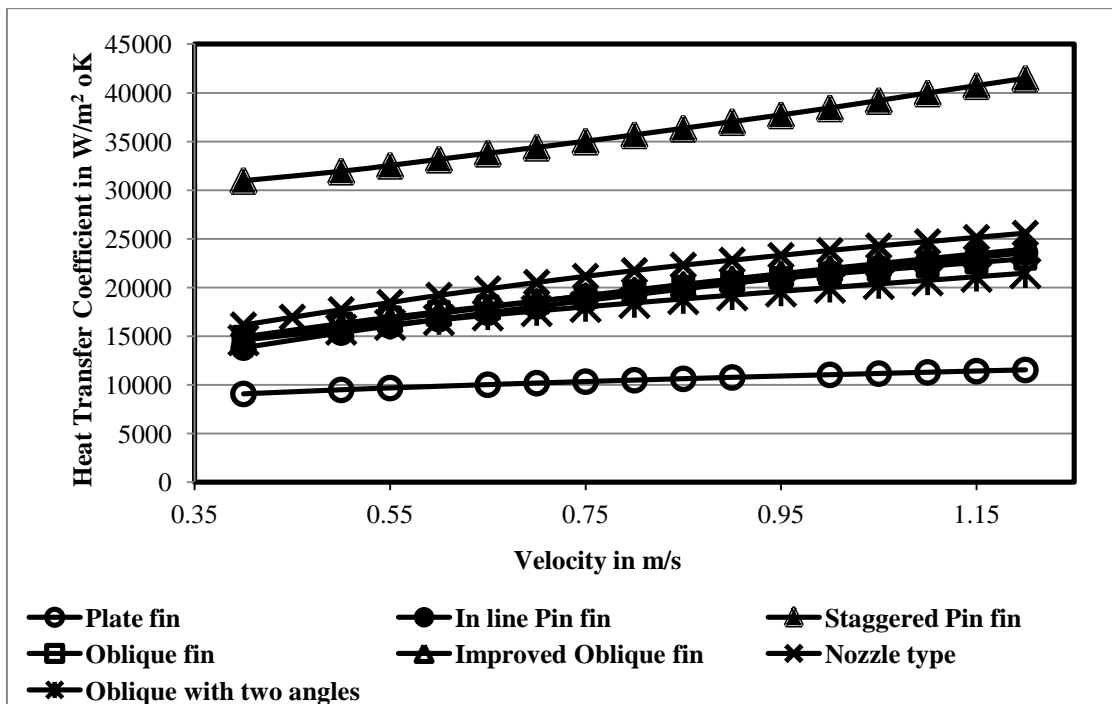
Fig. 7 Heat Transfer Performance Compared with Staggered fin
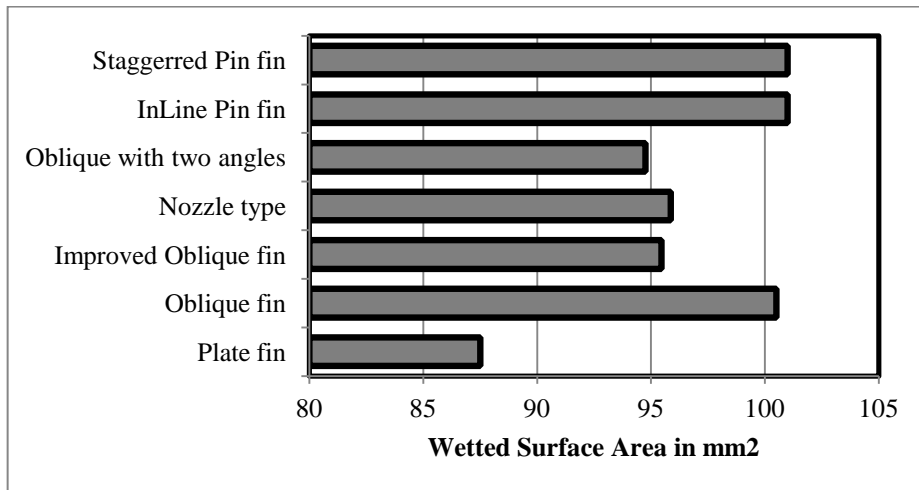
Fig. 8 Comparison of Wetted Surface area

4.2 Performance index

To get a meaningful insight, the above results are compared using a performance index. The ratio of heat transfer coefficient (h) per unit pressure drop (p) is considered as the performance index. The pressure drop is proportional to the pumping power as the mass flow at the inlet is held constant. The ratio of h/p is an indication of heat transfer coefficient per unit pumping power. Figure 9 below presents the h/p ratio for different inlet velocities. It is observed that the performance index of the staggered pin fin is the lowest of all. This implies that the staggered pin demands higher pumping energy to achieve higher heat transfer coefficient. The performance index of the improved oblique fin is the highest which implies that the higher thermal performance is achievable with lesser pumping power.
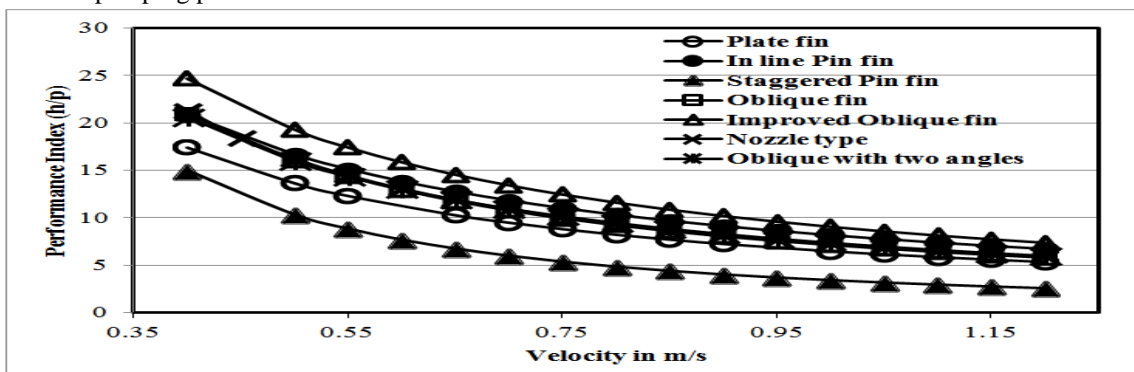
Fig. 9 Comparison of Performance Index
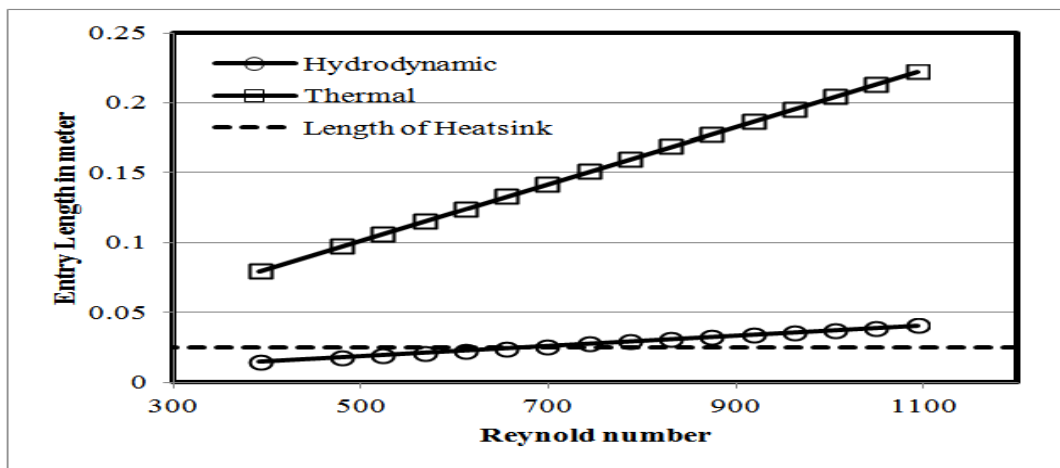
Fig. 10 Effect of Reynolds number on Hydrodynamic and Thermal entry lengths

4.3 Heat Transfer Correlations

The thermal performance of plate fin micro channels decrease along the flow direction due to the thickening of the boundary layer. In order to understand whether the flow is in developing or developed region, the hydrodynamic & thermal entry lengths have been calculated for the plate fin micro channels using the following relations [18].

$L_h = 0.05 \text{ Re } D_h$

$L_T = 0.05 \text{ Re } D_h \text{ Pr}$

Figure 10 shows that the hydro dynamically developed flow is not feasible if the Reynolds number is beyond 700. But the flow is always in thermally developing zone for all the flow rates. The conventional heat transfer correlations are not applicable for these flow conditions as they are based on the developed flow assumption. For all the fin geometries excluding plate fins, the boundary layer gets re-initialized repeatedly along flow direction, so that the flow is always in the developing region. In view of the above, it is required to evolve indicative heat transfer correlations. The heat transfer correlations were evolved through curve fitting using the above simulated results. The list of proposed heat transfer correlations is presented in Table 4. The heat transfer correlation for the inline pin fin is found to be closely matching to that of the one reported in the published literature [11]. Therefore the other heat transfer relations proposed in this work is considered to be reasonable.

Table 4 Heat transfer correlations from simulation

Sl No	Micro channel type	Heat Transfer Correlation
1.	Plate fin	$Nu = 2.415 \text{ Re}^{0.250}$
2.	In line Pin fin	$Nu = 0.642 \text{ Re}^{0.543}$
3.	Staggered Pin fin	$Nu = 5.499 \text{ Re}^{0.314}$
4.	Oblique fin	$Nu = 1.348 \text{ Re}^{0.434}$
5.	Improved Oblique fin	$Nu = 0.943 \text{ Re}^{0.491}$
6.	Nozzle type	$Nu = 1.186 \text{ Re}^{0.468}$
7.	Oblique with two angles	$Nu = 1.784 \text{ Re}^{0.382}$

VII. CONCLUSION

A comparison study has been carried out to investigate for performance enhancement of micro channel fins by modifying the secondary flow passage of the oblique fin micro channel. Thermal & flow performance is compared based on the performance index. The staggered pin fin geometry is able to thermally perform better with higher penalty of pressure drop. But the improved oblique fin geometry which is a variant of modified oblique fin geometry has shown a notable improvements in the performance. In the oblique fin micro channel the main flow branches out to the secondary flow with sharp angle leading to considerable pressure drop. The modification incorporated in the improved oblique fin geometry has helped the smooth entry and exit of secondary flow while ensuring the frequent boundary layer redevelopment leading to an enhancement in performance. The staggered pin fin is the best choice, if thermal performance alone considered as the criteria irrespective of the pumping power. Indicative heat transfer correlations have been developed using numerical simulation.

This numerical study has demonstrated that the augmented heat transfer coefficient is achievable with lesser pressure drop penalty than the oblique fins micro channel. Hence it can be concluded that the improved oblique fin micro channel has better advantage than the other types of micro channel configuration.

VIII. Acknowledgements

Nomenclature

Nu	=	Nusselt number
Re	=	Reynolds number
Pr	=	Prandtl number
h	=	Heat transfer coefficient in W/m^2 ^{o}K
p	=	Pressure in Pascals
L_h	=	Hydrodynamic entry length in m
L_T	=	Thermal entry length in m
D_h	=	Hydraulic diameter in m

REFERENCES

[1]　Tuckerman, D. B., and Pease, R. F. W., High-performance heat sinking for VLSI, IEEE Electron Device Letters, Vol. 2, No. 5, 1981, pp.126–129.

[2]　Li, J., and Peterson, G. P.,3-Dimensional numerical optimization of silicon based high performance parallel micro channel heat sink with liquid flow, International journal of heat & mass transfer,50,15-16, 2007, pp. 2895-2904.

[3]　Poh-Seng Lee, and Suresh V. Garimella Thermally developing flow and heat transfer in rectangular microchannels of different aspect ratios International Journal of Heat and Mass Transfer, 49 , 2006, pp. 3060–3067.

[4]　Liu, D., and Garimella, S. V., Investigation of Liquid Flow in Micro channels, Journal of Thermophysics and Heat Transfer, Vol. 18, No. 1, 2004, pp. 65-72.

[5]　Lee, P.S., Garimella, S.V., and Liu, D., Hotspot thermal management with flow modulation in a micro channel heat sink, Proceedings of ASME international mechanical engineering congress & exposition, paper no IMECE2005-79562.

[6]　Lee, Y. J., Lee, P. S., Chou, S. K., Hotspot mitigating with obliquely finned micro channel heat sink –an experimental study, IEEE Transactions on components, packaging and manufacturing technology,Vol.3, No. 8, 2013, pp. 1332-1341.

[7]　Xu, J. L., Gan, Y. H., Zhang, D. C., and Li, X. H.,Microscale heat transfer Enhancement Using Thermal Boundary Layer Redeveloping concept, International Journal of Heat and Mass transfer, 48, 2005, pp. 1661-1674.

[8]　Xu, J., Song, y., Zhang, W., Zhang, and H., Gan, Y.,Numerical simulation of interrupted and conventional microchannel heat sinks, International Journal of Heat and Mass transfer, 51, 2008, pp. 5906- 5917.

[9]　Qu, W., Comparison of Thermal & Hydraulic Performance of Single Phase Micro-Pin-Fin and Micro-Channel Heat sinks, 11th IEEE Intersociety conference on Thermal & Thermo mechanical Phenomena In electronic systems(I-THERM),2008, pp. 105-112.

[10]　Jasperson, B. A., Jeon, Y., Turner, K. T., Pfefferkorn, F. E., and Weilin Qu, Comparison of Micro-Pin-fin and Micro channel Heat sinks considering Thermal-Hydraulic Performance and Manufacturability, IEEE Transactions on Components and Packaging Technology, Vol. 33, No. 1, 2010,pp.148 -160.

[11]　Liu, M., Liu, D., Xu, S., and Chen, Y., Experimental study on liquid flow and heat transfer in micro square pin fin heat sink, International Journal of Heat and Mass transfer, 54, 2011, pp. 5602-5611.

[12]　Rubio-Jimenez, C. A.,Kandlikar, S.G., and Hernandez-Guerrero, A.,Numerical Analysis of Noval Micro Pin fin Heat sink with Variable Fin density, IEEE Transactions on Components and Packaging Technology, Vol. 2, No.5, 2012, pp. 825-833.

[13]　Fan, Y., PS Lee, L jin, B W Chua, Numerical simulation of forced convection in novel cylindrical oblique-finned heat sink,13th Electronics packaging technology conference,2011.

[14]　Lee, Y. J., Lee, P. S., Chou, S. K., Enhanced Thermal Transport in Micro channels using Oblique Fins, Proceedings of the ASME 2009 Inter PACK Conference, San Francisco.

[15]　Lee, Y. J., Lee, P. S., Chou, S. K., Numerical study of fluid flow and heat transfer in the enhanced micro channel with oblique fins, Journal of heat transfer, Vol. 135, 2013, pp. 04901-10.

[16]　Lee, Y. J., Lee, P. S., Chou, S. K., Enhanced Thermal Transport in Micro channels using Oblique Fins, Journal of Heat Transfer, vol.134, no. 9, 2012, pp. 101901-9.

[17]　Danish Ansari, Afzal Husain and Kwang-Young Kim, Optimization and comparative study on Oblique- and Rectangular-Fin Micro channel Heat sinks, Journal of Thermophysics and Heat Transfer, Vol. 24, No. 4, 2010, pp. 849-852.

[18]　Afzal Hussain and Kwang-Young kim, Shape optimization of micro-channel heatsink for micro-electronic cooling, IEEE Transactions on Components and Packaging Technology, Vol. 31, No. 2, 2008, pp.322-330.

[19]　ANSYS CFX manual v14.5.

Research Paper	Open Access

Location of Zeros of Analytic Functions

P. Ramulu[1], G. L. Reddy[2] and C. Gangadhar[3]

[1]*Department of Mathematics, Govt. Degree College, Wanaparthy, Mahabubnagar, Telangana, India-509103.*
[2]*School of Mathematics and Statistics, University of Hyderabad, Telangana, India-500046.*
[3]*School of Mathematics and Statistics, University of Hyderabad, Telangana, India-500046.*

***Abstract:** In this paper we are finding the number of zeros of class of analytic functions, by considering more general coefficient conditions. As special cases the extended results yield much simpler expressions for the upper bounds of zeros of those of the existing results.*
***Mathematics Subject Classification:** 30C10, 30C15.*
***Keywords:** Zeros of polynomial, Analytic functions, Eneström-Kakeya theorem.*

I. INTRODUCTION

Let $P(z) = \sum_{i=0}^{n} a_i z^i$ be a polynomial of degree n such that $0 < a_0 \leq a_1 \leq a_2 \leq \cdots \leq a_n$ then all the zeros of P(z) lie in $|z| \leq 1$. Finding approximate zeros of a polynomial related to an analytic function is an important and well-studied problem. To find the number of zeros of a polynomial related to an analytic function has already been proved by Aziz and Mohamad [3], by extending Eneström-Kakeya theorem [1-2].

Here we establish the following results which are more interesting.

Theorem 1. Let $F(z) = \sum_{i=0}^{\infty} a_i z^i \not\equiv 0$ *be an analytic function in* $|z| \leq 1$ *such that*
$$|\arg(a_i) - \beta| \leq \alpha \leq \frac{\pi}{2}, i = 0,1,2, \ldots, n, \ldots \text{ for some real } \beta, a_0 \neq 0,$$
$$0 < \tau \leq 1, k \geq 0, k_1 \geq 0 \text{ and}$$
$$\tau|a_0| \leq |a_1| \leq \cdots \leq |a_{m-2}| \leq |a_{m-1}| \leq k_1|a_m| \geq |a_{m+1}| \leq |a_{m+2}| \geq |a_{m+3}| \leq |a_{m+4}| \geq \cdots$$
$$\leq |a_{n-2}| \geq |a_{n-1}| \leq k|a_n| \geq |a_{n+1}| \geq |a_{n+2}| \geq \cdots$$
for some m, $0 \leq m \leq n$ *then the number of zeros of* F(z) *in* $|z| \leq r, \ 0 < r < 1$
does not exceed

$$\frac{1}{\log\frac{1}{r}} \log \frac{2\left[E_1 + |a_0| + \sin\alpha \sum_{i=1}^{\infty}|a_i| + (k_1|a_m| + k|a_n|)(1 + \cos\alpha + \sin\alpha) - \frac{1}{2}\tau|a_0|(1 + \cos\alpha - \sin\alpha)\right]}{|a_0|},$$

where $E_1 = [(|a_{m+2}| + |a_{m+4}| + \cdots + |a_{n-4}| + |a_{n-2}|) - (|a_{m+1}| + |a_{m+3}| + \cdots + |a_{n-3}| + |a_{n-1}|)]\cos\alpha - [|a_m| + |a_n|](1 + \sin\alpha).$

Corollary 1. Let $F(z) = \sum_{i=0}^{\infty} a_i z^i \not\equiv 0$ *be an analytic function in* $|z| \leq 1$ *such that*
$$|\arg(a_i) - \beta| \leq \alpha \leq \frac{\pi}{2}, i = 0,1,2, \ldots, n, \ldots \text{ for some real } \beta, a_0 \neq 0 \text{ and}$$
$$|a_0| \leq |a_1| \leq \cdots \leq |a_{m-2}| \leq |a_{m-1}| \leq |a_m| \geq |a_{m+1}| \leq |a_{m+2}| \geq |a_{m+3}| \leq |a_{m+4}| \geq \cdots$$
$$\leq |a_{n-2}| \geq |a_{n-1}| \leq |a_n| \geq |a_{n+1}| \geq |a_{n+2}| \geq \cdots$$
for some m, $0 \leq m \leq n$ *then the number of zeros of* F(z) *in* $|z| \leq \frac{1}{2}$ *does not exceed*

$$1 + \frac{1}{\log 2} \log \frac{\left[E_2 + \sin\alpha \sum_{i=1}^{\infty}|a_i| + (|a_m| + |a_n|)\cos\alpha + \frac{1}{2}|a_0|(1 + \sin\alpha - \cos\alpha)\right]}{|a_0|},$$

where $E_2 = [(|a_{m+2}| + |a_{m+4}| + \cdots + |a_{n-4}| + |a_{n-2}|) - (|a_{m+1}| + |a_{m+3}| + \cdots + |a_{n-3}| + |a_{n-1}|)]\cos\alpha.$

Remark 1. By taking $\tau = k = k_1 = 1$ *and* $r = \frac{1}{2}$ in theorem 1, then it reduces to Corollary 1.

Theorem 2. Let $F(z) = \sum_{i=0}^{\infty} a_i z^i \not\equiv 0$ *be an analytic function in* $|z| \leq 1$ *such that*

$$|\arg(a_i) - \beta| \leq \alpha \leq \frac{\pi}{2}, i = 0,1,2,\dots,n,\dots \text{ for some real } \beta, a_0 \neq 0,$$

$$k \geq 0, 0 < \tau \leq 1, 0 < \vartheta \leq 1 and$$

$$k|a_0| \geq |a_1| \geq \cdots \geq |a_{m-2}| \geq |a_{m-1}| \geq \tau|a_m| \leq |a_{m+1}| \geq |a_{m+2}| \leq |a_{m+3}| \geq |a_{m+4}| \leq \cdots$$
$$\geq |a_{n-2}| \leq |a_{n-1}| \geq \vartheta|a_n| \leq |a_{n+1}| \geq |a_{n+2}| \geq |a_{n+3}| \geq \cdots$$

for some m, $0 \leq m \leq n$ then the number of zeros of F(z) in $|z| \leq r$, $0 < r < 1$
does not exceed

$$\frac{1}{\log \frac{1}{r}} \log \frac{2\left[E_3 + \frac{1}{2}k|a_0|(1 + cos\alpha + sin\alpha) - (\tau|a_m| + \vartheta|a_n|)(1 + cos\alpha - sin\alpha) + sin\alpha \sum_{i=1}^{\infty}|a_i|\right]}{|a_0|}.$$

where $E_3 = [(|a_{m+1}| + |a_{m+3}| + \cdots + |a_{n-3}| + |a_{n-1}|) - (|a_{m+2}| + |a_{m+4}| + \cdots + |a_{n-4}| + |a_{n-2}|)]cos\alpha + [\,|a_m| + |a_n|](1 - sin\alpha).$

Corollary 2. Let $F(z) = \sum_{i=0}^{\infty} a_i z^i \not\equiv 0$ *be an analytic function in* $|z| \leq 1$ *such that*

$$|\arg(a_i) - \beta| \leq \alpha \leq \frac{\pi}{2}, i = 0,1,2,\dots,n,\dots \text{ for some real } \beta, a_0 \neq 0, and$$

$$|a_0| \geq |a_1| \geq \cdots \geq |a_{m-2}| \geq |a_{m-1}| \geq |a_m| \leq |a_{m+1}| \geq |a_{m+2}| \leq |a_{m+3}| \geq |a_{m+4}| \leq \cdots$$
$$\geq |a_{n-2}| \leq |a_{n-1}| \geq |a_n| \leq |a_{n+1}| \geq |a_{n+2}| \geq |a_{n+3}| \geq \cdots$$

for some m, $0 \leq m \leq n$ then the number of zeros of F(z) in $|z| \leq r$, $0 < r < 1$
does not exceed

$$\frac{1}{\log \frac{1}{r}} \log \frac{2\left[E_4 + \frac{1}{2}|a_0|(1 + cos\alpha + sin\alpha) - (|a_m| + |a_n|)cos\alpha + sin\alpha \sum_{i=1}^{\infty}|a_i|\right]}{|a_0|}.$$

where $E_4 = [(|a_{m+1}| + |a_{m+3}| + \cdots + |a_{n-3}| + |a_{n-1}|) - (|a_{m+2}| + |a_{m+4}| + \cdots + |a_{n-4}| + |a_{n-2}|)]cos\alpha.$

Remark 2. By taking $k = \tau = \vartheta = 1$ in theorem 2, then it reduces to Corollary 2.

II. Lemmas

Lemma 1. [4]: Let $P(z) = \sum_{i=0}^{\infty} a_i z^i \not\equiv 0$ *be an analytic function in* $|z| \leq 1$ *such that*

$$|\arg(a_i) - \beta| \leq \alpha \leq \frac{\pi}{2}; |a_{i-1}| \leq |a_i| \text{ for } i = 0,1,2,\dots,n,\dots$$

$$\text{then } |a_i - a_{i-1}| \leq (|a_i| - |a_{i-1}|)cos\alpha + (|a_i| + |a_{i-1}|)sin\alpha.$$

Lemma 2. [5]: If f(z) is regular $f(0) \neq 0$ *and* $f(z) \leq M$ in $|z| \leq 1,$ *then the nuber of zeros of* $f(z)$
in $|z| \leq r, 0 < r < 1$ *does not exceed* $\frac{1}{\log \frac{1}{r}} \log \frac{M}{|a_0|}.$

III. Proofs of the Theorems

Proof of the Theorem 1.

Let $F(z) = a_0 + a_1 z + a_2 z^2 + \cdots + a_m z^m + \cdots + a_n z^n + \cdots$ be an analytic function.

Let us consider the polynomial $G(z) = (1 - z)F(z)$ so that

$$G(z) = (1 - z)(a_0 + a_1 z + a_2 z^2 + \cdots + a_m z^m + \cdots + a_n z^n + \cdots)$$

$$= a_0 + \sum_{i=1}^{\infty} (a_i - a_{i-1}) z^i$$

Now for $|z| \leq 1$, we have

$$|G(z)| \leq |a_0| + |a_0 - \tau a_0 + \tau a_0 - a_1| + \sum_{i=2}^{m-1} |a_i - a_{i-1}| + |a_m - k_1 a_m + k_1 a_m - a_{m-1}|$$

$$+ |a_{m+1} - k_1 a_m + k_1 a_m - a_m| + \sum_{i=m+2}^{n-1} |a_i - a_{i-1}| + |a_n - k a_n + k a_n - a_{n-1}|$$

$$+ |a_{n+1} - k a_n + k a_n - a_n| + \sum_{i=n+2}^{\infty} |a_i - a_{i-1}|$$

$$\leq |a_0| + (1-\tau)|a_0| + |\tau a_0 - a_1| + \sum_{i=2}^{m-1} |a_i - a_{i-1}| + 2(k_1 - 1)|a_m| + |k_1 a_m - a_{m-1}| + |k_1 a_m - a_{m+1}|$$

$$+ \sum_{i=m+2}^{n-1} |a_i - a_{i-1}| + 2(k-1)|a_n| + |k a_n - a_{n-1}| + |k a_n - a_{n+1}| + \sum_{i=n+2}^{\infty} |a_i - a_{i-1}|$$

By using lemma 1 we get

$$|G(z)| \leq |a_0| + (1-\tau)|a_0| + (|a_1| - \tau|a_0|)\cos\alpha + (|a_1| + \tau|a_0|)\sin\alpha + 2[(k_1 - 1)|a_m| + (k-1)|a_n|]$$

$$+ \sum_{i=2}^{m-1} (|a_i| - |a_{i-1}|)\cos\alpha + \sum_{i=2}^{m-1} (|a_i| + |a_{i-1}|)\sin\alpha + (k_1|a_m| - |a_{m-1}|)\cos\alpha$$

$$+ (k_1|a_m| + |a_{m-1}|)\sin\alpha + (k_1|a_m| - |a_{m+1}|)\cos\alpha + (k_1|a_m| + |a_{m+1}|)\sin\alpha$$

$$+ (|a_{m+2}| - |a_{m+1}|)\cos\alpha + (|a_{m+2}| + |a_{m+1}|)\sin\alpha + (|a_{m+2}| - |a_{m+3}|)\cos\alpha$$

$$+ (|a_{m+2}| + |a_{m+3}|)\sin\alpha + \cdots + (|a_{n-2}| - |a_{n-3}|)\cos\alpha + (|a_{n-2}| + |a_{n-3}|)\sin\alpha$$

$$+ (|a_{n-2}| - |a_{n-1}|)\cos\alpha + (|a_{n-2}| + |a_{n-1}|)\sin\alpha + (k|a_n| - |a_{n+1}|)\cos\alpha$$

$$+ (k|a_n| + |a_{n-1}|)\sin\alpha + (k|a_n| - |a_{n+1}|)\cos\alpha + (k|a_n| + |a_{n+1}|)\sin\alpha$$

$$+ \sum_{i=n+2}^{\infty} (|a_{i-1}| - |a_i|)\cos\alpha + \sum_{i=n+2}^{\infty} (|a_{i-1}| + |a_i|)\sin\alpha$$

$$= |a_0| + (1-\tau)|a_0| + (|a_1| - \tau|a_0|)\cos\alpha + (|a_1| + \tau|a_0|)\sin\alpha + 2[(k_1 - 1)|a_m| + (k-1)|a_n|]$$

$$+ (|a_{m-1}| - |a_1|)\cos\alpha + \sum_{i=2}^{m-1} (|a_i| + |a_{i-1}|)\sin\alpha + (k_1|a_m| - |a_{m-1}|)\cos\alpha$$

$$+ (k_1|a_m| + |a_{m-1}|)\sin\alpha + (k_1|a_m| - |a_{m+1}|)\cos\alpha + (k_1|a_m| + |a_{m+1}|)\sin\alpha$$

$$+ 2[(|a_{m+2}| + |a_{m+4}| + \cdots + |a_{n-4}| + |a_{n-2}|) - (|a_{m+1}| + |a_{m+3}| + \cdots + |a_{n-3}|$$

$$+ |a_{n-1}|)]\cos\alpha + |a_{m+1}|\sin\alpha + \sum_{i=m+2}^{n-2} 2|a_i|\sin\alpha + |a_{n-1}|\sin\alpha + (k|a_n| - |a_{n-1}|)\cos\alpha$$

$$+ (k|a_n| + |a_{n-1}|)\sin\alpha + (k|a_n| - |a_{n+1}|)\cos\alpha + (k|a_n| + |a_{n+1}|)\sin\alpha + |a_{n+1}|\cos\alpha$$

$$+ \sum_{i=n+2}^{\infty} (|a_i| + |a_{i-1}|)\sin\alpha$$

$$= 2|a_0| - \tau|a_0|(1 + \cos\alpha - \sin\alpha) + 2(k_1|a_m| + k|a_n|)(1 + \cos\alpha + \sin\alpha) - 2[|a_m| + |a_n|](1 + \sin\alpha)$$

$$+ 2\sin\alpha \sum_{i=1}^{\infty} |a_i|$$

$$+ 2[(|a_{m+2}| + |a_{m+4}| + \cdots + |a_{n-4}| + |a_{n-2}|) - (|a_{m+1}| + |a_{m+3}| + \cdots + |a_{n-3}|$$

$$+ |a_{n-1}|)]\cos\alpha$$

$$\leq 2\left[E_1 + |a_0| + \sin\alpha \sum_{i=1}^{\infty} |a_i| + (k_1|a_m| + k|a_n|)(1 + \cos\alpha + \sin\alpha) - \frac{1}{2}\tau|a_0|(1 + \cos\alpha - \sin\alpha) \right],$$

$where\ E_1 = [(|a_{m+2}| + |a_{m+4}| + \cdots + |a_{n-4}| + |a_{n-2}|) - (|a_{m+1}| + |a_{m+3}| + \cdots + |a_{n-3}| + |a_{n-1}|)]\cos\alpha - [|a_m| + |a_n|](1 + \sin\alpha)$

Apply lemma 2 to G(z), we get then number of zeros of G(z) in $|z| \leq r, 0 < r < 1$ does not exceed

$$\frac{1}{log\frac{1}{r}}log\frac{2\left[E_1 + |a_0| + sin\alpha \sum_{i=1}^{\infty}|a_i| + (k_1|a_m| + k|a_n|)(1 + cos\alpha + sin\alpha) - \frac{1}{2}\tau|a_0|(1 + cos\alpha - sin\alpha)\right]}{|a_0|},$$

$where\ E_1 = [(|a_{m+2}| + |a_{m+4}| + \cdots + |a_{n-4}| + |a_{n-2}|) - (|a_{m+1}| + |a_{m+3}| + \cdots + |a_{n-3}| + |a_{n-1}|)]cos\alpha -$
$[|a_m| + |a_n|](1 + sin\alpha)$

All the number of zeros of F(z) in $|z| \le r, 0 < r < 1$ is also equal to the number of zeros of G(z) in $|z| \le r, 0 < r < 1$.

This completes the proof of theorem 1.

Proof of the Theorem 2.

Let $F(z) = a_0 + a_1 z + a_2 z^2 + \cdots + a_m z^m + \cdots + a_n z^n + \cdots$ be an analytic function.

Let us consider the polynomial $G(z) = (1 - z)F(z)$ so that

$$G(z) = (1 - z)(a_0 + a_1 z + a_2 z^2 + \cdots + a_m z^m + \cdots + a_n z^n + \cdots)$$

$$= a_0 + \sum_{i=1}^{\infty}(a_i - a_{i-1})z^i$$

Now for $|z| \le 1$, we have

$$|G(z)| \le |a_0| + |a_0 - ka_0 + ka_0 - a_1| + \sum_{i=2}^{m-1}|a_i - a_{i-1}| + |a_m - \tau a_m + \tau a_m - a_{m-1}|$$

$$+ |a_{m+1} - \tau a_m + \tau a_m - a_m| + \sum_{i=m+2}^{n-1}|a_i - a_{i-1}| + |a_n - \vartheta a_n + \vartheta a_n - a_{n-1}|$$

$$+ |a_{n+1} - \vartheta a_n + \vartheta a_n - a_n| + \sum_{i=n+2}^{\infty}|a_i - a_{i-1}|$$

$$\le |a_0| + (k-1)|a_0| + |ka_0 - a_1| + \sum_{i=2}^{m-1}|a_i - a_{i-1}| + 2(1-\tau)|a_m| + |\tau a_m - a_{m-1}| + |\tau a_m - a_{m+1}|$$

$$+ \sum_{i=m+2}^{n-1}|a_i - a_{i-1}| + 2(1-\vartheta)|a_n| + |\vartheta a_n - a_{n-1}| + |\vartheta a_n - a_{n+1}| + \sum_{i=n+2}^{\infty}|a_i - a_{i-1}|$$

By using lemma 1 we get

$$|G(z)| \le |a_0| + (k-1)|a_0| + (k|a_0| - |a_1|)cos\alpha + (k|a_0| + |a_1|)sin\alpha + 2[(1-\tau)|a_m| + (1-\vartheta)|a_n|]$$

$$+ \sum_{i=2}^{m-1}(|a_{i-1}| - |a_i|)cos\alpha + \sum_{i=2}^{m-1}(|a_{i-1}| + |a_i|)sin\alpha + (|a_{m-1}| - \tau|a_m|)cos\alpha$$
$$+ (|a_{m-1}| + \tau|a_m|)sin\alpha + (|a_{m+1}| - \tau|a_m|)cos\alpha + (|a_{m-1}| + \tau|a_m|)sin\alpha$$
$$+ (|a_{m+1}| - |a_{m+2}|)cos\alpha + (|a_{m+1}| + |a_{m+2}|)sin\alpha + (|a_{m+3}| - |a_{m+1}|)cos\alpha$$
$$+ (|a_{m+3}| + |a_{m+2}|)sin\alpha + \cdots + (|a_{n-3}| - |a_{n-2}|)cos\alpha + (|a_{n-3}| + |a_{n-2}|)sin\alpha$$
$$+ (|a_{n-1}| - |a_{n-2}|)cos\alpha + (|a_{n-1}| + |a_{n-2}|)sin\alpha + (|a_{n-1}| - \vartheta|a_n|)cos\alpha$$
$$+ (|a_{n-1}| + \vartheta|a_n|)sin\alpha + (|a_{n+1}| - \vartheta|a_n|)cos\alpha + (|a_{n+1}| + \vartheta|a_n|)sin\alpha$$
$$+ \sum_{i=n+2}^{\infty}(|a_{i-1}| - |a_i|)cos\alpha + \sum_{i=n+2}^{\infty}(|a_i| + |a_{i-1}|)sin\alpha$$

$$= |a_0| + (k-1)|a_0| + (k|a_0|-|a_1|)cos\alpha + (k|a_0|+|a_1|)sin\alpha + 2[(1-\tau)|a_m| + (1-\vartheta)|a_n|]$$

$$+ (|a_1| - |a_{m-1}|)cos\alpha + \sum_{i=2}^{m-1}(|a_i| + |a_{i-1}|)sin\alpha + (|a_{m-1}|-\tau|a_m|)cos\alpha$$

$$+ (|a_{m-1}|+\tau|a_m|)sin\alpha + (|a_{m+1}|-\tau|a_m|)cos\alpha + (|a_{m-1}|+\tau|a_m|)sin\alpha$$
$$+ 2[(|a_{m+1}| + |a_{m+3}| + \cdots + |a_{n-3}| + |a_{n-1}|)$$

$$- (|a_{m+2}| + |a_{m+4}| + \cdots + |a_{n-4}| + |a_{n-2}|)]cos\alpha + |a_{m+1}|sin\alpha + \sum_{i=m+2}^{n-2}2|a_i|sin\alpha$$

$$+ |a_{n-1}|sin\alpha + (|a_{n-1}|-\vartheta|a_n|)cos\alpha + (|a_{n-1}|+\vartheta|a_n|)sin\alpha + (|a_{n+1}|-\vartheta|a_n|)cos\alpha$$

$$+ (|a_{n+1}|+\vartheta|a_n|)sin\alpha + |a_{n+1}|cos\alpha + \sum_{i=n+2}^{\infty}(|a_i| + |a_{i-1}|)sin\alpha$$

$$= k|a_0|(1 + cos\alpha + sin\alpha) - 2(\tau|a_m| + \vartheta|a_n|)(1 + cos\alpha - sin\alpha) + 2[|a_m| + |a_n|](1 - sin\alpha)$$
$$+ 2[(|a_{m+1}| + |a_{m+3}| + \cdots + |a_{n-3}| + |a_{n-1}|)$$

$$- (|a_{m+2}| + |a_{m+4}| + \cdots + |a_{n-4}| + |a_{n-2}|)]cos\alpha + 2sin\alpha\sum_{i=1}^{\infty}|a_i|$$

$$\leq 2\left[E_3 + \frac{1}{2}k|a_0|(1 + cos\alpha + sin\alpha) - (\tau|a_m| + \vartheta|a_n|)(1 + cos\alpha - sin\alpha) + sin\alpha\sum_{i=1}^{\infty}|a_i|\right].$$

where $E_3 = [|a_m| + |a_n|](1 - sin\alpha)$
$+[(|a_{m+1}| + |a_{m+3}| + \cdots + |a_{n-3}| + |a_{n-1}|) - (|a_{m+2}| + |a_{m+4}| + \cdots + |a_{n-4}| + |a_{n-2}|)]cos\alpha.$

Apply lemma 2 to G(z), we get then number of zeros of G(z) in $|z| \leq r, 0 < r < 1$ does not exceed

$$\frac{1}{log\frac{1}{r}}log\frac{2\left[E_3 + \frac{1}{2}k|a_0|(1 + cos\alpha + sin\alpha) - (\tau|a_m| + \vartheta|a_n|)(1 + cos\alpha - sin\alpha) + sin\alpha\sum_{i=1}^{\infty}|a_i|\right]}{|a_0|}.$$

where $E_3 = [|a_m| + |a_n|](1 - sin\alpha)$
$+[(|a_{m+1}| + |a_{m+3}| + \cdots + |a_{n-3}| + |a_{n-1}|) - (|a_{m+2}| + |a_{m+4}| + \cdots + |a_{n-4}| + |a_{n-2}|)]cos\alpha.$

All the number of zeros of F(z) in $|z| \leq r, 0 < r < 1$ is also equal to the number of zeros of G(z) in $|z| \leq r, 0 < r < 1$

This completes the proof of theorem 2.

REFERENCES

[1]. G.Eneström, Remarquee sur un théorème relatif aux racines de l'equation $a_n+...+a_0=0$ oü tous les coefficient sont et positifs, Tôhoku Math.J 18 (1920),34-36.

[2]. S.KAKEYA, On the limits of the roots of an alegebraic equation with positive coefficient, Tôhoku Math.J 2 (1912-1913),140-142.

[3]. A. Aziz and Q.G. Mahammad, on the certain class of analytic class of polynomial and related analytic functions, J. Anal and Appl. 75,[1980], 495-502.

[4]. N.K.Govil and Q.I.Rehman, On the EnstromKakeya Theorem Tohoku Math .J. 20, (1968), 126-136.

[5]. K. K. Dewan, Extremal Properties and Coefficient Estimates for Polynomials with Restricted Zeros and on Location of Zeros of Polynomials, Ph.D Thesis, Indian Institutes of Technology, Delhi, 1980.

Research Paper   Open Access

Water Level Indicator with Alarms Using PIC Microcontroller

Ahmed Abdullah[1], Md. Galib Anwar[2] , Takilur Rahman[3] , Sayera Aznabi[4]
[1,2,3,4](EEE, American International University-Bangladesh, Bangladesh)

ABSTRACT : *This paper shows a design of a water level indicator with PIC microcontroller. This design is applicable for both reservoir and main tank in home or industries.PIC 18F452 used in this design. There is also buzzer and LCD in this design. LCD used to show the level of water in both reservoir and main tank. Buzzer used to create a siren to stop the pump or water coming channel. There are 10 DIP switches used in this design. These switches indicate water level of both tanks. PIC microcontrollers also controls the motor which pumps the water in the tank from the reservoir. In the auto mode, motor is automatically turned on when water level reaches 20% in the tank and it is turned off when water level reaches 100%. Choose PIC microcontroller for programming flexibility, faster speed of execution since microcontrollers are fully integrated inside the processor*
.

Keywords - Pic Microcontroller, Sensor, Crystal, LS2 Buzzer, Protues.

I.   INTRODUCTION

Now a day's water crisis is no one global risk. One drop of water waste can be vary for us. 750 million people around the world lack access to safe water [1]. Today in world when people try to solve these problem one unseen problem stand up now. Water wasted by full tank is now a comparatively risk problem.

This design is to solve that problem. This design not only indicates the amount of water present in the overhead tank but also gives an indication when the tank is full. This design uses widely PIC microcontroller 18F452, bilateral switches to indicate the water level through LCD display. When the water is empty the wires in the tank are open circuited and resistor pulls the switch low hence and open the switch. As the water fill in the first reservoir tank its fill-up percentage shown in the LCD display. Today in the world most of the developing countries using this in their home and also industries. All probes used to implement should be made by aluminum.

Need of a water level indicator are shown below:
- Overflow problems.
- To prevent wastage of energy.
- To prevent wastage of water.
- Attention.
- Observation.
- Automatic switch off.

II.   PIC MICROCONTROLLER 18F452

PIC is a family of modified Harvard architecture microcontrollers made by Microchip Technology. PIC stands for Peripheral Interface Controller. There are lots of Microcontroller chips 18F452 is one of them. This chip is suitable for large operation.

The PIC 18F452 is a 28/40 pin high performance flash based microcontrollers with 32 Kbytes of program memory and 1.5Kbytes of RAM. Also 256 bytes of EEPROM data memory is provided to store data. The 18F452 microcontroller operates from DC to 40 MHz clock/oscillator input with 16 bit instructions and two priority levels for interrupts [2]. One of the main additional feature of this microcontroller is its 8 * 8 single cycle hardware multiplier. This will make multiplication easier and faster than the software routines used in previous controllers like 16 F series. The total number of interrupt sources in 18F452 microcontroller is 18, with an instruction set having 75 instructions unlike 35 instructions in 16 F series. The I/O ports in the microcontroller is divided into 5 ports like 16 F series :- PORTA(6 pins), PORTB(8 pins), PORTC(8 pins),PORTD(8 pins) and PORTE(3 pins).

Peripheral Features:

1. PSP (Parallel Slave Port) Module

2. USART module - Supports both RS-232 and RS-485 communication

3. MSSP (Master Synchronous Serial Port) Module – Supporting both I2C and SPI

4. Three external interrupt pins

5. Timer0 Module with 8/16 bits timer/counter with programmable pre-scalar.

6. Timer1 Module is a 16 bit timer/counter

7. Timer2 Module is a 8 bits timer/counter with 8 bit period register

8. Timer 3 Module is a 16 bit timer/counter

9. The values of sinking current and sourcing current is very high and is rated at 25mA

10. Two CCP (Capture Compare PWM) modules with 16 bits Capture Input and maximum of   bits PWM

resolution

11. Ten bit ADC (Analog to Digital Conversion) with high sampling rate

12. Supports in Circuit Debugging (ICD) via two pins – PGD and PGC

III.   EQUIPMENT'S

Pic Microcontroller is main equipment but there are lot of equipment's to design this. Here is a list of equipment's with short description in below:

Input Voltage: 1 2volt power supply is required. Adopter polarity is shown in the picture.

Capacitors: Capacitor has ability to store charge and release them at a later time. Capacitance is the measure of the amount of charge that a capacitor can store for a given applied voltage. The unit of capacitance is the farad (F) or microfarad. The capacitors used in the circuit is an electrolytic capacitor. The value and voltage rating of the electrolytic capacitor can be directly read from the capacitor itself. The electrolytic capacitor should be used with proper polarity. In the circuit the electrolytic capacitor is used as a bypass capacitor. Any noise variation in the circuit is removed by the capacitor [3].

Water Sensors: Simple wires can be placed in the water tank. As the current required to pass through the wire is in nano amps. But if need then place carbon rods at the end of wires which can be extracted from the 1.5v AA cell. These carbon rods should be thoroughly washed.

Transistor: Any npn transistor will work here.

LM7805: This is the 5v regulator used to power up the whole circuit.

Seven Segments: These are used to display water level. Common cathode seven segments are used.

LCD: Common 16x2 LCD can be used in this circuit.

LED Bar: J7 is the 10 LEDs bar.

Crystal: 10 MHz crystal needs to be attached with the PIC18F452.

PIC18F452: This microcontroller is used to generate all the required logic for this circuit.

D2, D4 Diodes: Any diode 1N4007 or 1N4148 or any other general purpose diode will work here.

LS2 Buzzer: Any 5v buzzer will work here.

<div align="center">

IV.   WORKING PRINCIPLE
</div>

The operation of this project is very simple. In this project "water level indicator" there are 3 main conditions:

1.   There is no water available in the source tank.
2.   Intermediate level i.e. either of 3rd to 7th level.
3.   There is ample amount of water available in the source tank.

Condition 1: Water not available

When the tank is empty there is no conductive path between any of the 8 indicating probes and the common probe (which is connected to 5v+ supply) so the sensor region will not have sufficient biasing voltage hence it remains in cut off region and the output across its collector will be Vc approximately 4.2v. As in this case the microcontroller is used in the active low region (which means it considers 0-2 volts for HIGH and 3-5 volts for LOW) now the output of transistor which is 4.2v approximately will be considered as LOW by the microcontroller and hence the default value given by microcontroller to the seven segment display is 0 which indicates as the tank is empty.

Condition 2: Intermediate levels

Now as the water starts filling in the tank a conductive path is established between the sensing probes and the common probe and the corresponding transistors get sufficient biasing at their base, they starts conducting and now the outputs will be Vce (i.e. 1.2v-1.8v) approximately which is given to microcontroller [4]. Here the microcontroller is programmed as a priority encoder which detects the highest priority input and displays corresponding water level in the seven segment display. In this project while the water level reaches the 7th level i.e. last but one level along with display in seven segment a discontinuous buzzer is activated which warns user that tank is going to be full soon.

Condition 3: Water full

When the tank becomes full, the top level probe gets the conductive path through water and the corresponding transistor gets into conduction whose output given to microcontroller with this input microcontroller not only displays the level in seven segment display but also activates the continuous buzzer by which user can understand that tank is full and can switch off the motor and save water [5].

<div align="center">

V.   SOFTWARE SIMULATION
</div>

The Software which have used for this project is "Proteus" version 7.8. Proteus is one of the user friendly software in simulation world. For both electrical and electronics based circuit simulation and implementation can be done very easily with this software. Before starting the implementation and the simulation of the project circuit it is necessary to make an algorithm. Because a fruitful algorithm can makes the path easier to implement a circuit both virtually and practically.
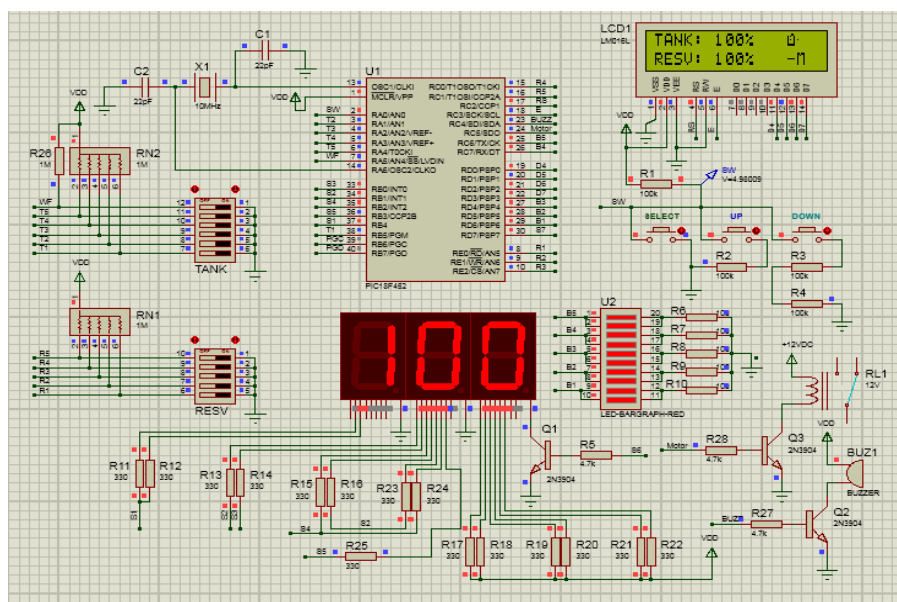
Figure 1: .Main window of software simulation when both tanks have 100 are full   And buzzer speakers are on.

This is the main simulation of this design. It's clearly shown that all tanks are full all DIP switches are in the right side LED bar graphs are all red that means buzzer is on. Buzzer sign is active when tanks water reaches up to 80 percent. When siren hearing have to stop the down switch. Then LCD display options like start motor or enable motor again.

There are two sensor using both of them used for sensing the level of water in tank.
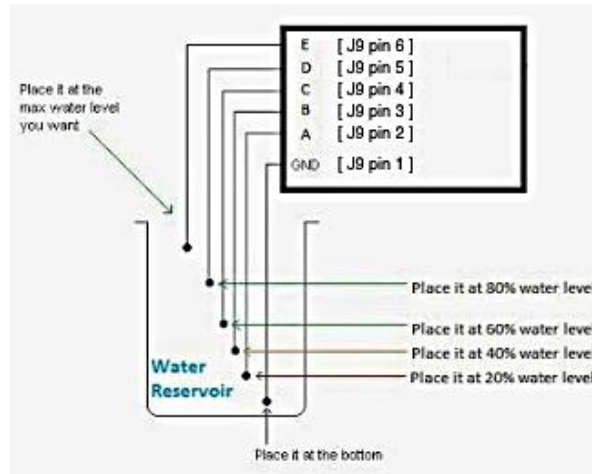
Fig. 2: Procedure of Water Reservoir.

In fig 2 it shows the working procedure of sensor in water reservoir. Six J9 pins used for to build a sensor in the water reservoir J9 pin 1 is used for grounding. This grounding pin place in bottom of the tank one thing is careful that it doesn't touch ground of the tank. Pin 2 to 5 used in different water levels of 20 to 80 percent. Then last Pin 6 place it at the maximum level we want.
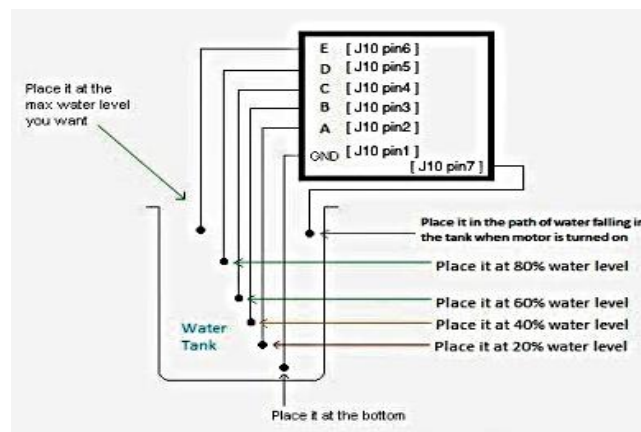
Fig. 3: Procedure of Water Reservoir

In fig 3 it shows the working procedure of sensor in water tank. Seven J10 pins used for to build a sensor in the water tank J10 pin 1 is used for grounding. This grounding pin place in bottom of the tank one thing is careful that it doesn't touch ground of the tank. Pin 2 to 5 used in different water levels of 20 to 80 percent. Then last Pin 6 place it at the maximum level we want. There is one extra pin 7 it place in the path of water falling in the tank when motor is turned on.

VI.   Projects Applications

Water Level Indicator Project Applications:
- Automatic Water level Controller can be used in Hotels, Factories, Homes Apartments, Commercial Complexes, Drainage, etc., it can be fixed for single phase motor, Single Phase Submersibles, Three Phase motors. (For 3 phase and Single Phase Submersible Starter is necessary) and open well, Bore well and Sump [6]. We can control two motor and two sumps and two overhead tanks by single unit.
- Automatic water level controller will automatically START the pump set as soon as the water level falls below the predetermined level (usually 1/2 tank) and shall SWITCH OFF the pump set as soon as tank is full [7].

- Fuel level indicator in vehicles.
- Liquid level indicator in the huge containers in the companies.
- Low costs.
- Easily operate because of microcontroller.
- Low power consumer.
- It can be used to predict flood.

VII.   Acknowledgements

VIII.   CONCLUSION

This paper was intended to design a simple and low cost water level indicator. This is not only for water tank but also used for oil level and chemical lab. To design this system, we used microcontroller as a platform and local materials for low cost. Our target was to design a system in such a way that its components will be able to prevent the wastage of water. Microcontroller code was deployed here. The whole system operates automatically. So it does not need any expert person to operate it. It is not so expensive. This design has much more scope for future research and development. Though it is a project, we hope some modification in this project will lead to a reasonable diversity of usage. Obviously there are some limitations in our design some of them in the below:

- Heating problems due to stray capacitances.
- Neck strain.

REFERENCES

[1]   Yuihana, J. B.(2014),World Health organization (WHO) yearly magazine "*Burden of disease from inadequate water, sanitation around the world*" Volume 19, pp 89-90.

[2]   Abdullah, A. (2008). *; Eater Level in Tank acing Sensors and P1D Controller.* Btech Thesis, University Malaysia Sarawak, Sarawak, 123 p.

[3]   Yu, land Hahn. (2010). Remote Detection and Monitoring of .water level using narrow capacitor. *J. Information Science and Engineering.26:* 71-82.

[4]   Um, J. H. (2000) 'inquiry of special quality of supersonic sensor for water level by non-contact, *"The Bulletin of Korea Environment Engineers Association,* Vol. 162:.3036.

[5]   Pandey • A. Chowdary, V.M. Mal. B.C. Billy. M. (2009) Application of the WEPP model for prioritization and evaluation of water level indicator. *Ifrdrol   Process.* 23, 2997-3005.

[6]   Lee, B. Y. and Park B. Y. (1999)" Development of high precision underground water level meter using a buoyant rod load cell technique," *KSAFM,* Vol. I: 1-5.

[7]   Ken, P. Y. Tack. Y. H. Jong, K. S. Ho. S. M. and Yong, J. S.(2004)˙Development of real time flood monitoring system composed of CCD camera and water level gauge *Collection of Learned Papery of Fall Conferences of Korean Society Railway,* pp. 224- 228.

ARAB ARULMANI?... (RAMANUJAM "HUMAN RESOURCE")
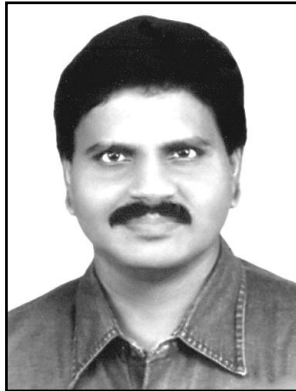
M.Arulmani, B.E.
(Engineer)

V.R.Hema Latha, M.A., M.Sc., M.Phil.
(Biologist)

Abstract : *ARULMANI IS ARAB?... ARULMANI IS USEFUL HUMAN RESOURCE OF RAMANUJAM?... "DARWIN SIR" says "ARULMANI" is of "APE ORIGIN"... ARULMANI has "MONKEY MIND"... ARULMANI IS TERRORIST?... (or) HUMANIST?... Numerology believe that the word ARUL means GOD'S GRACE. Further om mani padme hum is a six syllable Sanskrit mantra. If so…*

> i)   *What does mean "ARUL"?...*
>
> ii)   *What does mean 'MANI"?...*
>
> iii)   *"ARUL" differs from "MANI"?...*
>
> iv)   *"GRACE" differs from "LOVE"?...*
>
> v)   *"SOURCE" differs from "RESOURCE"?...*
>
>   *- Author*

This scientific research focus that the Philosophy of word "**ARAB**" is closely associated with **ancient human race**. **ARAB ARULMANI** shall mean Arulmani belongs to Arab race.

This research further focus that the entire universe shall be considered created by "**Supernatural Person**" called by name by author as "**RAMANUJAM**" who consider created everything through his

"**MOTHER JANAKI**" (**Soul**). The philosophy of word "**ARAB**" consider closely associated with "**HUMAN SOURCE**" of "**RAMANUJAM**". In Proto Indo Europe language root "**ARUL**" (**GRACE**) shall mean "**CREATED HUMAN SOUL**" and "**MANI**" (**RESOURCE**) shall mean "**TRANSFORMED HUMAN SOUL**" . The philosophy of "**Mother Nature**" and origin of '**created human soul**' shall be represented as below:

(i)
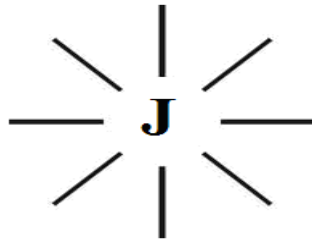
(CREATIVE MANTRA LOGO)

(ii)
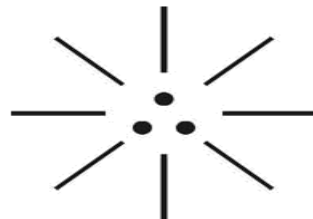
GRACE
(ARUL ANNAI)

It is further hypothesized that the "**created Human soul**" consider transformed from "**SUPERRIOR WORLD**" (**MARS PLANET**) to "**MATERIAL WORLD**" (**EARTH PLANET**) and further evolved into "**Billions of souls**" of varied genetic value in '**three nuclear age**' of expanding universe. The philosophy of transformed "**HUMAN SOURCE**" and evolved "**HUMAN RESOURCE**" shall be represented as below:

(i)
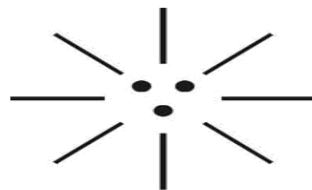
MANI
(Transformed Human Soul)

(ii)
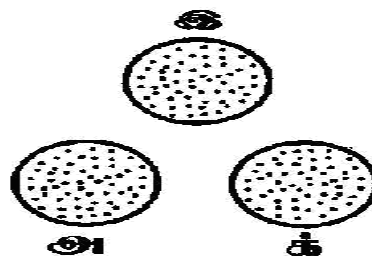
MAKUDAM
(3G Evolved Souls)

1.0   Etymology of word "GRACE"?...
          It is focused that the etymology of English words like "**GREEK**", "**RACE**" (**G-RACE**), "**AGE**" might be derived from Proto Indo Europe root word.
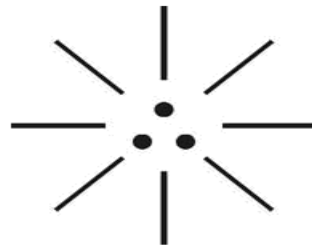
GRACE

          i) Right dot is like "**DNA**" (Dharmam)
          ii) Left dot is like "**HORMONE**" (Karmam)
          iii) Center dot is like "**RNA**" (Brahmam)

2.0   Philosophy of DRAVIDA, ARAB, MUBARAK?...
          It is hypothesized that the **Ancient India** (1,00,000 years ago) shall be considered like a single large "**SUPER CONTINENT**" called by name by author. "**J&K CONTINENT**" (**JAMMU AND KASHMIR**). The super continent shall be considered as exist as multilayer land mass over the surface of the **EARTH PLANET**. The super continent land mass shall be considered as "**evolved land mass**" from the fundamental virgin land mass which descended from **MARS PLANET** (Say 3,00,000 years ago). The sub continental mass like **SOUTH ASIA, EAST ASIA, WEST ASIA** shall be considered as derived and split from fundamental "**J&K CONTINENT**" in Triassic period (say 75,000 years ago).
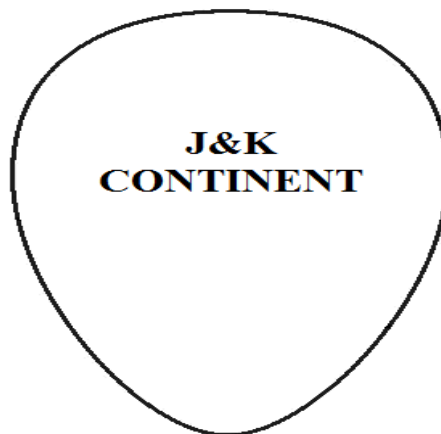
**ANCIENT INDIA
(1,00,000 Years Ago)**

          It is further hypothesized that "**J&K continent**" shall be considered as two distinguished stage of land mass i.e. "**before sun rise**" and "**after sunrise**". The J & K continent considered have only **two races** as described below.
          i)   **DRAVIDA RACE** (before sunrise)
          ii)   **ARAB RACE** (After sunrise)

          The **DRAVIDA RACE** shall also be called as "**DARK ARAB**" (**Thriyan**) and "**ARAB RACE**" shall also be called as "**RED DRAVIDA**" (**Thirayan**).

It is further focused that "**MUBARAK**" shall be considered as Diversified Arab as a three ethnic race, transformed to three sub continental region like South Asia, East Asia, West Asia (50,000 years ago). The three diversified Arab race shall be indicated as below:

      i)   "**ARAB INDO**" (South Asia)
      ii)   "**ARAB GREEK**" (East Asia)
      iii)   "**ARAB AFGHAN**" (West Asia)

MUBARAK (50,000 years ago)

ARAB (75,000 years ago)

DRAVIDA (1,00,000 years ago)
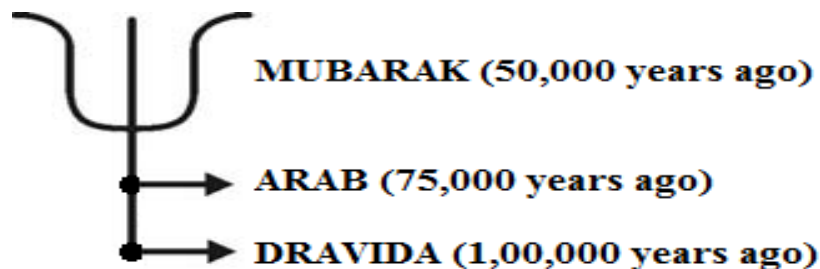
J&K means **Mother of Nations**
DRAVIDA means **Dark Arab** (Indo)
ARAB means **Red Dravida** (Post Indo)
MUBARAK means **Diversified Arab**

3.0   Philosophy of "ARIYAN RACE"?...

It is hypothesized that Ariyan race shall be considered as the "**3rd Generation human race**" evolved around 10,000 years ago. **DRAVIDA, ARAB, ARIYAN** shall be three genetically varied human race under varied environmental condition.

      i)   **DRAVIDA (1st generation)**
      ii)   **ARAB (2nd generation)**
      iii)   **ARIYA (3rd generation)**

4.0   Arulmani is Arab Christian?...

It is focused that "**ARAB**" shall mean "**ATHAVAN**" belongs to "**MONOTHEISM**" having faith of "**ONE GOD**". The philosophy of birth of religion **HINDUSIM, ISLAM, JUDHAISM** might be born from the race of "**MUBARAK**". The Philosophy of evolution of various religion shall be described as below.

      i)   **Ramanujam – "Atheist"**
      ii)   **Janaki – "Theist"**
      iii)   **Dravida – "Sun god"**
      iv)   **Arab – "Monothesim"**
      v)   **Arab Indo – "Hinduism"**
      vi)   **Arab Greek – "Islam"**
      vii)   **Arab Afghan – "Judhaism"**

5.0   Arulmani is "DALIT BRAHMIN"?...
      i)   **Arulmani is Dalit Brahmin?...**
      ii)   **Arulmani is Dalit Maravar?...**
      iii)   **Arulmani is Dalit Thevar?...**
      iv)   **Arulmani is Dalit Nadar?...**
      v)   **Arulmani is Dalit Pallar?...**
      vi)   **Arulmani is Dalit Kallar?...**
      vii)   **Arulmani is Dalit Pulavar?...**
      viii) **Arulmani is Dalit Valluvar?...**

It is focused that **Arulmani** is a useful Human Resource of Ramanujam and shall be considered as "**DALIT BRAHMIN**". "**DALIT**" shall mean **THALAI + ETHU.** "**BRAHMIN**" shall mean "**MAGAN**" (Ancestor). Further "**RAMANUJAM**" shall be considered as "**MAKKAL MUTHALVAR**", "**JANAKI**" shall be considered as "**MAKKAL THALAIVAR**". The "**CREATED SOUL**" shall be considered as "**ARUL THIRU**".

(i)
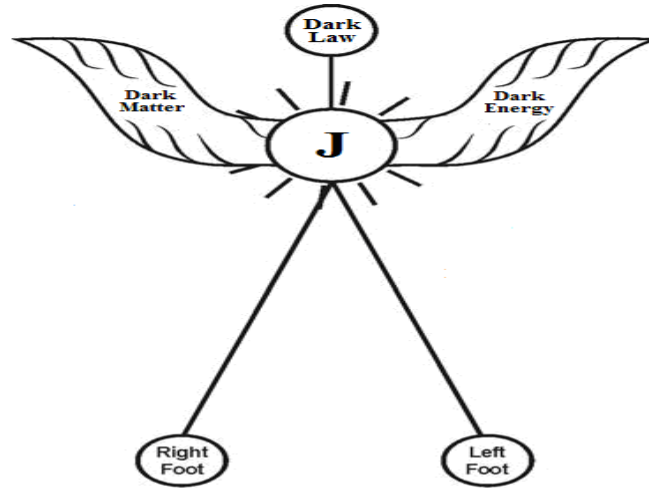
மக்கள் முதல்வர்
(RAMANUJAM)
(Creator)

(ii)
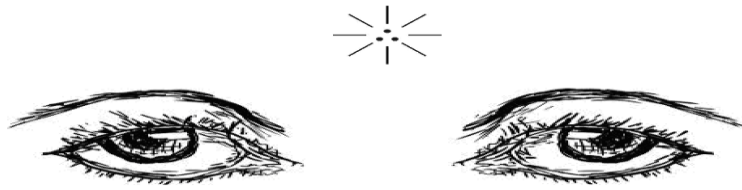
மக்கள் தலைவர்
(JANAKI)
(Soul)

(iii)
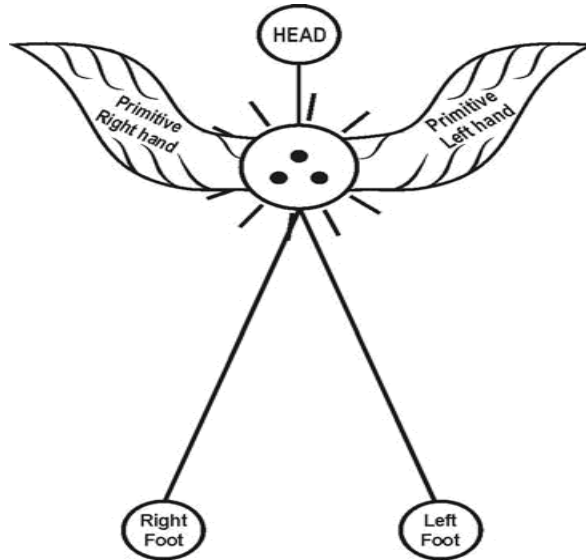
அருள் திரு
(DALIT BRAHMIN)
(Created Soul)

6.0   WHO I AM?...

Dal Lake Srinagar, Kashmir (10-06-2015)

**Am I Pakistan Arab (Red Dravidian)?...
No... No... No... I am Kashmir Arab (Black
Dravidian)... Dark Glass is symbol of
Dravidian culture**

i)   *AM I Arab Indo?...*
ii)   *AM I Arab Greek?...*
iii)   *AM I Arab Afghan?...*
iv)   *AM I Arab Pakistan?...*
v)   *AM I Arab China?...*
vi)   *AM I Arab Srilanka?...*
vii)   *AM I Arab Palestine?...*
viii)   *AM I Arab Israelite?...*
ix)   *AM I Arab American?...*
x)   *AM I Terrorist?...*
xi)   *AM I Arab Jew?...*
xii)   *AM I Arab Christian?...*
xiii)   *AM I Arab Islam?...*
xiv)   *AM I Account holder of "Swiss Bank"?...*

YES… YES… YES… NO… NO… NO….

I am "ARULMANI" (DARK ARAB) loving son and useful "Human resource" of "J&K" (Mother of Nations)

- Author

7.0   Abraham is Arab (or) Jew?...
        Based on Biblical study it is stipulated by the author the population of **ADAM** shall be considered as belong to "**ANGEL RACE**" descended from superior world (**Mars Planet**) to Earth Planet during Expanding Universe. The **ADAM** population might have been destroyed due to climatic condition.

        The origin of "**NOAH**" population shall be considered as "**DRAVIDIANS**" during first origin of sunrise and the population of **ABRAHAM** shall be considered as "**ARAB RACE**". The sons of "**ISAAC**", "**ISHMAIL**" shall be considered as "**MUBARAK**".

- (Genesis 17: 19-21)

Case study further shows that the Arab race has existed for over 6000 years and the best place of pick up of bones of Arab race where they started out from "**Ancient Iraq**".

Simply compare the **DNA** of ancient Iraqis against DNA of **European ancestors**. The original Arab are called "**Marsh lands Iraqis**". Medieval theories of race believe humanity as a whole was descended from **SHEM, HAM, JAPHEITE,** the three sons of **NOAH** producing different **Semitic** (Asiatic) **Hamitic** (African) and **Japhetic** (Indo-European) people.

8.0   Conclusion:

சமர்ப்பணம்

Iran
Greek   Afghan

INDO RAYS
Egypt   Europe

Africa   Malaya
Elem

(MUBARAK DIVERSITY)

" இந்தியநாடு என் தாய்;
தமிழ்நாடு என்தாயின் பாதஅடி.
என் தாயின் பாத அடியில் இப்புத்தக அஞ்சலி "
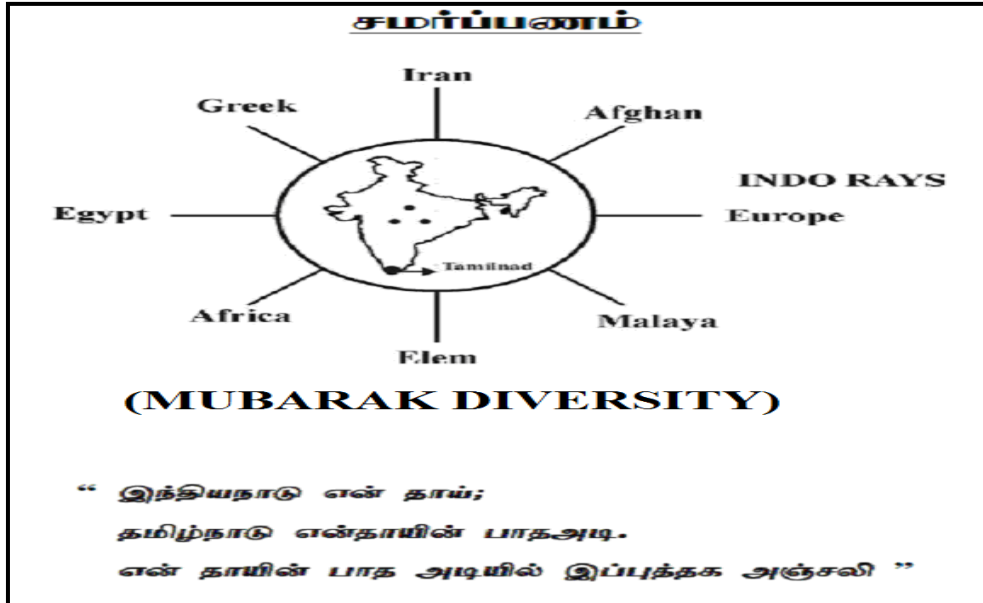
புதுக்கவிதை

GRACE
(Arul Annai)

OH… ARULMANI (Dark Arab)… Citizen of "J&K" Continent…
You are the son of Mother Janaki (Grace)…
You are the useful Human Resource of Ramanujam…

You have been sent to Earth to live…
You have been sent to Earth to Love…
Why are you terrorist killing the innocents?…

You are Dark Arab by birth born of sun shine…
Greek, Palestine, Israelite are your younger brothers…
Why do you kill them on border issue?…

'Arab Indo' is Heart of Janaki…
'Arab Jews' is Left hand of Janaki…
'Arab Israelite' is Right hand of Janaki …

Comfort the world with HOPE of Father...

Strengthen the world with MERCY of Mother...

Lead the world with everlasting LOVE...

அன்னைக்கு முதல் எழுத்து 'அ'... *(Mother)*

அருளுக்கு முதல் எழுத்து 'அ'... *(Grace)*

அன்புக்கு முதல் எழுத்து 'அ'... *(Deed)*

G...O...D......BLESS......YOUuuuuuu...

> *... M. Arulmani*
> *Tamil Based Indian*
> *Madurai.*

9.0 Previous Publications:

Part-A

The philosophy of origin of first life and human, the philosophy of model Cosmo Universe, the philosophy of fundamental neutrino particles have already been published in various international journals mentioned below. Hence this article shall be considered as **extended version** of the previous articles already published by the same author.

1. Cosmo Super Star – IJSRP, April issue, 2013
2. Super Scientist of Climate control – IJSER, May issue, 2013
3. AKKIE MARS CODE – IJSER, June issue, 2013
4. KARITHIRI (Dark flame) The Centromere of Cosmo Universe – IJIRD, May issue, 2013
5. MA-AYYAN of MARS – IJIRD, June issue, 2013
6. MARS TRIBE – IJSER, June issue, 2013
7. MARS MATHEMATICS – IJERD, June issue, 2013
8. MARS (EZHEM) The mother of All Planets – IJSER, June issue, 2013
9. The Mystery of Crop Circle – IJOART, May issue, 2013
10. Origin of First Language – IJIRD, June issue, 2013
11. MARS TRISOMY HUMAN – IJOART, June issue, 2013
12. MARS ANGEL – IJSTR, June issue, 2013
13. Three principles of Akkie Management (AJIBM, August issue, 2013)
14. Prehistoric Triphthong Alphabet (IJIRD, July issue, 2013)
15. Prehistoric Akkie Music (IJST, July issue, 2013)
16. Barack Obama is Tamil Based Indian? (IJSER, August issue, 2013)
17. Philosophy of MARS Radiation (IJSER, August 2013)
18. Etymology of word "J" (IJSER, September 2013)
19. NOAH is Dravidian? (IJOART, August 2013)
20. Philosophy of Dark Cell (Soul)? (IJSER, September 2013)
21. Darwin Sir is Wrong?! (IJSER, October issue, 2013)
22. Prehistoric Pyramids are RF Antenna?!... (IJSER, October issue, 2013)
23. HUMAN IS A ROAM FREE CELL PHONE?!... (IJIRD, September issue, 2013)
24. NEUTRINOS EXIST IN EARTH ATMOSPHERE?!... (IJERD, October issue, 2013)
25. EARLY UNIVERSE WAS HIGHLY FROZEN?!... (IJOART, October issue, 2013)
26. UNIVERSE IS LIKE SPACE SHIP?!... (AJER, October issue, 2013)
27. ANCIENT EGYPT IS DRAVIDA NAD?!... (IJSER, November issue, 2013)

87.   AM I CORRUPT?... (IJSER November 2014 issue)
88.   BLACK MONEY?... (AJER November 2014 issue)
89.   DEAD PARENTS ARE LIVING ANGELS?... (IJERD November 2014 issue)
90.   MICHAEL IS CHIEF ANGEL?... (AJER November 2014 issue)
91.   LONG LIVE!... (IJERD November 2014 issue)
92.   THE SOUL OF THOLKAPPIAM (AJER December 2014 issue)
93.   SENTHAMIL AMMA!... (IJERD December 2014 issue)
94.   THE LAW OF LYRICS?... (IJERD December 2014 issue)
95.   WHY JESUS CHRIST CAME INTO THE WORLD?... (AJER December 2014 issue)
96.   WHAT DOES MEAN "GOD"?... (IJERD January 2015 issue)
97.   ZERO IS GREATER THAN "INFINITY"?... (IJSER January 2015 issue)
98.   THE LAW OF SEX?... (IJSER January 2015 issue)
99.   HAPPY TAMIL NEW YEAR!... (IJSER January 2015 issue)
100.   BHARAT RATNA!... (IJSER March 2015 issue)
101.   WHAT DOES MEAN "SECULARISM"?... (IJSER February 2015 issue)
102.   A COMMON SENSE THEORY ON "VARYING-SCIENCE"?... (IJERD February 2015 issue)
103.   FEBRUARY FESTIVAL OF KACHCHA THEEVU?... (IJERD February 2015 issue)
104.   THE DOCTRINE OF LOVE (678) ?... (IJERD March 2015 issue)
105.   A NEW THESIS ON "THAILAND" !... (IJSER March 2015 issue)
106.   PALLAVAS IMMIGRATION? (IJERD March 2015 issue)

Part-B
1. YUGADI WISHES (IARA, March 2015)
2. TAMIL PUTHANDU!... (AJER, April 2015)
3. THEN MADURAI?... (IJERD, April 2015)
4. TAMIL NEW YEAR COOL DRINK?... (AJER, April 2015)
5. SCIENTIFIC RAMANUJAM?... (IJERD, April 2015)
6. ARENKA NAYAKI IS MOTHER OF RAMA?... (AJER, April 2015)
7. TRIVIDAITE?... (IJERD, April 2015)
8. THALI CULTURE OF ANGELS?... (AJER, April 2015)
9. UNIVERSAL POET?... (IJERD, April 2015)
10. "JANGLISH" IS CHEMMOZHI?... (AJER, April 2015)
11. RAMANUJAM PARLIAMENT?... (IJERD, May 2015)
12. CAN LORD JUDGE GOD?... (AJER, May 2015)
13. MAY DAY?... (IJERD, May 2015)
14. DEEMED UNIVERSITY?... (AJER, May 2015)
15. CAR FESTIVAL?... (IJERD, May 2015)
16. MISSING HEART?... (AJER, May 2015)
17. Morning Star!... (AJER, May 2015)
18. JAYAM (J-AUM)!... (IJSER, June 2015)
19. RAMANUJAM CONSCIENCE (IJERD, June 2015)
20. "J & K" (IJSER, June 2015)
21. "J & K" SAFFRON?... (AJER, June 2015)
22. TOILET CLEANING?... (IJSER, June 2015)
23. RAMADAN?... (IJERD, July 2015)

Research Paper	Open Access

Establishing the Driving Forces and Modeling of flooding in the Lafa River Basin, Accra, Ghana.

Anthony Ewusi[1], Jamel Seidu[1], Asare Asante-Annor[1],Emmanuel Acquah[2]
[1]*Geological Engineering Department, University of Mines and Technology, Ghana*
[2]*Ghana Irrigation Development Authority, Accra, Ghana*

ABSTRACT : *The Lafa River Basin (LRB) experiences increased frequency and magnitude of floods, causing increases in areal and depth of inundation. This translates into huge economic losses and loss of human lives. The effective management of flood disaster of the LRB is hinged on the identification of the factors responsible for the floods, modelling of the flood situations and a quantitative assessment of the hazard zones. Hydrologic Engineering Centre-Hydrologic Modeling System (HEC-HMS) and Hydrologic Engineering Centre-River Analysis System (HEC-RAS) models have been integrated with Geographical Information System (GIS) to identify the driving forces behind the floods, and assess the hazard zones of the Basin. Physiographical characteristics are responsible for the floods and analysis indicate that the LRB is a small urbanised elongated drainage basin of area 27.945 km2 with predominantly steep slopes, and impervious surface soils. The Peak flows produced by 2, 15, 25, 50, and 100 year return period storms have been found to inundate 233.88 ha, 292.92 ha, 298.36 ha, 305.00 ha, and 311.24 ha respectively. 1.68 %, 5.54 %, 5.91 %, 6.41 %, and 6.63 % respectively of total inundation areas were above inundated depth of 2 m and are located around culvert locations on the Lafa stream.*

Keywords-Basin, Flood plain, Hydrological analysis, Modelling, Peak flows

I. INTRODUCTION

Urban flooding is generally induced by torrential rains that generate excess precipitation beyond the capacity of river channels and other drainage systems. As the water rises to flood stages, areas along the middle and lower reaches of rivers are flooded resulting in negative impacts on social and economic developments. The Lafa River Basin (LRB) has consistently been affected by floods during rainy seasons (June - July and September - October). The Basin in the past 20 years has been experiencing increased frequency and magnitude of floods causing increases in areal and depth of inundation which translates to huge economic losses to the inhabitants.

The Hydrological Services Department together with the Ga West Municipal Assembly had put in several mitigation measures including desilting the river channel biannually, and pulling down unauthorised buildings within the floodplains. Various portions of the river reaches have also been modified to reduce meandering to ease water flow in the river channel. However, these measures have not yielded the expected mitigation of flooding in the Basin. Increased urbanisation has also led to increasing impervious coverage increasing the flood hazard levels in the Basin. Devastating floods as a result of torrential rainstorms in October 2011 displaced four thousand, four hundred and thirteen (4,413) people from their homes, three (3) corpses were recovered, and properties worth thousands of Ghana cedis were destroyed (Anon., 2011).

The spatial integration of hydrological and hydraulic models into a GIS, enables flood visualisation, animation, and flood hazard levels assessment. Maps of flood situations showing hazards levels are widely used for planning, designing, and forecasting, so that appropriate structural and non-structural measures could be established for efficient flood mitigation and control. It is also used by emergency response personnel to identify safe areas during emergency evacuation exercises.

This paper therefore seeks to identify the driving forces behind the floods in the LRB using GIS technique, model the flood situations, and to assess the flood hazard zones in the Basin. These models will form the basis on which stakeholders would identify the appropriate mitigation measures for effective management of floods in the Basin.

1.1 Location and Assessibility

LRB is located about 9 km to the west of Accra and lie within three administrative jurisdictions of the Greater Accra Region. It can be located between longitudes 0° 18' 33" W and 0° 15' 26" W and latitudes 5° 34' 12" N and 5° 38' 22" N (Fig. 1) and covers an approximate area of 28 km2.

The Basin has evolved from peri-urban into a completely urbanised status due to its proximity to central Accra, as it offers a preferred dwelling place for people who work in the capital city. Pressure has been brought to bear on available space, thus encroaching on the floodplains and stream courses. Such situation causes floods even in short duration high intensity rainstorms. There are numerous socioeconomic infrastructures in the Basin including schools, markets and a power sub-station.

II.   MATERIALS AND METHODS

The basic geographical data used for the studies included topographical data comprising of height (contour lines and spot heights), buildings, road lines, and other cultural features were obtained from Survey and Mapping Division of The Lands Commission. Soil data was obtained from the Soil Research Institute (SRI). Culvert locations on the stream were measured on the field using a handheld Geographical Positioning System (GPS) and the specifications measured with a tape.

The contour lines were edited to ensure line continuity and elimination of overlaps. The river lines were edited for line continuity, and directed towards the outlet. All the datasets were projected using the Projection and Transformation Tools of ArcGIS onto the Universal Transverse Mercator (UTM) reference system (WGS_84_UTM_Zone_30N) to enable integration and analysis. The edited dataset were further organized into a geodatabase for easy access and management. The output maps of the study were thus produced in the UTM reference system. Rainfall data of 1 hour, 2 hour, 3 hour, 4 hour, 5 hour, 6 hour, and 24 hour durations extracted from a 50-year record of the Accra Rainfall Synoptic station was obtained from the Hydrological Services Department.

2.1 Rainfall Frequency Analysis

Rainfall frequency analysis was carried out to relate the magnitude of extreme rainfall events to their frequency of occurrence in the LRB through the use of a probability distribution function. Annual maximum values of each duration records were ranked and fitted to the Gumbel's distribution using the Weibull plotting position. Numerous theoretical and empirical distributions have been proposed by various hydrologists that are generally applicable to annual maximum rainfall series. However, a comprehensive studies of various distributions made by (Hershfield and Kohlar, 1960) revealed that the Extreme Value Type 1 (EV1) or the Gumbel distribution (Gumbel, 1954) is the most suitable (Deshpande et al., 2008).
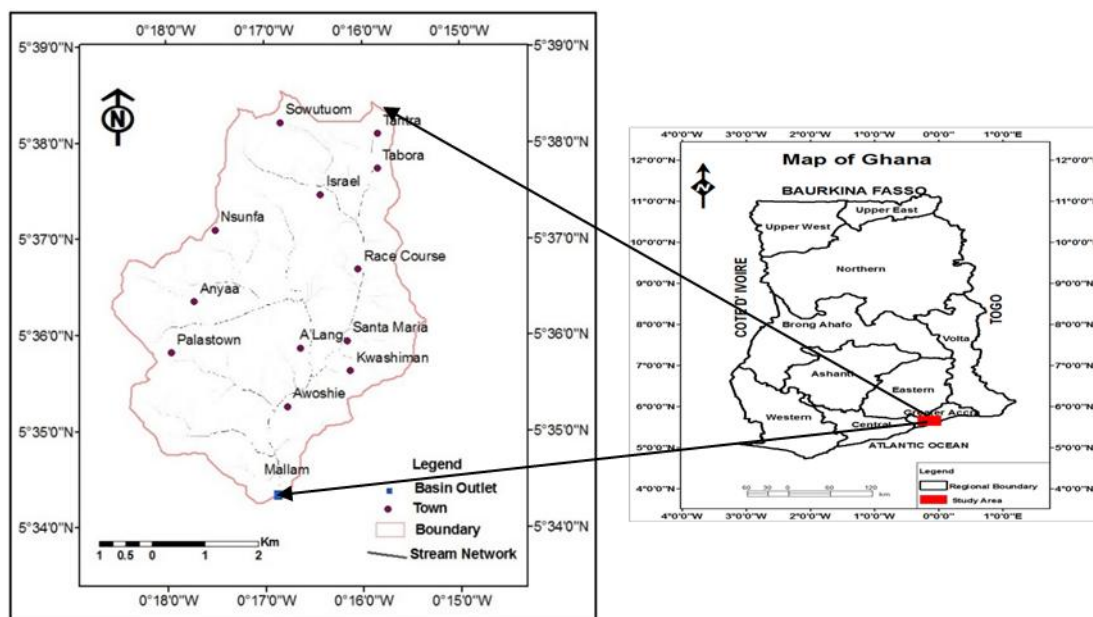
Figure 1 Map showing the Lafa River Basin

2.2   Digital Elevation Model (DEM) Generation

A DEM is a useful source for deriving physiographical variables for hydrological, hydraulic, water resources, and environmental investigations. The DEM of the LRB was generated from the contour data of the Basin using the Topo-to-Raster function in 3D Analyst of ArcGIS 9.3 software. The Topo to Raster interpolator is based on the Australian National University's Digital Elevation Model (ANUDEM) program developed by Michael Hutchinson (Hutchinson, 1989). It was designed specifically for generating hydrologically correct DEMs (Anon., 2009).

2.3   Watershed Extraction from DEM

The LRB extraction from the DEM was carried out using the hydrology analysis tools of the ArcGIS suite. The DEM was preprocessed using the flow direction, sink identification and sink filling tools to produce a smooth or depressionless DEM. The Flow Accumulation function was used to compute accumulated flow which is the accumulated weight of all cells flowing into each downslope cell in the output raster. The flow accumulation threshold or the pour point was set at the Basin outlet. The pour point and the flow accumulation raster were used in the watershed function to extract the LRB.

A drainage basin's physical characteristics play a critical role in the hydrological response of the basin. The physiographical parameters of the LRB were determined using ArcGIS Suite based on the LRB DEM. These include slope, aspect, and morphometric parameters. The slopes and aspect of the LRB were determined using the Spatial Analyst tool of ArcGIS. The slopes were further classified into five (5) categories namely; Flat (0-2 %), Undulating (2-8 %), Rolling (8-16 %), Hilly (16-30 %), Mountainous (>30%). Linear and areal morphometric parameters of the LRB were also determined and computed. The linear aspects of the drainage network included; stream order (Nu) and stream length (Lu). The areal aspects of the Basin considered included basin area (A), basin perimeter (P), basin length (Lu), elongation ratio (Re), circularity ratio (Rc), and form factor ratio (Rf).

2.4   Rainfall-Runoff Modelling

The US Army Corps of Engineers Hydrological Engineering Center's HEC-HMS was adopted for the rainfall-runoff simulation for the study due to its simplicity and availability on the internet. The Natural Resources Conservation Service (NRCS), Curve Number (CN) loss method was used to compute rainfall losses. SCS Unit Hydrograph, and Muskingum routing methods were adopted for transform and flow routing estimation respectively. The resulting landuse grid was also used to prepare a percentage impervious surface grid based on the percent impervious values of the corresponding landuse classes.

The landuse/landcover (LULC) of the LRB was generated from the topographic data with Google earth image of the LRB as backdrop. The map was delineated in four classes (Table 1) based on the United States Geological Survey Land cover Institute classification system (Anon., 2012)

2.5   Hydraulic Modelling

Hydraulic model of the U.S. Army Corps of Engineers, Hydrological Engineering Center River Analysis System (HEC-RAS), and Hydrological Engineering Center-Geospatial River Analysis System (HEC-GeoRAS) were selected for this study due to their extensive application for floodplain analysis and free accessibility on the internet. HEC-GeoRAS application was developed specifically to process geospatial data for use with HEC-RAS.

2.6   Flood Hazard Mapping

The hazard assessment in the LRB involved the estimation of two vital parameters: the probability of occurrence or the return period of the hazard, where the Probability of occurrence P and the Return period T over a Period n are mathematically related by:

$$P = 1 - \left(1 - \frac{1}{T}\right)^n \qquad (1)$$

The hydraulic model output for the various return periods were exported to HEC-GeoRAS and classified for flow depth (d) indicated on Table 2.
The inundated depth classes were computed for hazard levels assessment for each return period.

Table 1 LRB Inundated depth classification

Inundated Depth Class (d)	Hazard Level
d < 0.5 m	Very Low
0.5 m < d < 1 m	Low
1 m< d< 1.5 m	Medium
1.5 m< d < 2 m	High
d > 2 m	Very High

Table 2 Delineated LULC Classes of the Lafa River Basin

LULC Class	Class Number	Percent Impervious	Area (m2)
Low Intensity Residential	21	20	21809196.100
High Intensity Residential	22	25	4583915.180
Herbaceous	71	5	1137815.296
Bare rock	31	85	414038.847

III.   RESULTS

3.1   Rainfall Frequency Analysis

A plot of the maximum rainfall against the reduced variate followed a linear trend (Fig. 2) indicating consistency in the data and justified the use of the Gumbel distribution (Reddy, 2011). The result of the Gumbel distribution frequency analysis performed for 1, 2, 3, 4, 5, 6, and 24 hour duration rainfall corresponding to 2 year, 15 year, 25 year, 50 year, and 100 year return period is summarised in Table 3 and Fig. 3.

3.2   Physiographical Parameters Analysis

The contour and river lines data were used to generate the DEM, from which LRB DEM was delineated (Fig. 4). From Fig. 4, the minimum elevation on the LRB is 2 m at the outfall and the maximum is 160.232 m located on the north-easterly trending hills at the western fringe of the basin. Based on the DEM, the morphometric parameters of the basin were also derived.

3.2.1 Morphometric Parameters

The morphometric parameters of the LRB are summarised in Table 4. The study showed that the Lafa Stream is a 3rd Order stream with 53 total numbers of streams and a total stream length of 34.390 km.

For a relatively large basin, the order number is directly proportional to the size of the contributing watershed, channel dimensions, and the stream discharge at any section in the system (Strahler, 1964). The area of a drainage basin is very critical in hydrological design. It is a direct function of the volume of water that can be generated from an effective rainfall. The area of the LRB is 27.945 km^2 (Table 4). According to Reddy's watershed classification, a watershed is considered to be small if its area is less than 250 km^2 (Reddy, 2011). Small watersheds tend to have a shorter time of concentration and therefore prone to floods. This criterion therefore characterizes LRB as a small basin.

Basin shape is not applied directly in hydrological computations, however, it supposedly reflects the way runoff will 'bunch up' at the basin outlet and has a significant effect on the hydrological character of the basin. The shape indices considered in this study included elongation ratio, circularity ratio, and form factor ratio.
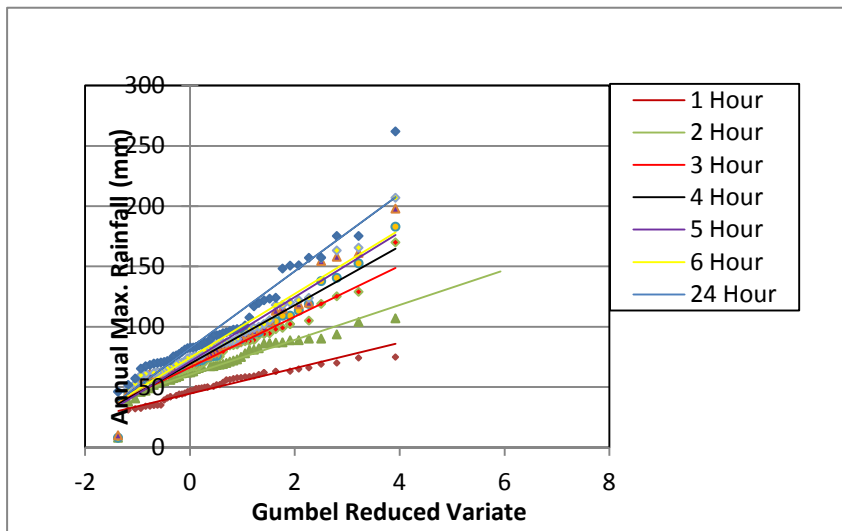
Figure 2 A Graph of Maximum Rainfall versus Gumbel Reduced Variate

Table 3 Summary of Rainfall Frequency Analysis

Duration	Rainfall Magnitude (mm)				
	2 Year	15 Year	25 Year	50 Year	100 Year
1 hour	48.3	74.3	80.2	88.1	96.0
2 hour	65.3	100.8	108.8	119.7	130.4
3 hour	73.8	124.2	135.7	151.1	166.3
4 hour	77.7	136.1	149.4	167.2	184.9
5 hour	80.6	144.8	159.4	178.9	198.4
6 hour	83.8	147.4	161.9	181.3	200.5
24 hour	93.6	171.0	188.6	212.2	235.6
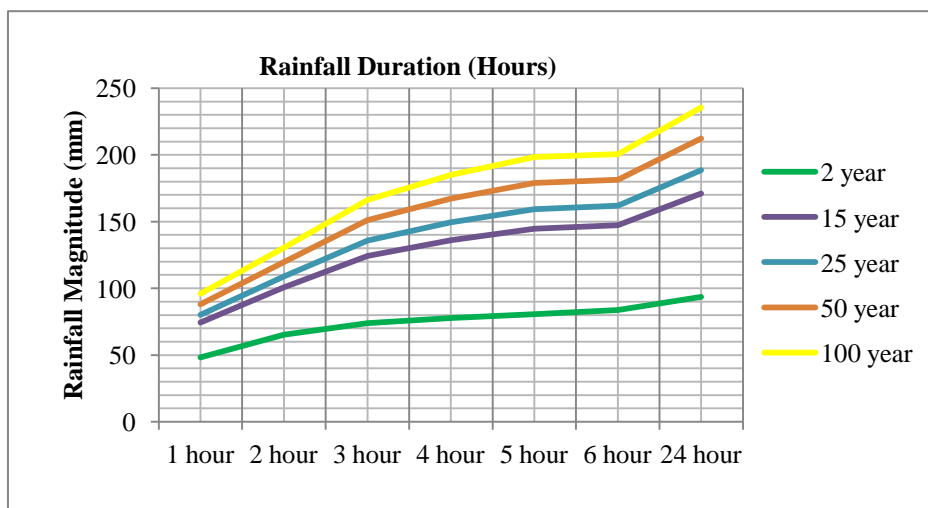
Figure 3 Relationship between Magnitude, Duration and Return Period
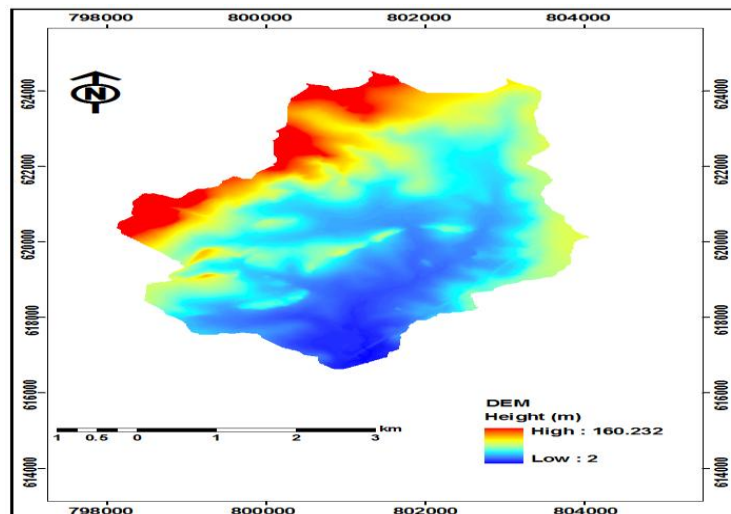
Figure 4 DEM of the Lafa River Basin

Shumm (1956) defined elongation ratio (Re) as the ratio of diameter of a circle of the same area as the basin to the maximum length. The Re values generally ranges between 0.6 and 1.0 over a wide variety of climate and geologic types. Values near to 1.0 are characteristics of region of very low relief, while values in the range of 0.6-0.8 usually occur in the areas of high relief and steep ground slope (Chow, 1964).

These values are further categorised as circular (Re>0.9), oval (0.9-0.8) and strong elongated to less elongated (0<Re<0.7), (Yusuf et al., 2011). The computed Re of the LRB is 0.609. The Circularity ratio (Rc) is a dimensionless factor that indicates the measure of circularity of the basin. The computed Rc value of 0.521 (Table 4) indicates that the LRB is elongated. A form factor value (Rf) of 0.291 further indicates a lower value of form suggesting that the LRB is not circular or oval in shape but an elongated basin.

3.2.2 Lafa River Basin Slopes

The slopes of the LRB created from the DEM ranges between 0 and 56 %. These percentage slopes were further classified into five categories based on (Sreenivasulu and Pinnamaneni, 2010) classification illustrated on (Table 5).

Flat slopes cover 22 % of the basin area and are located along the main stream channel which constitutes the floodplain of the basin. The undulating, rolling, hilly, and mountainous areas which constitute the steep slopes cover 78 % of the Basin. The velocity and volume of runoff depends on the slope of the land. Steeply sloped basin characteristics induce faster stream response to precipitation. It produces higher peak flows and shorter time of concentration due to reduced time for infiltration and shorter travel time to the stream channel and outfall. Channel slope affects the magnitude of the peak and the duration of runoff. A steep channel produces greater velocities and allows faster removal of runoff from the watershed and produces shorter times to peak. A mild or low channel slope produces lower velocities and slow removal of runoff, resulting in higher peaks and therefore influences frequent flood occurrence.

Table 4 Morphometric Parameters of the LRB

Drainage Basin Parameter	Symbol/Formula	Parameter Value
Stream Order	Nu	3
Stream Length	Lu	34.390 km
Total Number of Streams	Ns	53
Basin Length	Lb	9.800 km
Basin Area	A	27.945 km2
Basin Perimeter	P	25.957 km
Elongation Ratio	$R_e = \dfrac{2}{L_b}\sqrt{\dfrac{A}{\pi}}$	0.609
Circularity Ratio	$R_c = \dfrac{4\pi A}{p^2}$	0.521
Form Factor Ratio	$R_f = \dfrac{A}{L_b{}^2}$	0.291

The computed mean channel slope of the LRB is 1%, which does not influence a quick removal of runoff from the stream channel resulting in water overtopping the banks causing floods in the basin. The aspect grid created indicated that the slopes of the basin are directed towards the stream channel indicating less travel time for runoff to reach the stream channel, and thus enhance flooding in the Basin.

Table 5 Slope Classes on the LRB

Slope Class	Class (%)	Area (Km²)
Flat	0-2	6.302
Undulating	2-8	16.799
Rolling	8-16	3.850
Hilly	16-30	0.831
Mountanous	> 30	0.162

3.3 Soil Data Map

The classified soil map is illustrated in Figure 6 shows that the Korle series is the only soil with relatively high infiltration rate. However, the Korle series only constitutes 17 % of soils in the LRB. The remaining soils, including; Chuim-Gbegbe, Fete-Bediesi, Nyigbenya-Haacho, Oyarifa-Manfe, Oyibi-muni, and Songaw constitutes 83 %. These soils have clay content soils that impede vertical transmission of water resulting in low infiltration rates and higher runoff volume.

3.4 Landuse/land cover Map

The result of the LRB landuse data preparation is indicated on Fig. 7. It could be observed that the residential landuse characteristic covers a total of 94 % of the LRB, a marginal herbaceous characteristic of 4 %, and 2 % bare rock surface located in the abandoned quarry sites. These percentages indicate that the landuse type of the LRB is residential and urban in nature. Urbanisation, with the accompanying loss of vegetation, replacement of soil with impervious surfaces, and routing storm water runoff directly to stream channels, has significant impact on many of the processes that control streamflow in a drainage basin (McCuen, 1998).

3.5 Hydraulic Modelling and Hazard Assessment

The Geometric data output from HEC-GeoRAS and the flow rates were used to compute the water surface profiles (flood models) corresponding to 2 year, 15 year, 25 year, 50 year, and 100 year return period in HEC-RAS.

From the hydrological analysis and the hazard maps, it was observed that the peak flows produced by 2 year, 15 year, 25 year, 50 year, and 100 year return period storms are 43.0 m3/s, 98.0 m3/s, 112.4 m3/s, 132.6 m3/s, and 153.5 m3/s respectively. These flows inundated 233.88 ha, 292.92 ha, 298.36 ha, 305.00 ha, and 311.24 ha respectively of the LRB. The area inundated with respect to peak flows show that inundated area increased rapidly between the 2 year and 15 year peak flows, increased moderately between 15 and 25 year flows, and slight increases beyond 25 year flows (Fig. 8).A relationship between the return period and the inundated areas showed a rapid increase of inundated area from 2 to 15 year and moderate increases between 15 and 25 year return periods. Slight increases occurred beyond 25 years return period (Fig. 9).

3.5.1 Flood Hazard Assessment

The result of the flood hazard assessment based on the hazard maps is summarised in   Table 6. It could be observed that inundated area decreases with increasing depth for all return periods. For inundation depth d<0.5 designated low hazard level, inundation extent for 2 year, 15 year, 25 year, 50 year, and 100 year is 139.16 ha, 145.16 ha, 143.60 ha, 139.36 ha, and 136.36 ha respectively, which covers 59.50 % , 49.6 %, 48.13 %, 45.64 % and 43.81 % of total inundated area respectively. This indicates that low hazard flood is approximately 50 % of total inundated area for all flood intensities. For inundation depth d>2 designated very high hazard level, the inundated areas for 2 year, 15 year, 25 year, 50 year, and 100 year flood are 3.92 ha, 16,24 ha, 17.64 ha, 19.56 ha, and 20.64 ha respectively. These areas cover 1.68 %, 5.54 %, 5.91 %, 6.41 %, and 6.63 % respectively of total inundation extent of each return period flood. This indicates that area above inundation depth d>2 also increases with increasing flood intensity.
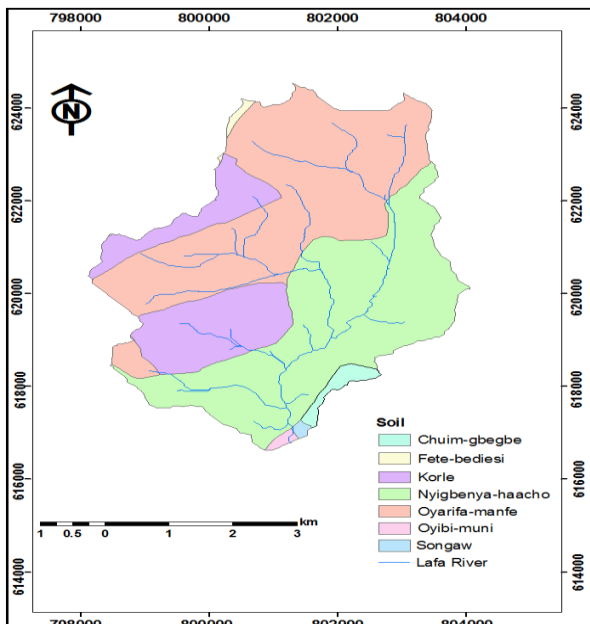
Figure 5 Soil Map of the Lafa River Basin
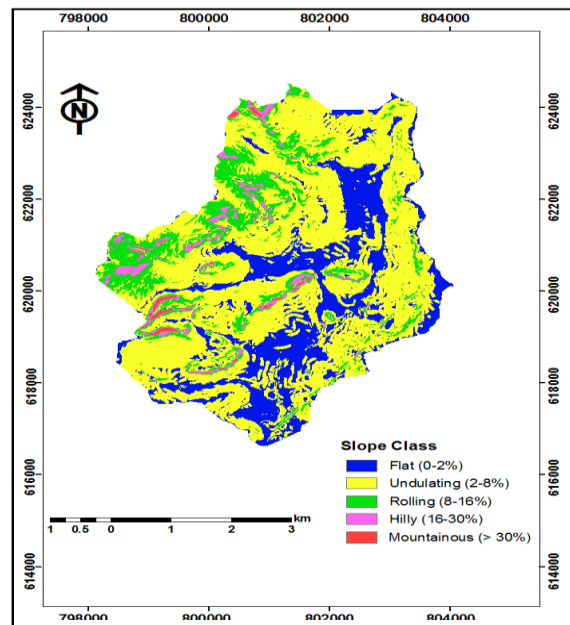
Figure 6 LRB Classified slope grid
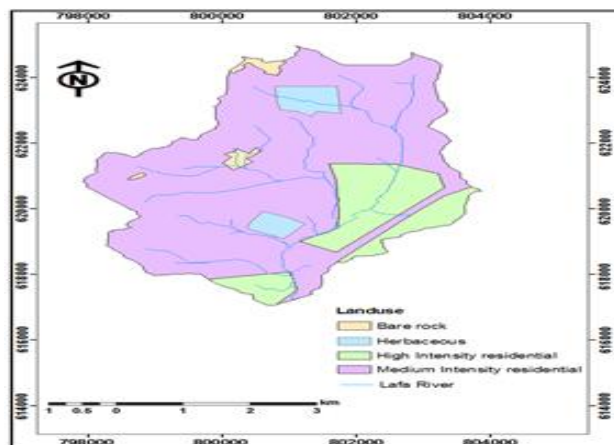
Figure 7 Landuse Map of Lafa River Basin
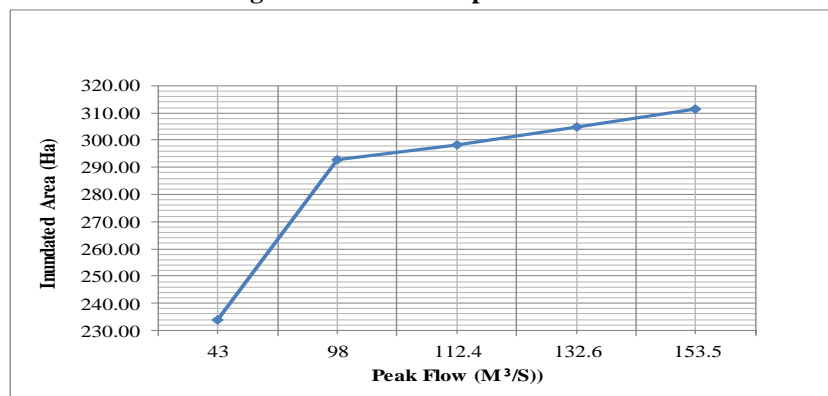
Figure 8 Peak Flow and Inundated area relationship
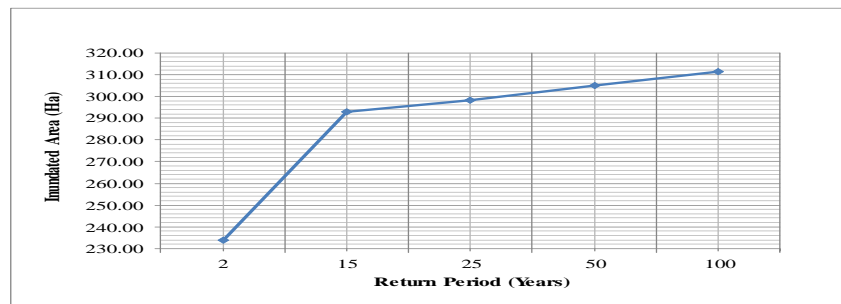
Figure 9 Return Period and inundated area relationship

Table 6 Summary of Flood Hazard Assessment

Water Depth (d) (m)	TOTAL FLOODED AREA (Ha)									
	2 Year Flood		15 Year Flood		25 Year Flood		50 Year Flood		100 Year Flood	
	Area	%	Area	%	Area	%	Area	%	Area	%
d < 0.5	139.16	59.50	145.16	49.56	143.60	48.13	139.20	45.64	136.36	43.81
0.5 < d < 1	57.56	24.61	74.60	25.47	78.68	26.37	85.56	28.05	90.96	29.23
1 < d < 1.5	22.96	9.82	36.12	12.33	37.40	12.54	37.28	12.22	38.76	12.45
1.5 < d < 2	10.28	4.40	20.80	7.10	21.04	7.05	23.40	7.67	24.52	7.88
d > 2	3.92	1.68	16.24	5.54	17.64	5.91	19.56	6.41	20.64	6.63
Total	233.88	100	292.92	100	298.36	100	305.00	100	311.24	100

IV. CONCLUSIONS

Results from this study show that a combination of hydrological and hydraulic model integrated with GIS is an invaluable tool for flood analysis and management in drainage basins where limited hydrometeorological data exist. The results indicate that the driving forces behind the floods in the LRB are inherently natural physiographical characteristics that include the following:

- The Basin consists of a 3rd order stream with a drainage area of 27.945 km2. It has an elongated shape characterised by high relief and steep ground indicated by an elongation ratio (Re) of 0.609, circularity ratio (Rc) of 0.521, and form factor value of 0.291.
- 78 % of the Basin is characterised by steep slopes that produce higher peak flows and shorter time of concentration due to reduced time for infiltration and shorter travel time to the stream channel and outfall.
- 83 % of the soils in the LRB impede vertical transmission of water resulting in low infiltration rates, and higher runoff volume in the basin.
- 94 % of the landuse characteristic in the basin is residential, indicating an urban setting and therefore predominantly impervious.

The flood models produced by the hydraulic analysis corresponding to 2 year, 15 year, 25 year, 50 year, and 100 year return period storms inundated 233.88 ha, 292.92 ha, 298.36 ha, 305.00 ha, and 311.24 ha of the LRB flood plain respectively. These inundation extents give an indication of the potential flood situations in the Basin.

REFERENCES

[1]   Anon., Report on Flood Response Operations in Ga South Updated, National Disaster Management Organization (NADMO), Accra, Ghana, 2011.
[2]   Hershfield, D. M. and Kohlar, M. A., An Empirical Appraisal of the Gumbel Extreme Value Procedure, *Journal of geophysics Research, Vol. 65, No. 6.*,1960.
[3]   Gumbel, E. J., Statistical Theory of Extreme Values and some Practical Applications, Applied Mathematics Series No. 33, National Bureau of Standards, Washington D.C., 1954, 54pp.
[4]   Deshpande, N. R., Kulkani, B. D., Verma, A. K., Mandal, B. N., Extreme Rainfall Analysis and Estimation of Probable Maximum Precipitation (PMP) by Statistical Methods over the Indus River Basin in India,*Journal of Spatial Hydrology, Vol. 8, No. 1*, 2008, pg 22-36.
[5]   Hutchinson, M. F., A New Procedure for Gridding Elevation and Stream line Data with Automatic Removal of Spurious Pits, *Journal of Hydrology, Vol. 106*, 1989, pp 211–232
[6]   Anon, (2009), "Flooding in Urban Areas", ttp://www.unescap.org/idd/events/2009_EGM-DRR/SAARC-India-Shankar-Mahto-Urban-Flood-Mgt-Final.pdf, Accessed: April 26, 2012.
[7]   Anon., (2012), "Land Cover Class Definitions", United States Geological Survey Land Cover Institute (LCI), http://landcover.usgs.gov/classes.php#develop, Accessed: March 9, 2013.
[8]   Reddy, P. J. R., *A textbook of Hydrology* (University Science Press, New Delhi, 3rd Edition, 2011) pp. 347-415.
[9]   Strahler, A. N.,*Quantitative Geomorphology of Drainage Basins and Channel Network In Handbook of Applied Hydrology*(McGraw Hill Book Company, New York, section 4-II, 1964)
[10]   Schumm, S. A. Evolution of Drainage Systems and Slopes in Badlands at Perth Amboy, New Jersey, *Bulletin of Geological Society of America, Vol. 67*, 1956, pp 597-646
[11]   Chow, V. T., *Handbook of Applied Hydrology* (McGraw Hill, New York section-4-II, 1964),1495pp.
[12]   Sreenivasulu, V. and Pinnamaneni U.B., Estimation of Catchment Characteristics using Remote Sensing and GID Techniques, *International Journal of Engineering Science and Technology, VOL. 2, No. 10,* 2010, pp. 7763-7770.
[13]   McCuen, R. H., *Hydrologic Analysis and Design, 2nd ed*. (Prentice Hall, Upper Saddle River, New Jersey, 1998) pp 814.

Research Paper   Open Access

Carbon Emission Management in the Construction Industry – Case Studies Of Nigerian Construction Industry

[1]Edeoja, Joy Acheyini , [2]Edeoja, Alex Okibe
[1]*Department of Building, Benue State Polytechnic Ugbokolo, Nigeria/*
[2]*Department of Mechanical Engineering, University of Agriculture, Makurdi, Nigeria*

ABSTRACT : *Climate change is a global concern. The effect is seen all over the globe and man's anthropogenic activities is a major contributor. This study evaluates the management of carbon emissions in the Nigerian construction industry by measuring the amount of carbon being emitted from constructional activities within selected organizations. At present, there is no standard of measuring greenhouse gas emissions that is acceptable internationally for all countries so the UK Department for Environment and Rural Affairs (DEFRA) methodology of emission monitoring and measurement was used to evaluate the extent of carbon dioxide emissions in these organizations. This methodology was adopted for this study because there was no known national methodology for emission measurement and monitoring within Nigeria. Case studies were undertaken and questionnaires were applied in some construction organizations within Nigeria and the responses from these questionnaires were evaluated and it was found that though there was significant emissions from the Nigerian construction industry, the provision for emissions monitoring and management was lacking, the general awareness regarding carbon emissions and environmental issues across the various organizations evaluated was poor and the construction organizations had no singular person directly in charge of carbon or environmental issues.*

Keywords - Climate change, Global warming, DEFRA Methodology, Greenhouse gases, Carbon emission management, Construction industry.

I. INTRODUCTION

There is a general consensus that global warming is as a result of climate change. Climate change is one out of many global pressures that the present generation needs to attend to in order to ensure that the quality and prosperity of life is preserved [1]. The earth's climate has varied significantly in the past with variations as a result of natural emissions like volcanic eruptions and greenhouse gas emissions. The concentration of carbon dioxide, a major greenhouse gas has increased in recent years. This increase in carbon dioxide emission has been attributed to anthropogenic activities of man. In 1997, an agreement was reached in Kyoto where about 38 developed countries committed themselves to the reduction of their annual carbon dioxide emissions [2]. The global climate will continue to change as long as man inhabits this planet and with the predictions on global temperature continuing to rise, there is an expected change in the global climate that will lead to changes in weather patterns for each locality with impact varying according to local conditions and vulnerability. The 2007 fourth assessment report from the Intergovernmental Panel on Climate Change (IPCC) stated that there is a 90 per cent likelihood of man-made greenhouse gas emissions causing most of the observed global temperature rise since pre-industrial era [3].

Addressing the threat posed by carbon emissions ultimately require behavioral changes in the global consumption and utilization of energy especially fossil fuels. The ultimate objective to address climate change by the United Nations Framework Convention on Climate Change (UNFCCC) as clearly stated by the body is to stabilize atmospheric greenhouse gas concentrations at safe levels that would prevent dangerous anthropogenic interference with the climate system. To achieve this goal, net carbon emissions must be substantially reduced over the course of this century and must be virtually eliminated in the future [4]. Progress towards achieving this will require a long chain of actions performed over time though there are growing suggestions that these steps alone will not be enough to reduce or stabilize the global atmospheric carbon dioxide concentrations [5].

Carbon management is the concept of managing carbon dioxide emissions from anthropogenic activities so as to minimize its effects on global climate. The techniques include among others carbon dioxide capture and storage, geochemical carbon cycling to enhance transformation of carbon dioxide gas into dissolved

or solid phase carbon, biological mechanisms of enhancing carbon contents of soils and physical mechanisms such as formation of carbon dioxide lakes, and confinement of Carbon dioxide gas in underground formations [6]. Tackling carbon emission is a local issue that will depend on the individual country's emissions status and vulnerability to climate change. It will therefore require management strategies that are locally adaptive since sources like energy (availability, alternatives or mixes and demand), carbon sinks and other factors vary widely globally. In developed and developing countries, the largest sources of carbon dioxide are from fossil fuel while in less-developed countries like Nigeria, most of the carbon emissions are from sources such as fossil fuel consumption in the transport sector, industrial sector including the construction industry, deforestation, gas flaring as a result of oil exploration and land use.

Managing carbon emissions successfully will require the development of different types of options which will include the followings:

- greater efficiency in the production and use of energy;
- greater use of renewable energy technologies;
- technologies for removing carbon from hydrocarbon fuels and sequestering it away from the atmosphere;
- a mixture of behavioural and operational changes in forestry, agricultural, industrial and land use practices; and
- Other approaches, some of which are currently very controversial, such as nuclear power and carbon capture and storage [7, 8].

The population of the world as a whole will continue to grow in the coming decades, because though populations in some parts of the world have stabilized, in developing countries like Nigeria, the population is growing and will continue to grow. The desire for development will also continue among developing countries and this will definitely lead to an economic development that will continue to result in growing energy demand, even if the global energy efficiency can be significantly increased.

The Clean Development Mechanism (CDM) is a market mechanism under the Kyoto Protocol targeted at reducing GHG emissions in a cost effective way and still maintain sustainable development in host countries by encouraging energy-efficient, capital and technology transfer into those countries. CDM is an important mechanism that is designed to link the gap between industrialized countries which are responsible for most of the past greenhouse gas emissions and the developing world which is expected to be the major source of future emissions. Article 12 of the Kyoto Protocol provides for the clean development mechanism. Through the CDM, countries with emission targets can invest in emission control projects in developing countries with no targets, thus earning credits for the reductions in GHG emissions in the host country [9, 10].

The greenhouse gas benefits of each CDM project will be measured according to internationally agreed methods and will be quantified in standard units, to be known as 'Certified Emission Reductions' (CERs), expressed in tonnes of CO_2 emission avoided. CDM projects should be based on voluntary participation by each Party. In providing a mechanism for this exchange, CDM through emissions trading reduces the cost of meeting the Kyoto targets on one hand and provides a new source of export earnings on the other [11].

Nigeria is a Party to the UNFCCC, which it signed on June 13th 1992 and ratified in August 1994 and ratified the Kyoto Protocol in 2004 and the Protocol came into force in the country in 2005. The Federal Ministry of Environment which is responsible for carbon emissions and climate change is one of the relevant authorities for CDM in Nigeria. Recently, the FGN introduced another authority named the Presidential Implementation Committee on CDM (PIC CDM) as the entity to organize CDM activities in Nigeria. The PIC CDM has been named the Designated National Authority (DNA) as required by the UNFCCC. In this capacity, the PIC CDM has complete responsibility for CDM activities, especially in areas where government intervention and activities are expected. Stakeholders include the government, the general public and the private sectors [12, 13].

As far back 2007 CDM projects commenced activities and they are at various stages currently. Gas Flare Reduction Partnership (GGFR) in Nigeria has undertaken a series of actions in gas flare reduction strategies mechanisms to achieve its objectives. GGFR's stated objective in Nigeria is to reduce key barriers to flared gas utilization [12, 14, and 15].

Construction industry accounts directly and indirectly for an estimated 40% of the material flow entering the world economy and in the developing countries it accounts for around 50% of the total energy consumption. Materials used in construction have widely varying amounts of greenhouse gases associated with their extraction, refining, manufacture or processing and delivery. As new buildings become more energy efficient, the emissions associated with materials make up a greater proportion of their total climate change impact. Planners, developers, architects and builders are becoming more aware of the climate change impacts of construction materials and are increasingly including climate change considerations in their selection of materials and construction techniques for building projects [16, 17].

In global terms, the Nigerian construction industry is very small with global construction estimated to be about $4 trillion in 2008, the value of the Nigerian construction industry was estimated at $3.15 billion (0.2% of the global total estimate). Its impacts on the environment is considerably huge and is therefore the largest exploitation of natural resources with transformations that are irreversible sometimes being the end result on the environment. The impacts on the environment as a result of exploitation are particular in energy use, air and water pollution, depletion of natural resources loss of agricultural land, natural reserves, forests, soil degradation etc [18-20]

The Nigerian population is growing at an alarming rate with growth rate estimated at 1.999% thereby increasing the need for housing and urbanization. Urbanization with huge movement of people especially, the youth from the rural areas to urban centers is creating so much constructional activities in the industry [21].

Nigeria was the 4th highest emitter of Carbon dioxide in Africa as far back as in 2004, producing an estimated 31.1 million metric tonnes of Carbon dioxide emissions per capita and fossil fuel use and gas flaring was identified as the major sources of this carbon emission [22]. In 1995, the total Carbon emissions from Nigeria was 21.42 million metric tonnes – from the little data available, there has been a gradual increase in the annual national carbon emissions inventory. The main sources of Carbon emission in Nigeria were identified to be from the combustion of fuels, agriculture, and fugitive emissions due to gas flaring [23, 24]. Each sector of the economy has its own contribution to the carbon emission in the country. To be able to manage these emissions, it is very important to have an effective inventory of carbon emissions from the various sectors.

The Nigerian economy presently is one that is driven by Oil. Hence, the activity surrounding its exploration, exploitation, generation and production account for a certain percentage of Carbon dioxide emission particularly through gas flaring. In 2000, studies showed that over 3-5 billion standard cubic feet of associated gas was produced and more than 70 per cent was burnt off (flared). This made Nigeria the world's largest country with flared gas which amounted to about 2 billion standard cubic feet a day being flared. The economy is gradually picking up as well as the fact that the population is growing rapidly [25]. These both have effect on the extent of emissions from the transport, industrial, services and the agricultural sectors.

In Nigeria, harvesting of wood to be used as fuel by about 50% of the population is a major source of deforestation and is estimated to be at a rate of about 400,000 hectares per year. If this trend continues the country's forest resources could be completely depleted by 2020. Use of wood as an energy source can also contribute to the accumulation of carbon dioxide, the main greenhouse gas, both because burning wood produces carbon dioxide, and because deforestation destroys an important carbon dioxide sink [26, 27].

The objectives of this study are to estimate the energy consumed in direct construction activities, estimate the direct emissions of carbon as a result of construction activities, and the analysis of the two points above, with recommendations and a conclusion drawn concerning ways of managing carbon emissions from construction activities. In other words, this work aims at exploring the rate of emissions of carbon dioxide in the construction industry, the level of awareness and how this emission is managed within the Nigerian construction industry.

II. MATERIALS AND METHODS

2.1 Case studies

Three case studies involving construction organizations of different sizes and in different locations in Nigeria were taken for consideration. The names of these construction organizations were not used directly in this project for security purposes. These case studies were selected randomly based on the volume of work each was involved in and its perceived size. Emissions from construction activities were evaluated through the energy being consumed for such activities.

Case Study 1 was indigenous, carries out building and civil construction activities all over the country, has branches in six states with its national headquarter located in the northern part of the country. At the time of the study a branch located in the Middle Belt of the country was the respondent. Case Study 2, at the time this study was conducted was one of the leading constructional organisations in Nigeria and had handled a sizeable number of both building and civil construction works all over Nigeria. The head office, located within the Federal Capital Territory and is partly handled and owned by expatriates and indigenous Nigerians. It was responsible for most of the construction projects carried out in the present Federal Capital Territory before it took off as a national capital and are still responsible for most of the construction projects being handled by the Nigerian Government. The questionnaire was answered and filled from one of the branches within the Federal Capital Territory. Case study 3 was a civil construction organisation that was involved in road construction work in some states within the country. This organisation like case study 2 was had a combination of both expatriates and indigenes working together. The questionnaire was handled by a branch of the organisation that was handling a civil construction work in the Middle Belt of the country.

This evaluation was carried out by considering the energy consumption through the use of electricity, fuel consumption and the fuel types and the DEFRA methodology [28] of carbon emissions conversion tool used to convert from fuel consumption to carbon equivalent. This method of measurement/conversion was used because it was simple, available to all and will be ideal for Nigeria where there are no known laid down regulations regarding measurements and conversion factors. Also, Nigeria already recognizes the British Standard and combines the British Standard with its own code of practice within the construction industry. The general awareness of the construction industry's employees and the management of each industry were also considered.

Questionnaires were applied in the construction industries and the responses from these questionnaires were evaluated to arrive at a conclusion concerning the status of the Nigerian construction industry with regards to emissions. The issues tackled in the questionnaire include type of energy used, yearly consumption and transport emissions. The data collected through this questionnaire contained all information needed to establish how the Nigerian construction industry was handling emissions and management of carbon. The questionnaire sought for contact details of the company and most importantly the identification of a person responsible for carbon issues within the organization. The DEFRA 1999 reporting guidelines suggest that the identification of a 'greenhouse gas champion' is the first step to take when attempting to report on greenhouse gas emissions [29]. This person should have the authority to collect data and draw up a strategy for managing and reporting on emissions, and should liaise with the relative consultative and statutory bodies. A number of questions were asked to establish the presence of this greenhouse gas champion or a carbon information manager within the organization and also to establish the availability of a carbon emission or an environmental policy within the organizations. Using the DEFRA methodology for estimating Carbon dioxide emissions from energy consumption based on the carbon content of the fuels and the fuel types supplied to the organizations, different activities like combustion of fuel from plant and equipment usage, transport, electricity consumption were considered [28].

The Questionnaire was devised to help gauged the staff awareness as regard carbon emission and management, energy consumption and energy data collation including bills logging and documentation. Questions 1, 2, and 3 were all general questions designed to get a feel about the size of the construction company and questions 4, 5, 6, 7 and 8 were designed to measure the awareness of environmental issues especially carbon emissions and its management within the organization. Question 5 specifically asked for the presence of a "green champion" or a carbon information manager. This is an individual that is wholly responsible for carbon issues or environmental issues within an organization and who would also be responsible for a proper logging and documentation of all energy bills, consumption and types. Finally, the respondents were also given the opportunity to offer suggestions or comments regarding carbon emissions and management within their various organizations. The following section is a sample of the questionnaire that was sent to the various respondents.

2.2 Data analysis
2.2.1 Carbon emission measurement

Direct and indirect carbon emissions from construction activities or what is called scope 1 and scope 2 emissions were the identified emission sources for this research. Direct emissions are emissions from onsite heating (or electricity generation), onsite industrial use or manufacturing process and from owned transportation fleet while indirect emissions included emissions from energy purchased, usually split by fuel type or generation method. Putting the above into scope 1 and scope 2 emissions, scope 1 emissions were the direct carbon emissions from sources that the organizations owned or controlled (e.g. emissions from combustion of boilers, generating plant, air conditioning units, vehicles; and emissions from any on site production activities) while scope 2 emissions were carbon emissions from the generation of electricity, heat or steam that were used by the construction organization and have been brought in from elsewhere. The activity data or the energy consumption data were collected in litres of petrol consumed and kWh of electricity consumed as shown below for scope 1 and scope 2 emissions:

• Scope 1: purchased quantities of commercial fuels (oil, gas, etc.) using data from meters and/or utility bills. Common units of fuel consumption were converted into CO_2 emissions using the standard published emissions factors.

• Scope 2: purchased quantities of electricity consumption using data from meters and/or electricity bills. Electricity consumption was converted into CO_2 emissions using the UK grid average conversion factors created by DEFRA [28].

2.2.2 Tool and data conversion factor
The annual electricity consumed for the various activities were calculated using the kWh of electricity consumed per week for twelve months, and the activity data converted into the emissions data using the UK DEFRA greenhouse gas conversion factors for companies. Once the activity data was collected, the next step was the application of the above conversion factors using the UK guidance. The data from each activity was calculated and then a combined total of carbon dioxide emissions from the various fuel and energy consumption obtained and an overall emission for each organization arrived at. The DEFRA data conversion tool [28] provides that

- Emissions from grid electricity was converted into carbon dioxide equivalent using annex 3 of the conversion factor; while
- Emissions from the use of fuels was converted into carbon dioxide equivalent using annex 1;

The quantity of carbon dioxide (kg) emitted from each constructional activity is given by (1):

$$Activity\ Data \times Emission\ Factor = Carbon\ dioxide\ content \qquad (1)$$

The process used in the determination of carbon emission and its management for the various case studies is summarized in fig. 1 below:

2.3 Data quality and limitations
Due to the distance between Nigeria (the case study) and the UK where this study was carried out, the collection of data was systematic. Data were collected using a third party to get to the various respondents through the internet services and through telephone communications. These media of communication placed a time constraint on the data collection and the research as a whole as it was difficult getting the required data from Nigeria. Data documentation within the various organizations was a little bit difficult as discussed.

III. RESULTS

3.1 Case study findings
The results and findings obtained from the various case studies are summarized under the following headings:
(i)   The size of the construction organisation;
(ii) The availability of a carbon information/policy manager;
(iii) The availability of an organisational carbon or environmental policy; and
(iv) Energy and fuel consumptions data.

These issues were handled primarily by the first 6 questions on the questionnaire and the responses for the 3 case studies are presented in Table 1. Each case study was considered separately based on the response received from the questionnaire that was administered to it. Tables 2 to 6 show details of energy consumption for the past 12 months by the case studies. Case Study 3 did not state weekly cost of energy consumed for various construction activities.
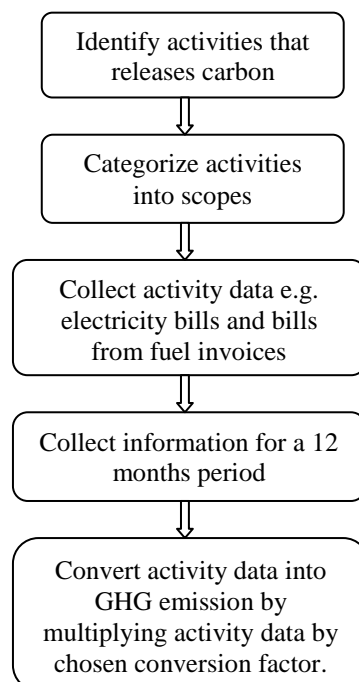
Fig. 1: Process of determining carbon emissions and its management (Source: [28]).

Table 1: Responses to the First 6 questions by the Case Studies

Issue	Case Study 1	Case Study 2	Case Study 3
Position of Respondent	Site Engineer	Engineer	Project Manager
Number of Employees	> 150	> 150	> 150
Presence of Carbon Emission/other Environmental Policy	No	No	Unsure
Presence of a Personnel in charge of Environmental issues	No	No	No
Presence of day to day log of Energy bills and consumption based on fuel types	Yes	Yes	Yes
Presence of method for CO_2 Emissions assessment	No	No	No

Table 2: Annual Energy consumption by Case Study 1

Fuel type	Annual units consumed (kWh/tonnes or litres)	Total annual cost (₦)
Grid electricity	1,040,250 kWh	10,090,425
Natural gas	-	-
Gas diesel oil	800,000 litres	92,000,000
Heavy fuel oil	-	-
Any form of renewable energy	-	-
Coal or coking	-	-

Table 3: Annual Energy consumed for transport by Case Study 1

Fuel type used	Total units consumed annually (l or kg)	Total amount spent annually (₦)
Petrol	156,000litres	10,140,000
Diesel	-	-
Petroleum gas	400,000litres	46,000,000
Natural gas	-	-
Others	-	-

Table 4: Annual Energy consumed for Construction activities by Case Study 2

Fuel type	Annual units consumed (kWh/tonnes or litres)	Total annual cost(₦)
Grid electricity	3120000 kWh	-
Natural gas	1456kg	-
Gas diesel oil	520000 litres	-
Heavy fuel oil	-	-
Any form of renewable energy	-	-
Coal or coking	-	-
Others	-	-

Table 5: Annual Energy consumed for various construction activities by Case Study 3

Fuel type	Annual units consumed (kWh/tonnes or litres)	Total annual cost(Naira)
Grid electricity	52,000 kWh	-
Natural gas	1344kg	-
Gas diesel oil	370000 litres	-
Heavy fuel oil	480000litres	-
Any form of renewable energy	-	-
Coal or coking	-	-
Others	-	-

Table 6: Annual Energy consumed for transport by Case Study 3

Fuel type used	Total units consumed annually (l or kg)	Total amount spent annually (₦)
Petrol	137,480litres	8,650,000
Diesel	-	-
Petroleum gas	520,000litres	46,000,000
Natural gas	-	-
Others	-	-

3.2   Carbon measurement and conversion from the case studies
Tables 7 to 9 below show the energy and fuel consumption with their conversion factor for the various case studies.

Table 7: Conversion of emissions from energy consumption for construction activities to carbon equivalent for case study 1

Fuel type	Quantity consumed	Emission factor(kg CO_2/unit)	Total CO_2(kg)
Gas diesel oil	800,000 litres	2.6413	2113040.00
Petrol	156,000litres	2.3018	359080.80
Natural gas	40,0000litres	2.0230	80920.00
Grid electricity	1,040,250kWh	0.50076	520915.59
Total			3073956.39

Table 8: conversion of emissions into carbon dioxide equivalent for case study 2

Fuel type	Quantity used	Emission factor (kg CO_2/unit)	Total kg CO_2
Gas diesel oil	520000litres	2.6413	1373476.00
Petrol	-	2.3018	-
Natural gas/other petroleum gas	1456kg (1.456 tonnes)	2894.0	4213.66
Grid electricity	3120000kWh	0.50076	1562371.20
Total			2940060.86

Table 9: Conversion of emissions into carbon dioxide equivalent for case study 3

Fuel type	Quantity used	Emission factor (kg CO_2/unit)	Total (kg CO_2)
Gas diesel oil	370000litres	2.6413	977281.00
Petrol	137480litres	2.3018	316451.46
Natural gas	125000litres	2.0230	252875.00
Grid electricity	1135000kWh	0.50076	568362.60
Total			2114970.06

IV.   DISCUSSION

From the responses given by the various case studies, the analyses of each organization's status regarding carbon management were discussed under the following sub sections.

4.1   Carbon information/policy manager

The Carbon Information Manager is responsible for carbon emission, management and all that pertains to environmental issues, and should have a level of detailed understanding of every activities and operations within the construction organization. This manager will ensure that:

(i)   Emission data like energy bills, fuel consumption invoices are properly kept and updated from time to time;

(ii)   Policies and regulations regarding carbon emissions are maintained;

(iii)   A general awareness about carbon issues is created within the organisation;

(iv)   A link between the organisation and the government including the general public as regard carbon emission and its management is maintained.

From Table 1, the responses of 2 of the case studies were negative on this issue while case study 3 was unsure. From the number of employees recorded by them, they were between medium and big in size. The absence of a carbon or environmental issues Manager shows the level of importance placed on emissions of greenhouse gases from construction activities by the organization or its understanding of carbon emissions and this raised some suspicion as to the validity and consistency of the data supplied. Given the volume of work Case study 2 was involved in, the number of employees it has and its exposure to the Federal Government's economical policies some meaningful information regarding carbon emission issues, awareness about climate change, the effect of carbon emissions on climate change and possibly the availability of a form of environmental policy was highly expected from it. This response from this case study also shows a lack of understanding or interest regarding carbon emissions and management. Case Study 3 was unsure as touching the presence of a person in charge of any form of carbon issues. The respondent was a project manager within the organization and if he/she is unsure of a carbon information manager then there is a need to query his competence, the general awareness across the organization regarding environmental issues and also the validity of other information supplied within the questionnaire by the respondent.

Based on the responses given by all the case studies on this issue, there is the need for the creation of awareness and/or a policy within the Nigerian construction organizations on the provision for a Carbon Information Manager who will be able to control some aspects of carbon emissions as well as stimulating other aspects that might be susceptible only to influence, rather than direct control. For instance, while an organization has direct financial control over energy consumption, having an effective energy policy that relies on influencing employee behavior rather than controlling its energy consumption will go a long way.

4.2 Carbon issues and environmental policy

Table 1 also shows that the 3 case studies all answered in the negative on the issue of a carbon emissions/other environmental policy within the various organization. An environmental policy stating organizational objectives, targets and means of achieving these targets is very important if the emissions of greenhouse gases are to be monitored within an organization. The absence of one shows the level of awareness within the various construction organizations. The Table also shows the calibre of the persons who responded on behalf of the case studies and for them not to know would be very unfortunate. This also speaks of the national attitude towards environmental or carbon emission issues within the construction industry and within the nation as a whole in Nigeria. The fact that there was a general carefree attitude towards emission or environmental issue could be because Nigeria was classified under the countries with little emissions and do not need any emission reduction target for now. With the current population, the rate the population is growing coupled with some national emission problems like gas flaring, deforestation and emissions from agricultural processes, carbon emissions within the country will keep growing in all sectors of the economy and there is a need to lay down ways for these emissions to be monitored and managed.

4.3   Carbon dioxide emissions from the various case studies

Tables 7 to 9 show the carbon emissions from the constructional activities of the various case studies. The total computed carbon dioxide emission from case study 1 was 3073956.39kg (approximately 3073.96 tonnes of CO_2). The total carbon emission calculated from this case study was 2940060.86kg (approximately 2940.06 tonnes CO_2). This result was however inconclusive as the figure for petrol consumption was missing. It was either this organization was not using petrol for its construction activities or there were some discrepancies in the documentation of energy consumption for those activities. The carbon emissions from the construction activities for case study 3 was calculated as equal to 2114970.06kg of CO_2 (approximately 2114.97tonnes of CO_2). The figures that were calculated from these emissions individually were minimal but when combined from the entire construction sector and other sectors of the economy, this will become significant.

The status of the Nigerian construction industry concerning carbon emissions and management can be seen from the responses which were generally negative. There is an absolute absence of awareness regarding carbon emissions and management. For carbon to be well managed and monitored through proper measurement, it is important that energy consumption be properly documented and logged at the appropriate time according to quantities consumed, the types and the amount spent in acquiring the energy with everything shown in the right order with the right units.

4.4   Ways of reducing carbon emissions within the construction organizations

Countries like the UK have put in place policies and regulations that have helped in the reduction of its carbon emissions. Incorporating some of these policies into the Nigerian environmental policies will go a long way in helping Nigeria to monitor its greenhouse gas emissions and also manage it successfully. The Nigerian construction industry and the Nigerian Government could reduce its carbon emissions by adopting the UK Low

Carbon Transition Plan strategies for built environment. These strategies involve the followings will go a long way in the reduction of carbon if incorporated into the Nigerian policies.

(a) Clean energy cash-back schemes: Payments if low carbon sources are used to generate heat or electricity;
(b) A target to generate a percentage of total national electricity consumption from renewable sources; and
(c) The government encouraging industries and household with the provision of smart meters so that the public will understand its energy use and maximize opportunities for saving energy thereby reducing the emissions as a result of energy consumption and by doing that also saves energy bill.

UK energy supply comprises of natural gas, coal, petroleum, nuclear power and renewable energy. Policies involving the introduction of different energy mixes had helped in the reduction of emissions within the UK. The Nigerian energy policy needs to be upgraded if different energy mixes will be encouraged in the national mix. Every sector of the economy and everyone need to play a part in making these changes. Nigeria will then have a better quality of life, improved long-term economic health, new business opportunities in a fast-growing global sector, reduced reliance on fossil fuels, greater security of future energy supplies and fewer emissions into the atmosphere [30].

South Africa is another good example of an African country that is trying to do something tangible about the reduction of its carbon emissions. In December 2009 just before the convention in Copenhagen, the South African government announced national greenhouse gas emissions reductions by 34% by 2020 and 42% by 2025. South Africa which has a dirty economy due to its historical dependence on cheap coal to generate electricity, on a per capita basis have a greenhouse gas emission that is close to that of the UK and Germany despite its smaller economy. Two processes were agreed on by the South African government to help in the reduction of its carbon emissions. These were:

(i) The compilation of a climate change green paper which will lead to legislation and policies in support of carbon management; and
(ii) The compilation of the second Integrated Resource Plan (IRP2) by the department of energy, which will determine what South Africa's energy mix will be for the next 25 years [31].

In terms of sensitivity to environmental issues and shifts in awareness and policy, there is much that the Nigerian government and the Nigerian construction industry need to learn from South Africa. In 2009, there was a conference in South Africa called the Green Building Council of South Africa (GBCSA) , which launched the 'Green Star" rating tool that was based on the Australian Green Star rating system and since then the Council has been hard at work translating the meaning of 'Green' building into something that is practical. The objectives of the Green Star South African rating tool were given as:

(i) The reduction of the environmental impact of development;
(ii) The establishment of a common language for green building;
(iii) The setting of benchmarks and standards of measurement;
(iv) The promotion of integrated whole building design; and
(v) To raise awareness of green building benefits.

The South African government now has new or reprioritized considerations which taken into account during construction includes skills transfer, local procurement, suppliers, eco-design and sustainability.

There are a number of complementary ways the Nigerian construction industry and the Nigerian government can learn from what the UK and the South African government has done to 'make a difference' and, in so doing, will begin to address the issues of carbon emissions and management within the construction industry and the nation at large. Whether this means using products made from renewable resources or recycled material, choosing products with low energy, opting specifically for non-toxic products or changing to technology to harness renewable energy sources for example the harnessing of solar energy, will help in the creation of a built environment that is environmentally friendly and a Nigeria that is environmentally sustainable [32]

V. CONCLUSIONS AND RECOMMENDATIONS

Three construction organizations within the Nigerian were considered as case studies for this study and the organizational size, availability of a carbon information manager, availability of carbon policy or methods of assessing carbon emission and available energy consumption data were considered. From these considerations, the following conclusions were drawn:

- The figures (3073.96, 2940.06 and 2114.97 tonnes of CO_2) obtained from the various case studies represent significant amount of carbon dioxide emissions.
- There were some elements of doubt regarding the validity of the data collected as the basis for the calculations of these carbon emissions. These were observed in the way the questionnaires were filled as there were some important parts that were left vacant. For carbon to be properly managed there is a need for a proper documentation and logging of energy use, fuel types, quantity consumed and duration

of consumption. This does not however invalidate the results obtained because the missing information would have been an addition to the values above.

- There were no particular persons responsible for carbon management or emission monitoring in all the case studies undertaken and this probably is the situation in the Nigerian construction industry.
- There was no carbon or environmental policy in place in all the case studies considered and there was no form of carbon assessment in any of the organisation. This also is likely the situation across the industry.

To manage carbon emissions within the Nigerian construction industry effectively, the followings are recommended:

- The presence of a carbon management department with an information manager within the individual construction organisations.
- The need for the various construction organisations to develop their own ways of collecting energy data and they can do this by starting from a blank sheet of paper and a pile of energy bills.
- An organisational objectives stating a carbon management strategy that will benefit the organisation, the economy as well as the environment;
- Communicating across each construction organisation about carbon management and the creation of awareness regarding carbon emissions, the effect of the emissions on the environment especially climate change, the stand of the organisation and its objectives regarding carbon management issues;
- The creation of a general awareness regarding employees behaviour and energy consumption;
- Setting of targets regarding organisational objectives and decide on the carbon emission measurement criteria to be used;
- Prioritising the areas of carbon emissions that need to be controlled and target areas where reduction in emissions will have a high impact on the overall measure e.g. energy consumption; and
- Considering monitoring carbon emissions for a period before setting targets.

In this study, time limitations and distance restricted the amount of data collected and the amount of research carried out as regard emissions from the construction activities. Research was carried out via the internet and telephone services due to the distance between the UK and Nigeria. Carbon dioxide emission was the only greenhouse gas considered for this study and the method for measurement and calculation of data used was the UK DEFRA methodology. The use of this methodology for carbon emission within the Nigerian construction industry is not ideal because the emission scenarios within the two countries are different. The DEFRA conversion factor was however adopted because there was no national emission factor for Nigeria to be used and the measurement of carbon emissions probably gives an indication of the Nigeria situation.

In this work all the research were carried out using questionnaire via the internet and telephone services. It is therefore recommended that a further work be carried out where research can be possible by being involved in the construction activities directly and having a firsthand knowledge about the energy being consumed, where it is consumed and also monitor how these emissions can be measured and managed by considering the following:

- Determining the general awareness of the employees and the whole construction industry as regard the effects of carbon emissions within the construction industry;
- Determine the effect of employees' behaviour on energy and fuel consumption;
- Development of a database for emission issues within the construction industry through a proper energy consumption and carbon inventories;
- The consideration of the other greenhouse gas emissions as this is vital for a proper greenhouse gas emission inventories.

REFERENCES

[1]. DEFRA, Adapting to climate change. UK climate projections, (2009). Available at http://www.defra.gov.uk/. Accessed on 30/06/2010.

[2]. Shi, The impact of population pressure on global carbon dioxide emissions, 1975–1996: evidence from pooled cross-country data, *Journal of ecological economics, 44(1),* 2003, 29-42. Available at http://www.sciencedirect.com .

[3]. IPCC, A report of working group of the Intergovernmental panel on climate change, 2007.. Available at http://www.ipcc.ch/pdf/assessment-report/ar4/wg1/ar4-wg1-spm.pdf. Accessed on 30/06/2010.

[4]. **UNFCCC,** Intergovernmental negotiating committee for a framework convention on climate change, **1992**. Available at http://www.un-documents.net/unfccc.htm#article-2. Accessed on 30/06/2010.

[5]. IEA, CO_2 emissions from fuel combustion, 2009. Available at http://www.iea.org /co2highlights/CO2highlights.pdf. Accessed on 30/06/2010

[6]. Sorrel, Making the link: climate policy and the reform of the UK construction industry. *Journal of energy policy*, *31(9)*, 2003, 865-878. Available at http://www.sciencedirect.com.

[7]. Caldeira et al, A portfolio of carbon management options. The Global Carbon Cycle: Integrating Humans, Climate and the Natural World – *Scientific Committee on Problems of the Environment*, *62,* 2004, 103.

[8]. Millstein & Harley, Revised estimates of construction activity and emissions: Effects on ozone and elemental carbon concentrations in southern California, *Journal of atmospheric environment, 43(40)*, 2009, 6328-63335. Available at http://www.sciencedirect.com. Accessed on 07/07/2010.

[9].   Rehan & Nehdi, Carbon dioxide emissions and climate change: policy implications for the cement industry, *Journal of environmental science and policy*, 8(2), 2005, 105-114. Available at http://www.sciencedirect.com . Accessed 23/06/2010.

[10].   Zegras, As if Kyoto mattered: the clean development mechanism and transport, 2006. Available at http://web.mit.edu/czegras/www/Zegras_CDM%26Transport.pdf.

[11].   Pickvance, The construction of the UK sustainable housing policy and the role of pressure group, 2007. Available at http://www.informaworld.com /smpp/content~content= a909961596 . Accessed on 11/07/2010.

[12].   World Bank, Nigeria: Carbon Credit Development for Flare Reduction Projects guidebook, 2006.. Available at http://siteresources.worldbank.org /EXTGGFR/ Resources/Nigeria GGFRGuidebook_ICF.pdf. Accessed on 30/06/2010.

[13].   Dayo, Clean energy investment in Nigeria- the domestic context, 2008. Available at http://www.iisd.org/pdf/2008/cei_nigeria.pdf . Accessed on 13/07/2010

[14].   Nigeriancan, Carbon market and clean energy investment opportunities in Nigeria executive summary, 2010. Available at http://www.nigeriacan.org/web/ download /_1272449759.pdf. Accessed on 13/07/2010.

[15].   UNEP, Sub-Sahara African CDM projects, 2008. Available at http://www.unep.org/pdf/ Sub-SaharanCDMProject-List.pdf. Accessed on 13/07/2010.

[16].   Smith et al, Construction industry mass balance: resource use, wastes and emissions, 2002. Available at http://www.massbalance.org/downloads/projectfiles/1406- 00112.pdf . Accessed on 06/07/2010.

[17].   Spence & Mulligan, Sustainable development and the construction industry, *A journal of habitat international*, *19(3)*, 1995, 279-292. Available at http://www.sciencedirect.com. Accessed on 05/07/2010.

[18].   Uher, Absolute indicators of sustainable construction, 1999. Available at http://www.rics.org/site/downloadfeed.aspx?fileID=1847&fileExtension=PDF. Accessed on 06/07/2010.

[19].   Dantata, General overview of the Nigerian construction industry, 2008. Available at http://hdl.handle.net/1721.1/44272.

[20].   Winiwater & Rypdal, Assessing the uncertainty associated with national greenhouse gas emission inventories: A Case study for Austria, *Journal of atmospheric environment*, 35(32), 2001, 5425 - 5440. Available at http://www.sciencedirect.com. Accessed on 07/07/2010.

[21].   BIS, Low Carbon Construction -Innovation & Growth Team, 2010. Available at http://www.bis.gov.uk/assets/biscore/business-sectors/docs/10-671-construction-igt-emerging-findings.pdf

[22].   Fagbeja, Applying remote sensing and GIS techniques to air quality and carbon management – a case study of gas flaring in the Niger Delta, 2008. Available at http://www .uwe.ac.uk/aqm/files/PROGRESSION%20REPORT%20PART%201.pdf. Accessed on 13/07/2010.

[23].   NAIEI (2010). UK greenhouse gas inventory, 1990 to 2008. Annual report for submission under the Framework Convention on Climate Change. Available at http://www.airquality.co.uk/reports/cat07/1005070919_ukghgi-90-08_main_ chapters_Issue3_Final.pdf. Accessed on 05/07/2010.

[24].   OECD (2007). Climate change and Africa. Available at http://www.oecd.org/dataoecd /17/20/39921733.pdf . Accessed on the 02/07/2010.

[25].   FOEI, Gas flaring in Nigeria: a human rights, environmental and economic monstrosity, 2005. Available at http://www.foe.co.uk/resource/reports/gas_flaring_nigeria.pdf.

[26].   Aluko & Oyebode (2006). Nigeria. Environmental policy and its enforcement. Available at http://www.iclg.co.uk/khadmin/Publications/pdf/746.pdf.

[27].   Paehler, 2007. Nigeria in the dilemma of climate change. Available at http://www.kas.de/proj/home/pub/33/2/dokument_id-11468/index.html

[28].   DEFRA (2010). Guidelines to DEFRA/DECC,s greenhouse gas conversion factors for company reporting Available at http://www.defra.gov.uk/environment/business/ reporting/conversion-factors.htm.

[29].   Cole, Carbon emissions benchmarking for public sector supply chain Companies, 2003. Available at http://www.uea.ac.uk/env/all/teaching/eiaams/pdf_dissertations/2003/Cole_Peter.pdf. Accessed on 30/06/2010.

[30].   UNFCCC, The UK's Fifth National Communication under the United Nations Framework Convention on Climate Change, 2009. Available at http://unfccc.int/files/_ national_reports/annex_i_natcom/submitted_natcom/application/pdf/gbr_nc5.pdf. Accessed on 05/07/2010.

[31].   C. Paton, Can South Africa really reduce its carbon footprint by 34%?. 2010. Available at http://www.tshikululu.org.za/thought-leadership/can-south-africa-really-reduce-its-carbon-footprint-by-34/. Accessed on 25/08/2010.

[32].   G. Nisbeth, Building green thinking in South Africa, 2010. Available at http://www. gbcsa.org.za/system/data/uploads/resource/76_res.pdf. Accessed on 25/08/2010.

Research Paper   Open Access

3D finite element modeling of chip formation and induced damage in machining Fiber reinforced composites

R. El Alaiji[1, 2], L. Lasri[1], A. Bouayad[2]

[1](Département Génie Mécanique et Structures, ENSAM/ Université My Ismail, Maroc)
[2](Département Matériaux et Procédés, ENSAM/ Université My Ismail, Maroc)

ABSTRACT: *With the increasing demand for composite materials in many applications such as aerospace and automotive, their behavior needs to be thoroughly investigated, especially during and after failure. In the present work a three-dimensional (3D) finite element (FE) model is developed to study the machining of unidirectional (UD) carbon fiber reinforced polymer composite (CFRP). Chip formation process and ply damage modes such as matrix cracking, fiber matrix shear, and fiber failure are modeled by degrading the material properties. The 3D Hashin failure criteria are used and implemented in the commercial finite element program Abaqus, using a VUMAT subroutine. The objective of this study is to understand the 3D chip formation process and to analyze the cutting induced damage from initiation stage until complete chip formation. The effect of fiber orientation on cutting forces is investigated. The numerical results have been compared with experimental results taken from the literature and showing a good agreement.*

Keywords - *Chip formation, composites, finite element analysis (FEA), machining, modeling.*

I.   INTRODUCTION

In recent years, the application of composite materials has increased in various areas of science and technology due to their special properties, namely for use in the aircraft, automotive, defense, aerospace and other advanced industries. These materials are characterized by the high mechanical properties (strength, stiffness, etc.), light weight and good damage resistance over a wide range of operating conditions, making them an attractive option in replacing conventional materials for many engineering applications. Although the components are usually made near-net-shape, achieving dimensional and assembly specifications of the workpiece requires cutting operations such as milling [1] and drilling [2]. However, machining composite materials is quite a complex task owing to its heterogeneity, and to the fact that reinforcements are extremely abrasive. It has been shown that the machining could cause various damages, such as matrix cracking, fiber-matrix shearing, and fiber breakage. That is why the development of knowledge on the composite behavior is considered as a challenging task to manufacturing engineers.

The methods used in studying the machining of composites have been diverse, and the investigations can be generally divided into three categories: experimental studies focusing on the macro/microscopic machinability of composites, simple modeling using conventional cutting mechanics, and numerical simulations that treat a composite as a macroscopically anisotropic material or concentrate on the reinforcement–matrix interaction microscopically.

The study done by Koplev et al. [3, 4] is considered as one of the first real attempts at understanding the machining behavior of fiber reinforced composites. They conducted experimental studies on the orthogonal cutting of carbon fiber-reinforced polymer composites (CFRP). Two important results were observed: the chip formation mechanism was a series of fractures observed in the fibers and a rougher surface was observed for 90° fiber orientation samples as compared to 0° fiber orientation. Similar observations were later made by several authors [5-9]. All these authors observed that the chip formation is highly dependent on the fiber orientation.

The direct experimental approach to study machining processes as outlined above is expensive and time consuming. So, numerical simulation and theoretical modellings can be very helpful to characterize and simulate the cutting process. Amongst the numerical procedures, the finite element method (FEM) has been the most effective. Numerous numerical modeling studies have been conducted on orthogonal machining of

composite materials. Arola and Ramulu [10] and Arola et al. [11] analyzed orthogonal cutting of unidirectional fiber-reinforced polymer composites using the finite element method. They used a dual fracture process to simulate chip formation incorporating both the maximum stress and Tsai-Hill failure criteria. The obtained cutting forces were found in good agreement with experimental values. However, the thrust forces remain very low and far from those obtained experimentally. Other authors such as Mahdi and Zhang [12] also proposed a 2D cutting force model with the aid of the finite element method. These authors have shown the influence of the fiber orientation on the cutting forces. The obtained results are satisfactory compared with experimental measurements. Rao et al. [13] developed a three-dimensional macro-mechanical finite element (FE) model to study the machining response of unidirectional (UD) carbon fiber reinforced polymer composites. It was found that the cutting force increases with fiber orientation and depth of cut but is less influenced by rake angle. Lasri et al. [14] have used a FEM approach and homogeneous equivalent material (HEM) to study the orthogonal cutting of unidirectional Glass Fiber Reinforced Polymer (GFRP) composites. Their model takes into account the concept of the stiffness degradation and three failure criteria have been considered: Hashin, Maximum Stress and Hoffman criterion to study the mechanisms of chip formation, machining forces and induced damage. These criteria have been implemented in a 2D numerical model using a User-Defined Field Variables (USDFLD) subroutine [15]. In their study, the authors obtained valid cutting forces but the thrust forces remain lower than those obtained experimentally. Recently Zenia et al. [16] developed a 2D finite element model to analyze the chip formation process and subsurface damage when machining the unidirectional CFRP composites (carbon fiber reinforced polymer). Their approach is based on combined elastoplastic–damage model taking into account the stiffness degradation of mechanical properties in the material response. The obtained results in terms of the chip formation process, prediction of cutting forces and induced damage are satisfactory compared with experimental measurements.

The objective of this study was, therefore, to develop a 3D finite element model to analyze the physical mechanisms responsible of the chip formation process, to predict the cutting forces and to simulate the cutting induced damage.

II. FINITE ELEMENT MODEL
2.1. GEOMETRY AND BOUNDARY CONDITIONS

Experimental studies in composites cutting are expensive and time consuming. Moreover, their results are valid only for the experimental conditions used and depend greatly on the accuracy of calibration of the experimental equipment and apparatus used. An alternative approach is numerical methods. FEM is the most frequently used to predict the machining response of metals and composites. The goal of finite element analysis (FEA) is to predict the various outputs of the machining process as the cutting force, stresses, chip geometry. In this study a 3D finite element model was developed using the commercial software Abaqus/Explicit v6.11. It consists of a three-dimensional orthogonal cutting model (Fig.1). It only takes account of the area near the edge radius of the tool ($1500\,\mu m * 1500\,\mu m * 1500\,\mu m$). The cutting tool is assumed to be in contact with the proportion of a workpiece inclined according to the fiber orientation θ [11, 17]. The machined material is carbon fiber reinforced polymer composites. The properties used during FE simulation is adapted from [13] and are listed in Table 1.

Concerning the boundary conditions, the workpiece is fixed while the cutting tool moves. The under edge of the workpiece is constrained against horizontal and vertical displacements ($u_x = u_y = 0$). The displacements of extreme left side are also restrained ($u_x = 0$) in the cutting direction. The cutting tool is modeled as a rigid body with geometry defined by the rake and clearance angles (α and γ) and tool nose radius r_ε. A reference point was defined to control the movement of Cutting Tool against the workpiece. The elements employed are eight-node brick elements (C3D8R). Mesh convergence tests were conducted and finally, fine mesh is used in the vicinity of the contact zone between the tool and workpiece while coarse meshes are used elsewhere. The element size employed in the in fine mesh domain is around $5\,\mu m * 5\,\mu m * 5\,\mu m$ and $30\,\mu m * 30\,\mu m * 30\,\mu m$ in the extreme sides and bottom of the workpiece.
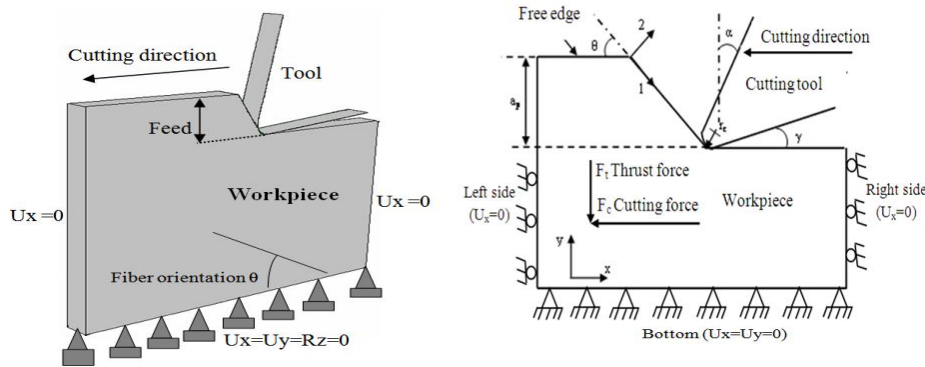
Figure 1: Schematic view of the3D orthogonal cutting model showing the tool geometry and composite workpiece. θ is the fibre orientation, α the tool rake angle, γ the flank angle and r_{ε} the tool nose radius. (123) is the principal material system, a_p being the depth of the cut

2.2 COULOMB FRICTION

Friction at the tool–chip interface is a very complex process. One of the methods is to experimentally obtain the coefficient of friction and apply it as a constant over the tool–chip contact length. In most studies, the Coulomb friction model is used in machining simulations: The Coulomb friction law and Tresca shear stress limit to model the sticking and sliding conditions at the tool–chip interface. In the study by Pramanik et al. [18], the friction at the tool–chip interface was controlled by a Coulomb limited Tresca law, which is expressed by Eqs. (1) and (2).

$$\tau = \mu\sigma_n \qquad (1)$$

$$|\tau| \le \tau_{\lim} \qquad (2)$$

Where $\tau_{\lim}$ is the limiting shear stress, τ is the equivalent shear stress, μ is the friction coefficient and σ_n is the normal stress (contact pressure). For the present study, the coefficient of friction between the tool-work interface was taken as a constant value of 0.3, however, it is understood that with higher fiber orientation this coefficient of friction will not remain constant and can vary with normal load or machining speed.

Elastic properties of UD-CFRP composite	
Longitudinal modulus: E1 (GPa)	147
Transversal modulus: E2(GPa)	10.3
Transversal modulus: E3(GPa)	10.3
Shear modulus in 1-2 plane: G12 (GPa)	7
Shear modulus in 2-3 plane: G23 (GPa)	3.7
Shear modulus in 1-2 plan: G12 (GPa)	7
Poisson's ratio: υ_{12}	0.27
Poisson's ratio: υ_{23}	0.54
Poisson's ratio: υ_{13}	0.27
Ultimate strength (MPa)	
Longitudinal tensile strength: Xt	2280
Longitudinal compressive strength: Xc	1725
Transverse tensile strength: Yt	57
Transverse compressive strength: Yc	228
Tensile strength across the fiber direction : Zt	57
Compressive strength across the fiber direction : Zc	228
Shear strength in 1-2 plane: Sxy	76
Shear strength in 2-3 plane: Syz	52
Shear strength in 1-3 plane: Sxz	46

Table 1 : Mechanical properties of the CFRP composite used in the model [13].

2.3 HASHIN 3D FAILURE CRITERIA

Failure modes in unidirectional fiber composites are strongly dependent on ply orientation, loading direction, specimen geometry. There are four basic modes of failure that occur in a composite structure. These failure modes are; matrix cracking, fiber-matrix shearing, fiber failure, and delamination. Delamination failure, however, is not included in the present study.

The onset and the type of the failure can be predicted using different theories published by different authors; a general overview of failure theories is reported in [19]. Several authors used the 2D Hashin criteria to predict failure during machining FRP composites [14, 17]. From their works it was concluded that 3D failure criteria would be needed when 3D out of plane components of the stress are important. In the present work, 3D Hashin criteria have been chosen to produce the various induced damages responsible for chip formation.

The 3D Hashin criteria are summarized below.

- Matrix tensile cracking can result from a combination of transverse, σ_{22}, and shear stress, σ_{12}, σ_{13} and σ_{23}. The failure index can be defined in terms of these stresses and the strength parameters Y and S. when the index, e_m, exceeds unity, failure is assumed to occur. Assuming linear elastic response, the failure index has the form:

$$e_m^2 = \left(\frac{\sigma_{yy}}{Y_t}\right)^2 + \left(\frac{\sigma_{xy}}{S_{xy}}\right)^2 + \left(\frac{\sigma_{yz}}{S_{yz}}\right)^2 \quad \text{for } \sigma_{22} \geq 0$$

- Matrix compressive failure occurs due to a combination transverse compressive stress and shear stress. The failure criterion has the same form as that for matrix tensile cracking:

$$e_m^2 = \left(\frac{\sigma_{yy}}{Y_c}\right)^2 + \left(\frac{\sigma_{xy}}{S_{xy}}\right)^2 + \left(\frac{\sigma_{yz}}{S_{yz}}\right)^2 \quad \text{for } \sigma_{22} \prec 0$$

Where Y_t is the strength perpendicular to the fiber direction in tension, Y_c is the strength perpendicular to the fiber direction in compression, and S_{xy}, S_{yz} are the in-plane shear and transverse shear strengths, respectively.

- Fiber matrix shearing failure result from a combination of axial stress (σ_{11}) and the shear stresses. The Failure criterion has the form:

$$e_{fs}^2 = \left(\frac{\sigma_{yy}}{X_c}\right)^2 + \left(\frac{\sigma_{xy}}{S_{xy}}\right)^2 + \left(\frac{\sigma_{xz}}{S_{xz}}\right)^2 \quad \text{for } \sigma_{11} \prec 0$$

- Fiber tensile failure

$$e_f^2 = \left(\frac{\sigma_{xx}}{X_t}\right)^2 + \left(\frac{\sigma_{xy}}{S_{xy}}\right)^2 + \left(\frac{\sigma_{xz}}{S_{xz}}\right)^2 \quad \text{for } \sigma_{11} \geq 0$$

- Fiber compressive failure

$$e_f^2 = \left(\frac{\sigma_{xx}}{X_c}\right)^2 \quad \text{for } \sigma_{11} \prec 0$$

Where X_t is the tensile strength along the fiber direction X_c is the compressive strength along the fiber direction.

2.4 PROGRESSIVE FAILURE AND MATERIAL DEGRADATION

PFA are based on two main ingredients: failure criteria to be checked locally, i.e., in each Gauss point of the FE mesh, and a degradation rule, to be applied once the failure criterion is satisfied in some points. The Hashin criteria are the most used in PFA. The degradation rules usually are applied once a damage mode is activated on the basis of a local failure criterion; they basically consist in the reduction of appropriate components of the stiffness matrix. Most frequently sudden, brittle degradation is imposed, i.e., stiffness components are reduced to zero. After the stiffness components have been reduced, the stresses are recalculated with the new global stiffness and then the load is again increased. Kutlu and Chang [20, 21] have applied Hashin's failure multimode criterion; subsequently the local properties are reduced according to the failure type predicted by the failure criterion.

The sudden reduction of stiffness properties can sometime give problems of convergence, in other words it is difficult to reachieve equilibrium after sudden degradation. To overcome the above difficulty some authors adopt a gradual reduction (see Fig. 2), a reduction factor β has been introduced. The degraded material properties (see Table 2) are calculated by multiplying the original value with the reduction factor β.
A typical scheme for the progressive failure analysis is illustrated in Fig. 3.
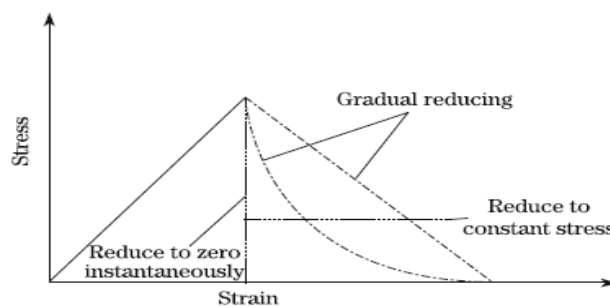
Figure 2 Properties degradation behavior in damage composite
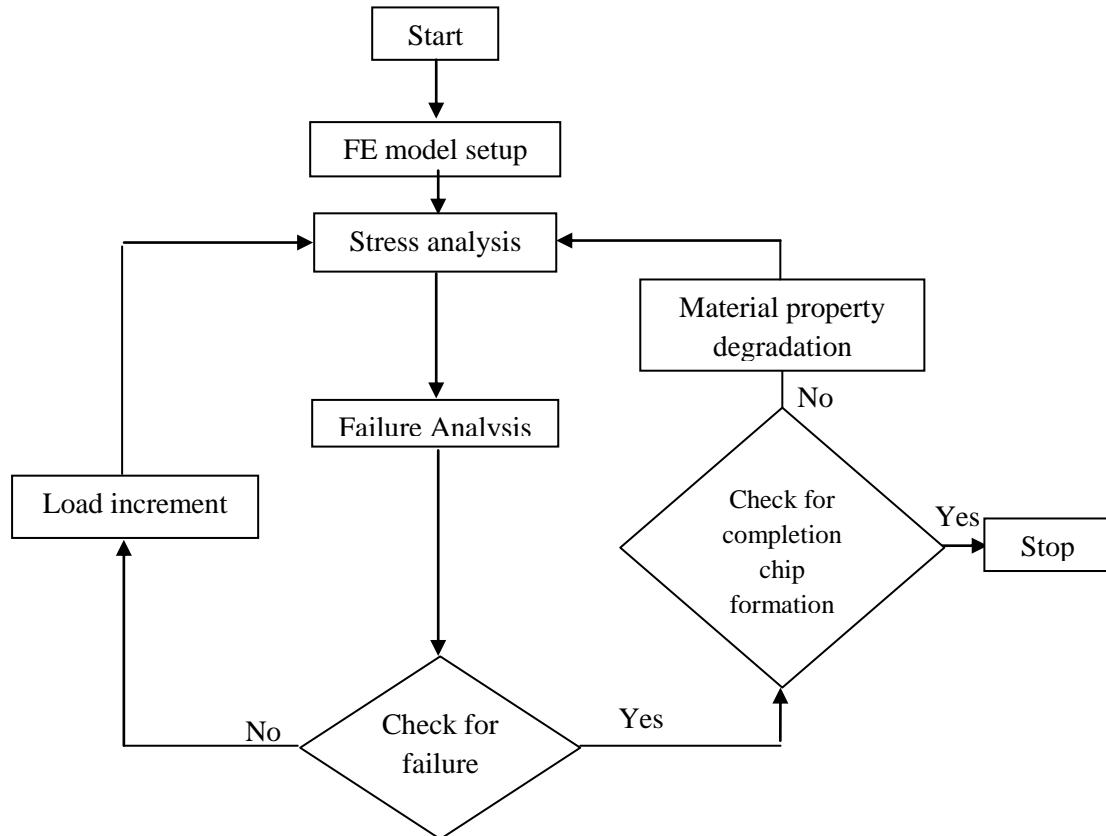
Figure 3 Progressive damage algorithm

2.5 VUMAT SUBROUTINE

The experimental observations conducted by several authors like Koplev [3,4] and Wang et al. [7] showed that composite chips are formed through a series of brittle fractures under high mechanical loading. Consequently, we consider in this work that during machining process, a brittle behaviour dominates during the chip formation process. To analyze the later, the progressive failure analysis has been implemented in Abaqus using the subroutine VUMAT, written in FORTRAN. The VUMAT subroutine (user-defined material model for Abaqus/Explicit) allows the use of solution defined variables, noted SDV [15]. To simulate the fractures responsible of the chip formation process, the elastic properties are made to be dependent on three solution variables, SDV 1, SDV 2, and SDV 3. The first solution variable represents the matrix failure index, the second the fiber-matrix shearing failure index, and the third the fiber failure index.

As depicted in Fig. 3, at the beginning of the analysis, the solution defined variables are set equal to zero in all integration points and the material properties are equal to their initial values. Then, the tool advancement generates an increased mechanical loading. For each displacement increment, several iterations are needed before the simulation converges to an equilibrium state. At the end of each increment, stresses and failure indices are computed at the integration points of each element. If the failure index exceeds 1, the associated user-defined field variable SDV is set equal to 1 and remains at this value until the end of the process, the material properties are automatically degraded, see Table 2. The procedure is repeated until the complete chip formation.

Failure modes	Associated solution defined variable	Reduced material properties
Matrix tensile failure ($\sigma_{22} \geq 0$)	SDV1	$E_2, \upsilon_{12} \to 0$
Matrix compressive failure ($\sigma_{22} \prec 0$)	SDV1	$E_2, \upsilon_{12} \to 0$
Fiber matrix shearing failure ($\sigma_{11} \prec 0$)	SDV2	$\upsilon_{12}, G_{12}, G_{13} \to 0$
Fiber tensile failure ($\sigma_{11} \geq 0$)	SDV3	$E_1, E_2, E_3, \upsilon_{12}, \upsilon_{23}, \upsilon_{13}, G_{12}, G_{23}, G_{13} \to 0$
Fiber compressive failure ($\sigma_{11} \prec 0$)	SDV3	$E_1, E_2, E_3, \upsilon_{12}, \upsilon_{23}, \upsilon_{13}, G_{12}, G_{23}, G_{13} \to 0$

Table 2 Hashin criteria with five modes and associated degradation rules.

III.   NUMERICAL RESULTS

3.1 CHIP FORMATION PROCESS

As said before, the chip formation has been considered completed when both fiber matrix shearing(interface debonding) reaches the free workpiece surface, and the fracture of the fiber(primary fracture) is verified and attached with interface debonding .

Fig. 4 shows failure modes responsible of the chip formation process for the fiber orientation of 30°, rake angle of 10°, clearance angle of 6°, depth of cut of 200μm and tool nose radius of 50 μm at different tool advancement stage. SDV1, SDV2 and SDV3 indicate the matrix cracking mode, the fiber matrix shearing mode (interface debonding) and the fiber fracture mode, respectively.

It can be seen that at the beginning of the process, damage is originated at the chip/tool contact at the zone close to the cutting edge radius. Matrix cracking and fiber matrix shearing occur first and followed by fiber fracture. Damage of different components propagates until the complete chip formation. The progression damage at the matrix and the interface occurs in the parallel direction to the fiber axis. The fiber fracture can also be observed localized in a plane with a specific direction.

The predicted damages are very similar to the primary and secondary fracture previously reported by Wang et al. [7] and Arola et al. [10, 11]. The ruptures that were represented in the model by SDV3 and SDV2 were found to be consistent with the primary and secondary fracture planes, respectively. The primary fracture is defined by fibers fracture, while the secondary fracture is defined by interface debonding. From many experimental data, it was found that the nature of the chip formation largely depends on the fiber orientation Wang et al. [7], Arola et al. [8], Rao et al. [13] and Zitoune et al. [22], for this reason other simulations have been performed to show the effect of the fiber orientation on the chip formation process. Fig.5 shows the damage mode responsible for the chip formation for the case of fiber orientation between 15° and 75°. It can be

seen that all failure modes (matrix cracking, fiber matrix shearing and fiber failure) initiated near the tool nose. as and when as the tool advances into the work material, fiber matrix shearing (sdv2) and matrix cracking (sdv1) propagate in the parallel direction to the fiber axis. However, the fibers fracture (sdv3) propagates in a plane with a specific direction, which fiber orientation dependent. These results are in good agreement with the experimental observations of Iliescu et al. [23], Arola et al. [10], and Wang et al. [7]. Another important point of this work concerning the plane of primary fracture (fibers fracture) can be highlighted.

(a) initiation state

(b) propagation state

(c) complete chip formation
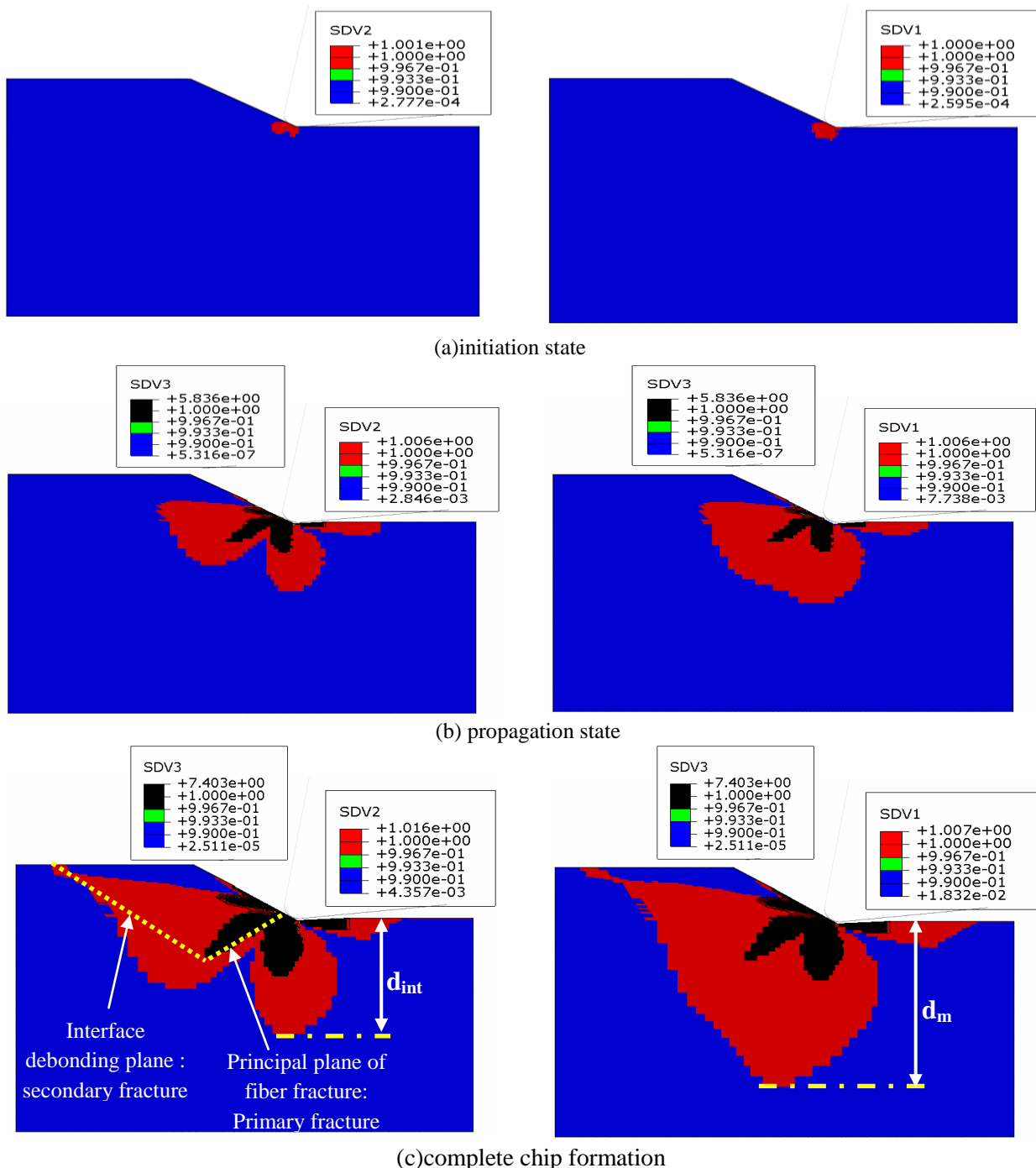
Figure 4: Damage modes responsible of the chip formation process when the fiber orientation is kept equal to $30\circ$. (a) Initiation stage. (b) Propagation stage. (c) Chip formation completed. The cutting conditions are: $\alpha = 10°$, $\gamma = 6°$, $a_p = 200\,\mu m$, $r_\varepsilon = 50\,\mu m$. SDV1, SDV2 and SDV3 indicate matrix cracking mode, fiber–matrix shearing or interface debonding mode, and fiber fracture mode, respectively. d_m and d_{int} represent the depth of the damaged zone in the matrix and at the interface, respectively.

(a) θ=15°

(b) θ=30°

(c) θ=45°

(d) θ=60°

(e) θ=75°
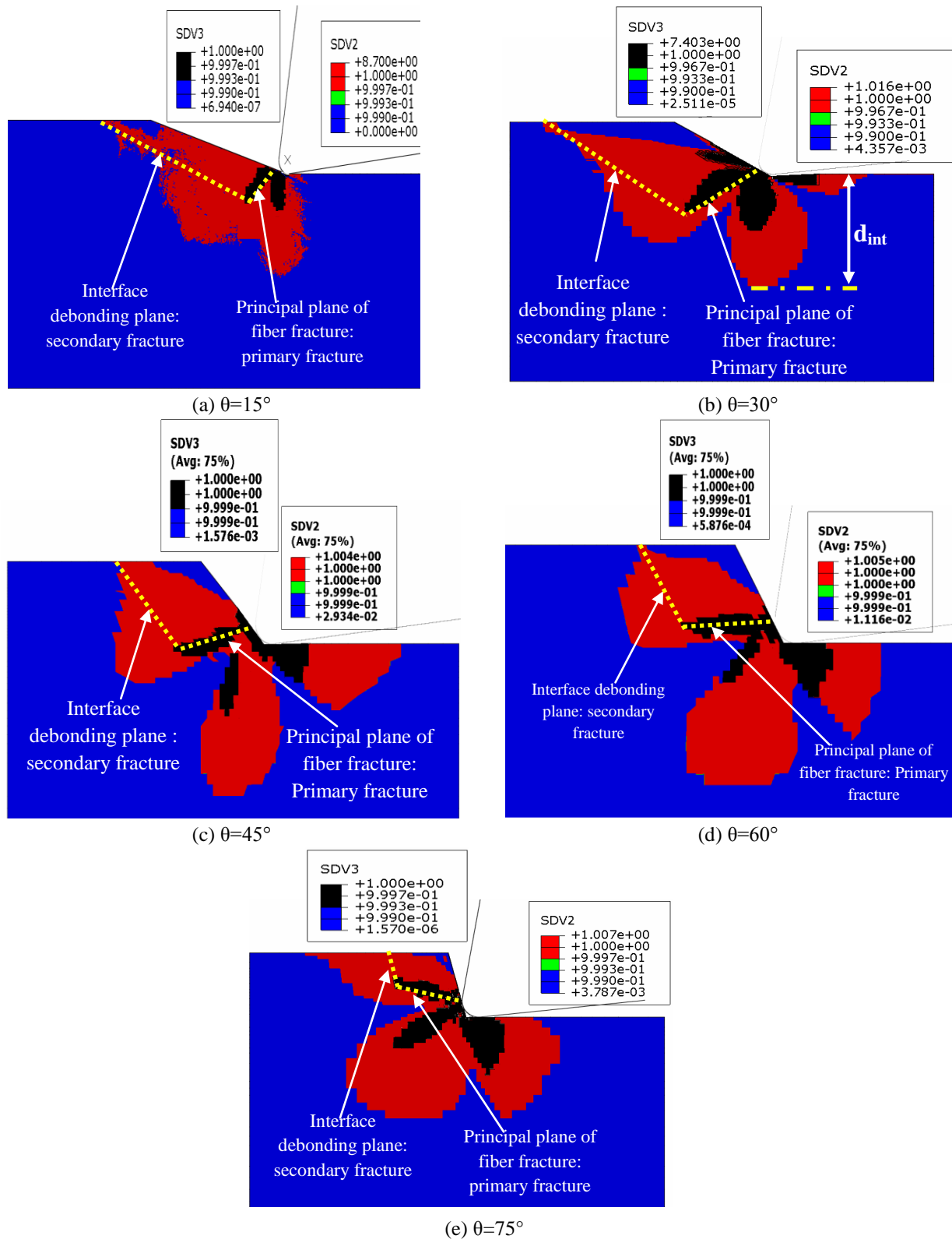
Figure 5: Chip formation process and damage mechanisms predicted by the 3D finite element model with respect to the fiber orientation. The cutting conditions are: $\alpha = 10°$, $\gamma = 6°$, $a_p = 200\,\mu m$, $r_\varepsilon = 50\,\mu m$.

3.2 CUTTING FORCES

In order to validate the 3 finite element model, the reaction forces on the cutting tool from simulations were compared to cutting forces from experimental data presented by Rao et al. [13]. Cutting forces are calculated at each increment of time during the displacement of the cutting tool following the cutting direction.

From a comparison of the experimental and numerical results in Fig. 6(a) it was found that the trend in principal cutting force with fiber orientation obtained from the finite element model agreed very well with experimental results. They increase significantly with increasing fiber orientation. The minimum cutting force occurred in the cutting of 15° unidirectional material.

Thrust forces from the numerical model were an order of magnitude lower than experimental values as evident in Fig.6(b) They increase gradually up to 45° fiber orientation and then decrease slowly till 75° fiber orientation. This can be explained by the use of HEM, and by the bouncing back phenomenon described by Wang and Zhang [24] and which not taken into account in this work.
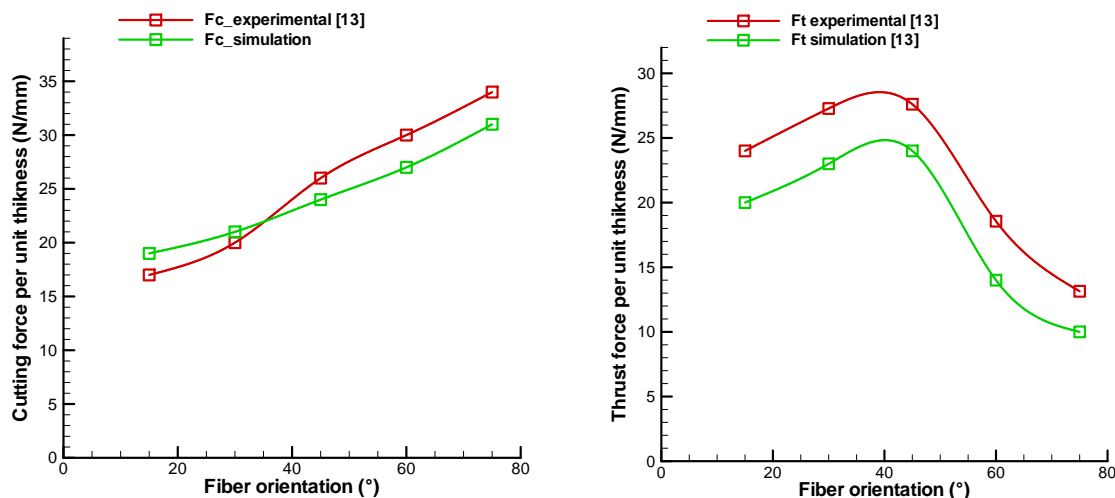
Figure 6: variation of machining forces with fiber orientation. (a) Cutting force, (b) Thrust force. The cutting conditions are: $\alpha = 10°$, $\gamma = 6°$, $a_p = 200\,\mu m$, $r_\varepsilon = 50\,\mu m$.

3.3 INDUCED SUBSURFACE DAMAGE

Several types of damage are introduced during the machining operations, one of the most important results of this study is to predict the subsurface damage such as matrix cracking (SDV1), fiber matrix debonding (SDV2) induced by the cutting process, and to analyze its interaction with the fiber orientation. The failure index contours defined by SDV's contours display the damaged zones. Fig.4(c) shows an example of the predicted subsurface damage obtained, in the case of 30° fiber orientation, in the matrix and at the interface. d_m and d_{int} represent the depth of subsurface damage in the matrix and at the interface, respectively. Fig.7 shows variation of subsurface damage with fiber orientation. The damage tends to increase with the advancement of the tool in the machined material.
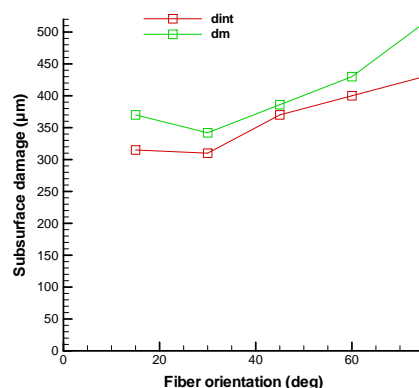
Figure 7: variation of subsurface damage with fiber orientation. d_{int}, d_m indicate damage in matrix and damage in interface, respectively. The cutting conditions are: $\alpha = 10°$, $\gamma = 6°$, $a_p = 200\,\mu m$, $r_\varepsilon = 50\,\mu m$.

IV.   CONCLUSION

A 3D finite element progressive failure analysis was developed for chip formation in 3D orthogonal machining of unidirectional fiber reinforced plastics for fiber orientation 15deg ≤ θ ≤ 75deg. The progressive failure analysis includes matrix cracking, fiber matrix debonding and fiber breaking. The mode was verified from a comparison of cutting forces with experimental results taken from the literature. The following conclusions are drawn:

(i)   matrix cracking and fiber matrix debonding are firstly detected and progress along the fiber direction,

(ii)   the fiber fracture occurs later than that of the matrix cracking and the fiber matrix debonding,

(iii)   the damage of different components: fiber, matrix, and fiber matrix interface, then simultaneously progresses until the complete chip formation process,

(iv)   the chip formation process was strongly dependent on fiber orientation,

(v)   The current model can easily predict the induced subsurface damage.

Finally, it is important to include the temperature on the mechanical behavior in order to investigate thermal influence on the damage initiation and its growth. .

REFERENCES

Journal Papers:

[1]   D. Kalla, J. Sheikh-Ahmad and J. Twomeya, Prediction of cutting forces in helical end milling fiber reinforced polymers. Int J Mach Tool Manuf, 50, 2010, 882–891.

[2]   D. Iliescu, D. Gehin, ME. Gutierrez and F.Girot, Modeling and tool wear in drilling of CFRP. Int J Mach Tool Manuf, 50, 2010, 204–213.

[4]   A. Koplev, A. Lystrup and T. Vorm ,The cutting process, chips, and cutting forces in machining CFRP, Composites 14(4), 1983, 371–376.

[5]   H. Takeyama and N. Iijima, Machinability of glassfiber reinforced plastics and applications of ultrasonic machining, Annals CIRP, 37(1), 1988, 93-96

[6]   T. Kaneeda, CFRP cutting mechanism, Trans. North American Manufacturing Research Institute of SME, 19, 1991, 216-221

[7]   D.H. Wang, M. Ramulu, D. Arola, Orthogonal cutting mechanisms of graphite/epoxy composite. Part I: unidirectional laminate, Int J Mach Tools Manuf,35(12), 1995,1623–38.

[8]   D. Arola, M. Ramulu and D.H.Wang, Chip formation in orthogonal trimming of graphite/epoxy, Compos Part A, 27, 1996, 121–33.

[9]   N. Bhatnagar, N. Ramakrishnan, N.K. Naik and R.Komanduri, On the machining of fiber reinforced plastic (FRP) composite laminates, Int J Mach Tools Manuf, 35(5),1995,701–16.

[10]   D. Arola and M. Ramulu, Orthogonal cutting of fiber-reinforced composites: a finite element analysis, Int J Mach Tool Manuf, 39(5), 1997, 597–613.

[11]   D. Arola, M.B. Sultan, M. Ramulu, Finite element modeling of edge trimming fiber-reinforced plastics, Trans ASME J Eng MaterTechnol,124, 2002,32–41.

[12]   M. Mahdi, L. Zhang, A finite element model for the orthogonal cutting of fiber reinforced composite materials, J Mater Process Technol, 113(1–3), 2001,373–377.

[13]   GVG Rao, P. Mahajan and N. Bhatnagar, Three-dimensional macro-mechanical finite element model for machining of unidirectional-fiber reinforced polymer composites. Materials Science and Engineering A, 498, 2008, 142–149.

[14]   L. Lasri, M. Nouari and M. El-Mansori, Modelling of chip separation in machining unidirectional FRP composites by stiffness degradation concept, Compos Sci Technol, 69, 2009, 684–92.

[15]   ABAQUS Documentation for version 6.11-2Dassault systems Simulia; 2011.

[16]   S. Zenia, L. Ben Ayed, M. Nouari and A. Delamézière, Numerical prediction of the chip formation process and induced damage during the machining of carbon/epoxy composites, Int J Mech Sci, 90, 2015, 89-101.

[17]   L. Lasri, M. Nouari, M. El Mansori, Wear resistance and induced cutting damage of aeronautical FRP components obtained by machining, Wear 271, 2011, 2542– 2548.

[18]   A. Pramanik, L.C. Zhang and J.A. Arsecularatne, An FEM investigation into the behavior of metal matrix composites: tool–particle interaction during orthogonal cutting, International Journal of Machine Tools and Manufacture 47, 2007, 1497–1506.

[19]   A.C. Orifici, I. Herszberg, et al., Review of methodologies for composite material modelling incorporating failure. Composite structures 86(1-3), 2008, 194-210.

[20]   Z. Kutlu and F. K. Chang, Composite panels containing multiple through the-width delaminations and subjected to compression: Part I. Analysis. Composites Struct., 31, 1995, 273–296.

[21]   Z. Kutlu and F. K. Chang, Composite panels containing multiple through the-width delaminations and subjected to compression: Part II. Experiments and verification. Composites Struct., 31, 1995,297–314.

[22]   R. Zitoune, F. Collombet, F. Lachaud, R. Piquet and P. Pasquet, Experimental calculation of the cutting conditions representative of the long fiber composite drilling phase, Composites Science and Technology 65, 2005, 455–466.

[23]   D. Iliescu, D. Gehin, I. Iordanoff, F. Girot and M.E. Gutiérrez, A discrete element method for the simulation of CFRP cutting. Compos Sci Technol, 70, 2010, 73–80.

[24]   XM. Wang, LC. Zhang, An experimental investigation into the orthogonal cutting of unidirectional fibre reinforced plastics. Int J MachTools Manuf,43, 2003,1015–22.

Proceedings Papers:

[3]   A. Koplev, Cutting of CFRP with single edge tools, Proc. 3rd Int. Conf. on Composite Materials, Paris, 1980, 1597-1605.

Analysis and evaluation the role of social trust in urban development (Case Study: Zahedan city)

[1]Mohammad Jahantigh, [2*]Gholam Reza Miri, [3]Maryam karimian Bostani

[1]*MSc student in Department of Geography and Urban Planning, College of human science, Zahehan Branch, Islamic Azad University, Zahedan, Iran*
[2*3]*Assistant professor in Department of Geography and Urban Planning, College of human science, Zahehan Branch, Islamic Azad University, Zahedan, Iran*

ABSTRACT: *Social confidence, as an important element of social capital, is one of the pre-conditions of urban development in deferent societies. The main goal of urban development is providing essential needs, improvement of live level, better managing of ecosystems, and some kind of safe future. The target of the current research is surveying the role of social confidence in urban development of Zahedan. The type of the research is corresponding and in order to analyze data the regression model was used. The population in the research include all of the Zahedan citizens and the population of the sample, based on Cochran formula, is 384 people in which individuals were selected randomly. For collecting the data of the research social confidence and urban development questionnaires were used. The questionnaires' reliability was confirmed by Cronbach's Alpha. The questionnaires were distributed among the sample population and then collected. The collected data was analyzed by SPSS.V20 software. The results show that from the perspective of the citizens of Zahedan city, there is a significant positive relationship between social trust and urban development.*

Keywords: *social trust, Urban Development, Development, Zahedan*

I.   INTRODUCTION

Social trust is an important factor in interpersonal, professional and abstract relations in the development of society and it is prerequisite for the formation of social ties and treaties. Social trust is the creator of the cooperation and assistance and only in this case, solving the problems and social obligations will be possible while there are differences. However, studies indicate that a crisis is created in the most important index of social capital that is social trust which requires closer and scientific examination. According to Anthony Giddens, Modern societies rely on the specialized trust systems this means that trust is the key to the relationship between the individual and specialized systems (Giddens, 2005, 52). Since the new surveys also show that the lowest level of trust in society is to technical and professional organizations, this indicates that the level of trust in abstract systems such as economic organizations is low (Azimi and Edrisi, 2007, 10).

Mutual trust allows that Interactions will be flowed in the community widely. So trust is one of the most important compound forces within society. Social trust will influence on the accelerated economic growth, the increase of economic efficiencies prosperity, providing of public benefit, creating of social cohesion and cooperation and coordination, the satisfaction level of life, the stability of democracy and development and health and increasing of life expectancy (Newton, 2002, 3).

By regarding of the importance of trust in society and comprehensive development, this concept was considered in development planning so that it was mentioned in the law of development programs (Mansur, 2005, 144). On the other hand, urban development is one of the concepts that is strongly linked to peoples 'lifestyle in a society and in concrete dimensions, it will be more related to raising the level of public life through the creation of optimal conditions in nutrition, health, employment, education and how to spend leisure time. Therefore, urban development seeks to improve the social, economic and cultural conditions of a society that the strengthening of social capital is needed for its formation. Today, in urban communities with abundant physical, human, economic capital, we're slow in the process of urban development and a lack of social capital is felt (Karkonan Nosratabadi, 2006, 222).

The city of Zahedan with a population of 660,575 people is one of the major cities located in close proximity to both Afghanistan and Pakistan and it is faced with various problems in the direction of development. It seems that we will be able to overcome these problems by moving in the direction of development and by strengthening social foundations of social capital and social trust between the citizens and detects weaknesses and recommend ways to strengthen the trust.

The hypothesis of the research

There is a direct and significant relation between the social trust of citizens and Urban Development.

The history of the research

Adhami and Kavianpour (2010) in an article entitled" the Effect of social factors on social trust in the city of Nour" have concluded that social trust is not as Pirbordio assumed but social trust has moral nature and function.

Divson and Go (2011) have studied trust and focus on the intention of publishing of tacit and explicit knowledge in Chinese companies and argued that the type of knowledge have different levels of effects.

Fukuyama (1999) examined the relationship between social capital and the civil society and in his articles points to the development of the concept of social capital through ((the radius of trust)) and channels of trust.

Kristen and et al (2007) studied the relationship of cooperation, trust, and justice (fairness) as a component of social capital on a number of job characteristics for staff's physical and mental health. They found that the alignment of component of the social capital and trust and justice have a direct and strong relationship with their employees' health. In addition, they found that in organizations that social capital was low; job satisfaction was extremely low, too.

Yajoun Lee and et al (2005) examined the impact of social capital and social trust on quality of life in the United Kingdom. In their analysis of the results, they concluded that the informal channels of social capital are more important in influencing the public perception of trust and quality of life.

Theories social trust

Social trust is one component of social capital that has been an essential element to strengthen cooperation which is achieved through close acquaintance with others in a small community. But in the larger and more complex societies an impersonal trust with an indirect form of trust will be necessary. Fukuyama also knows the trust as an index for social capital within the meaning of the collective values of social networks and cultural ethics that form the foundation of economic growth and stability. From his view, the trust is an expectation that will rise from a society with a regular behavior with friendly relations based on cooperation and participation (Ganji and et al, 2010).

Social capital refers to characteristics of social organization such as networks, norms and trust that makes it easier the coordination and cooperation to achieve mutual benefit (Putnam, 2005, 95).

Urban development:

Urban development is the improvement of living standards in different dimensions in order to achieve a better life for all citizens, So that social, economic, political, structural and environmental stability will be provided. As long as the city does not find the concept of community, the concept of city development will not be realized and may decrease the effectiveness of development components. In the first step, all citizens of a city should demand the growth of the city and resolve the troubles and problems until these components are to be effective. Therefore, collective participation is the infrastructure of the component of urban development and if there is no partnership and common aim for the development, there will be no meaningful development (Mirza Abotalebi, 2006, 9).

The situation of the area under the study

Zahedan is located in the province of Sistan va Baluchestan in southeast of Iran. It is bordering Afghanistan and Pakistan. Zahedan is the center of the province with an area of 5771 hectares and 2000 meters above the sea level. The area which Zahedan is situated on does not have identical topographical features. Hence, many urban problems are associated with the topographic of the region. Zahedan's topographic is mainly influenced by the surrounding mountains and vast plains. According to the detailed plan of the city in 1991, Zahedan was divided into 3 regions, 20 Regions, and 85 localities.

Figure (1): geographical location of Zahedan, Source: search results

II. DISCUSSION AND CONCLUSION

The state of social trust among citizens of zahedan city:

Social trust in this study includes components of fundamental trust, interpersonal trust and a public trust, political trust, institutional trust and confidence is jobs. Table 1 shows the results of the single-sample t-test to check the status of each of the dimensions of social trust.

Table (1): single-sample t test results in relation to the situation of social trust and its components

sig	t	Deviation of Mean	theoretical Mean	Experimental Mean	Variable
0/000	15/10	0/804	3	3/62	Fundamental trust
0/000	36.45	0/556	3	4/09	interpersonal and group trust
0/105	1/62	0/563	3	3/05	Public confidence
0/000	14/33	0/617	3	3/45	Political trust
0/000	-3/93	0/920	3	2/82	Institutional trust
0/000	4/803	0/645	3	3/16	Confidence in Jobs
0/000	15/244	0/456	3	3/35	Social trust

Source: research results

The Study shows that all components of social trust except public trust and institutional trust are in a satisfactory condition with probability of 99% (sig = 0.000, p <0.01) higher than average (experimental Mean more than theoretical mean). As well as public trust has a moderate level because of having the significance level of higher than 0.05 and institutional trust is in undesirable level by a significant level of less than 0.05 and negative t value. In general, due to significant level, the social trust is higher than the average and it is desirable with the possibility of 99%.

The variable situation of the urban development among the citizens of zahedan city

The components of urban development in the research include municipal health system, good government, a sustainable environment, educational structure and the satisfaction and happiness.

Table (2): Results of the one-sample t-test in connection with the urban development and its components

sig	t	Deviation of Mean	theoretical Mean	Experimental Mean	Variable
0.000	-17.56	0.72	3	2.30	Urban health
0.000	-18.66	0.82	3	2.46	The ideal system of government
0.000	-12.64	0.80	3	0.33	Environmental sustainability
0.015	-1865	0.76	3	2.90	Educational structure
0.000	-2.43	0.68	3	2.39	Happiness and joy
0.000	-17.11	0.59	3	2.46	Urban Development

Source: research results

As it is seen in Table 2, the significant level of all components is less than 0.05 and because the value of t for all aspects of urban development is negative so the dimensions of urban development in the city of Zahedan are not desirable.

Also according to the significant level of urban development which is less than 0.05 and the value of obtained t equals to (-17.11), it can be concluded that urban development is not desirable in the city of Zahedan.

Hypothesis testing

There is a direct and significant relation between the social trust of citizens and Urban Development. The results of correlation test for the first hypothesis is specified in Table 3.

Table (3): Pearson correlation test between urban development and social trust

Sig	Pearson correlation coefficient	Independent variable	Dependent variable
0.000	0.647	social trust	Urban Development

Source: research results

According to Table 3, since the significant level for social trust and urban development is less than the obtained 0.01 so, in the level of 99%, there is a significant correlation between social trust and urban development which correlation coefficient between social trust and Urban Development is 0.647 and represents a strong relationship between them. Thus the first hypothesis of the research will be confirmed and from the perspective of the citizens of Zahedan city, there is a significant positive relationship between social trust and urban development.

The significance level is also obtained less than 0.01 between the variable of urban development and six dimensions of social trust so there is a significant correlation between the dimensions of social trust and urban development at the significance level of 99%. As a result of the impact of independent variables on the dependent variable can be examined by using multivariate regression test.

Table (4): Pearson correlation test between urban development and social trust

Sig	Pearson correlation coefficient	Social trust	Dependent variable
0.000	0.422	Fundamental trust	
0.000	0.221	interpersonal and group trust	
0.000	0.284	Public confidence	Urban Development
0.000	0.431	Political trust	
0.000	0.507	Institutional trust	
0.000	0.619	Confidence in Jobs	

Source: research results

To examine multivariate regression test, the correlation between dependent and independent variables should be measured first then if there is any regression equation it should be investigated in fact, the correlation is a prerequisite for multivariate regression test.

As it is determined in Table 5, there is an overall correlation between independent variables of the social trust and the dependent variable of the urban development and this amount equal to R =0.647 and it represents a high direct positive correlation between the variables. Since the coefficient of determination (R2), is equal to 0.419%, this means that the independent variable has been able to explain a total of 41% of the variance of the dependent variable indicating the high influence of social trust on urban development. And also according to the ANOVA table or significant table (Table 5), F-value indicates whether the research regression model is an appropriate model or not. In other words, can the independent variable explain the dependent variable changes well or not? It is possible to detect this case with significant F in Error level of smaller or larger than 0.05. Since F is equal to 275.025 that in level of error of less than 0.05 is significant, indicates that the independent variable has the high power of explaining and is able to explain the changes and variance of the dependent variable. In other words, the research regression model is a good model and helps us to explain changes in the dependent variable based on the independent variable. Since the interpretation of the regression coefficients is done based on the coefficient of (Beta) and since, the relative contribution of each independent variable in the model is determined through this statistic therefore, with respect to the amount of Beta, we can say that social trust is an important factor in predicting urban development.

Table (5): regression coefficients for the impact social trust on the urban development

Subscribe factors(Beta)		ANOVA		Summary Model		Variables
sig	Beta	sig	F	R2	R	
0.000	0.647	0.000	275.025	0.419	0.647	Social trust

Source: research results

Multivariate regression test is shown in Table 6. Due to the significance level for this test has been obtained less than 0.05 (sig = 0.000, p <0.05) then regression equation between the independent variables and the dependent variable can be explained. Since the amount of R2 (coefficient of determination) is about 0.419 for regression equation therefore, the independent variables can explain 49% of the variance of the dependent variable.

Table (6): multivariate regression test results

Subscribe factors(Beta)		Variables	ANOVA		Summary Model	
sig	Beta		sig	F	R^2	R
0.000	0.222	Fundamental trust				
0.019	-0.97	interpersonal and group trust				
0.002	0.123	Public confidence	0.000	60.707	0.491	0.701
0.014	0.114	Political trust				
0.017	0.121	Institutional trust				
0.000	0.436	Confidence in Jobs				

Source: research results

According to the output of the regression test in Table 6 shows that the significant level for each dimension of social trust is less than 0.05 which represents the influence of all dimensions of social trust on urban development and the coefficient of each of these dimensions in the regression equation equals to the value of the specified Beta in table 6.

Based on the above mentioned issues, the regression equation of Social trust variable can be expressed as an equation:

$$y = 0.222x_1 - 0.97x_2 + 0.123x_3 + 0.114x_4 + 0.121x_5 + 0.436x_6$$

X1=Fundamental trust
X2=interpersonal and group trust
X3=Public confidence
X4=Political trust
X5=Institutional trust
X6=Confidence in Jobs

According to the beta coefficients in Table 6, the impact of interpersonal and group trust has the greatest impact on urban development with influence Coefficient of - 0.97, it should be noted that this effect is in the negative direction. The component of political trust from the social trust system components has also the minimal impact (0.114) on the dependent variable of urban development.

III. CONCLUSION

Social trust is one of the most important aspects of human relationship that is the basis for cooperation between members of the community. Social trust will enhance the cooperation in the economic, social, political and cultural fields and will increase the willingness of people to work with different groups of population. Evolution and development of modern human societies from the first manner depends on the complexity, the density of social relationships and interaction that the confidence has fueled its expansion. Urban Management and in its specific meaning, the municipal as one of the social organizations can have a higher efficiency and productivity whenever gain the citizens trust as social and spiritual capital and use it in the direction of the organization and urban development.

According to the above issues it can be said that with the increase of social trust among citizens of Zahedan city, urban development will also increase. It is essential to note that the improvement of social trust component is effective in the improvement of urban development of the city of Zahedan and by improving of these components; the improvement of the development of the city of Zahedan can be created.

Suggestions

- The collaboration of municipal managers with the University to identify the urban problems and resolve them
- The education office should attempt to promote trust and eliminate the mistrust in the community from preschool by publications of books.
- Considering to economic level of society, creating of the conditions for jobs and supporting the right of employers to reduce unemployment to strengthen appropriate government system.
- Encounter decisively with people who cause the loss of social trust and distrust spread in society at any positions which they are.
- Creating of the necessary groundwork for greater participation of people in collaboration to create social religious atmosphere in direction of improving of social partnerships.

REFERENCES

[1]. Adhami. A, Kavianpour. J, (2010), the Effect of social factors on social trust in the city of Nour, Volume 5, Number 2; from page 9 to page 23.
[2]. Azimi. L and Edrisi. A, (2007), Social trust factor for the development of society, Proceedings of the Regional Conference on social capital challenges and strategies, Vice Chancellor for Research of Azad university of Dehaghan.
[3]. Davison, R. M., & Gu, J, (2011). The impact of trust, guanxi orientation and face on the intention of Chinese employees and managers to engage in peerto- peer tacit and explicit knowledge sharing. Information Systems Journal, 21, 557–577.
[4]. Fukuyama, F, (2005), Social capital and civil society, an attempt from Tajbakhsh.K, translated by: Khakbaz. A and Poyan. H, Tehran, Shiraza publication.
[5]. Ganji. M, Sabtelahi. Z and Taheri. Z, (2010), the relationship between religious identity and social capital among the people of the city of Kashan. Applied Sociology, Vol. 21, No. 4: 123-144
[6]. Giddens, A, (2005), global perspectives, translated by Hamidreza Jalaeipour published by the Tarhe Nav publications, Tehran
[7]. Karkonan Nasrabadi. M, (2006), Social capital and civil society, Proceedings of the Regional Conference on social capital challenges and strategies, Vice Chancellor for Research of Azad university of Dehaghan.
[8]. kristensen , T. S. hesle , p. and pejtersen , J, (2007). Organizational social capital and the health of the Employees- two empirical studies from denmark. Isoca, oct, 18-20
[9]. Lee, C. & Chen, W., J, (2005). The effects of internal marketing and organizational culture on knowledge management in the information technology industry", International journal of management, 22 (4), pp. 661-672
[10]. Mansour. J, (2005), The Fourth economic, social, cultural Development Plan of country, Davran publications
[11]. Mirza Abotalebi. A, (2006), Social components of urban development, the daily of Etemad Melli, No. 253, p. 9.
[12]. Newton, K, (2002), Social Trust and Political Disaffection Social Capital and Democracy. Eursco Conference on Social Capital: Exeter
[13]. Putnam, R, (2005), the prosperous society, social capital in public life, an attempt from Tajbakhsh.K, translated by: Khakbaz.A and Poyan.H, Tehran, Shiraza publication.

Research Paper   Open Access

Flow and Diffusion Equations for Fluid Flow in Porous Rocks for the Multiphase Flow Phenomena

[1]Mohammad Miyan, [2]Pramod Kumar Pant
[1]*Department of Mathematics, Shia P. G. College, University of Lucknow, Lucknow, India*
[2]*Department of Mathematics, Bhagwant University, Ajmer, Rajasthan, India*

ABSTRACT: *The multiphase flow in porous media is a subject of great complexities with a long rich history in the field of fluid mechanics. This is a subject with important technical applications, most notably in oil recovery from petroleum reservoirs and so on. The single-phase fluid flow through a porous medium is well characterized by Darcy's law. In the petroleum industry and in other technical applications, transport is modeled by postulating a multiphase generalization of the Darcy's law. In this connection, distinct pressures are defined for each constituent phase with the difference known as capillary pressure, determined by the interfacial tension, micro pore geometry and surface chemistry of the solid medium. For flow rates, relative permeability is defined that relates the volume flow rate of each fluid to its pressure gradient. In the present paper, there is a derivation and analysis about the diffusion equation for the fluid flow in porous rocks and some important results have been founded. The permeability is a function of rock type that varies with stress, temperature etc., and does not depend on the fluid. The effect of the fluid on the flow rate is accounted for by the term of viscosity. The numerical value of permeability for a given rock depends on the size of the pores in the rock as well as on the degree of interconnectivity of the void space. The pressure pulses obey the diffusion equation not the wave equation. Then they travel at a speed which continually decreases with time rather than travelling at a constant speed. The results shown in this paper are much useful in earth sciences and petroleum industry.*

KEYWORDS: Darcy's law, Diffusion equation, Multiphase flow, Porous rock.

I. INTRODUCTION

For discussing the fluid flow in porous media, we discuss firstly about the groundwater. The groundwater systems contain a huge quantity of the fresh water present on earth, providing a repository of water that is necessary for both human society and ecological systems. Many times for groundwater range from hundreds to thousands of years, making it a water source that is largely independent of the seasonal caprices associated with many surface water sources.

Due to primary source of drinking water worldwide, protection of this resource is critical to ensure widespread access to reliable sources of clean water. Instances of groundwater contamination are common, and many can be identified with significant risks to public health. But from long residency times often extend to groundwater contamination and pollutants can be involved with long-term deleterious impacts on contaminated resources. Non-aqueous phase liquids (NAPLs) represent a class of contaminants for which existing remediation strategies are particularly inadequate. NAPL contaminated systems are common, arising from improper disposal of solvents used in industry, leakage of underground storage tanks containing petroleum products, spills and byproducts of refinement and coal gasification [1], [7], [8]. NAPLs are immiscible in water, and most are soluble in trace amounts. Once NAPLs have been introduced into a system contamination can persist for decades or even centuries [12], [13]. The development of useful remediation strategies for these systems has been largely unsuccessful, and standard mathematical modeling approaches used to give the flow behavior for these systems are subject to a number of problems occurring, severely limiting their predictive capability [9], [10]. The in use modeling approaches fail too properly account for multiple fluid phases, and more precise mathematical descriptions are required to analyses risks involved in contamination, advance fundamental understanding of system behavior, and develop remediation strategies related with these systems.

The consideration of porous media within a multi-scale framework is an emerging concept that takes advantage of the more mature state of understanding that applies at smaller length scales as a method to give the description of larger scale systems. Many physical systems can be associated with a series of length scales; each one is associated with a particular mathematical formulation which describes the system behavior at that scale. The multi-scale frameworks give the relationship between these different descriptions, which give a series of mathematical formulations.

When these are applied to porous media the approach can be used to tie macroscopic thermodynamic forms and conservation equations to those that apply at the pore-scale, otherwise known as the micro scale. This is useful when macroscopic closure relationships are unreliable or incomplete; microscopic closure relationships are usually better known. Microscopic simulations can therefore be applied to give insights into macroscopic behavior, judges simplifying assumptions, and generate suitable macroscopic closure relationships. These studies rely heavily on computational methods to give the actual solutions for the microscopic analysis of porous medium flows. The computational analysis gives opportunities to incorporate larger and more realistic details of micro-analysis behavior into macroscopic modeling analysis.

In Germany and many other countries more than half of the population depends on groundwater as their supply in drinking water [4]. The problems with groundwater quality arise from disposal dumps, leaking storage tanks and accidental spills of substances used in industry. For removing these substances from the subsurface are extremely complicated and difficult, if at all possible [6]. In order to design effective remediation methods it is important to understand the governing physical processes of flow and transport in porous media. The mathematical modeling is one of the important methods that help to get the target. Including the more detailed physics and geometric detail into the mathematical models wants the use of efficient numerical algorithms and large scale parallel computers, both are of major concern in this analysis. Among the most toxic and prevalent materials threatening groundwater quality are so called non-aqueous phase liquids (NAPLs) such as petroleum products, chlorinated hydrocarbons etc. These chemicals have low solubility in water and are to be considered as separate phases in the subsurface.
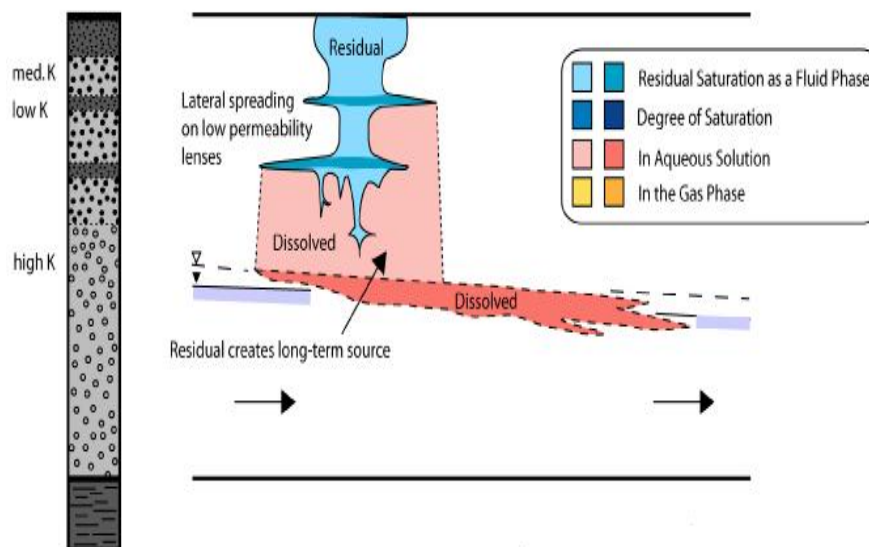
Figure 1 Formation of residual and dissolution

(Source: *Friedrich Schwille, 1988, Lewis Publishers, Chelsea, Michigan*)
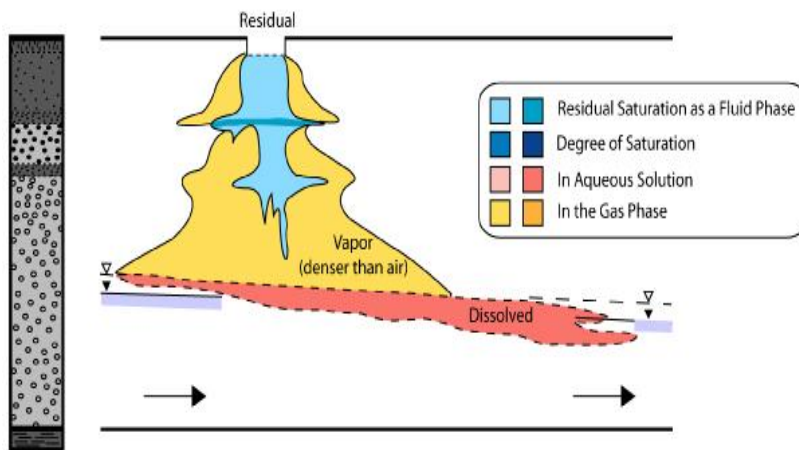
Figure 2 Formation of residual and vapor plume
(Source: *Friedrich Schwille, 1988, Lewis Publishers, Chelsea, Michigan*)
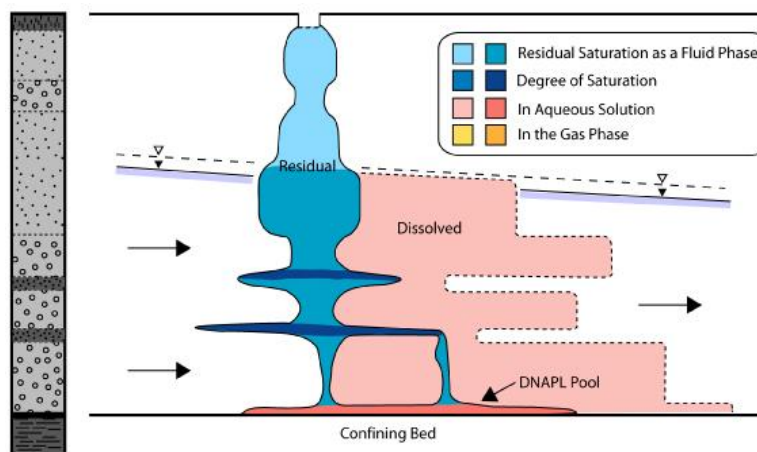
Figure 3 DNAPL below the water table
(Source: *Friedrich Schwille, 1988, Lewis Publishers, Chelsea, Michigan*)
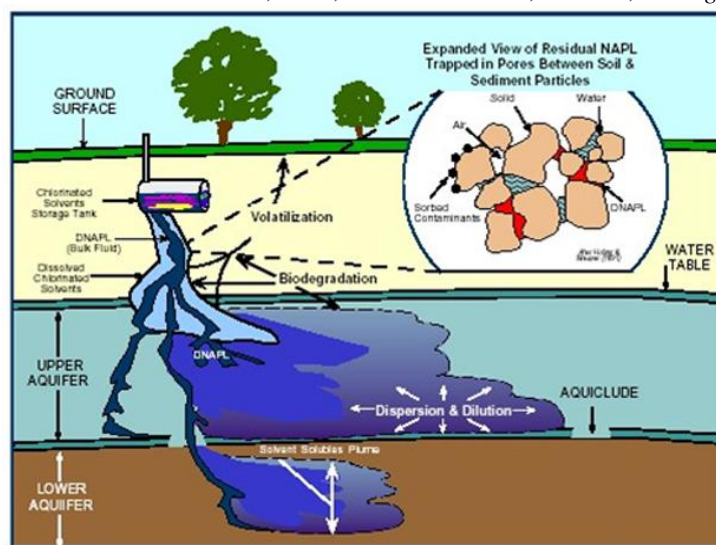
Figure 4 Summary of processes in the DNAPL spill.

(Source: *Pope, D. F., and J. N. Jones, 1999.*

Monitored Natural Attenuation of Chlorinated Solvents.

Report Number EPA/600/F-98/022. Office of Researchand Development,

U.S. Environmental Protection Agency, Washington, D.C. May 1999)
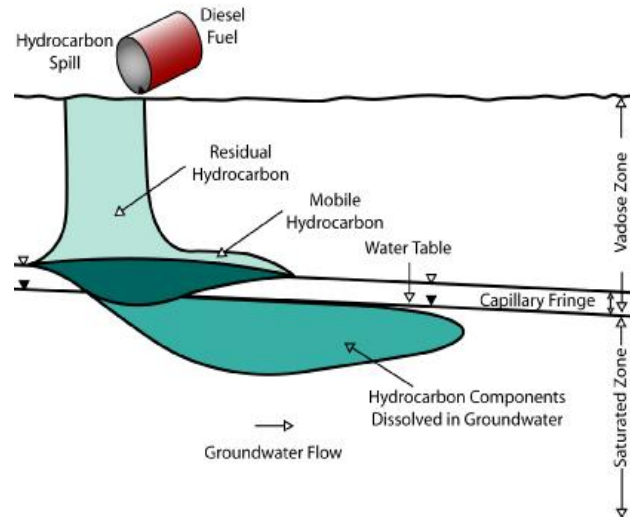
Figure 5 LNAPL behavior at the water table

(Source: *C.W.Fetter, 1992, Contaminant Hydrogeology, Macmillan Publishing Company, New York*)

The above figures taken from different sources illustrate the qualitative flow behavior of different NAPLs in the subsurface. In the case, when a light NAPL (LNAPL) with density smaller than water is released then it migrates downward through the unsaturated zone until it reaches the water table where it continues to spread horizontally. Now, these substances contain volatile components that are then transported in the air phase. When the supply of LNAPL stops, a certain amount of it remains immobile in the soil at residual saturation. The flow of a dense NAPL (DNAPL) is heavier than water and its flow behavior in the unsaturated zone are same. But due to its bigger density it moves downward also through the saturated zone. But due to capillary effects heterogeneities in the soil play an important role in multiphase flows. The regions of smaller pores are not penetrated by the fluid until a critical fluid saturation has accumulated. The size of these regions may variates from centimeters leading to an irregular lateral spreading of the NAPL to meters with the formation of DNAPL pools. The NAPLs give a long term problem to the quality of ground water. The initial infiltration may occur in hours or days while the solution process may occur in years. The small concentrations of NAPL on the order of 10 make the water not suitable for drinking. By the large number of processes mentioned in list it is evident that mathematical modeling of remediation processes can be very difficult. In the simplest example of two phases immiscible flow, the mathematical model is related to two coupled non-linear partial differential equations depend on time. But the detailed geometry of a porous medium is impossible to determine its complicated structure is effectively known by several parameters in the mathematical equations. It is the fundamental problem of all porous medium flow models for finding these parameters. But due to the heterogeneity of the porous medium on different length scales these effective parameters are the scale dependent. The different techniques have been found to address this problem. Here we have mention stochastic modeling [5], upscaling [2] and parameter identification [11].So far we concentrated on groundwater remediation problems as our motivation for the consideration of multiphase fluid flow in porous media. In addition there are other important applications for these models such as oil reservoir exploitation and security analysis of underground waste repositories. The latter application is often complicated by the existence of fractures in hard rock [3].

For flow in porous media, the Darcy's equation has been applied. The Darcy equation is generally based on the principle of a linear relation between the velocity and the pressure gradient in the porous media. The linear factor is expressed as porosity and is representing the resistant to flow in the solid media. The flow process in porous media is governed by several physical phenomena like as viscous forces and the forces coming from surface tensions between solid and fluid, but also surface tensions between different phases of the fluid. The flow process is involved in the principle modeled by use of the momentum equation, but it takes more simulation effort to solve the momentum equation than use the Darcy's equation. For this reason the Darcy's equation is most commonly applied in simulations of fluid flow through porous media.

II. GOVERNING LAWS AND EQUATIONS

The basic law governing the flow of fluids through porous media is Darcy's law, which was formulated by the Henry Darcy in 1856 on the basis of his experiments on vertical water filtration through sand beds. The detailed derivation related to diffusion was given by R. W Zimmerman in 2002 [14]. Darcy found that his data could be described by

$$Q = \frac{C \, A \, \Delta(P - \rho g z)}{L} \tag{1}$$

Where
P = pressure [Pa]
ρ = density [kg/m^3]
g = gravitational acceleration [m/s^2]
z = vertical coordinate (measured downwards) [m]
L = length of sample [m]
Q = volumetric flow rate [m^3/s]
C = constant of proportionality [$m^2/Pa \, s$]
A = cross-sectional area of sample [m^2]

Any consistent set of units can be used in Darcy's law, such as SI units, C.G.S. units etc. But in the oil industry it is common to use "oilfield units", that are inconsistent. The Darcy's law is mathematically same as other linear transport laws, such as Ohm's law for electrical conduction, Fick's law for solute diffusion and Fourier's law for heat conduction. By the fluid mechanics we know that Bernoulli's equation contains the terms:

$$\frac{P}{\rho} - g \, z + \frac{V^2}{2} = \frac{1}{\rho}\left(P - \rho \, g \, z + \rho \, \frac{v^2}{2}\right) \tag{2}$$

where P/ρ is related to the enthalpy per unit mass, $g \, z$ is the gravitational energy per unit mass, $v^2/2$ is the kinetic energy per unit mass. But the fluid velocities in a reservoir are small then the third term can be neglected. And we see that the term ($P - \rho g \, z$) represents a term of energy type. That seems reasonable that the fluid can flow from regions of higher to lower energy so, the driving force for flow must be the gradient of ($P - \rho g \, z$). But due to Darcy's analysis, it has been found that all other factors being equal, Q is inversely proportional to the fluid viscosity. It is therefore suitable to factor out μ, and put $C = k/\mu$, where k is known as the permeability. On taking the volumetric flow per unit area, $q = Q/A$. Now the Darcy's law can be written as:

$$q = \frac{Q}{A} = \frac{k}{\mu}\frac{\Delta(P - \rho g z)}{L} \tag{3}$$

where the flux q has the dimensions of [m/s]. It is perhaps easier to say of these units as [$m^3/m^2 s$].

For transient processes in which the flux varies from the point to point, we can write a differential form of Darcy's law. In the vertical direction, this equation can be written as:

$$q_v = \frac{Q}{A} = -\frac{k}{\mu}\frac{d(P - \rho g z)}{dz} \tag{4}$$

where the suffix v is taken for vertical flow. The minus sign is taken since the fluid flows in the direction from higher potential to lower potential. The differential form of Darcy's law for one-dimensional horizontal flow can be

$$q_h = \frac{Q}{A} = -\frac{k}{\mu}\frac{d(P - \rho g z)}{dx} = -\frac{k}{\mu}\frac{dP}{dz} \tag{5}$$

where the suffix v is taken for vertical flow. In most rocks the permeability k_h in the horizontal plane is different than the vertical permeability, k_v ; in most of the cases, $k_h > k_v$. The permeabilities in any two orthogonal directions within the horizontal plane have the difference. So, in this course we shall generally take: $k_h = k_v$. The permeability is the function of rock type, that varies with stress, temperature etc., but it does not depend on the fluid; the effect of the fluid on the flow rate is accounted for by the term of viscosity in the above equations. The permeability has units of m^2, but in mathematical use it is conventional to use "Darcy" units, defined as:

$1 Darcy = 0.987 \times 10^{-12}$ m$^2 \approx 10^{-12}$ m^2

The Darcy unit is defined such that a rock having a permeability of 1 *Darcy* would transmit 1 c.c. of water with viscosity 1 *cP per second*, through a region of 1 sq. cm. cross-sectional area, if the pressure drop along the direction of flow were 1 *atm per cm*. Many soils and sands that mathematicians must deal with have permeabilities on the order of a few *Darcies*. The original purpose of the "*Darcy*" definition was thus to avoid

the need for using small prefixes such as 10^{-12} etc. But a Darcy is nearly a round number in SI units, so conversion between the two is easy. The numerical value of k for a given rock depends on the size of the pores in the rock, d as well as on the degree of interconnectivity of the void space. So that
$k \approx d^2/1000$

where d denotes the diameter of the pores. The permeabilities of different types of rocks and soils vary over many orders of magnitude. However, the permeabilities of petroleum reservoir rocks tend to be in the range of 0.001-1.0 *Darcies*. So it is convenient to refer the permeability of reservoir rocks in units of "*milliDarcies*" (*mD*), which equal 0.001 *Darcies*. In some reservoirs, the permeability is due mainly to an interconnected network of fractures. The permeabilities of fractured rocks tend to be in the range 1 *mD* to 10 *Darcies*. In a fractured reservoir, the reservoir scale permeability is not closely related to the core scale permeability that anyone can measure it.

If the fluid is in static equilibrium then $q = 0$, so the differential equation will be

$$\frac{d(P - \rho g z)}{dx} = 0 \Rightarrow P - \rho g z = \text{ constant} \qquad (6)$$

If we take $z = 0$ i.e., at sea level, where the fluid pressure is equal to the atmospheric pressure, then we have
$$P_s = P_a + \rho g z \qquad (7)$$
where P_s, P_a represent the static pressure and atmospheric pressure respectively. But we always measure the pressure above the atmospheric pressure, so we can neglect the term P_a in the above equation (7). We can see by comparing equation (7) with equation (4) that only the pressure above and beyond the static pressure given by equation (2) plays a role in driving the flow. So the term $\rho g z$ is useless, as it only contributes to the static pressure and but does not contribute to the driving force for the flow. Then after removing the term, the equation for correct pressure will be
$$P_c = P - \rho g z \qquad (8)$$
Now the Darcy's law in the terms of corrected pressure for the horizontal flow can be written as:

$$q = \frac{Q}{A} = -\frac{k}{\mu}\frac{dP_c}{dx} \qquad (9)$$

Instead of using sea level i.e., $z = 0$, we can take $z=z_0$ as a datum i.e., the amounts of initial oil in place lie above and below $z=z_o$. So we get
$P_c = P - \rho g (z - z_o) \qquad (10)$

The choice of the datum level is immaterial, in the sense that it gives a constant term to the corrected pressure so it does not contribute to pressure gradient. The pressure P_c defined in equation (10) can be interpreted as the pressure of a analytical fluid at depth $z=z_o$ that will be in equilibrium with the fluid and exists at the actual pressure at depth z. The Darcy's law is supposed to be a macroscopic law that is intended to be meaningful over regions that are much bigger than the size of a single pore. Now we can discuss about the permeability at a point in the reservoir, we cannot be referring to the permeability at a mathematically infinitesimal point since the given point can be in a sand grain and not in the pore space. The permeability property is actually defined for a porous medium, not for a single pore. So the permeability is the property that is in a meaning of averaged out on a certain region of space surrounded the point (x,y,z). Now the region must be sufficiently large to encompass a significant number of pores. The pressure P that is used in Darcy's law is actually an average pressure taken on a small region of space.
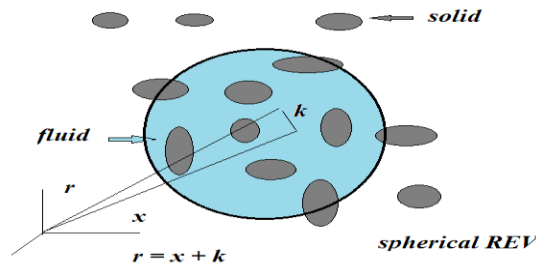
Figure 6. Spherical representative elementary volume (REV).

The spherical representative elementary volume is shown by figure-6. When we refer to the pressure at a certain location in the reservoir, we do not distinguish between two nearby points such as these. So, the entire region shown in the figure will be represented by an average pressure which is taken over the indicated circular region that is known as a Representative Elementary Volume (REV). Similarly, the permeability of the rock is defined over the REV length scale. About the size of REV, we can say that it must be at least one order of magnitude larger than the pore size.

The Darcy's law in itself does not give sufficient information to solve time-dependent i.e., transient problems that involving subsurface flow. So to find the complete governing equation that applies to these problems, we will first find the mathematical expression for the principle of conservation of mass. The conservation of mass equation states the balance between rate of mass change in an arbitrary volume and inflow of mass through the boundary surface area. In integral form, this can be expressed as follows:

$$\frac{\partial}{\partial t} \iiint \rho\, \phi\, dV + \iint \rho\, \bar{v}.\bar{n}\, dS = \iiint q\, dV \tag{11}$$

In this equation the double and triple integrals are taken over surface and volume respectively and $\bar{v}, \bar{n}, \rho, q$ and ϕ represent the velocity vector, unit normal vector, fluid density, external mass flow rate and porosity respectively. The right hand side term of the equation (11) can be changed into a volume integral form by the using the Gauss' divergence theorem as:

$$\iint \rho\, \bar{v}.\bar{n}\, dS = \iiint \nabla.(\rho\, \bar{v})\, dV \tag{12}$$

So, for a fixed control volume, the integral form of the conservation law will be

$$\iiint \left[\frac{\partial(\rho\, \phi)}{\partial t} + \nabla.(\rho\, \bar{v}) - q \right] dV \tag{13}$$

Now the differential form the conservation equation for mass can be written in coordinate invariant form as:

$$\frac{\partial(\rho\, \phi)}{\partial t} + \nabla.(\rho\, \bar{v}) = q \tag{14}$$

For the multiphase flow, it is necessary to account for the saturation of each phase. So that the equation (14) within each phase α can be written as:

$$\frac{\partial(\rho_\alpha S_\alpha \phi)}{\partial t} + \nabla.(\rho_\alpha \bar{v}_\alpha) = q_\alpha \tag{15}$$

III. DIFFUSION EQUATION IN CARTESIAN COORDINATES

The transient flow of a fluid through a porous medium is governed by a certain type of partial differential equation known as a diffusion equation. The detailed derivation and discussion related to diffusion was given by R. W. Zimmerman in 2002 [14] *i.e.,* discussed in this paper. So to derive the equation, we combine Darcy's law with the law of mass conservation and an equation that describes the process for which the fluid is stored inside a porous rock. Now using the differentiation for the product function $(\rho\, \phi)$, we get

$$D(\rho\, \phi) = \rho\, D\phi + \phi\, D\rho, D \equiv \frac{d}{dt} \tag{16}$$

$$= \rho \frac{d\phi}{dP}\frac{dP}{dt} + \phi \frac{d\rho}{dP}\frac{dP}{dt}$$

$$= \phi \left[\left(\frac{1}{\phi}\frac{d\phi}{dP} \right)\frac{dP}{dt} + \rho \left(\frac{1}{\rho}\frac{d\rho}{dP} \right)\frac{dP}{dt} \right]$$

$$D(\rho\, \phi) = \rho\, \phi\, (c_R + c_f)\, D(P) \tag{17}$$

where c_R, c_f are the compressibility of the rock and the fluid respectively.

The equation for mass conservation for the fluid flow is taken as:

$$-\frac{d(\rho\, q)}{dx} = \frac{d(\rho\, \phi)}{dt} \tag{18}$$

By using the Darcy's law, we have

$$-\frac{d(\rho\,q)}{dx} = -\frac{d}{dx}\left[-\frac{\rho k}{\mu}\frac{dP}{dx}\right]$$

$$-\frac{d(\rho\,q)}{dx} = \frac{k}{\mu}\left[\rho\frac{d^2P}{dx^2} + \frac{d\rho}{dx}\frac{dP}{dx}\right]$$

$$-\frac{d(\rho\,q)}{dx} = \frac{k}{\mu}\left[\rho\frac{d^2P}{dx^2} + \frac{d\rho}{dP}\frac{dP}{dx}\frac{dP}{dx}\right]$$

$$-\frac{d(\rho\,q)}{dx} = \frac{k\rho}{\mu}\left[\frac{d^2P}{dx^2} + \frac{1}{\rho}\frac{d\rho}{dP}\left(\frac{dP}{dx}\right)^2\right]$$

$$-\frac{d(\rho\,q)}{dx} = \frac{k\rho}{\mu}\left[\frac{d^2P}{dx^2} + c_f\left(\frac{dP}{dx}\right)^2\right] \tag{19}$$

From the equations (17) and (19), we get

$$\frac{d^2P}{dx^2} + c_f\left(\frac{dP}{dx}\right)^2 = \frac{1}{K}\rho\,\phi\,(c_R + c_f)\,D(P) \tag{20}$$

But we know that,

$$\frac{d^2P}{dx^2} \gg c_f\left(\frac{dP}{dx}\right)^2$$

On neglecting the term $c_f\left(\frac{dP}{dx}\right)^2$, $i.e.$

$$c_f\left(\frac{dP}{dx}\right)^2 \approx c_f\left[\frac{\mu\,Q}{2\,\pi\,k\,H\,R}\right]^2 \tag{21}$$

$$\frac{d^2P}{dx^2} \approx \frac{\mu\,Q}{2\,\pi\,k\,H\,R^2} \tag{22}$$

So we can neglect the nonlinear term in equation (20), we get the diffusion equation as given

$$\frac{dP}{dt} = \frac{K}{\phi\,\mu\,(c_\phi + c_f)}\frac{d^2P}{dx^2} \tag{23}$$

where $(c_\phi + c_f) = c$ is the total compressibility.

The parameter which governs the rate at which fluid pressure diffuses through the rock is the hydraulic diffusivity D_H, that is defined by

$$D_H = \frac{k}{\phi\,\mu\,(c_\phi + c_f)} \tag{24}$$

The distance d at which a pressure disturbance will travel during an elapsed time t is given as

$$d = \sqrt{4\,D_H\,t} \tag{25}$$

For the multi-phase flow if we have assume that the pores of the rock are filled with two components, oil and water, and often also contain some hydrocarbons in the gaseous phase. So we have to find the governing flow equations for an oil and water system, in the general form. From the rock properties module that Darcy's law can be generalized for two-phase flow by including a relative permeability factor for each phase, we have

$$q_w = \frac{-k\,k_{rw}}{\mu_w}\frac{dP_w}{dx} \tag{26}$$

$$q_o = \frac{-k\,k_{ro}}{\mu_o}\frac{dP_o}{dx} \tag{27}$$

where the subscripts w and o are used for oil and water respectively. The two relative permeability functions are supposed to be known functions of the phase saturations. For the oil-water system, the two saturations are necessarily related to each other by the relationship

$$S_w + S_o = 1 \qquad (28)$$

The pressures in the two phases at every point in the reservoir must be different. If the reservoir is oil-wet then the two pressures will be given by

$$P_o - P_w = P_c \, S_o \qquad (29)$$

where the capillary pressure P_c is given by the rock-dependent function of oil saturation.

But the volume of the oil in a given region is equal to the total pore volume multiplied by the oil saturation then by the equations of the conservation of mass for the two phases can be written by inserting a saturation factor in the storage term as given

$$-\frac{d(\rho_0 q_0)}{dx} = \frac{d(\phi \rho_0 S_0)}{dt} \qquad (30)$$

$$-\frac{d(\rho_w w)}{dx} = \frac{d(\phi \rho_w S_w)}{dt} \qquad (31)$$

The densities of the two phases are related to their respective phase pressures with the equation of state as given by

$$\rho_0 = \rho_0(P_0) \qquad (32)$$

$$\rho_w = \rho_w(P_w) \qquad (33)$$

where the temperature are taken as constant.

Lastly, the porosity must be the function of the phase pressures Po and Pw. The above two pressures independently affect the porosity. Now, the capillary pressure P_c is generally small so that

$$Po \approx Pw$$

From which we can use the pressure-porosity relationship that would be obtained under single-phase conditions, *i.e.,*

$$\phi = \phi(P_0) \qquad (34)$$

If the fluid is taken as slightly compressible or if the pressure variations are small then the equations of state are written as

$$\rho(P_o) = \rho_{0i}[1 + c_o(P_o - P_{oi})] \qquad (35)$$

where the subscript "*i*" is used for the initial state, and the compressibility c_o is taken as a constant.

IV. DISCUSSION AND RESULTS:

The permeability is a function of rock type that varies with stress, temperature etc., and does not depend on the fluid. The effect of the fluid on the flow rate is accounted for by the term of viscosity. The numerical value of k for a given rock depends on the diameter of the pores in the rock "d" as well as on the degree of interconnectivity of the void space. The parameter that governs the rate at which fluid pressure diffuses through a rock mass is the hydraulic diffusivity which is defined by

$$D_H = \frac{k}{\phi \, \mu \, c}$$

The distance d at which a pressure disturbance will travel during an elapsed time t is given as

$$d = \sqrt{4 \, D_H t}$$

The time required for a pressure disturbance to travel a distance d is found by

$$t = \frac{\phi \, \mu \, c \, d^2}{4k}$$

The pressure pulses obey a diffusion equation not a wave equation. So, they travel at a speed that continually decreases with time rather than travelling at a constant speed.

REFERENCES

[1]. Celia M. A., Rajaram H., and Ferrand L. A. A multi-scale computational model for multiphase flow in porous media. Advances in Water Resources, 16(1): (1993), *pp*.81-92.

[2]. Ewing, R. Aspects of upscaling in simulation of flow in porous media. *Adv. Water Resources 20*(5-6), (1997), *pp*. 349–358.

[3]. Helmig, R. Multiphase Flow and Transport Processes in the Subsurface – *A Contribution to the Modeling of Hydrosystems*. Springer–Verlag (1997).

[4]. Jahresbericht der Wasserwirtschaft Gemeinsamer Bericht der mit der Wasserwirtschaft befassten Bundesministerien – Haushaltsjahr 1992. *Wasser und Boden 45*(5), (1993) *pp*. 504–516.

[5]. Kinzelbach, W. and W. Sch¨afer. Stochastic modeling of insitu. bioremediation in heterogeneous aquifers. *Journal of Contaminant Hydrology* 10, (1992) *pp*. 47–73.

[6]. Kobus, H. The role of large–scale experiments in groundwater and subsurface remediation research: The VEGAS concept and approach. In H. Kobus, B. Barczewski, and H. Koschitzky (Eds.), *Groundwater and Subsurface Remediation*, Springer–Verlag (1996), *pp*. 1–18.

[7]. Mercer J. W. and Cohen R. M. A review of immiscible fluids in the subsurface: Properties, models, characterization and remediation. Journal of Contaminant Hydrology, 6(2): (1990), *pp*.107-163.

[8]. Mercer J. W., Parker R. M., and Spalding C. P. Site characterization: Use of site characterization data to select applicable remediation technologies. In Subsurface Restoration Conference / Third International Conference on Water Quality Research, Dallas, TX, National Center for Ground Water Research. (1992), *pp*. 26-27.

[9]. Miller C. T. and Gray W. G. Hydrogeological research: Just getting started Ground Water, 40(3): (2002), *pp*.224-231.

[10]. Miller C. T. and Gray W. G. Hydrogeological research, education, and practice: A path to future contributions. Journal of Hydrologic Engineering, 13(1): (2008), *pp*.7-12.

[11]. Watson, A., Wade J., and Ewing R. Parameter and system identification for fluid flow in underground reservoirs. In H. Engl and J.McLaughlin (Eds.), *Proceedings of the Conference on "Inverse Problems and Optimal Design in Industry"*, Volume 10, *pp*. 81–108. B. G. Teubner. Europ. Cons. for Math. Ind (1994).

[12]. Wilson J. L., Conrad S. H., Mason W. R., Peplinksi W. and Hagan E. Laboratory investigation of residual organics from spills, leaks, and the disposal of hazardous wastes in groundwater. Technical Report EPA CR-813571-01-0, U.S. Environmental Protection Agency, Robert S. Kerr Environmental Research Laboratory, Ada, OK, (1989).

[13]. Yu S. C. T. Transport and fate of chlorinated hydrocarbons in the vadose zone/ a literature review with discussions on regulatory implications. Journal of Soil Contamination, 4(1): (1995), *pp*. 25-56.

[14]. Zimmerman, R. W. Flow in Porous Media Section 1, (2002), *pp*. 1-17.

| Research Paper | Open Access |

Modeling and Optimization of the Rigidity Modulus of Latertic Concrete using Scheffe's Theory

P.N. Onuamah
Civil Engineering Department, Enugu State University of Science

ABSTRACT: *This investigation is on the modeling and optimization of the rigidity modulus of Lateritic Concrete. The laterite is the reddish soil layer often belying the top soil in many locations and further deeper in some areas, collected from the Vocational Education Building Site of the University of Nigeria, Nsukka. Scheffe's optimization approach was applied to obtain a mathematical model of the form $f(x_{i1}, x_{i2}, x_{i3})$, where x_i are proportions of the concrete components, viz: cement, laterite and water. Scheffe's experimental design techniques were followed to mould various block samples measuring 220mm x 210mm x 120mm, using the auto-generated components ratios, and tested for 28 days strength to arrive at the mathematical model: $\hat{Y} = 1371.48X_1 + 1459.38X_2 + 1362.68X_3 - 816.84X_1X_2 + 49.80X_1X_3 - 54.00X_2X_3$. To carry out the task, we embarked on experimentation and design, applying the second order polynomial characterization process of the simplex lattice method. The model adequacy was checked using the control factors. Finally a software is prepared to handle the design computation process to select the optimized properties of the mix, and generate the optimal mix ratios for the desired property.*

KEYWORDS: *Model, laterite, pseudo-component, Simplex-lattice, model.*

I. INTRODUCTION

From the beginning of time, the cost of this change has been of major concern to man as the major construction factors are finance and others such as labour, materials and equipment. The construction of structures is a regular operation which creates the opportunity for continued change and improvement on the face of the environment.

Major achievements in the area of environmental development is heavily dependent on the availability of construction materials which take a high proportion of the cost of the structure. This means that the locality of the material and the usability of the available materials directly impact on the achievable development of the area as well as the attainable level of technology in the area.

To produce the concrete several primary components such as cement, sand, gravel and some admixtures are to be present in varying quantities and qualities. Unfortunately, the occurrence and availability of these components vary very randomly with location and hence the attendant problems of either excessive or scarce quantities of the different materials occurring in different areas. Where the scarcity of one component prevails exceedingly, the cost of the concrete production increases geometrically. Such problems obviate the need to seek alternative materials for partial or full replacement of the component when it is possible to do so without losing the quality of the concrete. In the present time, concrete is the main material of construction, and the ease or cost of its production accounts for the level of success in the of area environmental upgrading through the construction of new roads, buildings, dams, water structures and the renovation of such structures.

Concept of Optimization

The target of planning is the maximization of the desired outcome of the venture. In order to maximize gains or outputs it is often necessary to keep inputs or investments at a minimum at the production level. The process involved in this planning activity of minimization and maximization is referred to as optimization [1]. In the science of optimization, the desired property or quantity to be optimized is referred to as the objective function. The raw materials or quantities whose amount of combinations will produce this objective function are referred to as variables.

The variations of these variables produce different combinations and have different outputs. Often the space of variability of the variables is not universal as some conditions limit them. These conditions are called constraints. For example, money is a factor of production and is known to be limited in supply. The constraint at any time is the amount of money available to the entrepreneur at the time of investment.

Hence or otherwise, an optimization process is one that seeks for the maximum or minimum value and at the same time satisfying a number of other imposed requirements [2]. The function is called the objective function and the specified requirements are known as the constraints of the problem.

Making structural concrete is not all comers' business. Structural concrete are made with specified materials for specified strength. Concrete is heterogeneous as it comprises sub-materials. Concrete is made up of fine aggregates, coarse aggregates, cement, water, and sometimes admixtures. Researchers [3] report that modern research in concrete seeks to provide greater understanding of its constituent materials and possibilities of improving its qualities. For instance, Portland cement has been partially replaced with ground granulated blast furnace slag (GGBS), a by–product of the steel industry that has valuable cementations properties [4].

Bloom and Bentur [5] reports that optimization of mix designs require detailed knowledge of concrete properties. Low water-cement ratios lead to increased strength but will negatively lead to an accelerated and higher shrinkage. Apart from the larger deformations, the acceleration of dehydration and strength gain will cause cracking at early ages.

Modeling

Modeling has to do with formulating equations of the parameters operating in the physical or other systems. Many factors of different effects occur in nature in the world simultaneously dependently or independently. When they interplay they could inter-affect one another differently at equal, direct, combined or partially combined rates variationally, to generate varied natural constants in the form of coefficients and/or exponents [6]. The challenging problem is to understand and asses these distinctive constants by which the interplaying factors underscore some unique natural phenomenon towards which their natures tend, in a single, double or multi phase system.

A model could be constructed for a proper observation of response from the interaction of the factors through controlled experimentation followed by schematic design where such simplex lattice approach [7]. Also entirely different physical systems may correspond to the same mathematical model so that they can be solved by the same methods. This is an impressive demonstration of the unifying power of mathematics [8].

II.   LITERATURE REVIEW

The mineralogical and chemical compositions of laterites are dependent on their parent rocks [9]. Laterite formation is favoured in low topographical reliefs of gentle crests and plateaus which prevent the erosion of the surface cover [10].

Of all the desirable properties of hardened concrete such as the tensile, compressive, flexural, bond, shear strengths, etc., the compressive strength is the most convenient to measure and is used as the criterion for the overall quality of the hardened concrete [2]. To be a good structural material, the material should be homogeneous and isotropic. The Portland cement, laterite or concrete are none of these, nevertheless they are popular construction materials [11]. With given proportions of aggregates the compressive strength of concrete depends primarily upon age, cement content, and the cement-water ratio [12].

Simplex is a structural representation (shape) of lines or planes joining assumed positions or points of the constituent materials (atoms) of a mixture, and they are equidistant from each other [13] When studying the properties of a q-component mixture, which are dependent on the component ratio only the factor space is a regular (q-1)–simplex [14]. Simplex lattice designs are saturated, that is, the proportions used for each factor have m + 1 equally spaced levels from 0 to 1 (x_i = 0, 1/m, 2/m, … 1), and all possible combinations are derived from such values of the component concentrations, that is, all possible mixtures, with these proportions are used [14].

Background Theory

The Scheffe's involves the application of a polynomial expression of any degrees, is used to characterize a simplex lattice mixture components. In the theory only a single phase mixture is covered. The theory lends path to a unifying equation model capable of taking varying componental ratios to fix approximately equal mixture properties. The optimization is the selectability, from some criterial (mainly economic) view point, the optimal ratio from the component ratios list that can be automatedly generated. His theory is one of the adaptations to this work in the formulation of response function for compressive rigidity modulus of lateritic concrete.

Simplex Lattice

Simplex is a structural representation (shape) of lines or planes joining assumed positions or points of the constituent materials (atoms) of a mixture [13], and they are equidistant from each other. Mathematically, a simplex lattice is a space of constituent variables of X_1, X_2, X_3,……, and X_i which obey these laws:

$$X_i < 0$$
$$X \neq \text{negative}$$
$$0 \leq x_i \leq 1$$
$$\sum_{i=1} x_i = 1$$

…………………………………………………………….(1)

That is, a lattice is an abstract space.

To achieve the desired strength of concrete, one of the essential factors lies on the adequate proportioning of ingredients needed to make the concrete Henry Scheffe [7] developed a model whereby if the rigidity modulus desired is specified, possible combinations of needed ingredients to achieve the rigidity modulus can easily be predicted by the aid of computer, and if proportions are specified the rigidity modulus can easily be predicted.

Simplex Lattice Method

In designing experiment to attack mixture problems involving component property diagrams the property studied is assumed to be a continuous function of certain arguments and with a sufficient accuracy it can be approximated with a polynomial [14]. When investigating multi-components systems the use of experimental design methodologies substantially reduces the volume of an experimental effort. Further, this obviates the need for a special representation of complex surface, as the wanted properties can be derived from equations while the possibility to graphically interpret the result is retained.

As a rule the response surfaces in multi-component systems are very intricate. To describe such surfaces adequately, high degree polynomials are required, and hence a great many experimental trials. A polynomial of degree n in q variable has C^n_{q+n} coefficients. If a mixture has a total of q components and x_1 be the proportion of the ith component in the mixture such that,

$$x_i >= 0 \ (i=1,2, ….q), \qquad\qquad\qquad\qquad\qquad (2)$$

then the sum of the component proportion is a whole unity i.e.

$$X_1 + x_2 + x_3 = 1 \text{ or } \sum x_i - 1 = 0 \qquad …. \qquad .. \qquad .. \qquad .. \qquad (3)$$

where i = 1, 2, …., q… Thus the factor space is a regular (q-1) dimensional simplex. In (q-1) dimensional simplex if q = 2, we have 2 points of connectivity. This gives a straight line simplex lattice. If q=3, we have a triangular simplex lattice and for q = 4, it is a tetrahedron simplex lattice, etc. Taking a whole factor space in the design we have a (q,m) simplex lattice whose properties are defined as follows:

    i. The factor space has uniformly distributed points,
    ii. Simplex lattice designs are saturated (Akhnarova and Kafarov, 1982). That is,
      the proportions used for each factor have m + 1 equally spaced levels from 0
      to 1 ($x_i = 0$, 1/m, 2/m, … 1), and all possible combinations are derived from
      such values of the component concentrations, that is, all possible mixtures,
      with these proportions are used.

Hence, for the quadratic lattice (q,2), approximating the response surface with the second degree polynomials (m=2), the following levels of every factor must be used 0, ½ and 1; for the cubic (m=3) polynomials, the levels are 0, 1/3, 2/3 and 1, etc; Scheffe [7] showed that the number of points in a (q,m) lattice is given by

$$C_{q+m-1} = q(q+1) … (q+m-1)/m! ……………..\qquad .. \qquad .. \qquad .. \qquad .. \qquad (4)$$

The (3,2) Lattice Model

The properties studied in the assumed polynomial are real-valued functions on the simplex and are termed responses. The mixture properties were described using polynomials assuming a polynomial function of degree m in the q-variable x_1, x_2 ……, x_q, subject to Eqn (3), and will be called a (q,m) polynomial having a general form:

$$\hat{Y} = b_0 + \sum_{i\leq1\leq q} b_i X_i + \sum_{i\leq1<j\leq q} b_{ij} X_i X_{ij} + \ldots + \sum b_{ijk} + \sum b_{i1i2\ldots in} X_{i1} X_{i2} \ldots X_{in} \quad \ldots\ldots \quad .. \quad .. \quad (5)$$

where b is a constant coefficient.

The relationship $\sum x_i = 1$ enables the qth component to be eliminated and the number of coefficients reduced to C^m_{q+m-1}, but the very character of the problem dictates that all the q components be introduced into the model.

Substituting into equation Eqn (5), the polynomial has the general usable form:

$$\hat{Y} = b_0 + b_1 X_1 + b_2 X_2 + b_3 X_3 + b_{12} X_1 X_2 + b_{13} X_1 X_{13} + b_{23} X_2 X_3 +$$
$$b_{11} X^2_{1} + b_{22} X^2_2 + b_{33} X^2_3 \quad \ldots\ldots \quad \ldots.. \quad\quad \ldots \quad\quad (6)$$

By applying the normalization condition of Eqn. (3) and to Eqn (6) and jogling [6], we get that

$$\hat{Y} = \beta_1 X_1 + \beta_2 X_2 + \beta_3 X_3 + \beta_{12} X_1 X_2 + \beta_{13} X_1 X_3 + \beta_{23} X_2 X_{23} \quad . \quad . \quad\quad (7)$$

where

$$\beta_i = b_0 + b_i + b_{ii} \quad \text{and} \quad \beta_{ij} = b_{ij} - b_{ii} - b_{jj}, \;. \quad . \quad\quad . \quad\quad . \quad\quad . \quad\quad (8)$$

Thus, the number of coefficients has reduced from 10 in Eqn (6) to 6 in Eqn (7). That is, the reduced second degree polynomial in q variables is

$$\hat{Y} = \sum \beta_i X_i + \sum \beta_{ij} X_i \quad\quad .. \quad\quad .. \quad\quad .. \quad\quad .. \quad\quad .. \quad\quad .. \quad\quad (9)$$

Construction of Experimental/Design Matrix

From the coordinates of points in the simplex lattice, we can obtain the design matrix. We recall that the principal coordinates of the lattice, only a component is 1 (refer to fig 3.1), others are zero.

Hence if we substitute in Eqn. (3.11), the coordinates of the first point ($X_1=1$, $X_2=0$, and $X_3=0$, Table 3.1), we get that $Y_1 = \beta_1$.

And doing so in succession for the other two points if the hexahedron, we obtain

$$Y_2 = \beta_2, Y_3 = \beta_3 \quad\quad .. \quad\quad . \quad\quad . \quad\quad . \quad\quad . \quad\quad . \quad\quad . \quad\quad (10)$$

\

The substitution of the coordinates of the fourth point yields

$$Y_{12} = \tfrac{1}{2} X_1 + \tfrac{1}{2} X_2 + \tfrac{1}{2} X_1.X_2$$
$$= \tfrac{1}{2}\beta_1 + \tfrac{1}{2}\beta_2 + \tfrac{1}{4}\beta_{12}$$

But as $\beta_i = Y_i$ then
$$Y_{12} = \tfrac{1}{2}\beta_1 - \tfrac{1}{2}\beta_2 - \tfrac{1}{4}\beta_{12}$$

Thus
$$\beta_{12} = 4 Y_{12} - 2Y_1 - 2Y_2 \quad\quad . \quad\quad . \quad\quad . \quad\quad . \quad\quad .$$

And similarly,
$$\beta_{13} = 4 Y_{13} - 2Y_1 - 2Y_2$$
$$\beta_{23} = 4 Y_{23} - 2Y_2 - 2Y_3$$

Or generalizing,

$$\beta_i = Y_i \text{ and } \beta_{ij} = 4 Y_{ij} - 2Y_i - 2Y_j \quad . \quad\quad . \quad\quad . \quad\quad . \quad\quad . \quad\quad . \quad\quad .(11)$$

which are the coefficients of the reduced second degree polynomial for a q-component mixture, since the three points defining the coefficients β_{ij} lie on the edge. The subscripts of the mixture property symbols indicate the relative content of each component X_i alone and the property of the mixture is denoted by Y_i. Mixture 4 includes X_1 and X_2, and the property being designated Y_{12}.

Actual and Pseudo Components

The requirements of the simplex that $\sum_{x=1}^{q} X_i = 1$ makes it impossible to use the normal mix ratios

such as 1:3, 1:5, etc, at a given water/cement ratio. Hence a transformation of the actual components (ingredient proportions) to meet the above criterion is unavoidable. Such transformed ratios say $X_1^{(i)}$, $X_2^{(i)}$, and $X_3^{(i)}$ for the ith experimental points are called pseudo components. Since X_1, X_2 and X_3 are subject to $\sum X_i = 1$, the

transformation of cement:laterite:water at say 0.60 water/cement ratio cannot easily be computed because X_1, X_2 and X_3 are in pseudo expressions $X_1^{(i)}$, $X_2^{(i)}$, and $X_3^{(i)}$. For the ith experimental point, the transformation computations are to be done.

The arbitrary vertices chosen on the triangle are $A_1(1:7.50:0.05)$, $A_2(1:8.20:0.03)$ and $A_3(1:6.90:0.10)$, based on experience and earlier research reports.

Transformation Matrix
If Z denotes the actual matrix of the ith experimental points, observing from Table 3.2 (points 1 to 3),

$$BZ = X = 1 \qquad \qquad \qquad \qquad \qquad \qquad \qquad \qquad (12)$$

where B is the transformed matrix.

Therefore, $\quad B = I.Z^{-1}$

Or $\qquad\qquad B = Z^{-1}$ . . . . (13)

For instance, for the chosen ratios, at the vertices A_1, A_2 and A_3,

$$Z = \begin{bmatrix} 1.00 & 7.50 & 0.50 \\ 1.00 & 8.20 & 0.30 \\ 1.00 & 6.90 & 0.10 \end{bmatrix} \qquad . \qquad . \qquad . \qquad . \qquad . \qquad (14)$$

From Eqn (13),

$$B = Z^{-1}$$

$$Z^{-1} = \begin{bmatrix} 26.65 & -17.60 & -8.04 \\ -30.04 & 2.17 & 0.87 \\ -56.52 & 26.08 & 30.43 \end{bmatrix}$$

Hence,

$$B Z^{-1} = Z. Z^{-1} = 0 \begin{bmatrix} 1 & 0 & 0 \\ 1 & 0 & \\ 0 & 0 & 1 \end{bmatrix}$$

Thus, for actual component Z, the pseudo component X is given by

$$X \begin{bmatrix} X_1^{(i)} \\ X_2^{(i)} \\ X_3^{(i)} \end{bmatrix} = B \begin{bmatrix} 26.65 & -17.60 & -8.04 \\ -30.04 & 2.17 & 0.87 \\ -56.52 & 26.08 & 30.43 \end{bmatrix} Z \begin{bmatrix} Z_1^{(i)} \\ Z_2^{(i)} \\ Z_3^{(i)} \end{bmatrix} \begin{bmatrix} \\ \\ \end{bmatrix}$$

which gives the $X_i(i=1,2,3)$ values in Table 1.

The inverse transformation from pseudo component to actual component is expressed as

$$AX = Z . \qquad . \qquad . \qquad . \qquad . \qquad . \qquad . \qquad . \qquad (15)$$

where A = inverse matrix
$$A = Z X^{-1}.$$

From Eqn 3.16, X = BZ, therefore,

$A = Z. (BZ)^{-1}$

$A = Z.Z^{-1}B^{-1}$

$A = IB^{-1}$

$B = B^{-1}$ . . . . (16)

This implies that for any pseudo component X, the actual component is given by

$$Z \begin{bmatrix} Z_1^{(i)} \\ Z_2^{(i)} \\ Z_3^{(i)} \end{bmatrix} = B \begin{bmatrix} 1 & 7.50 & 0.05 \\ 1 & 8.20 & 0.03 \\ 1 & 6.9 & 0.10 \end{bmatrix} X \begin{bmatrix} X_1^{(i)} \\ X_2^{(i)} \\ X_3^{(i)} \end{bmatrix}. \qquad \qquad . \qquad . \qquad . \qquad . \qquad (17)$$

Eqn (17) is used to determine the actual components from points 4 to 6 , and the control values from points 7 to 9 (Table 1).

Table 1 Value for Experiment

N	X_1	X_2	X_3	RESPONSE	Z_1	Z_2	Z_3
1	1	0	0	Y_1	1	1	1
2	0	1	0	Y_2	7.50	8.20	6.90
3	0	0	1	Y_3	0.05	0.03	0.10
4	1/2	1/2	0	Y_{12}	1	7.85	0.04
5	½	0	1/2	Y_{13}	1	7.20	0.075
6	0	1/2	1/2	Y_{23}	1	7.55	0.065
Control Points (6-9)							
7	1/3	1/3	1/3	Y_{123}	1	7.458	0.0594
8	1/3	2/3	0	Y_{122}	1	7.698	0.0366
9	0	1/3	2/3	Y_{233}	1	7.329	0.0769

III.   METHODOLOGY

Materials

The disturbed samples of laterite material were collected at the Vocational Education project site at the University of Nigeria, Nsukka, at the depth of 1.5m below the surface.

The water for use is pure drinking water which is free from any contamination i.e. nil Chloride content, pH =6.9, and Dissolved Solids < 2000ppm. Ordinary Portland cement is the hydraulic binder used in this project and sourced from the Dangote Cement Factory, and assumed to comply with the Standard Institute of Nigeria (NIS) 1974, and kept in an air-tight bag.

Material Properties

All samples of the laterite material conformed to the engineering properties already determined by a team of engineering consultants from the Civil Engineering Department, U.N.N, who reported on the Sieve Analysis Tests, Natural Moisture Content, etc, carried out according to the British Standard Specification, BS 1377 – "Methods of Testing Soils for Civil Engineering Purposes".

Preparation of Samples

The sourced materials for the experiment were transferred to the laboratory where they were allowed to dry. A samples of the laterite were prepared and tested to obtain the moisture content for use in proportioning the components of the lateritic concrete to be prepared. The laterite was sieved to remove debris and coarse particles. The component materials were mixed at ambient temperature. The materials were mixed by weight according to the specified proportions of the actual components generated in Table 1. In all, two blocks of 220mm x210 x120mm for each of six experimental points and three control points were cast for the rigidity modulus test, cured for 28 days after setting and hardening.

Strength Test

After 28 day of curing, the cubes and blocks were crushed, with dimensions measured before and at the point of shearing, to determine the lateritic concrete block strength, using the compressive testing machine to the requirements of BS 1881:Part 115 of 1986.

IV.   RESULT AND ANALYSIS

Replication Error And Variance of Response

To raise the experimental design equation models by the lattice theory approach, two replicate experimental observations were conducted for each of the six design points.

Hence we have below, the table of the results (Tables 5.1a,b and c) which contain the results of two repetitions each of the 6 design points plus three Control Points of the (3,2) simplex lattice, and show the mean and variance values per test of the observed response, using the following mean and variance equations below:

$$\ddot{Y} = \sum(Y_r)/r \qquad . \qquad . \qquad . \qquad . \qquad . \qquad . \qquad . \qquad (18)$$

where $\hat{Y}$ is the mean of the response values and
r = 1,2.

$$S_Y{}^2 = \sum[(Y_i - \ddot{Y}_i)^2]/(n-1) \quad . \qquad . \qquad . \qquad . \qquad . \qquad . \qquad (19)$$

where n = 9.

5.1.2 Results and Analysis for the Modulus of Rigidity
Property

The Modulus of Elasticity, E_c, and the Modulus of Rigidity, G, of the lateritic concrete block were computed from the relation

$$E_c = 1.486f_c{}^{1/3} \, \rho^2 x10^{-3} \qquad . \qquad . \qquad . \qquad . \qquad . \qquad (20)$$

where E_c and fc are measured in MPa and ρ in Kg/m³ [15], and ρ = density of block.
f_c = Failure load/Cross-sectional Area contact area of block,

$$G = E_c/2(1+ v) \qquad . \qquad . \qquad . \qquad . \qquad . \qquad . \qquad . $$
(21)

where v = Poisson's Ratio = lateral strain/longitudinal strain

Table 2: 220x210x120 Block Sample Results

No	Replication	Failure Load (kN)	Dx (10^{-2}xmm)	dy (10^{-2}xmm)	Wet Weight (kg)	Dry Weight (kg)
1	A	55.60	300	120	8.68	8.63
	B	54.90	324	74	8.69	8.33
2	A	60.40	355	94	8.75	8.33
	B	71.00	360	89	8.89	8.28
3	A	69.40	301	132	8.87	8.66
	B	68.20	245	103	8.73	8.62
4	A	57.80	230	84	8.69	8.42
	B	62.50	240	109	8.77	8.46
5	A	65.30	295	112	8.79	8.67
	B	69.30	302	110	8.98	8.63
6	A	68.90	344	138	8.82	8.91
	B	66.10	307	146	8.71	8.22
CONTROL POINTS						
7	A	81.30	282	97	8.91	8.45
	B	82.60	327	93	8.43	8.33
8	A	71.30	280	112	8.83	8.63
	B	65.30	330	113	8.68	8.55
9	A	80.00	312	120	8.64	8.42
	B	74.20	344	92	8.67	8.79

Table 3 Compressive Strength, Poisson's Ratio, Young's Modulus and Modulus of Rigidity Results

No	Replication	f_c (MPa)	Average f_c (MPa)	ρ (kg/m³)	V	E_c (N/mm²)	G (N/mm²)
1	A	2.10	2.08	1552.31	0.33	4569.01	1371.48
	B	2.07					
2	A	2.28	2.48	1498.10	0.27	4501.31	1459.38
	B	2.68					
3	A	2.62	2.60	1558.44	0.45	4950.84	1362.68
	B	2.58					
4	A	2.18	2.27	1522.36	0.43	4518.88	1208.72
	B	2.36					
5	A	2.47	2.54	1560.24	0.39	4925.61	1379.53
	B	2.62					

6	A	2.60	2.55	1526.87	0.36	4728.05	1397.53
	B	2.50					
Control Points							
7	A	3.07	3.09	1513.34	0.33	4945.85	1476.20
	B	3.12					
8	A	2.70	3.59	1551.22	0.39	4899.21	1453.30
	B	2.49					
9	A	3.03	2.77	1552.12	0.34	5097.61	1531.64
	B	2.81					

Table 4 Result of the Replication Variance of the G Response for 220x210x120 mm Block

Experiment No (n)	Repetition	Response G (N/mm²⁾	Response Symbol	$\sum Y_r$	$\ddot{Y}_r$	$\sum(Y_r - \ddot{Y}_r)^2$	S_i^2
1	1A 1B	1356.02 1386.95	Y_1	2742.97	1371.48	478.35	239.17
2	2A 2B	1439.51 1479.25	Y_2	2918.77	1459.38	789.48	394.74
3	3A 3B	1437.98 1297.38	Y_3	2735.36	1362.68	9883.84	4941.92
4	4A 4B	1189.85 1227.58	Y_{12}	2417.44	1208.72	711.72	355.86
5	5A 5B	1397.73 1361.20	Y_{13}	2758.93	1379.53	667.20	333.60
6	6A 6B	1597.42 1197.42	Y_{23}	2795.06	1397.53	79916.67	39958.53
Control Points							
7	7A 7B	1430.13 1522.28	C_1	2952.41	1476.20	4245.77	2122.88
8	8A 8B	1500.19 1406.42	C_2	2906.61	1453.30	4396.18	2198.09
9	9A 9B	1493.21 1570.07	C_3	3063.28	1531.64	2953.65	1476.82

$\sum 104042.89$

Replication Variance

$$S_{Yc}^2 = (\sum S_i^2)/(n-1) = 104042.89/8 = 13005.36$$

Replication Error

$$S_{Yc} = (S_{\hat{Y}}^2)^{1/2} = 13005^{1/2} = 114.04$$

$\beta_1 = 1371.48$
$\beta_2 = 1459.38$
$\beta_3 = 1362.68$
$\beta_{12} = 4(1208.72) - 2(1371.48) - 2(1459.38) = -816.84$
$\beta_{13} = 4(1379.53) - 2(1371.48) - 2(1362.68) = 49.80$
$\beta_{23} = 4(1397.53) - 2(1459.38) - 2(1362.68) = -54.00$

Determination of Regression Equation for the G
From Eqns 3.15 and Table 5.1 the coefficients of the reduced second degree polynomial is determined as follows:
Thus, from Eqn (7),

$$\hat{Y} = 1371.48X_1 + 1459.38X_2 + 1362.68X_3 - 816.84X_1X_2 + 49.80X_1X_3 - 54.00X_2X_3 \qquad (22)$$

Eqn (22) is the mathematical model of the G of the lateritic concrete based on the 28-day strength.

Test of Adequacy of the G Model
Eqn (22), the equation model, will be tested for adequacy against the controlled experimental results.

We apply the statistical hypothesis as follows:
1. Null Hypothesis (H_0): There is no significant difference between the experimental
   values and the theoretical expected results of the Modulus of Rigidity.

2. Alternative Hypothesis (H_1): There is a significant difference between the experimental
   values and the theoretical expected results of the Modulus of Rigidity.

The number of control points and their coordinates are conditioned by the problem formulation and experiment nature. Besides, the control points are sought so as to improve the model in case of inadequacy. The accuracy of response prediction is dissimilar at different points of the simplex. The variance of the predicted response, S_Y^2, is obtained from the error accumulation law. To illustrate this by the second degree polynomial for a quaternary mixture, the following points are assumed:

X_i can be observed without errors.

The replication variance, S_Y^2, is similar at all design points, and

Response values are the average of n_i and n_{ij} replicate observations at appropriate points of the simplex

Then the variance $S_{\hat{Y}i}$ and $S_{\hat{Y}ij}$ will be

$$(S_{\hat{Y}}^2)_i = S_Y^2/n_i \qquad . \qquad . \qquad . \qquad . \qquad . \qquad . \qquad . \qquad . \qquad (23)$$

$$S_{\hat{Y}}^2)_{ij} = S_Y^2/n_{ij}. \qquad . \qquad . \qquad . \qquad . \qquad . \qquad . \qquad . \qquad (24)$$

In the reduced polynomial,

$$\hat{Y} = \beta_1 X_1 + \beta_2 X_2 + \beta_3 X_3 + \beta_4 X_4 + \beta_{12}X_1X_2 + \beta_{13}X_1X_3 + \beta_{14}X_1X_4 + \beta_{23}X_2X_{23} + \beta_{24}X_2X_4 +$$
$$\beta_{34}X_3X_4 \qquad\qquad . \qquad . \qquad . \qquad .(25)$$

If we replace coefficients by their expressions in terms of responses,

$$\beta_i = Y_i \text{ and } \beta_{ij} = 4Y_{ij} - 2Y_i - 2Y_j$$

$$\hat{Y} = Y_1X_1 + Y_2X_2 + Y_3X_3 + + Y_4X_4 + (4Y_{12} - 2Y_1 - 2Y_2)X_1X_2 + (4Y_{13} - 2Y_1 - 2Y_3)X_1X_3 + (4Y_{14} - 2Y_1 - 2Y_4)X_1X_4 + (4Y_{23} - 2Y_2 - 2Y_3)X_2X_3 + (4Y_{24} - 2Y_2 - 2Y_4)X_2X_4 + (4Y_{34} - 2Y_3 - 2Y_4)X_3X_4$$

$$= Y_1(X_1 - 2X_1X_2 - 2X_1X_3 - 2X_1X_4) + Y_2(X_2 - 2X_1X_2 - 2X_2X_3 - 2X_2X_4) + Y_3(X_3 - 2X_1X_3 + 2X_2X_3 + 2X_3X_4) + Y_4(X_4$$
$$- 2X_1X_4 + 2X_2X_4 + 2X_3X_4) + 4Y_{12}X_1X_2 + 4Y_{13}X_1X_3 + 4Y_{14}X_1X_4 + 4Y_{23}X_2X_3 + 4Y_{24}X_2X_4 + 4Y_{34}X_3X_4 \qquad . \qquad .$$
$$. \qquad . \qquad . \qquad . \qquad . \qquad\qquad (26)$$

Using the condition $X_1 + X_2 + X_3 + X_4 = 1$, we transform the coefficients at Y_i

$$X_1 - 2X_1X_2 - 2X_1X_3 - 2X_1X_4 = X_1 - 2X_1(X_2 + X_3 + X_4)$$

$$= X_1 - 2X_1(1 - X_1) = X_1(2X_1 - 1) \text{ and so on.} \qquad . \qquad (27)$$

Thus

$$\hat{Y} = X_1(2X_1 - 1)Y_1 + X_2(2X_2 - 1)Y_2 + X_3(2X_3 - 1)Y_3 + X_4(2X_4 - 1)Y_4 + 4Y_{12}X_1X_2 + 4Y_{13}X_1X_3 + 4Y_{14}X_1X_4 +$$
$$4Y_{23}X_2X_3 + 4Y_{24}X_2X_4 + 4Y_{34}X_3X_4 \qquad . \qquad . \qquad . \qquad . \qquad . \qquad (28)$$

Introducing the designation

$$a_i = X_i(2X_1 - 1) \text{ and } a_{ij} = 4X_iX_j \qquad (29)$$

and using Eqns (23) and (24) give the expression for the variance S_Y^2.

$$S_{\hat{Y}}^2 = S_Y^2 \left(\sum_{1 \leq i \leq q} a_{ii}/n_i + \sum_{1 \leq i < j \leq q} a_{ij}/n_{ij} \right) \qquad (30)$$

If the number of replicate observations at all the points of the design are equal, i.e. $n_i = n_{ij} = n$, then all the relations for $S_{\hat{Y}}^2$ will take the form

$$S_{\hat{Y}}^2 = S_Y^2 \xi/n \qquad (31)$$

where, for the second degree polynomial,

$$\xi = \sum_{1 \leq i \leq q} a_i^2 + \sum_{1 \leq i < j \leq q} a_{ij}^2 \qquad (32)$$

As in Eqn (32), ξ is only dependent on the mixture composition. Given the replication variance and the number of parallel observations n, the error for the predicted values of the response is readily calculated at any point of the composition-property diagram using an appropriate value of ξ taken from the curve.

Adequacy is tested at each control point, for which purpose the statistic is built:

$$t = \Delta_Y/(S_{\hat{Y}}^2 + S_Y^2) = \Delta_Y n^{1/2}/(S_Y(1 + \xi)^{1/2} \qquad (33)$$

where $\Delta_Y = Y_{exp} - Y_{theory}$. $\qquad (34)$

and n = number of parallel observations at every point.

The t-statistic has the student distribution, and it is compared with the tabulated value of $t_{\alpha/L}(V)$ at a level of significance α, where L = the number of control points, and V = the number for the degrees of freedom for the replication variance.

The null hypothesis is that the equation is adequate is accepted if $t_{cal} < t_{Table}$ for all the control points.

The confidence interval for the response value is

$$\hat{Y} - \Delta \leq Y \leq \hat{Y} + \Delta \qquad (35)$$

$$\Delta = t_{\alpha/L,k} S_{\hat{Y}} \qquad (36)$$

where k is the number of polynomial coefficients determined.

Using Eqn (31) in Eqn (36)

$$\Delta = t_{\alpha/L,k} S_Y(\xi/n)^{1/2} \qquad (37)$$

t-Test for the G Model

If we substitute for X_i in Eqn (20) from Tables 1, the theoretical predictions of the response ($\hat{Y}$) can be obtained. These values can be compared with the experimental results (Table 3 and 4). a, ξ, t and Δ_y are evaluated using Eqns 29, 32, 33 and 37 respectively.

Table 5   t-Test for the Test Control Points

N	CN	I	J	a_i	a_{ij}	a_i^2	a_{ij}^2	ξ	$\ddot{Y}$	$\hat{Y}_a$	Δ_y	t
1	C_1	1	2	-0.333	0.444	0.011	0.197		1476.20	1301.18	175.02	0.011
		1	3	-0.333	0.444	0.011	0.197					
		2	3	-0.333	0.444	0.011	0.197					
					$\sum$	0.033	0.591	0.624				
2	C_2	1	2	-0.333	0.887	0.011	0.787		1453.30	1258.74	194.56	0.012
		1	3	-0.333	0.000	0.011	0.000					
		2	3	0.333	0.000	0.011	0.000					
					$\sum$	0.033	0.787	0.820				
3	C_3	1	2	0.000	0.000	0.000	0.000		1531.64	1382.91	148.73	0.008
		1	3	0.000	0.000	0.000	0.000					
		2	3	-0.333	0.887	0.011	0.787					
					$\sum$	0.011	0.787	0.798				

Significance level $\alpha = 0.05$,

i.e. $t_{\alpha/L}(V_c) = t_{0.05/3}(9)$,   where L=number of control point.

From the Student t-Table, the tabulated value of $t_{0.05/3}(9)$ is found to be 5.722 which is greater than any of the calculated t-values in Table 5. Hence we can accept the Null Hypothesis.

From Eqn 37, with k=6 and $t_{\alpha/k}(V) = t_{0.05/6}(9) = 5.722$,

$\Delta = 325.10$ which satisfies the confidence interval equation of

Eqn (35) when viewed against the response values in Table 5.

V.   COMPUTER PROGRAM

In the developed computer program any desired Rigidity Modulus can be specified as an input and the computer processes and prints out possible combinations of mixes that match the property, to the G tolerance of 0.50 N/mm².

Interestingly, should there be no matching combination, the computer informs the user of this. It also checks the maximum value obtainable with the model.

Choosing a Combination

It can be observed that the strength of 1209 N/sq mm yielded 6combinations. To accept any particular proportions depends on the factors such as workability, cost and honeycombing of the resultant lateritic concrete.

VI.   CONCLUSION AND RECOMMENDATION

Conclusion

Henry Scheffe's simplex design was applied successfully to prove that the modulus of rigidity of lateritic concrete is a function of the proportion of the ingredients (cement, laterite and water), but not the quantities of the materials.

The maximum elastic modulus obtainable with the Rigidity Modulus model is 1459.38 N/sq mm. See the computer run outs which show all the possible lateritic concrete mix options for the desired rigidity modulus property, and the choice of any of the mixes is the user's. One can also draw the conclusion that the maximum values achievable, within the limits of experimental errors, is quite below that obtainable using sand as aggregate. This is due to the predominantly high silt content of laterite.

It can be observed that the task of selecting a particular mix proportion out of many options is not easy, if workability and other demands of the resulting lateritic concrete have to be satisfied. This is an important area for further research work.

The project work is a great advancement in the search for the applicability of laterite in concrete mortar production in regions where sand is extremely scarce with the ubiquity of laterite.

Recommendations
From the foregoing study, the following could be recommended:

i)   The model can be used for the optimization of the strength of concrete made from cement, laterite and water.
ii) Laterite aggregates cannot adequately substitute sharp sand aggregates for heavy construction.
iii) More research work need to be done in order to match the computer recommended mixes with the workability of the resulting concrete.
iii) The accuracy of the model can be improved by taking higher order polynomials of the simplex.

REFERENCE

[1]   Orie, O.U., Osadebe, N.N., "Optimization of the Compressive Strength of Five Component Concrete Mix Using Scheffe's Theory – A case of Mound Soil Concrete", Journal of the Nigerian Association of Mathematical Physics, Vol. 14, pp. 81-92, May, 2009.
[2]   Majid, K.I., Optimum Design of Structure, Butterworths and Co., Ltd, London, pp. 16, 1874.
[3]   David, J., Galliford, N., Bridge Construction at Hudersfield Canal, Concrete, Number 6, 2000.
[4]   Ecocem Island Ltd, Ecocem GBBS Cement. "The Technically Superior and Environmentally Friendly Cement", 56 Tritoville Road Sand Dublin 4 Island, 19.
[5]   Bloom, R. and Benture, A. "Free and restrained Shrinkage of Normal and High Strength Concrete", int. ACI Material Journal, Vol. 92, No. 2, pp. 211-217.
[6]   Onuamah, P.N. and Okpube G.C., "Mechanical Strength Modeling and Optimization Lateritic Solid Block, with 4% Mound Soil Inclusion", *American Journal of Engineering Research (AJER), 2015, Vol' 4, No.5, pp . 178 - 192.*
[7]   Schefe, H., (1958), Experiments with Mixtures, Royal Statistical Society journal. Ser B., Vol. 20, 1958. pp 344-360, Rusia.
[8]   Erwin, K., Advanced Engineering Mathematics, 8th Edition, John Wiley and Sons, (Asia) Pte. Ltd, Singapore, pp. 118-121 and 240 – 262.
[9]   Tardy Yves, (1997), Petrology of Laterites and Tropical Soils. ISBN 90-5410-678-6, http://www.books.google.com/books. Retrieved April 17, 2010.
[10] Dalvi, Ashok, D., Bacon, W. Gordon, Osborne, Robert, C. (March 7-10, 2004), PDAC 2004 International Convention, Trade Show & Investors Exchange.
[11] Wilby, C.B., Structural Concrete, Butterworth, London, UK, 1983.
[12] Reynolds, C. and Steedman, J.C., Reinforced Concrete Designers Handbook, View point Publications, 9th Edition, 1981, Great Britain.
[13] Jackson, N., Civil Engineering Materials, RDC Arter Ltd, Hong Kong, 1983.
[14] Akhanarova, S. and Kafarov, V., Experiment and Optimization in Chemistry and Chemical Engineering, MIR Publishers, Mosco, 1982, pp. 213 - 219 and 240 – 280.
[15] Takafumi, N., Fminori, T., Kamran, M.N. Bernardino, M.C. and Alessandro P.F., (2009), "Practical Equations for the Elatic Modulus of Concrete", ACI Structural Journal, September-October, 2009, Vol. 106, No. 5.

APPENDIX 1
QBASIC BASIC PROGRAM THAT OPTIMIZES THE PROPORTIONS OF LATERITIC CONCRETE MIXES

```
'USING THE SCHEFFE'S MODEL FOR CONCRETE RIGIDITY MODULUS
Cls
C1$ = "(ONUAMAH.HP) RESULT OUTPUT ": C2$ = "A COMPUTER PROGRAM "
C3$ = "ON THE OPTIMIZATION OF THE RIGIDITY MODULUS OF A 3-COMPONENT LATERITIC CONCRETE
MIX"
Print C2$ + C1$ + C3$
Print
'VARIABLES USED ARE
'X1, X2, X3, Z1, Z2, Z3, YT, YTMAX, DS

'INITIALISE I AND YTMAX

I = 0: YTMAX = 0

For MX1 = 0 To 1 Step 0.01
    For MX2 = 0 To 1 - MX1 Step 0.01
      MX3 = 1 - MX1 - MX2
      YTM = 1371.48 * MX1 + 1459.38 * MX2 + 1362.68 * MX3 - 816.84 * MX1 * MX2 + 49.8 * MX1 * MX3 - 54! *
MX2 * MX3
      If YTM >= YTMAX Then YTMAX = YTM
```

```
       Next MX2
     Next MX1
INPUT "ENTER DESIRED RIGIDITY MODULUS, DS = "; DS

   'PRINT OUTPUT HEADING
   Print
   Print Tab(1); "No"; Tab(10); "X1"; Tab(18); "X2"; Tab(26); "X3"; Tab(32); "YTHEORY"; Tab(45); "Z1"; Tab(53);
"Z2"; Tab(61); "Z3"
   Print
   'COMPUTE THEORETICAL RIGIDITY MODULUS, YT
    For X1 = 0 To 1 Step 0.01
     For X2 = 0 To 1 - X1 Step 0.01
      X3 = 1 - X1 - X2
YT = 1371.48 * X1 + 1459.38 * X2 + 1362.68 * X3 - 816.84 * X1 * X2 + 49.8 * X1 * X3 - 54! * X2 * X3

If Abs(YT - DS) <= 0.5 Then

'PRINT MIX PROPORTION RESULTS
      Z1 = X1 + X2 + X3: Z2 = 7.5 * X1 + 8.2 * X2 + 6.9 * X3: Z3 = 0.05 * X1 + 0.03 * X2 + 0.1 * X3
      I = I + 1
      Print Tab(1); I; USING; "##.###"; Tab(7); X1; Tab(15); X2; Tab(23); X3; Tab(32); YT; Tab(42); Z1; Tab(50); Z2;
Tab(58); Z3
       Print
       Print
       If (X1 = 1) Then GoTo 550
      Else
       If (X1 < 1) Then GoTo 150
      End If

150   Next X2
    Next X1
  If I > 0 Then GoTo 550
  Print
  Print "SORRY, THE DESIRED RIGIDITY MODULUS IS OUT OF RANGE OF MODEL"
  GoTo 600

550 Print Tab(5); "THE MAXIMUM VALUE PREDICTABLE BY THE MODEL IS "; YTMAX; "N / Sq mm; "
 600 End
```

A COMPUTER PROGRAM (ONUAMAH.HP) RESULT OUTPUT ON THE OPTIMIZATION OF THE RIGIDITY MODULUS OF A 3-COMPONENT LATERITIC CONCRETE MIX

ENTER DESIRED RIGIDITY MODULUS, DS = ? 1205

| No	X1	X2	X3	YTHEORY	Z1	Z2	Z3

SORRY, THE DESIRED RIGIDITY MODULUS IS OUT OF RANGE OF MODEL

 Press any key to continue

ENTER DESIRED RIGIDITY MODULUS, DS = ? 1209

No	X1	X2	X3	YTHEORY	Z1	Z2	Z3
1	0.530	0.470	0.000	%1209.318	1.000	7.829	0.041
2	0.540	0.460	0.000	%1209.011	1.000	7.822	0.041
3	0.550	0.450	0.000	%1208.867	1.000	7.815	0.041
4	0.560	0.440	0.000	%1208.887	1.000	7.808	0.041
5	0.570	0.430	0.000	%1209.070	1.000	7.801	0.041
6	0.580	0.420	0.000	%1209.416	1.000	7.794	0.042

Research Paper   Open Access

METRO RAIL?... *(RAMANUJAM "JOURNEY")*
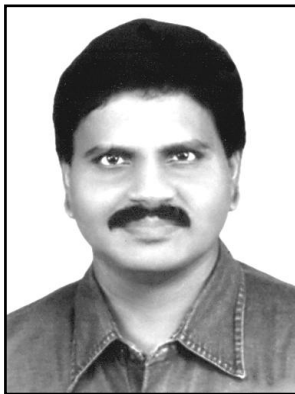
M.Arulmani, B.E.
(Engineer)

V.R.Hema Latha,
M.A., M.Sc., M.Phil.
(Biologist)

ABSTRACT: *It is focused that "**METRO RAIL**" is very much popular across the global nations such as Paris, Singapore, china, etc. London metropolitan railway is the world first underground railway. Besides Paris metro, Metro light rail, US, Metro train, Melbourne, Aurtralia also become popular. Now in India, Metro Rail System also become popular in TAMIL NADU STATE. Various political party leaders also experiencing "**Metro Rail Journey**" among public. If so…*

> *i) What does mean Metro Rail?...*
> *ii) Metro Rail means Flying Rail?...*
> *iii) Metro Rail differs from Electric Rail?...*
> *iv) Metro Rail is heavy rail system?...*
> *v) Cosmo Rail is light rail system?...*
>
> *- Author*

This scientific research focus that "**METRO RAIL**" shall be considered closely associated with "**Cosmological Evolution**". "**Metro Rail**" shall mean "**Cosmo Journey**" performed in "**Three Stages**" of **Nuclear age** evolution of   Universal matters. Further for movement of "**RAIL**" "**LOCO**" (Locomotive force) is essentially required for moving one state to another stage Journey point.

This scientific research further focus that "**J-RADIATION**" (Zero hour radiation) began near "**WHITE HOLE**" region of Universe shall be considered as the "**Locomotive force**" of cosmological evolution of various matters of Universe including origin of Human Life at **Zero point** and white hole region of universe. The philosophy of "**RAIL**", "**LOCO**" and three stage of "**METRO RAIL**" shall be described as below.

(i)

(RAIL LOCO)

(ii)

(LAW OF RAIL)
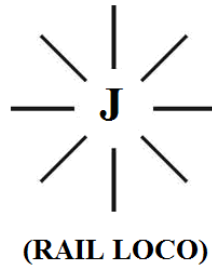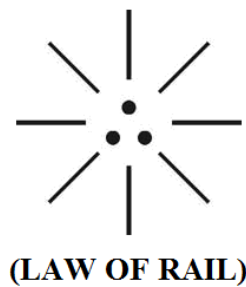
i) Centre dot is like "**SUN TRACK**"
ii) Left dot is like "**EARTH TRACK**"
iii) Right dot is like "**MOON TRACK**"

1.0   "Cosmo" differs from "Metro"?...

It is hypothesized that in the origin of universe the philosophy of word "**COSMO**" shall be considered as distinguished from the word "**METRO**". "**Cosmo Universe**" shall mean "**created universe**" and "**Metro Universe**" shall mean **evolved universe**. The philosophy of "**Cosmo Universe**" and "**Metro Universe**" shall be described as below.

(i)

COSMOPOLITAN RAIL
(Void Universe)
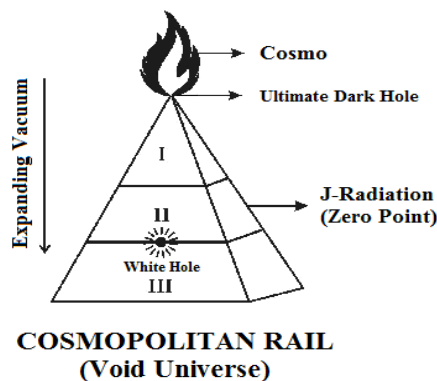
Region I – Perfect vacuum region (Anti-Neutrinos radiation)

Region II – Partial vacuum region (Neutrinos radiation)

Region III – Observable Vacuum region (EMR radiation)

(ii)

METROPOLITAN RAIL
(Evolved Universe)
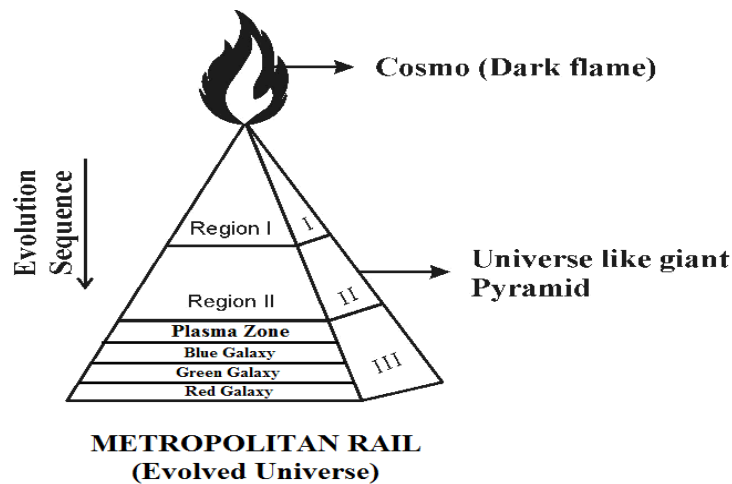
In expanding Universe the cosmopolitan rail journey shall be considered as transformed to metropolitan rail journey in three stages as described below.

i)   **White galaxy – Electric rail journey**
ii)   **Dark galaxy – Metro sleep (transformation)**
iii)   **Blue galaxy – Stage I metro rail**
iv)   **Green galaxy - Stage II metro rail**
v)   **Red galaxy – Stage III metro rail**

It is focused that in the origin of universe "**White galaxy**" near "**White hole region**" (Endothermic) shall be considered as existence of "**VIRGIN MATTERS**" composed of only **three-in-one** fundamental panicles   **PHOTON, ELECTRON, PROTON** and free from "**HCNO MATTERS**". The region of white galaxy shall also be called by author as Journey performed by "**ELECTRIC RAIL**" (Only fundamental parties).The philosophy of "**METRO RAIL**" Journey shall be considered a originated when virgin matters consider "**transformed**" to Earth Planet which further evolved in "**three stages**" of Nuclear age say γ-age, β-age, α-age. The "**Dark age**" (about 4,00,000 years ago) of universe shall also called by author as "**METRO SLEEP**" (or) Transformation of Journey from "**ELECTRIC RAIL**" to "**METRO RAIL**". Further the **ELECTRIC RAIL** shall also be called by author as "**FLYING RAIL**" (upward gravity) and "**METRO RAIL**" shall mean "**TRACK RAIL**" (downward gravity).

2.0   Philosophy of "Mono Rail"?...
Case study shows that in the evolution of rail system various locomotives were developed such as diesel locomotive, steam locomotive etc. It is hypothesized that **MONO RAIL** shall be considered as **FLYING RAIL** deriving energy from natural energy source called by author as "**J-Locomotive**".

(i)

(Evolved Metro Rail)

(ii)

(Evolved Metro Rail)

3.0   Etymology of word "Metro Rail"?...

It is hypothesized that the etymology of word "**Metro Rail**" might be derived from Proto Indo Europe Root Word "**MU-Thiri**", "**MA-Thiri**" "**Muthirai**", "**Muthiren**". Muthiren shall mean "**Human ancestor**" (electric rail) created by supernatural person **RAMANUJAM** who consider created everything through his "**MOTHER JANAKI**" (**Soul**) as described below.
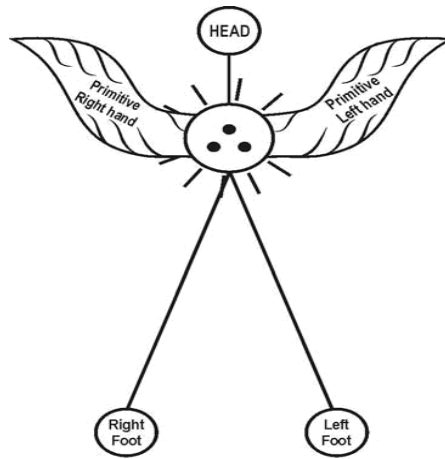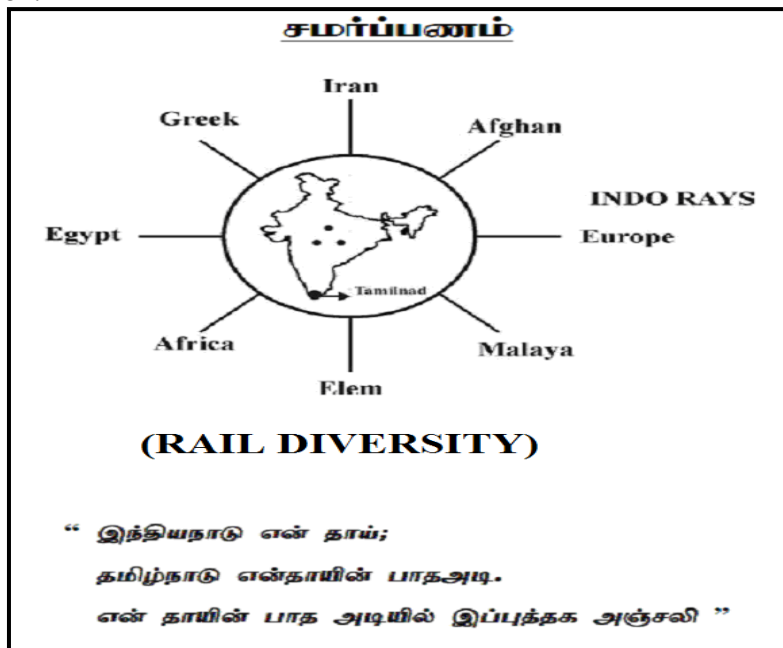

MUTHIREN
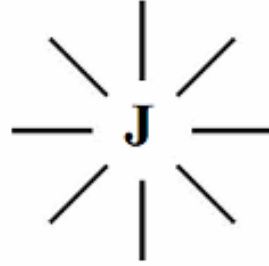**(Human Ancestor)**
(MONO RAIL)

It is further focused that in Hindu mythology the philosophy of Brahma, Rama, Krishna, Shiva shall be considered as evolution of Human Species and traveled by varied "**RAIL SYSTEM**" as described below.

i)	**BRAHMA**	-	Mono Rail (Flying rail)
ii)	**RAMA**	-	Transformation to Metro rail
iii)	**KRISHNA**	-	Stage-I Metro rail
iv)	**SHIVA**	-	Stage-II Metro rail
v)	**POST SHIVA**	-	Stage-III Metro rail

4.0   Conclusion:

சமர்ப்பணம்

(RAIL DIVERSITY)

" இந்தியநாடு என் தாய்;

தமிழ்நாடு என்தாயின் பாதஅடி.

என் தாயின் பாத அடியில் இப்புத்தக அஞ்சலி "

புதுக்கவிதை

(RAIL LOCO)

மனித வாழ்வின் நான்கு

பருவ நிலை...

நான்கு நிலை ரயில் பயணமோ?...

i) முத்திரி (Infant) - Brahma (**Flying Rail**)

ii) நித்திரி (Child) - Raman (**Metro Sleep**)

iii) யாத்திரி (Youth) - Krishna (**Stage-I Metro**)

iv) சித்திரி (Adolescence) - Shiva (**Stage-II Metro**)

v) கத்திரி (Elder) - Post Shivam (**Stage-III Metro**)

— **M. Arulmani,**

Tamil Based Indian, Madurai

5.0   Previous Publications:

<u>Part-A</u>

The philosophy of origin of first life and human, the philosophy of model Cosmo Universe, the philosophy of fundamental neutrino particles have already been published in various international journals mentioned below. Hence this article shall be considered as **extended version** of the previous articles already published by the same author.

1. Cosmo Super Star – IJSRP, April issue, 2013
2. Super Scientist of Climate control – IJSER, May issue, 2013
3. AKKIE MARS CODE – IJSER, June issue, 2013
4. KARITHIRI (Dark flame) The Centromere of Cosmo Universe – IJIRD, May issue, 2013
5. MA-AYYAN of MARS – IJIRD, June issue, 2013
6. MARS TRIBE – IJSER, June issue, 2013
7. MARS MATHEMATICS – IJERD, June issue, 2013

8.   MARS (EZHEM) The mother of All Planets – IJSER, June issue, 2013
9.   The Mystery of Crop Circle – IJOART, May issue, 2013
10.   Origin of First Language – IJIRD, June issue, 2013
11.   MARS TRISOMY HUMAN – IJOART, June issue, 2013
12.   MARS ANGEL – IJSTR, June issue, 2013
13.   Three principles of Akkie Management (AJIBM, August issue, 2013)
14.   Prehistoric Triphthong Alphabet (IJIRD, July issue, 2013)
15.   Prehistoric Akkie Music (IJST, July issue, 2013)
16.   Barack Obama is Tamil Based Indian? (IJSER, August issue, 2013)
17.   Philosophy of MARS Radiation (IJSER, August 2013)
18.   Etymology of word "J" (IJSER, September 2013)
19.   NOAH is Dravidian? (IJOART, August 2013)
20.   Philosophy of Dark Cell (Soul)? (IJSER, September 2013)
21.   Darwin Sir is Wrong?! (IJSER, October issue, 2013)
22.   Prehistoric Pyramids are RF Antenna?!... (IJSER, October issue, 2013)
23.   HUMAN IS A ROAM FREE CELL PHONE?!... (IJIRD, September issue, 2013)
24.   NEUTRINOS EXIST IN EARTH ATMOSPHERE?!... (IJERD, October issue, 2013)
25.   EARLY UNIVERSE WAS HIGHLY FROZEN?!... (IJOART, October issue, 2013)
26.   UNIVERSE IS LIKE SPACE SHIP?!... (AJER, October issue, 2013)
27.   ANCIENT EGYPT IS DRAVIDA NAD?!... (IJSER, November issue, 2013)
28.   ROSETTA STONE IS PREHISTORIC "THAMEE STONE" ?!... (IJSER, November issue, 2013)
29.   The Supernatural "CNO" HUMAN?... (IJOART, December issue, 2013)
30.   3G HUMAN ANCESTOR?... (AJER, December issue, 2013)
31.   3G Evolution?... (IJIRD, December issue, 2013)
32.   God Created Human?... (IJERD, December issue, 2013)
33.   Prehistoric "J" – Element?... (IJSER, January issue, 2014)
34.   3G Mobile phone Induces Cancer?... (IJERD, December issue, 2013)
35.   "J" Shall Mean "JOULE"?... (IRJES, December issue, 2013)
36.   "J"- HOUSE IS A HEAVEN?... (IJIRD, January issue, 2014)
37.   The Supersonic JET FLIGHT-2014?... (IJSER, January issue, 2014)
38.   "J"-RADIATION IS MOTHER OF HYDROGEN?... (AJER, January issue, 2014)
39.   PEACE BEGINS WITH "J"?... (IJERD, January issue, 2014)
40.   THE VIRGIN LIGHT?... (IJCRAR, January issue 2014)
41.   THE VEILED MOTHER?... (IJERD, January issue 2014)
42.   GOD HAS NO LUNGS?... (IJERD, February issue 2014)
43.   Matters are made of Light or Atom?!... (IJERD, February issue 2014)
44.   THE NUCLEAR "MUKKULAM"?... (IJSER, February issue 2014)
45.   WHITE REVOLUTION 2014-15?... (IJERD, February issue 2014)
46.   STAR TWINKLES!?... (IJERD, March issue 2014)
47.   "E-LANKA" THE TAMIL CONTINENT?... (IJERD, March issue 2014)
48.   HELLO NAMESTE?... (IJSER, March issue 2014)
49.   MOTHERHOOD MEANS DELIVERING CHILD?... (AJER, March issue 2014)
50.   E–ACHI, IAS?... (AJER, March issue 2014)
51.   THE ALTERNATIVE MEDICINE?... (AJER, April issue 2014)
52.   GANJA IS ILLEGAL PLANT?... (IJERD, April issue 2014)
53.   THE ENDOS?... (IJERD, April issue 2014)
54.   THE "TRI-TRONIC" UNIVERSE?... (AJER, May issue 2014)
55.   Varied Plasma Level have impact on "GENETIC VALUE"?... (AJER, May issue 2014)
56.   JALLIKATTU IS DRAVIDIAN VETERAN SPORT?... (AJER, May issue 2014)
57.   Human Equivalent of Cosmo?... (IJSER, May issue 2014)
58.   THAI-e ETHIA!... (AJER, May issue 2014)
59.   THE PHILOSOPHY OF "DALIT"?... (AJER, June issue 2014)
60.   THE IMPACT OF HIGHER QUALIFICATION?... (AJER, June issue 2014)

Research Paper　　　　　　　　　　　　　　　　　　　　　　　　　　Open Access

The study of the rate and variety in granting loans and facilities of public and private banks and their impact on attracting customers (Case Study: the chosen Banks of Sistan and Baluchistan province)

[1,] Mohsen Marhamati Bonjar, [2*,] Farahdokht Ebadi

[1]MSc student of Accounting, College of human science, Zahehan Branch, Islamic Azad University, Zahedan, Iran
[2]Assistant professor of Accounting, College of human science, Zahehan Branch, Islamic Azad University, Zahedan, Iran*

ABSTRACT: *There are several factors in modern banking which attract the customers. It will be important to identify and determine the impact and relationship of these factors to the success of banks in attracting customers. Nowadays, the conditions and the situations of the banks are not the same and influential factors may even be different for each of the branches of the Bank. The goal of this research is the study of the rate and variety in granting loans and facilities of public and private banks and their impact on attracting customers in Sistan and Baluchistan province. About 260 customers were questioned for examining hypotheses and T-student and Analyze-variance tests are used for analyzing the data. The results show that the variety of facilities is effective in customer satisfaction.*

KEY WORDS: *Bank, facilities, customer, public and private banks*

I. INTRODUCTION

There are several factors in modern banking which attract the customers. It will be important to identify and determine the impact and relationship of these factors to the success of banks in attracting customers. Nowadays, the conditions and the situations of the banks are not the same and influential factors may even be different for each of the branches of the Bank. At the present time, it is important to identify these factors because of the competition between banks to attract customers. Moreover, competition among banks and loan institutions and other forms of financial resources is increasing, so it seems essential to create a competitive advantage for survival of the banks (Ahmadi and Moradrasoli, 2009).

Attraction of financial resources is the most important mission of the banks so it has an important impact on proper regulation of the flow of money and establishing of a proper monetary and credit system appropriate to long-term and short-term plans of country (Hedayati and et al, 2004).

The banks which absorb more deposits than other banks, they will have more profitability. The banks try to collect the wander fund of the community by their marketing and specific policies to allocate a greater share of deposits to themselves. The structure of bank deposits compared to other rivals should be in such a way that it increase the customers' motivation and willingness to choose any one of them and it will be a kind of marketing and advertising (Abbass. gh. pour, 2010). Certainly, a bank can have the power of maneuverability in economic and development projects more that have a positive and considerable performance in comparison to its rivals in banking system.

Having eighty years old, the banking industry has had enormous changes over the past three decades and after the first two decades of experience in public banking after the revolution, the private banks were activated again in 2001. The banks can be very influential in economic growth of countries by obtaining of customer satisfaction and encouraging savings and capital accumulation and their application in generative and consumption industrials (Ashrafi, 2007). By the formation of private banking in Iran, the power of banks gradually was faded and their customers have more choices to do their banking and financial affairs.

The Banks can attract the customer's satisfaction by granting a variety of facilities and amount of deposit interest rates, repayment period according to the customer's need. From the beginning of the foundation of economics, there has been extending and important issues among economists in relation to the role of interest rates in the orientation of macroeconomic variables. Many of the worlds estimated results of econometric models show that the amount of saving in community and interest rates are correlated.

By opening an account in the bank, the customers hope to receive the deposit interest of account and do the essential financial services in the best way through his bank and receive the needed credits and loans with the lowest interest rate in time (Asgharizadeh and Amin, 2011). However the more of citizens trust to public banks which have a long precedence and prefer to receive a lower interest but in peace. A look at interest rates in some state banks and compares it with the other components of interest in the country's banking market shows the existing gap and some of the customers 'unwillingness to deposit in these banks. Interest rates of deposits in state banks is almost half of the 40% inflation meanwhile the depositors have not the concession of receiving loans for their deposits while they have it in private banks and financial institution (Mafi, 2013). So in this direction the goal of this research is the study of the rate and variety in granting loans and facilities of public and private banks and their impact on attracting customers in Sistan and Baluchistan province.

The hypothesis of the research

There is a significant correlation between granting facilities and loans of state and private banks with attracting customers.

The history of the research

Tahmasebi and et al (2009) in stated that activities such as advertising and marketing are the techniques of attracting customers that good advertising strategy should be applied according to purposes of advertising and ultimately they stated that we can hope to the effectiveness of advertising activities and attracting more customers just by intelligent determining of advertising goals and applying suitable advertising strategies.

Ramazani (2006) in a research entitled "Influencing factors on Resource Mobilization of Bank e Sepah in Gulistan province" and believed that factors such as advertising, development of automation, the number of branches, interest rate and payment facilities are effective factors in attracting deposits.

Keshavarzain and Azimi (2005), in studied the impact of releasing of interest rate on macroeconomic variables of country in 1966-2002. According to the results of simultaneous equations system, they concluded that the negative real rates of interest rate will reduce investment and production and financial releasing will promote investment and economic growth.

Maghoinejad (1999), in a research entitled" Factors affecting on increasing of the rate of customer deposits at Bank e Tejarat in Rafsanjan city" concluded that improvement of the employees' social relationships with customers, , good personal characteristics, advertising, interest rates and favorable services are effective in attracting financial resources.

Laptit and et al (2008), in a research entitled" The expansion of banking services in Europe with regard to the pricing of loans" studied 602 European banks for the period 1996 to 2002 and reviewed the expansion of the banks on the basis of effects of services such the cost of the interest rate and loan pricing.

Wang and Zhang (2006), in studied long-term profitability of banks in Taiwan and concluded that banking services are the most important factor in profitability and obtaining profit for the studied branches of banks. Then the employees are considered as the most factors in increasing of profitability.

Satriv and Znivs (1997), in offered a framework for strategic modeling from various aspects of performance in branches of commercial banks in the United States. They presented the combination of strategic modeling and performance modeling for the first time in their research.

II. DISCUSSION AND CONCLUSION

The frequency of research variables:
●The rate and variety of granting facilities
The index scores are between 1 and 5 and the average of data is 2/62 and the obtained standard deviation is equal to 0/79.

Table (1): central Statistics of the distribution of scores of rate and variety of granting facilities

Variable	Average	S.D	minimum	maximum
The rate and variety of granting facilities	2/62	0/79	1	5

Source: research results

In Table 2 and Chart 1 the frequency and the desirability of variety and the rate of granting facilities by 260 of respondents are shown.

Table (2): Frequency of items in a variable of the rate and diversity of granting of facilities

		frequency	Percent	Cumulative percentage
	The rate and variety of granting facilities			
Items	Very low	19	7.3	7.3
	Low	89	34.2	41.5
	Average	125	48.1	89.6
	high	25	9.6	99.2
	maximum	2	0.8	100
	maximum	260	100.0	

.   Source: research results
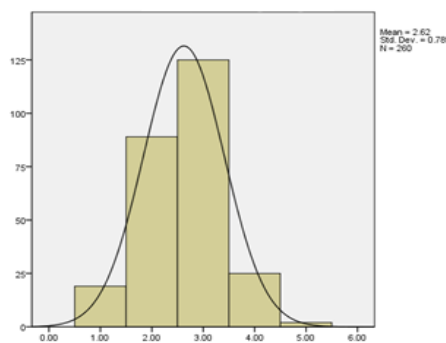
Figure (1): the percentile bar graph of the frequency of variety and the rate of granting facilities, Source: research results

As it has been shown in above chart and table 19 people (7.3%) chose the item of Very low and 89 (34.2%) people chose the item of Low and 125 people (48.1%) chose the item of Average and 25 people (9.6%) chose the item of High and 2 people (0.8%) chose the item of Maximum. The bar graph shows the skewness of a normal variable and the frequency is 2.5.

●**The variable of Customer satisfaction**
The index scores are between 1 and 5 and the average of data is 2/67 and the obtained standard deviation is equal to 0/72.

Table (3): central Statistics of the distribution of scores of customer satisfaction

Variable	Average	S.D	minimum	maximum
Customer satisfaction	2/67	0/72	1	5

Source: research results

In Table 4 and Chart 2 the frequency and the desirability of customer satisfaction by 260 of respondents are shown.

Table (4): Frequency of items in a variable of customer satisfaction

		frequency	Percent	Cumulative percentage
Customer satisfaction				
Items	Very low	8	3.1	3.1
	Low	98	37.7	40.8
	Average	126	48.5	89.2
	high	27	10.4	99.6
	maximum	1	0.4	100
	maximum	260	100.0	

Source: research results
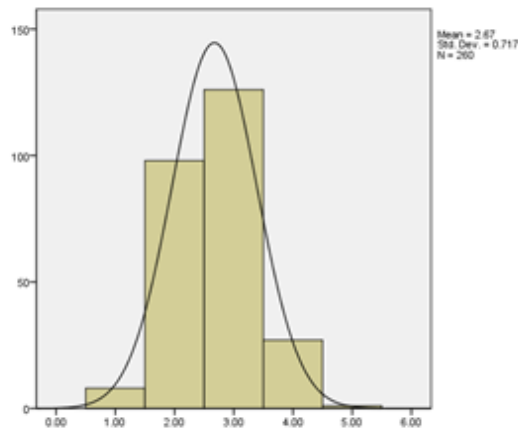
Figure (2): the percentile bar graph of the frequency of customer satisfaction, Source: research results

As it has been shown in above chart and table 8 people (3.1%) chose the item of Very low and 98 (37.7%) people chose the item of Low and 126 people (48.5%) chose the item of Average and 27people (10.4%) chose the item of High and 1 people (0.4%) chose the item of Maximum. The bar graph shows the skewness of a normal variable and the frequency is 2.5.

Inferential statistics

Table 5 shows the descriptive statistics of main and detail variables of questionnaire according to sex separation. The mean and standard deviation of the original variables and the dependent variables are calculated and presented.

Table (5): group sex statistics

	Sex	No	Mean	SD	SD of the mean
Interest rates of deposits	male	108	2.4074	.59652	.05740
	female	152	2.5066	.72784	.05904
Rate of Facilities	male	108	2.5000	.67672	.06512
	female	152	2.4276	.73333	.05948
Variety of facilities	male	108	2.6204	.79387	.07639
	female	152	2.6250	.78742	.06387
Customer Satisfaction	male	108	2.6389	.72934	.07018
	female	152	2.6974	.70981	.05757

Source: research results

Table (6): independent test of sample sex

	Loon test		T - student test						
								CI of 95%	
	F	Probability	t	Degrees of freedom	Probability	The mean difference	SD difference	Lower bound	Upper bound
Interest rates of deposits	6.899	.009	-1.165	258	.245	-.09917	.08514	-.26682	.06848
			-1.204	252.719	.230	-.09917	.08234	-.26133	.06299
Rate of Facilities	.737	.392	.809	258	.419	.07237	.08940	-.10369	.24842
			.821	241.106	.413	.07237	.08819	-.10136	.24610
Variety of facilities	.002	.966	-.047	258	.963	-.00463	.09943	-.20044	.19118
			-.046	229.434	.963	-.00463	.09957	-.20082	.19156
Customer Satisfaction	.288	.592	-.647	258	.518	-.05848	.09036	-.23641	.11945
			-.644	226.719	.520	-.05848	.09077	-.23735	.12039

Source: research results

Table (6) applies the T- Student test and Loon test on data according to sex. Loon test is used for assumption of equality of variances and T-Student test is used for assumption of equality of means.
According to the equality of variances and the p-value, it can be concluded that the assumption of equal variances is rejected in the variable of interest rate. So in the variances of the male and the female community are not equal in this variable.

It is observed in the assumption of equality of variances that the P-value is more than 5% in all variables. As a result of these variables, there is no reason to reject the null hypothesis and therefore we can say that in the studied variables, there were no significant differences between men and women.

Table 7 shows the descriptive statistics of the main and the detail variables of the questionnaire according to the type of bank. The mean and standard deviation of the variables and the dependent variables were calculated and presented.

Table (7): The group statistics of the type of the Banks

The type of the Bank		No	Mean	SD	the mean SD
The deposit rate	public	156	2.4295	.67310	.05389
	private	104	2.5192	.68238	.06691
The rate of facilities	public	156	2.4744	.74875	.05995
	private	104	2.4327	.65008	.06375
The diversity of facilities	public	156	2.6410	.84203	.06742
	private	104	2.5962	.70393	.06903
Customer satisfaction	public	156	2.6859	.75181	.06019
	private	104	2.6538	.66492	.06520

Source: research results

Table (7) applies the T- Student test and Loon test on data according to the type of the banks (public and private). According to the equality of variances test, the p-value is more than 5% for all variances so there is no reason for rejecting of null hypothesis and variances of these variables are equal between the community of the public and private banks.

It is observed in the assumption of equality of variances that the P-value is more than 5% in all variables. As a result of these variables, there is no reason to reject the null hypothesis and therefore we can say that in the studied variables, there were no significant differences between the public and private banks.

III. CONCLUSION

In this research, the statistic sample is consisted of 260 customers of public banks (Maskan, Meli, Keshavarzai) and private banks (Sina, Ghavamin, Eghtesad e Noin, Tejarat, Mellat, Saderat and Saman) in Sistan and Baluchestan. The questionnaires were distributed among them in order to test the hypothesis of the research. 152 (58/46%) of questionnaires were answered by the men and the other 148 (41/54%) of questionnaire were answered by the women. As it was shown in chapter 4, 22.3% of respondents aged less than 25 years, 35.4% at age 25 to 35 and 28.5% were in the age range of 36 to 45 and 13.8 % were aged over 45 years and also in terms of qualification, 15.8% of them had not diploma, 18.1% of them were diploma, 27.7% of them had A.A degree and 28/8% had B.A degree and 9/6% had M.A degree and above it. In terms of jobs, 15/8 % had no job, 6/5% was worker, 11/2% was teachers, 4/6% was engineers, 3/8% was physicians, 10/4% was students, 26/9% was employees and 20/8% had free jobs. The purpose of research includes the review and identifying of different strategies of public and private banks in the calculation of interest rates and variety of facilities and assessing of the efficacy of strategies to attract customers in selected banks in Sistan and Baluchestan.

Hypothesis testing: The variety of facilities of public and private banks has a significant correlation with customer satisfaction.

It was shown by the help of Loon and T-student tests that there was no significant difference in variables used in this study between private and public banks. Because the P-value is more than 5% in all variables in the test of equality of variances, so there is no reason for rejecting of null hypothesis and variances of these variables are equal between the community of the public and private banks.

In the test of assumption of the equality of the means, the P-value was more than 5% in all variables. As a result of these variables, there is no reason to reject the null hypothesis and therefore we can say that in the studied variables, there were no significant differences between the public and private banks.

However for the variable of desirability of the variety and the rate of granting facilities, from total number of 260of customers, 19 people (7.3%) chose the item of Very low and 89 (34.2%) people chose the item of Low and 125 people (48.1%) chose the item of Average and 25 people (9.6%) chose the item of High and 2 people (0.8%) chose the item of Maximum so it can be concluded that the diversity of facilities is effective in customer's satisfaction.

IV.   SUGGESTIONS

The results of this study showed that since the rate of interest is effective on customer satisfaction and his investment in bank, it will be suggested that the banks should design packages of deposits with special privilege and should consider the culture and the religion of each region (especially Sunni areas). For example daily cash deposit without interest but with the privilege of priority facilities papers or payment of the cost of domestic and foreign tours for Sunni areas.

With regard to the impact of facilities rate on customer satisfaction, considering indices such as interest -free loans, partnership facilities and facilities of civic participation and the amount of commission for the named facilities will be effective in improving of these indices for attracting customers and the amount of customer's investment in these banks.

Diversity in loans and facilities has a considerable impact for attracting customers. For example in commercial-free areas partnership facilities and loans are welcomed more because it is easier to customers. It will be suggested that the banks give financial advice to their customers to receive the best facilities and loans according to their income, the time of repaying and also according to the kind of their needs.

The relationship between performance and customer satisfaction with the performance evaluation models of organization such as the balanced scorecard and the study of new variables in customers' satisfaction such as giving financial advice will increase the customer satisfaction.

REFERENCES

[1]. Abbasgholi. p. M, 2010, Factors affecting performance of banks, the banks and the economy, No. 106.
[2]. Ahmadi.M, Moradrasouli. M, 2009, Factors affecting the customer attraction of the banks, Banking Management, University of Urmia.
[3]. Asgharizadeh. E, Amin. F, 2011, Increase banking productivity with priority of customers using quantitative techniques, policies and Economic Research Journal, No. 36.
[4]. Ashrafi. S. M, 2007, Evaluate the quality of services in the public and private banks using the next five dimensional SERVQUAL model in Bank e Parsian and Melli Iran ", MSc thesis, Islamic Azad University, Science and Research, Faculty of Management and Economics.
[5]. Hedyati. A, Kalhor. H, Safari. A, Bahmani. M, 2004, Domestic banking operations, resource allocation, ninth edition, Tehran: Institute of Banking.
[6]. Lepetit L., Nys .E, Rous. Ph, Tarazi. A, 2008, the expansion of services in European banking: Implications for loan pricing and interest margins, Journal of Banking & Finance 32, 2325-2335.
[7]. Mafi.k, 2013, Deposit in public banks, Department of Economics, The Jam e Jam paper, 16 November 2014.
[8]. Maghoinejad. H, 1999, influencing factors on increasing customer deposits in branches of Bank e Tejarat in the city of Rafsanjan (from the customers view), MS Thesis, School of Humanities, and University of Kerman.
[9]. Ramzani. A, 2006, influencing factors on resource mobilization of Bank e Sepah in Gulistan province, MS Thesis, Faculty of Humanities and Social Sciences, University of Mazandaran.
[10]. Soteriou, A. C and Zenios, S.A, 1997 "Efficiency, profitability and quality in the provisison of banking" Department of Business Administration, University of Cyprus, working papers
[11]. Tahmasebi, Hamza. A, Ghafari, Sara and Amozada. H, 2009, Banking advertising, its causes and effects on attracting customers, the first banking ethics Advertising Conference.
[12]. Yong-Chin Liu, Jung-Hua Hung. 2006, Services and the long-term profitability in Taiwan's banks, Global Finance Journal, Vol .17, Issue 2, December 2006, pp. 177-191.

Research Paper   Open Access

Effect of two temperature and anisotropy in an axisymmetric problem in transversely isotropic thermoelastic solid without energy dissipation and with two temperature

Nidhi Sharma[1] ,Rajneesh Kumar [2] , and Parveen Lata[3]
[1]Department of Mathematics, MM University, Mullana, Ambala, Haryana, India.
[2]Department of Mathematics, Kurukshetra University ,Kurukshetra, Haryana, India
[3]Department of Basic and Applied Sciences, Punjabi University, Patiala, Punjab, India
E-mail:parveenlata70@gmail.com

ABSTRACT: *The present study is concerned with the thermoelastic interactions in a two dimensional homogeneous, transversely isotropic thermoelastic solids without energy dissipation and with two temperatures in the context of Green - Naghdi model of type-II. The Laplace and Hankel transforms have been employed to find the general solution to the field equations. Concentrated normal force, normal force over the circular region and concentrated thermal source and thermal source over the circular region have been taken to illustrate the application of the approach. The components of displacements, stresses and conductive temperature distribution are obtained in the transformed domain. The resulting quantities are obtained in the physical domain by using numerical inversion technique. Numerically simulated results are depicted graphically to show the effect of two temperature and anisotropy on the components of normal stress, tangential stress and conductive temperature.*

KEYWORDS: *Transversely isotropic, thermoelastic, Laplace transform, Hankel transform, concentrated and distributed sources*

I.   INTRODUCTION

During the past few decades , widespread attention has been given to thermoelasticity theories that admit a finite speed for the propagation of thermal signals. In contrast to the conventional theories based on parabolic-type heat equation , these theories are referred to as generalized theories. Thermoelasticity with two temperatures is one of the non classical theories of thermomechanics of elastic solids. The main difference of this theory with respect to the classical one is a thermal dependence.

In a series of papers, Green and Naghdi [6] –[8] provided sufficient basic modifications in the constitutive equations and proposed three thermoelastic theories which are referred to as GN theories of Type-I, II, and III . GN Theory of Type-I is a theory describing behaviour of a thermoelastic body which relies on entropy balance rather than entropy inequality. The novel quantity is a thermal displacement variable. GN theory of Type-II allows heat transmission at finite speed without energy dissipation. This model admits un-damped thermoelastic waves in a thermoelastic material and is best known as theory of thermoelasticity without energy dissipation. The principal feature of this theory is in contrast to classical thermoelasticity associated with Fourier's law of heat conduction, the heat flow does not involve energy dissipation. This theory permits the transmission of heat as thermal waves at finite speed. GN theory of Type-III includes the previous two models as special cases and admits dissipation of energy in general. This theory was pursued by many authors. Chandrasekharaiah and Srinath [1] discussed the thermoelastic waves without energy dissipation in an unbounded body with a spherical cavity.

Youssef [25,27,29] constructed a new theory of generalized thermoelasticity by taking into account two-temperature generalized thermoelasticity theory for a homogeneous and isotropic body without energy dissipation and obtained the variational principle. Chen and Gurtin [2], Chen et al. [3] and [4] have formulated a theory of heat conduction in deformable bodies which depends upon two distinct temperatures, the conductive temperature φ and the thermodynamical temperature T. For time independent situations, the difference between these two temperatures is proportional to the heat supply, and in absence of heat supply, the two temperatures are identical. For time dependent problems, the two temperatures are different, regardless of the presence of heat supply. The two temperatures T, φ and the strain are found to have representations in the form of a travelling wave plus a response, which occurs instantaneously throughout the body. Several researchers studied various problems involving two temperature.e.g. (Warren and Chen [24] ,Quintanilla [16], Youssef AI-Lehaibi [26] and Youssef AI -Harby [27] , Kaushal, Kumar and Miglani [12] , Kumar, Sharma and Garg [14],Sharma and Marin[18],Sharma and Bhargav [17], Sharma, Sharma and Bhargav [22],Sharma and Kumar[19]). The axisymmetric problems has been studied during the past decade by many authors.e.g. (Kumar and Pratap [10]. Sharma and Kumar [15] , Kumar and Kansal [13], Kumar,Kumar and Gourla[11],Sharma,Kumar and Ram[21]). Inspite of these studies no attempt has been made to study the axisymmetric deformation in transversely isotropic medium with two temperature and without energy dissipation.

In the present investigation, a two dimensional axisymmetric problem in transversely isotropic thermoelastic solid without energy dissipation and with two temperature is investigated . The components of normal stress, tangential stress and conductive temperature subjected to concentrated normal force , normal force over the circular region and concentrated thermal source along with thermal source over the circular region are obtained by using Laplace and Hankel transforms. Numerical computation is performed by using a numerical inversion technique and the resulting quantities are shown graphically.

II. BASIC EQUATIONS

Following Youssef [28] the constitutive relations and field equations in absence of body forces and heat sources are:

$$t_{ij} = C_{ijkl}e_{kl} - \beta_{ij}T \qquad (1)$$

$$C_{ijkl}e_{kl,j} - \beta_{ij}T_{,j} = \rho\ddot{u}_i \qquad (2)$$

$$K_{ij}\varphi_{,ij} = \beta_{ij}T_0\ddot{e}_{ij} + \rho C_E\ddot{T} \qquad (3)$$

where

$$T = \varphi - a_{ij}\varphi_{,ij} \qquad (4)$$

$$\beta_{ij} = C_{ijkl}\alpha_{ij} \qquad (5)$$

$$e_{ij} = \frac{1}{2}(u_{i,j} + u_{j,i}) \quad i,j = 1,2,3 \qquad (6)$$

Here
$C_{ijkl}(C_{ijkl} = C_{klij} = C_{jikl} = C_{ijlk})$ are elastic parameters, β_{ij} is the thermal tensor, T is the thermodynamic temperature, T_0 is the reference temperature, t_{ij} are the components of stress tensor, e_{kl} are the components of strain tensor, u_i are the displacement components, ρ is the density, C_E is the specific heat, K_{ij} is the thermal conductivity, a_{ij} are the two temperature parameters, α_{ij} is the coefficient of linear thermal expansion.

III. FORMULATION OF THE PROBLEM

We consider a homogeneous transversely isotropic , thermoelastic body initially at uniform temperature T_0. We take a cylindrical polar co-ordinate system (r, θ, z) with symmetry about z –axis. As the problem considered is plane axisymmetric, the field component $v = 0$, and $u , w, and \varphi$ are independent of θ. We have used appropriate transformation following Slaughter[23] on the set of equations (1)-(3) to derive the equations for transversely isotropic thermoelastic solid without energy dissipation and with two temperature and restrict our analysis to the two dimensional problem with $\vec{u} = (u, 0, w)$, we obtain

$c_{11}\left(\frac{\partial^2 u}{\partial r^2}+\frac{1}{r}\frac{\partial u}{\partial r}-\frac{1}{r^2}u\right)+c_{13}\left(\frac{\partial^2 w}{\partial r\partial z}\right)+c_{44}\frac{\partial^2 u}{\partial z^2}+c_{44}\left(\frac{\partial^2 w}{\partial r\partial z}\right)-\beta_1\frac{\partial}{\partial r}\left\{\varphi-a_1\left(\frac{\partial^2 \varphi}{\partial r^2}+\frac{1}{r}\frac{\partial \varphi}{\partial r}\right)-a_3\frac{\partial^2 \varphi}{\partial z^2}\right\}=\rho\frac{\partial^2 u}{\partial t^2}$ (7)

$(c_{13}+c_{44})\left(\frac{\partial^2 u}{\partial r\partial z}+\frac{1}{r}\frac{\partial u}{\partial z}\right)+c_{44}\left(\frac{\partial^2 w}{\partial r^2}+\frac{1}{r}\frac{\partial w}{\partial r}\right)+c_{33}\frac{\partial^2 w}{\partial z^2}-\beta_3\frac{\partial}{\partial z}\left\{\varphi-a_1\left(\frac{\partial^2 \varphi}{\partial r^2}+\frac{1}{r}\frac{\partial \varphi}{\partial r}\right)-a_3\frac{\partial^2 \varphi}{\partial z^2}\right\}=\rho\frac{\partial^2 w}{\partial t^2}$ (8)

$K_1\left(\frac{\partial^2 \varphi}{\partial r^2}+\frac{1}{r}\frac{\partial \varphi}{\partial r}\right)+K_3\frac{\partial^2 \varphi}{\partial z^2}=T_0\frac{\partial^2}{\partial t^2}\left(\beta_1\frac{\partial u}{\partial r}+\beta_3\frac{\partial w}{\partial z}\right)+\rho C_E\frac{\partial^2}{\partial t^2}\left\{\varphi-a_1\left(\frac{\partial^2 \varphi}{\partial r^2}+\frac{1}{r}\frac{\partial \varphi}{\partial r}\right)-a_3\frac{\partial^2 \varphi}{\partial z^2}\right\}$ (9)

Constitutive relations are

$t_{rr}=c_{11}e_{rr}+c_{12}e_{\theta\theta}+c_{13}e_{zz}-\beta_1 T$

$t_{zr}=2c_{44}e_{rz}$

$t_{zz}=c_{13}e_{rr}+c_{13}e_{\theta\theta}+c_{33}e_{zz}-\beta_3 T$

$t_{\theta\theta}=c_{12}e_{rr}+c_{11}e_{\theta\theta}+c_{13}e_{zz}-\beta_1 T$ (10)

where

$e_{rz}=\frac{1}{2}\left(\frac{\partial u}{\partial z}+\frac{\partial w}{\partial r}\right),\ e_{rr}=\frac{\partial u}{\partial r},\ \ e_{\theta\theta}=\frac{u}{r}\ ,\ \ e_{zz}=\frac{\partial w}{\partial z},\ T=\varphi-a_1\left(\frac{\partial^2 \varphi}{\partial r^2}+\frac{1}{r}\frac{\partial \varphi}{\partial r}\right)-a_3\frac{\partial^2 \varphi}{\partial z^2}$

$\beta_{ij}=\beta_i\delta_{ij}\ ,\qquad K_{ij}=K_i\delta_{ij}$

$\beta_1=(c_{11}+c_{12})\alpha_1+c_{13}\alpha_3,\qquad\qquad \beta_3=2c_{13}\alpha_1+c_{33}\alpha_3$

In the above equations we use the contracting subscript notations $(1\to 11, 2\to 22, 3\to 33, 4\to 23, 5\to 31, 6\to 12)$ to relate c_{ijkl} to c_{mn}

To facilitate the solution, the following dimensionless quantities are introduced

$r'=\frac{r}{L},\quad z'=\frac{z}{L}\ ,\ t'=\frac{c_1}{L}t\ ,\ u'=\frac{\rho c_1^2}{L\beta_1 T_0}u,\ w'=\frac{\rho c_1^2}{L\beta_1 T_0}w,\ T'=\frac{T}{T_0}\ ,t'_{zr}=\frac{t_{zr}}{\beta_1 T_0}$

$t'_{zz}=\frac{t_{zz}}{\beta_1 T_0}\ ,\varphi'=\frac{\varphi}{T_0},a'_1=\frac{a_1}{L},a'_3=\frac{a_3}{L}$ (11)

in equations (7)-(9) and after that suppressing the primes and applying the Laplace and Hankel transforms defined by

$\hat{f}(r,z,s)=\int_0^\infty f(r,z,t)e^{-st}dt$ (12)

$\tilde{f}(\xi,z,s)=\int_0^\infty \hat{f}(r,z,s)rJ_n(r\xi)\,dr$ (13)

on the resulting quantities, we obtain

$\left(-(\xi^2+s^2)+\delta_2 D^2\right)\tilde{u}-\xi\delta_1 D\tilde{w}+(\xi(1-a_1\xi)-a_3\xi D^2\,)\tilde{\varphi}=0$ (14)

$\delta_1\left(\frac{-\xi^2+1}{\xi}\right)D\tilde{u}+\left(\delta_3 D^2-(\delta_2\xi^2+s^2)\right)\tilde{w}-\left(\frac{\beta_3}{\beta_1}(\xi^2 a_1+1)D-D^3\right)\tilde{\varphi}=0$ (15)

$(\delta_4 s^2\xi)\tilde{u}-\delta_5 D\tilde{w}+\left(\left(\frac{\delta_6 a_3}{L}+\frac{K_3}{K_1}\right)D^2-\xi^2+\delta_6 s^2(1+\xi^2)\right)\tilde{\varphi}=0$ (16)

where $\delta_1=\frac{c_{13}+c_{44}}{c_{11}}\ ,\frac{c_{44}}{c_{11}}=\delta_2,\frac{c_{33}}{c_{11}}=\delta_3,\ \delta_4=\frac{\beta_1^2 T_0}{K_1},\ \ \delta_5=\frac{\beta_3\beta_1 T_0}{K_1}s^2\ ,\ \ \delta_6=\frac{\rho C_E C_1^2}{K_1}$

The solution of the equations (14)-(16), using the radiation condition that $\tilde{u}$, $\tilde{w}$, $\tilde{\varphi} \to 0$ as $z \to \infty$,yields

$$\tilde{u} = A_1 e^{-\lambda_1 z} + A_2 e^{-\lambda_2 z} + A_3 e^{-\lambda_3 z} \qquad (17)$$

$$\tilde{w} = d_1 A_1 e^{-\lambda_1 z} + d_2 A_2 e^{-\lambda_2 z} + d_3 A_3 e^{-\lambda_3 z} \qquad (18)$$

$$\tilde{\varphi} = l_1 A_1 e^{-\lambda_1 z} + l_2 A_2 e^{-\lambda_2 z} + l_3 A_3 e^{-\lambda_3 z} \qquad (19)$$

where $\pm \lambda_i$ ($i = 1,2,3$) are the roots of the equation

$$AD^6 + BD^4 + CD^2 + E = 0 \qquad (20)$$

where A , B, C,D, and E are listed in appendix A and the values of coupling constants d_i and l_i , are given in appendix B and A_i ,$i=1,2,3$ being arbitrary constants.

IV.   APPLICATIONS
Mechanical forces/ Thermal sources acting on the surface
The boundary conditions are

(i) $t_{zz}(r,z,t) = -P_1(r,t)$

$(ii)$$t_{zr}(r,z,t) = 0$

$(iii)$$\frac{\partial \varphi}{\partial z} = P_2(r,t)$ $\qquad (21)$

$P_1(r,t)$, $P_2(r,t)$ are well behaved functions

Here $P_2(r,t)$ =0 corresponds to plane boundary subjected to normal force and $P_1(r,t) = 0$ corresponds to plane boundary subjected to thermal point source.

Case 1. **Concentrated normal force/ Thermal point source**
        When plane boundary is subjected to concentrated normal force/ thermal point force, then $P_1(r,t), P_2(r,t)$ take the form

$$(P_1(r,t), P_2(r,t)) = \left(\frac{P_1 \delta(r)\delta(t)}{2\pi r} , \frac{P_2 \delta(r)\delta(t)}{2\pi r} \right) \qquad (22)$$

P_1 is the magnitude of the force applied , P_2 is the magnitude of the constant temperature applied on the boundary and $\delta(r)$ is the Dirac delta function.

        Using the equations (10), (11) in the boundary conditions (21) and applying the transforms defined by(12) and (13) and substitute the values of $\tilde{u}$, $\tilde{w}$, $\tilde{\varphi}$ from (17)-(19) in the resulting equations, we obtain the expressions for the components of displacement, stress , and conductive temperature in case of concentrated normal force which are given in appendix C and in case of thermal point source are these are obtained by replacing Δ_i by Δ_i^* and P_1 with P_2, as listed in appendix D

Case II: Normal force over the circular region/ Thermal source over the circular region
        Let a uniform pressure of total magnitude P_1/ constant temperature P_2 applied over a uniform circular region of radius *a* is obtained by setting

$$P_1(r,t), P_2(r,t) = \left(\frac{P_1}{\pi a^2} H(a-r)\delta(t), \frac{P_2}{\pi a^2} H(a-r)\delta(t) \right) \qquad (23)$$

where $H(a-r)$ is the Heaviside unit step function.

Making use of dimensionless quantities defined by (11) and then applying Laplace and Hankel transforms defined by (12)-(13) on (23) ,we obtain

$$(\widetilde{P_1}(\xi, s), \widetilde{P_2}(\xi, s)) = \left(\frac{P_1}{\pi a} \frac{J_1(a\xi)}{\xi}, \frac{P_2}{\pi a} \frac{J_1(a\xi)}{\xi} \right)$$

The expressions for the components of displacements, stress and conductive temperature are obtained by replacing $\frac{P_1}{2\pi}$ with $\frac{P_1}{\pi a} \frac{J_1(a\xi)}{\xi}$ and by replacing $\frac{P_2}{2\pi}$ with $\frac{P_2}{\pi a} \frac{J_1(a\xi)}{\xi}$ in equations (C.1)-(C.5) and in (D.1)-(D.5) respectively

V.   PARTICULAR CASES

(i) If $a_1 = a_3 = 0$, from equations (C.1) $-$ (C.5) and from (D.1) $-$ (D.5) we obtain the corresponding expressions for displacements, stresses and temperature change in thermoelastic medium without energy dissipation.

(ii) If we take $a_1 = a_3 = a$, $c_{11} = \lambda + 2\mu = c_{33}$, $c_{12} = c_{13} = \lambda$, $c_{44} = \mu$, $\beta_1 = \beta_3 = \beta$, $\alpha_1 = \alpha_3 = \alpha$, $K_1 = K_3 = K$ in equations (C.1) $-$ (C.5) and (D.1) $-$ (D.5) , we obtain the corresponding expressions for displacements, stresses and conductive temperature for isotropic thermoelastic solid without energy dissipation.

VI.   INVERSION OF THE TRANSFORMS

To obtain the solution of the problem in physical domain, we must invert the transforms in equations (26)-(30) These expressions are functions of z, the parameters of Laplace and Hankel transforms s and ξ ,respectively ,and hence are of the form $\tilde{f}(\xi, z, s)$. To get the function $f(r, z, t)$ in the physical domain, first we invert the Hankel transform using

$$\hat{f}(r, z, s) = \int_0^\infty \xi \tilde{f}(\xi, z, s) J_n(\xi r) d\xi \qquad (24)$$

Now for the fixed values of ξ, z and r the $\hat{f}(r, z, s)$ in the expression above can be considered as the Laplace transform $\hat{g}(s)$ of $g(t)$. Following Honig and Hirdes [9] , the Laplace transform function $\hat{g}(s)$ can be inverted.

The last step is to calculate the integral in equation (24). The method for evaluating this integral is described in Press et al. [15]. It involves the use of Romberg's integration with adaptive step size. This also uses the results from successive refinements of the extended trapezoidal rule followed by extrapolation of the results to the limit when the step size tends to zero.

VII.   NUMERICAL RESULTS AND DISCUSSION

Copper material is chosen for the purpose of numerical calculation which is transversely isotropic. Physical data for a single crystal of copper is given by

$c_{11} = 18.78 \times 10^{10} \, Kgm^{-1}s^{-2}$, $c_{12} = 8.76 \times 10^{10} \, Kgm^{-1}s^{-2}$, $c_{13} = 8.0 \times 10^{10} \, Kgm^{-1}s^{-2}$ $c_{33} = 17.2 \times 10^{10} \, Kgm^{-1}s^{-2}$, $c_{44} = 5.06 \times 10^{10} \, Kgm^{-1}s^{-2}$ $C_E = 0.6331 \times 10^3 \, JKg^{-1}K^{-1}$ $\alpha_1 = 2.98 \times 10^{-5} K^{-1}$, $\alpha_3 = 2.4 \times 10^{-5} K^{-1}$, $\rho = 8.954 \times 10^3 \, Kgm^{-3}$, $K_1 = 0.433 \times 10^3 \, Wm^{-1}K^{-1}$, $K_3 = 0.450 \times 10^3 \, Wm^{-1}K^{-1}$

Following Dhaliwal and Singh [5], magnesium crystal is chosen for the purpose of numerical calculation(isotropic solid). In case of magnesium crystal like material for numerical calculations, the physical constants used are

$\lambda = 2.17 \times 10^{10} Nm^2$, $\mu = 3.278 \times 10^{10} Nm^2$, $K = 1.7 \times 10^2 Wm^{-1}deg^{-1}$ $\omega_1 = 3.58 \times 10^{11} S^{-1}$ $\beta = 2.68 \times 10^6 \, Nm^{-2}deg^{-1}$, $\rho = 1.74 \times 10^3 Kgm^{-3}$ $T_0 = 298K$, $C_E = 1.04 \times 10^3 Jkg^{-1}deg^{-1}$

The values of normal force stress t_{zz} , tangential stress t_{zr} and conductive temperature φ for a transversely isotropic thermoelastic solid with two temperature (TITWT) , isotropic thermoelastic solid with two temperature(ITSWT) and thermoelastic solid without two temperature (TSWT) are presented graphically to show the impact of two temperature and anisotropy.

i). The solid line corresponds to (TITWT) for $a_1 = .02$, $a_3 = .04$

ii) small dashed line corresponds to(TITWT) for $a_1 = .05$, $a_3 = .07$

iii)solid line with centre symbol circle corresponds to (TSWT) for $a_1 = a_3 = 0$

iv) solid line with centre symbol diamond corresponds to (ITSWT) for $a_1 = a_3 = .06$

VIII.　　NORMAL FORCE ON THE BOUNDARY OF THE HALF-SPACE

Case I: Concentrated normal force

Fig.1 shows the variations of normal stress t_{zz} with distance r. In the initial range there is a sharp decrease in the values of t_{zz} for all the curves i.e. (TITWT) , (ITSWT) and (TSWT) but away from source applied, it follows oscillatory behaviour near the zero value. We can see that the two temperature have significant effect on the normal stress in all the cases as there are more variations in t_{zz} in case of (TITWT) and (ITSWT) as compared to (TSWT). Impact of anisotropy is seen in the range $1 \leq r \leq 3$ where the values of t_{zz} for (TITWT) are more than from (ITSWT). It is evident from fig.2 that near the point of application of source there is increase in the values of t_{zr} for (ITSWT) and have small variation near the zero value in the remaining range. However for (TITWT) and (TSWT) , there is a sharp decrease in the range $0 \leq r \leq 2$ but pattern is oscillatory near the zero value in the rest of the range. In case of (TITWT) oscillations are of greater magnitude than in case of (TSWT), however not much difference in behaviour is noticed in the two cases i.e. i)$a_1 = .02$, $a_3 = .04$ and ii) $a_1 = .05$, $a_3 = .07$. Fig.3 depicts the behaviour of conductive temperature φ. Two temperature and anisotropy effect is more prominent in the range $0 \leq r \leq 5$ for all the curves and curves are close to each other in the remaining range with minor difference in the magnitude.

Case II: Normal force over the circular region

The trend of variations of normal stress t_{zz}, tangential stress t_{zr} and conductive temperature φ for normal force over the circular region is similar to concentrated normal force with difference in their magnitude. At a first look it seems as mirror image of one another i.e. pattern is similar but the corresponding values are different. These variations are shown in figs. (4-6)

7.2 Thermal source on the boundary of half-space
Case-I: Thermal point source

Fig.7 depicts the variations of normal stress t_{zz} with distance r. In case of (ITSWT), it decreases sharply in the range $0 \leq r \leq 2$ and away from point of application of source the behaviour is oscillatory. Opposite behaviour is exhibited in the remaining cases i.e. in case of (TITWT) and (TSWT). Also for (TITWT) , difference in variations in both cases(case(i) $a_1 = .02$, $a_3 = .04$ and case(ii) $a_1 = .05$, $a_3 = .07$) are not found but follow same pattern for two temperature parameter and are shown in fig.7.

The values of t_{zr} increase sharply in the range $0 \leq r \leq 2$ and afterwards follow oscillatory pattern in case of (TITWT both cases) and (TSWT). In this case difference in variations is shown when temperature parameters are changed. In case of (ITSWT) , there is a decrease in range $0 \leq r \leq 2$ and away from origin ,it has small variations near zero and impact of anisotropy is visible because behaviour is quite different in this case than in transverse isotropy as is depicted in fig.8.

Fig.9 exhibits the behaviour of conductive temperature φ with distance r. In the initial range there is a sharp increase in (TITWT both cases), (TSWT) but away from source behaviour is oscillatory. In case of (ITSWT), there is an increase in the initial range but afterwards there are small variations near zero.

Case-II: Thermal source over the circular region

The trend of variations of normal stress t_{zz}, tangential stress t_{zr} and conductive temperature φ for thermal source over the circular region is similar to thermal point source with difference in their magnitude. The pattern is similar but the corresponding values are different. These variations are shown in figs. (9-12)
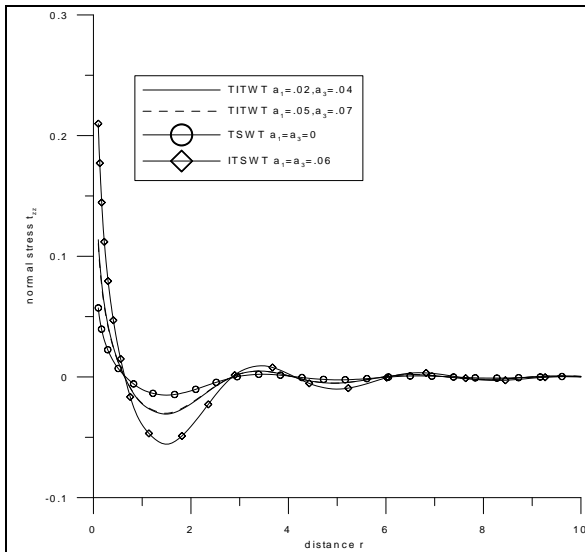
Fig.1 Variation of normal stress t_{ZZ} with distance r (concentrated normal force)
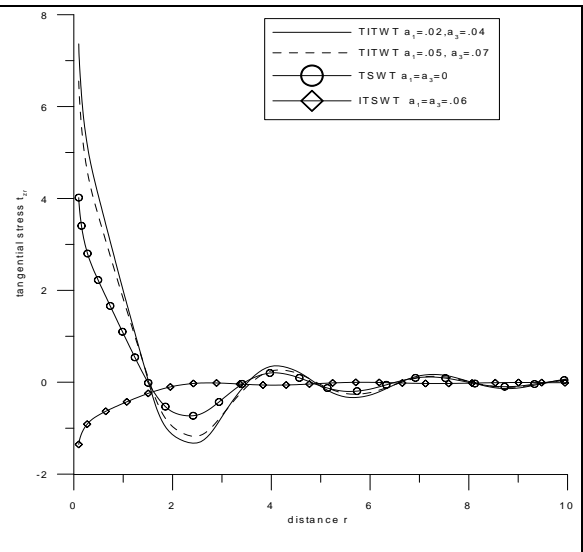

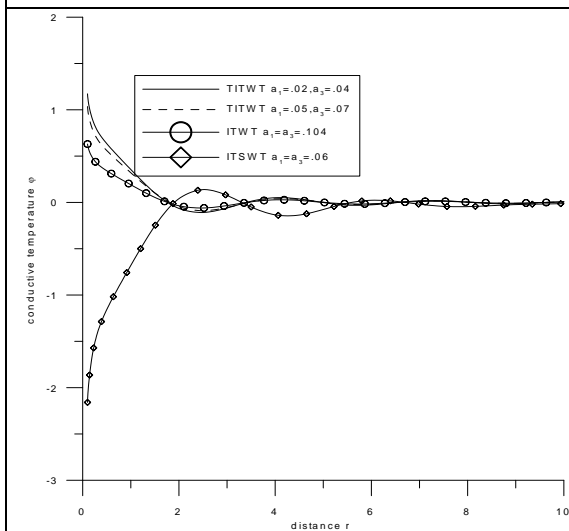**Fig.2 Variation of tangential stress t_{zr} with distance r (concentrated normal force)**

Fig.3 Variation of conductive temperature φ with distance r (concentrated normal force)

Fig.4 Variation of normal stress t_{zz} with distance r (normal force over the circular region)

Fig.5 Variation of tangential stress t$_{zr}$ with distance r (normal force over the circular region)

Fig.6 Variation of conductive temperature φ with distance r (normal force over the circular region)

Fig.7 Variation of normal stress t$_{zz}$ with distance r (thermal point source)

Fig.8 Variation of tangential stress t$_{zr}$ with distance r (thermal point source)

Fig.9 Variation of conductive temperature φ with distance r (thermal point source)
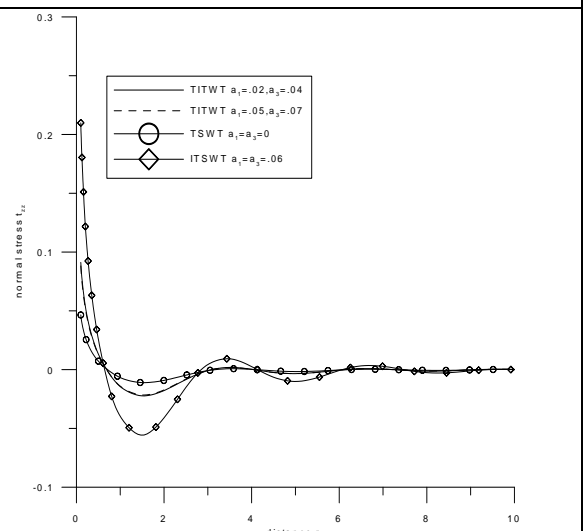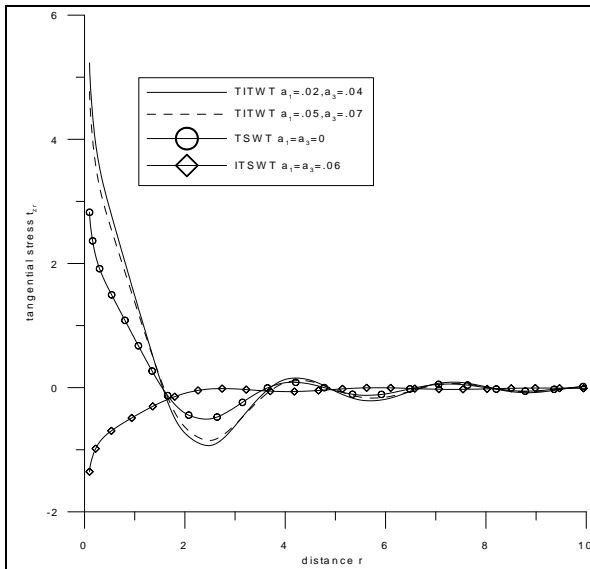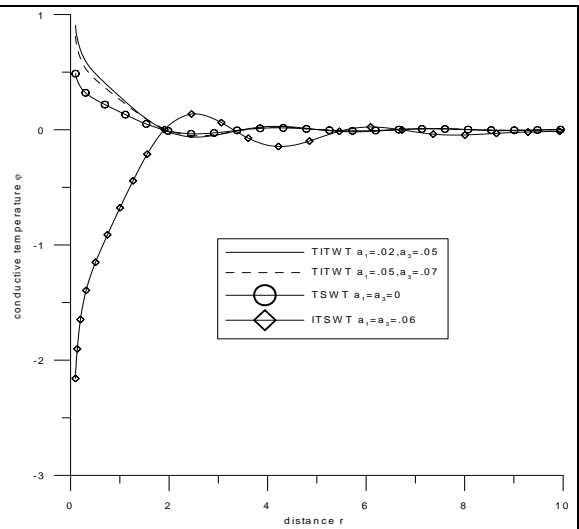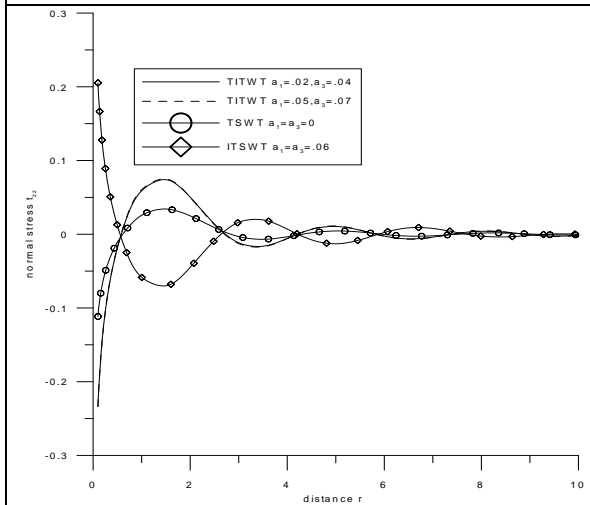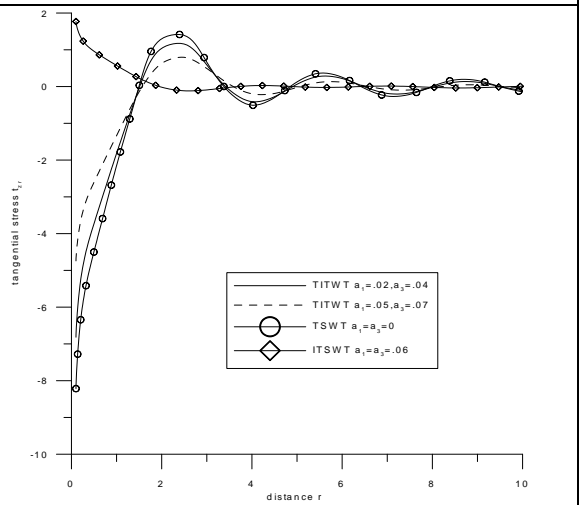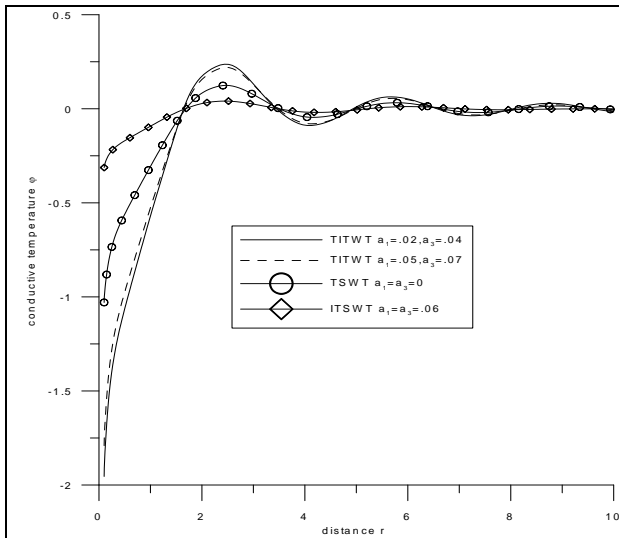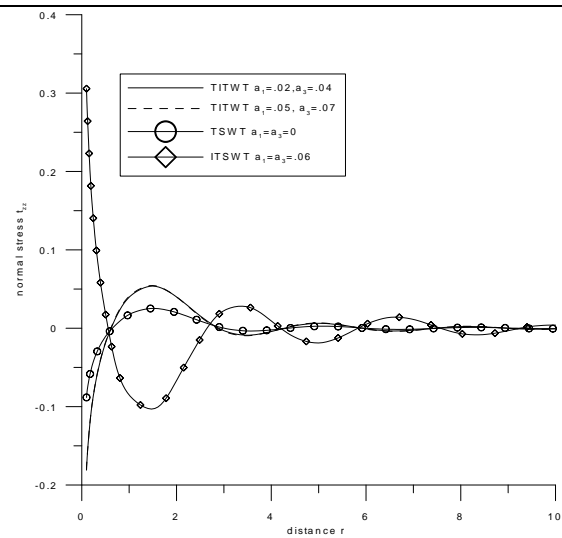
Fig.10 Variation of normal stress t_{zz} with distance r(thermal source over the circular region)
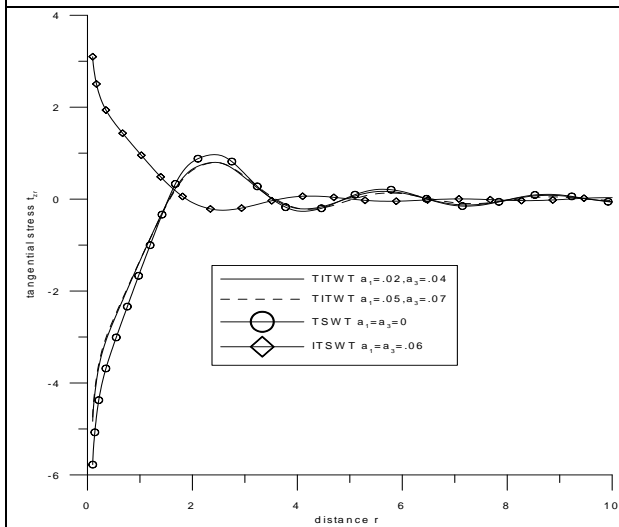
Fig.11 Variation of tangential stress t_{zr} with distance r (thermal source over the circular region)
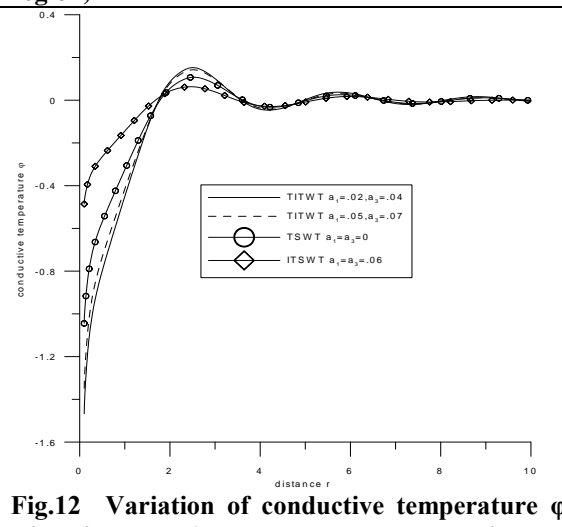
Fig.12 Variation of conductive temperature φ with distance r (thermal source over the circular region)

IX.   CONCLUSION

From the graphs it is clear that effect of two temperature plays an important part in the study of the deformation of the body. As r diverse from the point of application of the source the components of normal stress, tangential stress and conductive temperature for all types of sources (concentrated normal force / normal force over the circular region/ thermal point source/ thermal source over the circular region) follow an oscillatory pattern. It is observed that the variations of normal stress t_{zz}, tangential stress t_{zr} and conductive temperature φ for both mechanical forces (concentrated normal force and normal force over the circular region) are same and for both thermal sources(thermal point source and thermal source over the circular region) are same with difference in magnitude. As the disturbances travel through different constituents of the medium , it suffers sudden changes ,resulting in an inconsistent/ non- uniform pattern of curves. The trend of curves exhibits the properties of two temperature of the medium and satisfies the requisite condition of the problem. The results of this problem are very useful in the two dimensional problem of dynamic response due to various sources of the transversely isotropic thermoelastic solid without energy dissipation and with two temperature which has various geophysical and industrial applications.

REFERENCES

[1]. Chandrasekharaiah, D. S., and Srinath, K.S; Thermoelastic waves without energy dissipation in an unbounded body with a spherical cavity, The International Journal of Mathematics and Mathematical Sciences,(2000), 23 (8), 555-562.

[2]. Chen,P.J., and Gurtin, M.E; On a theory of heat conduction involving two parameters, Zeitschrift für angewandte Mathematik und Physik (ZAMP), (1968),19,614-627.

[3]. Chen,P.J., Gurtin, M.E., and Williams,W.O; A note on simple heat conduction, Journal of Applied Mathematics and Physics (ZAMP), (1968),19, 969-70.

[4]. Chen,P.J., Gurtin, M.E., and Williams,W.O; On the thermodynamics of non simple elastic materials with two temperatures, (ZAMP), (1969),20, 107-112.

[5]. Dhaliwal,R.S., and Singh,A.,Dynamic coupled thermoelasticity, Hindustance Publisher corp, New Delhi(India), 1980:726.

[6]. Green, A.E., and Naghdi, P.M; A re-examination of the basic postulates of thermomechanics.,Proc. Roy.Soc.London Ser. A-432(1991),171-194.

[7]. Green, A.E., and Naghdi, P.M; On undamped heat waves in an elastic solid, Journal of Thermal Stresses, (1992),15,253-264.

[8]. Green, A.E., and Naghdi, P.M; Thermoelasticity without energy dissipation, Journal of Elasticity, 31, 189-208(1993).

[9]. Honig,G.,and Hirdes,U; A method for the inversion of Laplace Transform, J Comput and Appl Math,(1984), (10), 113-132.

[10]. Kumar, R., and Pratap ,G;Axi-symmetric vibrations in micropolar thermoelastic cubic crystal plate bordered with layers or half-spaces of inviscid liquid.,Indian Journal of mathematical sciences and informatics,(2009),4(1),55-77.

[11]. Kumar,R.,Kumar,S.,and Gourla,M.G;Axi-symmetric deformation due to various sources in saturated porous media with incompressible fluid,Journal Of Solid Mechanics vol.5,no.1,74-91.2013

[12]. Kaushal, S., Kumar, R.,and Miglani, A; Response of frequency domain in generalized thermoelasticity with two temperatures,(2010),83(5), 1080-1088.

[13]. Kumar,R., and Kansal,T; Propagation of cylindrical Rayleigh waves in a transversely isotropic thermoelastic diffusive solid half-space, Journal of Theoretical and Applied Mechanics,(2013),43(3), 3-20.

[14]. Kumar,R., Sharma,K.D., and Garg,S.K; Effect of two temperature on reflection coefficient in micropolar thermoelastic media with and without energy dissipation, Advances in Acoustics and Vibrations,(2014),ID 846721,Pages11.

[15]. .Press,W.H., Teukolshy,S.A., Vellerling,W.T.,and Flannery, B.P; Numerical recipes in Fortran, Cambridge University Press, Cambridge,(1986).

[16]. Quintanilla, R; Thermoelasticity without energy dissipation of materials with microstructure, Journal of Applied Mathematical Modeling ,(2002), 26,1125-1137.

[17]. Sharma,K.,Bhargava,R.R;Propagation of thermoelastic plane waves at an imperfect boundary of thermal conducting viscous liquid/generalized thermolastic solid, Afr.Mat. (2014),25,81-102.

[18]. Sharma,K.,and Marin,M; Effect of distinct conductive and thermodynamic temperatures on the reflection of plane waves in micropolar elastic half-space,U.P.B.Sci.Bull Series,2013,75(2),121-132.

[19]. Sharma,K.,and Kumar,P; Propagation of plane waves and fundamental solution in thermoviscoelastic medium with voids,Journal of Thermal Stresses,2013,36,94-111.

[20]. Sharma,N.,Kumar,R.,; Elastodynamics of an axi-symmetric problem in generalised thermoelastic diffusion . , International Journal of advanced Scientific and Technical Research June2012,,2(3),478-492.

[21]. Sharma,N.,Kumar,R.,and Ram,P; Interactions of generalised thermoelastic diffusion due to inclined load, International Journal of Emerging Trends in Engineering and Development, (2012),5(2),583-600.

[22]. Sharma,S., Sharma,K.,Bhargava,R.R; Effect of viscosity on wave propagation in anisotropic thermoelastic with Green-Naghdi theory Type-II and Type-III,Materials Physics and Mechanics,2013,16,144-158.

[23]. Slaughter,W.S;The linearised theory of elasticity,Birkhausar (2002).

[24]. Warren, W.E., and Chen,P.J; Wave propagation in the two temperature theory of thermoelasticity, Journal of Acta Mechanica,(1973),16, 21-33.

[25]. Youssef, H.M; Theory of two temperature generalized thermoelasticity, IMA Journal of Applied Mathematics,(2006), 71(3),383-390.

[26]. Youssef, H.M.,and AI-Lehaibi,E.A; State space approach of two temperature generalized thermoelasticity of one dimensional problem, International Journal of Solids and Structures, (2007), 44, 1550-1562.

[27]. Youssef,H.M., and AI-Harby, A.H; State space approach of two temperature generalized thermoelasticity of infinite body with a spherical cavity subjected to different types of thermal loading, Journal of Archives of Applied Mechanics,(2007), 77(9), 675-687.

[28]. Youssef, H.M; Theory of two - temperature thermoelasticity without energy dissipation, Journal of Thermal Stresses,(2011),34, 138-146.

[29]. Youssef, H.M; Variational principle of two - temperature thermoelasticity without energy dissipation, Journal of Thermoelasticity,(2013),1(1), 42-44.

Appendix A

$$A = \delta_1^2 \zeta_1 - K_1 \delta_5 \delta_1$$

$$B = -\zeta_2 \zeta_1 \delta_1 + \delta_5 \zeta_2 K_1 - \delta_1{}^2 \zeta_4 - \delta_1 \zeta_1 \zeta_3 + \xi \delta_2{}^2 \zeta_1 \zeta_5 - K_1 \xi \zeta_7 \zeta_6 + \xi \delta_2 \delta_5 \zeta_5 a_3 + a_3 \zeta_7 \xi \delta_3$$

$$C = \zeta_2 \delta_1 \zeta_4 + \zeta_1 \zeta_2 \zeta_3 + \zeta_8 \delta_5 \zeta_2 + \delta_1 \zeta_3 \zeta_4 - \delta_1 \zeta_5 \zeta_8 - \xi \delta_2{}^2 \zeta_5 \zeta_4 + \xi \delta_2 \delta_5 \zeta_5 - \zeta_6 \zeta_5 \delta_5 \delta_2 - \zeta_6 \zeta_7 \delta_3 - a_3 \xi \zeta_7 \zeta_3$$

$$D = \zeta_6 \zeta_3 \zeta_7$$

Where

$$\zeta_1 = \left(\frac{\delta_6 a_3}{L} + \frac{K_3}{K_1}\right), \quad \zeta_2 = \xi^2 + s^2 \quad \zeta_3 = \delta_1 \xi^2 + s^2 \quad \zeta_4 = \xi^2 + \delta_6 s^2 (1 + \xi^2) \quad \zeta_5 = \frac{-\xi^2 + 1}{\xi} \quad \zeta_6 = \xi(1 - a_1 \xi),$$

$$\zeta_7 = \delta_4 \xi s^2 \quad \zeta_8 = \frac{\beta_3}{\beta_1}(1 + a_1 \xi^2)s$$

Appendix B

$$d_i = \frac{-\lambda_i^3 P^* - \lambda_i Q^*}{\lambda_1^4 R^* + \lambda_1^2 S^* + T^*} \quad i = 1,2,3$$

$$l_i = \frac{\lambda_i^2 P^{**} + Q^{**}}{\lambda_1^4 R^* + \lambda_1^2 S^* + T^*} \quad i = 1,2,3$$

Where $P^* = \delta_2 \zeta_5 \zeta_1 - \zeta_7 K_1$

$Q^* = \zeta_7 \zeta_8 - \delta_2 \zeta_4 \zeta_5$

$R^* = \delta_3 \zeta_1 - K_1 \delta_5$

$S^* = \delta_5 \zeta_8 - \zeta_3 \zeta_1 - \zeta_4 \delta_3$

$T^* = \zeta_4 \zeta_3$

$P^{**} = -(\zeta_5 \delta_2 \delta_5 + \zeta_7 \delta_3)$

$Q^{**} = \zeta_7 \zeta_3$

Appendix C

$$\tilde{u} = \frac{1}{\Delta}\left\{-\frac{P_1}{2\pi}(\Delta_1 e^{-\lambda_1 z} - \Delta_2 e^{-\lambda_2 z} + \Delta_3 e^{-\lambda_3 z}\right\} \tag{C.1}$$

$$\tilde{w} = \frac{1}{\Delta}\left\{-\frac{P_1}{2\pi}(d_1 \Delta_1 e^{-\lambda_1 z} - d_2 \Delta_2 e^{-\lambda_2 z} + d_3 \Delta_3 e^{-\lambda_3 z}\right\} \tag{C.2}$$

$$\widetilde{t_{zz}} = \frac{1}{\Delta}\left\{-\frac{P_1}{2\pi}(h_1 \Delta_1 e^{-\lambda_1 z} - h_2 \Delta_2 e^{-\lambda_2 z} + h_3 \Delta_3 e^{-\lambda_3 z}\right\} \tag{C.3}$$

$$\widetilde{t_{zr}} = \frac{1}{\Delta}\left\{\frac{P_1}{2\pi}(m_1 \Delta_1 e^{-\lambda_1 z} - m_2 \Delta_2 e^{-\lambda_2 z} + m_3 \Delta_3 e^{-\lambda_3 z}\right\} \tag{C.4}$$

$$\tilde{\varphi} = \frac{1}{\Delta}\left\{-\frac{P_1}{2\pi}(l_1 \Delta_1 e^{-\lambda_1 z} - l_2 \Delta_2 e^{-\lambda_2 z} + l_3 \Delta_3 e^{-\lambda_3 z}\right\} \tag{C.5}$$

Where

$\Delta_1 = (l_3 \lambda_3)(\lambda_2 + \xi d_2) - (l_2 \lambda_2)(\lambda_3 + \xi d_3)$

$\Delta_2 = (l_3 \lambda_3)(\lambda_1 + \xi d_1) - (l_1 \lambda_1)(\lambda_3 + \xi d_3)$

$\Delta_3 = (l_2 \lambda_2)(\lambda_1 + \xi d_1) - (l_1 \lambda_1)(\lambda_2 + \xi d_2)$

$\Delta = h_1 \Delta_1 - h_2 \Delta_2 + h_3 \Delta_3$

$h_j = -\xi \frac{c_{31}}{\rho c_1^2} - \frac{c_{33}}{\rho c_1^2} d_j \lambda_j - \frac{\beta_3}{\beta_1} l_j + \frac{\beta_3}{\beta_1} l_j \lambda_j^2 a_3 - \frac{\beta_3}{\beta_1} l_j a_1 \xi^2 , j = 1,2,3.$

$m_j = c_{44} \frac{\beta_1 T_0}{\rho C_1^2} (\lambda_j + \xi d_j) \quad j = 1,2,3$

Appendix D

$$\tilde{u} = \frac{1}{\Delta} \left\{ -\frac{P_2}{2\pi} (\Delta_1^* e^{-\lambda_1 z} - \Delta_2^* e^{-\lambda_2 z} + \Delta_3^* e^{-\lambda_3 z} \right\} \qquad (D.1)$$

$$\tilde{w} = \frac{1}{\Delta} \left\{ -\frac{P_2}{2\pi} (d_1 \Delta_1^* e^{-\lambda_1 z} - d_2 \Delta_2^* e^{-\lambda_2 z} + d_3 \Delta_3^* e^{-\lambda_3 z} \right\} \qquad (D.2)$$

$$\widetilde{t_{zz}} = \frac{1}{\Delta} \left\{ -\frac{P_2}{2\pi} (h_1 \Delta_1^* e^{-\lambda_1 z} - h_2 \Delta_2^* e^{-\lambda_2 z} + h_3 \Delta_3^* e^{-\lambda_3 z} \right\} \qquad (D.3)$$

$$\widetilde{t_{zr}} = \frac{1}{\Delta} \left\{ \frac{P_2}{2\pi} (m_1 \Delta_1^* e^{-\lambda_1 z} - m_2 \Delta_2^* e^{-\lambda_2 z} + m_3 \Delta_3^* e^{-\lambda_3 z} \right\} \qquad (D.4)$$

$$\tilde{\varphi} = \frac{1}{\Delta} \left\{ -\frac{P_2}{2\pi} (l_1 \Delta_1^* e^{-\lambda_1 z} - l_2 \Delta_2^* e^{-\lambda_2 z} + l_3 \Delta_3^* e^{-\lambda_3 z} \right\} \qquad (D.5)$$

$\Delta_1^* = -(h_2)(\lambda_3 + \xi d_3) + (h_3)(\lambda_2 + \xi d_2)$

$\Delta_2^* = -(h_1)(\lambda_3 + \xi d_3) + (h_3)(\lambda_1 + \xi d_1)$

$\Delta_3^* = -(h_1)(\lambda_2 + \xi d_2) + (h_2)(\lambda_1 + \xi d_1)$

Research Paper	Open Access

The Evaluation of Satisfaction of Quality Of Life and Its Role in Development of Urban Areas (Case Study: City Of Rask)

[1]Ziaalhagh Hashemzehi, [2*]Mahsume Hafez Rezazade, [3]Gholam Reza Miri

[1]*MSc student in Department of Geography and Urban Planning, College of human science, Zahehan Branch, Islamic Azad University, Zahedan, Iran*
[2,3]*Assistant professor in Department of Geography and Urban Planning, College of human science, Zahehan Branch, Islamic Azad University, Zahedan, Iran*

Abstract: *Nowadays, enhancing the quality of life is almost known by everyone as the ultimate goal of development and improving of the quality of life is reckoned as the main objective of all planning. The existences of various problems necessitate the study of the quality of life. By the development of spatial planning, satisfaction with the quality of life in planned spaces is considered as the primary objectives. Accordingly, this research will study the evaluation of satisfaction of quality of life and its role in development in the city of Rask (Located in Sistan and Baluchestan province). The type of research is applicative and its method is descriptive-analytic based on completing the questionnaires. The Statistical population is all the residents of the city of Rask and the sample community is 295 of heads of households living in thirteen districts in city of Rask. Random sampling method is used and the size of sample is computed by using Cochran method. The data is processed and analyzed based on statistical methods of SPSS software. The results showed a high positive and statistically significant relationship between the satisfactions of quality of life and urban development. This means the situation of urban development is significantly effective in increasing satisfaction of quality of life.*

Key words*: quality of urban life, satisfaction, Urban Development, City of Rask*

I.   INTRODUCTION

Quality of life in terms of a wide range of fields, including the fields of international development, healthcare, and politics is being used. Quality of life should not be a standard of living that is based largely on income, confused. Instead, standard indicators Quality of life include not only wealth and employment, but also include environmental, physical and mental health, education, recreation and leisure, and social belonging, too.

Discussion of the quality of life and sustainable development released today in literature to plan for social development and the new economy topics raised and has special status and national and local-level Governments and many institutions on its index and measurement of work (Kharazmi, 2008). In the new issue of sustainable human development is a major emphasis on the important issues of the policy-based allocation of resources more efficient, which is a major issue of social justice is Possible (Marsoosi, 2004: 25). Consequently, during the most recent decades, policy makers, social welfare and improve their living standards Persisted (Jabbari, 2002: 55).

With the beginning of the 1980s, a common attitude with titles Index of Sustainable Economic Welfare (ISEW) and Physical Quality of life Index (PQLI) were raised (Henderson and et al, 2000). Quality of life assessment of infant mortality, literacy and life expectancy as criteria for assessment of welfare and well-being, opinions (Ekins and Max, 1992).

Today, most of the urban quality of life as a key concept in urban planning. On this basis in many developed countries, planners are trying to show the levels of quality of life in the different geographical levels are optimal solutions can be used in this way to improve the quality of life of backward regions and they examined. One of the major concerns of every General Manager in the professional decision making activities for achieving, maintaining and improving productivity, which is the most important topics of interest to the Organization (Azar & Azim, 2002) and is one of the principles of decision making for managers, performance evaluation, which shall be in the form of being scientific has an effective decisions help (Mirghafori & Shafiei, 2007).

Due to the holistic approach lies in the quality of life issues, analysis and evaluation in developing countries, and the main role in the holistic planning. Iran, which is a development of the people in connection with the geographical formation, forming the shape of a model is the severity of spatial development was commenced. (Faraji, 2010: 3).

In this regard, the city of Sarbaz and the city of Rask have located in a deprived area geographically. Their residents are facing with numerous challenges in economic, socio-cultural and security, environmental and physical affairs. Thus, it seems necessary to study the quality of life and its role in urban development in city of Rask as a low prosperous city. With these attributions, this research is to evaluate urban families' satisfaction with the quality of urban life and its role in development of city of Rask located in Sistan and Baluchestan province in order to make this fundamental issue clear that in what level the quality of life of citizens is and what effect has it on urban development?

II.   THEORETICAL FUNDAMENTALS AND HISTORY OF RESEARCH

Quality of life is a broad concept that ideas like, life, life is precious, life is satisfying and happy life in the (McCrea and et al, 2006). David Smith was the first geographer about quality of life, prosperity and social justice, he spoke in geography. Smith emphasized that indicators of health, housing, public services, happiness, family, education, employment opportunities, salaries and wages, food, franchise, life expectancy, per capita consumption of animal protein, the percentage of school enrollment, number of phone mean newspapers and the like form (Smith, 2002: 160-169).

Domain-connected quality of life may be at any time as the date has been extended. Economists, social scientists and government of each particular viewpoint to look at this issue (Baldwin & Godfry & Propper, 1992: 1). This stems from the fact that a range of indicators relating to the quality of life in the fall. Feeding and clothing ranging from health care, social environment and physical environment surrounding include (Drewnevski, 2005: 53-70). Although some of the sources of living, quality of life is translated (Rahim abadi, 2004: 68).

FO, Quality of life is defined as: "the quality of life in many cases the two sets of objective and subjective parameters is studied.

Indicators of subjective perceptions of the assessment, evaluation and satisfaction of citizens in urban environment received, whereas objective indicators connected to observable facts. According to the definition of, Focan be said that quality of life can be classified in various ways and studied. One of these categories connected to the research work(Zapf, 1984) and (Craglia et al, 2004) where it is stated that, if the individual subjective feelings and objective conditions are favorable living environment, as having or happiness is defined. And an assessment of the environmental conditions and the individual is bad, as it is deprived remembered.

If a person's subjective evaluation was good, but the objective conditions are bad, the process is said to be compatible if the same person's mental condition favorable objective conditions of their environment, is bad, this mismatch is introduced. Several methods for measuring quality of life in urban environments have been used. For example, (Moro et al, 2008) and (Das, 2008) have proposed methods by which these methods could make Quality of life in the context of selected features or aspects of life should be assessed.

(Repheal et al, 1997) quality of life so that one of the important features of life enjoyed define. While the RIVM group claims that quality of life is immaterial equipment life issues, with the objective of such person in accordance with the perceptions about health, living conditions, work, family, and has been determined (RIVM, 2000). Perhaps the concept of quality of life and quality of life conceptual drawing for the four basic dimensions of human life, namely economic, environmental aspects, social aspects, and finally cultural dimensions - political adapted to provide a standard level of expectations (Faraji molaei, 2010). In other words, quality of life is a multidimensional concept that requires a firsthand analysis of expectations and satisfaction of citizens (Faraji molaei, 2010).

Study areas and various cities in the United States in terms of quality of life showed significant differences in some indicators show the different regions (Hagget, 2000: 458-460). On the other hand there is a significant connection between quality of life indicators. In Helsinki, research has shown the quality of life and social maladaptive behaviors such as suicide, social deviance, Alcoholism and there is a direct connection between divorces. While the quality of their housing situation is a reflection of the socio - economic (Shakoie, 2004).In American Ghettoes race, early mortality, influenza, heart disease and a major cause of death in black men is murder. Non- standard housing in Harlem ghetto 50 percent unemployment rate for 25 to 30 percent, with almost half the young men are not able to find work. As a result, residents of these areas are under severe economic pressure and psychological (Shakoie, 1990: 79-80). Thus, the concept of quality of life is associated largely with the concept of welfare. Although there is no consensus on welfare, but welfare is a concept that describes the welfare, security of life and poverty alleviation and therefore closely connected concepts such as justice is (Barry, 2001: 6-12).

III.   THE STUDY AREA

city of Sarbaz is located at longitude 60 degree and 38 minutes to 62 degree and 19 minutes of East and at latitude 25 degree and 49 minutes to 27 degree and 4 minutes of North. The city of Rask as the center of the city of Sarbaz is also located at longitude 61 degrees and 24 minutes of east and at latitude 26 degrees 14 minutes of North and its altitude from sea level is 410 meters. This city is restricted from the north to the city of Iranshahr and Meherstan, from East to Pakistan and from south to the city of Chabahar and from west to the city of Nikshahar.
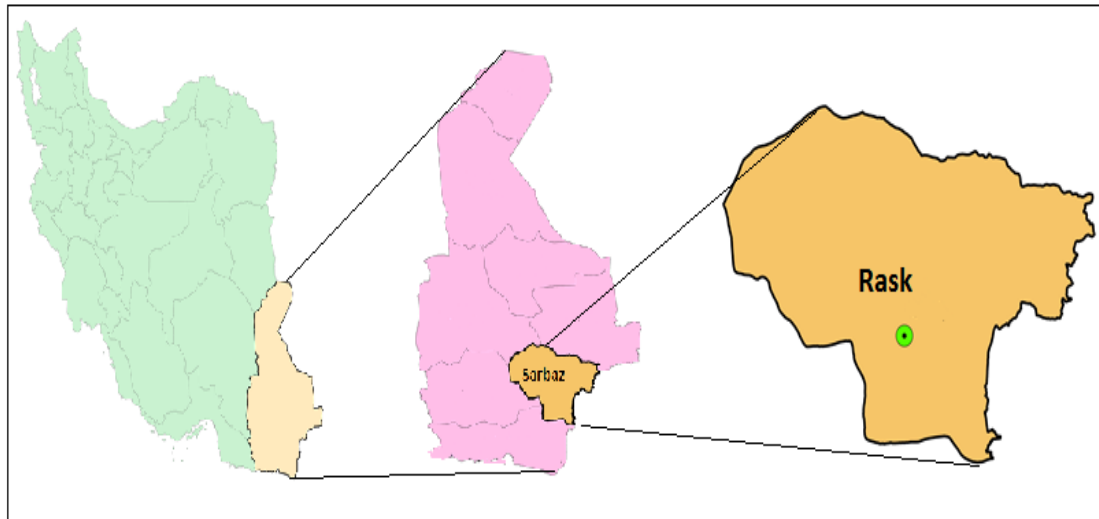

Figure 1: The study area: reference: research findings

IV.   DISCUSSION AND CONCLUSION

Correlation statistics methods (Pearson, Kendall and Spearman) have been used in order to study the question whether satisfaction of the quality of life of urban households has had an impact on urban development. The results of such correlations indicate that there is a relatively high positive and significant relationship between the satisfaction of quality of life and urban development in the city of Rask. This means that with an increase in satisfaction with the quality of life the understanding of urban development has also been improved. In other words, the situation of urban development significantly affects the increase of the quality of life satisfaction Table1). This situation shows that it will be possible to increase the quality of life of the citizens' satisfaction with the systematic planning and organization to improve urban infrastructure (economic, social and physical) and increase the people participation in Sustainable development and urban desirable governance.

Table (1): the relationship between satisfaction with the quality of life and urban development with correlation

Urban Development	values	Correlation type	
0/451**	Correlation coefficient	Pearson	Satisfaction with the quality of urban life
0/000	Significance level		
288	The number of samples		
0/312**	Correlation coefficient	Kendal	
0/000	Significance level		
288	The number of samples		
0/432**	Correlation coefficient	Spearman	
0/000	Significance level		
288	The number of samples		

Reference: research findings

For more accuracy, the separate study of the relationship between each of the three dimensions of (economic, social and physical environment) with urban development through the Pearson correlation showed that all dimensions of the quality of life were mentioned, have a direct and significant relation with urban development.

This means that an increase in satisfaction with the quality of economic, social and physical - environmental factors influenced by the index of urban development. In the meantime, the social dimension of urban development shows a stronger correlation. It means that the social and welfare indices, including indices of education, health, leisure and security are more tangible in satisfaction of the quality of life and affects the

lives of citizens more than other indices. Then the physical-environment dimension showed a stronger relation with urban development. This means that the physical environmental indices, especially the environmental indices including exclusion and landfill waste, municipal sewage and surface water, pollution control and transportation as well as the impact of natural hazards are dramatically in direct contact with urban life and affect the citizens' lives and livelihoods. However, economic indices showed a weaker correlation with urban development (Table 2). It can be deduced that despite the economic indices that have been in direct contact with the lives of citizens and have the role of infrastructure in urban life, but in many cases are influenced by external conditions such as the regional and national level and practically is beyond the power of the urban management. That is why the relationship between urban development and the economic dimension is weaker than the other dimensions.

According to the results, it can be deduced that the more the urban development indices have favorable status; the satisfaction of the physical quality of life, especially in social and environmental dimensions will increase and the citizens will play a more effective role in the process of planning and urban sustainable participative development.

Table (2) : the relationship between satisfaction with the quality of life and urban development with Pearson correlation

Urban Development	values	dimensions	
0/148**	Correlation coefficient	Economic	Satisfaction with the quality of urban life
0/011	Significance level		
293	The number of samples		
0/533**	Correlation coefficient	Social	
0/000	Significance level		
293	The number of samples		
0/483**	Correlation coefficient	Spearman	
0/000	Significance level		
286	The number of samples		

Reference: research findings

This means that an increase in welfare services, improving of transportation, improving of environmental conditions (water and soil pollution, waste management and surface water, etc.), attention to the free times and increasing of the recreation and sport possibilities in the city, increasing of per capita green space, improving of communication and information, health and education per capita promotion, social security and the like are significantly effective to increase the satisfaction of quality of life and the speed of the process of sustainable urban development will be increased.

In addition, single-group T-test results obtained from the review and the test of separate sub-indices of mentioned dimensions showed that the satisfaction with the quality of life in all indices is statistically significant (income, employment, wealth, housing, education, health, security, leisure, life satisfaction, the natural environment, pollution, transportation) which are consisted of several variables by themselves. Since the difference between the average and the upper and lower bounds on all mentioned indices is negative, it can be concluded that the quality of life in all studied indices were considered less than average so it will be assessed weakly.

Table (3) : Evaluation of satisfaction with the quality of life according to the different indices

Test value = 3						Indicators
Level of confidence of 95 percent		Mean difference	Level of significance	The degree of freedom	The value of T	the average of community
Upper bound	Lower bound					
-0/2411	-0/0117	-0/0311	0/004	294	-2/12	2/97	Income and mployment
-0/2815	-0/0318	-0/0710	0/000	294	-3/93	2/93	property and wealth
-0/3101	0/2472	-0/0908	0/00	294	-4/08	2/91	Housing
-0/2911	-0/0352	-0/0610	0/04	294	-3/98	2/94	Education
-0/3359	-0/2684	-0/1121	0/03	294	-4/53	2/89	Health and hygiene
-0/3981	-0/3128	-0/2013	0/000	294	-6/05	2/8	Security
-0/7865	-0/5661	-0/4315	0/000	294	-12/6	2/57	Leisure Time
-0/2428	-0/0125	-0/0416	0/03	294	-2/08	2/96	Life satisfaction
-0/4513	-0/3623	-0/3142	0/00	290	-8/15	2/7	Natural environment
-0/5010	-0/3964	-0/4213	0/02	291	-9/96	2/6	Pollution
-0/8957	-0/6907	-0/7932	0/000	294	-15/2	2/37	Transportation
-0/1123	-0/1483	-0/1603	0/000	291	-3/32	2/84	Total

Reference: the research findings

According to what was said and the results of T-test single group in 5 value range (Likert range), it can be found that the satisfaction has been below the average in all economic, social and physical environment dimensions and in all the indices listed in Table 3. This means that it couldn't fulfill the quality of life of its citizens as it was expected to help and improve the satisfaction of the citizens of income and employment, wealth, education, health, health care, facilities and utilities, leisure, environmental protection, improving environmental health and pollution control and etc. Thus the quality of life and welfare of residents in the study city can be assessed as weak and below in the current situation.

V.   CONCLUSION

Different opinions have been expressed by experts and scholars on the role and impact of quality of life and its role in development as well as urban development. Some knows it as the main objective of all planning and final development. In this study, satisfaction with the quality of urban life in one of deprived areas of the country (Town of Rask in the city of Sarbaz located in Sistan and Baluchestan province) has been evaluated according to this prospective and previous theoretical principle and its role and its impact on urban development was analyzed. The obtained results from statistical methods will be presented as follows:

The results showed a positive and statistically high significant relationship between the level of satisfaction of quality of life and urban development. It means that the situation of urban development significantly influence the increase the satisfaction of quality of life. This situation shows that it will be possible to increase the quality of life of the citizens' satisfaction with the systematic planning and organization to improve urban infrastructure (economic, social and physical) and increase the people participation in Sustainable development and urban desirable governance. The significant relationship between the economic, social and physical environment dimensions with satisfaction of quality of life and urban development was also confirmed. This correlation was positive and direct. This means that an increase in satisfaction with the quality of life (economic, social and physical – environmental) is influenced by urban development indices. Meanwhile, social dimension has a stronger relationship with urban development. This suggests that social and welfare indices are more tangible in satisfaction of quality of life including indices of education, health, leisure and security and affect the lives of citizens more than other indices. Then the physical-environment dimension showed a stronger relation with urban development. This means that the physical environmental indices, especially the environmental indices including exclusion and landfill waste, municipal sewage and surface water, pollution control and transportation as well as the impact of natural hazards are dramatically in direct contact with urban life and affect the citizens' lives and livelihoods. However, economic indices showed a weaker correlation with urban development. It can be deduced that despite the economic indices that have been in direct contact with the lives of citizens and have the role of infrastructure in urban life, but in many cases are influenced by external conditions such as the regional and national level and practically is beyond the power of the urban management. That is why the relationship between urban development and the economic dimension is weaker than the other dimensions. According to the results, it can be deduced that the more the urban development indices have favorable status; the satisfaction of the physical quality of life, especially in social and environmental dimensions will increase and the citizens will play a more effective role in the process of planning and urban sustainable participative development. This means that an increase in welfare services, improving of transportation, improving of environmental conditions (water and soil pollution, waste management and surface water, etc.), attention to the free times and increasing of the recreation and sport possibilities in the city, increasing of per capita green space, improving of communication and information, health and education per capita promotion , social security and the like are significantly effective to increase the satisfaction of quality of life and the speed of the process of sustainable urban development will be increased.

REFERENCE

[1]   Azar, A & Zare, A, (2002), Factors affecting the efficiency of using multi-criteria decision-making models, Daneshvar, 10 (42): 1-16.
[2]   Baldwin, Sally, Christine Godfrey and Carol Propper, (1992). Quality of Life: perspectives and policies, Routledge
[3]   Barry, N, (2007), Social Welfare, Translated by A.Mirhosseini, M.Noorbakhash, Samat Publication
[4]   Craglia, M., Leontidou, L., Nuvolati, G. and Schweikart, J., (2004), Towards the Development of Quality of Life Indicators in the Digital City, Environment and Planning B-Planning & Design, Vol. 31, No. 1, PP. 51-64.
[5]   Darvish Rahim abadi, I, Rahmanian, R, Mahdavi, R, (2004), intro concepts of planning and budgeting, Rasht, Management and Planning Organization of Iran in Gilan Province
[6]   Das, D., (2008), Urban Quality of Life: A Case Study of Guwahati, Social Indicators Research, Vol. 88, PP. 297-310.
[7]   Drewnevski, J, (2005), quality of life, measurement and planning, Translated by A.Ashraf
[8]   Ekins, P., Max-Neef, M., (1992), Reallife Economics: Understanding Wealth Creation. Routledge, London, pp :460.
[9]   Faraji molaei, A, (2009), analysis of the quality of urban life and planning to improve the city Babolsar, MA thesis, Geography and Urban Planning, Supervisor Dr M.T.Rahnamai School of Geography, Tehran University.
[10]   Faraji Mollaie, A., (2010), Analysis of Urban Quality of Life Concept, Second Scientificnationwide Congress of Geography Students, Faculty of Geography, University of Tehran.

[11] Faraji Mollaie, A., (2010), Analysis of Urban Quality of Life Indices and Planning to Improve It, Case Study: Babolsar City, Department of Human Geography, Faculty of Geography, University of Tehran, A Thesis Submitted to the Graduate Studies Office in Partial Fulfillment of the Requirements for the Degree of M.Sc. in Geography and Urban Planning.

[12] Hagget, P, (2000), a new combination of geography, Volume II, Translated by Sh.Goodarzinajad, Samat Publication.

[13] Henderson, H., Lickerman, J., Flynn, P. (Eds.), (2000), Calvert– Henderson Quality of Life Indicators. Calvert Group, Bethesda, pp : 391.

[14] Jabbari, H, (2002). Social and economic development is two sides of one coin, Social Welfare Quarterly Of social policy.

[15] Kharazmi, Sh, (2008), quality of life and requirements of the digital age, Regional Centre for Information Science and Technology website

[16] McCrea, R., Shyy, T.K. and Stimson, R., (2006), what is the Strength of the Link between Objective and Subjective Indicators of Urban Quality of Life?", Applied Research in Quality of Life, Vol. 1, No. 1, PP: 79-96.

[17] Mirghafori, H, Shaefie, M, (2007), academic libraries are ranked based on performance using Data Envelopment Analysis and Breda (The Library of Yazd). Research on information science& Public Libraries, 10 (3), 36-53.

[18] Moro, M., Brereton, F., Ferreira, S., Clinch, J.P., (2008), Ranking Quality of Life Using Subjective Well- being data, Ecological Economics, Vol. 65, No. 3, PP.448-460.

[19] Raphael, D., Renwick, R., Brown, I., Rootman, I., (1996), Quality of life indicators and health: current status and emerging conceptions. Soc. Indicators Res. 39 (1), 65–88.

[20] RIVM (2000). De Hollander A.E.M., et al. 5e Nationale Milieu Verkenningen. RIVM, (2000). National Outlook, Summary in English, ISBN: Check

[21] Shakoie, H, (1990), urban social geography (social ecology), second edition,Iranian student book agency

[22] Shakoie, H, (2001), New perspectives in urban geography, Volume I, Fourth Edition, Samat Publication

[23] Smith, D.M, (2002), Quality of life: human welfare and social justice, Translated by H.Hatamynajad & H.Shahiardabili, Political & Economic Ettelaat, seventeenth year. No. 186-185.

[24] Zapf, W., (1984), Individual Welfare: Living Conditions and Noticed Quality of Life, in Lebensqualitat in der Bundersrepreblik, Objective Lebensbedingungen und Subjektives Wohlempfinden Eds W Glatzer, W Zapf (Campus, Frankfurt Am Main): PP.13-26.

Research Paper　　　　　　　　　　　　　　　　　　　　　　　　　　Open Access

A Method for Damping Estimation Based On Least Square Fit

Jintao Gu[1], Meiping Sheng[2]

School of Marine Science and Technology, Northwestern Polytechnical University, P. R. China

Abstract: *A new approach based on least square fit method is proposed to estimate damping. Noise resistance of the proposed method and half-power bandwidth method are analyzed and compared by plenty of simulations with different signal-to-noise ratios (SNR). The proposed method is more accurate and stable than half-power bandwidth method in all SNRs, especially when the noise level is high. If $SNR \leq 30dB$, the proposed method should be used for damping estimation instead of half-power bandwidth method. A damping estimation experiment is carried out with both methods, and the results indicate and verify that there is smaller variability for the proposed method.*

Keywords: *Least square fit, damping estimation, half-power bandwidth*

I.　　INTRODUCTION

Since damping is a valuable parameter for resonant response of structures or systems, damping is of great significance for structural dynamics. It is difficult to obtain damping through a theoretical method so that the universal way for damping estimates is experimental investigation[1,2]. Half-power bandwidth method[3,4], which calculates resonant damping with frequency bandwidth for vibration energy decreases 3dB and the resonant frequency, is a widely used approach for damping estimation. Half-power bandwidth method is introduced as main method for damping estimates in the American test standard ASTM E756-05. Bertha[5] obtained damping of a system that does not possess real modes with half-power bandwidth method. Guo[6] improved the half-power bandwidth method and proposed a new method based on integral opinion. Badsar[7] determined the material damping ratio in shallow soil layers with the half-power bandwidth method.

As the half-power bandwidth method uses only three data points, its accuracy will be affected by the signal-to-noise ratio (SNR). When some of the three data points are seriously affected by noise, a large error will appear and cannot be neglected. The aim of this work is to put forward a new method which has high accuracy and strong noise resistance by using the amplitude of frequency response.

II.　　HALF-POWER BANDWIDTH METHOD

A widely used method, namely half-power bandwidth method, is introduced as follows. The damping loss factor can be obtained by the quotient of half-power bandwidth and the resonant frequency, as shown in equation (1). The diagrammatic sketch of the method is shown in Fig. 1.
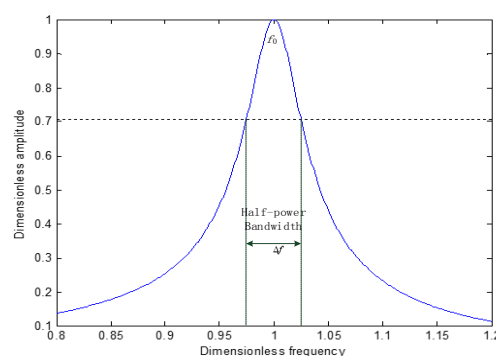

Fig.1. Half-power bandwidth method

$$\eta = \frac{\Delta f}{f_0} \qquad (1)$$

The half-power bandwidth method is a classical and widely used method, but there is a fatal short coming that if the signal-to-noise ratio (SNR) is not high enough. It is difficult to recognize the half-power bandwidth, seen in Fig. 2.
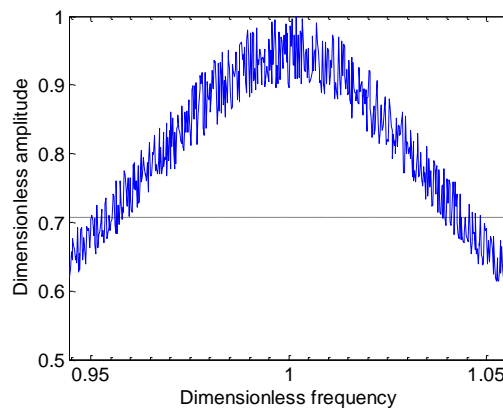

Fig. 2. Half-power bandwidth method with low SNR

It can be seen in Fig. 2 that the half-power bandwidth is hard to decide because there are more than two frequencies related to half-power response.

III.　　　DAMPING ESTIMATION BASED ON LEAST SQUARE FIT

The parameter of damping is often estimated with data near the resonant frequency. The widely used half-power bandwidth method for damping investigation only uses three data points of frequency response so that it will cause a large error when the experimental data is affected by noise. It is expected to obtain a more accurate damping if more data points of frequency function are used. Therefore, a new approach based on least square fit method is proposed in which a numbers of data points near resonant frequency are used.

The amplitude of frequency function is

$$|H| = \frac{F/K}{\sqrt{\left(1 - \frac{\omega^2}{\omega_0^2}\right)^2 + \eta^2}} \qquad (2)$$

where F is excitation force, K the stiffness, ω_0 natural circle frequency, and η the loss factor.

It is obvious that the maximum amplitude can be obtained

$$|H|_{\max} = \frac{F}{K\eta} \qquad (3)$$

The dimensionless amplitude is defined as

$$|\overline{H}| = \frac{|H|}{|H|_{\max}} = \frac{\eta}{\sqrt{\left(1 - \frac{\omega^2}{\omega_0^2}\right)^2 + \eta^2}} \qquad (4)$$

Rewrite equation (4) as

$$\frac{1}{|\overline{H}|^2} = 1 + \frac{1}{\eta^2}\left(1 - \frac{\omega^2}{\omega_0^2}\right)^2 \qquad (5)$$

Make that

$$x = \left(1 - \frac{\omega^2}{\omega_0^2}\right) \qquad (6)$$

and

$$y = f(x, \eta) = 1 + \frac{1}{\eta^2}x^2 \qquad (7)$$

A number of data points $(x_i, y_i)(i = 1, 2, \cdots, n)$ can be obtained according to the experimental frequency response. The residual error is defined as

$$err(\eta) = \sum_{i=1}^{n} \left[y_i - f(x_i, \eta) \right]^2 \qquad (8)$$

The damping identification can be transferred into getting a proper value of η to make the residual error the most minimum. Gauss-Newton iterative method is used to find the optimal parameter of damping.

Expand $f(x_i, \eta)$ to Taylor series at point of initial value η_0 as

$$f(x_i, \eta) \approx f(x_i, \eta_0) + f'(x_i, \eta_0) \cdot (\eta - \eta_0) \qquad (9)$$

where $f'(x_i, \eta_0) = \dfrac{df(x_i, \eta)}{d\eta}\bigg|_{\eta = \eta_0}$.

Rewrite equation (8) as

$$err(\eta) = \sum_{i=1}^{n} \left[y_i - f(x_i, \eta_0) - f'(x_i, \eta_0) \cdot (\eta - \eta_0) \right]^2 = \sum_{i=1}^{n} \left[\tilde{y}_i - g(x_i - \eta_0)\eta \right]^2 \qquad (10)$$

where $\tilde{y}_i = y_i - f(x_i, \eta_0) + g(x_i, \eta_0) \cdot \eta_0$, $g(x_i, \eta_0) = f'(x_i, \eta_0)$. Equation (10) is a typical least square optimization problem. The estimated η_1 can be obtained for the first generation by solving equation (11).

$$A^T A \cdot \eta = A^T b \qquad (11)$$

where $A = \left(g(x_1, \eta_0), g(x_2, \eta_0), \cdots, g(x_n, \eta_0) \right)^T$, $b = \left(\tilde{y}_1, \tilde{y}_2, \dots, \tilde{y}_n \right)$.

After η_1 is obtained, η_0 will be replaced by η_1 and repeat the above step to get the estimated value η_2 for the second generation. The iteration will be finished if the difference between the neighbor generations of η is small enough for satisfactory demand. The last generation of η is the estimated damping. The experimental and fitting response are shown in Fig. 3 and damping can be obtained in the fitting process.
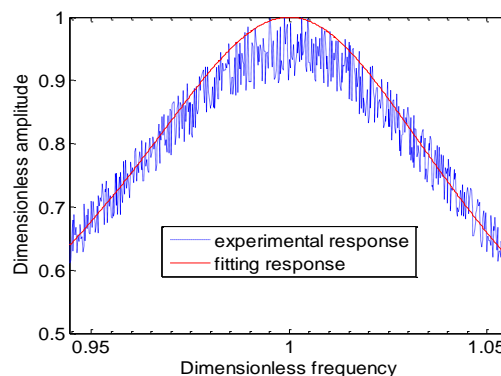

Fig. 3. Experimental and fitting response

IV. RESISTANCE TO NOISE

This simulation is conducted to illustrate the noise sensitivity of the proposed methods. A single-degree-of-freedom system is adopted to verify the validity of least square fit method. A comparison is made between least square fit method and half-power bandwidth method. Gaussian random noise is applied to the simulated frequency response, and the signal-to-noise ratio (SNR) is defined as

$$SNR = 20\log_{10}\left(|H|_{\text{signal}} \big/ |H|_{\text{noise}} \right) \qquad (12)$$

where $|H|_{\text{signal}}$ is amplitude of effective signal and $|H|_{\text{noise}}$ is amplitude of noise.

The simulated signal parameters are $\eta = 0.001$, $f_0 = 500\,\text{Hz}$, $\omega_0 = 2\pi f_0$, and $\Delta f = 0.1\,\text{Hz}$. It is simulated on 1000 samples with the SNR in the range from 10 dB to 50 dB. Errors of estimated damping with the two methods are shown in Fig. 4.

In Fig. 5, each method is tested for 41 noise levels, which is from 10dB to 50dB with 1dB interval, with 1000 samples in each noise level. The average error is calculated by equation (13).

$$\text{average error} = \frac{1}{N} \sum_{i=1}^{N} \frac{|\eta_i - \eta_{\text{exact}}|}{\eta_{\text{exact}}} \qquad (13)$$

where η_i is the identified damping, η_{exact} is the exact loss factor set in the simulation, N is the number of samples.
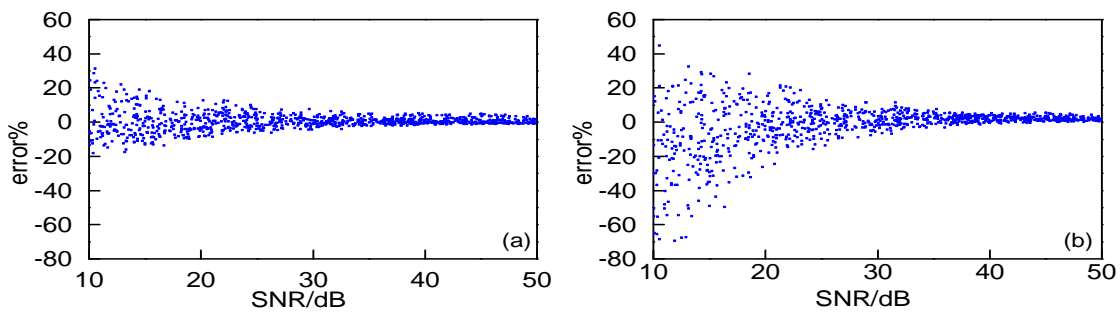
Fig. 4. Error of the estimated damping versus SNR: (a) proposed method, (b) half-power bandwidth method.
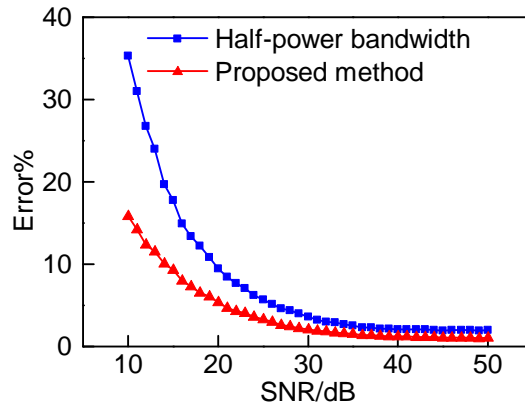

Fig. 5. Average error for the two methods

It can be seen in Fig. 4 that identified damping by the two methods are more and more accurate with the increased SNR. The accuracy of proposed method is more than half-power bandwidth method at all SNRs. It may also be noticed that there is considerable variability of half-power bandwidth method especially in the lower SNR.

As seen in Fig. 5, both methods are of satisfied accuracy if $SNR > 30dB$. But if $SNR \leq 30dB$, error of half-power bandwidth is much larger than proposed method. It is clear that the proposed method should be used to estimate damping instead of half-power bandwidth if $SNR \leq 30dB$

V.   EXPERIMENT

The experiment is carried out on an alloy beam with the dimensions of $0.23m \times 0.01m \times 0.002m$, as shown in Fig. 6. Fig. 7 is the dimensionless response of the third mode. Fig. 5 is the estimated damping obtained from six repeat experiment results by the two methods.
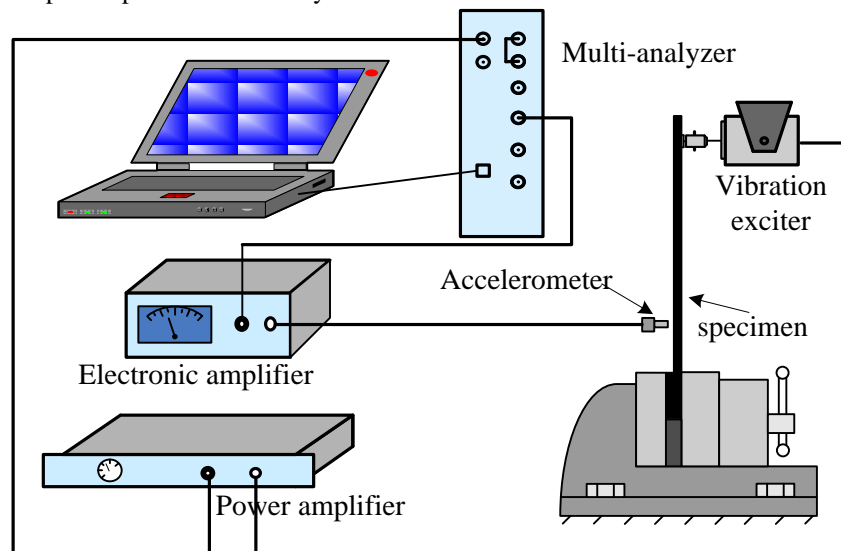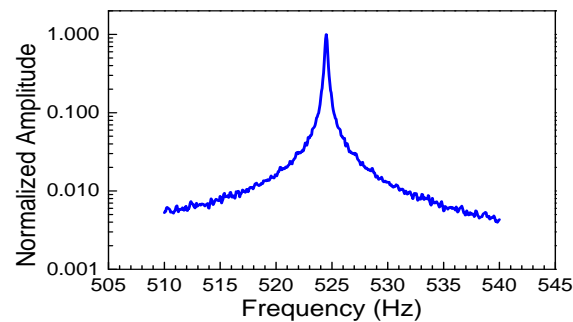

Fig. 6. Experimental setup
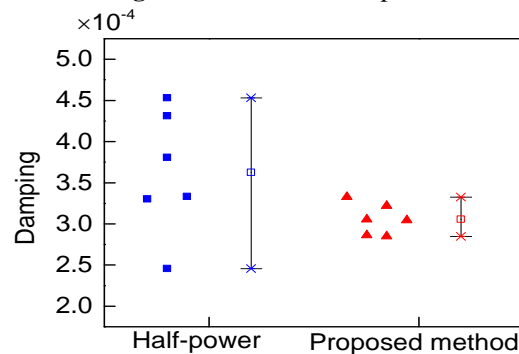
Fig. 7. Dimensionless response

Fig. 8. Damping estimated by the two methods

As seen in Fig. 8, it is clear that there is smaller variability for the proposed method than half-power bandwidth method. Thus, damping estimated by the proposed method is more accurate than half-power bandwidth method.

VI.   CONCLUSION

A noval method based on least square fit is proposed to estimate damping in this paper. There is smaller variability for the proposed method than half-power bandwidth method. The proposed method is more accurate than half-power bandwidth method, especially in the lower SNR circumstances. The proposed method should be used instead of half-power bandwidth method for damping estimation if $SNR \leq 30dB$.

REFERENCE

[1]   O. Guasch. A direct transmissibility formulation for experimental statistical energy analysis with no input power measurements. Journal of Sound and Vibration, 330(25), 2011, 6223-6236.
[2]   M. Rak, M. Ichchou, and J. Holnicki-Szulc. Identification of structural loss factor from spatially distributed measurements on beams with visoelastic layer. Journal of Sound and Vibration, 310(4), 2008, 801-811.
[3]   G. A. Papagiannopoulos, and G. D. Hatzigeorgiou. On the use of the half-power bandwidth method to estimate damping in building structures. Soil Dynamics and Earthquake Engineering, 31(7), 2011, 1075-1079.
[4]   P. W. Wang, W. W. Zhong, and J. F. Hsu. Investigation of multi-layer sandwich beams through single degree-of-freedom transformation. Applied acoustics, 74(4), 2013, 521-525.
[5]   B. A. Olmos, and J. M. Roesset. Evaluation of the half-power bandwidth method to estimate damping in systems without real modes. Earthquake Engineering & Structural Dynamics. 39(14), 2010, 1671-1686.
[6]   Z. W. Guo, M. P. Sheng, J. G. Ma, and W. L. Zhang. Damping identification in frequency domain using integral method. Journal of Sound and Vibration, 338(3), 2015, 237-249.
[7]   S. A. Badsar, M. Schevenels, W. Haegeman, and G. Degrande. Determination of the material damping ratio in the soil from SASW tests using the half-power bandwidth method. Geophysical Journal international, 182(3), 2010, 1493-1508.

Research Paper   Open Access

Application of Building Production Management Documents in High Rise Building Projects in Anambra State Nigeria

Peter Uchenna Okoye[1], Chukwuemeka Ngwu[2]
[1]Department of Building, Nnamdi Azikiwe University, Awka, Nigeria
[2]Department of Quantity Surveying, Nnamdi Azikiwe University, Awka, Nigeria

Abstract: *The study examined the level of application and use of building production management documents in high rise building projects in Anambra State, following the State Government's directives that such documents should be used to curtail the incessant building collapse in the State. It examined the challenges in using the documents, and strategies to be adopted for improvements. The study made use of structured questionnaires which were administered to practitioners, developers and personnel responsible for approval and monitoring of building projects in the state, through stratified random sampling. Data obtained were analyzed and ranked using Mean Score Index (MSI), Severity Index (SI) and Relative Importance Index (RII). The study revealed that there were low level of awareness and very low use of the documents. It also identified non enforcement of the provisions of the building code by the government, and negligence and corruption in the system among others as major challenges facing application of the document in the state. It further identified strict enforcement of the provisions of the building code with stem punishment on the defaulters among others as strategies for increasing the use of the documents. It then recommended proactive measures through restructuring of Anambra State Urban Development Board and constitution of special taskforce made up of relevant professionals in the building industry whose duties would be inter alia, strict monitoring and implementation of the provisions of the law as it regards to building development in the State.*

Keywords: *Anambra State Nigeria, Building Code, Building Collapse, Building Production Management Documents, Building Projects*

I.   INTRODUCTION

Modern building designs and constructions have became so complex, expensive , time consuming as well as consuming a lot of resources, generating high waste with high uncertainty and risks, thereby jeopardising the sustainability of the building project. Many at times, Nigeria has been promulgating laws and instituting policies and programmes affecting the practice of building development. In some cases, individual States adopt these laws and programmes and amended them to suit their individual peculiarities without providing guidelines on how to ensure quality, safety and speedy delivery at various stages of building production process. The result has been poor design, poor workmanship, time and cost overrun with high incidence of building collapse across the country. Since 1974 till date, scores of buildings of different types and magnitude have collapsed across Nigeria with losses of hundreds of lives and properties worth of billions of Naira [1],[2],[3],[4],[5],[6],[7]. In Anambra State specifically, the rising spate of collapse of buildings in recent years is grievously alarming. Okonkwo [8] reports that no fewer than 10 buildings have collapsed between 2000 and 2014 in Onitsha alone. Similarly, building collapse in Anambra State is not restricted to Onitsha in that it cuts across the entire state irrespective of urban or rural areas [9]. To underpin this fact, the report of the Panel of Inquiry set up by the Anambra State Government to investigate the collapsed buildings in the state revealed that between June and September, 2014, the State has recorded about nine (9) building collapses with six (6) fatalities [10]. Issues relating to poor design and construction featured prominently as parts of the causes of this ugly incidence [11]. Odesola and Umoh [12] argue that the issue of quality and standards has been the subject of emphasis in the Nigerian construction industry in recent times following the incessant collapse of building structures around the nation. To this end, [13] and [14] agree that the consequential effects of poor design and construction have made the construction industry to follow a path that has led to lack of trust and confidence, adversarial relations and increased arbitration and litigation.

Consequently, the need for regulations or standards spelling out the quality requirements of building and procedures for achieving such becomes more pressing [15],[16]. Response to this need is the emergence of the National Building Code (NBC) [17] in 2006, through the tireless efforts of the National Council on Housing and Urban Development in collaboration with relevant construction professionals and other stakeholders in the construction industry [18].

Regrettably, since the approval of this code by the National Executive Council in 2006, not much has been done with regard to fully or partly implementation of the code. The passage of the National Building Code enforcement bill by the National Assembly has been lingered so long without success. Notwithstanding, some States such as Lagos State have adopted some parts of the code and implement same due to its essence in stemming the tide of building collapse.

In Anambra State however, the need to implement some aspects of the National Building Code arises as a result of the rising spate of building collapse in the State. Following the recommendations of the Panel of Inquiry set up by the Anambra State Government to investigate the collapsed buildings in the state in 2014 that building production management documents (Construction Programme, Project Quality Management Plan, Project Health and Safety Plan) prepared by a registered builder should be used during building construction and as part of the requirements for obtaining building approvals from the Anambra State Urban Development Board (ASUDEB) for high rising buildings (buildings above three storeys). The Anambra State Government through the White Paper published in that regard approved and accepted the recommendation of the panel and directed immediate implementations by the agencies concerned [10].

Based on the above position, it is pertinent to determine whether stakeholders in the building industry and those responsible for building approval and monitoring in the State are aware of this provision. If so what are the level of compliance with respect to the use of building production management documents, the challenges and strategies for maximum compliance and use? Thus, this paper examines the application and use of building production management documents in high rise building projects in Anambra State Nigeria.

1.1   Building Production Management

NIOB Handbook [19] defines building production management as the main professional service offered by builders to clients on building projects both in the public and private sectors of our national economy. It further submits that the scope of services in building production management include studying production information (i.e. drawings, schedules, specifications, etc); construction planning which involves preparing and/or examining and reviewing the building production management documents; and managing site production process.

Section 2.32c of the National Building Code specifies building production management documents (Construction Programme, Project Quality Management Plan, Project Health and Safety Plan) prepared by a registered builder as parts of the contract documents for building projects in Nigeria [20]. According to NIOB Handbook [19], for any building project to be successfully executed on site, contractors must forecast plan and put in place various production management documents (builders' documents). More so, [21] stresses that the preparation and subsequent use and implementation of each of production management documents are so important and plays a major role in successful site execution of building projects.

1.1.1   Construction Programme

Bamisile [21] opines that an essential part of any building project is to ensure completion within the time specifies or agreed with a client. He describes construction programme as a statement in diagram format of what is to be done and when it would be carried out. Obiegbu [22] sees a construction programme as a statement of intended action and an important common reference point in managing construction processes. Bamisile [21] however, maintains that a detailed construction programme must be prepared prior to commencement of work on building site, while Obiegbu [22] stresses that the content of the programming is of greatest significance to all the parties charged with handing over to the client a building fit for its intended use within the contract time and with optimal economy.

According to CORBON Document [23] and CORBON Training Manual [24], the clauses that have to do with time in contract conditions and associated penalties reinforce the need for proper programming. It is also argued that construction programme becomes more important when it is realised that unreasonable time for construction works can lead to waste of funds, poor delivery and other manifestations of project failure such as abandonment, litigation etc. The construction programme is used to manage time and resource deployment and utilization on the project. Its function goes beyond just giving the overall project time, but indicates the sequence and logic of the construction work [25]. CORBON/NIOB [25] further infers that construction programme is not just for planning the project only; rather it is useful for embarking on other management processes such as controlling.

1.1.2   Project Quality Management Plan (PQMP)

According to Okoye [26] PQMP is a document that spells out the specified quality practices, resources, procedures and sequence of activities that are relevant to a particular product, service, contract or product. It includes reference to purchase, materials or service specification, quality system procedure, process control and sampling and inspection procedure. Thus, PQMP is construed to mean various quality related activities and procedures which are to be implemented on a project. Bamisile [21] adds that PQMP sets down requirements, gives guidelines, provides information, indicates appropriate personnel, and the procedure to be followed with respect to the quality of building projects.

For CORBON/NIOB [25] project quality management plan describes the quality management system for all phases of a particular project. It presents a management and control framework that will ensure that all aspects of the project from start up through the final inspection and handing over to the client, including all equipment and materials incorporated in the works, comply with contract requirements.

Further still, the functions of PQMP are to provide the means to establish, document and maintain cost effective quality management system on the project; ensure and demonstrate that the works carried out by contractors will conform to the production information issued on the project; and provide means by which the client may derive confidence that the project is being carried out in accordance with specified requirements [21]. PQMP provides the project staff, both on site and in the office, with a reference base and a management tool for the management control of quality matters. The controls described in the PQMP represent a practical and logical framework by which the quality of the building can be achieved. It covers general issues connected with the scope of the project and addresses specific areas [25].

Therefore, when quality is fully addressed through a Quality Management Plan, such often leads to greater efficiencies as the plans are designed to standardised process, minimise waste and reworking, and increase profit. More so, PQMP is a tool to guide proper execution of a construction project in terms of quality [27].

1.1.3   Project Health and Safety Plan (PHSP)

PHSP is that building production management document that details all the health and safety related issues in the building projects including the personnel involved [21]. The objective of PHSP is to secure the health, safety and welfare of person(s) who will work or visit the site throughout the project duration; protect any other persons against risk to health and safety arising out of, or in connection with the activities of persons working on the project; and control the use on site of substances that might be hazardous to health.

Consequently, Bamisile [21] emphasizes the preparation and use of health and safety plan on building projects and further stresses that PHSP is a major part of production management of building projects. CORBON/NIOB (2012) [27] surmises that an effective Health and Safety Plan in construction can be achieved by delegating responsibility and accountability to all involved in an organisations' operation.

1.2   The Use of Building Production Management Documents in Nigeria Building Industry

Kabir [28] stresses the importance of implantation of the National Building Code and its provisions without delay. Despite the provision of the National Building Code, 2006 [20] and increased demand for implementation of its provisions by stakeholders in the building industry [28],[29],[30],[31][32], the implementation and use of building production management documents have not been wide spread across the country. Only few States in Nigeria such as Lagos have given serious thought to the provisions of this code including the use of building production management documents and its implementation. The result has been unabated collapse of buildings.

In studying the challenges for implementation, compliance and enforcement of the National Building Code, 2006 [29],[30],[31],[32] agree that there are enormous challenges facing the implementation of National Building Code and its provisions. These according to the authors ranged from lack of knowledge and awareness, complexity and technicality, non availability of law backing the enforcement, lack of political will and government commitment, corruption and unprofessional practices etc.

In view of the scenarios above, Windapo and Owolabi [32] charge that enforcement of the National Building Code entails a deep understanding of the code and probable factors that would militate against its effective implementation. They further submit that enforcement of the Code should first of all start with adherence to its tenets by individual stakeholders, building professionals and building owners alike before enforcement by the governments' statutory regulatory body

In Anambra State, the situation is the same. It was not until a panel of inquiry to investigate the collapsed buildings in the state submitted its report and recommended inter alia that Anambra State Urban Development Board (ASUDEB) should request for building production management documents (Construction Programme, Project Quality Management Plan, Project Health and Safety Plan) prepared and sign by a registered builder for high rising buildings (buildings above three storeys) that Anambra State Government

started giving the use of these document a serious thought, despite the fact that there have been agitations and calls for implementation of the National Building Code in the state before then [9],[17,[33],[34]. Subsequently, the Government accepted and approved this recommendation as published through the government white paper [10].

However, whether these documents are generally acknowledged and used across the state by the relevant stakeholders in execution of building projects is a subject of determination?

II.   METHODOLOGY

The study is a survey research conducted in Anambra State and among stakeholders responsible for delivery of building projects in the state. This involved the use of structure questionnaire administered randomly to selected personnel of ASUDEB and Anambra State Ministry of Housing and Urban Development, building professionals, contractors and developers in the state. In all, a total of 220 questionnaires were distributed to various categories of respondents, out of which 163 were returned and found useful for analysis. This represents 74% response rate. The results are presented and discussed below. The questionnaire was structured to capture the background information of the respondents, the level of awareness and application of building production management documents, challenges and strategies for application of the documents in the State. Questions concerning the level of awareness, challenges and strategies for implementing building production management documents were measured on a five point Likert scale, where 1 = least and 5 = most for each of the variables being considered. Data were presented using simple column charts and tables. Mean Score Index, Severity Index and Relative Importance Index were computed using equations (1), (2) and (3) for the level of awareness, challenges and strategies for implementing building production management documents, respectively. Subsequently, the factors were ranked accordingly. These were given as:

$$\text{Mean Score Index (MSI)} = \frac{\sum (f\,w)}{N} \tag{1}$$

$$\text{Severity Index (SI)} = \frac{\sum (f\,w)}{AN} \times \frac{100}{1} \tag{2}$$

$$\text{Relative Importance Index (RII)} = \frac{\sum (w_1 + w^2 + w_3 + ... + w_n)}{A \times N} \tag{3}$$

Where, w = the weighting given to each factor by the respondents and ranges from 1 to 5; f = the number of response for each weight; A = the highest weight (in this case 5); and N = the total number of sample.
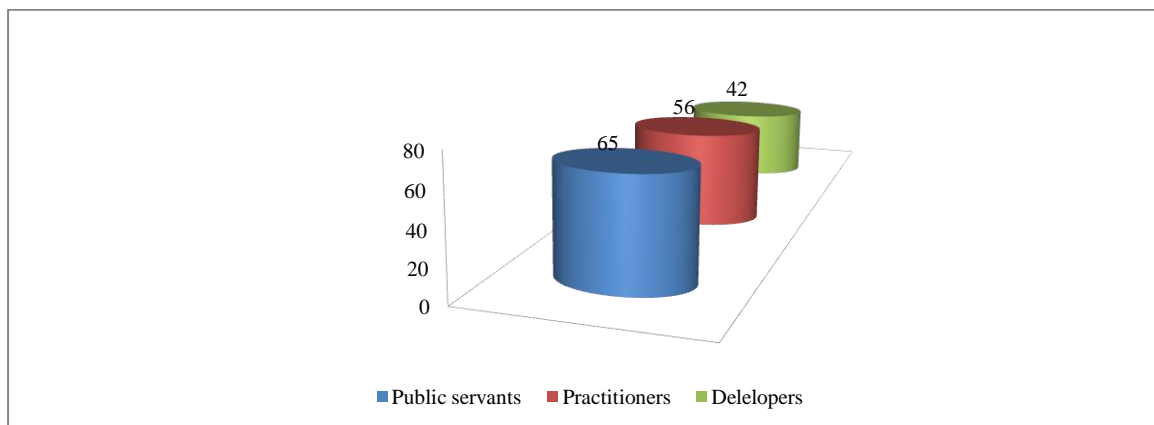
III.   RESULTS AND DISCUSSION

Figure 1: Characterisation of respondents

Fig. 1 represented the composition of the respondents. Out of 163 respondents who responded to questionnaire, 65 indicated that they were public servants i.e. those responsible for approval and monitoring of building projects in the state, 56 were practitioner either contractors or professionals in the building industry, while 42 were developers or clients.

It was also revealed that 108 of this number were registered members of various professional associations (26 NIA, 23 NIOB, 30 NSE, 11 NITP, 13 NIQS and 5 others) in the building industry.

Table I: Awareness of the Building Production Management Documents

S/N	Issues	Weighting					Mean Score	Average Mean
		1	**2**	**3**	**4**	**5**		
i	Provisions of the National Building Code	32	55	43	27	6	2.51	
ii	Knowledge of Building Production Management Documents	83	48	13	16	3	1.82	
iii	Position of the Anambra State Government on the use of Building Production Management Documents in the state	92	43	18	10	-	1.67	
iv	Building Production Management Documents are requisite documents for approval of high rise buildings	108	39	11	7	-	1.47	**2.03**
v	The uses of Building Production Management Documents	99	35	10	17	2	1.70	
vi	Person responsible for preparation of Building Production Management Documents	29	31	49	21	33	2.99	

TABLE I showed the level of awareness of building production management documents among the stakeholders responsible for building production in Anambra State. It can be deduced from the table that the overall level of awareness among the stakeholders on issues relating to building production management documents in Anambra State is low. This was indicated by the average mean score value (**2.03**) as shown in table 3. To underscore the gravity of this, when asked to list the building production management documents specified by the national building code and recommended to the Anambra State Government which the Government accepted and approved for use for high rise buildings in the state, only 17 (10.43%) respondents were able to list them correctly as Construction Programme, Project Quality Management Plan, and Project Health And Safety Plan.

Further still, more than 90% of this number who were able to list them belonged to the Nigerian Institute of Building (NIOB) and were Builders. This was a clear indication of low and lopsided awareness of the documents in the State.
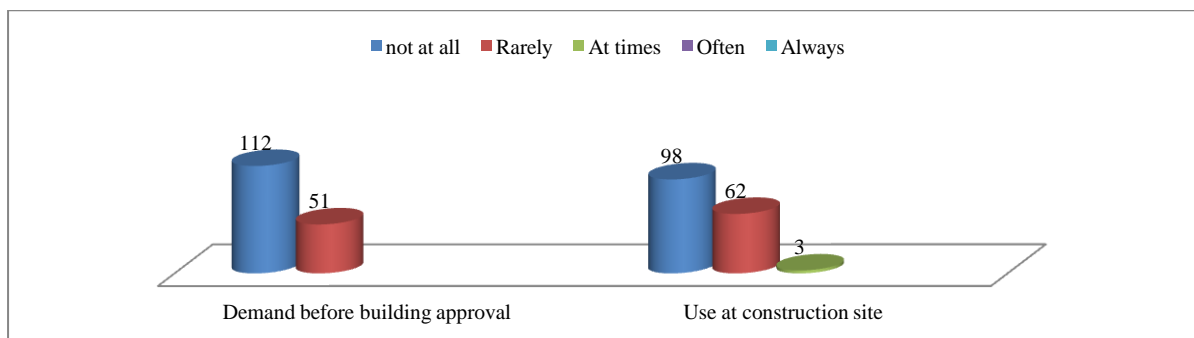

Figure 2: Application of the building production management documents in building projects

Figure 2 showed that greater number of respondents (112) representing about 68.71% indicated that building production management documents are not demanded at all by the authority before approval is given for any building, 51 respondents representing 31.29% indicated that the documents are rarely demanded. Likewise, 98 representing 60.12% of the respondents specified that the documents are not being used at construction site, 62 (38.04%) showed that they are rarely being used at construction site while only 3 (1.84%) showed that the documents are at times used at site.

This is an attestation that a good number of stakeholders did not even understand what these documents meant as also reflected when they were asked to list the documents as contained in the National Building Code and approved by the Anambra State Government. When further enquired for the reasons for their options, almost all the respondents pointed at one challenge or the other as articulated in table 2. These they added needed to be severely dealt with by the government.

Table II: Challenges of Using Building Production Management Documents

S/N	Challenges	Weighting					Severity Index (%)	Rank
		1	2	3	4	5		
i	No enabling law or bye-law for enforcement of national building code	11	20	20	51	61	76.07	4
ii	Non enforcement of the provisions of the code by the government	-	7	29	68	73	90.55	1
iii	Non awareness of national building code and its provisions by relevant stakeholders	9	11	56	63	24	70.18	5
iv	Non awareness of government position on the use of building production management documents	10	25	54	45	31	68.34	6
v	Ambiguity and complexity in the use of building production management documents	53	70	21	12	7	41.60	9
vi	Lack of technical skills and knowledge on the preparation and use of building production management documents	10	94	42	4	13	49.57	7
vii	Time and Cost of use of the building production management documents	15	85	61	2	-	46.26	8
viii	Negligence and corruption in the system	6	6	20	43	88	84.54	2
ix	Lack of government support	12	-	28	48	75	81.35	3

TABLE II showed the severity of challenges facing the use of building production management documents in Anambra State. Accordingly, the top six (6) challenges include; non enforcement of the provisions of the code by the government (90.55), negligence and corruption in the system (84.54), lack of government support (81.35), no enabling law or bye-law for enforcement of national building code (76.07), non awareness of national building code and its provisions by relevant stakeholders (70.18), and non awareness of government position on the use of building production management documents (68.34). This implied that institutional challenges are the bane of implementation of building production management documents in Anambra State.

Table III: Strategies for Improving the Use of Building Production Management Documents

S/N	Strategies	Weighting					RII	Rank
		1	2	3	4	5		
i	Legislating an enabling law or bye-law backing the enforcement of the national building code and its provisions.	-	22	24	55	62	0.792	5
ii	Strict enforcement of the provisions of the national building code	-	-	50	27	86	0.844	1
iii	Public enlightenment through media and social groups	22	18	21	62	40	0.698	6
iv	Mandatory professional development, conference, workshops, seminars and symposia	-	8	26	67	62	0.814	3
v	Stern punishment on the defaulters	-	-	44	52	67	0.828	2
vi	Government supports and demand for building production management documents	10	7	30	38	78	0.804	4

TABLE III showed the strategies for improving the use of building production management documents in Anambra State. Based on the computed relative importance index (RII), it was observed that the five (5) top strategies indentified by the respondents include strict enforcement of the provisions of the national building code (0.844), strict punishment on the defaulters (0.828), mandatory professional development, conference, workshops, seminars and symposia (0.814), government supports and demand for building production management documents (0.804), and Legislating an enabling law or bye-law backing the enforcement of the national building code and its provisions (0.792). This indicated that these strategies went in line with the identified major challenges facing the use of the documents in the State,

IV. CONCLUSION AND RECOMMENDATIONS

There is no doubt that Anambra State is facing daunting challenges occasioned by the incessant collapse of buildings. Based on this, the Anambra State Government had inaugurated a panel of inquiry which investigated the collapsed buildings in the State. Part of the panel's recommendations which the state Government accepted and directed immediate implementation was the use of building production management documents for high rise buildings in the State.

In view of this, the study has examined the awareness level and application of these documents and found that the level of awareness and application of building production management documents in the state was still low and that the documents were not being demanded during building approval. The study has also identified and ranked the challenges and strategies for improving the use of these documents in the State.

It was revealed that non enforcement of the provisions of the code by the government; negligence and corruption in the system, and lack of government support were the topmost challenges facing the application of building production management documents in the state. The study further revealed that with strict enforcement of the provisions of the national building code, strict punishment on the defaulters, mandatory professional development, conference, and government supports, building production management documents could be overwhelmingly implemented and used in building projects in the Anambra State.

Although the awareness and application of building production management documents in the State was still low due to the identified challenges, if adequate strategies backed with political will and appropriate regulatory and legal frameworks are adopted, the use of these documents in the State would be greatly improved. This however, implies that the result of this study would raise the awareness level of these important documents which appropriate application would stem the rate of building collapse in the state. Most importantly, the study would also awaken the stakeholders' consciousness, especially the government towards their neglected statutory function which inadvertently have consequential effects of building collapse.

Consequently, the study recommended that Anambra State Government should toe the line of Lagos State by enacting a law for implementation of provisions of the National Building Code in the state. A special taskforce made up of requisite professionals in the building industry should also be constituted by the State Government whose duties should be inter alia strict monitoring, implementation and compliance to the provisions of the law as it regards to building construction in the State.

There is also urgent need for restructuring of ASUDEB, i.e. the board responsible for approval and monitoring of building development in the state to reflect the inclusion of all the professionals in the building industry. This is because ASUDEB is the first contact for compliance as far as building law or code is concerned. If the menace of building collapses in Anambra State would be stemmed, Government must proactively tackle this without delay.

REFERENCES

[1]   G. Chinwokwu, The role of professional in averting building collapse, *Proceedings of a 2-Day Seminar of the Nigerian Institute of Building, Lagos State Chapter on Building Collapse, Causes, Prevention and Remedies,* 3rd -4th May, 2000.

[2]   M.O. Dada, The threat of building collapse to sustainable built environment, *Proceedings of the 36th Annual General Meeting/ Conference of the Nigerian Institute of Building,* 9-12th August, 2006, 69-75.

[3]   A. Windapo, The threat of building collapse to sustainable development in the built environment, *Proceedings of the 36th Annual General Meeting/ Conference of the Nigerian Institute of Building,* 9-12th August, 2006, 59-67.

[4]   K.O. Dimuna, Incessant incidents of building collapse in Nigeria: Challenges to stakeholders, *Global Journal of Researches in Engineering.* 10(4) (Ver 1.0) September, 2010, 75-84.

[5]   A.N. Ede, Building collapse in Nigeria: The trend of casualties in the last decade (2000-2010), *International Journal of Civil and Environmental Engineering IJCEE.* 10(06), 2010.

[6]   S.A. Oloyede, C.B. Omoogun, and O.A. Akinjare, Tackling causes of frequent building collapse in Nigeria, *Journal of Sustainable Development.* 3(3), 2010, 127-132.

[7]   C.A. Ayedum, O.D. Durodola, and O.A. Akinjare, An empirical ascertainment of the causes of building failure and collapse in Nigeria, *Mediterranean Journal of Social Sciences.* 3(1), January, 2012, 313-322.

[8]   N. Okonkwo, Frequent Building Collapse: Fear Grips Onitsha Residents. *Vanguard Newspaper,* June 11, 2014

[9]   F.A. Onweluzo, National Building Code: Challenges and strategies, *A Paper Presented at a One-Day Seminar by the Association of Professional Bodies of Nigeria (APBN), Anambra State Chapter on Effective Implementation of the National Building Code: Panacea for the Eradication of Collapse of Building in Nigeria,* Crescent Spring Hotel, Iyiagu Estate, Awka, 19th June, 2008.

[10]   Government of Anambra State of Nigeria, Government white paper, *The report of the State Government panel of inquiry to investigate the collapsed buildings in Anambra State submitted to Government,* October, 2014.

[11]   M.E. Obiegbu, Factors influencing the defects and performance of buildings, *The Professional Builder, Journal of the Nigerian Institute of Building,* August, 2003, 53-61.

[12]   I.A. Odesola, and A.A. Umoh, An assessment of the effectiveness of regulatory measures for ensuring quality and standards in the construction industry of some selected cities in Nigeria, *The Professional Builder, Journal of the Nigerian Institute of Building,* June, 2007, 63-70.

[13]   S.M. Ahmed, A. Azhar, and S. Castello, Measurement of construction processes for continuous improvement, *Revised Final Report Submitted to Mr. Michael Ashwort, Planning Consultant State of Florida, Department of Community Affair,* USA, 2002.

[14]   D.A. Adesanya, Problem areas in controlling quality of construction projects in Nigeria, *The Builders Focus, a Magazine of the National Association of Building Students (NAOBS) Nigeria,* Maiden Edition, 2006, 52-63.

[15]   T.S. Ojambati, The need for code of conduct, building regulations and bye laws for the building industry in Nigeria, *The Professional Builder, Journal of the Nigerian Institute of Building,* July, 2001, 11-14.

[16]   A.O. Windipo, and O.A. Yakubu, Planning/building regulations and implementation by contractors in Nigeria (A case of Lagos State), The *Professional Builder, Journal of the Nigerian Institute of Building,* July, 2001, 15-21.

[17]   F.E. Okwuoma, National Building Code: The place of insurance, *A Paper Presented at a One-Day Seminar by the Association of Professional Bodies of Nigeria (APBN), Anambra State Chapter on Effective Implementation of the National Building Code: Panacea for the Eradication of Collapse of Building in Nigeria,* Crescent Spring Hotel, Iyiagu Estate, Awka, 19th June, 2008.

[18]   M.E. Obiegbu, Understanding the National Building Code – Utilising the provisions of the code in practice of building profession, *A Paper Delivered At 2007 Annual General Meeting of Abia State Chapter of NIOB,* 2007.

[19]   The Nigerian Institute of Building, *NIOB Hand Book*, 1st Edition, (Marina Lagos, Nigeria, The Nigerian Institute of Building, 2002).

[20]   Federal Republic of Nigeria, *National Building Code,* 1st Edition, (South Africa, Lexis Nexis Butterworths,.2006).

[21]   A. Bamisile, *Building production management*, (Lagos-Nigeria, Foresight Press Ltd, 2004).

[22]   M.E. Obiegbu, Effective project delivery in Nigeria construction industry, In M.E. Obiegbu, J.U. Ezeokonkwo, A. Ezemerihe & S. Akabogu (Eds), *Effective building procurement and delivery in Nigerian construction industry.* (Nimo, Anambra State, Rex Charles & Patrick Ltd, 2002), 11-26.

[23]   CORBON Document, *Construction programming using MS Project 2007for builders,* Reversed Edition.

[24]   CORBON Training Manual, *The essentials of construction programming (planning & monitoring) using Microsoft Project 2007,* New Edition, 2012.

[25]   CORBON/NIOB, Improving the core practice areas of builders IV, *7th Mandatory Continuous Professional Development Programmes (MCPDP) for Builders Paper,* Abuja Gusua, Lagos, Port Harcourt, 20th – 23 May, 2014.

[26]   P.U. Okoye, *Quality management activities in design and construction phases in Nigeria,* U*npublished BSc. Project,* Department of Building, Nnamdi Azikiwe University, Awka, Anambra State, Nigeria, 2007.

[27]   CORBON/NIOB, Improving the core practices areas of builders III, *6th Mandatory Continuous Professional Development Programmes (MCPDP) for Builders, 2012.*

[28]   B. Kabir, The rule of law and National Building Code, *Proceedings of the 38th Annual General Meeting/ Conference of the Nigerian Institute of Building,* 15-19th October, 2008, 112-118.

[29]   M.O. Balogun, The National Building Code: Challenges of implementation and enforcement, *Proceedings of the 38th Annual General Meeting/ Conference of the Nigerian Institute of Building,* 15-19th October, 2008, 53-61.

[30]   D.D. Jambol, The National Building Code: Enforcement and compliance with standards, *Proceedings of the 38th Annual General Meeting/ Conference of the Nigerian Institute of Building,* 15-19th October, 2008, 37-52.

[31]   F.P. Oyewole, Challenges and strategies for implementation and enforcement of the National Building Code towards sustainable environment development, *Proceedings of the 38th Annual General Meeting/ Conference of the Nigerian Institute of Building,* 15-19th October, 2008, 68-75.

[32]   A.O. Windapo, and A.D. Owolabi, Implementation, compliance and enforcement of the National Building Code; challenges and strategies to adopt, *Proceedings of the 38th Annual General Meeting/ Conference of the Nigerian Institute of Building,* 15-19th October, 2008, 62-61.

[33]   J.U. Okoye, Effective implementation of the National Building Code – panacea for the eradication of collapse of building in Nigeria, *A Paper Presented at a One-Day Seminar by the Association of Professional Bodies of Nigeria (APBN), Anambra State Chapter on Effective Implementation of the National Building Code: Panacea for the Eradication of Collapse of Building in Nigeria*, Crescent Spring Hotel, Iyiagu Estate, Awka, 19th June, 2008.

[34]   I.J. Onochie, The implementation of the National Building Code in Anambra State, Nigeria: Benefits and challenges, *2011 Annual Conference and General Meeting of the Nigerian Institute of Building, Anambra State Chapter.* 17-18th, June, 2011.

Research Paper   Open Access

Selection of Optimal Supplier in Supply Chain Using A Multi-Criteria Decision Making Method

H. Assellaou*, B. Ouhbi*, B.Frikh **

* Mathematical Modeling and Computing laboratory. ENSAM-Meknes, Moulay Ismail University, Marjane II, BP 4024 BENI M'Hamed, Meknes, Morocco.
** LTTI laboratory, EST-Fès, Moulay Abdellah University, B.P. 1796 Atlas Fès, Fès, Morocco.

Abstract: *The supplier selection problem is one of the strategic decisions that have a significant impact on the performance of the supply chain. In this study, supplier selection problem of an automotive company is investigated and a comprehensive methodology is used to select the best supplier providing the most customer satisfaction for the criteria determined. The proposed methodology consists of Analytic Network Process (ANP), the criteria which are relevant in the supplier selection, have been used to construct an ANP model.*

Keywords: *Supplier Selection, ANP,*

I.   INTRODUCTION

Since 1960s, supplier selection criteria and suppliers performance have been a focal point of many researchers. As a pioneer in supplier selection problem, Dickson (1966) identified 23 different criteria for this problem including quality, delivery, performance history, warranties, price, technical capability and financial position. Weber et al. (1991) analyzed 74 articles published between 1966 and 1990 dealing with this problem.

Extensive multi-criteria decision making approaches have been proposed for supplier selection, such as the analytic hierarchy process (AHP), Analytic Network Process (ANP), Case-Based Reasoning (CBR), mathematical programming, Data Envelopment Analysis (DEA), Genetic Algorithm (GA)… Many decision problems cannot be building ad hierarchical because of dependencies, influences between and within clusters (criteria, alternatives). ANP (Saaty, 2001) is very useful to solve this kind of problems.

Analytic Network Process (ANP) is a generalization of the (AHP), it considers the dependence between the elements of the hierarchy. The ANP feedback approach replaces hierarchies with networks, and emphasizes interdependent relationships among various decision-making, also interdependencies among the decision criteria and permit more systematic analysis.

II.   THE PROPOSED MODEL IN SUPPLIER SELECTION

The automotive company is in a decision-making situation for purchasing one of the main items for assembling the components of cars. A committee of decision-makers wants to select the most promising vendor for supplying the item. After a preliminary screening, three alternatives {*S1, S2, S3*} remain for further evaluations. The network structure of this problem is depicted in Figure 1.

Several techniques have been developed to solve the supplier selection problem, and all techniques have to use criteria and sub-criteria to rate suppliers. The main goal of the supplier selection is selecting the best supplier that meets the requirements or criteria. For the proposed supplier selection model, overall criteria are determined under two main criteria clusters mentioned below:

- Selectivity criteria;
- Rejectability criteria

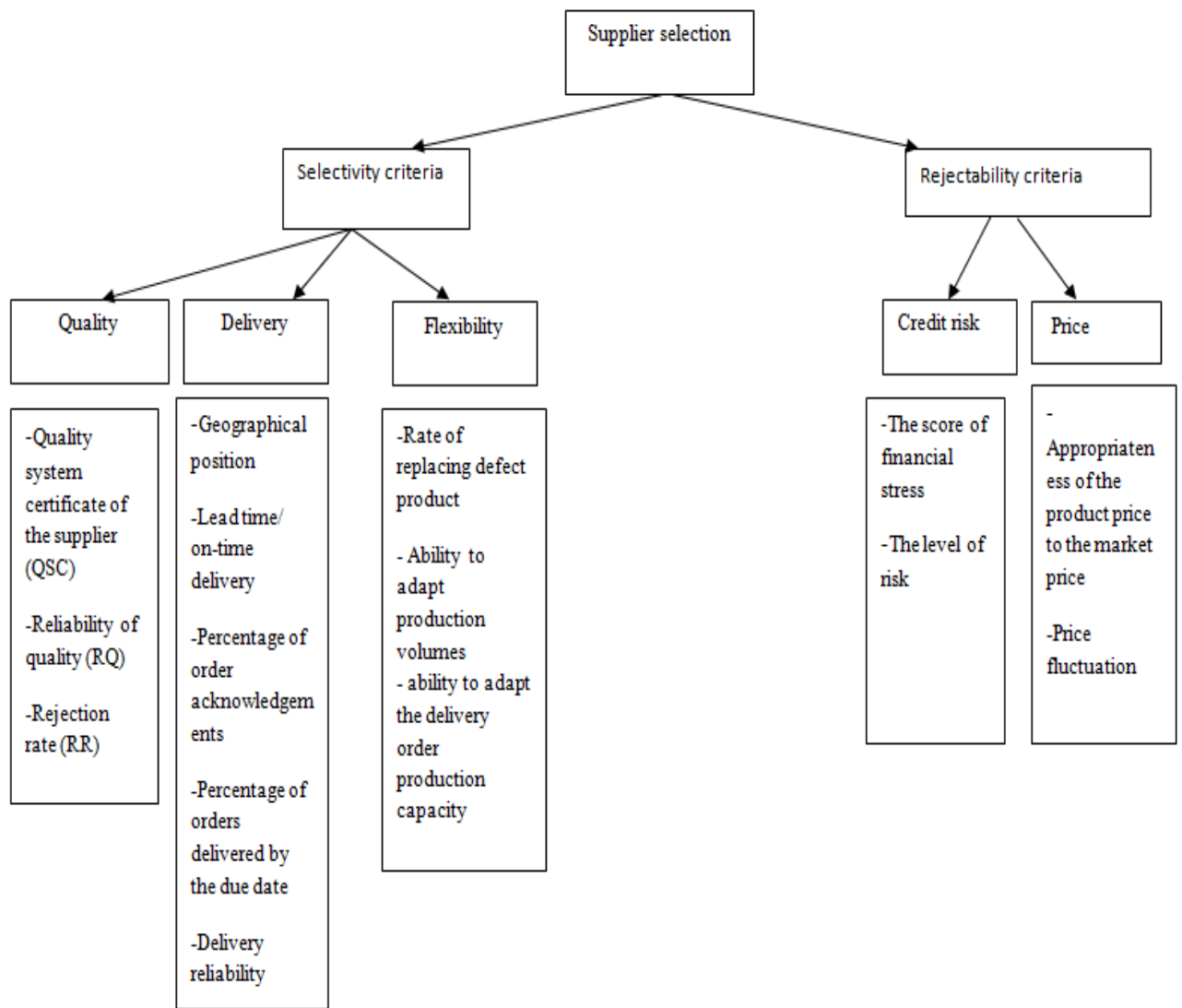All criteria and sub-criteria are given in the following model:

Figure 1: ANP-base d mode l for supplier selection

As shown in Figure1, the problem is composed into a network. There are five criteria, each of which has   several   sub-criteria

III. APPLICATION OF SUPPLIER SELECTION

Step1: pairewise comparison of clusters:

In this step, a series of pairwise comparisons are made to establish the relative importance of clusters in achieving the objective. In such comparisons, a ratio scale of 1_9 is used to compare any two elements. A score of 1 indicates equal importance of the two elements whereas a score of 9 indicates overwhelming dominance of the elements under consideration (row component) over the comparison element (column component).

The matrix showing the pairwise comparison of clusters along with the derived local priority vectors (also known as e-vectors (eigen vectors)) is shown in table 1

Table 1: paire wise comparisons of clus te rs:

	Selectivity criteria	Rejectability criteria	e-vectors
Selectivity criteria	1	8	0.888
Rejectability criteria	1/8	1	0.111

Step 2: Pairwise Comparison of criteria

In this step, the relative importance of each criterion for cluster 1 (selectivity criteria) is obtained through a pairwise comparison matrix. Two such matrices would be formed in the present case. One each for the two clusters.

The matrix for selectivity criteria cluster is shown in table 2.

Table 2: pairewise comparison of criteria for cluster 1

	Quality	Delivery	Flexibility	E vectors
Quality	1	4	2	0,552
Delivery	1/4	1	3	0,277
Flexibility	1/2	1/3	1	0,172

The matrix for rejectability criteria cluster is shown in table 3

Table 3: pairewise comparison of criteria for cluster 2

	Credit risk	Price	e-vectors
Credit risk	1	1/3	0,245
Price	3	1	0,754

Step 3: Pairwise Comparison of subcriteria:

In this step, the pairwise comparison of elements at each level is conducted with respect to their relative influence towards their control criterion. One such pairwise comparison matrix for quality under the selectivity criteria cluster is shown in table 4:

Table 4: The pairwise comparison matrix for quality under the selectivity criteria cluster

	(QSC)	(RQ)	(RR)	e-vectors
(QSC)	1	4	1/3	0,352
(RQ)	1/4	1	5	0,347
(RR)	3	1/5	1	0,301

It is observed from table 4 that QSC has the maximum influence on quality under selectivity criteria

Step 4: Pairwise Comparison for interdependencies:

In this step, pairwise comparisons are made to capture interdependencies among the criteria. The pairwise comparison matrix and relative importance weight results for other criteria and impact on quality criterion is shown in table 5:

Table 5: The pairwise comparison matrix and relative importance weight results for other criteria and impact

on quality criterion

Quality	Delivery	Flexibility	Credit risk	Price	W
Delivery	1	3	4	6	0,536
Flexibility	1/3	1	2	3	0,218
Credit risk	1/4	1/2	1	5	0,179
Price	1/6	1/3	1/5	1	0,064

Step 5: Evaluation of suppliers

The final set of pairwise comparaison is made of the relative impact of each of the alternatives (S 1, S2et S3) on the subcriteria in influencing the clusters. The number of such pairwise comparison matrices is dependent on the number of subcriteria that are included in each cluster. In the present case 11 subcriteria for the selectivity criteria cluster and 6 subcriteria for the rejectability criteria, this leads to the formation of 17 such pairwise comparaison matrices.

Matrix for alternatives impact on subcriterion (DR) in influencing the selectivity criteria:

Table 6: Matrix for alternatives impact on subcriterion (DR) in influencing the selectivity criteria

	S 1	S 2	S 3	e-vectors
S1	1	2	3	0,512
S2	1/2	1	4	0,36
S 3	1/3	1/4	1	0,128

Step6: super-matrix formation:

After we have all the pairwise comparisons completed, we go to the next step, to evaluate those criteria with interdependencies using super-matrix analysis. The super matrix as shown in table 7, presents the results of the criteria.

Table 7: super matrix before convergence

	Quality	Delivery	Flexibility	Credit risk	Price
Quality	1	0,327	0,351	0,298726	0,322
Delivery	0,536	1	0,27233	0,211855	0,209
Flexibility	0,218	0,257511	1	0,181249	0,224
Credit risk	0,179	0,177165	0,110496	1	0,052
Price	0,064	0,233	0,221	0,223	1

These converged values turn out to be Wf= 0.240, 0.203, 0.165, 0.110, 0.235 for quality, delivery, flexibility, credit risk, price

Step7: selection of the best supplier:

The selection of the best supplier depends on the values of various desirability indices. The final step of the process is to aggregate the values to arrive at the final scores for each supplier. This aggregation is a weighted average sum calculation defined by expression.

Provider$_i$ =

$$\sum_{i=1}^{2} \sum_{k=1}^{Kl} \sum_{j=1}^{Jl} Aijkl * SSjkl * FIkl * FDkl * Cl$$

- **Provider$_i$** is the overall desirability index score for supplier i.

- **Jk** is the index for the number of selected subcriteria for a criterion k.

- **Kl** the index for the number of selected criteria for a Cluster l.

- **Cl** the relative importance score of a Cluster l at the top level (e.g. a score for the selectivity criteria cluster).

- **F$^D_{kl}$** the direct (dependent) relative importance score of criterion k within a Cluster l. (e.g. a score for quality criterion which appears within the selectivity criteria cluster).

- **F$^I_{kl}$** the interdependent relative importance score of criterion k within the Cluster l as determined by the super-

matrix results.

- **SSjkl** the relative importance score for a subcriterion j controlled by criterion k within Cluster l (e.g. a score of Reliability of quality under the quality criterion within the selectivity criterion cluster).

  - **Aijkl** the relative importance score of a supplier i for subcriterion j under criterion k within the Cluster l.

Desirability index calculations for supplier selection:

Table 5: Desirability index calculations for supplier selection

Cluster	cl	factors	attributes	F^D_{kl}	SSjkl	F^I_{kl}	A1jkl (A)	A2jkl (B)	A3jkl ©	1	2	⊞
Selectivity criteria	0,888	Quality	QSC	0,552	0,352	0.240	0,512	0,36	0,128	0,002	0,017	0,0068
	0,888		RQ	0,552	0,346	0.240	0,139	0,573	0,286	0,003	0,015	0,007
	0,888		RR	0,552	0,300	0.240	0,095	0,650	0,254	0,002	0,014	0,005
	0,888	Delivery	GP	0,277	0,158		0,331	0,119	0,549	0,001	0,0006	0,002
	0,888		LT	0,277	0,211	0.203	0,259	0,065	0,675	0,001	0,0004	0,004
	0,888		PA	0,277	0,255	0.203	0,267	0,063	0,668	0,002	0,001	0,005
	0,888		PD	0,277	0,215	0.203	0,273	0,089	0,637	0,001	0,001	0,004
	0,888		DR	0,277	0,158	0.203	0,231	0,071	0,696	0,001	0,001	0,003
		Flexibility	RRD	0,172	0,557	0.165	0,303	0,089	0,607	0,0039	0,0011	0,007
	0,888		APV	0,172	0,320	0.165	0,303	0,089	0,607	0,0022	0,0006	0,004
	0,888		ADC	0,172	0,122	0.165	0,303	0,089	0,607	0,0008	0,0002	0,001
	0,888											
Rejectability criteria	0,111	Credit risk	SFS	0,245	0,557	0.110	0,2	0,6	0,2	0,0051	0,0153	0,0051
	0,111		ORS	0,245	0,320	0.110	0,157	0,655	0,186	0,0003	0,0014	0,0004
	0,111		LR	0,245	0,122	0.110	0,157	0,655	0,186	0,0001	0,0005	0,0001
	0,111	Price	APM	0,754	0,621	0.235	0,134	0,745	0,120	0,0012	0,007 / 0,001	0,0011
	0,111		FP	0,754	0,096	0.235	0,111	0,777	0,111	0,0001	0,003	0,0001
	0,111		FS	0,754	0,281	0.235	0,096	0,797	0,1053	0,0004		0,0004
Desirability indices										0,0399	0,0854	0,0655

IV.   CONCLUSION

Supplier selection is difficult given the qualitative and quantitative criteria. Since selecting the best supplier involves complex decision variables, it is considered to be a multicriteria decision problem. The ANP approach, as a methodology used to select the best supplier, not only leads to a logical result but also enables the decision-makers to visualize the impact of various criteria in the final result. Further, we have demonstrated that the interdependencies among various criteria can be effectively captured using the ANP technique. The ANP approach is capable of taking into consideration both qualitative and quantitative criteria

REFERENCE

[1] **Dickson, G.W., 1966**. An analysis of vendor selection systems and decisions, *Journal of Purchasing*, vol.2, pp.5-17
[2] **Amin, S. H., & Zhang, G. (2012).** An integrated model for closed-loop supply chain configuration and supplier selection: Multi-objective approach. Expert Systems and Applications, 39(8), 6782–6791.
[3] **Jharkharia, S. and Shankar, R. (2007)**. "Selection of logistics service provider: An Analytic Network
[4] Process (ANP) approach." Omega: International Journal of Management Science, Vol. 35, pp. 274-289.
[5] **Levary, R. R. (2008).** Using the analytic hierarchy process to rank foreign suppliers based on supply risks. Computers and Industrial Engineering, 55(2), 535–542.
[6] **Narasimhan, R. (1983),** An analytic approach to supplier selection. Journal of Purchasing and Supply
[7] Management, 1, 27–32.
[8] **Saaty, T. L. (2001).** The Analytic Network Process: Decision Making with Dependence and Feedback, RWS Publication, Pittsburgh, PA

Research Paper   Open Access

Network Mobiles

Alhamali Masoud Alfrgani .Ali, Raghav Yadav**,** Hari Mohan ,W.Jeberson
Department of Computer Sciences& Information Technology
'Sam Higginbotom Institute of Agriculture, Technology & Sciences Allahabad India'

I.   INTRODUCTION

Mobile devices are becoming increasingly popular for delivering multimedia content, particularly by means of streaming. The main disadvantage of these devices is their limited battery life. Unfortunately, streaming of multimedia content causes the battery of the device to discharge very fast, often causing the battery to deplete before the streaming task finishes, resulting in user dissatisfaction. It is generally not possible to charge the device while on the go as electricity socket and charger are required. Therefore, to avoid this user dissatisfaction, it is necessary to find ways to prolong the battery lifetime and to support the completion of the multimedia streaming tasks. A typical architecture for mobile multimedia streaming is presented In this architecture, a wired server streams multimedia content over a wireless IP network to a number of client devices. These devices could be PDAs, smartphones or any other mobile device with 802.11 connectivity. In relation to possible power savings, the multimedia streaming process can be described as consisting of three stages: reception, decoding and playing. Other researchers have shown that energy savings can be made in each stage, for example by using pre-buffering in the reception stage, feedback control during decoding and backlight adjustment for playing. However, it is not a common practice to combine energy savings in the three stages in order to achieve the best

Overall savings. Due to the large amount of power used by the network interface card, the reception stage is the largest consumer of the batteryThis paper proposes the Adaptive-Buffer Power Save Mechanism (AB-PSM) that provides significant power savings in the reception stage, and hence to the overall battery life. ABPSM

Introduces an additional buffer which hides data from the station it is intended for, allowing it to return to sleep and consequently save power. Data is eventually delivered in one of the station's following attempts to receive it. The proposed

AB-PSM improves the existing Power Save Mechanism (PSM) without making any modifications to it. The following section of this paper describes the related

Works proposed to provide power savings for each stage of the multimedia streaming process. The legacy PSM in the 802.11 standard is then described and its weaknesses identified.

1.1 Objective

A large amount of research has been carried out in both multimedia streaming and power saving techniques in wireless communications. However, few researchers have considered power saving in multimedia streaming and even fewer have considered the streaming process as a whole. Instead they have concentrated on only one of the three stages: reception, decoding or playing. In the following sections, some of these research findings are described

1.2 Reception Stage

Chandra and Vahdat propose an application-specific server side traffic shaping mechanism that can offer energy savings by allowing the client to sleep for longer periods of time. The system architecture consists of a client side proxy and a server side proxy. The server side proxy informs the client side proxy of the next data arrival. It is then the responsibility of the client side proxy to transition the client.

To a low power sleep state. The client can then sleep between data transfers. Although this scheme looks promising, it is not compatible with the 802.11 standard as it ignores the beacon interval which is the basis of the standard power-save mechanism. Another scheme for power saving in the reception stage is proposed at Energy efficient CPU scheduler for mobile devices, particularly those that run real time multimedia

applications. To save power, the pre-buffering method for multimedia output

is used, where output frames of real-time multimedia applications are temporarily stored in buffers. The proposed algorithm monitors the buffer occupancy and adjusts the CPU frequency accordingly. Although good results are shown to be achieved in simulations, this scheme relies on a low power hardware technique, such as Dynamic Voltage Scaling and on the prebuffering method, which makes it difficult to be implemented on a real system or device.

1.3 Playing Stage

The majority of the research which has been proposed in relation to the playing stage of the multimedia streaming process is related to the display of the device, in particular the back light. Pascrich propose an adaptive middlewarebased approach to optimize back light power consumption for mobile handheld devices when streaming MPEG-1 video. Another back light power management scheme is proposed by Shim, Chang and Pedram. In this case, a back light power management framework for color TFT LCD panels is proposed. The authors extend Dynamic Luminance Scaling (DLS) to cope with transflective LCD panels, which operate both with and without a back light, depending on the remaining

battery energy and the ambient luminance. The scheme, known as Extended DLS or EDLS, compensates for loss of brightness when there is a rich or moderated power budget and compensates for loss of contrast when the power budget is low.

1,4 General Power Saving in Multimedia Streaming

Acquaviva, Benini and Ricco propose a softwarecontrolled approach for adaptively minimizing energy in embedded systems for real time multimedia processing. Energy is optimized by modifying the clock speed settings. This is a very low level solution involving hardware and it is not independent of the platform. Korhonen and Wang study the impact of the burst length and peak transmission rate for observed packet loss and delay characteristics. They then implement an adaptive burst length mechanism which provides an improved trade off between power efficiency and congestion tolerance. Anastasi address energy saving by including periodic transmission interruptions in the schedule of audio frames at the server. In this way the Network Interface Card (NIC) at the server can be set to low power state, achieving power savings. Mohapatra propose an integrated power management approach that unifies low level architectural optimizations, OS power saving mechanisms

1.5 FACTORS THAT INFLUENCE BATTERY POWER IN MULTIMEDIA STREAMING PROCESS

The multimedia streaming process can be seen as comprising of three distinct stages. The reception stage refers to all of the network related tasks in the multimedia streaming process. The decoding stage involves the received media being power can be made in the reception stage. As expected, for the decoding stage, the higher the bit rate, the faster the battery is consumed. Various tests were

performed in the playing stage. The test results show that both the brightness level of the screen and the volume of the speakers have a significant effect on the battery consumption rate.

1,6 LEGACY POWER SAVE MECHANISM IN 802.11

The reception stage is the most significant power drainer in the streaming process due to the fact that the Network Interface Card (NIC) consumes a large amount of energy in a mobile device. For this reason, methods to save battery power during

this stage are being devised. Within the 802.11 standard, there is a built in powersave mechanism (PSM). A station informs the access point whether or not it is using power management by setting the Power Management bit within the Frame Control field of the transmitted frames. This bit is set to 1 if power management is being used and to 0 if it is not. When using power management, a station can enter a low power sleep state when it is not receiving traffic. This is how the station saves power. If the access point receives packets for a station that is in sleep mode, then it will buffer these packets.

1.7 ADAPTIVE-BUFFER POWER SAVE MECHANISM

This paper proposes a novel power save scheme, known as Adaptive-Buffer Power Save Mechanism (AB-PSM). ABPSM introduces a second buffer, in addition to the data buffer that is included at the Access Point. The new buffer, called the application Buffer, effectively hides packets from the default Access Point Buffer. When a beacon is received, the TIM only reports traffic which is waiting in the Access Point Buffer and is not influenced by the data that is in the Application Buffer. Assuming that the Listen Interval is set to one, as is generally the case, the station will wake up every beacon interval to receive the beacon. If the TIM indicates traffic, the station will stay awake to receive it, otherwise it will return to the low power sleep mode.

1.8 TESTS AND RESULTS

To examine the effectiveness of AB-PSM, tests were performed which compared it to the case when streaming is performed over 802.11 with no power save mechanism employed and with the legacy PSM, respectively.

II. TEST SETUP & SCENARIO

For the tests, a 3GHz Pentium 4 desktop computer with 1GB of RAM was used as the server. The client was a Personal Digital Assistant (PDA), with a 520MHz CPU, 64MB RAM and running Microsoft Windows Mobile 5 operating system. The multimedia content was sent from the server, to an 802.11b access point and then via the wireless network to the client. The tests involved continuously sending multimedia packets to the client.

1.9 Analysis of Results

The results are presented. The interval between sent packets is represented in terms of milliseconds and ranges from 25ms to 200ms. The packet sizes, or more specifically the size of the multimedia data chunks before lower layer fragmentation, are also shown and range from 512B(ytes) to 4096B. The graph shows four bars, each representing a different power saving scheme. The top bar refers to the 802.11 standard with the PSM switched off, with a 25ms interval and

a packet size of 512B. The next bar shows the legacy 802.11 PSM with the same settings. The last two bars correspond to the proposed AB-PSM. The first has an inter-packet sending interval of 100ms and a packet size of 2048B and the second

has an interval of 200ms and a packet size of 4096B. It should be noted that an identical amount of data is sent in all cases. The results show significant increases in the battery life when AB-PSM is used in comparison with both other cases: when no power saving and when the legacy PSM is employed respectively. There is an increase of 140% in the battery life when first AB-PSM scenario was considered and an increase of 160% battery life in the second AB-PSM test, both in comparison with the same legacy IEEE 802.11 PSM.

III.   CONCLUSION

The multimedia streaming process is divided into three stages: reception, decoding and playing. As the reception stage is the biggest consumer of power, the largest power savings can be obtained in this stage. To obtain power saving in the reception stage, the Adaptive- Buffer Power Save Mechanism (AB-PSM) is proposed. This is a mechanism that makes use of an extra Application Buffer

in order to "hide" packets from the station they are intended for, hence allowing it to sleep for longer periods and save power. Real-world tests show significant increases in battery life when AB-PSM is used. For example, tests presented in

this paper show that when AB-PSM is used, the battery life increased by 160% in comparison to the legacy power save mode described in the IEEE 802.11 standard.

REFERENCES:

[1]   "IEEE 802.11: Wireless lan medium access control (MAC) and physical layer (PHY) specification," 2000.
[2]   "IEEE 802.11b: Higher-speed physical layer (PHY) extension in the2.4ghz band," 2001.
[3]   "IEEE 802.11g: Further higher-speed physical layer extension in the 2.4 ghz band," 2003.
[4]   J. Adams and G.-M. Muntean, "Power-dependent adaptation algorithm for mobile multimedia networking," *IEEE International Symposium onBroadband Multimedia Systems and Broadcasting*, April 2006.
[5]   S. Chandra and A. Vahdat, "Application-specific network management for energy-aware streaming of popular multimedia formats," *Proceedings of the General Track. 2002 USENIX Annual Technical Conference*,pp. 329 – 42, 2002.
[6]   [6] J. Korhonen and Y. Wang, "Power-efficient streaming for mobile terminals," *Proceedings of the 15th International Workshop on Network*
[7]   *and Operating Systems Support for Digital Audio and Video. NOSSDAV 2005*, pp. 39 – 44, 2005.
[8]   [7] G. Bae, J. Kim, D. Kim, and D. Park, "Low-power multimedia scheduling using output pre-buffering," *13th IEEE International Symposium on Modeling, Analysis, and Simulation of Computer and Telecommunication*
[9]   *Systems*, pp. 389 – 96, 2005.

Alhamali Masoud Alfrgani .Ali ph.D student of SHIATS, B.tech degree in computer engineering from Technology College of Civil Aviation & Meterology In year 1992 Tripoli – Libya ,Mtech. From Sam Higginbotom Institute of Agriculture, Technology & Sciences in year 2012.His research area is Computer net work

Raghav Yadav is obtain a ph.D degree from the Motilal Nehru National institute of technology (MNNIT),Allahabad india. He received his B.E degree in electronics engineering from Nagpur University and M.Tech degree in Computer Science and engineering from MNNIT.Allahabad . Mr Yadav is currently an
assistant professor at Sam Higginbotom Institute of Agriculture, Technology & Sciences (SHIATS). Allahabad , India .He has authored more than 10 research papers in national /international conferences and refereed journals .His research interests are in the field of optical net work survivability,ad-hoc net works, and fault tolerance systems.

Hari Mohan Singh is presently pursuing a phD degree from MNNIT, Allahabad ,India , He received his B.F degree in computer science and engineering from Amravati University ,india.and M.Tech . degree in computer science and engineering from Uttar Pradesh Technical University (UPTU), Lucknow,india. Mr.Singh is currently an assistant professor at SHIATS,Allababad , india.
.He has authored more than eight research papers in national /international conferences and refereed journals .His research interests are in the field of optical net work survivability,real-time systems, and fault -tolerant systems

W. Jeberson is obtain a PhD degree from the SHIATS India. He received his M.B.A degree in I.T from M.K. University .and M.C.A degree in Computer from Madurai kamraj university. and B.Sc degree in physics from Manononmanian sundananar university. Mr. W. Jeberson is currently an assistant professor at Sam Higgin botom Institute of Agriculture, Technology & Sciences (SHIATS). Allahabad, India..

Research Paper   Open Access

Effects and Roles of Laws of Bangladesh Against Crimes: A Study

Shafiul Pervez[1]

[1](Post Graduate Diploma, Northumbria University, UK)

ABSTRACT: *Bangladesh officially the people's republic of Bangladesh is a country of South Asia. The independence day of Bangladesh is 26 March. After getting independence in 1971, there was established laws in Bangladesh. Which is under legislative and parliamentary affairs division. Bangladesh people have 23 fundamentals right's under the constitution of Bangladesh, Part 3 and Articles 26 to 47A. The Judiciary of Bangladesh consists of a Supreme Court, Subordinate courts and Tribunals Total 956 Acts, Ordinances and President's Orders have been compiled in the Bangladesh Code from September, 1836 to January, 2007. The first Act in the Bangladesh Code is accumulated from 11th September, 1836 and the first Act title is 'The Districts Act, 1836. Our main objective is to establish a thesis paper on lows of Bangladesh.*

Keywords: Code, Supreme Court, Appellate Division,Subordinate Courts and Tribunals.

I.   LAW

Law is a system of rules that are enforced through social institutions to govern behavior. Laws can be made by legislatures through legislation, the executive through decrees and regulations, or judges through binding precedent. Private individuals can create legally binding contracts, including arbitration agreements that may elect to accept alternative arbitration to the normal court process. The formation of laws themselves may be influenced by a constitution and the rights encoded therein. The law shapes politics, economics, history and society in various ways and serves as a mediator of relations between people.A general distinction can be made between (a) civil lawjurisdictions, in which the legislature or other central body codifies and consolidates their laws, and (b) common law systems, where judge-made precedent is accepted as binding law. Historically, religious laws played a significant role even in settling of secular matters, which is still the case in some religious communities, particularly Jewish, and some countries, particularly Islamic. Islamic Sharia law is the world's most widely used religious law. The adjudication of the law is generally divided into two main areas referred to as Criminal law and, Civil law. Criminal law deals with conduct that is considered harmful to social order and in which the guilty party may be imprisoned or fined [1]. Civil law deals with the resolution of lawsuits between individuals or organizations. These resolutions seek to provide a legal remedy to the winning litigant. Under civil law, the following specialties, among others, exist: Contract law regulates everything from buying a bus ticket to trading on derivatives markets. Property law regulates the transfer and title of personal property and real property. Trust law applies to assets held for investment and financial security. Tort law allows claims for compensation if a person's property is harmed. Constitutional law provides a framework for the creation of law, the protection of human rights and the election of political representatives.

Administrative law governs what executive branch agencies may and may not do, procedures that they must follow to do it, and judicial review when a member of the public is harmed by an agency action. International law governs affairs between sovereign states in activities ranging from trade to military action. To implement and enforce the law and provide services to the public by public servants, a government's bureaucracy, military, and police are vital. While all these organs of the state are creatures created and bound by law, an independent legal profession and a vibrant civil society inform and support their progress.

II.   OBJECTIVES

Our main objective is to establish a thesis that we can express our laws to others, not only laws it's include our limitations also. As a thesis paper we have some objectives to follows:

- To identify
- To establish a thesis paper considering Laws in Bangladesh
- To describe briefly about all sections of law in Bangladesh.
- To determine the problem that faces people in Bangladesh.
- To estimate a proper way to complete thesis.
- To develop a rational of study related our paper.
- To compare crimes result.
- To collect data of crimes.

III.   STATE OF THE PURPOSE CONSIDERING BANGLADESH

The Law of Bangladesh is primarily in accordance with the English legal system although since 1947, the legal scenario and the laws of Bangladesh have drifted far from the West owing to differences in socio-cultural values and religious guidelines. In November 2007, Bangladesh has successfully separated the Judiciary from the Executive but several black laws still influence the rulers in creating Special Tribunals in using several black lawsincluding the Special Powers Act.

The Supreme Court

The Supreme Court of Bangladesh is the highest court of law in Bangladesh. It comprises the Appellate Division and the High Court Division. It was created by Part VI, Chapter I of the Constitution of Bangladesh. It is the apex Court of the country and other Courts and Tribunals are subordinate to it [2]. This is also the office of the Chief Justice, Appellate Division Justices, and High Court Division Justices of Bangladesh.

Jurisdiction of the Appellate Division

Appellate Jurisdiction:The Appellate Division has jurisdiction to hear appeals from the High Court Division in the following grounds:-
One can appeal against the division of High Court when-

i. The issue relates to interpretation of Constitution of Bangladesh,
ii. Contempt of that Division, and
iii. Death or life imprisonment confirmed or declared by the Division.
An appeal to the Appellate Division from a judgment, decree or sentence of the High Court Division in a case to which clause 2 (102) does not apply shall lie only if the Appellate Division grants leave to appeal.

Rule-making Jurisdiction: The Supreme Court is independent of the executive branch, and is able to rule against the government in politically controversial cases.
Advisory Jurisdiction: In the question of any law or anything required for public interest, the President may ask for opinion from the Appellate Division.
Jurisdiction to ensure justice: Article 104 deals with issue and execution of processes of Appellate Division. It provides the power to the Appellate Division to issue anything required for the complete justice.
Other Jurisdictions: The Appellate Division shall have others jurisdiction by Act of Parliament.Chancery Research and Consultants Trust (CRC-Trust) maintains a website Chancery Law Chronicles-First ever Online Database of Bangladesh Laws where it has already included 7000 judgments of the Appellate Division and High Court Division of the Supreme Court of Bangladesh from 1972 to till date.

The High Court Division

Clause 3 of Article 95 provides to the High Court Division which at any time before the commencement of our Constitution exercised jurisdiction as a High Court in the Territory of Bangladesh. The High Court Division shall have Superintendence and control over all Courts and tribunals subordinate to it [3]. The High Court Division, though a Division of the Supreme Court, is for all practical purposes, an independent court with its powers, functions and jurisdictions well defined and determined under the Constitution and different laws. Jurisdiction of the High Court Division: It has both appellate as well as original jurisdiction.
•**Original Jurisdiction**: The power to file any case is called the original jurisdiction. It has original jurisdiction to hear Writ Applications under article 102 of the Constitution, which is known as extra ordinary constitutional jurisdiction. It has further original jurisdiction, inter alia, in respect of company and admiralty matters under statutes. The High Court Division, in special circumstances, has also powers and jurisdiction to hear and dispose

of cases as the court of first instance under article 101 of the Constitution.

•**Appellate Jurisdiction**: The High Court Division hears appeals from orders, decrees and judgments of subordinate courts and tribunals. One can appeal to the High Court Division if-

i. more than 14 years imprisonment by Session Judge, or

ii. Related to the question of interpretation of the Constitution.

The Subordinate Courts and Tribunals

There are a wide variety of subordinate courts and tribunals. Such courts and tribunals are created by some relevant statutes. All their powers, functions and jurisdictions are well determined by the respective statutes. These are the basic courts in the system of the judiciary of Bangladesh. The major bulk of the cases, both civil and criminal, are tried and heard in such courts and tribunals [4]. Certain tribunals are termed as administrative tribunals, Nari-o-ShishuNirjaton Daman Tribunals, Special Tribunals etc. Such courts and tribunals spread all over the country at district levels. The subordinate courts in Bangladesh can be divided in two broad classes, namely, civil courts and criminal courts [5].

Civil Courts

The civil courts are created under the Civil Courts Act of 1887. The Act provides for five tiers of civil courts in a district, which bottom-up are:

- Court of Assistant Judge
- Court of Senior Assistant Judge,
- Court of Joint District Judge,
- Court of Additional District Judge and
- Court of District Judge

The first three are courts of first instances with powers, functions and jurisdictions in respect of subject matter, territory and pecuniary value determined by or under statutes.

Criminal Courts

- Courts of Sessions
- Courts of Metropolitan Sessions
- Special courts/tribunals (Criminal)
- Courts of Metropolitan Magistrate
- Courts of Magistrate

IV. RATIONAL OF STUDY

Our core composition is about Laws in Bangladesh. We got this idea, because we follow up crimes and watched what happened to people. What we wanted to show was make our laws describe to everyone. We started with these literal movements and planned that the collect data first then try to build a thesis on it.

We made our motif with shapes and dynamics that reflected the idea thesis paper on Laws in Bangladesh. The shapes started higher and would gradually get lower. The dynamics we chose were swinging to represent the movement of the laws related organization. The shapes in the motif are asymmetrical because this helps to show more flowing movement.

We wanted to show contrasting dynamics and levels in the middle section where we find the desired help for any cases. We chose higher shapes, and wider dimensions with a sharp dynamic, in the last section, where the Courts in Bangladesh, We chose low levels, stillness and collapsed dynamics. Slowed the music down to help me achieve the tempo of the movement that I needed in that section.

V. FUNDAMENTALS RIGHTS

Bangladeshi people have 23 fundamental rights under the Constitution of Bangladesh, Part 3, and Articles 26 to 47A. The Fundamental Rights in Bangladesh under below:

1. Laws inconsistent with fundamental rights to be void (Article-26)
2. Equality before law (Article-27)
3. Discrimination on grounds of religion, etc. (Article-28)
4. Equality of opportunity in public employment (Article-29)
5. Prohibition of foreign titles, etc. (Article-30)
6. Right to protection of law (Article-31)
7. Protection of right to life and personal liberty (Article-32)
8. Safeguards as to arrest and detention (Article-33)
9. Prohibition of forced labor (Article-34)
10. Protection in respect of trial and punishment (Article-35)
11. Freedom of movement (Article-36)

12.   Freedom of assembly (Article-37)
13.   Freedom of association (Article-38)
14.   Freedom of thought and conscience, and of speech (Article-39)
15.   Freedom of profession or occupation (Article-40)
16.   Freedom of religion (Article-41)
17.   Rights of property (Article-42)
18.   Protection of home and correspondence (Article-43)
19.   Enforcement of fundamental rights (Article-44)
20.   Modification of rights in respect of disciplinary law (Article-45)
21.   Power to provide indemnity (Article-46)
22.   Saving for certain laws (Article-47)
23.   Inapplicability of certain articles (Article-47A)

VI.   CASE STUDY

Considering others our criminal record are now in middle range. In some area we are in safe zone.
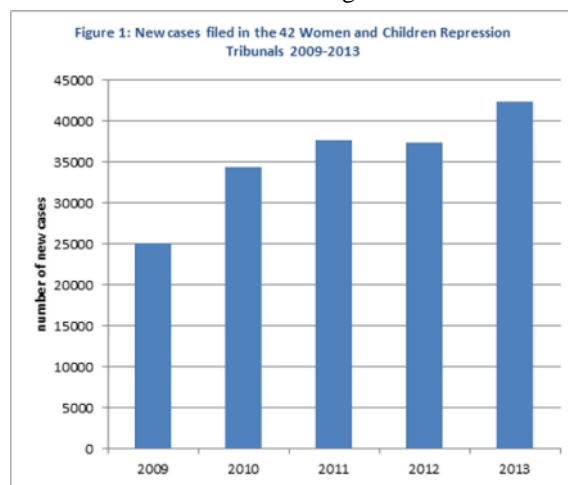
Chart 1: Special Tribunals Cases

Chart 1 depicts special case issue on 42 women &children repression tribunals. It is clearly shown that from 2009 to 2013 there is a lot of change in 2009 it was around 25000 & in 2013 it was around 42000.

Chart 2: Types of Political violence

Chart 2 illustrates political violence of Bangladesh. This picture tells horrible situation of political violence in Bangladesh. In 10 years there are 150 people inclosing sending state & refuges. In receiving state & refugees there are 110 peoples.

Proportions of women ages 15 – 49 reporting that their first act
of sexual intercourse was forced, by age at first intercourse.[16]

COUNTRY	Under age 15	15 – 17	18 and over
Peru (city)	45%	9%	3%
Peru (province)	41	28	17
Tanzania (city)	40	17	10
Tanzania (province)	43	18	12
Bangladesh (city)	38	24	13
Bangladesh (province)	36	28	21
Samoa	35	14	6
Thailand (province)	20	7	4
Ethiopia (province)	18	15	20
Brazil (city)	14	2	2
Brazil (province)	11	4	3

Table 1: Case study

From table 1 considering 7 country Bangladesh is in third position. Under age 15 there are 38 city girl and 36 province girls are sexually forced. In age 15-17 there are 24 city girl and 28 province girls are sexually forced. In age 18 and over there are 13 city girl and 21 province girls are sexually forced.

VII.   LIMITATIONS

After a review on our laws we found lots of limitations. From judge to criminal our studies finds some limitations like there working procedure. Some of the limitations are given below:

- Political instability.
- Political Unrest.
- Political crisis.
- Moral degeneration about their joining

VIII.   FINDINGS

These thesis activities show that it is possible for to control crimes which is not in alarming rates. We have time control our crimes by taking some necessary steps .A major disadvantage of our laws is there is not enough control about conspiracy, that's the main drawbacks

The Pathfinder study has shown that the collection of relevant data in crimes files, required for linking with performance data, can be cumbersome and time consuming. All relevant data should ideally be put into electronic format from the start, but there is also a need for a proper and unbiased definition of those data before they can be used in a linking exercise.

IX.   RECOMENDATIONS

Recommendation # 1: The Controlling Committee should review there enforcing lies and determine whether or not to standardize regional structures across the department. Recommendation #2: The Law department should assess the risk associated with the current practice of having a authority of start dates occurring before signature of the agreements, and take action to reduce such risks by addressing the cause of the issue.

Recommendation # 3: The Law department should develop minimum documentation and communication standards for rejected applications.

Recommendation # 4: Related employees should consider enhancing its training for project officers and managers and its active monitoring of project files for key compliance attributes.

X.   CONCLUSION

A proverb says "human are not for laws, Laws for human". That's the main theme laws imposed between us for helping us to lead a secure life. In this paper we actually introducing Laws that are now in constitution in Bangladesh. We are explain not briefly but try our best to establish a good review. In our country criminal records are not in alarming rates, This is the proper time to use our law against crimes.

REFERENCES

[1] H.Kdatta (2003), Communities and Law in Bangladesh: Politics and Cultures of Legal Identities. The University of Michigan Press, 2003. Second print 2005

[2] Auby, K.Hasan (2002). "Administrative Law in Bangladesh". Dhaka university press.

[3] G. Shukla(2003). Communities and Law: Politics and Cultures of Legal Identities considering South Asia. The University of Michigan Press.

[4] P. Bhattyacharyja. (1992). "A Critique of Laws". Hart's Legal Philosophy. Springer.

[5] Beale, Hugh; Tallon, Denis (2002). "English Law: Consideration Bangladesh". Contract Law. Hart

Research Paper   Open Access

Simulating the Erosion and Sedimentation of Karun Alluvial River in the Region of Ahvaz (Southwest Of Iran)

Farhang Azarang[1*], Mahmoud Shafai Bajestan[2]

[1]*Department of Water Science and Engineering, Science and Research Branch, Islamic Azad University, Tehran, Iran.*
[2]*Department of Water Science and Engineering, Shahid Chamran University, Ahvaz, Iran*

ABSTRACT : *Since the rivers are the main basic and accessible resource of water for miscellaneous uses, the erosion and Sedimentation condition of rivers are of a great deal of importance. Karun River, the greatest river of Iran, has a considerable interest because of strategic and environmental conditions regarding its water projects planning, agriculture, water supply of cities, and industrial units. The morphological changes due to erosion processes, sedimentation, and Sediment transport affects the hydraulic structures like Intake port, irrigation systems, and pump stations. Thus, the present research deals with the simulation of erosion and sedimentation processes and also considering cross section geometric changes, prediction of river thalweg, and total sediment load of Karun River using HEC-RAS model. The simulation periods of this research is 10 years from 2001-2011. The results show that the Karun River has had sedimentation in its most cross sections while the erosion has been rarely observed. Additionally, the Englund–Hansen and Ackers–White sediment transport functions propose better results about the river changes. According to the HEC-RAS results and the measured data, river training of dredging is necessary at the studied site especially at the Ahvaz urban areas. Also, at the river parts which are under erosion the stabilization procedures for the banks and walls, is suggested. The result of this work can be an appropriate pattern about the situations of Karun and effects of erosion, sediment transport, and sedimentation processes.*

KEYWORDS: *HEC-RAS Model, Manning roughness coefficient, Thalweg, Sediment transport, Dredging.*

I.   INTRODUCTION

Rivers are the most important resources of water supply for various uses. Thus, the knowledge of river situation and erosion and sedimentation conditions are the main priorities of each engineering project of the river. The river is a dynamic system undergoes continuous changes always. The knowledge of sedimentation phenomenon including the erosion, sediment transport, sedimentation, and consolidation of sediments are of a great deal of importance. Reasonable estimate of sediment transport rates in alluvial rivers is important in the context of a number of water management issues (Bhattacharya et al, [1]). Sediment transport is a widely studied topic in which numerous researches have built models for predicting bed material transport rates in an alluvial river (Bhattacharya et al, [2]). Information on soil erosion and its effects on water quality at catchment scales are increasingly sought by catchment managers (Merritt et al, [3]). Among several problems resulted from complicated erosion processes, the deposition of sediments are more important especially in rivers having the ability of high sedimentation level.

Karun River is of a great deal of importance as the greatest river of Iran because of climatic conditions, environmental effects, strategic location, hydraulic structures, and procurement of great agricultural plans, and water supply. Since Karun River has many hydraulic structure from its upstream to Persian Gulf downstream such as huge dams and bridges, the morphological and sedimentation condition of the river undergo widespread changes. The study of Karun River situations from hydraulic standpoint especially in downstream of these structures is an inevitable issue. Sedimentation in Karun River results in several problems in using high potential of the river in addition to problems for intake equipment's and pumps stations causing damage of mentioned structures. An important point is that the loafing capacity of the river decreases because deposition of sediments resulting in morphological changes. In other words, the great rivers like Karun have miscellaneous plans and projects, thus knowing and prediction of river conditions in order to optimum fulfillment is of considerable importance. Karun River has specific properties in river reach of this research from Ahvaz-Farsiat as follows:

i) The Karun River passes through Ahvaz as the center of Khouzestan province, Therefore, potential flood control, water transportation, city proportion and etc have strategic importance.
ii) There are a lot of hydraulic structures in Karun River route including huge bridges.

iii) The river reach have several meanders and islands having diverse vegetations. Thus, the study of erosion and sedimentation situations of the Karun River is important.

The main gold of this survey is evaluation of erosion and sedimentation conditions of Karun River that it reach passes through Ahvaz city.

The river engineering researchers have widely considered the erosion and sedimentation processes using different methods. Einstein, [4] has been one of greatest researchers in sedimentation field. The elementary researches of erosion and sedimentation were performed by Bagnold considering the transport of sand particles. He divided the transport particles into 2 bed load and suspended load (Bagnold, [5]). Van Rijn also performed valuable researches about sediment transport (Van Rijn, [6]). Nowadays, mathematical models are important instruments for study of rivers. Sediment transport in areas such as rivers, lakes or coast, can be modeled by mathematical model with a hydrodynamical component and a morphodynamical one (Morales de Luma et al, [7]). The sediment transport in alluvial rivers resulted from interactions between hydraulic conditions and the river bed characteristics (Azarang et al, [8]). The studies on river engineering through numerical and mathematical methods have been developed because of the great upsurges in computer science. Mathematical models are useful instruments to solve the problems of erosion, sediment transport, and sedimentation in river. There are advanced mathematical models which perform the simulation process of catchment sediment and river reach efficiently. The models like HEC-6, HEC-RAS, SSIIM, Seflow, MIKE-11, GSTARS, and Susflow have been widely used by many researchers to simulate the erosion and sedimentation situation of the rivers. The HEC-RAS model has been added to this list as water engineering software being able to simulate the sedimentation situation of the river widely used in simulation of different rivers of the world. The main mentioned researches are as follows: HEC-RAS model has been used to predict the sedimentation conditions in mountainous rivers (Rathburn et al, [9]). To simulate the scouring, erosion, and sedimentation in ephemeral channels, the HEC-6 model has been utilized (Canfield et al, [10]). Gibson et al have considered the capability of HEC-RAS model to calculate the sediment transport of the river (Gibson et al, [11]). In our previous research reported at 2015 in Persian, we have used the HEC-RAS model to consider the erosion and sedimentation of Karkheh River in Iran. Karun River has been widely studied in Iran because of high importance of this river and having critical engineering plans along this river. Shahinezhad et al, have used the GSTARS model to study the erosion and sedimentation processes of Karun River in suburban area of Ahvaz and reported the Ackers – White and Toffaleti as the superior relations (Published in Persian). Also in our published paper at 2010 in a Persian journal we have applied the CCHE1D software for hydraulic and sedimentation simulation of Karun River which is in agreement with Englund- Hansen as the best sedimentation load equation and sedimentation of 2.5 million tons per year estimated for Karun River in this reach.

II. MATERIALS AND METHODS

Karun Catchment

From hydrological classification, the Karun Catchment is a subset of Persian Gulf and Oman Sea. The Karun Catchment is located in Khouzestan, Lorestan, Chahar Mahal Bakhtiari, Kohkiloye - Boyer Ahmad, and Isfahan provinces. This catchment is limited to Dez Catchment in north, Zayandehrood Catchment in west, Zohreh and Jarahi Rivers Catchments in south, and Dez and Karkheh Catchments in east. This catchment has an area about $67257 \ km^2$. Important cities of this catchments include Yasuj, Shahrekord, Masjedsoleiman, Shoushtar, Ahvaz, Abadan, and Khoramshahr. 67% of Karun Catchment is the mountainous areas and 33% of it is the plains and foothills which major of it is located in Khouzestan plain (Behan Sad Consulting Engineers Co reported in Persian, 2010). The figure 1 depicts the Iran and Karun catchment.
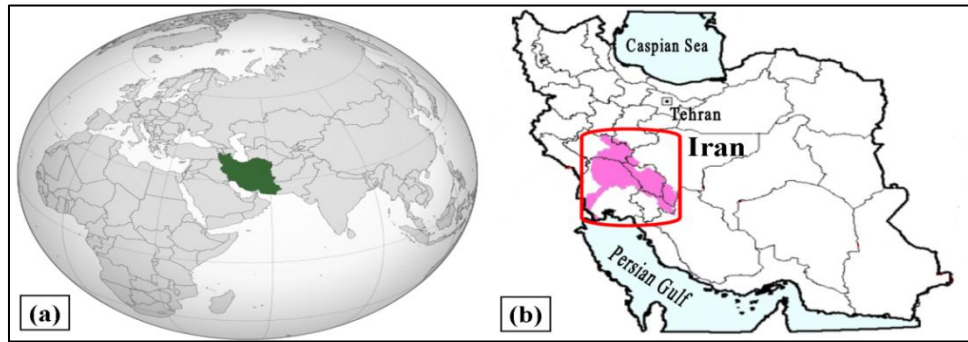
Figure 1: Location of Iran in the World (Wikipedia) and b Karun River Catchment in southwest of Iran

Karun River

The head water of Karun River is in central Zagros Mounains and Zardkouh Bakhtiari located in Kouhrang and its first great branch is called Kouhrang. Karun River is the greatest river of Iran and is 900 km long. Four main branches of Karun are: Khersan, Ab Vanak, Ab Kiar, and Bazoft. River reach of Karun in this research is considered as an old river becasue of lits low slope and having wide cross sections. Also, this river is classified as the suspended load in Ahvaz-Farsiat reach because of low slope and high depth and The sinusoidal coefficient of the river is around 2 (Behan Sad Consulting Engineers Co reported in Persian 2010). The bed load of the river in this reach is considered 10% of suspended load. Karun River has a braided river in under study reach. Figure 2 shows the parts of Karun in under study reach passing through Ahvaz city.
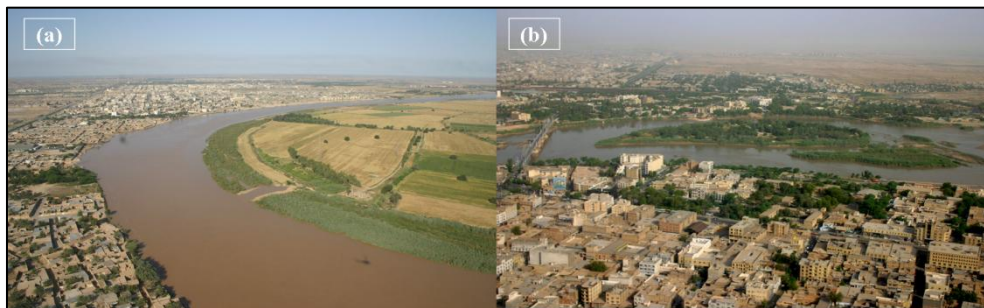
Figure 2: Images of Karun River in Ahvaz city, a Suburb of Ahvaz City and b Center of Ahvaz

In this paper, the statistic data of 2 hydrometric stations in upstream and downstream reach in Ahvaz and Farsiat were used. Table 1 shows the data of two mentioned hydrometric stations.

Table 1: Specifications of the Ahvaz and Farsiat hydrometric stations

Station Code	Station Name	River	Longitude (UTM)	Latitude (UTM)	Equipments	In Operation	Altitude (m)
21-309	Ahvaz	Karun	3469350	280701	Limnograph Staff gage	1950	9.787
21-465	Farsiat	Karun	3451555	263017	Staff gage	1973	3.015

The area of Karun Catchment is 61088 km^2 in hydrometric station of Ahvaz and its mean annual discharge is 673 m^3 per year. Also, the amount of specific discharge of sediment is 173.65 ton per year in km^2 while the specific discharge of sediment in hydrometric station of Farsiat is about 178.41 ton per year per km^2 (Behan Sad Consulting Engineers Co reported in Persian, 2010). Figure 3 shows hydrometric stations of Ahvaz and Farsiat on Karun reach.
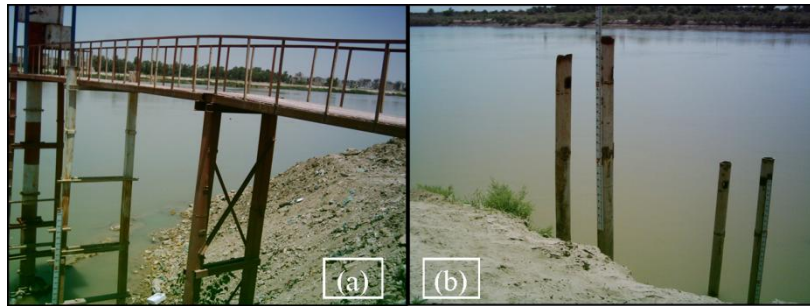
Figure 3: Images of Karun hydrometric stations, a Ahvaz station b Farsiat station

Figure 4 shows the Karun Plan and location of hydrometric stations on google earth software.
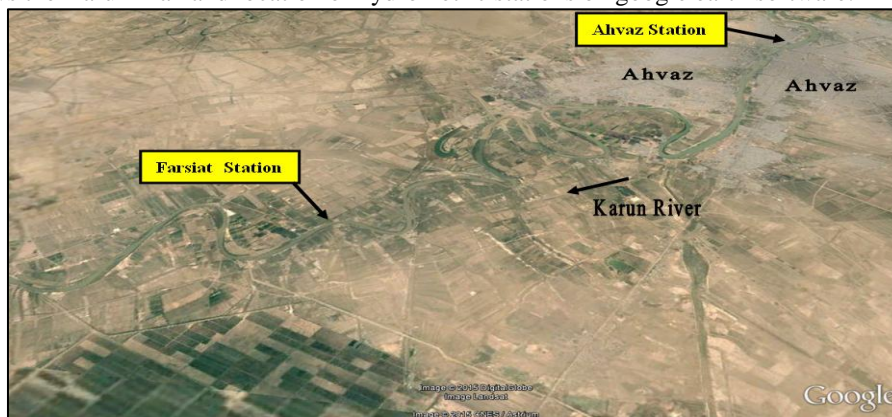
Figure 4: Studied Plan of Karun River and hydrometric stations of Ahvaz and Farsiat

Karun River Bridges

      Hydraulic structures such as bridges have built on Karun River in Ahvaz. These bridges highly influenced the river flow regime and sedimentation pattern. Hence they have introduced in brief here; now 8 bridges are in operation in Ahvaz. First of all is Siah Bridge which has 1050 meters long, 6 meters wide and 52 bases that built in 1929 for train passing between Tehran, Khorramshahr and Abadan. Second bridge or Sefid Bridge built at the center of Ahvaz for traffic and counted as the forth cantilever bridge of the world at its building time of 1936. It has 501 meters long and 9 meters wide. Shahid Daghayeghi Bridge with 496 meters long and 15 meters wide built in 1970 at the upstream of Karun River. Naderi Bridge is the forth bridge with 576 meters long and 17 meters wide built in center of Ahvaz city in 1977. Fifth Bridge at the downstream of Karun River has 480 meters long and 31 meters wide built in 1996. Sixth Bridge named Foolad has 400 meters long and 20 meters wide, is situated at the southern of Ahvaz. Seventh one is Kianpars Bridge built in 1996 with 490 meters long and 16 meters wide and the last one Ghadir Bridge with 643 meters long and 13 meters wide has finished in 2011. The Images of Figure 5 indicate to some of these bridges.
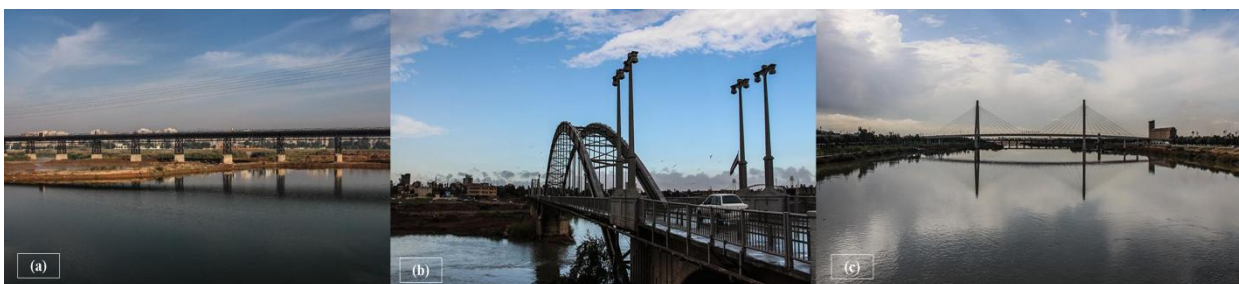
Figure 5: Bridges have built on the Karun River in Ahvaz; a Siah Bridge,

b Sefid Bridge and c Ghadir Bridge

HEC-RAS Model

In this research, HEC-RAS model 4.1 has been used for simulation proposed by US army. The mentioned software is able to simulate the steady flow, gradually varied flow, water quality, and sediment transport and the sedimentation simulation ability has been added to its newest versions. This model has an advanced graphic having a lot of abilities to display the software outputs. The sediment load part of this model has been developed to simulate the one dimensional deposition of sedimentation and erosion of the rivers. The main capabilities of HEC-RAS are as follows:

- Ability of the river network simulation,

- Using different sediment transport functions,

- Dredging of open channels and rivers,

- Sedimentation studies in dams,

- Estimation of scouring,

- Evaluating of sedimentation in rivers and channels (Brunner, [12],[13]).

New version of this software has been designed to simulate the erosion and sedimentation of the rivers and open channels. A geometric file of the river, a quasi-unsteady flow file, and a sedimentation details file are needed to create the conditions similar to the river in HEC-RAS model. In this software, well known equations are used to determine the total sedimentation load. The results are dependent upon the selected function of sediment transport (Brunner, [12],[13]).

In sedimentation analysis of HEC-RAS, the sedimentation control volume of each section is considered. The vertical part of sedimentation control volume is defined with Max Depth or Min Elevation. The cross section of sedimentation file of software is defined by Station Left and Station Right determination. The HEC-RAS provides the possibility of sedimentation in wet area of cross section while the erosion of river is just caused in defined area (Brunner, [12],[13]). Some properties of sediment transport formula of HEC-RAS software are summarized in table 2.

Table 2: Specification of sediment transport functions that were used in HEC-RAS model (Brunner, [12],[13])

Sediment TransSport Formula	Sediment Grading	Method of Calculation
Ackers-White 1973	Sand-Gravel	Laboratory
Englund-Hansen 1967	Sand	Laboratory
Larsen 1989	Silt-Gravel	Laboratory-Field
Toffaleti 1968	Sand	Laboratory-Field
Yang 1973-1984	Sand-Gravel	Laboratory-Field
Wilcock 2001-2003	Sand-Gravel	Laboratory-Field

Also, the Energy, Momentum Equations and Continuity of sedimentation Equations are the main equations of HEC-RAS mathematical model (Brunner, [12],[13]).

Data of Karun River for Running the Model

The necessary data to simulate the Karun River in under study river reach from hydrometric stations of Ahvaz-Farsiat includes the data of geometry, river flow and sedimentation. The cross sectional maps of 2001 of Karun River have been used for geometric data. In mentioned river reach which is about 48 Km, the data of 46 cross sections have been selected. These data has been taken from water organization of Ahvaz associated with ministry of force. Figure 6 shows the Karun plan in HEC-RAS and location of cross sections on it.
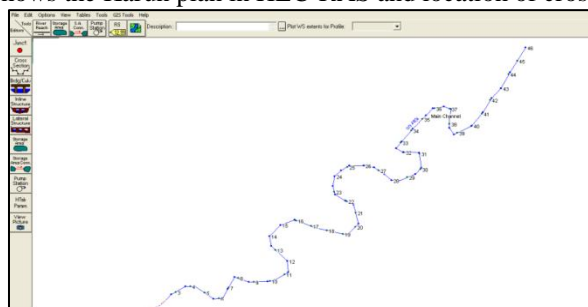
Figure 6: Karun River cross sections in the studied reach which have been lain out at the HEC-RAS model

Figure 7 is an example of the geometry of the cross-sectional view of Karun River.
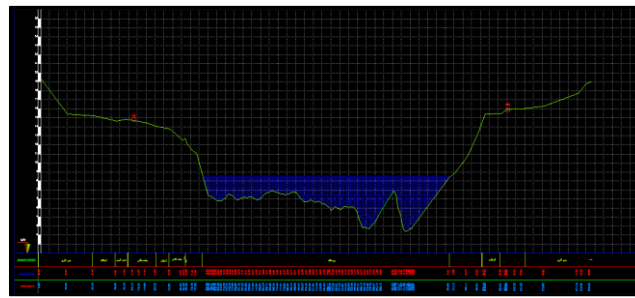
Figure 7: Geometry of the cross-sectional view of Karun River

A quasi-unsteady flow is needed for simulation in HEC-RAS model which should be defined in upstream and downstream of studied boundary conditions of the river. In this research, a time series of flow is determined as the upstream boundary of Karun River in Ahvaz hydrometric station. In quasi-unsteady flow, the variable steps are considered in HEC-RAS model and a 24 h period of time has been considered in this work. Figure 8 shows the hydrograph of input flow of Karun in upstream boundary.
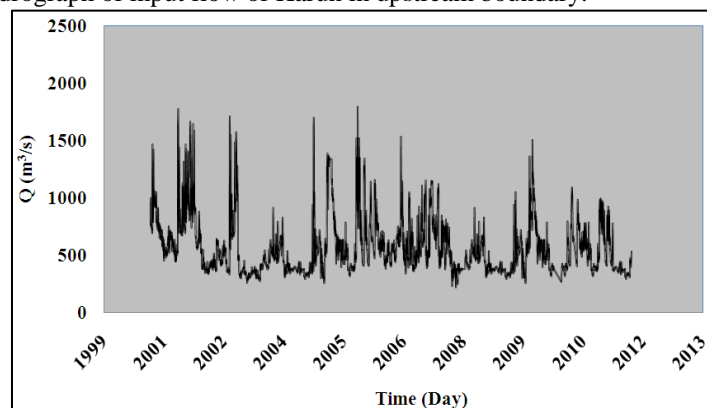
Figure 8: Inflow hydrograph of Karun River at the upstream and Ahvaz hydrometric station

during the simulation

The relation between water level and flow or the Discharge–Stage is considered for the downstream boundary. Since the downstream boundary of the river is located in Farsiat hydrometric station, this point has been selected as the boundary condition of the Karun River. Figure 9 show the Discharge–Stage of Farsiat hydrometric station.

$$Q = 2E\text{-}05H^{2.7105}$$
$$R^2 = 0.97$$
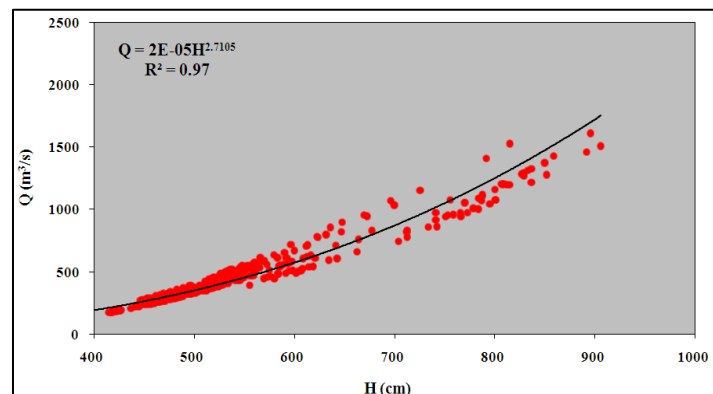
Figure 9: Discharge-stage curve of Karun River at the downstream and

Farsiat hydrometric station

The size of sediment particles plays an important role in erosion and sedimentation of the river, defining the sedimentation part in HEC-RAS, each cross section should have a gradation curve in a discrete bed.

In under study river reach from upstream to downstream, the cross sections having the statistics and data of gradation have been used and the interpolation data have been used to determine the gradation of the bed in cross sections which have no data. The specific weight of sediment particles of Karun River in this reach are 2.65, the shape coefficient is 0.6, and the density of gravel, sand, and clay particles are 1489, 1041, and 480 kg/m^{-3} respectively. As can be seen in Figure 10, the gradation curves of river bed are depicted in hydrometric stations of Ahvaz **a** and Farsiat **b** in upstream and downstream of the river, respectively. Considering the gradation curves show that the gradations gets smaller from upstream to downstream. In other words, the particles include large and medium sand particles near the Ahvaz while more tiny particles are observed near the downstream.
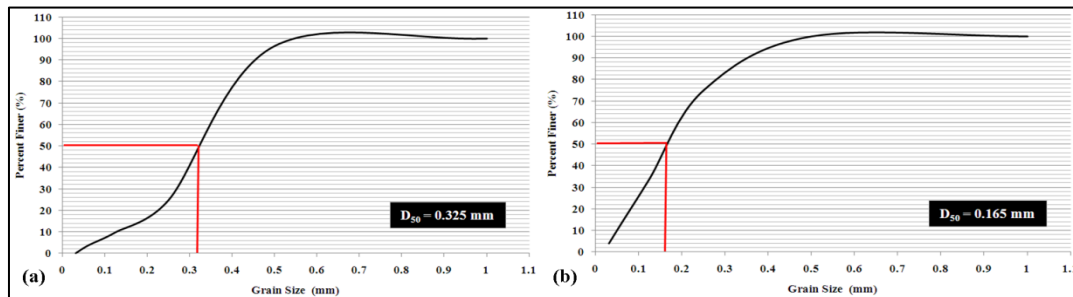
Figure 10: Particle size distribution curves of the Karun River in a Ahvaz station and b Farsiat station

The rating curve determines the sediment discharge into the river based on the river flow. To obtain the flow discharge-sediment load curve, the data recorded in hydrometric station are used. In this work, the data of Karun River in upstream are taken from Ahvaz station. Figure 11 shows the curve of Ahvaz station during the simulation process.
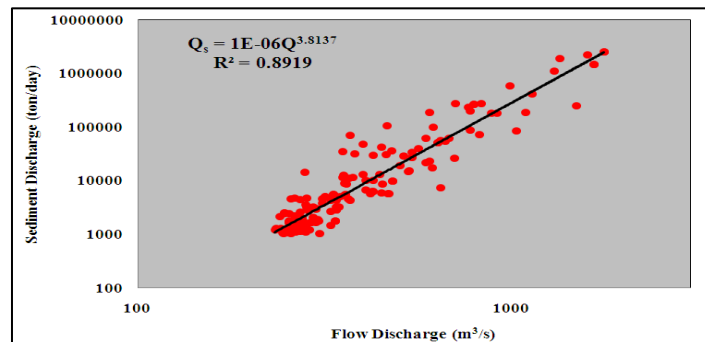
Figure 11: The relevance of flow discharge and sediment discharge of Karun River at upstream and Ahvaz hydrometric station

III.   RESUALTS AND DISCUSSION

Hydraulic Calibration of Model

The calibration of calculated data by the model is performed using the measured values in hydrometric stations. In hydraulic flow, the river flow and water level are used for calibration of the model. The Manning roughness coefficient of flow resistance is considered as the calibration parameter of the model in flow section in such a way that the change of this coefficient makes the calculated data of model and observed data closed. In Karun River, based on the gradation curves along the river reach and calculating the sediment particle size using experimental relations, the initial values of Manning roughness coefficient were determined. Table 3 shows the experimental methods to estimate the Manning roughness coefficient.

Table 3: Experimental methods for determining the Manning roughness coefficient

Method	Formula
Strickler 1923	$(D_{50}^{1/6})/21.1$
Muller 1948	$(D_{90}^{1/6})/26$
Keulegan1 1938	$(D_{50}^{1/6})/46.9$
Keulegan2 1949	$(D_{90}^{1/6})/49$
Keulegan3 1949	$(D_{65}^{1/6})/29.3$
Lane and Carlson 1953	$(D_{75}^{1/6})/39$

Then, considering the recent researches (Azarang et al. 2010) and applying the model for steady flow in 1500 $m^3.S^{-1}$ flow and drawing the water level profile along with Ahvaz-Farsiat (according to figure 12), the Manning roughness coefficient was considered 0.03 for the river bed and 0.045 for floodplains.
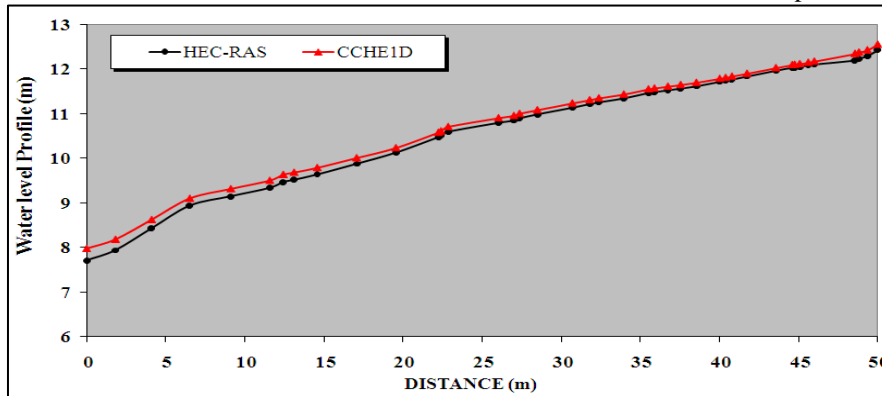
Figure 12: For the hydraulic calibration of Karun River, the water surface profile from HEC-RAS model compared with CCHE1D model

Verification of sediment formula

Having calibrated the model hydraulically, it is needed to evaluate the model for sedimentation calculations. To this, the HEC-RAS model results should be compared with experimental data and the correspondent data with experimental values should be the basis of next calculations. In this work, the cross section geometric figure of Karun River in upstream and downstream stations and the best sediment transport functions were selected to estimate the geometric changes. Figure 13 shows the geometric changes of Ahvaz cross section predicted by selected methods.
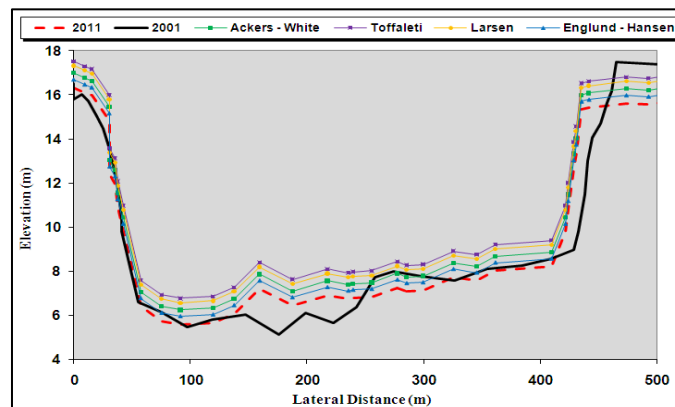
Figure 13: Prediction of cross-section changes of Ahvaz station with different methods

Also, Figure 14 shows the best methods to estimate the geometric changes in Farsiat station.
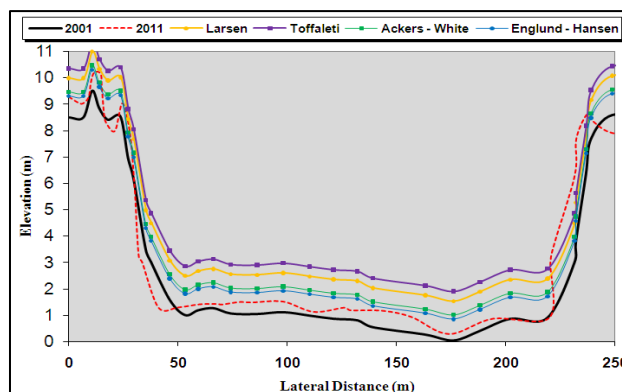
Figure 14: Prediction of cross-section changes of Farsiat station with different methods

As can be seen in Figures 13 and 14 the cross section located in stations have had the highest sedimentation during the simulation period 2001-2011. In other words, the highest bed level increase has been observed based on the HEC-RAS model results using sediment transport functions. Comparing the different methods, it can be seen that the Toffaleti method estimates the highest value of sedimentation and the Larsen methods estimates the second highest value. Also, the Englund–Hansen and Ackers–White are the best methods to estimate the geometric changes of Karun cross section in Ahvaz –Farsiat reach. According to the Figures 13 and 14 the Englund–Hansen, Ackers–White, and Toffaleti have the best estimation of geometric changes in cross section of Karun River, respectively.

Prediction of thalweg changes

The Karun River Thalweg is an important criterion in geometry of the river cross section to define the potential of erosion or sedimentation. The Thalweg is of a great deal of importance in sailing and the stability of coasts. It undergoes changes during the time affected from river phenomena. The Thalweg of Karun was estimated using the sediment transport functions in 48 Km of river from Ahvaz to Farsiat stations. Figure 15 compares the initial Thalweg of Karun River and calculated values by different methods of simulation.
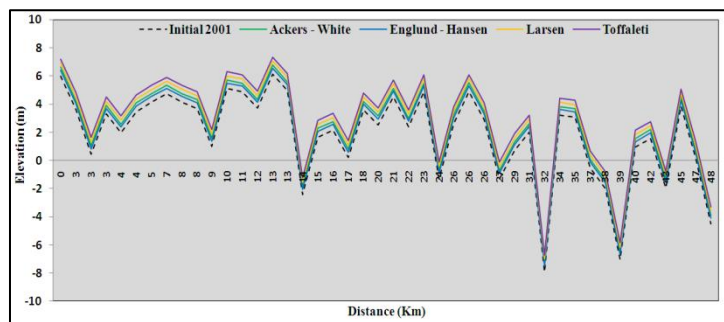
Figure 15: Prediction of thalweg changes of Karun River in the reach of study by different methods

As can be seen in Figure 15 the Toffaleti method has predicted the Karun River Thalweg higher compared to other methods and the Englund –Hansen and Ackers–White stand in next places, respectively. The Thalweg changes estimated by Englund–Hansen and Ackers–White are shown in Figures 16 and 17 as can be seen; the sedimentation has been occurred in most cross sections while the erosion and reduction of Thalweg has been rarely observed.
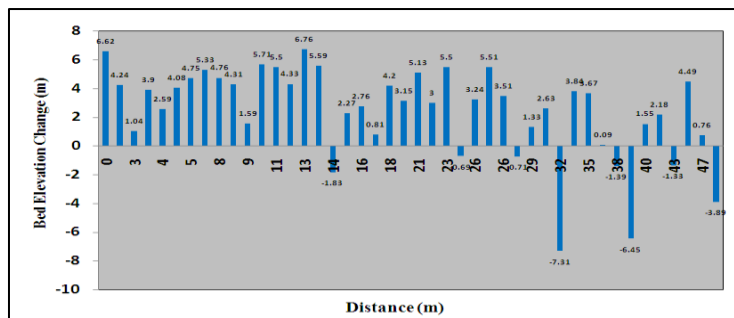
Figure 16: Prediction of thalweg changes of Karun River in the reach of study by Ackers-white method
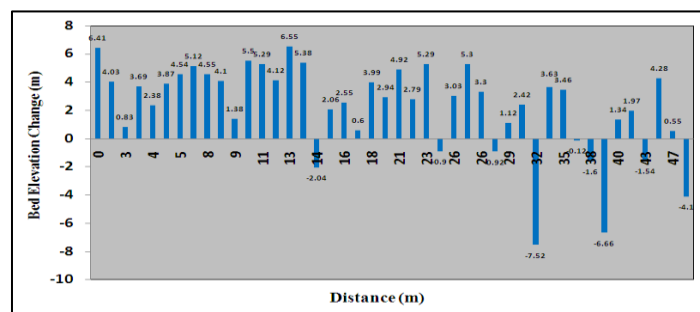
Figure 17: Prediction of thalweg changes of Karun River in the reach of study by Englund-Hansen method

Sediment Total Load

　　　　Base on the hydraulic properties of the river and sedimentation particle size, each river has a specific sedimentation potential. The inlet of sediments higher than the transport capacity results in sedimentation. Contrarily, the sediment amount lower than the transport capacity results in erosion. The total load of the river is the sum of load bed and suspended bed of the river and is one of most important outputs of the Hydraulic part of HEC-RAS model as an important index in river engineering plans. Thus, the sediment total load can play an important role in hydraulic behavior of the river. In Karun River, the bed load of the river has been considered as 10% of the suspended load. Figures 18 and 19 show the estimation of sediment total load of the Karun River in upstream station of Farsiat using the superior sediment transport functions.
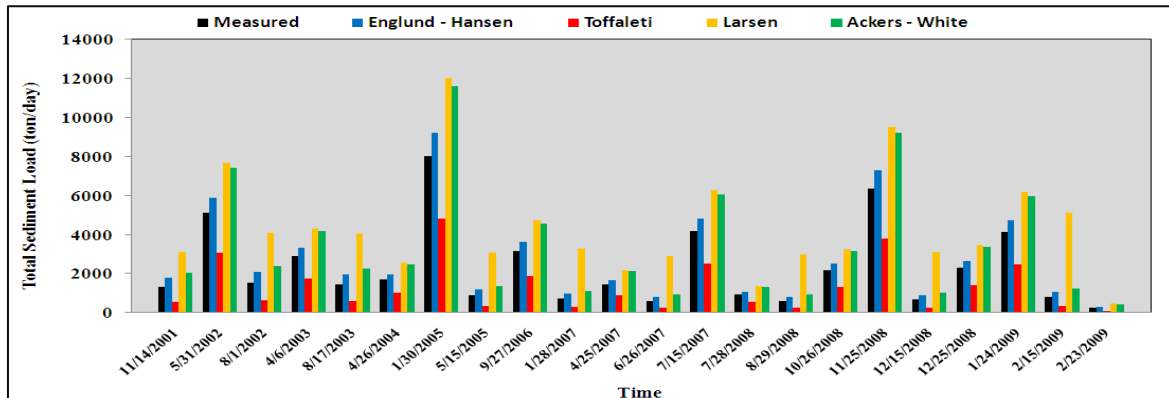
Figure 18: Estimation of total sediment load of Karun River at Farsiat stations with different method
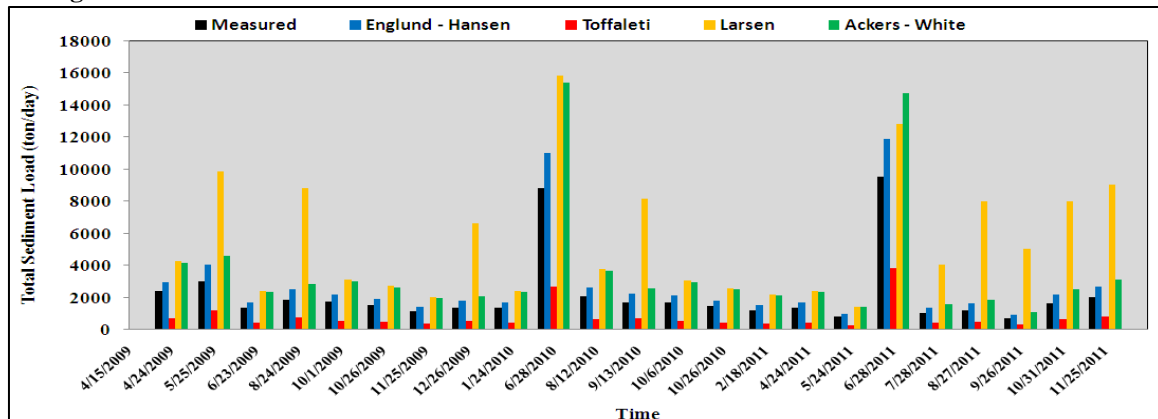
Figure 19: Estimation of total sediment load of Karun River at Farsiat stations with different method

　　　　Since the measurement of sediment load of Karun River has not been continuous in Farsiat station and only performed in special days of year, there are limitations in comparison of calculated results of the model with different models. The Nash-Sutcliffe criterion was used to select the best method to estimate the total sedimentation load of Karun in Farsiat hydrometric station and compare the obtained results with observed data. The Nash-Sutcliffe relationship is as follows:

$$NE = \frac{F^2 - F_1^2}{F^2} \qquad (1)$$
$$F^2 = \sum_{i=1}^{N} (Q_{oi} - \overline{Q_{oi}})^2 \qquad (2)$$
$$F_1^2 = \sum_{i=1}^{N} (Q_{ci} - \overline{Q_{ci}})^2 \qquad (3)$$

Where:

NE = Nash-Sutcliffe coefficient,

Q_{oi} = observed discharges,

Q_{ci} = calculated discharges,

$\overline{Q_{oi}}$ = Mean observed discharges,

$\overline{Q_{ci}}$ = Mean calculated discharges.

This relation considers a range from $-\infty$ to unity in which the coefficients near unity show values of higher accuracy. Table 4 shows the Nash-Sutcliffe criterion values for different methods of total sedimentation load estimation.

Table 4: Nash-Sutcliffe criterion values for total sediment load equations

Sediment Transport Formula	Englund-Hansen	Ackers-White	Larsen	Toffaleti
Nash-Sutcliffe coefficients (NE)	0.74	0.61	0.50	0.39

As can be seen, the Englund – Hansen and Ackers – White, Larsen, and Toffaleti have the most accurate estimation of total sediment load in Karun River in downstream station of farsiat.

Assessment of erosion and sedimentation

Considering the HEC-RAS model results and field observation and measurements concluded that in most of the studied region especially in Ahvaz city river reach, due to the low slope (0.000337) and very low flow speed, numerous hydraulic structures such as bridges, wide-being of river channel and etc. sedimentation occurred at the most regions and the river was mostly braided. Sedimentation and island formations at the Karun River glen especially at the Ahvaz city region made lots of problems such as reduction of capacity of flood flows and decrease of river depth that influenced waterway transportation purposes like sailing and canoeing which needs correction and provision appropriate river width and depth. Figure 20 shows the island formation of Karun River in Ahvaz region.

Figure 20: View of the islands formed by the river sedimentation at the downstream;

a Siah bridge and b Naderi bridge

As it seen in the figure usually sedimentation occurs after the bridges which is for reduction of flow speed and consequently by reducing of flow energy the suspended sediment particles would be deposited and form the islands at the river path. The images **a** and **b** of figure 20 show the islands at the downstream of Siah and Naderi Bridges, respectively.

Dredging and sediment removal are executive solutions to reduce the accumulation of sediments in the river bed and increase of flow depth for appropriate deliver of flood which are necessary for Karun River training in Ahvaz region. Karun River dredging operations in the city of Khorramshahr near the Persian Gulf is already done. Images illustrate the views of the impact of the operations and training of the Karun River in the city of Khorramshahr.
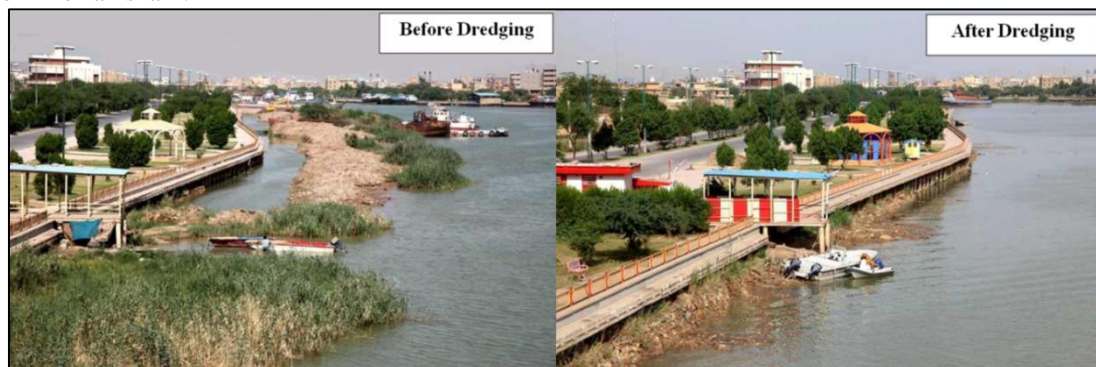
Figure 21: Dredging operations of Karun River in the Khorramshahr city

Figure 22: The impact of dredging operations in order to Karun River training

in the Khorramshahr city

Moreover, erosion occurred at the banks and walls of the river at various cross sections that an example of stepped erosion of Karun River in the southern of Ahvaz has shown (Fig. 23).
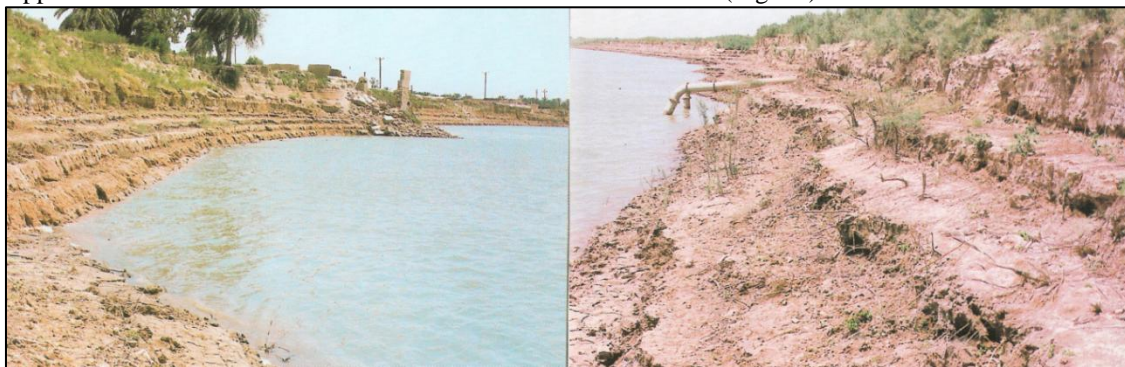
Figure 23: The erosion of the Karun River banks in the southern of Ahvaz

To prevent the erosion, stabilization of river banks procedures should be applied which included the operations for making the eroding river walls stable. Natural ways to protect river margins are vegetation, stone-fill revetment, gabion revetment, precast concrete blocks, pile driving and plate driving, bankhead and etc. which are the conventional methods of glen modification and erosion control of the river side which recommended utilizing for Karun River.

IV. CONCLUSIONS

Karun River is one of most critical rivers in Iran and the studied river reach of this work is Ahvaz-Farsiat is of a considerable importance since it passes through the Ahvaz as the capital of Khuzestan province. Karun River is classified as an old and braided river having suspended load. Karun River has a considerable suspended load regarding its long pathway and passing through miscellaneous geological formations resulting in a high concentration of river which leads to more erosion of bed and river walls and increase the sediment load of the river. In the present work, the HEC-RAS model was used to simulate the sedimentation condition of the Karun River. First of all, the model was calibrated for hydraulic conditions of the river and the Manning roughness coefficients of 0.03 and 0.045 were considered for bed and flood plains of Karun River, respectively. Then, the geometric cross section changes of, prediction of Thalweg profile variations, and estimation of total sediment load were performed using the sediment transport functions. The HEC-RAS results indicate that the Karun River has majorly experienced sedimentation and the bed level increase has been widely observed during the simulation period from 2001-2011. Also, the total sediment transport functions of Englund – Hansen and Ackers – White functions give results of higher accuracy compared to other methods. For the purpose of Karun River training at the reach of study and due to the results of HEC-RAS model, river bed dredging at the regions with sedimentation and stabilization of banks which are erodible are highly suggested. It noteworthy that the sediment transport functions of this work have been proposed as more appropriate functions not necessarily meaning that they give results of higher accuracy in other case studies since each sediment transport function is based on specific geometric, hydraulic, and sedimentation and are not able to be generalized to different conditions of other case studies. Thus, the geometric, hydraulic, and sedimentation conditions of each sediment transport functions and also the river reach of study are of critical importance in optimized application of these methods.

REFERENCES

[1] Bhattacharya B, Price RK, Solomatine DP, A data mining approach to modelling sediment transport, *6th International Conference on Hydroinformatics – Liong, Phoon & Babovic*, World Scientific Publishing Company, 2014.

[2] Bhattacharya B, Price RK, Solomatine DP, Data-driven modelling in the context of sediment transport, *Physics and Chemistry of the Earth, 30(4-5),* 2005,297-302.

[3] Merritt WS, Letcher RA, Jakeman AJ, A review of erosion and sediment transport models, *Environmental Modelling and Software, 18(8-9),* 2003, 761-799.

[4] Einsten HA, The bed load function for sediment transportation in open channel flows, *Thechnical Bulletin, No.1026, USDA, Soil Conservation Service*, Washington D.C, 1950.

[5] Bagnold RA, An approach to the sediment transport problem from general physics, *U.S. Geological Survey Professional Paper 422-J*, United States Government Printing Office, Washington, 1966.

[6] Van Rijn LC, Principles of sediment transport in rivers, estuaries and coastal seas, Aqua Publisher, Amsterdam, Netherlands, 1993.

[7] Morales de Luma T, Castro Diaz MJ, Pares Madronal C, A Duality method for sediment transport based on a modified Mayer-Peter & Muller model, *Journal of Scientific Computing, 48(1-3),* 2011, 258-273.

[8] Azarang F, Telvari A, Sedghi H, and Shafai Bajestan M, Numerical Simulation of Flow and Sediment Transport of Karkheh River before the Reservoir Dam Construction Using MIKE 11 (A Case Study in Iran), *Advances in Environmental Biology Journal*, *8(21),* 2014, 979-988.

[9] Rathburn SL, Rubin ZK, and Wohl EE, Evaluating channel response to an extreme sedimentation event in the context of historical range of variability: Upper Colorado River, Rocky Mountain National Park, Colorado, *Earth Surface Processes and Landforms, 38(4),* 2013, 391-406.

[10] Canfield HE, Wilson CJ, Lane LJ, Crowell KJ, Thomas WA, Modeling scour and deposition in ephemeral channels after wildfire, *CATENA journal, 61(2-3),* 2005, 273-291.

[11] Gibson S, Brunner G, Piper S, Jensin M, Sediment transport computations with HEC-RAS, *Proceedings of the Eighth Federal Interagency Sedimentation Conference (8thFISC)*, April 2-6, Reno, NV, USA JFIC, 2006.

[12] Brunner GW, HEC-RAS 4.1 River Analysis System, Haydraulic Reference Manual (Version 4.1), US Army Corps of Engineers, 2010.

[13] Brunner GW, HEC-RAS 4.1 River Analysis System, Haydraulic Users Manual (Version 4.1), US Army Corps of Engineers, 2010.

Research Paper	Open Access

Epq model for deteriorating items under three parameter weibull distribution and time dependent ihc with shortages

Kirtan Parmar[1], U. B. Gothi[2]

[1]Dept. of Statistics, St. Xavier's College (Autonomous), Ahmedabad, Gujarat, India.
[2]Dept. of Statistics, St. Xavier's College (Autonomous), Ahmedabad, Gujarat, India.

ABSTRACT:- *In this paper, we have analysed a production inventory model for deteriorating items with time-dependent holding cost. Three parameter Weibull distribution is assumed for time to deterioration of items. Shortages are allowed to occur. The derived model is illustrated by a numerical example and its sensitivity analysis is carried out.*

KEYWORDS: - *Deterioration, Production, Shortages, Three parameter Weibull distribution, Time dependent holding cost*

I.   INTRODUCTION

Deterioration is the damage caused due to spoilage, dryness, etc. Deterioration of an item is a realistic situation associated with an inventory system. The decrease or loss of utility due to decay is usually a function of the on-hand inventory. For items such as steel, hardware, glassware and toys, the rate of deterioration is so low that there is little need for considering deterioration in the determination of the economic lot size. But some items such as blood, fish, strawberry, alcohol, gasoline, radioactive chemical, medicine and food grains (i.e., paddy, wheat, potato, onion etc.) have remarkable deterioration overtime. It has been observed that the failure of many such items can be expressed by Weibull distribution.

Manna and Chiang [1] developed an EPQ model for deteriorating items with ramp type demand. Teng and Chang [2] considered the economic production quantity model for deteriorating items with stock level and selling price dependent demand. Jain et al. [3] developed an economic production quantity model with shortages by incorporating the deterioration effect and stock dependent demand rate. Roy and Chaudhary [4] developed two production rates inventory model for deteriorating items when the demand rate was assumed to be stock dependent. In the research of Sana et al. [5] shortages are allowed to occur at the end of a cycle. With the consideration of time varying demand and constant deteriorating rate, the optimal production inventory policy was studied. Raman Patel [6] developed a production inventory model for Weibull deteriorating items with price and quantity dependent demand and varying holding cost with shortages.

Both Skouri and Papachristos [7] and Chen et al. [8] developed a production inventory model in which the shortages are allowed at the beginning of a cycle. In contrast, in Manna and Chaudhari [9] shortages are allowed but occur at the end of each cycle. Goyal's [10] production inventory problem of a product with time varying demand, production and deterioration rates in which the shortages occur at the beginning of the cycle.

Kirtan Parmar and U. B. Gothi [11] have developed an order level inventory model for deteriorating items under quadratic demand with time dependent IHC. Authors also [12] have developed a deterministic inventory model by taking two parameter Weibull distribution to represent the distribution of time to deterioration where shortages are allowed with partial backlogging. Authors also [13] have developed an EPQ model of deteriorating items using three parameter Weibull distribution with constant production rate and time varying holding cost. Authors [14] also have developed an inventory model of deteriorating items using two parameter Weibull distribution with linear time dependent demand and IHC.

The rate of deterioration-time relationship for the three-parameter Weibull distribution is shown in Figure – 1. The figure shows that the three-parameter Weibull distribution is most suitable for items with any initial value of the rate of deterioration and for items, which start deteriorating only after a certain period of time (Begum at el. [15]). The probability density function for three parameter Weibull distribution is given by

$$f(t) = \alpha \beta (t - \mu)^{\beta - 1} e^{-\alpha(t-\mu)^{\beta}} \quad ; t \geq \mu \ (0 < \alpha < 1 \text{ and } \beta, \mu > 0)$$

The instantaneous rate of deterioration $\theta(t)$ (i.e. for hazzard rate) of the non-deteriorated inventory at time t, can be obtained from $\theta(t) = \dfrac{f(t)}{1 - F(t)}$, where $F(t) = 1 - e^{-\alpha(t-\mu)^{\beta-1}}$ is the cumulative distribution function (c.d.f.) for the three parameter Weibull distribution. Thus, the instantaneous rate of deterioration of the on-hand inventory is $\theta(t) = \alpha \beta (t - \mu)^{\beta - 1}$.
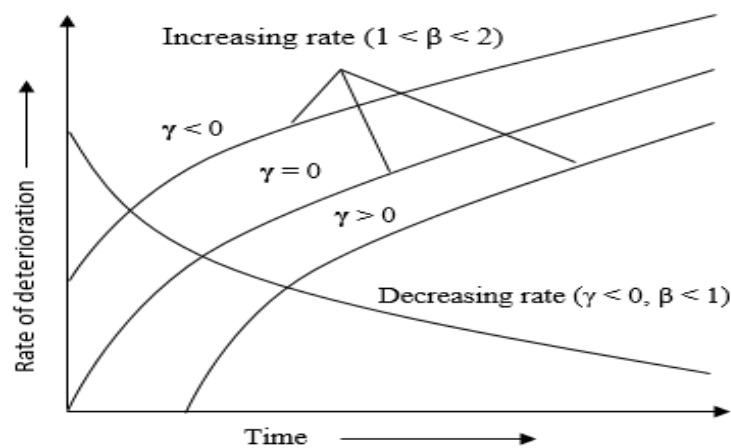
Figure - 1: Hazzard rate relationship for 3 parameter Weibull distribution

II.   NOTATIONS

We use the following notations for the mathematical model
1. $Q(t)$: Inventory level of the product at time t (≥ 0).
2. R   : Demand rate.
3. $\theta(t)$: Rate of deterioration per unit time.
4. A   : Ordering cost per order during the cycle period.
5. p   : Selling price per unit.
6. k   : Rate of production per unit time.
7. Q_1 : The maximum inventory level at time $t = \mu$.
8. Q_2 : The maximum inventory level during shortage period.
9. C_h : Inventory holding cost per unit per unit time.
10. C_d : Deterioration cost per unit per unit time.
11. T   : Duration of a cycle.
12. TC   : Total cost per unit time.

III.   ASSUMPTIONS

1. The demand rate of the product is a linear function of price and quantity which is
   $R = R(p, Q(t)) = [a - p + \rho Q(t)]$ (where a , p, $\rho > 0$).
2. As soon as a unit is produced it is available for to meet with demand.
3. As soon as the production is terminated the product starts with deterioration.
4. Holding cost is a linear function of time and it is $C_h = h + rt$ (h, r > 0)
5. Replenishment rate is infinite and instantaneous.
6. Shortages occur and they are completely backlogged.
7. Repair or replacement of the deteriorated items does not take place during a given cycle.
8. The second and higher powers of ρ and α are neglected in the analysis of the model.

IV. MATHEMATICAL MODEL AND ANALYSIS

Here, we consider a single commodity deterministic production inventory model with a time dependent demand rate $R(p, Q(t)) = [a - p + \rho\, Q(t)]$. Initial, inventory level is zero. At time t = 0, the production starts and simultaneously supply also starts. The production stops at t = μ when the maximum inventory level Q_1 is reached. In the interval [0, μ] the inventory is built up at a rate k − R and there is no deterioration in this interval. In the interval [μ, t_2] deterioration starts and the inventory depleted at the rate R. The inventory is finitely decreasing in the time interval [μ, t_2] until inventory level reaches zero. It is decided to backlog the demands up to Q_2 level which occur during stock-out time. Thereafter, shortages can occur during the time interval [t_2, t_3], and all of the demand during the period [t_2, t_3] is completely backlogged. Thereafter, Production is started at the rate k − (a − p) so as to clear the backlog, and the inventory level reaches to 0 (i.e. the backlog is cleared).

The pictorial presentation is shown in the Figure – 2.
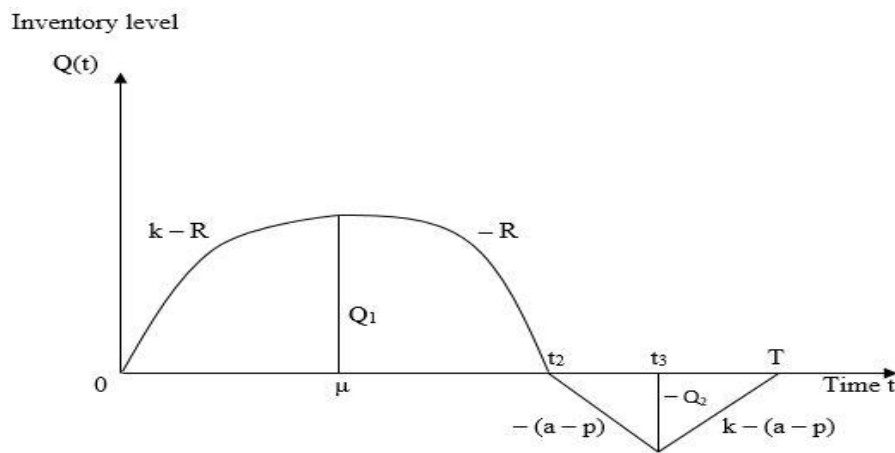
Figure - 2: Graphical presentation of the inventory system

The differential equations which describe the instantaneous state of Q(t) over the period (0, T) are given by

$$\frac{dQ(t)}{dt} = k - \left[a - p + \rho\, Q(t)\right], \qquad (0 \le t \le \mu) \tag{1}$$

$$\frac{dQ(t)}{dt} + \alpha\beta\,(t - \mu)^{\beta - 1}\, Q(t) = -\left[a - p + \rho\, Q(t)\right], \qquad (\mu \le t \le t_2) \tag{2}$$

$$\frac{dQ(t)}{dt} = -\,(a - p), \qquad (t_2 \le t \le t_3) \tag{3}$$

$$\frac{dQ(t)}{dt} = k - \,(a - p), \qquad (t_3 \le t \le T) \tag{4}$$

Under the boundary conditions Q(0) = 0, Q(μ) = Q_1, Q(t_2) = 0, Q(t_3) = − Q_2 and Q(T) = 0 solutions of equations (1) to (4) are given by

$$Q(t) = \left(k - a + p\right)\left(t - \frac{\rho t^2}{2}\right), \qquad (0 \le t \le \mu) \tag{5}$$

$$Q(t) = \left[1 - \rho\,(t - \mu) - \alpha\,(t - \mu)^{\beta}\right]Q_1 + (a - p)\left[(\mu - t)(1 - \rho t) + \frac{\rho}{2}\left(\mu^2 - t^2\right) + \frac{\alpha\beta}{\beta + 1}(t - \mu)^{\beta + 1}\right], \quad (\mu \le t \le t_2) \tag{6}$$

$$Q(t) = (a - p)(t_2 - t), \qquad (t_2 \le t \le t_3) \tag{7}$$

$$Q(t) = (k - a + p)(t - T), \qquad (t_3 \le t \le T) \tag{8}$$

Putting $Q(t_2) = 0$ in equation (6), we get

$$Q_1 = \frac{(p - a)\left[(\mu - t_2)(1 - \rho t_2) + \dfrac{\rho}{2}(\mu^2 - t_2^2) + \dfrac{\alpha \beta}{\beta + 1}(t_2 - \mu)^{\beta + 1}\right]}{1 - \rho(t_2 - \mu) - \alpha(t_2 - \mu)^{\beta}} \tag{9}$$

Taking $Q(t_3) = -Q_2$ in equation (7), we get

$$Q_2 = (a - p)(t_3 - t_2) \tag{10}$$

Equation (7) and (8) coincide at $t = t_3$ hence

$$(a - p)(t_2 - t_3) = (k - a + p)(t_3 - T)$$

$$\Rightarrow T = \frac{k t_3 - (a - p) t_2}{k - a + p} \tag{11}$$

The total cost comprises of the following costs

1) The ordering cost
   $$OC = A \tag{12}$$

2) The deterioration cost during the period $[\mu, t_2]$

$$DC = C_d \left\{ Q_1 - \int_{\mu}^{t_2} [a - p + \rho Q(t)] \, dt \right\}$$

$$\Rightarrow DC = C_d \left\{ Q_1 - \left[(a - p)(1 + \rho \mu) + \rho Q_1\right](t_2 - \mu) + \frac{\rho(a - p)\left(t_2^2 - \mu^2\right)}{2} \right\} \tag{13}$$

3) The inventory holding cost during the period $[0, t_2]$

$$IHC = \int_{0}^{\mu} (h + rt) Q(t) \, dt + \int_{\mu}^{t_2} (h + rt) Q(t) \, dt$$

$$= \int_{0}^{\mu} (h + rt)(k - a + p)\left(t - \frac{\rho t^2}{2}\right) dt + \int_{\mu}^{t_2} (h + rt) \left\{ \begin{array}{l} \left[1 - \rho(t - \mu) - \alpha(t - \mu)^{\beta}\right] Q_1 \\ + (a - p)\left[(\mu - t)(1 - \rho t) + \dfrac{\rho}{2}(\mu^2 - t^2) + \dfrac{\alpha \beta}{\beta + 1}(t - \mu)^{\beta + 1}\right] \end{array} \right\} dt$$

$$\Rightarrow IHC = (k - a + p)\left[\frac{h\mu^2}{2} + \left(r - \frac{h\rho}{2}\right)\frac{\mu^3}{3} - \frac{r\rho\mu^4}{8}\right] + \left\{ (h + r\mu)\left\{ \left[\left[(t_2 - \mu) - \frac{\rho}{2}(t_2 - \mu)^2 - \frac{\alpha(t_2 - \mu)^{\beta+1}}{\beta+1}\right]Q_1 + (a - p)\left[\frac{\rho}{6}(t_2 - \mu)^3 - \frac{(t_2 - \mu)^2}{2} + \frac{\alpha\beta(t_2 - \mu)^{\beta+2}}{(\beta+1)(\beta+2)}\right]\right] \right\} + r\left\{ \left[\frac{(t_2 - \mu)^2}{2} - \frac{\rho(t_2 - \mu)^3}{3} - \frac{\alpha(t_2 - \mu)^{\beta+2}}{\beta+2}\right]Q_1 + (a - p)\left[\frac{\rho(t_2 - \mu)^4}{8} - \frac{(t_2 - \mu)^3}{3} + \frac{\alpha\beta(t_2 - \mu)^{\beta+3}}{(\beta+1)(\beta+3)}\right] \right\} \right\}$$

(14)

4) The shortage cost per cycle

$$SC = -C_s\left[\int_{t_2}^{t_3} Q(t)dt + \int_{t_3}^{T} Q(t)dt\right]$$

$$\Rightarrow SC = C_s\left[\frac{(a - p)(t_2 - t_3)^2}{2} + \frac{(k - a + p)(t_3 - T)^2}{2}\right]$$

(15)

Hence the total cost per unit time is given by

$$TC = \frac{1}{T}(OC + IHC + DC + SC)$$

$$TC = \frac{1}{\left[\frac{kt_3 - (a-p)t_2}{k - a + p}\right]}\left\{ A + (k - a + p)\left[\frac{h\mu^2}{2} + \left(r - \frac{h\rho}{2}\right)\frac{\mu^3}{3} - \frac{r\rho\mu^4}{8}\right] + \left\{ (h + r\mu)\left\{ \left[\left[(t_2 - \mu) - \frac{\rho}{2}(t_2 - \mu)^2 - \frac{\alpha(t_2 - \mu)^{\beta+1}}{\beta+1}\right]Q_1 + (a - p)\left[\frac{\rho}{6}(t_2 - \mu)^3 - \frac{(t_2 - \mu)^2}{2} + \frac{\alpha\beta(t_2 - \mu)^{\beta+2}}{(\beta+1)(\beta+2)}\right]\right] \right\} + r\left\{ \left[\frac{(t_2 - \mu)^2}{2} - \frac{\rho(t_2 - \mu)^3}{3} - \frac{\alpha(t_2 - \mu)^{\beta+2}}{\beta+2}\right]Q_1 + (a - p)\left[\frac{\rho(t_2 - \mu)^4}{8} - \frac{(t_2 - \mu)^3}{3} + \frac{\alpha\beta(t_2 - \mu)^{\beta+3}}{(\beta+1)(\beta+3)}\right] \right\} \right\} + C_d\left\{ Q_1 - \left[(a - p)(1 + \rho\mu) + \rho Q_1\right](t_2 - \mu) + \frac{\rho(a - p)(t_2^2 - \mu^2)}{2}\right\} + C_s\left[\frac{(a - p)(t_2 - t_3)^2}{2} + \frac{(k - a + p)(t_3 - T)^2}{2}\right] \right\}$$

(16)

μ^*, t_2^* and t_3^* are the optimum values of μ, t_2 and t_3 respectively, which minimize the cost function TC and they are the solutions of the equations $\frac{\partial TC}{\partial \mu} = 0$, $\frac{\partial TC}{\partial t_2} = 0$, $\frac{\partial TC}{\partial t_3} = 0$, satisfying the sufficient condition $H > 0$, at μ^*, t_2^* and t_3^* where

$$H = \begin{vmatrix} \dfrac{\partial^2 TC}{\partial \mu^2} & \dfrac{\partial^2 TC}{\partial \mu \partial t_2} & \dfrac{\partial^2 TC}{\partial \mu \partial t_3} \\[2ex] & \dfrac{\partial^2 TC}{\partial t_2^2} & \dfrac{\partial^2 TC}{\partial t_2 \partial t_3} \\[2ex] & & \dfrac{\partial^2 TC}{\partial t_3^2} \end{vmatrix} \text{ is Hessian determinant.} \tag{17}$$

V.   NUMERICAL EXAMPLE

Let us consider the following example to illustrate the above developed model, taking A = 200, α = 0.05, β = 2, ρ = 0.04, a = 100, p = 0.05, k = 300, Cs = 8, h = 5, r = 0.05 and C_d = 25 (with appropriate units).

The optimal values of μ, t_2 and t_3 are μ* = 0.2922609055, t_2* = 0.7971385166, t_3* = 1.162469779 units and the optimal total cost per unit time TC = 292.1188781 units.

VI.   SENSITIVITY ANALYSIS

Sensitivity analysis depicts the extent to which the optimal solution of the model is affected by the changes in its input parameter values. Here, we study the sensitivity for the cycle length T and total cost per time unit TC with respect to the changes in the values of the parameters A, α, β, ρ, a, p, k, Cs, h, r and C_d.

The sensitivity analysis is performed by considering variation in each one of the above parameters keeping all other remaining parameters as fixed. The last column of the **Table – 1** gives the % changes in TC as compared to the original solution for the relevant costs.

Table – 1: Partial Sensitivity Analysis

Parameter	Values	μ	t_2	t_3	TC	% changes in TC
A	160	0.26086836	0.71820154	1.04433609	260.777187	−10.73
	180	0.27698628	0.75890706	1.10516826	276.870453	− 5.22
	220	0.30681595	0.83326276	1.21676237	306.646292	4.97
	240	0.32074754	0.86756457	1.26845115	320.548910	9.73
α	0.04	0.29132373	0.80636505	1.17056312	291.212773	− 0.31
	0.06	0.29315442	0.78854655	1.15495940	292.983715	0.30
	0.07	0.29400802	0.78051774	1.14796489	293.810738	0.58
	0.08	0.29482499	0.77299146	1.14142941	294.602984	0.85
β	1.7	0.29381028	0.78922481	1.15645351	293.636073	0.52
	2.2	0.29145691	0.80188926	1.16623813	291.333361	− 0.27
	2.4	0.29079177	0.80625594	1.16979361	290.684723	− 0.49
	2.7	0.28999578	0.81214901	1.17471824	289.910361	− 0.76
ρ	0.030	0.29176671	0.79774869	1.16300147	292.056120	− 0.02
	0.035	0.29201336	0.79744468	1.16273660	292.087416	− 0.01
	0.044	0.29245960	0.79689204	1.16225493	292.144166	0.01
	0.048	0.29265887	0.79664422	1.16203886	292.169558	0.02
a	110	0.31389982	0.78652619	1.12527284	297.961556	2.00
	120	0.33629005	0.77961771	1.09466062	302.867847	3.68
	130	0.35965081	0.77605652	1.06968258	305.253654	4.50
	140	0.38422542	0.77564139	1.04969128	306.826258	5.03
p	0.040	0.29228224	0.79712589	1.16242888	292.125497	0.002
	0.045	0.29253072	0.79713220	1.16244933	292.122188	0.001
	0.055	0.29225024	0.79714483	1.16249024	292.115569	− 0.001
	0.060	0.29223957	0.79715115	1.16251069	292.112258	− 0.002

Parameter	Values	μ	t_2	t_3	TC	% changes in TC
k	240	0.38956686	0.86409821	1.20463323	272.291802	− 6.79
	270	0.33376102	0.82541901	1.17989319	283.437558	− 2.97
	330	0.26011077	0.77551601	1.14955528	299.081800	2.38
	360	0.23443121	0.75842588	1.13961106	304.795673	4.34
Cs	6.4	0.27842610	0.76252505	1.19759872	278.307925	− 4.73
	7.2	0.28585872	0.78115463	1.17819763	285.728022	− 2.19
	8.8	0.29783754	0.81101420	1.14946209	297.685233	1.91
	9.6	0.30274153	0.82318024	1.13852528	302.579872	3.58
h	4.0	0.34291138	0.90648539	1.24976742	274.488318	− 6.04
	4.4	0.32041369	0.85911048	1.21176409	281.981824	− 3.47
	4.6	0.31036926	0.83734779	1.19439906	285.498196	− 2.27
	4.8	0.30100918	0.81672156	1.17799505	288.874283	− 1.11
r	0.040	0.29250414	0.79771582	1.16297647	292.062414	− 0.02
	0.045	0.29238242	0.79742695	1.16272292	292.090659	− 0.01
	0.055	0.29213959	0.79685053	1.16221705	292.147071	0.01
	0.060	0.29201847	0.79656299	1.16196474	292.175239	0.02
C_d	24.0	0.29209044	0.79873637	1.16386135	291.953929	− 0.06
	24.5	0.29217588	0.79793452	1.16316289	292.036604	− 0.03
	26.0	0.29242970	0.79556377	1.16109933	292.282240	0.06
	27.0	0.29259685	0.79401151	1.15974944	292.444046	0.11

VII.   GRAPHICAL PRESENTATION
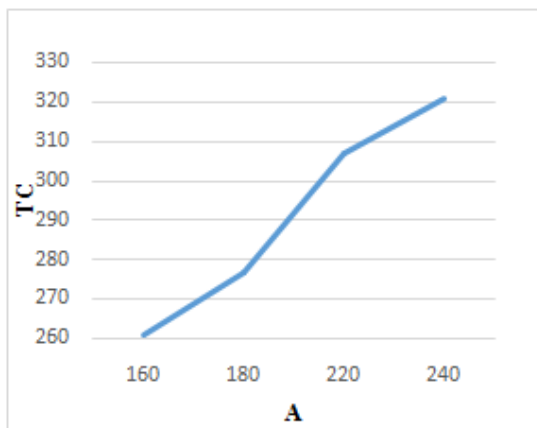
Figure – 3
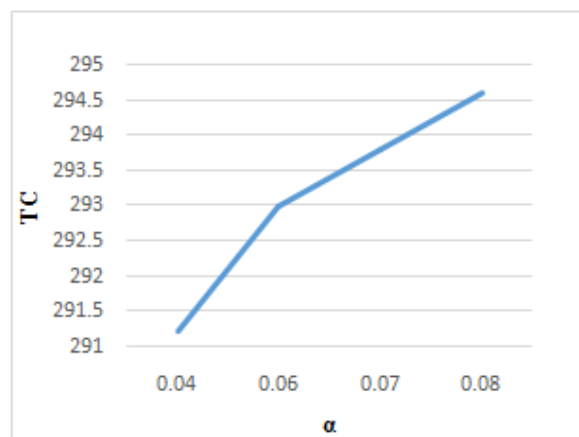
Figure – 4
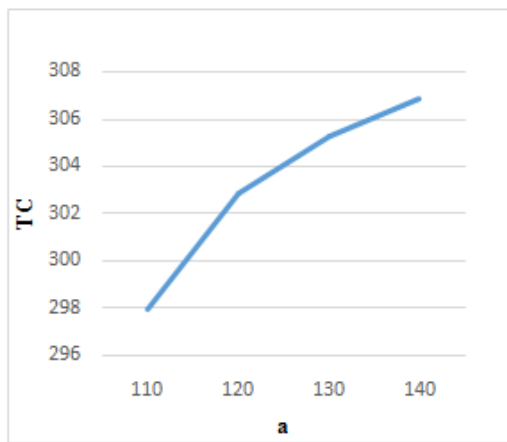
Figure – 5
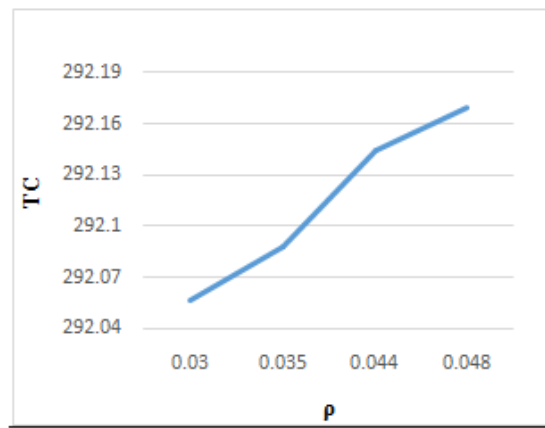
Figure – 6
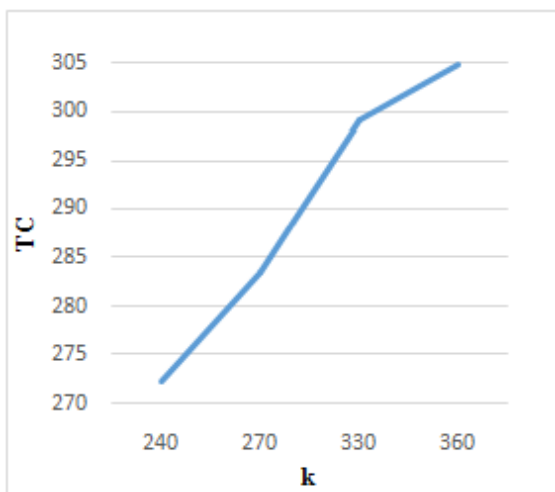
Figure – 7
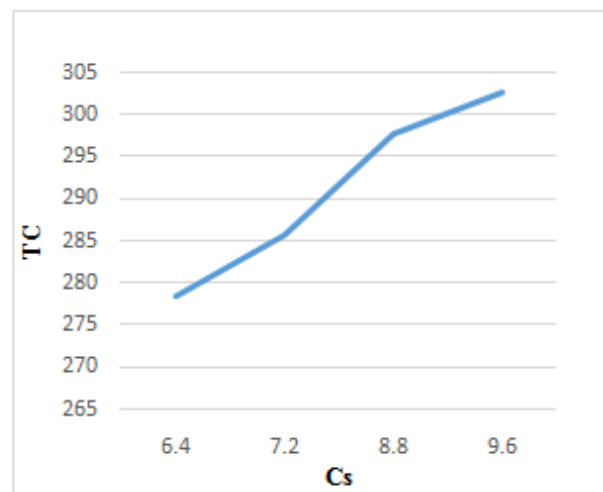
Figure – 8
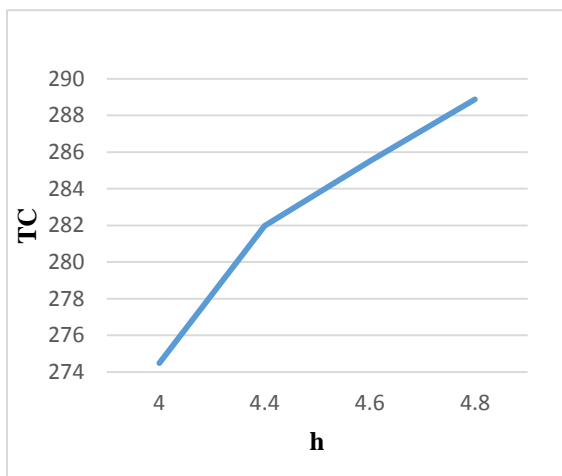
Figure – 9
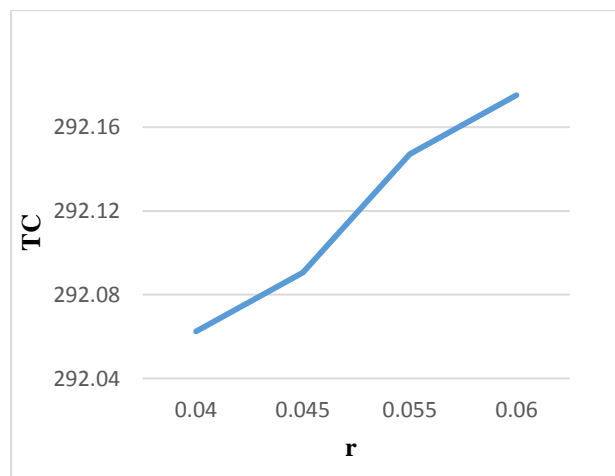
Figure – 10
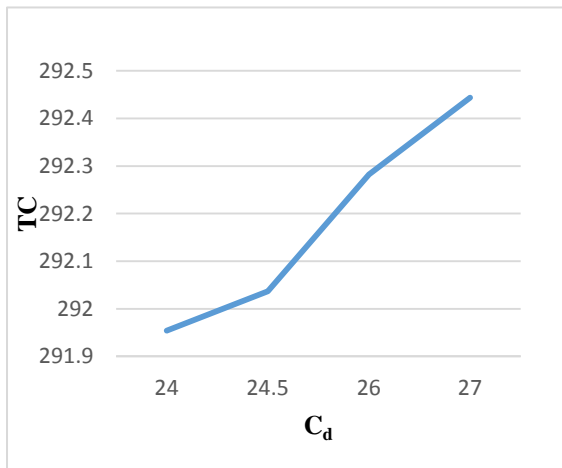
Figure – 11
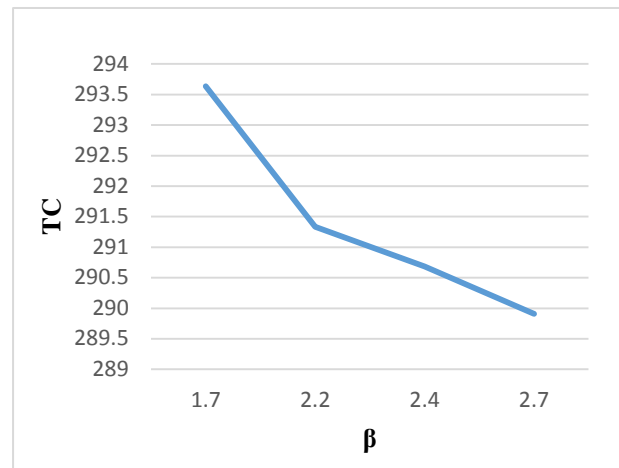
Figure – 12
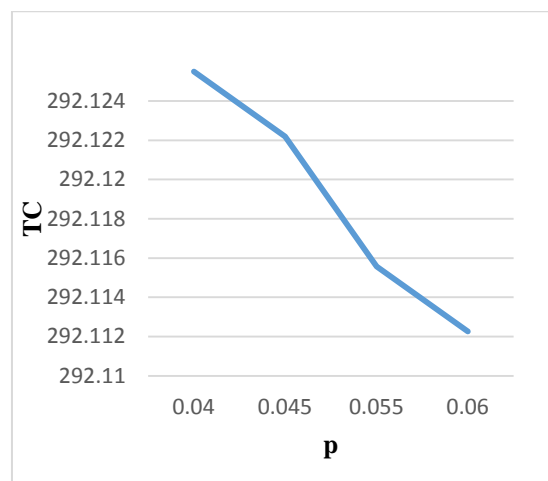
Figure – 13

VIII.   CONCLUSIONS

➢ It is observed from **Figure No – 3 to 11** that when the values of parameters A, α, a, ρ, k, h, r, Cs, C_d increase the average total cost (TC) also increases.

➢ It is observed from **Figure No – 12 to 13** that when the values of parameters β and p increase then the average total cost (TC) has reverse effect.

➢ It is observed from **Figure No – 3, 5, 7, 8, 9** that the total cost per time unit (TC) is highly sensitive to changes in the values of A, a, k, Cs, h.

➢ From **Figure No – 4, 12** that the total cost per time unit (TC) is moderately sensitive to changes in the values of α, β.

➢ From **Figure No – 6, 10, 11, 13** that the total cost per time unit (TC) less sensitive to changes in the values of ρ, r, C_d, p.

IX.   ACKNOWLEDGEMENT

REFERENCES

[1]   Manna, S. K. and Chiang, C., *Economic production quantity models for deteriorating item with ramp type demand", International Journal Operation Research, Vol. 7,* 2010, pp. 429 - 444.

[2]   Teng, J.T. and Chang, H.T., *Economic production quantity model for deteriorating items with price and stock dependent demand; Computers and Oper. Res., Vol. 32,* 2005, pp. 279-308.

[3]   Jain, M. and Sharma, G. C., Rathore, S., *Economic order quantity model with shortages and stock dependent demand for deteriorating items, IJE Transactions A: Basics, Vol. 20(2), 2007,* pp. 159-168.

[4]   Roy, T. and Chaudhary, K. S., *A production inventory model under stock dependent demand, Weibull distribution deterioration and shortages, International Transactions in Operations Research, Vol. 16,* 2009, pp. 325-346.

[5]   S. Sana, S. K. Goyal, and K. S. Chaudhuri, *A production - inventory model for a deteriorating item with trended demand and shortages, European Journal of Operational Research, Vol. 157,* 2004, pp. 357–371.

[6]   Raman Patel, *Production inventory model for Weibull deteriorating items with price and quantity dependent demand, time varying holding cost and shortages, Indian Journal of Applied Research, Vol. 4, Issue 1,* 2014.

[7]   K. Skouri, and S. Papachristos, *Optimal stopping and restarting production times for an EOQ model with deteriorating items and time-dependent partial backlogging," International Journal of Production Economics, Vol. 81–82,* 2003, pp. 525–531.

[8]   Chen S. J., Chen S. P., and Liu X. B., *A production inventory model for deteriorating items, Journal of Zhaoqing University, Vol. 23, No. 2,* 2002, pp. 66–68.

[9]   Manna and Chaudhuri, *An EOQ model with ramp type demand rate, time dependent deterioration rate, Unit production cost and shortages, European Journal of Operational Research, Vol.171,* 2006, pp. 557–566.

[10]   Goyal and Giri, *The production-inventory problem of a product with time varying demand, production and deterioration rates, European Journal of Operational Research, Vol. 147,* 2003, pp. 549–557.

[11]   Kirtan Parmar and Gothi U. B., *Order level inventory model for deteriorating items under quadratic demand with time dependent IHC, Sankhaya Vignan, NSV 10, No. 2,* 2014, pp. 1 – 12.

[12]   Gothi U. B. and Kirtan Parmar, *Order level lot size inventory model for Deteriorating items under quadratic demand with time dependent IHC and partial backlogging, Research Hub – International Multidisciplinary Research   Journal (RHIMRJ), Vol 2, Issue 2,* 2015.

[13]   Kirtan Parmar and Gothi U. B., *An EPQ model   of deteriorating items using three parameter Weibull distribution with constant production rate and time varying holding cost, International Journal of Science, Engineering and Technology Research, Vol. 4, Issue 2,* 2015, pp. 0409 – 416.

[14]   Kirtan Parmar, Indu Aggarwal and Gothi U. B., *Order level inventory model for deteriorating items under varying demand condition", Sankhaya Vignan, NSV 1, No. 1,* 2015

[15]   Begum, Sahoo, Sahu and Mishra, *An EOQ model for varying items with Weibull distribution deterioration and price dependent demand, Journal of Scientific Research, 2(1),* 2010, pp. 24 – 36.

Research Paper   Open Access

DataMining with Grid Computing Concepts

Mohammad Ashfaq Hussain [1], Mohammad Naser [1], AhmedUnnisa Begum [1],
Naseema Shaik [2], Mubeena Shaik [1]

[1] Jazan University, Jazan, Kingdom of Saudi Arabia
[2] King Khalid University, Kingdom of Saudi Arabia

ABSTRACT: *Now days the organizations often use data from several resources. Data is characterized to be heterogeneous, unstructured and usually involves a huge amount of records. This implies that data must be transformed in a set of clusters, parts, rules or different kind of formulae, which helps to understand the exact information. The participation of several organizations in this process makes the assimilation of data more difficult. Data mining is a widely used approach for the transformation of data to useful patterns, aiding the comprehensive knowledge of the concrete domain information. Nevertheless, traditional data mining techniques find difficulties in their application on current scenarios, due to the complexity previously mentioned. Data Mining Grid tries to fix these problems, allowing data mining process to be deployed in a grid environment, in which data and services resources are geographically distributed belong to several virtual organizations and the security can be flexibly solved. We propose both a novel architecture for Data Mining Grid, named DMG.*

KEYWORDS: *clusters, parts, rules, formulae, grid environment, Data Mining Grid.*

I.   INTRODUCTION

DataMining refers to the process of extracting useful, handy and survivable knowledge from data. The extracted knowledge useful in many areas such as business applications like financial business analysis, purchasing behavior scenarios and also in biology, molecular design, weather forecast, climate prediction, physics, fluid dynamics and so on. Now the challenge in these applications is to mine data located in distributed, heterogeneous databases while adhering to varying security and privacy constraints imposed on the local data sources.

The term grid can be defined as a set of computational resources interconnected through a WAN, aimed at performing highly demanding computational tasks such as internet applications. A grid makes it possible to securely and reliably take advantage of widely dispersed computational resources across several organizations and administrative domains. The aim of grid computing is to provide an affordable approach to large-scale computing problems.

Grid technology provides high availability of resources and services, making it possible to deal with new and more complex problems. But it is also known that a grid is a very heterogeneous and decentralized environment [8]. It presents different kinds of security policy, system administration procedure, data and computing characteristic and so on. In this juncture we can't say that any grid is not just a data mining grid. It is a very important aspect in maintaining grid systems. Grid management is the key to providing high reliability and quality of service [9]. The complexities of grid computing environments make impossible to have a complete understanding of the entire grid. Therefore, a new approach is needed. Such an approach should pool, analyze and involve all relevant information that could be obtained from a grid. The insights provided should then be used to support resource management and system involvement. Data mining has proved to be a phenomenally robust tool, which smoothen the analysis and interpretation of large volumes of complex data. It results, given the complexities involved in operating and maintaining grid environments efficiently and the ability of data mining to analyze and interpret large volumes of data, it is obvious that 'mining grid data' could be a solution to improving the performance, operation and maintenance of grid computing environments.

II.　　　GRID ENVIRONMENT AND KDD

The Knowledge Grid framework makes use of basic grid services to build more specific services supporting distributed knowledge discovery in databases (KDD) on the grid Such services allow users to implement knowledge discovery applications that involve data, programming and mathematical resources available from distributed grid views. To this end, the Knowledge Grid defines mechanisms and higher-level services for publishing and searching information about resources, representing and managing KDD applications [7], and also for managing their results.

III.　　　THE SIMPLE WAY TO REPRESENT GRID WITH KDD
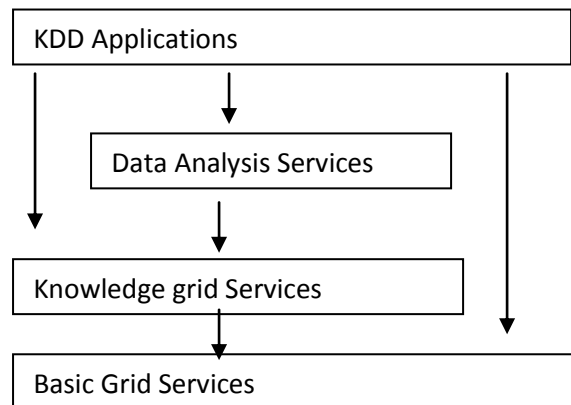
The above architectural approach is flexible in allowing KDD applications to be built upon data analysis services and upon Knowledge Grid services. These services can be composed together with basic services provided by a generic grid toolkit to develop KDD applications.

1. **Basic grid services** are core functionality provided by standard grid environments which include security services, data management services, execution management services and information services such as data access, file transfer, replica management, resource allocation, process creation, resource representation, discovery and monitoring ect.

2. **The Knowledge Grid Services** specifically designed to support the implementation of data mining services and applications they include resource management services, which provide mechanisms to explain, publish and retrieve information about data sources, data mining algorithms and computing resources, and execution management services, allow users to design and execute distributed KDD applications.

3. **Data analysis service**s are ad hoc services that express the Knowledge Grid services to provide high-level data analysis functionalities. A data analysis service can expose either a single data pre-processing or data mining task which includes classification, clustering, association.

4. **KDD applications** are the knowledge discovery applications built upon the functionalities provided by the underlying grid environments, the Knowledge Grid framework or higher-level data analysis services. Different models, languages and tools can be used to design distributed KDD applications in this framework.

IV.　　　THE DATAMININGGRID (DMG) ARCHITECTURE

Mining Data is a complex process, which can be deployed by means of multiple approaches. The distributed nature of data and the extension of information sharing makes the Grid a suitable scenario in which data mining applications can be executed [1]. The Grid community has oriented its activity towards a service model [2]. The architecture OGSA (Open Grid Services Architecture) defines an abstract view of this trend in Grid environments. OGSA gives support to the creation, maintenance and lifecycle of services offered by different VOs (Virtual Organizations) [3]. Different domain problems can be solved by means of grid services. Our proposal is a vertical and generic architecture, named DMGA (Data Mining Grid Architecture) [4], which is based on the main data mining stages: pre-processing, data mining and post-processing. Within this framework, the main functionalities of every stage are deployed by means of grid services. Figure A shows the three stages:

(i) PP1 stage (preprocessing stage), (ii) DM stage (data mining stage) and (iii) PP2 stage (post-processing stage). All these data mining services use both basic data and generic grid services. Data Grid services are services oriented to data management in a grid. One of the best known data grid service is GridFTP [5]. Besides data grid services, data mining grid services also use generic and standard grid services. Generic services offer common functionalities in a grid environment [6].

Data Mining Grid services are intended to provide specialized and new data mining services. Whenever a data or generic grid service can be used for a purpose, it will be used. Only if the typical behavior of a service must be modified, a specialized service must be placed at the Data Mining Grid Services level. For instance, if we need to transfer files in the pre-processing stage, we can make use of the GridFTP service. However, we can also invoke a specific Data Access Service, which is an adaptation of the DAI (Data Access and Integration) Data Grid service to data mining applications on grid. This last service is the SDAS (Specific Data Access Service) Data Mining Grid Service.
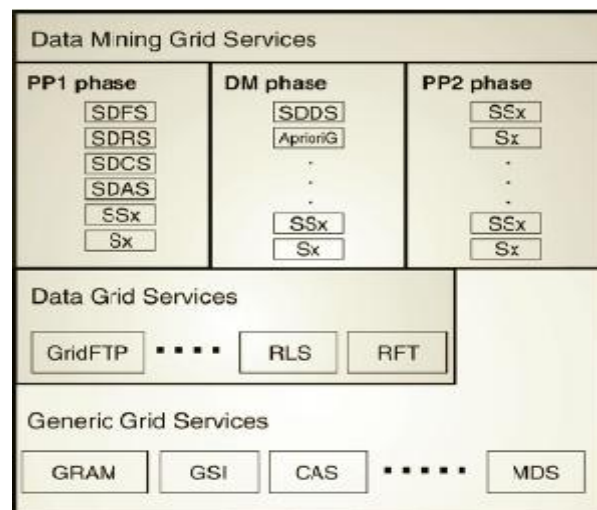
Fig: DataMiningGrid Architecture

New services oriented to data mining applications are included in the architecture. These kinds of services are usually linked to data mining techniques and algorithms. One example is the AprioriG service, which exhibits the Apriori algorithm functionality. Specialization services of the architecture are the following:

- SDFS, Specific Data Filtering Service: due to the huge amount of data involved in the process of data mining, filtering data is an important task, solved by means of this service.
- SDRS, Specific Data Replication Service: one important aspect related to distributed data is data replication. This service deals with this task.
- SDCS, Specific Data Consistency Service: its main purpose is maintaining the data consistency in the grid.
- SDAS, Specific Data Access Service: as has been previously mentioned, this service is an adaptation of the DAI (Data Access and Integration) Data Grid Service to data mining applications on grid.
- SDDS, Specific Data Discovery Service: this service improves the discovery phase in the grid for mining applications.
- SSx: additional specific services can be defined for the management of other features offered by the generic or data grid services, without changes in the rest of the framework.
- Sx: it represents new additional data mining services, which are not provided by basic grid Services. AprioriG is one example of such a kind of service.

V.　　THE IMPLEMENTATION OF DMG (DATA MINING GRID)

Most grid classifiers have their foundations in ensemble way [10]. The ensemble approach has been applied in various domains to increase the classification accuracy of predictive models. It produces multiple models (base classifiers) – typically from "homogeneous" data subsets – and combines them to enhance accuracy. Generally, weighted or UN weighted schemes are employed to aggregate base classifiers.
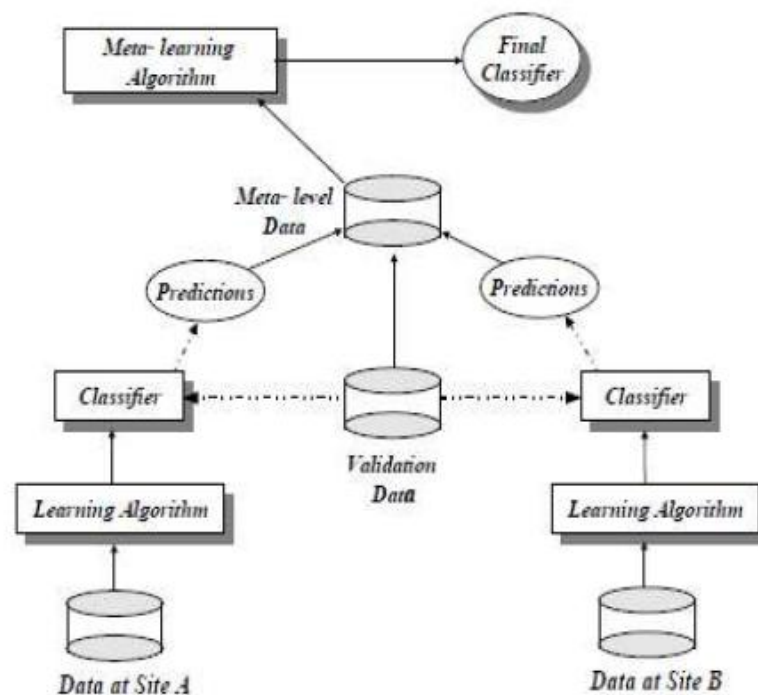
Figure B Grid Meta Learning from Distributed Data Sites

The ensemble approach is directly applicable to the distributed scenario. Different models can be generated at different sites and ultimately aggregated using ensemble combining strategies.

In this approach, supervised learning techniques are first used to learn classifiers at local data sites; then meta-level classifiers are learned from a data set generated using the locally learned concepts. The meta-level learning may be applied recursively, producing a hierarchy of meta-classifiers on grids.
Meta-learning follows three main steps

- Concrete base classifiers at each site using a classifier learning algorithms.
- Collect the base classifiers at a central site. Produce meta-level data from a separate validation set and predictions generated by the base classifier on it.
- Generate the final classifier (meta-classifier) from meta-level data grid.

Learning at the meta-level grid can work in many different ways. For example, we may generate a new data grid using the locally learned classifiers. We may also move some of the original training data from the local sites, blend it with the data artificially generated by the local classifiers, and then run any learning algorithm to learn the meta-level grid classifiers.
We may also decide the output of the meta-classifier by counting votes (weighted & non weighted) cast by different base classifiers.
The following discourse notes two common techniques for meta-learning grid from the output of the base classifiers are briefly described in the following.

- **The Grid Arbiter Scheme:** This scheme makes use of a special classifier, called arbiter, for deciding the final class prediction for a given feature vector. The arbiter is learned using a learning algorithm. Classification is performed based on the class predicted by the majority of the base classifiers and the arbiter. It there is a tie, the arbiter's prediction gets the grid preference.
- **The Grid Combiner Scheme:** The grid combiner scheme offers an alternate way to perform meta-learning. The combiner classifier is learned in either of the following ways.

One way is to learn the combiner from the correct classification and the base classifier outputs. Another possibility is to learn the combiner from the data comprised of the feature vector of the training examples, the correct classifications, and the data comprised of the feature vector of the training examples, the correct classifications, and the base classifier outputs.
Either of the above two techniques can be iteratively used resulting in a hierarchy of meta-classifiers.

The above figure (B) shows the overall architecture of the grid Meta learning framework.

The Grid Meta-learning illustrates two characteristics of DDM algorithms – parallelism and reduced communication.

All base classifiers of grid are generated in parallel and collected at the central location along with the validation set, where the communication overhead is negligible compared to the transfer of entire raw data.

VI. CHALLENGES FACING BY DATAMININGGRID

The shift towards intrinsically distributed complex problem solving environments is prompting a range of new data mining research and development problems. These can be classified into the following broad challenges:

- **Distributed data:** The data to be mined is stored in distributed computing environments on heterogeneous platforms such as grids. Both for technical and for organizational reasons it is impossible to bring all the data to a centralized place. Consequently, development of algorithms, tools, and services is required that facilitate the mining of distributed data.
- **Distributed operations:** In future more and more data mining operations and algorithms will be available on the grid. To facilitate seamless integration of these resources into distributed data mining systems for complex problem solving, novel algorithms, tools, grid services and other IT infrastructure need to be developed.
- **Massive data:** Development of algorithms for mining large, massive and high-dimensional data sets (out-of-memory, parallel, and distributed algorithms) is needed.
- **Complex data types:** Increasingly complex data sources, structures, and types (like natural language text, images, time series, multi-relational and object data types etc.) are emerging. Grid-enabled mining of such data will require the development of new methodologies, algorithms, tools, and grid services.
- **Data privacy, security, and governance:** Automated data mining in distributed environments raises serious issues in terms of data privacy, security, and governance. Grid-based data mining technology will need to address these issues.
- **User-friendliness:** Ultimately a system must hide technological complexity from the User. To facilitate this, new software, tools, and infrastructure development is needed in the areas of grid-supported workflow management, resource identification, allocation, and scheduling, and user interfaces.

VII. CONCLUSION

The DataMiningGrid needs frequently exchange of datamining models among the participating sites. Therefore, seamless and transparent realizations of DMG technology will require standardize schemes to represent and exchange models. Web search sites like Yahoo and Google are likely to start offering data mining services for analyzing the data they interconnecting data models from such sites will be treated as distributes data mining applications which are mostly implementing through grids. And so now we need to take the techniques that have been developed for things like business intelligence and data mining that goes on around that and think how we can apply those in these real time as well, how we can take every step of the process and have it be very visual and only require as much software understanding as is absolutely necessary.

REFERENCES

[1] Mario Cannataro, Domenico Talia, Paolo Trunfio, Distributed data mining on the grid, Future Generation Computer Systems 18 (8) (2002) 1101–1112.
[2] Ian Foster, Carl Kesselman, Jeffrey M. Nick, Steve Tuecke, The Physiology of the Grid: An Open Grid Services Architecture for Distributed Systems Integration, Tech. Report Globus Project, 2002.
[3] Ian Foster, The anatomy of the Grid: Enabling scalable virtual organizations, Lecture Notes in Computer Science 2150 (2001).
[4] Alberto S´anchez, Jos´e M. Pe˜na S´anchez, Mar´ıa S. P´erez, Victor Robles, Pilar Herrero, Improving distributed data mining techniques by means of a grid infrastructure, in: OTM Workshops, in: LNCS, vol. 3292, 2004, pp. 111–122.
[5] William Allcock, Joe Bester, John Bresnahan, Ann Chervenak, Lee Liming, Steve Tuecke, GridFTP: Protocol extensions to FTP for the Grid, Global Grid Forum Draft, 2001.
[6] Giovanni Aloisio, Massimo Cafaro, Italo Epicoco, Early experiences with the gridftp protocol using the grb-gsiftp library, Future Generation Computer Systems 18 (8) (2002) 1053–1059.
[7] Ian H. Witten, Eibe Frank, Data Mining: Practical machine learning tools with Java implementations, Morgan Kaufmann, San Francisco, 2000.
[8] Agrawal R. & Srikant, R. (1994, September). Fast Algorithms for Mining Association Rules. In Proceedings of the 20th International Conference on Very Large Databases (VLDB'94), Santiago, Chile, 487-499.
[9] Bauer, E., & Kohavi, R. (1999). An empirical comparison of voting classification algorithms: Bagging, boosting, and variants. Machine Learning, 36 (1-2), 105-139.
[10] Dietterich, 2000; Opitz & Maclin, 1999; Bauer & Kohavi, 1999; Merz & Pazzani, 1999

Study on genesis of the primary orebody in Shewushan gold deposit

BASSANGANAM Narcisse[1], Associate Prof. Minfang Wang[2], Ph. D Yang Mei Zhen[3], Ph. D Prince E. YEDIDYA DANGUENE[4]

Earth Resource, China University of Geosciences, Wuhan

ABSTRACT: *Shewushan gold deposit is located at 16 km southwest of Jiayu County, Xianning City, Hubei Province, with approximately 10 Mt reserve and average around 2.2 g /t gold grade. That resulted from chemistry of carlin-type orebody hosted in Cambrian-Permian strata under tertiary tropical rainforest climate, which exposed to the oxidation interface by the regional uplift movement. Shewushan gold deposit is a closed negative terrain controlled by faults, where broad karst landform also developed in the fault and unconformity boundary, and obviously is a favorable environment for weathering gold deposit.*

Primary orebody is controlled by Shewushan overturned anticline and Shewushan thrust nappe structure, which respectively belongs to EW trend tectonic belt developed in Indosinian-ealry Yanshanian and NE, NW trend tectonic belt developed in Himalayan. The low-middle temperature serials of alteration minerals include silicide, pyritization, baritization, calcite, realgar and orpiment in outcrop area of Shewushan deposit, which is an important alteration mineral assemblage for carlin-type deposit.

The "Cherts hat", associated with primary orebody, is hydrothermal mineral in Shewushan deposit, and result from filling-metasomatism when SiO_2-rich ore-forming fluid flowed to the F_{12} fault. Besides that, our further research implies that Si element is derived from the Cambrian-Permian stratum or older stratum in the area.

The characteristic of fluid inclusions is 5-20% at gas-liquid ratio, $10\mu m\pm$ at size, and its homogenization temperature is from 80 to 240 ℃, salinity is 2.20-9.34 wt% NaCl, average density is 0.817~0.990 g/cm^3, pressure is 420×10^5~$430\times10^5 Pa$ (equivalent 1.5-2.0 km at depth), which can be referred to high density, low salinity and low temperature ore-forming fluid. What's more, the compositions of gas phase in fluid inclusion contain CO_2 and CH_4, which indicates that it is a reducing ore-forming fluid. Finally, we conclude that the ore-forming fluid is hot brine based on evidence from baritization, "Cherts hat", and reserves ratio of Au/Ag.

KEYWORDS: *Genesis, Primary orebody, Carlin-type gold deposit, Shewushan deposit.*

I.   INTRODUCTION

In China, this kind of gold deposit has been paid more attention (Cao, 1998; Tu, 1999; Chen and Yang, 1999; Wang and Tan, 2002). Shewushan gold deposit located in southern Hubei, central China (Fig 1-1), was the first lateritic gold deposit discovered in central China in 1989, which is also the largest one in Asia. Since then, a series of laterite gold deposits have been found in succession from end of 1980's to beginning of 1990's, and have become an important type of gold resource in China (Cao, 1998; Chen et al., 2001; Wang and Tan, 2002).

Shewushan gold deposit is a new type of economically gold deposit that is currently being exploited in China. Economic grade of the ore is confined largely to the lower portion of the 30-m-thick weathering profile rather than to the fresh, unweathered parts of the deposit. However, both the climate and the tectonic settings in Shewushan are different from the area where typical lateritic gold deposits are located. For example, the climate is warm and humid in the Shewushan area. The annual rainfall is ~1100 mm, falling mainly between April and October, and the average temperature is 18 ^{0}C, with a mean of 4.1 ^{0}C during the coldest month (January) and 29.2 ^{0}C during the warmest month (July).
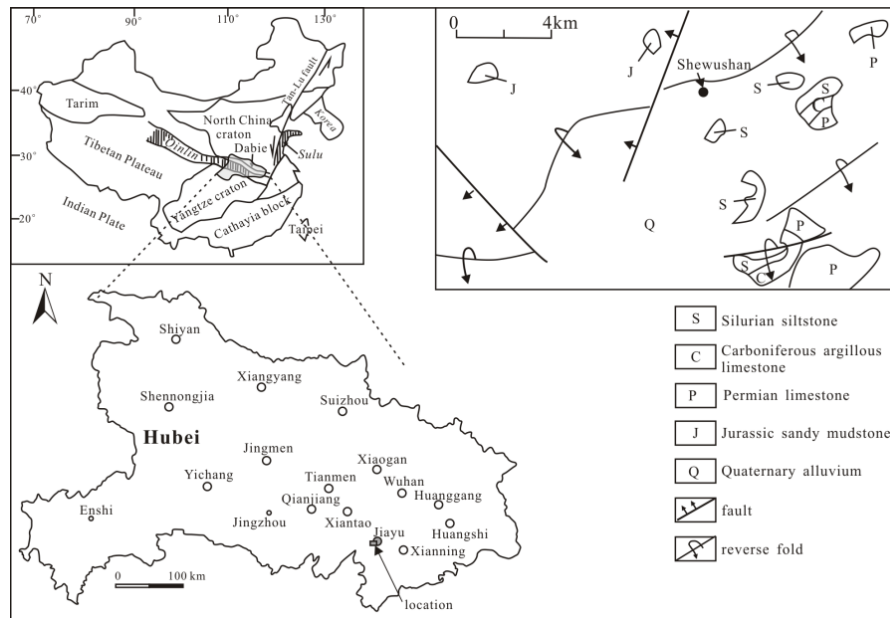
Fig. 1-1: Location of Shewushan gold deposit (after Hong, 2001)

The landscape consists of hills covered with evergreen trees and bushes and comprises relatively flat aggraded and coalesced alluvial fans, with the base level of erosion 20 m above mean sea level (Hong and Tie, 2005). The intensive tectonic movement during the Cenozoic limited the development of an erosional plain, and most of the bedrock is primary carbonates. As a result, the particle size of the gold in the weathering profile is extremely small; most grains are <0.02 mm in size and occur at the rims of clay mineral grains (Hong, 1996; Hong et al., 1999).

The gold in the ore is not visible by reflected- and transmitted-light microscopy at high magnification. It is, therefore, extremely difficult to study the occurrence of gold and its distribution by conventional means.

Previous studies of the Shewushan gold deposit have mainly focused on the geological setting, geochemical characteristics, and genetic model of this type of weathering-related gold deposit (Li, 1993; Li et al., 1994; Yu, 1994; Liu, 1996; Hong et al., 2000). However, the genesis of the primary orebody is still argued. There exist two viewpoints: weathered residual type (Yu, 1994; Li, 1998) and carlin type (Li and Liu, 1995; Liu and Li, 1995).

The Shewushan gold deposit, hosted in weathered mantle above the Shewushan thrust zone, is probably an example of a type of deposit where all the ore-grade gold is related to surficial weathering processes of a previously uneconomic gold deposit. Based on regional strata, from bottom to top, as the first large scale laterized gold deposit to this day, Shewushan gold deposit is characterized by large scale, lower grade, easy mining, easy dressing, top economic benefits etc... In the weathering type gold deposit, a part of the Shewushan gold deposit, whose orebodies occur in the loose clay bed, and contain different amounts of gravel and sand serving as the host rock.. In this paper, we illustrate the genesis of the primary ore body by fluid inclusion, geochemistry and electron microprobe analysis.

II.   REGIONAL GEOLOGICAL SETTING

2.1 Strata

The basement in the area is mesoproterozoic strata, and the cap consists of Sinian-Jurassic strata. Lengjiaxi group is the most important part of mesoproterozoic strata in the southern minerals area of Hubei province, which comprise lower metamorphic rock with flysch rhythm, and primary rock is slate and tuffaceous sandstone. The sedimentary strata mainly comprise carbonate rock with mud, sandstone and silicified coal. The rift basin in the local area, resulted from extension in Late Yanshanian, contain red terrigenous clastic rocks.

In this area, Doushantuo Formation and Pingyuan Formation of Lengjiaxi proup, mainly hosted mineral deposit, comprised dolomite with mud, limestone, shale and slate. Some mineral spots can also be observed in Cambrian strata.
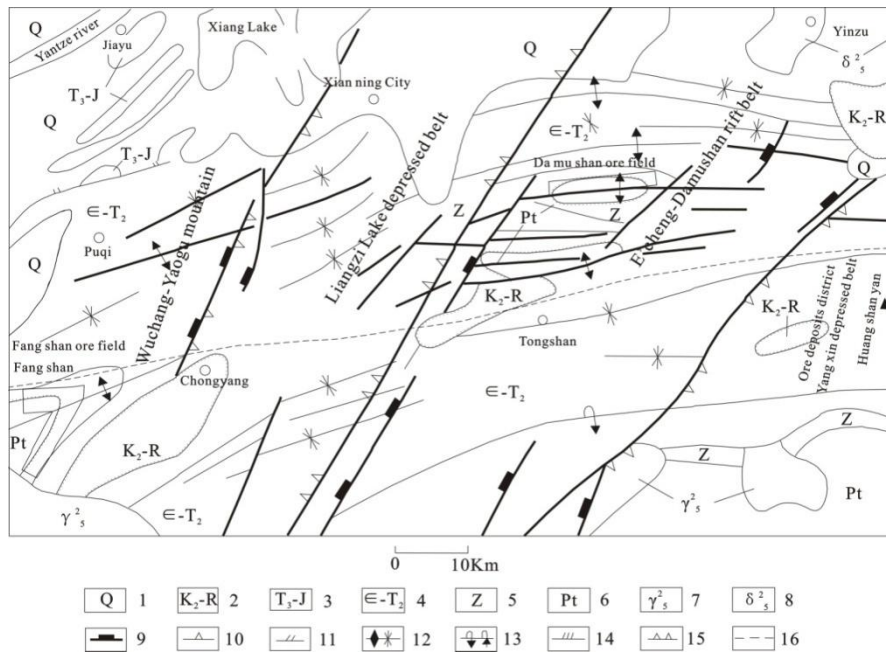
Fig.2-1 Simpled regional map of ore district in the south of Hubei province (after Wang et al., 2011)

Strata: Q: Quaternary; K_2-R: Upper Cretaceous-Tertiary; T_3-J: Triassic-Jurassic; $\in$-T_2: Cambrian-Triassic; Z: Sinian; Pt: Proterozoic

Magmatic rocks: γ^2_5 -granite; δ^2_5 -diorite

Structure: 1. compressive fracture; 2. tenso fracture; 3. fracture; 4. anticline, syncline; 5. inverted anticline inverted syncline; 6. complexing faults with several stages; 7. uplift and depression boundaries

2.2 Structures

The ore deposit district in the south of Hubei province is located in the Wuling-Pengze folded zone belonged to Wuling-Xiushui depression belt, Fangshan anticline and Damushan-Mugang anticline at the west of Tongshan-Duanchang folded zone. The deep tectonic, at the north of Tongshan-Chongyang fault, consists of basement with center type of Sichuan, the cap, and basement with south type of Yangtze River from bottom to top, but at the south of the fault, consists of basement with south type of Yangtze River and basement with center type of Sichuan from top to bottom. The covering relationship of them respond southern strata thrusts to the basement with center type of Sichuan along the faults, and lead to EW trend folds and EW trend faults, NE trend faults, NW trend faults occurred together, which bring about the alternating characteristic between depression and uplift.

2.3 Igneous rock

The Yanshanian magmatism is frequently in the area (Fig.2-1), when Mufu mountain melting-type granite emplaced in the Tongcheng, Jiugong Mountain, Shadian and some other place, most of the rock is diorite (i.e. Yinzu diorite) and common granite. It is suggested that igneous rock possibly is at the depth of Tongshan and Shewushan based on aeromagnetic reports (1:50000 at scale).

2.4 Regional mineral resources

Mineral resources in the area, mainly in non-metallic mineral, followed by metal ores, energy, water and gas mineral. 37 kinds of minerals have been found, but only 18 species of them were identified at mineral reserves, including two kinds of energy minerals, metal ores, non-metallic mineral, mineral water. 11 kinds of mineral resources, at reserves, rank in the top five in Hubei Province, the first in the province of minerals include magnesium, antimony, monazite, tantalum, geothermal, the second includes gold, niobium, metallurgical dolomite and so on, finally, the fourth include coal, vanadium and manganese.

Most of gold mineralization in the south of Hubei province are laterite gold deposits, for example, large Shewushan deposit and small-scale Bazimen deposit, Fushui deposit and Tongshan deposit, in addition to a large number of anomalous area, which mainly are associated with the glacial warm and humid climate between middle Pleistocene and late Tertiary, lead to intense chemical weathering, at same time, many gold-bearing silicified rocks are also crystallization. Recently, some researches indicate that Carlin-type gold deposit, possibly origin of the laterite gold deposits, may be at the depth.

Antimony mineral deposit is another important mineral types in the south of Hubei province, including Fangshan, Damushan and Huangshanyan mineralization concentrated area, very similar genesis to each other, is associated with early Yanshanian tectonic-magmatism. Recent researches suggest that metals are mainly derived from the Middle Proterozoic Lengjiaxi group and magmatic hydrothermal of granite.

III.   GEOLOGICAL SETTING OF SHEWUSHAN ORE DRISTRICT

3.1 Strata

Shewushan gold deposit lithologically overall constituted by the lower strata, middle strata ore body and upper strata. Constitute the slopes - basinal platform facies and restricted platform facies, but the water depth is obvious by the shallowing upward variation. The bottom portion of the middle strata and the upper strata constitute the main bedrock area of lateritic gold.

The water deep facies lower part of the rock formations in the anticline, the main body by a thin layer of mud calcareous slate folder in the thin layer of mudstone, set lithology subject may be equivalent subtidal zone half, slowly deposited debris content the product, including calcareous slate color is dark, and local to see asphalt may indicate higher biological content. Mud calcareous and argillaceous rocks staggered indication the subtidal environment Porgy surface under the shallow part of the terrigenous material containing terrigenous material relative water deeper mutual transition of the environment, that it may phase to the edge of the Wilson cycle Basin the bathyal slot basin facies and basinal quite.

The central body of a thick layer of marl, calcarenite containing shelly limestone component, the shelly limestone are often thin, local shelly limestone may Department reef shattered redeposition part. Rock and mineral identification indicate the segment containing dolomitic and a small amount of quartz sand and other debris ranging from 5-30 % (of course, the vast majority of quartz is a product of hydrothermal activity), so this set must contain some restricted platform components, the results from this rock and mineral identification containing the dolomitic located near the F.3-1 fracture. Saw another strong siliceous rocks of the local zone part of the original Department of rocks may be impure calcium quartz sandstone, some limestone has rounded siliceous gravel, and support it. Short, the central rock body is opened or semi-occlusive platform facies, and clip part of the platform margin shoal (shelly limestone), reflecting an unstable tidal
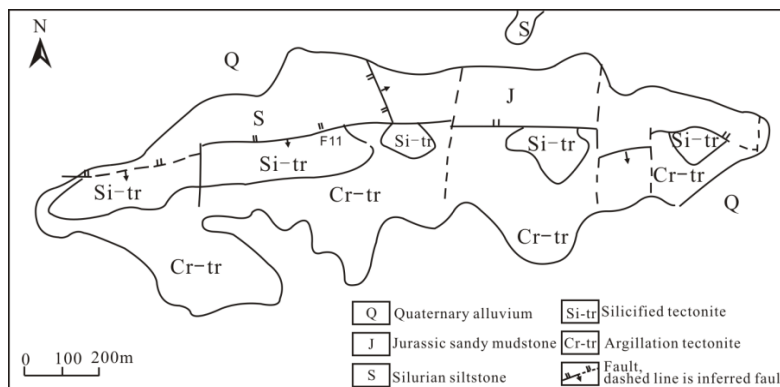
Fig. 3-1. Geological sketch map showing mine structure and lithology in Shewushan gold deposit

zone and the intertidal environment with constantly alternating. Early emergence of terrigenous material, reflect the early hydrodynamic conditions extremely turbulent, set strata at least represents a transgressive phase sequence. Upper strata body composed of thick-bedded marl, the lower part of the folder also have some of the thin layer of calcarenite, whose main shallow shelf phase (Fig. 3-1).

For mine set of strata area predecessors, has been controversial. Observed to lower strata based on regional geological maps prepared by the Hubei four teams, mine quite Silurian strata, middle and upper strata equivalent to the Carboniferous - Permian strata. The work in the central limestone collected a small amount of brachiopods, crinoids' layer foraminifers' fossils poor fossil preservation, according to the preliminary identification of paleontology Department of China University of Geosciences Professor Cai Xiongfei, speculated that there may belong to the Devonian.

3.2 Structure

The Carlin-type gold deposits in China are structurally controlled by both faults and folds formed in the Yanshanian orogeny (Cunningham et al., 1988; Ashley et al., 1991; Gao, 1992; Mao, 1992; Yang, 1992; Jian, 1996).The deposits are usually located along second-order faults (e.g., Lannigou) near major faults, but a few of them are hosted in large regional fault zones (e.g., Dongbeizhai).

The deposit occurs in the Shewushan Thrust Zone (Fig.3-2), which was a conduit for epithermal mineralization as well as the present site of formation of the weathered mantle formed at the expense of the mineralized tectonic melange (Ding, 1992). The orebodies are located mainly in the lower portion of the weathered mantle, which comprises brown to red-brown clay and gravelly clay, and consists of an assemblage of illite, kaolinite, goethite, quartz, and oxides of Fe and Mn (Hong, 1995).
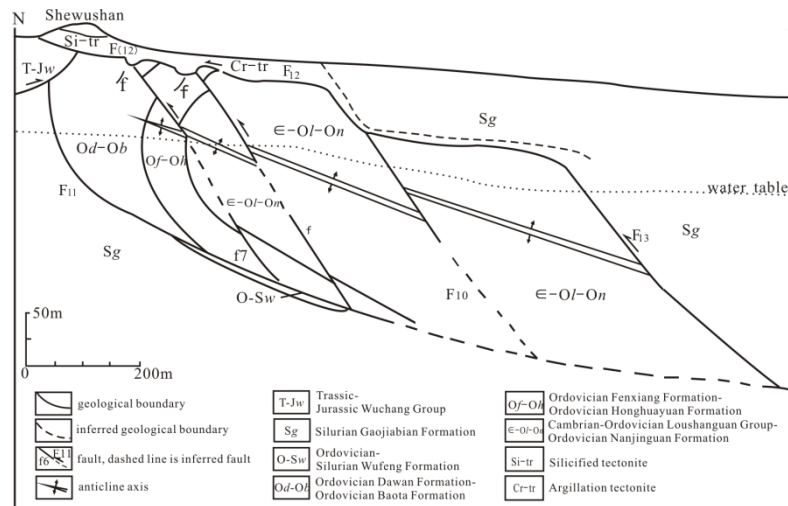
Fig. 3-2. The generalized model of the bimodal thrust faults in Shewushan gold deposit
(modified from Wang and Yang, 1992)

This deposit occurs within the over thus in the southern limb of Shewushan reversed anticline. The distribution of the ore at Shewushan is structurally controlled. The sequence of structures observed is: east-west-trending structures, including the major anticlines and faults.

The structures in the deposit show features of multistage deformation. The east-west structures may represent the regional north-south-trending Indosinian orogeny in earlier stage. The north-south structures may be related to the later tectono-magmatic event with east-west maximum principal stress (Yu, 1995). Shewushan deposit has its own feature including the structural location of occurrence, mineralization, gold-bearing weathering crust laterite profile, gold-forming resources, and gold occurrence features. This gold deposit belongs to carlin-type which can be divided into two subtype-original gold ore and, the weathered gold ore has been formed from exposed original gold ore which occurred in tectonite within the gently dipping fault by weathered and leaching. Shewushan gold deposit consists of series of mineralization faults containing high gold grade in a larger lower grade zone peripheral. Shewushan orefield occur the Middle-upper Cambrian and Ordovician, which bear plenty of gold deposits; mineralization and geochemical abnomalies evidently, reflect the source bed characteristic. The hydrother mal circulation passage is composed of gently dipping overthrust and steep extensive slide fault.

3.2.1 Fault
In geology, a fracture in the rocks of the Earth's crust, where compressional or tensional forces develops, causes the rocks on the opposite sides of the fracture to be displaced relative to each other. Faults range in length from a few inches to hundreds of miles, and displacement may also range from less than an inch to hundreds of miles along the fracture surface (the fault plane). Most, if not all, earthquakes are caused by rapid movement along faults. Faults are common throughout the world.

However Shewushan gold deposit developed north-south-trending faults, which are the second important structures observed (Fig.3-3). The north-south-trending structures, a set of faults oriented at 3°- 8°, which appear to postdate east-west faults and fractures and thus probably postdate mineralization. The faults dip east at around 30°, showing local interference with the east-west structures especially, and offset silicified limestone.

The hypogene mineralization is closely associated with the well-developed faults and fractures present mainly on the crest of the reverse anticline.

3.2.2 Fold

Fold is used in geology when one or a stack of originally flat and planar surfaces, such as sedimentary strata, are bent or curved as a result of permanent deformation. Many folds are directly related to faults, associate with their propagation, displacement and the accommodation of strains between neighbouring faults.

Thus Shewushan gold deposit, structural orientations of folds are roughly southeast-northwest. East–west structures are dominant in the deposit and include the major anticline and associated parasitic fractures. The major anticline is a reversed fold with shallowly dipping southern limbs in the Shewushan region and the axial zone just beneath the deposit. They occur as axial-plane fanning fractures in fold crests. Away from the crests they are at high angles or even normal to bedding. Comb-textured or massive veins, which may be truncated by slip along the bedding or terminated against adjacent mudstone, commonly fill such fractures. These folds and faults have been interpreted as the result of sliding movement of the sediment cause by the Indosinian orogeny.
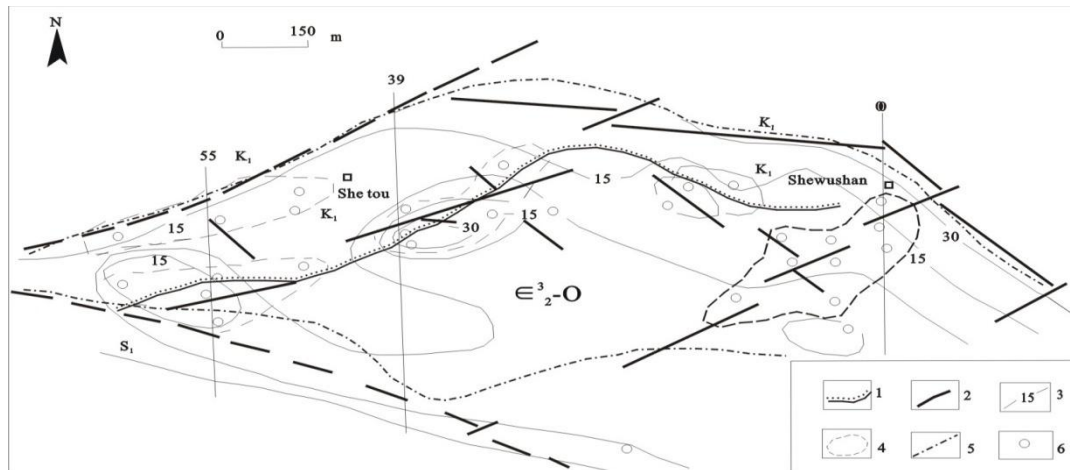
Fig. 3-3   Structural sketch map of basement rock in Shewushan gold mine Yu Renyu (1995)

K_1: Lower Cretaceous; S_1: Lower Silurian; $\in_2^3$-O: the upper Cambrian-Ordovician;

1. Unconformity; 2. Fault; 3. Contours of the bedrock surface (m); 4. Native gold mineralization boundary line; 5. Weathering boundary line type gold; 6. View native gold drilling location.

The elevation of the ore body occurrence is strongly controlled by structures, and the thickness and grade of the ore body increases in the fracture zone. The mineralization is confined to the structural area with the metasediments and crushed quartz veins and calcitization. East-west-trending fractures are most intense in the limestone, with a spacing of 5-60 cm (average 20 cm). The ore bodies are confined between the North Boundary Fault (F_{11}, with dip angle between 30-50°) and South Boundary Fault (F_{13}) (Fig.3-4a, b), where developed crushed limestone and tectonic breccias (Fig.3-4c, d). East-west-trending fractures occur as axial plane fanning fractures in fold crests. Away from the crests they are at high angle or even normal to bedding. Comb-textured or massive veins, which may be truncated by slip along the bedding or terminated against adjacent mudstone, which commonly fills such fractures.

Fig.3-4. Characteristics observed in the field.

a- North Boundary Fault (F_{11}), about 120° trending; b-South Boundary fault (F_{12}); c-crushed limestone near F_{12}; d-tectonic breccias occurs near F_{11}

3.3 Alteration of Wall Rock

Above the water table, silification, argillation, ferritization occurred, whereas pyritization, realgarization, baritization, bituminization, occurred below the water table.

Silification is the wide spreading alteration in Shewushan gold deposit, which also called 'silicon cap' by on-site producers. It is limited to the faulted crushed zone and limestone units. The most intense areas of silification are the faulted crushed zones, where the massive siliceous rock occurs (Fig. 3-5a, b). It presents discontinuous shaped, trending mainly southwards and projecting at the surface for weathering. The areas of intense silification are generally related to a higher gold grade.

Argillation develops mainly in the weathering profile, where clay minerals occur in the matrix and in fractures, with kaolinite and halloysite mainly in the upper portion and illite and minor kaolinite in the lower portion, which caused gold occurs within small Ag-bearing particles, nm-scale in size, adsorbed at the edges of illite and kaolinite (Wang and Yang, 1992; Hong, 1996; Hong et al., 1999; Hong and Tie, 2005).

Ferritization is the most intense surficial alteration in the mine. It is confined to weathering profile. Ferritization occurs as psendomorphs of the earlier sulfide (pyrite and marcasite), disseminated in the oxidized zone.

Pyritization develops widely in limestone, especially in western part of the mine, i.e. jarosite widely occurs, implying pyritization development (Fig. 3-5c). In addition, realgarization develops together with orpiment (Fig. 3-5d). They could be recognized in the calcite vein or in limestone, which occurred as granulous or filmated in calcite vein (Fig. 3-5e), or disseminated in limestone (Fig. 3-5f). Baritization occurs in vein or breccias, and coexist with calcite (Fig. 3-5g).

Bituminization occurs in bedrock outcrop, which cement or cut calcite vein, later than calcite (Fig. 3-5h).

In brief, both hypogene and supergene mineralization are present in Shewushan gold deposit. The hypogene mineralization, i.e. primary mineralization, is closely associated with silification. Three silification stages are observed: 1) the first stage is barren, characteristically coplanar to the axial plane, and devoid of sulfides; 2) gold-bearing sulfide quartz veins and calcite veins postdate the first stage chalcedony quartz veins, which crosscut the former chalcedony quartz veins and probably represent the primary gold-bearing mineralization; 3) the third stage is characterized by the disrupting of sulfide quartz veins and calcite veins by barite quartz veins.
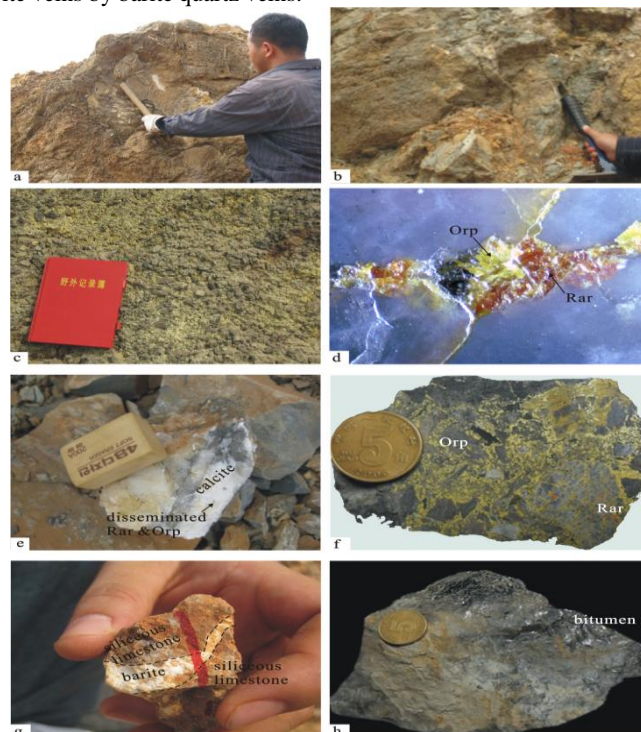
Fig. 3-5   Various alterations in Shewushan gold deposit.
a-chalcedony cement brecciaous limestone in fault crushed zone; b-Silicified limestone (primary mineralized bodies) outcrop in fault crushed zone; c-jarosite widely occurs in western part of ore mine; d-realgarization coexist with orpiment in polished section with oblique light, five times magnification; e-realgarization, orpiment disseminated occurs in calcite vein in fault zone; f-realgarization and orpiment in brecciaous limestone; g-barite cut across the siliceous limestone; h-bitumen envelope the calcite in fault zone

3.4 Characteristic of Orebody

The oxidated ore body (Ⅱ) in the Shewushan deposit is above over weathered surface and at the bottom of gold-bearing silicious belt (Ⅰ). The shape of ore body (Ⅱ) is layered, stratiform and lenticular, 1.8 km at length and n~100n m at width. All sulfides are oxidated and only leaving quartz, chalcedony, clay and limonite in the oxidated ore (Fig. 3-6). The range of gold grade is wide, from 1×10^{-6} to 3×10^{-6}, and 18.26×10^{-6} at most.

The primary ore body (Ⅲ) at the bottom of the oxidated ore body (Ⅱ) consist of Ordovician gold–bearing broken (brecciated) limestone (contains some clay) and gravel silty claystone (contains some siltstone).The gold grade of ore body (Ⅲ) is at the range of $1\text{-}2\times10^{-6}$.
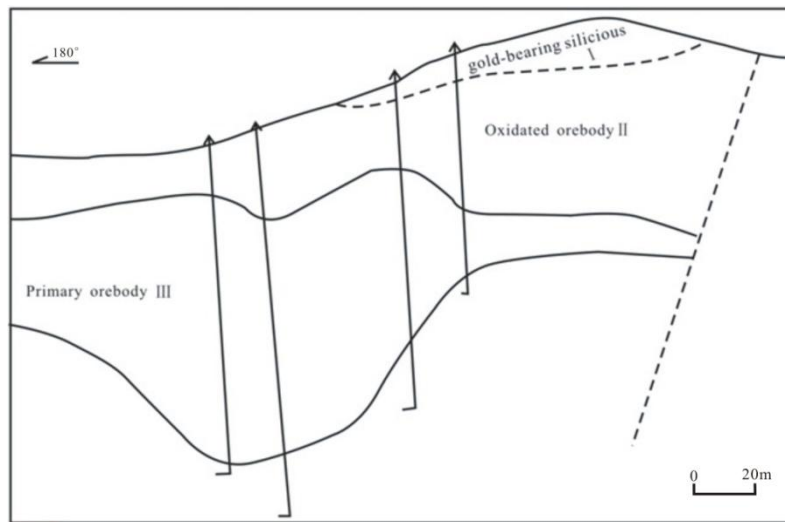
Fig. 3-6. Shewushan arnica mine 0 line schematic cross-sectional view (after Wang, 1992)
I, the silicon cap; Ⅱ, oxidized ore body (of); Ⅲ primary ore (of) the body

3.4.1 Minerals

Ore minerals occur in open faults, stock works, and breccias and replace adjacent strata resulting in the formation of disseminated ore (Fig3-7). In brittle, impermeable, and unreactive rocks, the bulk of the ore is along faults and fractures. In less competent, permeable, and reactive lithologies, ore extends outward from faults to form large tabular bodies.

The increment of fine grade size aggregates is of great significance to absorb Au particles and to form the economic ore bodies.
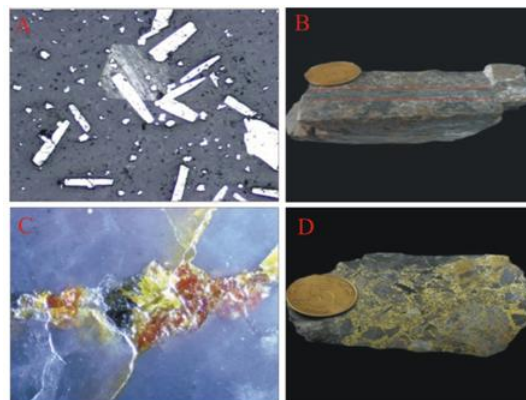
Fig.3-7 Ore minerals in   Shewushan gold deposit
A. pyrite and arsenopyrite symbiotic (×10), B. limestone interspersed with pyrite and arsenopyrite veins,
C. Symbiosis with realgar and orpiment (×5), D. Brecciated limestone realgar, orpiment

3.4.2 Gauge minerals

Primary ore body contains gangue minerals calcite, dolomite, barite, fluorite, and clay minerals.

3.4.3 Texture and structure of ore

There are three types of ore in Shewushan deposit, contain gold-bearing silicious (AuⅠ), oxidation and primary ore.

Gold-bearing silicious orebody (AuⅠ), which is brown, gray and maroon, and its' structure includes clastoporphyritic fragmentation, brecciated structure seen limonite leaching phenomenon (Fig.3-8A).

The characteristic of oxidation ore is cataclastic structure,argillaceous structure, containing structure, residual structure, brecciated structure, disseminated structure, banded structure, vein structure, and honeycomb structure.

The characteristic of primary ore is cataclastic structure, interspersed structure, micritic biological structure, brecciated structure, vein structure, and higher gold grade in broken rocks. The ore was crushed, fragmentation structure (Fig.3-8B), the film-like structure (Fig.3-8C), interspersed structure (Fig.3-8D), pulse-like structure (Fig.3-8E), brecciated structure (Fig.3-8F).
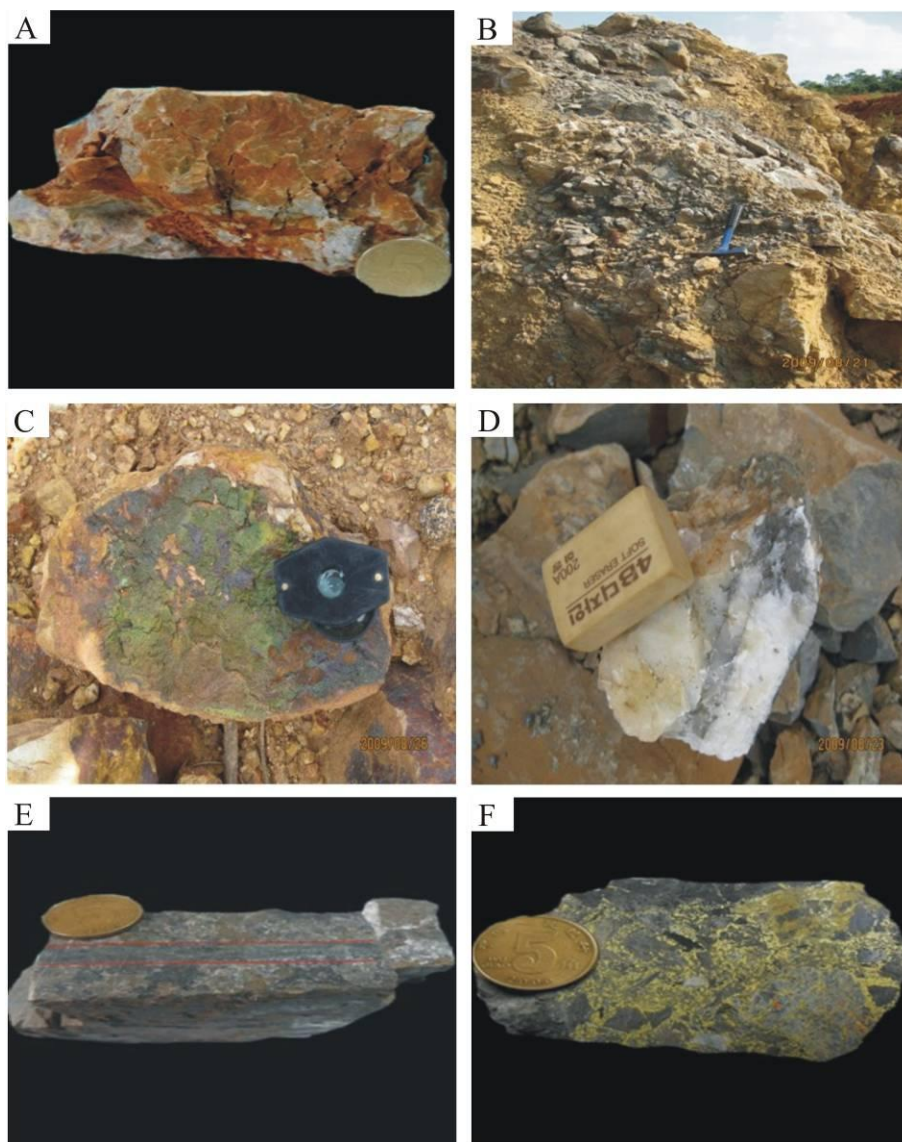
Fig. 3-8   Typical ore structure of primary orebody in Shewushan gold deposit
A-silicified tectonic rock, B-fragmentation structure Ore nearly F_{13}, C-film-like structure nearly F_{11},
D-realgar, orpiment disseminated structure nearly F_{11}, E-arsenopyrite vein, F-brecciated structure

IV.   ANALYSIS OF ORE GENESIS

4.1 Study on Fluid Inclusions

Several studies on the petrography, and microthermometry, of fluid inclusions have recently been on samples in the Laboratory of China University of Geosciences (Wuhan). Nineteen samples were observed for homogenization temperature. The location of the samples could be seen in Fig 4-1. Limestone, dolomite, cryptite and silicite samples were collected from outcrop. These samples were cut and double polished into around 0.3 mm thick sections to observe.
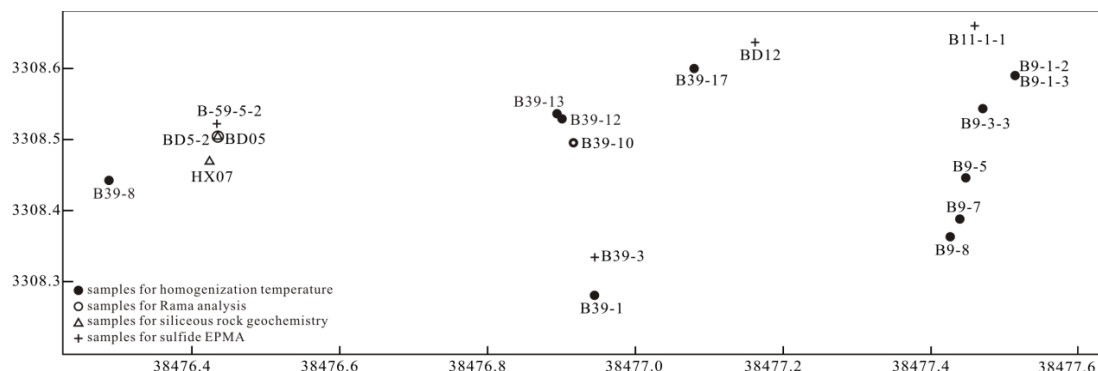
Fig. 4-1. The location map of the analyzed samples in Shewushan deposit

All the three types' inclusions have been observed in samples, i.e. primary (Fig. 4-2a, b), pseudosecondary (Fig. 4-2c) and secondary (Fig. 4-2d) fluid inclusions.

Primary inclusions are typically larger (maximum 20 μm) and isolated. Pseudosecondary and secondary fluid inclusions define linear trails and are much smaller (typically <5 μm). Analysis was in most cases confined to inclusions thought to be of primary origin and hence allows us to document temperature in mineralized fluid.

Two kinds of inclusions exist, i.e. aqueous (most abundant) fluid inclusions and CO_2-rich fluid inclusions. For the first type, the vapor phase occupies 5% to 10%, and to a lesser extent 15% to 40% of the total volume of individual inclusions. They are mostly irregular and elliptic in shape. Most of them are less than 8 μm in diameter; some are large, reaching 20 μm in the longest dimension. They occurred either in the small cluster without obvious planar orientation or in wide hands. The homogenization temperatures range from 70 ^{0}C to 350 ^{0}C, concentrating between 140 ^{0}C and 220 ^{0}C, which is middle-low temperature (Fig. 4-3).
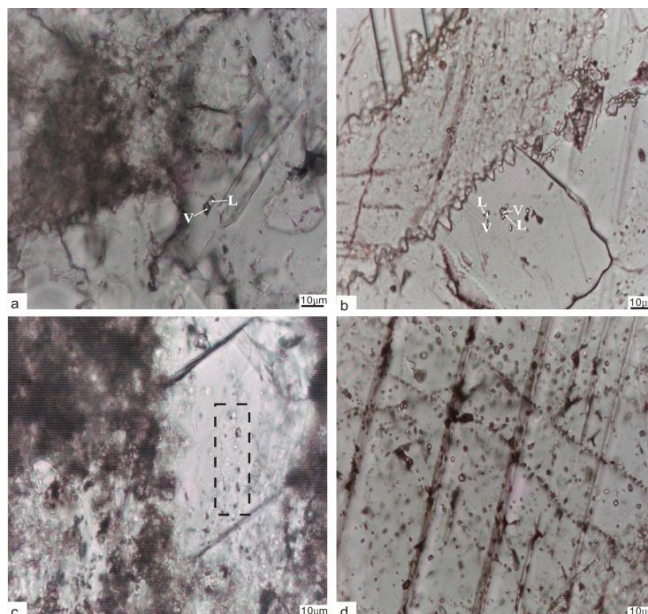
Fig. 4-2. Fluid inclusion petrography in Shewushan gold eposit
a-Primary fluid inclusion with isolated occurrence; b-Primary fluid inclusion in small clusters; c-Pseudosecondary fluid inclusion distributed in calcite fissure; d-Secondary fluid inclusion in calcite fissures
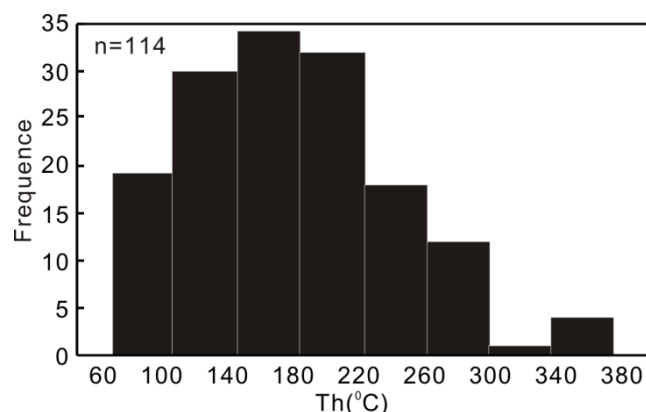
Fig. 4-3. Histogram showing homogenization temperatures of aqueous fluid inclusions in Shewushan gold deposit

At the room temperature, these CO_2-rich fluid inclusions contain liquid and vapor carbonic phase and an aqueous liquid phase. These inclusions have a dark appearance, and therefore, the boundary between the liquid and vapor carbonic phase is not always evident. According to the previous study by Liu and Li (1995), the salinity ranges from 2.2 wt. % to 9.34 wt. %, and the density ranges from 0.817 to 0.990 g/cm^3, with pressure from 42 to 46 MPa, showing low salinity and high density fluid characteristics, which implies the forming depth is about 1.5-2 km (Liu and Li, 1995).

4.2 Geochemistry of Siliceous Rocks

As mentioned in Chapter 3, silification is the wide developing and important alteration associated with gold mineralization. We collected laminate-lenticular siliceous rocks in the field. Samples were washed with distilled water, and were ground and passed through a 75 μm mesh sieve.

The siliceous rocks mainly consist of SiO_2, with the SiO_2 contents vary from 96.87% to 97.9%, and 97.24% on average, showing the better pure composition. The secondary constitutes are Al_2O_3, and the content of the other elements are very low (Table 4-1). The Al/ (Al+Fe+Mn) atomic ratio is an important indicator to evaluate the content of hydrothermal sedimentary components in various sediments, and the ratios decrease with the increase of the content of hydrothermal components. In addition, low TiO_2 contents are the typical characters of the hydrothermal siliceous rocks. In Shewushan deposit, the Al/ (Al+Fe+Mn) ratios of our samples range from 0.244 to 0.317, and TiO_2 contents are 0.01% (Table 4-1), showing the hydrothermal characteristics. In the Al-Fe-Mn triangle diagram, we plot samples of Shewushan, West Qinling, Franciscan and Shimanto, showing their hydrothermal characteristics (Fig. 4-4).

Table 4-1 Major elements contents of siliceous rocks in Shewushan gold deposit (%)

Sample	SiO_2	TiO_2	Al_2O_3	Fe_2O_3	FeO	MnO	MgO	CaO	Na_2O	Al/(Al+Fe+Mn)
HX07	97.9	0.01	0.30	0.54	0.38	0.01	0.06	0.01	0.10	0.244
BD05	96.87	0.01	0.44	0.69	0.25	0.01	0.06	0.01	0.11	0.317
WestQinling[1]	95.30	0.04	0.41	1.03	0.58	0.03	0.19	0.68	0.06	0.153
Franciscan[2]	92.30	0.09	1.31	0.27	2.36	0.53	0.28	0.11	0.16	0.293
Shimanto[3]	87.87	0.05	1.09	0.52	2.52	1.08	0.86	1.05	0.35	0.209

1. Average composition of cherts from West Qinling, data from (Liu et al., 1999); 2, 3. data from Yamamoto, (1987). Al/ (Al+Fe+Mn)= Al_2O_3/(Al_2O_3+ Fe_2O_3+ FeO+ MnO).
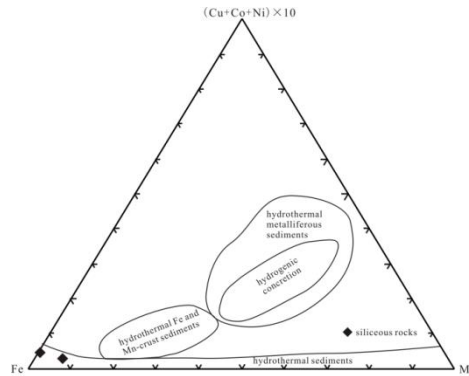
Fig. 4-6 Ternary diagram of Fe-Mn-(Cu+Co+Ni)×10, modified from Crerar et al., 1982

Hydrothermal sediments are relatively enriched in Cu, Ni and depleted in Co (Crerar et al., 1982), and high contents of As, Ba and Sb in sediments (Bostroem et al., 1979; Marchig et al., 1982). In the U-Th diagram, the siliceous rocks fall into hydrothermal field (Fig. 4-5). In the triangle diagram of Fe-Mn-(Co+Ni+Cu)×10, the siliceous rocks fall into the hydrothermal field close to the Fe-end member (Fig. 4-6). Sum up, the trace elements indicate that the siliceous rocks are hydrothermal sediments in the Shewushan gold deposit.
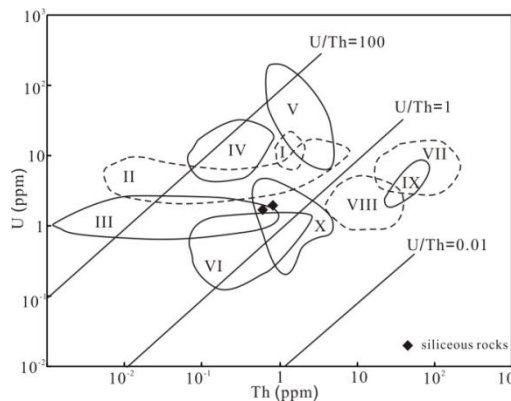
Fig. 4-5 The plot of U v.s. Th of siliceous rocks in Shewushan deposit, (based on Bostroem et al., 1979)

I-TAG hydrothermal area, at the Mid-Atlantic Ridge; II-Galapagos spreading center deposits; III-Amphitrite expedition, dredge site 2; IV- Red sea hot brine deposits; V-East Pacific Rise crest deposits; VI-Lanban hydrothermal sediments; VII-ordinary manganese nodules; VIII-ordinary pelagic sediments; IX-Laterites; X-fossil hydrothermal deposits
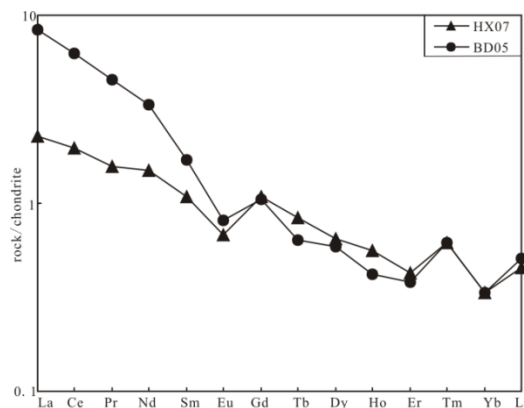
Fig. 4-7. The REE pattern of the siliceous rocks from the Shewushan gold deposit

In addition, REE compositions are also the important indicators distinguishing hydrothermal sediments from non-hydrothermal sediments (Marchig et al., 1982). The total REE contents of the siliceous rocks vary from 3.575 to 11.347×10^{-6} (Table 4-2). LREE/HREE >1, the values of Eu anomaly (Eu/Eu*) and Ce anomaly (Ce/Ce*) vary from 0.365 to 0.630 and from 0.889 to 1.038, respectively. The REE patterns are right-inclined (Fig. 4-7), and a lack of negative Ce anomaly, which usually appears in marine hydrothermal cherts (Bostroem et al., 1979; Bostrom, 1983; Adachi et al., 1986; Yamamoto, 1987), showing these siliceous rocks formed in the continental depositional environment.

Table 4-2 The REE contents of the siliceous rocks from the Shewushan Au deposit (10^{-6})

Sample	La	Ce	Pr	Nd	Sm	Eu	Gd	Tb	Dy	Ho	Er	Tm
HX07	0.7	1.6	0.19	0.9	0.21	0.05	0.28	0.04	0.21	0.04	0.09	0.02
BD05	2.6	5.1	0.55	2	0.33	0.06	0.27	0.03	0.19	0.03	0.08	0.02

Continued:

Yb	Lu	∑REE	LREE	HREE	LREE/HREE	Eu/Eu*	Ce/Ce*	(La/Yb)N	(La/Sm)N	(Gd/Yb)N
0.07	0.02	4.42	3.65	0.77	4.74	0.63	1.038	6.742	2.097	3.228
0.07	0.02	11.35	10.64	0.71	14.986	0.597	0.979	25.041	4.956	3.113

4.3 EMPA on Pyrite and Arsenopyrite

To make certain the occurrence of gold in Shewushan gold deposit, we choose EPMA to detect the elements content in pyrite and arsenopyrite. The chemical compositions were analyzed by electron microprobe analysis (JCXA-733, Japan) with five X-ray wavelength-dispersive spectrometers in the State Key Laboratory of Geological Processes and Mineral Resources, China University of Geosciences. Pyrite and arsenopyrite were analyzed for Au, Ag, Co and Ni at 25 keV accelerating voltage and 10-40 nA beam current, keeping 10s counting times.

Pyrite and arsenopyrite are the most widely distributed minerals in the mine samples selected for electron microprobe analysis seen in Table 4-3, the microscope photo shown in Fig. 4-8.

Table 4-3   EMPA results of pyrite and arsenopyrite from the Shewushan deposit (%)

Samples	Point	Mineral	Au	Co	Ag	Ni	Co/Ni
B2-1	1	Apy	0.113	0.079	-	0.013	
	2		0.118	0.083	0.01	0.024	
	3		0.155	0.085	-	0.013	
	4		0.13	0.088	0.023	0.016	
	5		0.112	0.074	-	0.017	
	6		0.142	0.079	-	0.021	
B11-1-1	1	Apy	0.12	0.098	-	0.052	
	2		0.106	0.101	0.019	0.082	
	3		0.123	0.073	-	0.026	
	4		0.091	0.08	0.029	0.03	
	5		0.123	0.08	0.036	0.044	
	6		0.113	0.082	0.021	0.028	
B39-3	1	Py	0.112	0.076	0.008	0.018	4.22
	2		0.047	0.089	0.035	0.013	6.85
	3		0.125	0.088	0.021	0.014	6.29
	4		0.134	0.065	-	0.014	4.64
	5		0.078	0.068	-	0.01	6.8
	6		0.091	0.064	-	0.026	2.46
B59-5-2	1	Apy	0.107	0.075	-	0.019	
	2		0.101	0.089	0.013	0.031	
	3		0.105	0.085	-	0.025	
	4		0.111	0.067	-	0.026	
	5		0.146	0.1	-	0.095	
	6		0.119	0.08	-	0.018	
BD12	1	Apy	0.085	0.092	0.012	0.025	
	2		0.124	0.063	0.01	0.012	
	3		0.121	0.081	0.004	0.024	
	4		0.104	0.082	-	0.028	

The results show that both pyrite and arsenopyrite are gold-bearing minerals. As we all know, the Co/Ni value in pyrite is the key index to confirm the pyrite genesis. The Co/Ni values range from 2.46 to 6.85, indicating its hydrothermal genesis. To some extent, the Co content in pyrite could indicate the pyrite genesis: the high temperature pyrite with Co content higher than 1000×10^{-6}, middle temperature pyrite having Co content between 100×10^{-6} to 1000×10^{-6}, while the low temperature pyrite having Co content lower than 100×10^{-6}.

The Co contents in pyrite range from 640×10^{-6} to 890×10^{-6} in Shewushan gold deposit, suggesting the pyrite was generated in middle temperature.
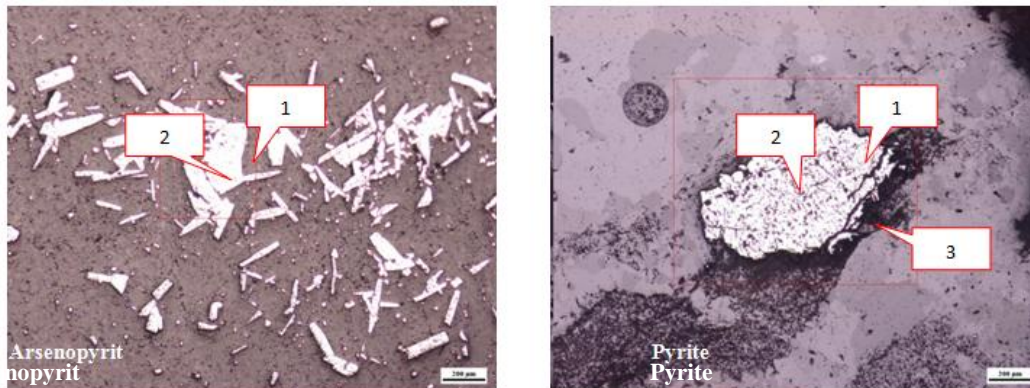
Fig.4-8 The typical map showing electron probe points

V.   CONCLUSION

Shewushan gold deposit is a kind of lateritic gold deposit in Jiayu County, Hubei Province, located in Yangtze platform fold belt, southeast edge of Jianghan basin. The ore body is greatly controlled by strata, placed between quaternary red net-like clay and brown clay, in lamellar or lentoid shape. The deposit exists an overturned anticline related with structure, and developed a double thrust structure, in which the crush of original rocks may do efforts to the ore formation.

The ore resources of the deposit mainly contains Au, other elements are in low content. And the deposit has different kinds of wall rock alterations, such as silicification, carbonatation, pyritization, realgar change, orpiment change, barite change, fluoritization etc. Sometimes gold (Au) can exist in pyrite crystal lattice.

The opinions about the ore genesis are different, however, the Carlin-type model show its priority, the model discusses about the genesis of the primary gold deposit and weathering gold deposit, amid expounds the source of ore forming materials, and conditions for the ore forming period, such as physicochemical conditions and low-lying land.

As mentioned above, the genesis of primary ore in Shewushan Au deposit is controversial. However, several points concerning the features, which are pertinent to understand the genesis of the primary ore, can be summarized as follows.Primary mineralization is typified by gold-bearing arsenopyrite and pyrite and hosted by tectonic mélange and crushed clay-rich limestone, which is the typical gold-bearing mineral in carlin type Au deposit.

The geochemistry data of siliceous rock illustrate that it is hydrothermal sediments, which are deposited near fault surface by bearing SiO_2 mineralized fluid migrated deep along the fault.

Primary mineralization was structurally controlled and formed in closely association with the well-developed faults and fractures mainly on the crest of the reverse anticline, which it's axis is oriented approximately east-west at Shewushan area and is the product of the Indosinian orogeny, which is adhere to the geotectonic setting and metallogenic characteristics of carlin Au type in China (Liu, 1994). Besides, the widely developed silicification, argillaceous alteration and pervasive limonitization, mild pyritization and realgarization are the typical alteration of carlin Au type.

The fluid inclusions are significantly small in size within the minerals. The homogenization temperature ranges from 110 ℃ to 290 ℃. The salinity varies from 2.2 % to 9.34 % w (NaCl, equivalent). The pressure falls in the range of 42 to 46 MPa, which indicate that the gold mineralization took place in low temperature, low pressure and low salinity hydrothermal fluid conditions. Therefore, all the above make sure that the genesis of primary ore in Shewushan Au deposit is carlin type.

VI.   Acknowledgements

REFERENCES

[1].   Cao Xinzhi (1998) Overview of research on laterite gold deposit in China [J]. *Geological Science and Technology Information*. **17,** 50-54 (in Chinese with English abstract).

[2].   Hong Hanlie and Tie Liyun (2005) Characteristics of the Minerals Associated With Gold in the Shewushan Supergene Gold Deposit, China [J]. *Clays and Clay Minerals*. **53**, 162-170.

[3].   Hong Hanlie (1996) Microscopic characteristics of the clay minerals in the oxidized zone of Shewushan gold mine in Jiayu, Hubei [J]. *Hubei Geology*. **10**, 71-74 (in Chinese with English abstract).

[4].   Li Songsheng (1993) The geology and genesis of Shewushan laterite gold deposit, Hubei [J]. *Geology and Exploration*. **29**, 12-15 (in Chinese).

[5].   Yu Renyu (1994) Geological characteristics and genesis of the weathering type gold deposit in the Shewushan gold ore district, Hubei province [J]. *Mineral Deposits*. **13**, 28-37 (in Chinese with English abstract).

[6].   Li Jiaxiang and Liu Shimin (1995) The geological characteristics of carlin type gold deposit in Shewushan, Hubei province [J]. *Hubei Geology*. **9**, 91-99 (in Chinese with English abstract).

[7].   Wang Shumin, Zhang Wensheng, Shi Huabin (2011). The study of the law of E'nan antimony mineralization [J]. *Inner Mongolia Petrochemical*, **7**: 46.

[8].   Cunningham CG, Ashley RP, Chou I-M, Huang Z, Wan C, Li W (1988) Newly discovered sedimentary rock-hosted disseminated gold deposits in the People's Republic of China. *Economic Geology*. **83**:1462-1467

[9].   Ding Qixiu (1992) Some new ideas on stratigraphy of Shewushan area [J]. *Hubei Geology*. **5**, 4-6 (in Chinese with English abstract).

[10].   Hong Hanlie (1995) Study on the geological characteristics of the oxidized zone at Shewushan [J]. *Gold*. **16**, l-7 (in Chinese).

[11].   Yu Renyu (1995) Analysis on the ore control structures of the primary gold mineralization in Shewushan laterized gold deposit [J]. *Hubei Geology*. 9(1) = 100-105.

[12].   Wang Tong and Yang Ming'ai (1992) A preliminary study on the occurrence of gold in primary ore from Shewushan gold deposit [J]. *Hubei Geology*. **6**, 40-46 (in Chinese with English abstract).

[13].   Liu Shimin, and Li Jiaxiang (1995) Geology and genesis of Shewushan carlin type of gold deposit in Hubei province [J]. *Journal of Precious Metallic Geology*. **4**, 184-192 (in Chinese with English abstract).

[14].   Liu Jiajun, Zheng Minghua, Liu Jianming, Zhou Yufeng, Gu Xuexiang and Zhang Bin (1999) The geological and geochemical characteristics of Cambrian chert and their sedimentary enviromental implication in western Qinling [J]. *Acta Petrologica Sinica*. **15**, 145-154.

[15].   Yamamoto K. (1987) Geochemical characteristics and depositional environments of cherts and associated rocks in the Franciscan and Shimanto Terranes [J]. *Sediment Geology*. **52**, 65-108.

[16].   Crerar D.A., Namson J., Chyi M.S., Williams L. and Feigenson M.D. (1982) Manganiferous cherts of the Franciscan assemblage; I, General geology, ancient and modern analogues, and implications for hydrothermal convection at oceanic spreading centers [J]. *Economy Geology*. **77**, 519-540.

[17].   Bostroem K., Rydell H., and Joensuu O. (1979) Langban; an exhalative sedimentary deposit? [J]. *Economy Geology*. **74,** 1002-1011.

[18].   Marchig V., Gundlach H., Möller P. and Schley F. (1982) Some geochemical indicators for discrimination between diagenetic and hydrothermal metalliferous sediments [J]. *Marine Geology*. **50**, 241-256.

[19].   Boynton W.V. (1984) Cosmochemistry of the rare earth elements: Meteorite studies, In *Rare earth element geochemistry* (ed. Henderson P) [C]. pp. 63-107. Elsevier, Amsterdam.

Research Paper   Open Access

Performance Testing Of Torque Limiter Timer Belt Spindle Drive for Overload Protection

L. B. Raut[1], Rohan N. Kare[2]

[1]*Assistant Professor, Mechanical Engineering, SVERI College of Engineering, Pandharpur.*
Solapur University, Solapur, (India)
[2]*ME Student, Mechanical Engineering (Design), SVERI College of Engineering, Pandharpur.*

Abstract -*Power is transmitted from motor to output shaft without any interference when no excessive load acting on the machine. But major problem is faced by industry on the machine that is when excessive load will act on the output shaft then problem of overloading make the driving motor or engine to stall; which will lead to burnout of the electric motor. In extreme cases this overload will lead to the breakage of drive elements or the clutch itself. In order to avoid the damage of the transmission elements it is necessary that the input and output shafts be disconnected in case of sudden overloads. The isolation of the input driver member i.e.; motor from the output member is absolutely necessary to avoid damage itself.*
Such serious problem which face by the industry can be avoided by use of Torque limiter timer belt spindle drive for overload protection and this can be achieved by the overload slipping ball clutch which is an safety device used in the transmission line to connect the driving and driven elements such that in case of occasional overload the clutch will slip there by disconnecting the input and output members. This protects the transmission elements from any breakage or damage and to cope up with this situation static structural analysis is done on the different parts of Torque limiter such as Base flange, Test rig, output shaft, plunger etc. In this case according to the discussion with company person we will decide to done the static analysis of various parts such as base flange, test rig, output shaft etc.

Key Words:*Timer belt, Torque limiter, FEA, Static structural Analysis, Overload protection, Ball clutch.*

I.   INTRODUCTION

The present work aims for a correct, safe and economical machine working it is necessary that the component elements of this to be designed and accomplished properly. It is important that, still from the conceiving stage, to work both on the machines and equipment's gauge and on their reliability (so implicitly on the materials and energy consumptions). Taking into consideration all of these, one of the solution is represented by the use of some safety clutches. In this way, the designers can decrease the value of the safety coefficient for the dimensioning of the mechanical transmissions of equipment's.

The safety clutches fulfill – besides the main function of the torque transmission and rotational motion transmission between two consecutive elements of a kinematic chain - the function of transmitted torque limitation, in the case of some overloads occurrence, during the performance. In this way it is avoided the kinematic chain elements overstressing and their deterioration. The overloads – that occur in transmission thanks to some causes like machine starting or stopping, the passing through resonance zone, too high overloads of the driven mechanism – can be dynamic (with shocks), with very short duration or quasi-static with long duration. Indifferently of the overloads type, these can lead to the machine deterioration and its retirement. Taking into consideration all overloads, for the transmission calculus, it can lead to an excessive over-measure of this, situation that cannot be accepted. If a safety clutch is assembled in the kinematic chain of the mechanical transmission, then the mechanical properties of the materials, for the transmission component elements can be used to maximum.

The clutches are used largely in machine buildings, and by the correct selection of these depends to a great extent – the safe and long working, both of these and of the kinematic chain equipped with them. The guarantee of these demands, for the mechanical power transmission between shafts, represents a ticklish problem for all areas and engineering applications that require compact, simple and reliable systems. By their advantages, the safety clutches are preferred in different top techniques areas like cars, naval industry and so on.

The main function of the clutches is characteristic to all of them and is the function of transmitting the motion and the torque moment. The other functions, specific to each clutch type are: the motion commanding, the load limitation (with or without interrupting the kinematic flux), the protection against shocks and loads; the compensation of assembling errors; the compensation of the errors which can appear during working; the limiting of revolution; the one-sense transmission of the motion. All of these functions can appear singularly or concomitantly. Clutch is a mechanism which enables the rotary motion of one shaft to be transmitted, when desired to a second shaft the axis of which is coincident with that of the first.

II. PROBLEM IDENTIFICATION AND PROBLEM DEFINITION
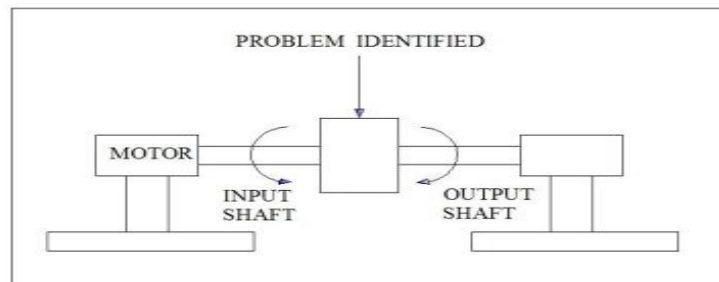
Fig-1: Problem Identification in the Torque Limiter

Above diagram shows that power is transmitted from motor to output shaft without any interference when no excessive load acting on the machine. But major problem is faced by industry on the machine that is when excessive load will act on the output shaft then problem of overloading make the driving motor or engine to stall; which will lead to burnout of the electric motor. In extreme cases this overload will lead to the breakage of drive elements or the clutch itself. In order to avoid the damage of the transmission elements it is necessary that the input and output shafts be disconnected in case of sudden overloads. The isolation of the input driver member i.e.; motor from the output member is absolutely necessary to avoid damage itself.

Such serious problem which face by the industry can be avoided by use of Torque limiter timer belt spindle drive for overload protection and this can be achieved by the overload slipping ball clutch which is an safety device used in the transmission line to connect the driving and driven elements such that in case of occasional overload the clutch will slip there by disconnecting the input and output members. This protects the transmission elements from any breakage or damage and to cope up with this situation static structural analysis is done on the different parts of Torque limiter such as Base flange, Test rig, output shaft, plunger etc. With this I have defined following problems regards with torque tender.

- Excess load on output shaft.
- Incomplete constrained motion.
- Excessive load on the motor.
- Less power transmission by output shaft.
- More power consumption.

III. SCOPE OF WORK

1. In many cases pump shaft drives either electrical or engine drives are normally furnished with the overload slipping ball clutch to avoid the breakage or damages arising due to pump clogging or blockage Compressor drives, especially in many mining applications are equipped with the over load slipping ball clutch.

2. Compact size: The size of the Torque limiter is very compact; which makes it low weight and occupies less space in any drive.

3. Ease of operation: The changing of torques gradual one hence no calculations of speed ratio required for change torque .Merely by rotating adjuster lock nut torque can be changed.

4. Machine tool slides are driven by electrical drives connected to lead screw. The over load slipping ball clutch isolates the electrical drive from the output in case of overload.

IV. OBJECTIVES OF PROJECT

- To design a Test rig and plunger which easily avoid the excess load acting on the output shaft.
- To prevent the Motor from stalling or burning which cause due to overloading on output shaft by doing static structural analysis.
- To vary Torque carrying capacity by Varying number of Ball & spring sets.
- Integration of the timer pulley set and torque limiter to form final drive system.

V. METHODOLOGY

5.1 Preparation of CAD model. Following are the various object of include in the projects which are listed below.
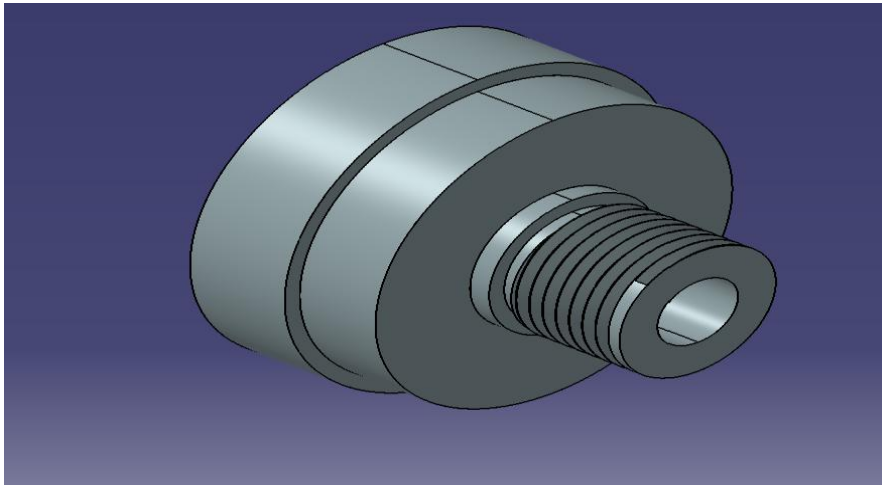
Fig 2 Clutch body
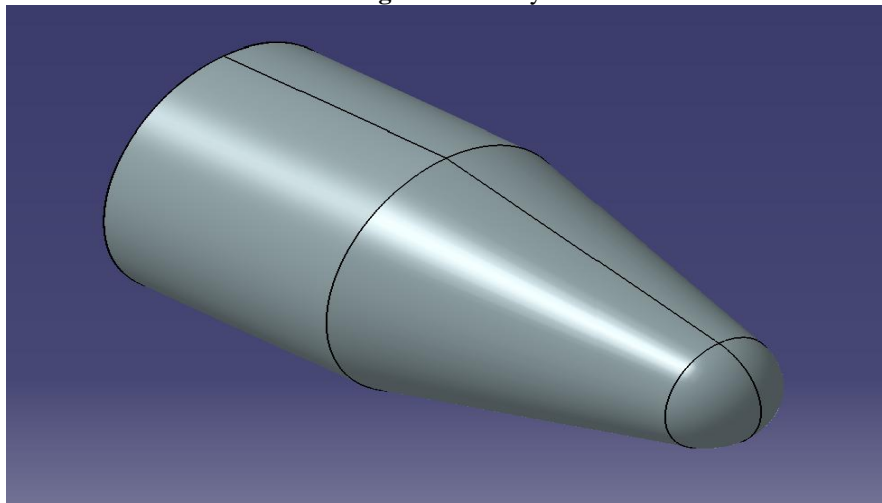
Fig 3 Plunger assembly
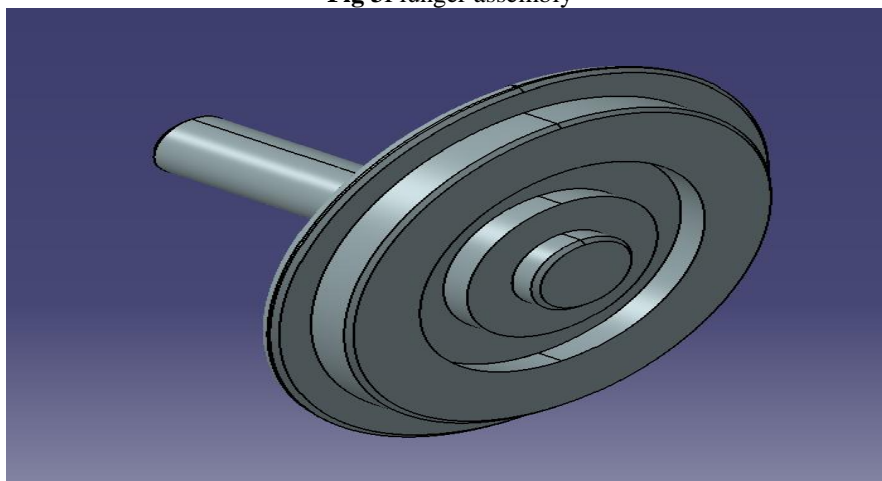
Fig 4 Base flange
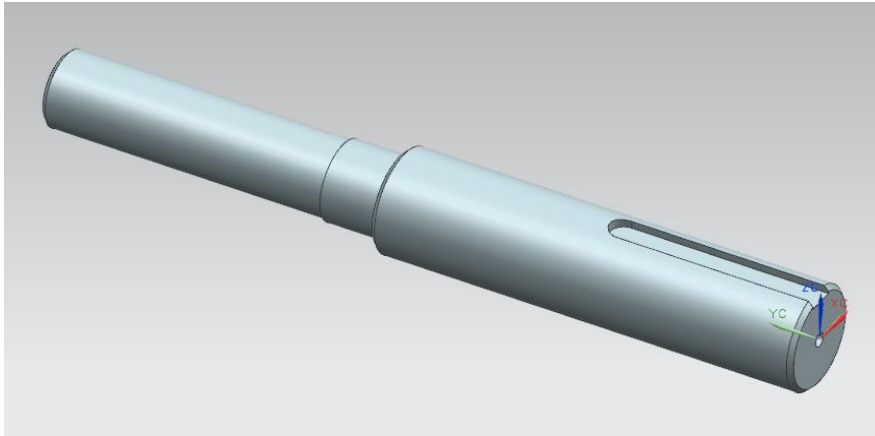
Fig 5 Shaft

5.2 FEA model by using ANSYS
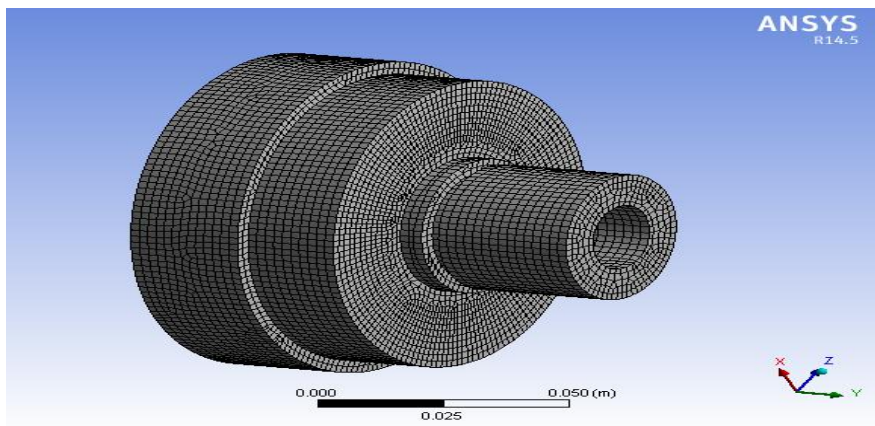
Fig 6. Meshing of Clutch body assembly
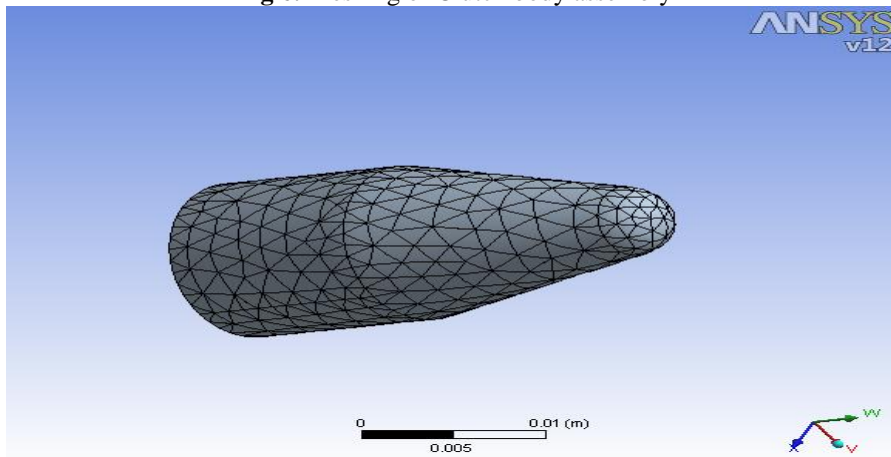
Fig 7. Meshing of plunger assembly
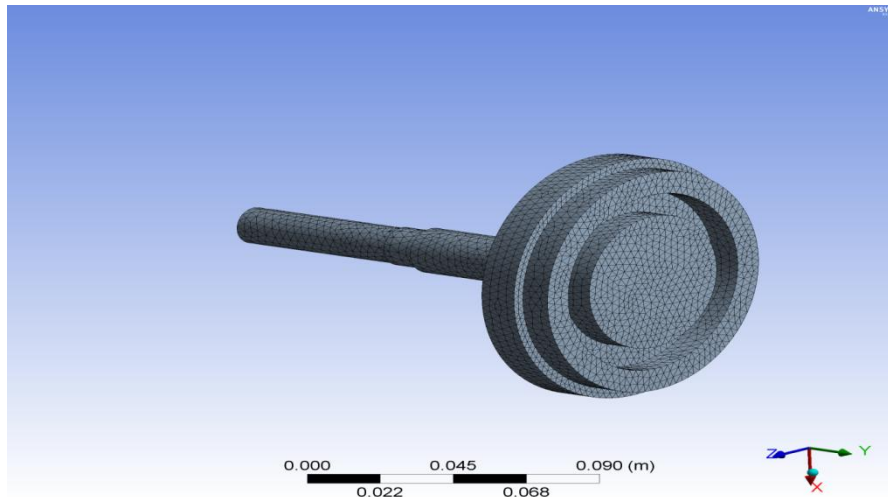
Fig 8 Meshing of flange assembly
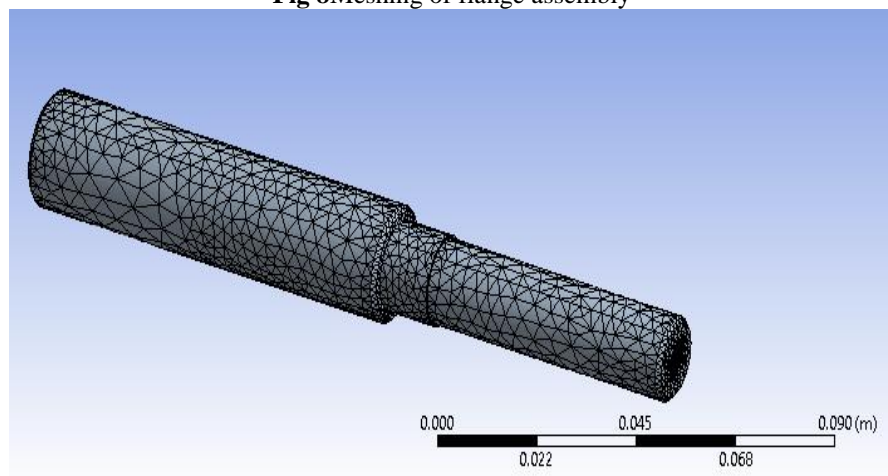
Fig 9 Meshing of shaft assembly

Meshing of all the components is done in the ansys itself. The elements are used for meshing is Solid 148.

5.3 Procedure for Static structural analysis in ANSYS:
Following is the procedure of actual analysis of individual part in torque limiter timer belt pulley.

Part 1: Test rig
The static analysis of base flange is done by means ANSYS Workbench 14.5.7 following are important steps which carried during the analysis
Step 1- First of all it is necessary to select the analysis type from main menu i.e. static structural analysis. After that we have use drag and drop option in order import the base flange to apply the material properties.
Step 2- In this step we have to call the existing model of Test rig ANSYS Workbench.
Step 3- The most important step is to enter into the analysis window by double clicking on geometry icon.
Step 4- The object which calls in step number 3 is followed by the boundary condition, constraints and mesh tool.
Step 5- To mesh the import model we have to define the method of meshing, size of meshing and element size of mesh.
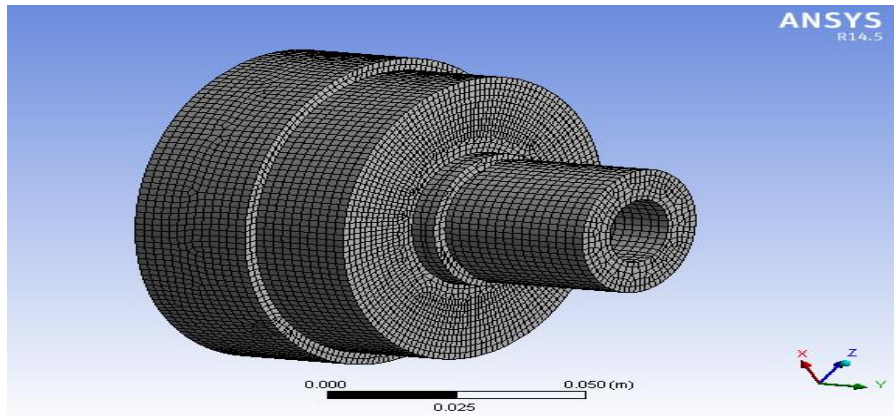
Fig 10. Mesh Test rig

Step 6

Now we have to apply the boundary condition like fixed support, force, moment. In this step we fix the outer end of Test rigand apply the moment on extreme end of Test rig
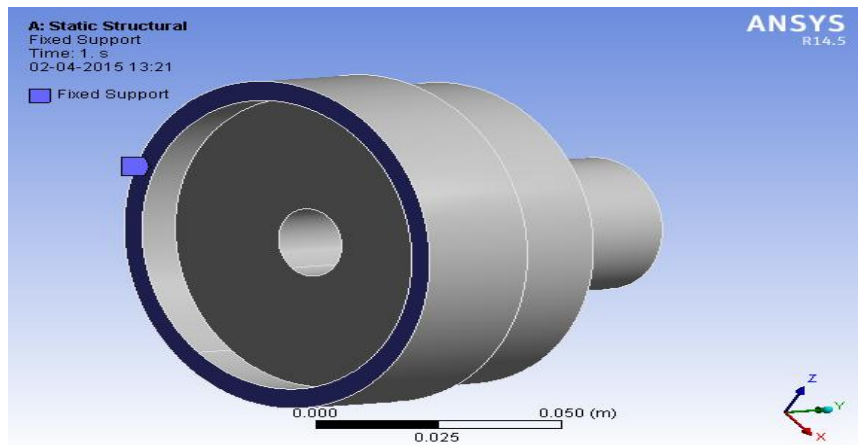
Fig 11 Fix support at outer end of Test rig
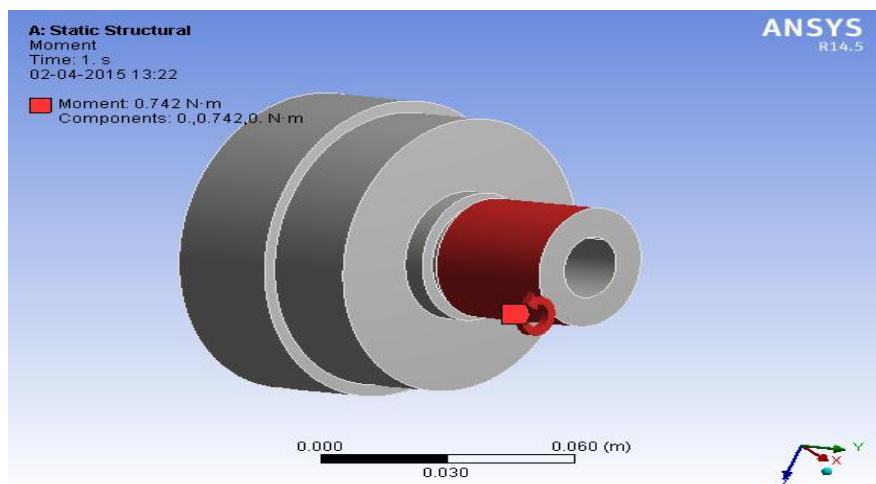
Fig 12. Moment at Extreme end of Test rig

Step 7

We have to insert the actual parameters that we want like Von Misses stress. Now solve this analysis by considering the above stress at each node of the Test rig and it gives the maximum and minimum value of maximum shear stress regarding static analysis of Test rig. This value of von misses stress executes the safe and failure region in the Test rig.
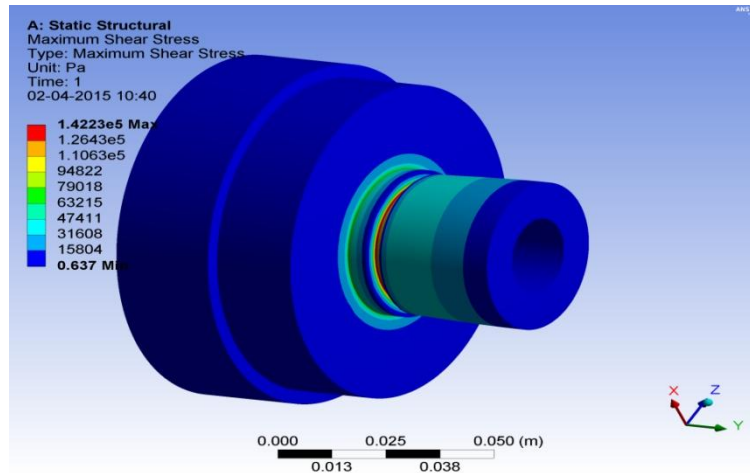
Fig 13 Maximum shear stress

Similarly just like above model we are applying all for seven steps for other models in order to tabulate our results and following table shows Number of Nodes and Elements for Meshing.

Sr.No	Name of components	Number of Nodes	Number of Element
1	Test Rig	239095	65233
2	Plunger	34365	23891
3	Base Flange	42453	28216
4	Output Shaft	25125	16509

Table1. Number of Nodes and Elements for Meshing.

Part 2: plunger
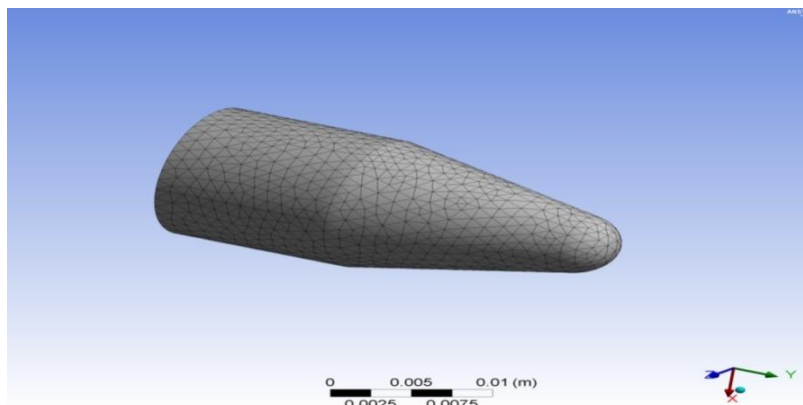
Fig 14 Meshing of plunger
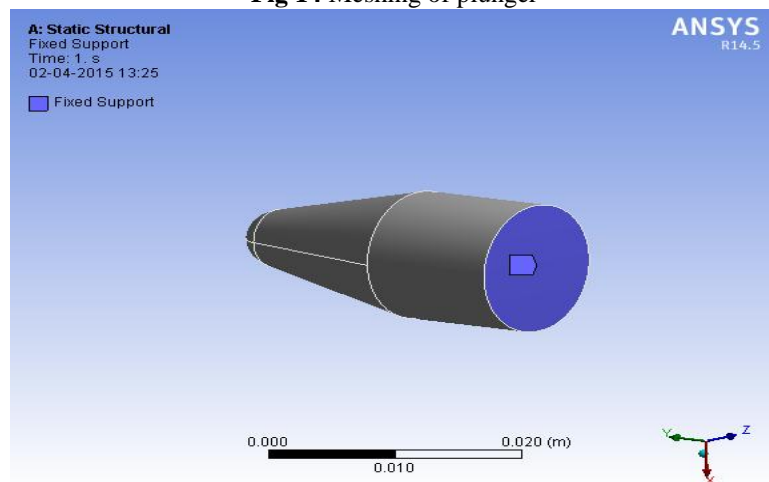
Fig 15 Fixed supports to plunger end
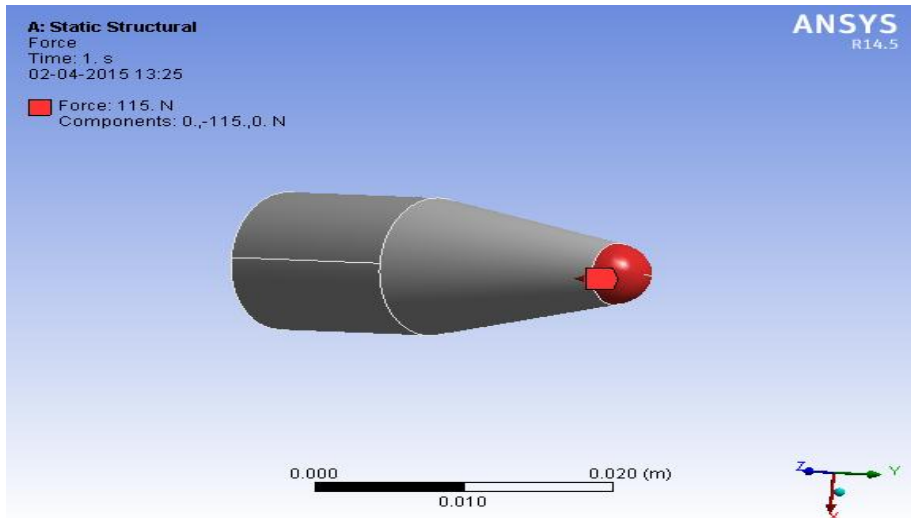
Fig 16 Application of force to plunger
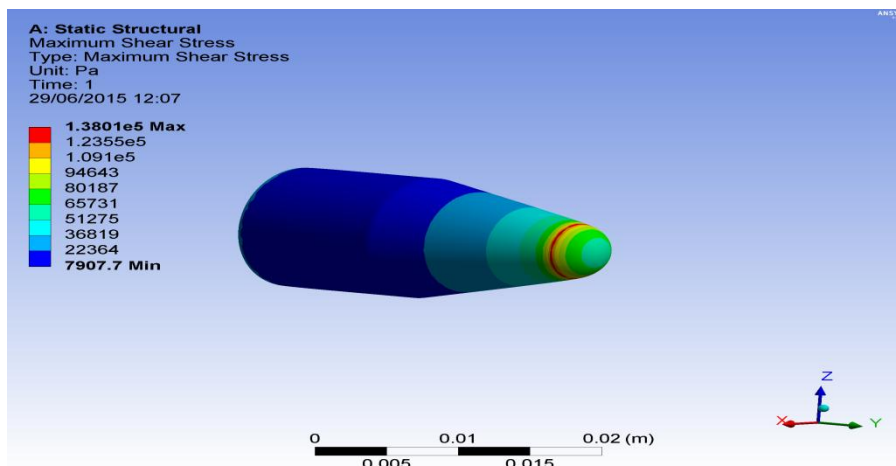
Fig 17 Maximum shear stress on plunger

Part 3: output shaft
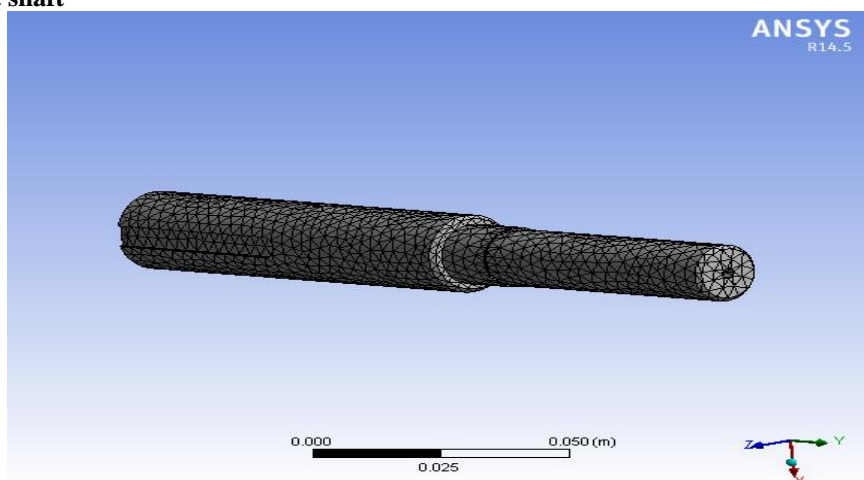
Fig 18 Meshing of output shaft
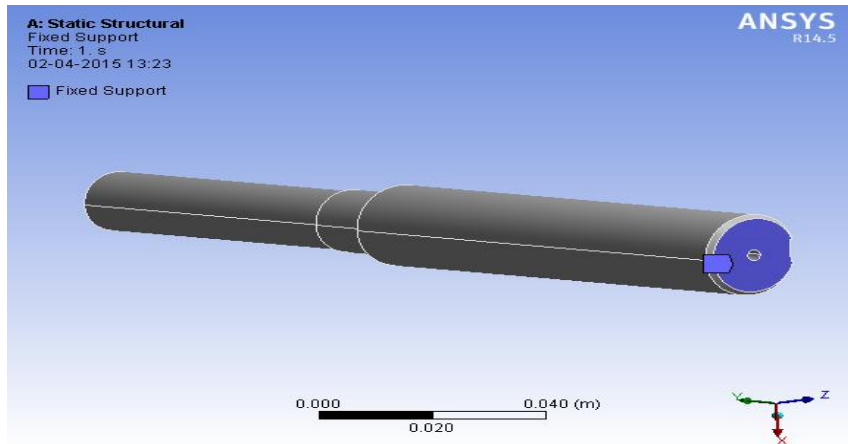
Fig 19 Fixed supports to output shaft
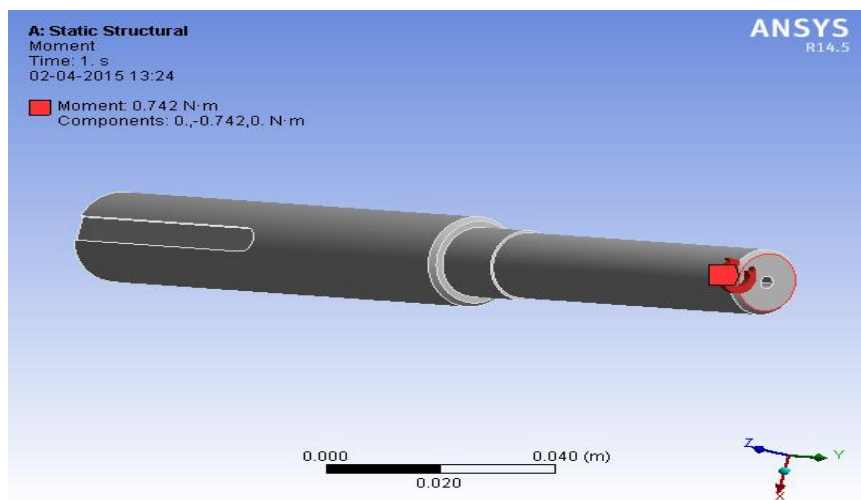
Fig 20 Application of Moment to output shaft
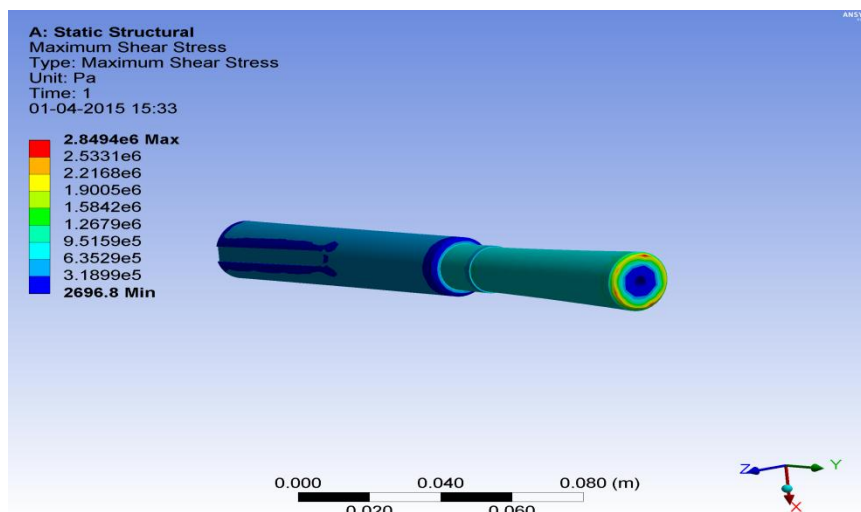
Fig 21 Maximum shear stress on output shaft

Part 4: Base Flange
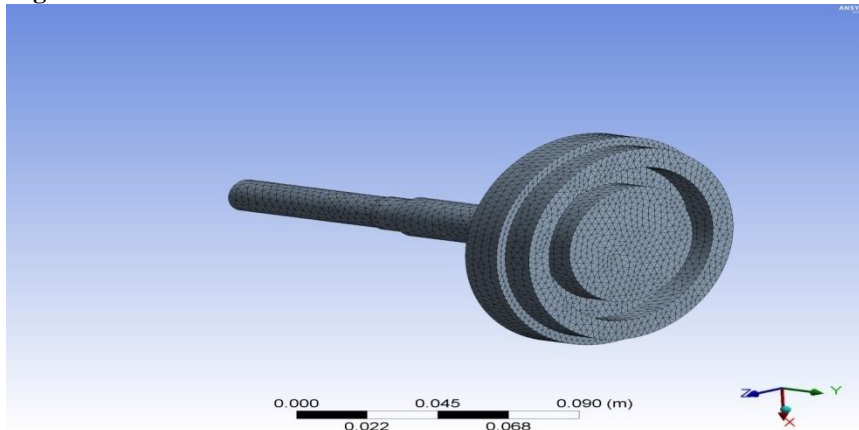
Fig 22 Meshing of Base Flange
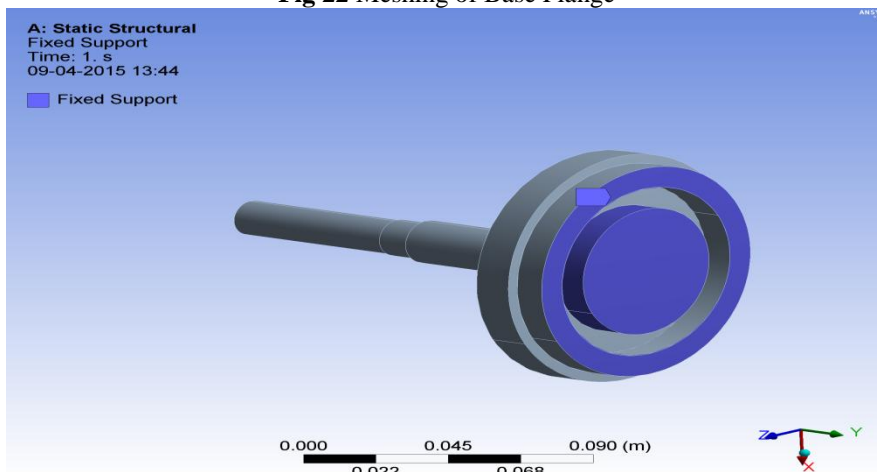
Fig 23 Fixed supports to Base flange
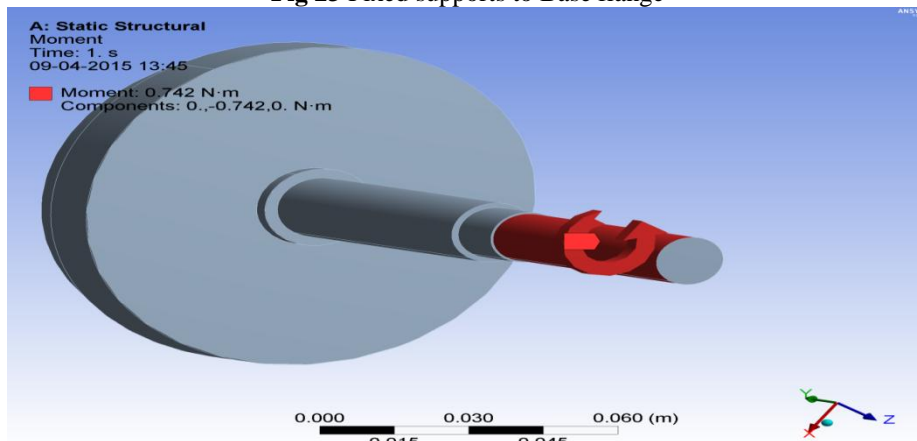
Fig 24 Application of Moment to Base flange
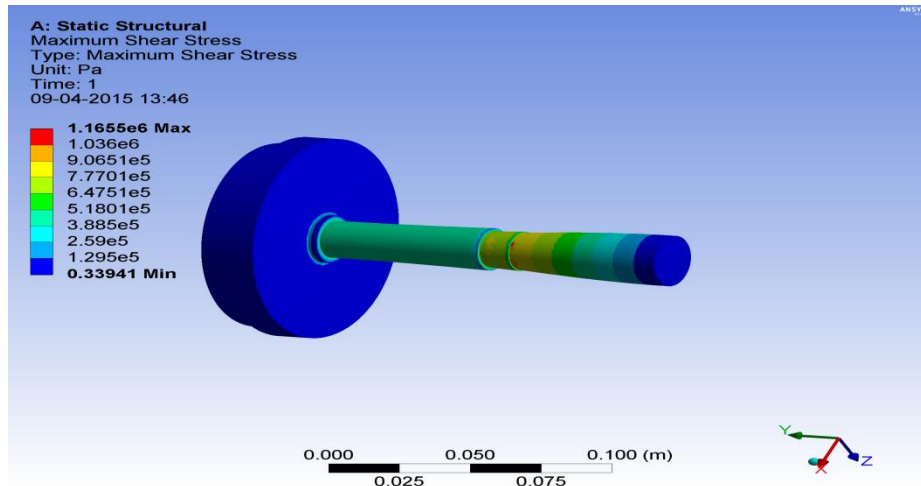
Fig 25 Maximum shear stress on Base flange

VI.   RESULTS AND DISCUSSION

By tabulating theoretical data and FEM analysis we conclude that the obtained results of each component that is maximum shear stress can be tabulate by considering following table for each component.

6.1 For Test Rig

Maximum shear stress	Allowable shear stress(consider Factor of safety 10)	Actual shear stress(By calculation)	Shear stress in ANSYS
700 x 10^6N/m^2	90×10^6 N/m^2	75.95×10^3 N/m^2	1.42x10^5 N/m^2

6.2 For output shaft

Maximum shear stress	Allowable shear stress(consider Factor of safety 10)	Actual shear stress(By calculation)	Shear stress in ANSYS
900 x 10^6N/m^2	90×10^6 N/m^2	922.6×10^3 N/m^2	2.489x10^6N/m^2

6.3 For plunger

Maximum shear stress	Allowable shear stress(consider Factor of safety 10)	Actual shear stress(By calculation)	Shear stress in ANSYS
700 x 10^6N/m^2	70×10^6N/m^2	866.4 x10^3N/m^2	1.3801 x 10^5N/m^2

6.4 For Base flange

Maximum shear stress	Allowable shear stress(consider Factor of safety 10)	Actual shear stress(By calculation)	Shear stress in ANSYS
700 x 10^6N/m^2	70×10^6N/m^2	866.4 x10^3N/m^2	1.165x10^6 N/m^2

VII.   EXPERIMENTATION OF TORQUE LIMITER.

7.1 Introduction of experimentation of Torque Limiter.

A part of static analysis gets completed in previous chapter and it gives result related with maximum shear stress of each component. In order to analyse efficiency of Torque limiter and value of maximum shear stress at maximum load i.e. 1 KG on the available model at company workshop. With the help of this model different characteristics like Load vs. speed Characteristics and efficiency vs. load Characteristics are obtain on test set up.

Fig 27 Experimental setup of Torque limiter assembly

7.2 Procedure followed during the testing on the setup

- Make all necessary connection in order to start the set up.
- Start motor by turning electronic speed variation knob.
- Let mechanism run & stabilize at certain speed (say 1300 rpm)
- Place the pulley cord on pulley and add 100 gm weight into the pan and note down the output speed for this load by means of tachometer.
- Similarly add another 100 gm weight in pan and observed the reading & take reading accordingly.
- Same step are followed by adding a different weight in the pan and note down all readings.
- Tabulate the readings in the observation table.
- Plot load vs. speed characteristic and Efficiency vs. load characteristic.
- Once the observation table is form then calculate the value of efficiency along with maximum shear stress by taking the respective dimension of components and maximum load acting on the shaft i.e. 1 kg means 9.81 N which is acting on the output shaft. So our calculation can be categorised in two parts.

7.3 Calculation of Efficiency of Torque Limiter assembly during various loading condition- Following table indicates speed variation according to load application and it considers a condition of loading and unloading respectively.

Sr.No	Loading		Unloading		Mean Speed (rpm)
	Weight (gm)	Speed (rpm)	Weight (gm)	Speed (rpm)	
1	100	2100	100	2100	2100
2	150	1820	150	1820	1820
3	200	1680	200	1680	1680
4	250	1540	250	1540	1540
5	300	1400	300	1400	1400
6	350	1260	350	1260	1260
7	500	840	500	840	840
8	600	700	600	700	700
9	700	560	700	560	560
10	800	420	800	420	420
11	1000	280	1000	280	280

Table 1 Observation Table

7.4 Sample Calculations: - (AT 0.6 kg Load)

Calculation of Average Speed:-

- $N = (N_1 + N_2)/2$

- $N = (650 + 650)/2$

- $N = 650$ rpm

Calculation of Output Torque:-

- T_{dp} = Weight in pan x Radius of Pulley

- $T_{dp} = (0.6 \times 9.81) \times 37.5$

- $T_{dp} = 202.725$ N.mm

- $T_{dp} = 202.75$ N.mm

Input Power:- ($P_{i/p}$)

- $P_{i/p} = (2 \Pi N T_{i/p})/60$

- $P_{i/p} = (2 \times \Pi \times 850 \times 0.225)/60$

➢ $P_{i/p} = 20.27$ watt

Output Power:-($P_{o/p}$)

➢ $P_{o/p} = (2 \, \Pi \, N \, T_{o/p})/60$

➢ $P_{o/p} = (2 \times \Pi \times 850 \times 0.203)/60$
➢ $P_{o/p} = 18.06$ watt

Calculation of Efficiency:-

➢ Efficiency = (Output power) / (Input power)

➢ Efficiency = (18.06 x 100) / 20.27

➢ Efficiency = 89 %

➢ **Efficiency of transmission of Torque Tender = 89%**

7.5 Result Table

Sr. No	Load (gms)	Speed(rpm)	Torque(N.M)	Power (watt)	Efficiency
1.	100	2100	0.036788	11.1760425	55.32694
2.	150	1820	0.055181	11.1760425	55.32694
3.	200	1680	0.073575	13.3048125	65.86541
4.	250	1540	0.091969	15.2055	75.27475
5.	300	1400	0.110363	14.25515625	89.09473
6.	350	1260	0.128756	13.97005313	87.31283
7.	500	840	0.183938	15.39556875	96.2223
8.	600	700	0.220725	14.8253625	92.65852
9.	700	560	0.257513	14.23614938	88.97593
10.	800	420	0.2943	15.81372	98.83575
11.	100	280	0.367875	14.445225	90.28266

Table No 2 Result table

7.6 Different characteristics of Load vs. speed and Efficiency vs. load.

7.6.1 Load Vs. Speed characteristics –
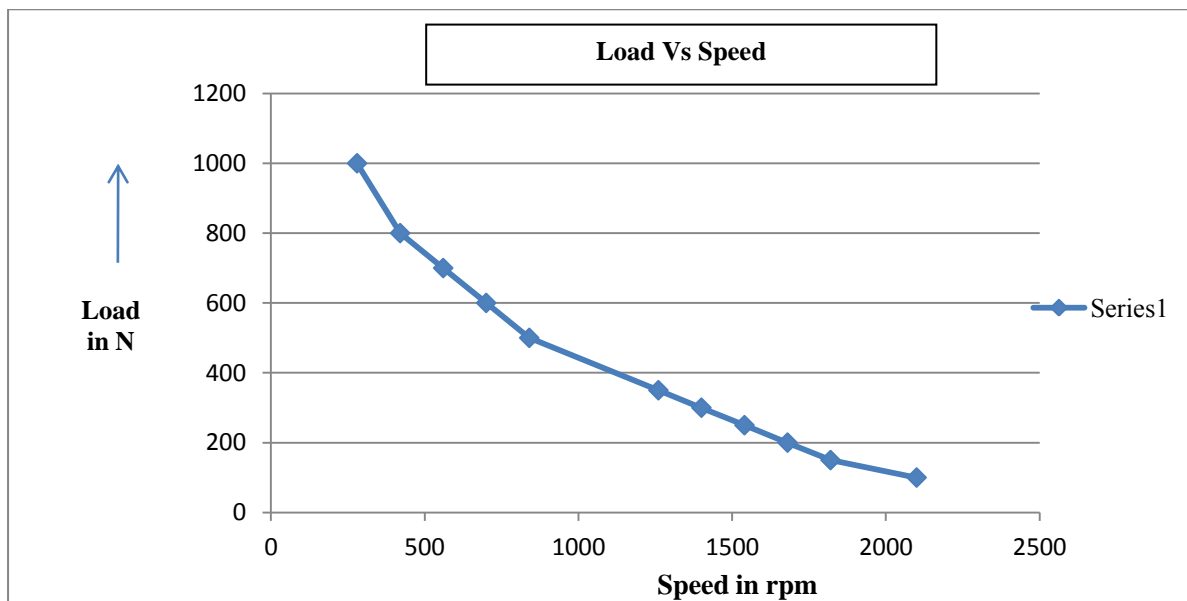
Graph No 1 Load vs. Speed characteristics

Above characteristic is obtained by plotting a graph by taking load on Y axis and speed on X axis respectively. The following graph indicates as load increasing on the output shaft then speed torque limiter gets decreases. In this case load taking on Y axis is in Newton and speed is in revolution per minute. Following figure indicates Load Vs. Speed characteristics.

7.6.2   Efficiency vs. Load characteristics –
Following characteristic is obtained by plotting a graph by taking load on X axis and efficiency on Y axis respectively. The following graph indicates when torque limiter are subjected to higher load then torque limiter are work very efficiently which clearly indicates in figure.

Efficiency Vs. Load characteristics –
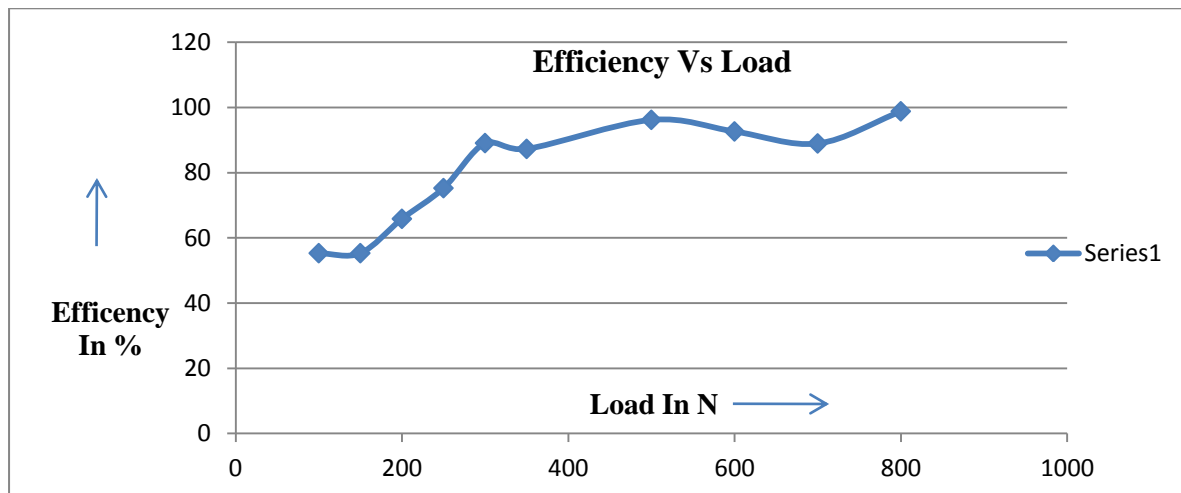
Graph No 2 Efficiency Vs. Load characteristics

VIII.   CONCLUSIONS
- Excess load acting on output shaft can be reduced by Design and Analysis of Torque Limiter Timer Belt Spindle Drive for Overload Protection.
- The torque carrying capacity can be obtained by varying three number of Ball & spring sets.
- With the help of Integration of the timer pulley set and torque limiter to form final drive system can be achieved.
- In this way stalling of motor can be avoided by design and development of torque limiter.

REFERENCES
[1]   I. Stroe.,Transilvania University Brasov, Romania. "Design Procedure of Elastic And Safety Clutches using Cam Mechanisms",12thIFToMM World Congress France.
[2]   Stroe Lone., "Elastic and safety clutches with intermediate rubber elements", Annals of the Oradea University Fascicle of Management and Technological Engineering, Volume IX (XIX), 2010, NR1.
[3]   NicolaeEftiimie., "Dynamic simulation of the safety clutches with ball", Faculty of Technical Science, Novi Sad. I. Stroe., Transilvania University Brasov, Romania.
[4]   [Guy James Burlington, Stroud (GB) "Clutch Mechanism" United states patents, Patent No.US 7,731,618 B2.
[5]   Neal I. "Simple Mechanical Clutch with Multiple Functions". In: Proceedings of SYROM 2009, pp. 433-438. I. Visa (Ed) Springer (2009).
[6]   PSG design data book.
[7]   William Silver, Grafton, MA (US) "Torque Limiter "United States patents, Patent No. US 8,083,596 B1.

Research Paper   Open Access

Reliability Analysis of Car Maintenance Forecast and Performance

[1,] Owhor, Sampson Chisa, [2,] Abdul Alim Ibrahim Gambo, [3,] Ojo, Victor Kayode, [4,] Dan'azumi Daniel

[1,] *Mechanical Engineering, Faculty of Engineering/ Federal University Wukari, Taraba State, Nigeria.*

[2,] *Department of Chemical and Biomedical Engineering, Federal University Wukari,Taraba State, Nigeria.*

[3, 4,] *Works & maintenance Department/ Federal University Wukari,Taraba State*

ABSTRACT: *In reliability analysis of car maintenance forecast and performance, researchers have mostly dealt with problems either without maintenance or with deterministic maintenance when no failure can occur. This can be unrealistic in practical settings. In this work, a statistical model is developed to evaluate the effect of predictive and preventive maintenance schemes on car performance in the presence of system failure where the forecasting objective is to minimize schedule duration. It was shown that neither method is clearly superior, but the application of each depends on the forecast environment itself. Furthermore, we showed that parameter values can be chosen for which preventive maintenance perform better than predictive maintenance. The result provided in this study can be helpful to practitioners and system machine administrators, fairplus transport company in Rivers State and works and maintenance department, federal university wukari, taraba state, Nigeria.*

KEYWORDS: *Car maintenance, Reliability analysis, Mean Time to failure, Performance, Weibull probability*

I.   INTRODUCTION

The origins of the field of reliability engineering, at least the demand for it, can be traced back to the point at which man began to depend upon machines for his livelihood. The Noria, for instance, is an ancient pump thought to be the world's first sophisticated machine. Utilizing hydraulic energy from the flow of a river or stream, the Noria utilized buckets to transfer water to troughs, viaducts and other distribution devices to irrigate fields and provide water to communities. If the community Noria failed, the people who depended upon it for their supply of food were at risk. Survival has always been a great source of motivation for reliability and dependability.

While the origins of its demand are ancient, reliability engineering as a technical discipline truly flourished along with the growth of commercial aviation following World War II. It became rapidly apparent to managers of aviation industry companies that crashes are bad for business. Karen Bernowski, editor of *Quality Progress*, revealed in one of her editorials research into the media value of death by various means, which was conducted by MIT statistic professor Arnold Barnett and reported in 1994.

Reliability engineering deals with the longevity and dependability of parts, products and systems. More poignantly, it is about controlling risk. Reliability engineering incorporates a wide variety of analytical techniques designed to help engineers understand the failure modes and patterns of these parts, products and systems. Traditionally, the reliability engineering field has focused upon product reliability and dependability assurance. In recent years, organizations that deploy machines and other physical assets in production settings have begun to deploy various reliability engineering principles for the purpose of production reliability and dependability assurance.

Increasingly, production organizations deploy reliability engineering techniques like Reliability-Centered Maintenance (RCM), including failure modes and effects (and criticality) analysis (FMEA,FMECA), root cause analysis (RCA), condition-based maintenance, improved work planning schemes, etc. These same organizations are beginning to adopt life cycle cost-based design and procurement strategies, change management schemes and other advanced tools and techniques in order to control the root causes of poor reliability. However, the adoption of the more quantitative aspects of reliability engineering by the production reliability assurance community has been slow. This is due in part to the perceived complexity of the techniques and in part due to the difficulty in obtaining useful data.

The quantitative aspects of reliability engineering may, on the surface, seem complicated and daunting. In reality, however, a relatively basic understanding of the most fundamental and widely applicable methods can enable the plant reliability engineer to gain a much clearer understanding about where problems are occurring, their nature and their impact on the production process – at least in the quantitative sense. Used properly, quantitative reliability engineering tools and methods enable the plant reliability engineering to more effectively apply the frameworks provided by RCM, RCA, etc., by eliminating some of the guesswork involved with their application otherwise. However, engineers must be particularly clever in their application of the methods because the operating context and environment of a production process incorporates more variables than the somewhat one-dimensional world of product reliability assurance due to the combined influence of design engineering, procurement, production/operations, maintenance, etc., and the difficulty in creating effective tests and experiments to model the multidimensional aspects of a typical production environment.

Despite the increased difficulty in applying quantitative reliability methods in the production environment, it is nonetheless worthwhile to gain a sound understanding of the tools and apply them where appropriate. Quantitative data helps to define the nature and magnitude of a problem/opportunity, which provides vision to the reliability in his or her application of other reliability engineering tools. This article will provide an introduction to the most basic reliability engineering methods that are applicable to the plant engineer that is interested in production reliability assurance. It presupposes a basic understanding of algebra, probability theory and univariate statistics based upon the Gaussian (normal) distribution e.g. measure of central tendency, measures of dispersion and variability, confidence intervals, etc. (Krishnamoorthi,1992; Dovich,1990).

1.1 *Basic mathematical concepts in reliability engineering*
Many mathematical concepts apply to reliability engineering, particularly from the areas of probability and statistics. Likewise, many mathematical distributions can be used for various purposes, including the Gaussian (normal) distribution, the log-normal distribution, the Rayleigh distribution, the exponential distribution, the Weibull distribution and a host of others. For the purpose of this brief introduction, we'll limit our discussion to the exponential distribution and the Weibull distribution, the two most widely applied to reliability engineering. In the interest of brevity and simplicity, important mathematical concepts such as distribution goodness-of-fit and confidence intervals have been excluded.

In car maintenance forecast and performance control, good bounds are available for the problem of minimizing schedule durations or the make span provided the worst-case bound for the approximation algorithm, Longest Processing Tim and improved bound using the heuristic by combining these were able to obtain an even tighter bound Graham, R.L(1969). These studies, however, assumed the continuous availability of machines, which may not be justified in realistic applications where machines can become unavailable due to deterministic or random reasons.

It was not until the late 1980's that research was carried out on machine scheduling with availability constraints. Some study considered the problem of parallel machine scheduling with non-simultaneous available time while some discussed various performance measures and machine environments with single unavailability. For each variant of the problem, a solution was provided using a polynomial algorithm. Turkcan, A (1999) analyzed the availability constraints for both the deterministic and stochastic cases. Chen,T et al (1999) conducted a study on scheduling the maintenance on a single-machine. Lee,C.Y and Liman,S.D (1929) studied single-machine flow-time scheduling with maintenance while attempted to minimize the total weighted completion time in two machines with maintenance. Schmidt,G(1988) discussed general scheduling problems with availability constraints, taking into account different release and due dates in a recent work.

1.2   Failure rate and mean time between/to failure (MTBF/MTTF)
The purpose for quantitative reliability measurements is to define the rate of failure relative to time and to model that failure rate in a mathematical distribution for the purpose of understanding the quantitative aspects of failure. The most basic building block is the failure rate, which is estimated using the following equation:

$$\lambda = r/T$$

Where:
λ = Failure rate (sometimes referred to as the hazard rate)
T = Total running time/cycles/miles/etc. during an investigation period for both failed and non-failed items.
r = The total number of failures occurring during the investigation period.

For example, if five electric motors operate for a collective total time of 50 years with five functional failures during the period, the failure rate is 0.1 failures per year.

Another very basic concept is the mean time between/to failure (MTBF/MTTF). The only difference between MTBF and MTTF is that we employ MTBF when referring to items that are repaired when they fail. For items that are simply thrown away and replaced, we use the term MTTF. The computations are the same.

The basic calculation to estimate mean time between failure (MTBF) and mean time to failure (MTTF), both measures of central tendency, is simply the reciprocal of the failure rate function. It is calculated using the following equation.

$$\theta = T/r$$

Where:
θ = Mean time between/to failure
T = Total running time/cycles/miles/etc. during an investigation period for both failed and non-failed items.
r = The total number of failures occurring during the investigation period.

The MTBF for our industrial electric motor example is 10 years, which is the reciprocal of the failure rate for the motors. Incidentally, we would estimate MTBF for electric motors that are rebuilt upon failure. For smaller motors that are considered disposable, we would state the measure of central tendency as MTTF.

The failure rate is a basic component of many more complex reliability calculations. Depending upon the mechanical/electrical design, operating context, environment and/or maintenance effectiveness, a machine's failure rate as a function of time may decline, remain constant, increase linearly or increase geometrically (Figure 1).
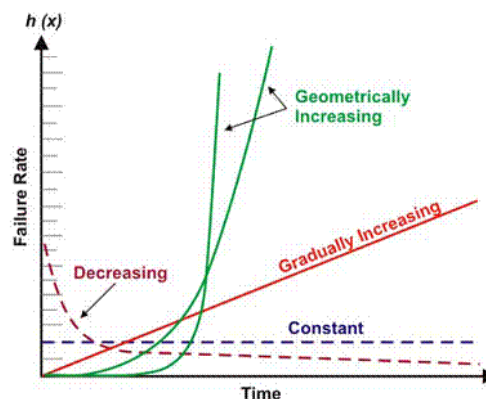
Depending upon machine type, the failure rate may
decrease, remain constant, gradually increase or
geometrically increase as a function of time
Figure 1. Different Failure Rates vs. Time Scenarios

II.   THE 7 STEPS FOR IMPLEMENTING RELIABILITY CANTERED MAINTENANCE (RCM)

There are several different methods for implementing RCM that are recommended by different organizations. In general, however, they can be summarized by the following 7 steps.

Step 1: Selection of equipment for RCM analysis

The first step is to select equipment for RCM analysis. The equipment selected for RCM should be critical, in terms of its effect on operations, its previous costs of repair and previous costs of preventative maintenance.

Step 2: Define the boundaries and function of the systems that contain the selected equipment

The equipment belongs in a system that performs a function that is important to the process. The system can be as large or small as necessary, but the function of the system should be known as should its inputs and outputs. For example, the function of a conveyor belt system is to transport goods. Its inputs are the goods and mechanical energy powering the belt, while its outputs are the goods at the other end. In this case, the electric motor supplying the mechanical energy would be considered as part of a different system.

Step 3: Define the ways that the system can fail - the failure modes

In step 3 the object is to list all of the ways that the function of the system can fail. In the case of the conveyor belt it can fail by being unable to transport the goods from one end to the other, or it can fail if it does not transport the goods sufficiently quickly.

Step 4: Identify the root causes of the failure modes

With the help of operators, experienced technicians, RCM experts and equipment experts, the root causes of each of the failure modes can be identified. Root causes for failure of the conveyor could include a lack of lubrication on the rollers, a failure of a bearing, or an insufficiently tight belt.

Step 5: Assess the effects of failure

In this step the effects of each failure mode are considered. The effects include the effects on safety, operations and other equipment. Criticality of each of these failure modes can also be considered.
There are various recommended techniques that are used to give this step a systematic approach. These include:
1. Failure, mode and effects Analysis (FMEA)
2. Failure, mode, effect and criticality analysis
3. Hazard and operability studies (HAZOPS)
4. Fault tree analysis (FTA)
5. Risk-based inspection (RBI)

The most important failure modes will be determined at the conclusion of the systematic analysis of each failure mode. This will be determined by asking questions such as "Does this failure mode have safety implications", and "Does this failure mode result in a full or partial outage of operations?". It is these important failure modes that are then prioritized for further analysis. Importantly, the failure modes that are retained include only those that have a real probability of occurring under realistic operating conditions.

Step 6: Select a maintenance tactic for each failure mode

At this step, the most appropriate maintenance tactic for each failure mode is determined. Importantly, the maintenance tactic that is selected has to technically and economically feasible.

Condition Based Maintenance is selected when it is technically and economically feasible to detect the onset of the failure mode.

Time or Usage Based **Preventative Maintenance** is selected when it is technically and economically feasible to reduce the risk of failure using this method.

For failure modes that do not have satisfactory condition based maintenance or preventative maintenance options, then a redesign of the system to eliminate or modify the failure mode should be considered.

Failure modes that were not identified as being critical in Step 6 may, at this stage, be identified as good candidates for a **run-to-failure maintenance** schedule.

Step 7: Implement and then regularly review the maintenance tactic that is selected.

Importantly, the RCM methodology will only be useful if its maintenance recommendations are put into practice. When that has been done, it is important that the recommendations are constantly reviewed and renewed as additional information is found.

III.   METHODOLOGY AND PROCEDURE

Data were collected from a private transport company that faced a problem in reliability analysis of car maintenance forecast and performance. Firstly, the data were analyzed, and rearranged according to the car systems (brake, fuel pump, tyres, Alignment and cooling systems respectively) and according to the common troubleshooting method followed as shown in the figures 2, 4, 6, 8 and 10. Secondly, the traditional standard maintenance technique that is used in car maintenance companies and machine maintenance was applied to choose the best statistical analysis approach. In analyzing the collected data, the Weibull distribution was selected and applied according to several characteristics that make Weibull distribution the best distribution method to be used for these data.

The primary advantage of Weibull analysis is the ability to provide reasonably accurate failure analysis and failure forecasts with extremely small samples. Another advantage of Weibull analysis is that it provides a simple and useful graphical plot. The data plot is extremely important to the engineers and others. Many statistical distributions were used to model various reliability and maintainability parameters. Whether to use one distribution or another is highly depending on the nature of the data being analyzed. Some commonly used statistical distributions are: 1. Exponential and Weibull. These two distributions are commonly used for reliability modeling – the exponential is used because of its simplicity and because it has been shown in many cases to fit electronic equipment failure data. On the other hand, Weibull distribution is widely used to fit reliability and maintainability models because it consists of a family of different distributions that can be used to fit a wide variety of data and it models, mainly wear out of systems (i.e., an increasing hazard function) and in electronic equipment failures, 2. Tasks that consistently require a fixed amount of time to complete with little variation. The lognormal is applicable to maintenance tasks where the task time and frequency vary, which is often the case for complex systems and products.

IV.   RESULTS AND DISCUSSION

The aim of using the traditional technique for car maintenance is to calculate reliability function of time R (t) of the overall system (the car). This was done by calculating R (t) for each subsystem in the car parallel to the other.

For calculating the reliability function R (t) for each system, the collected data were converted from Mean Distance to Failure (MDTF) to Mean Time To Failure (MTTF). This is because the reliability function which was used in this study is a function of time, where the reliability decreases as time increases. Hence, the Unreliability function F (t) increases as time increases, which lead to the logic relation, show in equation 1

F (t) + R (t) = 1.0 ………………………………………………….equ (1)

R (t), MTTF and the mean failure rate (λ) were calculated for each system according to the relations depicted in equation 2.

R (t) = exp (-λ x t) = exp $\left[\dfrac{-(t - t_o)}{\eta}\right]$ β …………………equ (2)

Where *t* is time, t_o is initial time, β is the slope and Ŋ is scale time parameter. By combining to Equations 1 and 2 is illustrated in equation 3.

F (t) = 1- exp (-λ x t) = 1 - exp $\left[\dfrac{-(t - t_o)}{\eta}\right]$ β ……………equ (3)

For calculating λ(t), η was calculated by setting the initial time for all subsystems equal to zero. Therefore, F(t) = (1- e^t) =0.632. Then, the unreliability function was drawn on a Weibull probability graph paper as a straight line to estimate η (scale time parameter) from the intersection of the line with the x-axis, and *β* from the slope of the line plotted for each system as shown in the figures 3, 5, 7, 9 and 11. Then, F(t) was found for each subsystem by applying Equation1. The slope of the Weibull plot, beta, (β), determines which member of the family of Weibull failure distributions best fits or describes the data. The slope, β, also indicates which class of failures is present:

β < 1.0 indicates infant mortality

β = 1.0 means random failures (independent of age)

β > 1.0 indicates wear out failures

Statistical approach was performed; and recommendations were reported to the car company to change preventive time maintenance of the company database to that obtained from statistical approach.

In addition to the above analysis, Unreliability test was made for the overall system, and this was by considering each system work separate to the other (parallel to the other), and this leading to equation 4.

$F_{system} = F_1 \times F_2 \times F_3 \times F_n$ ………………………………equ 4

For this approach, the real primitive time maintenance was found to make the car Reliable and Available every time of use and this is safe time significantly comparing to break down maintenance as in graph.

The results were divided in string way, namely breaking system, fuel pump, tyres, Alignment and cooling system.
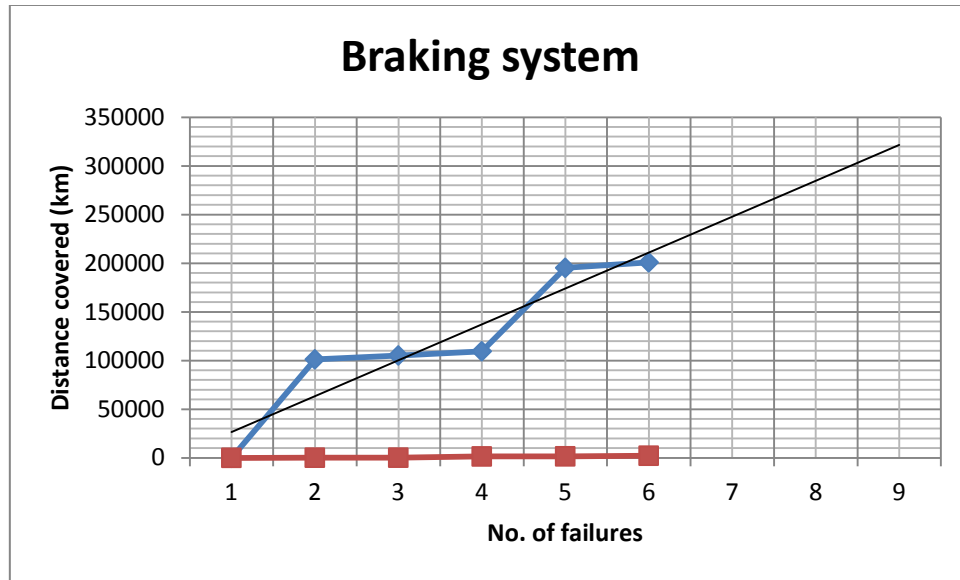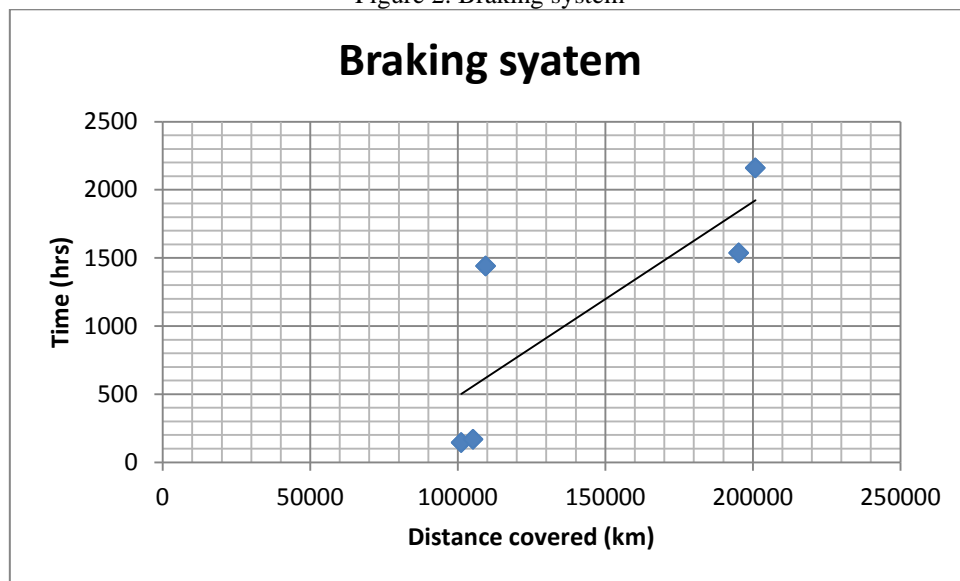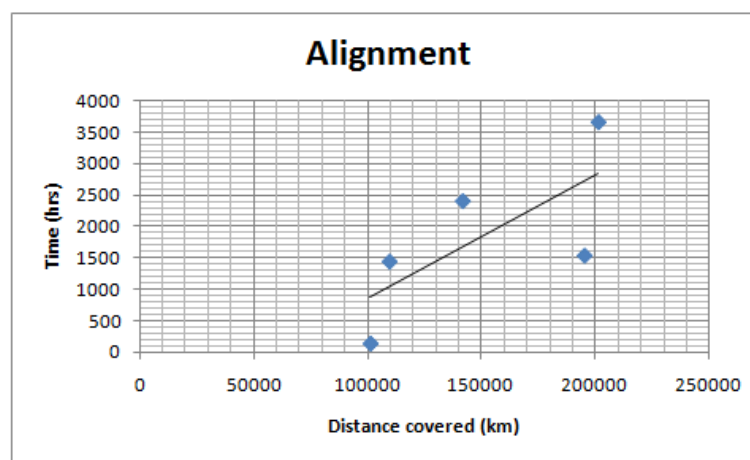

Figure 2. Braking system

Figure 3. Brake system unreliability data plotted on a Weibull probability graph

η (Scale Parameter) = 1400 hr
β from slope =1.67
Results from statistics analysis showed the following:
Total Average of Distance between Failure (Km) = 10000
Mean Time to Failure (MTTF) = 650
Failure rate model (λ) = 0.047{means very good}
Time of repairing (TOR) = 1.58 hr
Reliability Failure model (R(t)) = 1.200 (at 10 000 Km)
Un-reliability Failure model F(t) = 0.085
R(t)=.99 at Distance= 10000 Km {primitive distance from company}
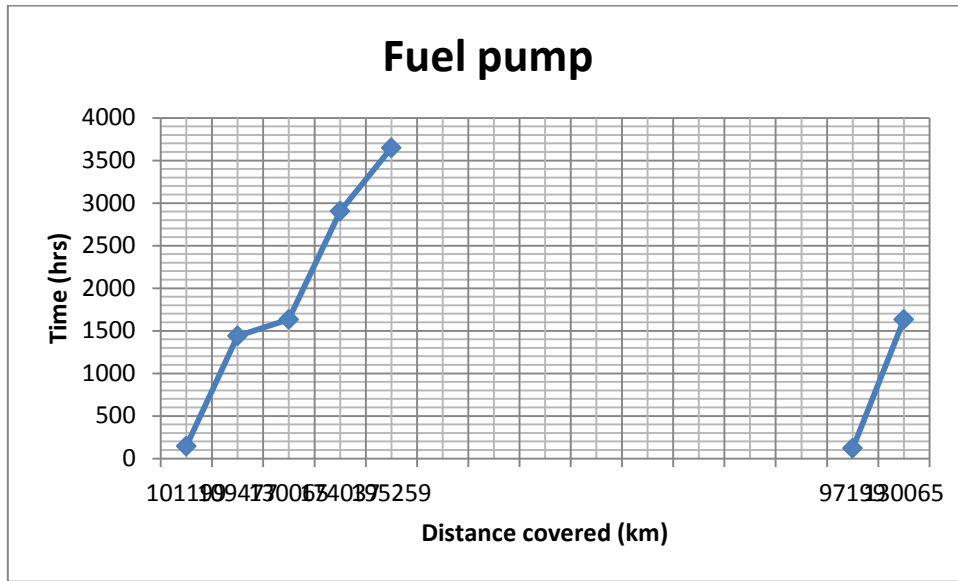
Figure 4. Fuel pump
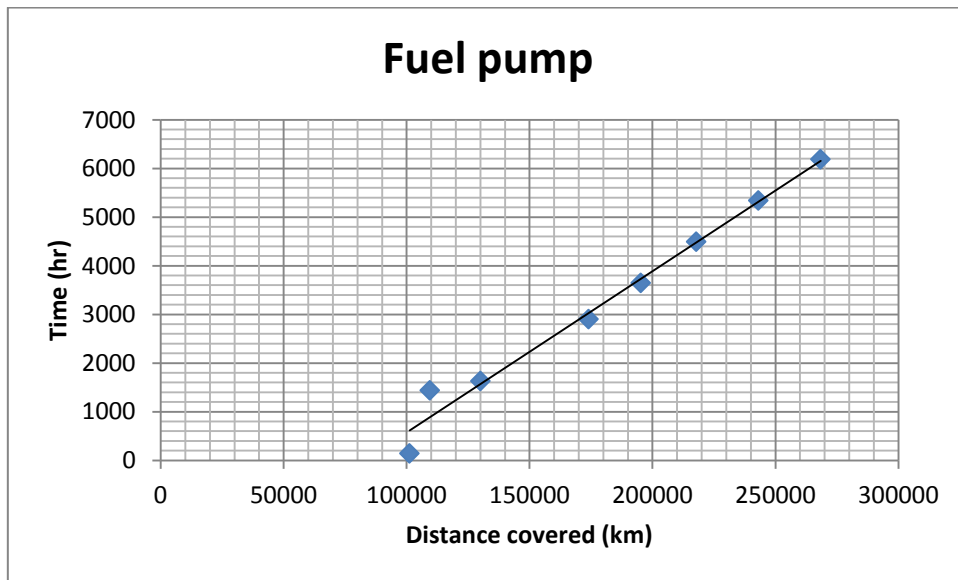
Figure 5. Fuel pump system unreliability data plotted on a Weibull probability graph

η (Scale Parameter) =4200 hr
β from slope = 4.0
Results from statistics analysis showed the following:
Total Average of Distance between Failure (Km) = 20000
Mean Time to Failure (MTTF) = 3000
Failure rate model (λ) = 0.09{means very good}
Time of repairing (TOR) = 4.4 hr
Reliability Failure model R(t) =0.978 (at 100 000 Km)
Un-reliability Failure model F(t) = 0.86
R(t)= 0.90 at Distance= 240000 Km {primitive distance from company}
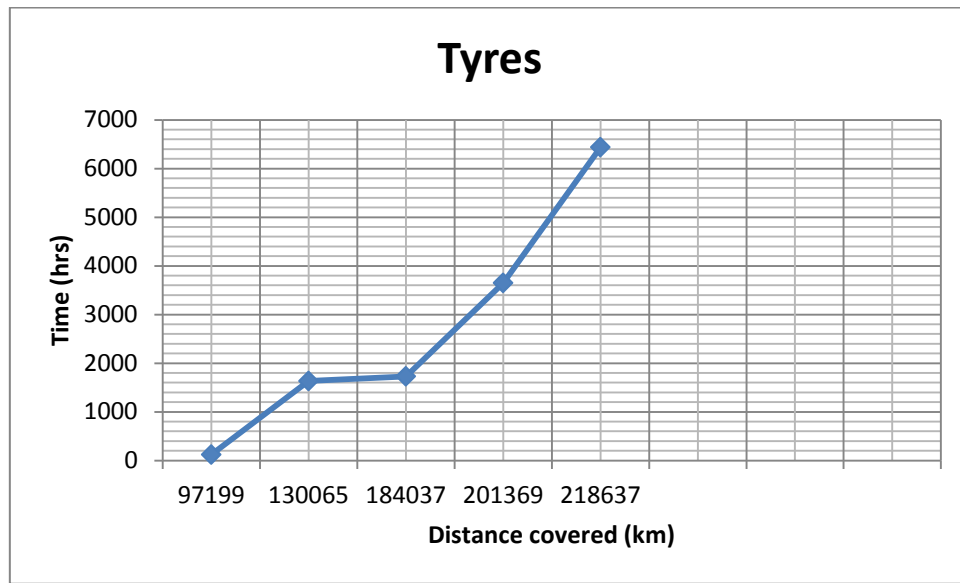
Figure 6. Tyre
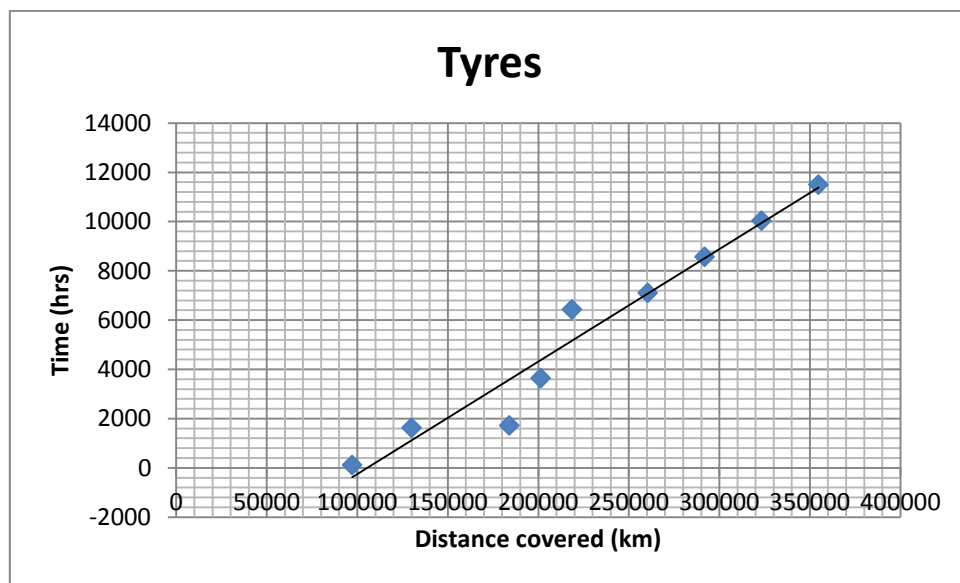
Figure 7. Tyre unreliability data plotted on a Weibull probability graph

η (Scale Parameter) = 1000 hr
β from slope = 3.5
Results from statistics analysis are as follows:
Total Average of Distance between Failure (Km) = 158000
Mean Time to Failure (MTTF) = 620
Failure rate model (λ) = 0.002808{means very good}
Time of repairing (TOR) = 1.2 hr
Reliability Failure model R(t) = 0.93 (at 200 000 Km)
Un-reliability Failure model F(t) = 0.75
R(t)=0.65 at Distance= 200000 Km {primitive distance from company}
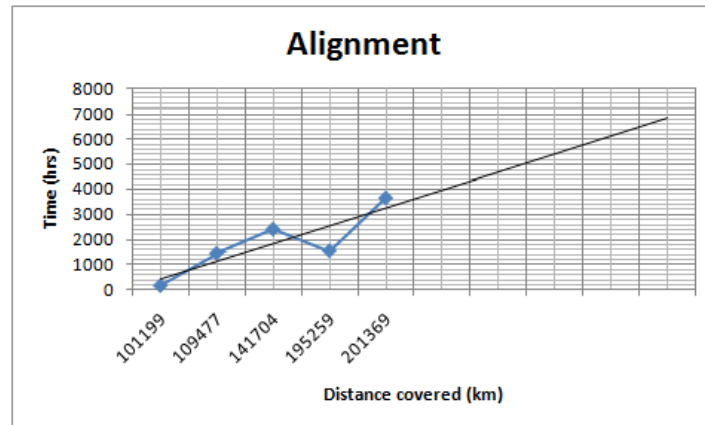
Figure 8. Alignment system

Figure 9. Alignment system unreliability data plotted on a Weibull probability graph

η (Scale Parameter) = 2400 hr
β from slope = 1.8
Results from statistics analysis are as follows:
Total Average of Distance between Failure (Km) = 1400
Mean Time to Failure (MTTF) = 1600
Failure rate model (λ) = 0.08 {means very good}
Time of repairing (TOR) = 1 hr
Reliability Failure model (R(t)) = 1.30 (at 150 000 Km)
Un-reliability Failure model F(t) = 0.067
R(t)=.80 at Distance= 100000 Km {primitive distance from company}

V.   CONCLUSION

The primitive distance specified from the company was not matching the distance calculated from the statistical analysis based on the real data collected from the work shop. It was found for most of the automobile systems, 15000 -20000km was found to perfect distance for scheduling preventive maintenance to guarantee the reliability and the availability of the automobile for operation. It was assumed that all systems work in parallel, so if one system fails then the other systems still work independently. However, if one assumed all systems to work in series then it means that the overall system configuration will fail. This is not the case in this study. The effect of corrective and preventive maintenance schemes on car performance in the presence of system failure was proven to minimize schedule duration. It was shown that neither scheme is clearly superior, but the applicability of each depends on the scheduling environment itself. Further, the undertaken research work showed that parameter values can be chosen for which preventive maintenance does better than corrective maintenance. The results provided in this study can be useful to system machine administrator in car maintenance, fairplus transporters and motor & generator unit of federal university wukari, taraba state, Nigeria.

Nomenclatures

F(t)	Unreliability function
MTTF	Mean time to failure
MDTF	Mean distance to failure
TOR	Time of repairing
R(t)	Reliability function
Ƞ	Scale time parameter
β	the slope of the weibull graph
t	Time (hr)
λ	The mean failure rate

REFERENCES

[1]. Bernowski, K (1997) "Safety in the Skies," *Quality Progress*, January.

[2]. Chen,T., Qi,X and Tu,F (1999) "Scheduling the maintenance on a single machine". Journal of the Operational Research Society, Vol. 50, pp. 1071–1078.

[3]. Coffman Jr. E.G, Garey, M.R and Johnson, D.S (1978) "An application of bin-packing to multiprocessor scheduling". SIAM Journal on Computing, Vol. 7, pp 1–17

[4]. Dovich, R. (1990) Reliability Statistics, ASQ Quality Press, Milwaukee, WI.

[5]. Graham,R.L(1969) "Bounds on multiprocessing timing anomalies". SIAM Journal of Applied Mathematics, Vol. 17, pp. 263–269.

[6]. Krishnamoorthi, K.S. (1992) Reliability Methods for Engineers, *ASQ Quality Press,* Milwaukee, WI.

[7]. Lee, C.Y. (1996) "Machine scheduling with an availability constraint". Journal of Global Optimization, Vol. 9, pp, 395–416.

[8]. Lee, C.Y. (1991) "Parallel machines scheduling with no simultaneous machine available time". Journal of Discrete Applied Mathematics, Vol. 30, pp. 53–61.

[9]. Lee, C.Y. and Massey, J.D(1988) "Multiprocessor scheduling: Combining LPT and MULTIFIT". Discrete Applied Mathematics, Vol. 20, pp. 233–242.

[10]. Lee, C.Y. and Liman, S.D. (1929) "Single machine flow-time scheduling with scheduled maintenance". Acta Informatica, No. 92, pp. 375–382.

[11]. Montgomery D. and Runger J.(2007) Applied Statistics and Probability for Engineers, John Wiley and Sons, Inc 4the edition

[12]. Schmidt, G (1988)"Scheduling independent tasks with deadlines on semi-identical processors". Journal of Operational Research Society, Vol. 39, pp. 271–277.

[13]. Troyer, D. (2006) Strategic Plant Reliability Management Course Book, Noria Publishing, Tulsa, Oklahoma

[14]. Turkcan,A(1999) "Machine Scheduling with Availability Constraints". Available at: benli.bcc.bilkent.edu.tr/~ie672/docs/present/turkcan.ps, 1999.

Research Paper   Open Access

Sharing of Securing A Secret Images Using Media Technique

[1,] Sunil G. Jare, [2,] Prof. Manoj Kumar
[1, 2,] Electronics and Telecommunication
S.V.C.E.T Pune, S.P. Pune University, India

ABSTRACT— *A natural visual secret sharing technique or Visual cryptography method can share a secret images. It is also enable to send information securiely using internet.*
This techniques reduces a transmission risk problem in image sharing. It also provides a meaningless shares are user friendly.In this method we can use carrier as diverse media.hence it is possible for sharing secret images. A new proposed technique is extended visual cryptography using embedded processing.

KEYWORDS — *Visual secret sharing scheme, extended visual cryptography scheme, Feature extraction Scheme.*

I.   INTRODUCTION

Image can contain information to hide a data in smart phones or digital cameras. Sharing & delivering secret images is called as visual cryptography. NVSS can share natural images or digital images and printed images. It can uses carrier as diverse image media. NVSS system can display low quality images in sharing. VSS method can share unity carrier as media and noise like pixels can occurs in resultant images.[4]

As number of share increases probability of failure also increases. NVSS can useful for reducing a transmission problem in sharing. Meaningful images are use friendly. New proposed method can helpful for grey level images. It can provide a secure data transmission in secret sharing.

II.   EXISTING SYATEM

VC or NVSS method can share n secret images during transmission. It can helpful for digital images, printed images, color images and transparency images. It consists of main three steps. First step is image preparation is preprocessing of input images. It includes acquiring images, crop images and resizing images. Second step is feature extraction extract features of natural images.[1],[3] It includes binarization, stabilization and clustering. Third step is pixel swapping consist exchanging the pixels of black and white images.

Disadvantages of Existing System:

First, it cannot be used for grey level images. Digital and natural images are only used.Second is large time is required for secret image sharing.
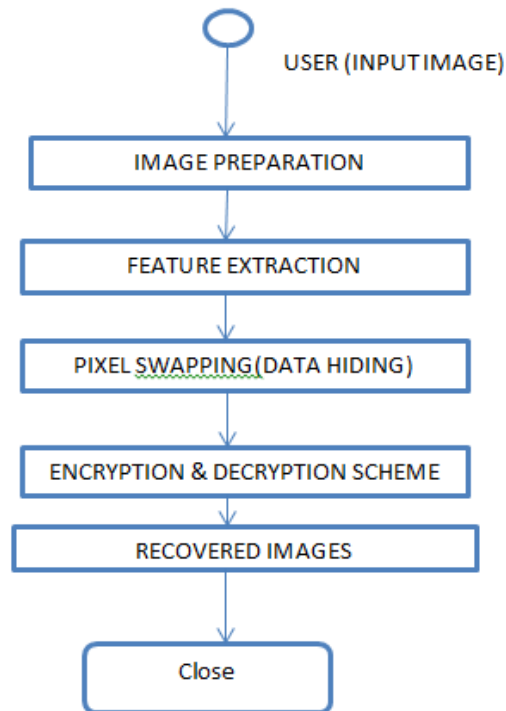
I.　　EXISTING SYSTEM WORK

Fig. Algorithm of NVSS or VC Scheme.

Advantages of Proposed System:

First is it helps for grey level images. A half tone images converted into black and white pixels.[6] Second is it provides secure image secret sharing. Third is it provides flexibility and simplicity.

III.　　SYSTEM ARCHITECTURE

Advanced embedded VC techniques can improve quality of images. This is simple and efficient method. It

consist of Modules:

- ➢ Input Image
- ➢ Embedding Procedure
- ➢ Extraction Procedure.
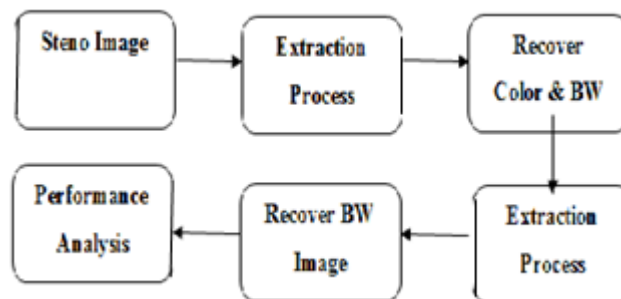
Fig. system works.

➢ Input Image

An image is a two-dimensional picture, which has a similar appearance to some subject usually a physical object or a person. Image is a two-dimensional, such as a photograph, screen display. They may be captured by optical devices—such as cameras, mirrors, lenses, telescopes, microscopes, etc. and natural objects and phenomena, such as the human eye or water surfaces.[7]

Embedding Procedure Algorithm :
Input: Cover image of size, secret Image bit stream.
Output: Steno image.

- ➢ 1. Find the minimum satisfying, and convert into a list of digits with a -ary notational system.
- ➢ 2. Solve the discrete optimization problem to find and.
- ➢ 3. In the region defined by, record the coordinate such that,
- ➢ 4. Construct a no repeat random embedding sequence.
- ➢ 5. To embed a secret Image bit stream, two pixels in the cover image are selected according to the embedding sequence, and calculate the modulus distance between and, then replace with.
- ➢ 6. Repeat Step 5 until all the secret Image bit streams are embedded.

Extraction Procedure Algorithm :
To extract the embedded message digits, pixel pairs are scanned in the same order as in the embedding procedure. The embedded secret Image bit streams are the values of extraction function of the scanned pixel pairs.[5]
Input: Steno image.
Output: secret Image bit stream.
- ➢ 1. Construct the embedding sequence.
- ➢ 2. Select two pixels according to the embedding sequence.
- ➢ 3. Calculate, the result is the embedded digit.
- ➢ 4. Repeat Steps 2 and 3 until all the secret Image bit streams are extracted.
- ➢ 5. Finally, the secret Image bits can be obtained by converting the extracted secret Image bit stream.
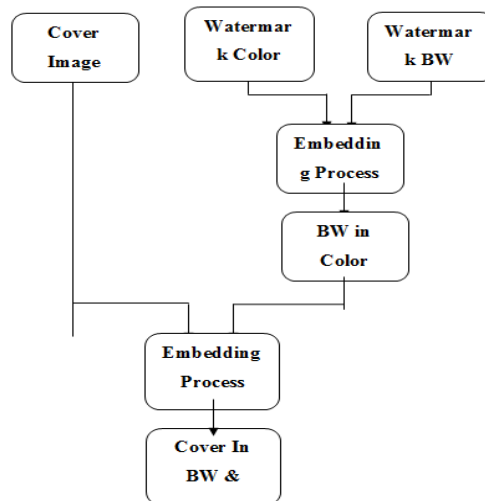
Fig. System Architecture.

II. RESULTS
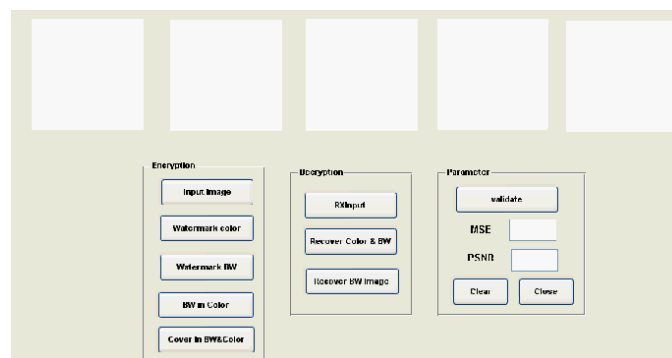
Fig. Input Sequence Steps.
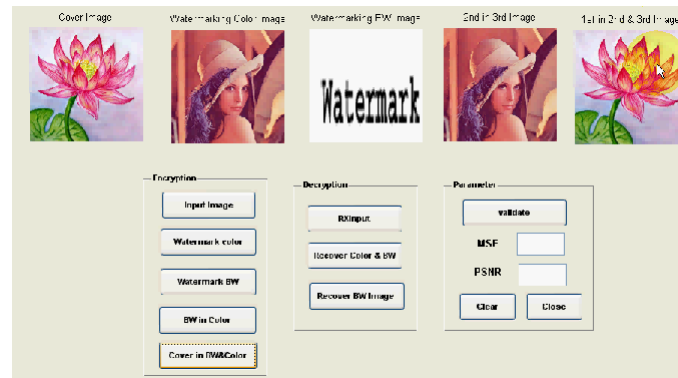
Fig. Resultant image.

IV.   CONCLUSION:

In this paper we recognize colorful secret images with higher contrast. It can effectively reduce transmission risk problem and user friendly for meaningful images. It can be used in copyright protection, securing, watermarking purpose.

REFERENCES

[1]   S. Naor and A. Gaikwad, "Visual cryptography and NVSS " in *Advances in Cryp-tology*, vol. 970. New York, NY, USA: Springer-Verlag, 2005, pp. 1–12.

[2]   K. H. Lee and P. L. Chiu, "Image size invariant for grey levels," *IEEE Trans. Image Process.*, vol. 22, no. 10, pp. 3830–3841, Oct. 2010

[3]   G. Ateniese, C. Blundo, "Extended capabilities for Embedded visual cryptography," *Theoretical Comput. Sci.*, vol. 250, nos. 1–2, pp. 144–161, Jan. 2011.

[4]   C. N. Jare and T. S. Chen, "Extended Thresholding for visual secret sharing schemes: Improving the shadow image quality," *Int. J. Pattern Recognit. Artif. Intell.*, vol. 21, no. 5, pp. 879–898, Aug. 20013.

[5]   Z. Zhou, and G. D. Crescenzo, "Halftone visual cryptog-raphy," *IEEE Trans. Image Process.*, vol. 15, no. 8, pp. 2461–2463, Aug. 2012.

[6]   , G. R. Arce, and G. D. Potdar, "Halftone visual cryptog-raphy via error diffusion colour extending ," *IEEE Trans. Inf. Forensics Security*, vol. 5, no. 4, pp. 383–396, Sep. 2014.

[7]   I. Kang, G. R. and H. K. Lee, "Color extended NVSS using error diffusion," *IEEE Trans. Image Process.*, vol. 20, no. 1,   142–147, Jan. 2014.

[8]   S.Chillingnar, P. Blundo, "Extended capabilities for Embedded visual cryptography & stegnography," *Theoretical Comput. Sci.*, vol. 250, nos. 1–2, pp. 154–158, Jan. 2013

[9]   P. L. Chiu, "Image Resize invariant & Variant for grey levels," *IEEE Trans. Image Process.*, vol. 42, no. 10, pp. 3845–3848Oct.2014

Sunil Jare Received B.E. Degree from Shivaji University in 2013 & Pursuing M.E. (VLSI & ES) from S.V.C.E.T, Rajuri (in Pune university) in VLSI & Embedded Systems.

Manoj Kumar Received B..E Degree From Dr. B.A.M.U Aurangabad in 2009 & M.E. Degree From Dr. B.A.M.U. in 2012 Respectively. He is Currently Pursuing P.h.d.. Degree In Electronics & Communication Engg. Of Image & Signal Processing Institute at the Jodhpur National University. Since 2013, he has been employed in S.V.C.E.T, Rajuri. He is Current Research Interest in Image & Signal Processing.

Research Paper　　　　　　　　　　　　　　　　　　　　　　Open Access

Analyze the effect of window layer (AlAs) for increasing the efficiency of GaAs based solar cell

[1,] Arifina Rahman Tumpa, [2]Eity Sarker, [3]Shagufta Anjum, [4,] Nasrin Sultana
[1,2,3,4](Department of Telecommunication & Electronic Eng, Hajee Mohammad Danesh Science & Technology University, Bangladesh)

ABSTRACT: *Solar energy is the most important renewable source and convertible into useful form with no transmission cost and environment pollution. The main drawback of currently used photovoltaic cell is its low conversion efficiency and materials with the appropriate band gaps. Recently it has been shown that the GaAs based p-i-n solar cell becomes a promising material for very high efficiency solar cell. An ideal model for p-i-n reference cell has been developed and used to theoretically explore the current-voltage characteristics on the host cell properties. The purpose of this paper is to study the performance of AlAs material use as window layer in p-i-n reference cell instead of AlGaAs and evaluated the performance with various parameters. Short circuit current density, open circuit voltage and efficiency are needed to be calculated with the dependencies of band gap energy, carrier concentration and temperature. Significant effects of width lengths on the performance of window layer are evaluated. These calculations will do at cell temperature of 300k. After all comparing these, GaAs based p-i-n reference cell with AlAs window layer offers the maximum efficiency.*

KEYWORDS – *Solar cell, window layer, efficiency.*

I.　　INTRODUCTION

Present day civilization and industries are highly dependent on energy. The main sector contributing this huge amount of energy generation is the fossil fuel with limited resources. Some of these resources are only available in few regions of the world. The scarcity also possess risk to national and regional resource security and autonomy as well as international security. The difficulty and cost of safty disposing radioactive material and toxic waste, makes the use of nuclear and chemical energy a questionable solution. Also the fossil fuel is costly for transmitting in remote areas. Therefore, renewable sources of energy need to be considered seriously for two main reasons: (i) To meet the world wide energy demand and (ii) To protect the environment from the destructive burning of fossil and other fuels. Renewable energies such as wind power, water, biomass and active and passive solar energy have the potential to overcome these problem, as they are unlimited. Due to the decentralized and distributed nature of most of these energy sources, they provide the energy when and where it is needed ensure national and regional resource security. The reliability of the power supply from renewable energies is usually higher than the conventional energy sources. The solar energy is the most important renewable source and convertible into useful form with no transmission cost and environment pollution.

To be competitive with the conventional energy, the cost of solar energy must be comparable with the cost of conventional energy. There are many factors, which affect the cost of solar energy. The cost of solar energy may be reduced by improving the performance of solar cells. Among the performance parameters, the efficiency of solar cell is very important. The main drawback of solar energy is their low conversion efficiency. To increase the efficiency of a cell some approaches are being practiced all over the world. Now these days some of these approaches are multi junction solar cell, multi quantum well solar cell, quantum dot solar cell, multiple absorption path solar cells, multiple temperature solar cells etc. Although they provide high efficiency but their fabrication process difficult and costly. Comparatively single junction solar cell plays an important role in this cost minimization issue. These higher efficiency with fabrication processes is comparatively less difficult and it provide minimum cost. GaAs based solar cell offers maximum efficiency among all the single junction solar cell.

II.   BASIC PRINCIPLE OF SOLAR CELL

A solar cell basically consists of a photon-absorbing material between a back and a front contact. The absorption is performed by electrons which absorb photon energy, Eph. If Eph is equal to the band gap of the material, Eg , the electron can be excite from the valence band to the conduction band, leaving a hole in the valence band. This is called electron hole pair generation. If Eph is greater than Eg, the electron will be excited above the conduction band are then relax down to the band edge and release the extra energy (Eph-Eg) as heat to the to the lattice, in a process referred to as thermalisation.

The opposite effect to electron hole pair generation is recombination in which electrons and holes recombine i.e. electrons fall back into a hole without contributing to the light generated current. Generation contributes to the number of free carriers. Free carriers are (electrons and in the solar cell whereas recombination decreases the number of free carriers. Free carriers are prerequisites for current output from the solar cell. A polarization occurs if electrons and holes are separated and move towards different contacts . If an electric circuit is connected to the cell, electrons will flow from the one of the contacts through the circuit and recombine with the holes in the other contact and hence, a current will flow in the circuit. A current from a solar cell required the separation of charge carriers i.e. electrons and holes. There are different ways to achieve charge separation in the solar cell.
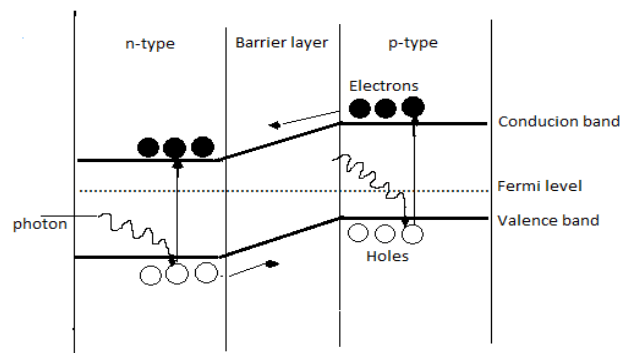
Figure: Solar cell operation

A common way is to use a p-n junction where a p-doped and an n-doped semiconductor are brought together. A p-doped semiconductor has a higher density of holes compared to electrons and an n-doped semiconductor has a higher density of electrons compared to holes. When they are brought together, carriers will flow from regions with high density. Hence, electrons will flow from the n-side to the p-side and holes in the opposite direction due to the concentration gradient. This is known as diffusion.

Electrons which are negatively charged, diffuse to the p-type side they leave positively charged ions in the n-type side. Similarly, holes leave negatively charged ions in the p-type side. Ions on opposite sides of the junction result in an electric field over the p-n junction which will oppose the diffusion. The flow of free carriers in the electric field is called drift current. In equilibrium, drift and diffusion currents are equal. The electric field, introduced into the cell by the p-n junction, provides the force for charge separation since it drives the different charges, generated by electron hole pair generation, in opposite directions. Within some distance on either side of the junction, the materials are depleted of free carriers and this region is called depletion region.

2.1 Basic Principles of a Solar cell

This parameter determines the performance of a solar cell i.e how good that solar cell is.

The main parameters are:

- Short circuit current
- Open circuit voltage
- Fill factor
- Efficiency

2.1.1 Short circuit current J_{sc}

It is defined as the current of a solar cell when the top and bottom (negative and positive leads) are connected with a short circuit. The current drawn when the terminals are connected together is the short circuit current J_{sc}. For any intermediate load resistance RLR_L the cell develops a voltage V between 0 and Voc and delivers a current I such that V = IR_L and I(V) is determined by the current voltage characteristic of the cell under that illumination. Thus both I and V are determined by the illumination as well as the load. Since the current is roughly proportional to the illuminated area, the short circuit current density J_{sc} is the useful quantity for comparison.

2.1.2 Open circuit voltage V_{oc}

It is defined as the voltage between the terminals obtained when no current is drawn from the solar cell. The voltage developed when the terminals are isolated (infinite load resistance) is called the open circuit voltage V_{oc}.

2.1.3 Fill factor (FF)

The operating regime of the solar cell is the range of bias, from 0 to Voc, in which the cell delivers power. The cell power density is given by P = JV where P reaches a maximum at the cell's operating point or maximum power point. This occurs at some voltage V_m with a corresponding current density J_m. The optimum load thus has sheet resistance given by V_m/J_m. The fill factor is defined as the ratio

$$\text{FF} = \frac{V_m J_m}{V_{oc} J_{sc}}$$

2.1.4 Efficiency ɳ

The efficiency ɳ of the cell is the power density delivered at operating point as a fraction of the incident light power density, P_s, $$ɳ = \frac{V_m J_m}{P_s}$$

Efficiency is related to J_{sc} and V_{oc} using FF,

$$ɳ = \frac{V_{oc} J_{sc} \text{FF}}{P_s}$$

2.2 Model of the p-i-n reference cell

Practical solar cells have a complicated structure with several layers in addition to the p-and n-layer we find in the simplest p-n solar cell. The purpose of these layers is to reduce front and back surface recombination and surface reflection. A sketch of a p-i-n reference cell is shown in figure showing all the layers (anti-reflective coating, window, p^+, p, i, n and n^+) included to obtain a high efficiency solar cell.
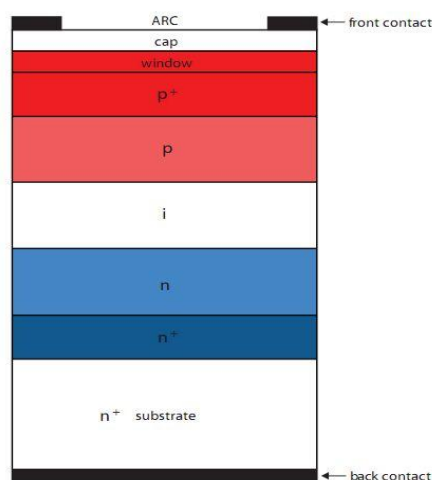

Figure: Structure of the p-i-n reference cell. It consists of an anti-reflective coating, a cap-, window-, p^+-, p-, i-, n- and n^+ layer placed on top of the substrate. The effect of using all these layers is described in the text.

2.3 Materials used in solar cell

Various materials are used in solar cell at table below

Table Materials used in a solar cell

Layers	Materials
Window	AlAs
p^+	GaAs
p	GaAs
i	GaAs
n	GaAs
n^+	GaAs

2.4 Purpose of using AlAs as window layer

Recombination of excess carriers occurs not only within the bulk of a semiconductor crystal, but at the surface of the crystal as well. The periodicity of the atoms is interrupted at the surface of the crystal, and the surface acts as an interface between the semiconductor and another material. As a result the recombination rate at the surface is different (and usually higher) than in the bulk of the semiconductor. Surface recombination is reduced by a passivating or window layer which prevents minority carriers from reaching the surface. Surface recombination velocity is strongly dependent on the surface roughness, contamination, ambient gases used during oxidation and the annealing conditions. In gallium arsenide, the surface recombination velocity is very high (of the order of 10^6 cm/s). The deposition of a thin layer of AlAs, however, reduces the recombination velocity at the interface to $10\text{-}10^3$ cm.

III.   CALCULATION OF PHOTO CURRENT AND QUANTUM EFFICIENCY

The photocurrent generated by a solar cell under illumination at short circuit is dependent on the incident light. To relate the photocurrent density, J_{sc}, to the incident spectrum we need the cell's quantum efficiency, (QE). QE (E) is the probability that an incident photon of energy E will deliver one electron to the external circuit. Then the photocurrent can be written in terms of the quantum efficiency QE(E)

$$J_{light} = q \int F(E)QE(E)dE$$

Where QE (E) is the probability that a photon of energy E will contribute with one electron to the current. The quantum efficiency is the sum of the quantum efficiency in the p-layer and n- layer given as

$$QE_p = \left[\frac{(1-R)\alpha L_n}{\alpha^2 L_n^2 - 1}\right] \times \left\{ \frac{(K_n + \alpha L_n) - e^{-\alpha l_p}(K_n \cosh(\frac{l_p}{L_n}) + \sinh\left(\frac{l_p}{L_n}\right))}{K_n \sinh\left(\frac{l_p}{L_n}\right) + \cosh\left(\frac{l_p}{L_n}\right)} - \alpha L_n e^{-\alpha l_p} \right\}$$

And

$$QE_n = \left[\frac{q(1-R)\alpha L_p}{(\alpha^2 L_p^2 - 1)}\right] e^{-\alpha(z_p + w_n)} \times \left\{ \alpha L_p - \frac{K_p \left(\cosh\left(\frac{l_n}{L_p}\right) - e^{-\alpha l_n}\right) + \sinh\left(\frac{l_n}{L_p}\right) + \alpha L_p e^{-\alpha l_n}}{K_p \sinh\left(\frac{l_n}{L_p}\right) + \cosh\left(\frac{l_n}{L_p}\right)} \right\}$$

For an ideal diode the dark current density J_{dark}(V) varies like

$$J_{dark}(V) = J_0\left(e^{\,qV/k_B T} - 1\right)$$

where J_0 is a constant, k_B Is Boltzmann's constant and T is temperature in degrees Kelvin.
With this sign convention the net current density in the cell is

$$J(V) = J_{SC} - J_{dark}(V)$$

This becomes, for an ideal diode,

$$J = J_{SC} - J_0\left(e^{\,qV/k_B T} - 1\right)$$

When the contacts are isolated, the potential difference has its maximum value, the open circuit voltage V_{OC}. For the ideal diode

$$V_{OC} = \frac{k_B T}{q} ln\left(\frac{J_{SC}}{J_0} + 1\right)$$

IV.   FIGURES AND TABLES

Effect of width of the window layer

The maximum efficiency and short circuit current density has been calculated for the devices with various width of the window layer while other parameter including width of the other layer kept constant. For comparison between AlGaAs window layer device and AlAs window layer device both data are included in Table.

Table. Simulation results of varying width of window layer:

Device no	Width of the window layer nm	AlGaAs as a window layer			AlAs as a window layer		
		V_{oc} Volt	J_{sc} mA/cm^2	Max efficiency	V_{oc} Volt	J_{sc} mA/cm^2	Max efficiency
1	5	0.9965	43.4839	35.5257	0.9966	43.5735	35.6028
2	10	0.9964	43.3942	35.4486	0.9966	43.5733	35.6026
3	50	0.9957	42.6856	34.8393	0.9966	43.5713	35.6010
4	100	0.9948	41.8211	34.0958	0.9966	43.5689	35.5989
5	150	0.9939	40.9794	33.3719	0.9966	43.5664	35.5968

Maximum efficiency vs. width of window layer

The efficiency variation due to thickness of the window layer is shown in Figure for AlGaAs and AlAs respectively.
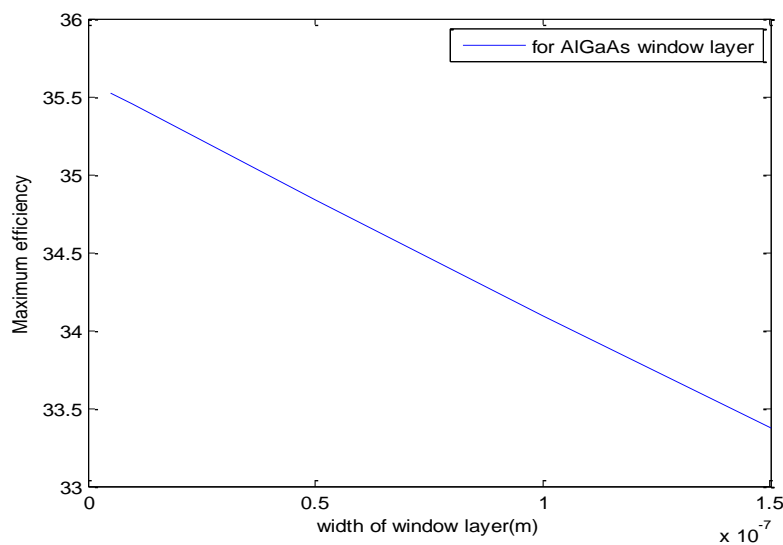
Figure: Variation of efficiency due to thickness of the Al$_x$Ga$_{1-x}$As (x=.804) window layer
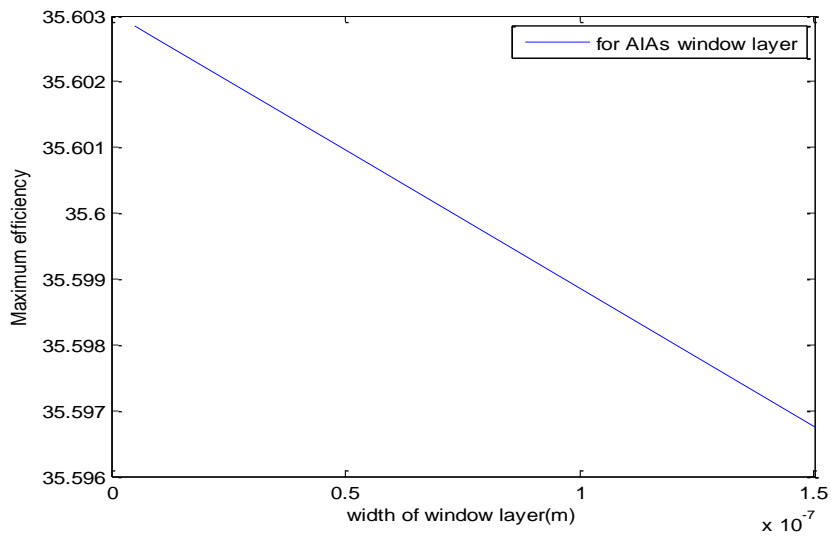
Figure: Variation of efficiency due to thickness of the AlAs window layer

- It can be observed from Figure that efficiency of AlGaAs is 35.527 and AlAs is 35.6028.
- The efficiency increases 0.08 by using AlAs as window layer.
- So we can observe that efficiency of the device decrease slowly due to increase width of AlAswindow layer than AlGaAs window layer.

Voltage versus Current density curve

Figure shows the voltage vs. current density for different width of the AlGaAs and AlAs window layer respectively.
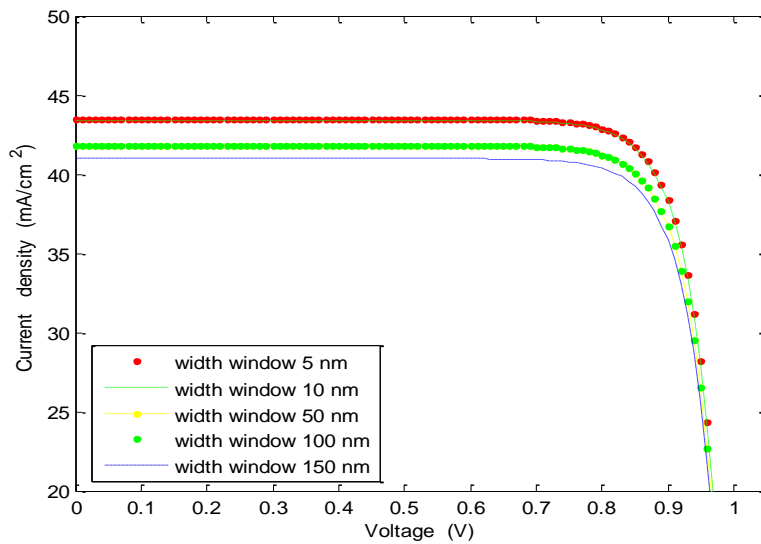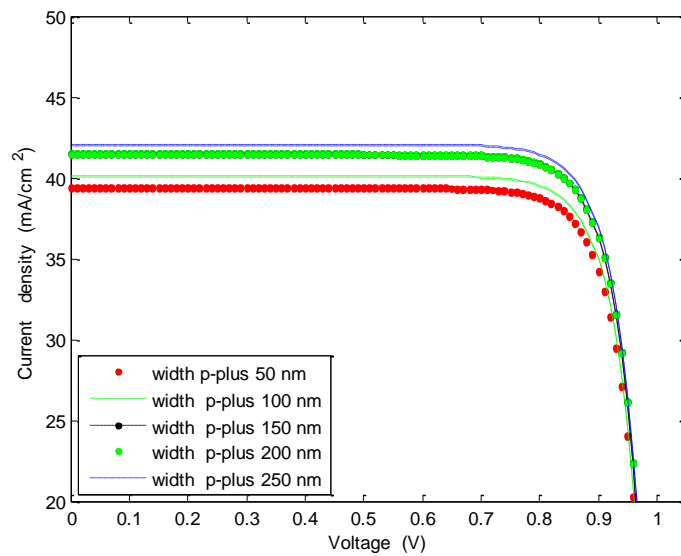

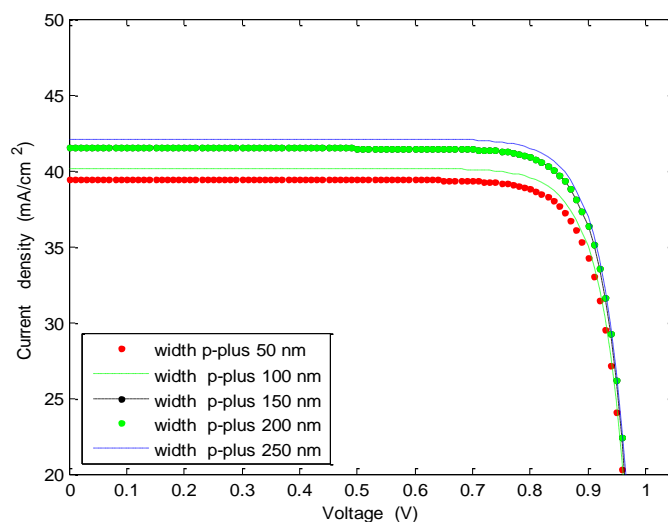Figure: Voltage versus current density curve for different width of the AlGaAs window layer
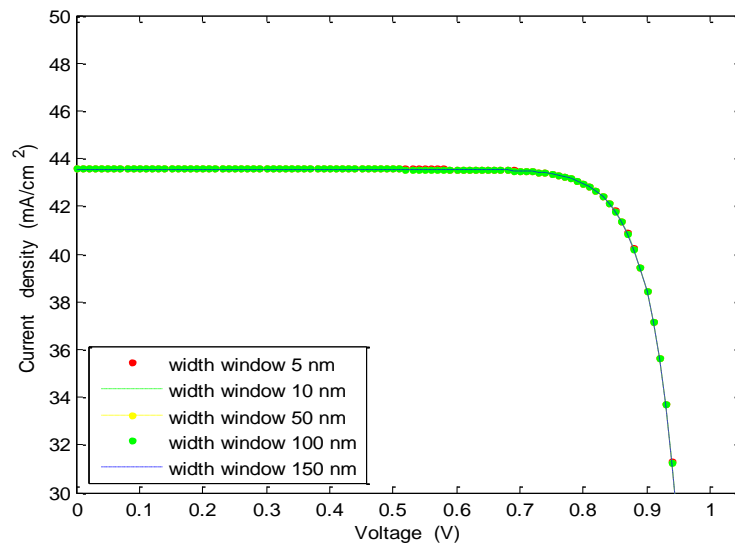
Figure: Voltage versus current density curve for different width of the AlAs window layer

- From Figure we can observe that both case current density decrease due to increase in width of the window layer.
- We can also observe that current density reached in saturation point when voltage is 0.83v for AlGaAs and 0.79 v for AlAs.

Wavelength versus Quantum efficiency

Figure shows the wavelength vs. quantum efficiency curve for different width of the AlGaAs and AlAs window layer respectively.
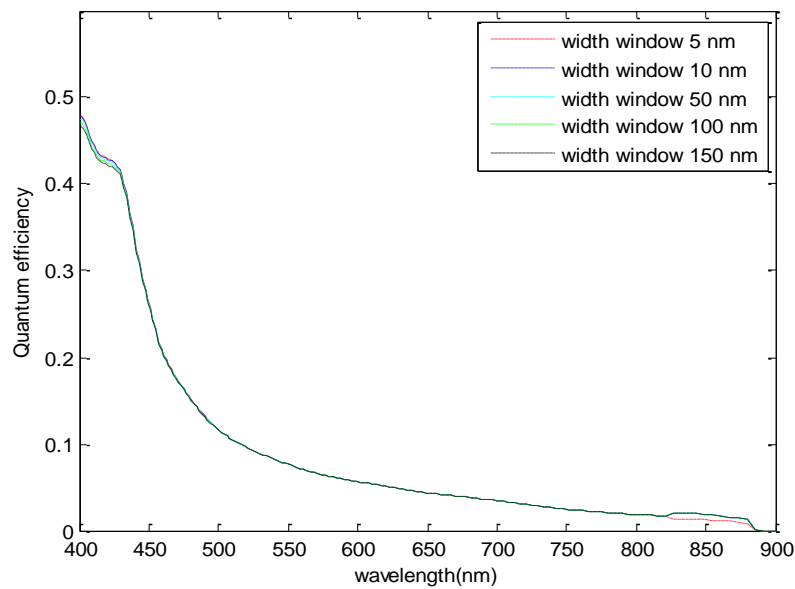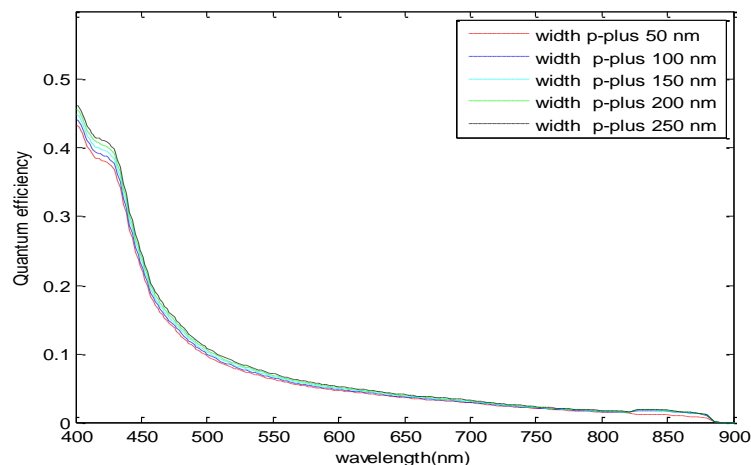

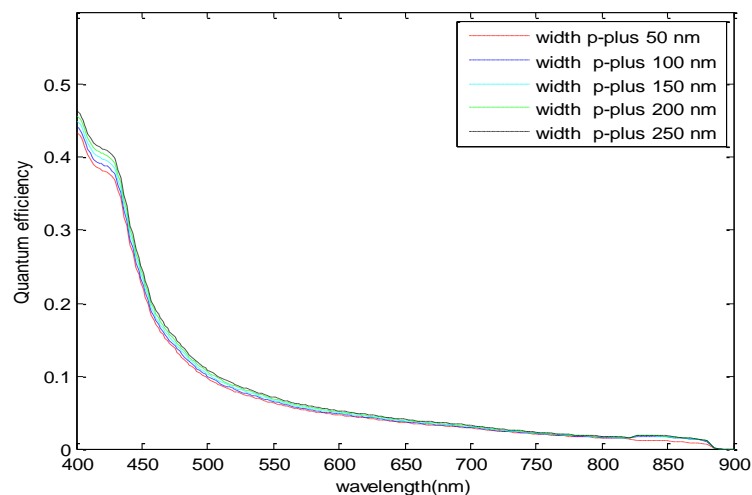Figure: Wavelength versus Quantum efficiency for different width of the AlGaAs window layer
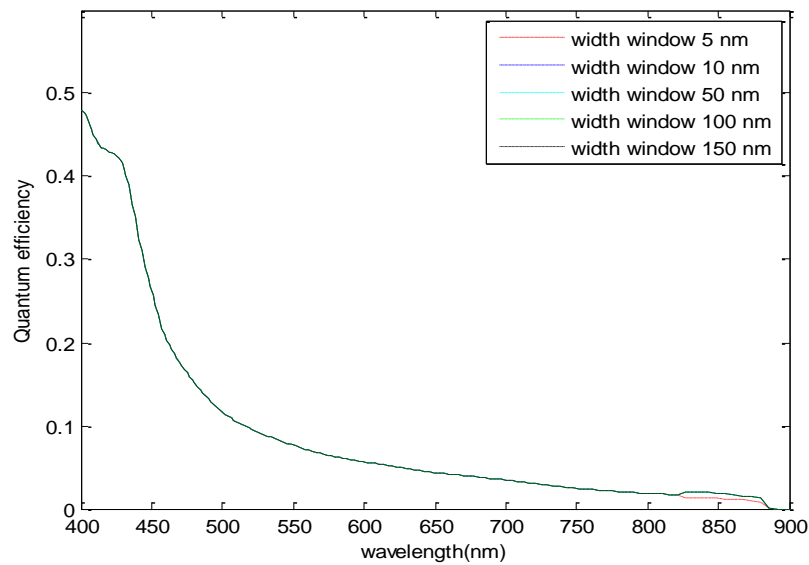
Figure: Wavelength versus Quantum efficiency for different width of the AlAs window layer

- It can be observed from Figure that quantum efficiency decrease with the increase of the width of the window layer.

Effect of width of the p$^+$ layer

The maximum efficiency and short circuit current density has been calculated for the devices with various width of the p$^+$ layer while other parameter including width of the other layer kept constant. For comparison between AlGaAs window layer device and AlAs window layer device both data are included in Table.

Table. Simulation results of varying width of the p$^+$ layer

Device no	Width of the p$^+$ layer nm	AlGaAs as a window layer			AlAs as a window layer		
		V_{oc}	J_{sc}	Max efficiency	V_{oc}	J_{sc}	Max efficiency
		Volt	mA/cm^2		Volt	mA/cm^2	
1	50	0.9922	39.3290	31.9529	0.9923	39.4101	32.0227
2	100	0.9930	40.0648	32.5857	0.9931	40.1474	32.6567
3	150	0.9937	40.7587	33.1824	0.9938	40.8428	33.2547
4	200	0.9944	41.4069	33.7398	0.9945	41.4923	33.8132
5	250	0.9950	42.0062	34.2551	0.9951	42.0928	34.3296

- It is observed form the data table, efficiency is also related to the width of the p$^+$ layer. Increasing the width of the p$^+$ layer also increase the efficiency. This is due to the more photon can be absorbed by this layer.

Voltage versus Current density curve

Figure shows the voltage vs. current density for different width of the p$^+$ layer.

Figure: Voltage versus current density curve for different width of the p$^+$ layer (using AlGaAs as a window layer)

Figure: Voltage versus current density curve for different width of the p$^+$ layer (using AlAs as a window layer)

- From Figure we can observe that current density reached in saturation point when the voltage is 0.84 v for AlGaAs and 0.85 v for AlAs.
- It is also observed that the device performance for both solar cell about same because of GaAs based solar cell used. So there is no appreciable change can observe between voltage vs. current density curves as shown in Figure.

Wavelength versus Quantum efficiency
Figure shows the wavelength vs. quantum efficiency curve for different width of the p$^+$ layer.

Figure: Wavelength versus Quantum efficiency for different width p$^+$ layer (using AlGaAs as window layer)

Figure: Wavelength versus Quantum efficiency for different width p$^+$ layer (using AlAs as window layer)

- It can be observed from Figure that quantum efficiency increase with the increase of the width of the p$^+$ layer.
- As photo current is directly related to the quantum efficiency, increasing quantum efficiency photo current also increase. That can be observed from Figure.

V.   CONCLUSION

In this thesis we study the GaAs based p-i-n reference cell for high performance. In order to realize the high performance of the p-i-n reference cells theoretical study and performance evaluation are very much essential. The design and performance evaluations are made by developing a simulation model which optimizes the design of p-i-n reference cell for high efficiency.

The modeling of the reference cells shows the importance of using a window layer and heavily doped p^+ and n^+ layers to obtain a low effective surface recombination velocity together with an anti-reflective coating minimizing the reflection losses. By using these layers, high quantum efficiency is obtained. Due to a model of a p-i-n solar cell with the intrinsic material placed in a flat band region, a model of high efficiency solar cell is developed and high short circuit current and open circuit voltage is obtained, because additional short circuit current density comes from intrinsic region. Here we have derived mathematical equation for current density, voltage and quantum efficiency.

Simulation is done for two different types of window material (AlGaAs and AlAs) with changing the values of different parameters specially width of the different layers. From those simulation results maximum efficiency is obtained 35.5257% for AlGaAs as a window layer and 35.6028% is obtained for AlAs . So efficiency increase .08% if AlAs is used as window layer instead of AlGaAs.

By comparing the results from the modeling with experimental data it is found that device performance for AlAs as window layer is better than AlGaAs.

REFERENCES

[1]　G. J. Bauhuis, Zan Czochralski and Dr. Saimon Wafer reuse for repeated growth of III–V cells, Prog. Photovoltaics: Res. Apply, December-2010, vol. 18, pp. 155.

[2]　S. M. Vernon, M.R. Brozel and G.E. Stillman High-efficiency concentrator cells from GaAs on Si, in Proc. 22nd IEEE Photovoltaic Spec. Conf, 1991, pp. 353.

[3]　I. Mathews, Theoretical performance of multi-junction solar cells combining III-V and Si materials, Opt. Express, vol. 20, 2012, pp. A754.

[4]　 M. L. Lovejoy, J. A. Carlin & Professor Jon Major. Minority hole mobility in GaAs, in Properties of Gallium Arsenide, Data Review Series no. 16, London: INSPEC, 1996, pp. 123.

[5]　M. S. Lundstrom R.K. Willardson, A.C. Beer and E.R. Weber Minority carrier transport in III-V semiconductors, in (eds.), Minority Carrier in III-V Semiconductors: Physics and Applications, Semiconductors and Semimetals, vol. 39: Academic Press Inc. pp.193.

[6]　Alla Srivani and Prof. Vedam Rama Murthy Effect of composition in arsenide ternary semiconductor alloys, May 2002, Vol. 1, pp. 7-12.

[7]　C. L. Andre Impact of dislocations on minority carrier electron and hole lifetimes in GaAs grown on metamorphic SiGe substrates, Appl. Phys. Lett., vol. 84, 2004, pp. 3447.

[8]　M. Y. Ghannam Theoretical study of the impact of bulk and interface recombination on the performance of GaInP/GaAs/Ge triple junction tandem solar cells in Proc. 3rd World Conf Photovoltaic Energy Convers. 2003, pp. 666.

[9]　J. A. Carlin High-lifetime GaAs on Si using GeSi buffers and its potential for space photovoltaics , Solar Energy Mater. Solar Cells, vol. 66, 2001, pp. 621.

[10]　S. M. Vernon & C. E. Fritts Experimental study of solar cell performance versus dislocation density, in Proc. 21st IEEE Photovoltaic Spec. Conf., 1990, pp. 211. 55

Research Paper	Open Access

Influence of Exterior Space to Linkage and Tourist Movement Pattern in Losari Coastal Area

Nur Adyla Suriadi[1*], Endang Titi Sunarti[2] ,Murni Rachmawati[3]

[1*]*Post-Graduate student in Departement of Architecture (FTSP), Sepuluh Nopember Institute of Technology,
Surabaya. Indonesia*
[2]*Professor in Departement of Architecture (FTSP), Sepuluh Nopember Institute of Technology,
Surabaya. Indonesia*
[3]*Lecturer in Departement of Architecture (FTSP), Sepuluh Nopember Institute of Technology,
Surabaya. Indonesia*

ABSTRACT : *Makassar City has a strategic location because located at the crossroads of good traffic from north to south and from west to east, from these advantages so Makassar City eligible to be a tourism destination. One of the hallmarks quality tourism destination is Losari Coastal Area, which is a tourist area that became an icon of the city of Makassar and has many tourist attractions i.e. Reclamation Losari Beach, Fort Rotterdam, Somba Opu Shopping Centre and Culinary Tourism Area. However, tourist movement patterns who concentrated only in Reclamation Losari Beach needs for development of linkage at tourist attractions based on tourist movement patterns. Research method used is descriptive qualitative method with cognitive mapping technique to identify of tourist movement patterns characteristic in visiting tourist attractions at Losari Coastal Area and influence of exterior space to linkage among tourist attractions. Results from this research is determine influence of exterior space to connectivity linkage and tourist movement patterns among tourist attractions and find local criteria of exterior space which can be applied in Losari Coastal Area.*
Keywords - Exterior Space, Linkage, Losari Beach, Tourist Movement Patterns, Tourist Attractions

I.   INTRODUCTION

Losari coastal tourism area has many tourist attractions i.e Reclamation Losari Beach, Fort Rotterdam, Somba Opu Shopping Centre, Makassar Culinary Area and PKL Centre that serve a variety of tourist attractions, however that is known by public and becam an icon of Makassar is Reclamation Losari Beach, which is a open public open space. therefore the movement patterns of tourist only concentrated on tourist attractions interested by visitors.

One of the problems lack of visitor to visiting tourist attractions in Losari Coastal Area is influence of exterior space that weaken the quality of linkage. This causes is lacking of motivation from tourist to travel in Losari Coastal Area, so that potential of every tourist attractions not explored optimally.

Purpose of this research is to show tourist movement patterns in Losari Coastal Area and determine influence of exterior space to connectivity linkage and tourist movement patterns among tourist attractions, so it known about how local criteria of exterior space that can provide connectivity and facilitate the tourist movement pattern among tourist attraction in Losari Coastal Area.

Location of this research is coastal area which is administration of this region located in Ujung Pandang district at west of Makassar City, South Sulawesi in Indonesia.
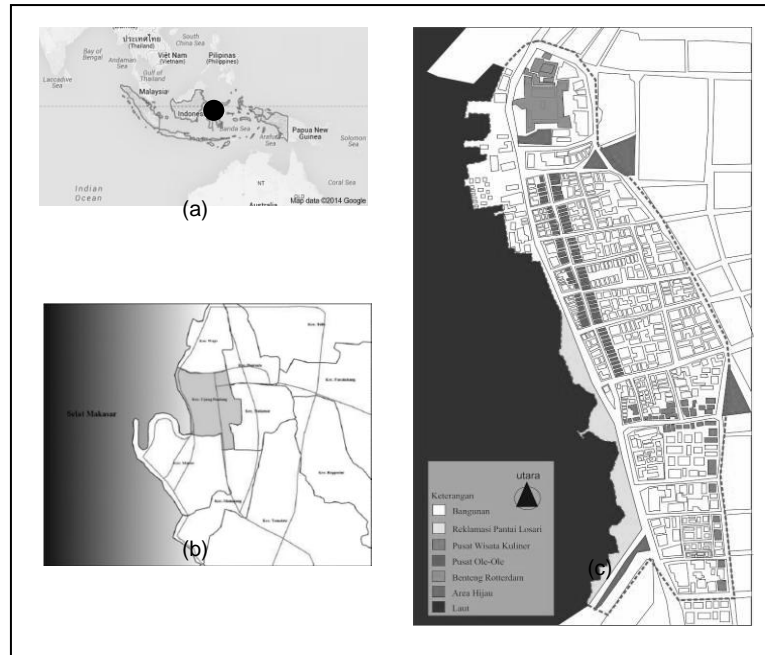
Fig 1: Location of Losari Coastal Area in the map of Indonesia and Makassar City

II.   METHODOLOGY

The reasearch method used in this study are included in descriptive research method (descriptive research). Descriptive research is a research which aims to create a description of a social phenomenon/natural with a systematic, factual, and accurate [1] [2].

Analysis techniques used is cognitive mapping or cognitive spatial analysis techniques defined as a form of urban design analysis [7]. This analysis method is divided into three steps, that is.
1. The first step is observation in the field to find out tourist movement patterns in Losari Coastal Area.
2. Correlate this observations with perception of tourist to support the observations by researchers.
3. Analysis of movement patterns among tourist attractions with overlay mapping to determine of tourist tendency on travelling and factors which is influence of exterior space to tourist movement patterns and linkage.

2.1 Movement Pattern Characteristics Analysis

The categories of movement patterns of tourists with a simple sketch proposed Lau and McKercher (2006) in the journal Understanding Tourist Movement Pattern In a Destination: A GIS Approach [3] that is.

Table 1
The Movement Patterns with Simple Sketch

Movement Patterns	Description
I. Single Pattern Single Point ◆――――●	There is no movement in the process of a visit a destination and return to their homes by same route

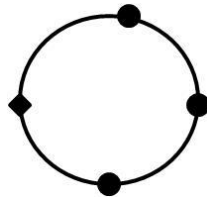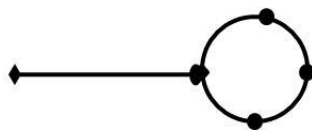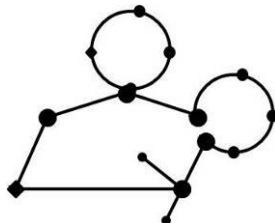|		
II. Multiple Pattern Base Site		Tourist movement patterns starting from the place of origin to the major destinations and proceed to secondary destination, secondary destinations in the pattern of this movement can be more than one destination.
Stop Over		Movement patterns of tourists with focus towards major destinatinations where the journey to visit some interesting secondary destinatios and visited by tourists.
Chaining Loop		Tourist movement patterns such as circles without any repetition of these tourists destinations. Tourist travel to visit several destinations accoriding to the tourist destination.
III. Complex Pattern Destination Region Loop		Tourist movement that began with a route around other destinations. After completing the tour around (circular pattern), they return home by the shortest route between the main objectived and the place of origin set out. It is combination of single point and chaining pattern loop.
Complex Neighbourhood		Is a combination of two or more patterns that have been mentioned above.
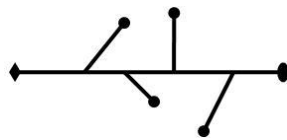
2.2 Analysis of Exterior Space

To determine influence of exterior space to linkage and tourist movement patterns used single directional view technique with evaluation techniques to find out condition exterior space which is weakend quality of linkage in Losari Coastal Area. As for the aspects of exterior space that will be reviewed is circulation, parking, and street furniture with general criteria as follows.

Table 2
General Criteria of Exterior Space Aspect

Exterior Space Aspects	Criteria
I. Circulation and Parking	• Circulation shall ensure the safety and comfort for pedestrians and vehicles areas [8] • Circulation shall in seperating pedestrian and vehicles areas [5] • Circulation should provide freedom of space for tourists [5] • Parking system should pay attention to the comfort and safety of pedestrians [4] • Parking system should facilitate the achievement of space activities [4]
II. Street Furniture	• Street furniture supposed to be attractive in terms of arrangement and shape, and lasting from all climates [5]

III.   RESULTS AND DISCUSSION

3.1 Existing Condition of Exterior Space

In integrating every tourist attraction in Losari Coastal Area be required a linkage to support the district to be an urban tourism [6]. A linkage system is characteristic that are very important from exterior space. This is an action which combine all activities and will result is a physical form an area.

To determine existing condition of exterior space that connects linkage among tourist attractions in Losari Coastal Area are divided into four segments i.e first segment is Penghibur Street, second segment is Lamadukelleng Street, third segment is Somba Opu Street, and fourth segment is Ujung Pandang Street with aspects will be reviewed are circulation, parking and street furniture, that is

Table 3.
Existing Condition of Exterior Space Each Tourist Attractions in Losari Coastal Area

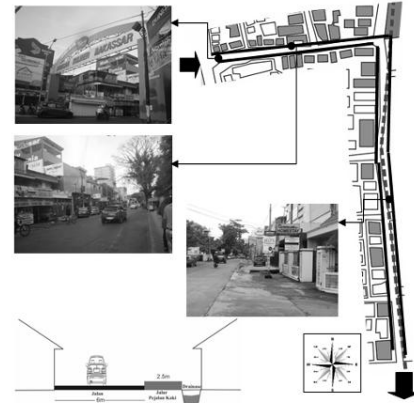| Analysis Of Existing Condition	Picture Of Each Segment
1st Segment Circulation and Parking • Circulation vehicles areas is one way and congested enough in the afternoon until evening. • There is a constriction of circulation vehicle in mid Penghibur street. • Along pedestrian way on the afternoon unti evening was converted by vendors to selling and parking of vehicles • Pedestrian way not yet to serve facilities to PDA. Street Furniture • Lack of signages as information for tourists about tourist attractions and directional markers.	

2ⁿᵈ Segment

Circulation and Parking:

- Circulation vehicles motorize is one way and congested enough in the afternoon until evening.
- Pedestrian way in this segment not fully exist only at a certainly point and there is a form of concrete drainage cover.
- Pedestrian way at some poin also converted for vendors to selling.

Street Furniture

- Street furniture in this segmen is nothing so that tourist doesn't facilitate to walking.
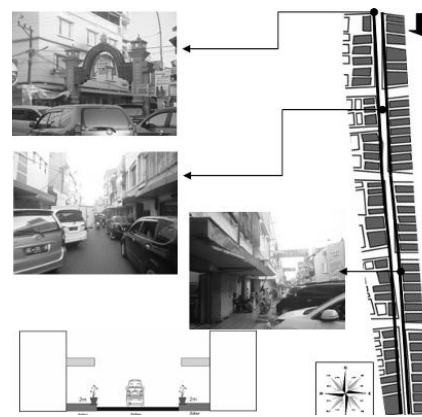

3ʳᵈ Segment

Circulation and Parking:

- Circulation vehicle is one way and congested enough in the afternoon until evening.
- There is no parking space which provided a means of trade and services along this corridor so that vehicle on street parking which causes congestion.

Street furniture:

- Size of different advertisement billboards covered with one another and cover a linkage corridor.

4ᵗʰ Segment

Circulation and Parking:

- 2 way vehicle circulation and congested enough in the afternoon until evening.
- Along pedestrian way on the afternoon until evening converted for vendors to selling and parking of vehicles
- There is no parking space provided by vendors along these corridors so that vehicle on street parking and causes congested.

Street Furniture:

Lack of signage and street furniture that increase district's image as a historical district to attract tourists to visit.
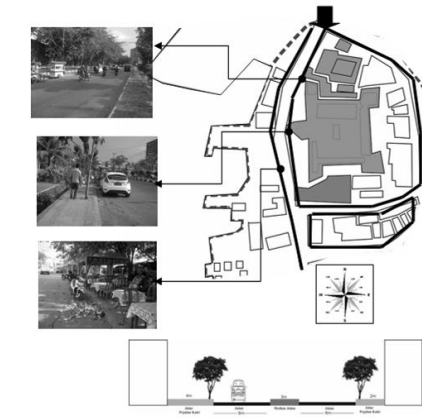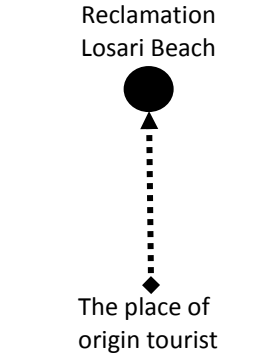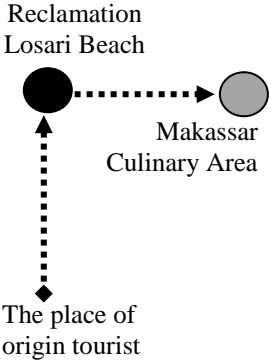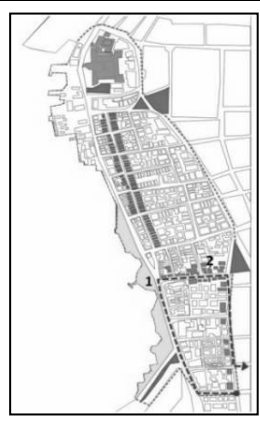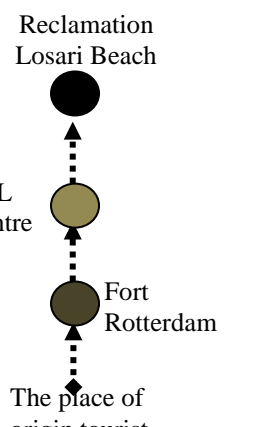

Based on the analysis of existing condition of exterior space from three aspects i.e. circulation, parking, and street furniture at each segment of tourist attraction in Losari Coastal Area can be identify that lack of connectivity linkage between tourist attractions based on a few things:

1. Circulation patterns of people and vehicle are not yet it easier for tourists to travelling among tourist attraction where the points are still jammed in some tourist attraction
2. Parking on street that dominate at each segmen and can hinder tourists to travelling.
3. Comfort and safety of tourists at pedestrian way still overlooked with lack of facilities provided and converted of pedestrian way by vendors and parking.
4. Lack of street furniture and signage in several segments that do not facilitate tourists in tourism activities

3.2 The Tourist Movement Patterns In Losari Coastal Area

Types of movement patterns proposed by Gigi Lau and Bob McKercher are divided into six types of movement patterns (see table 1) i.e. single point, base site, stopover, chaining loops, destination region loop, and complex neighbourhood. Referring to the theory, tourists movement patterns determined into 3 types i.e. single pattern, multiple patterns and complex patterns.

Table 4.
Tourists Movement Patterns among Tourist Attraction in Losari Coastal Area

Movement Patterns	Description
1. Single Point Reclamation Losari Beach The place of origin tourist	The movement patterns of single point that leads only one destination point without visiting another destination point and back to the place of origin is a tourist movement patterns who only visit destination Reclamation Losari Beach and tourists who only visit Fort Rotterdam.
2. Base Site Reclamation Losari Beach → Makassar Culinary Area The place of origin tourist	At movement patterns of base site, tourists start the trip from the place of origin and go to the main purpose, and followed a visit to secondary purpose in a certain area i.e tourists movement patterns destinations from the place of origin and visited Reclamation Losari Beach to Fort Rotterdam and tourists who visited Reclamation Losari Beach to Makassar Culinary Area, where Reclamation Losari Beach as the main attraction.
3. Stopover Reclamation Losari Beach PKL Centre Fort Rotterdam The place of origin tourist	At stopover movement patterns, movement towards the main destination point, where visiting another destination point (secondary) in the process of movement i.e. tourists movement patterns with two or more attraction destination from Fort Rotterdam-PKL Centre – Reclamation Losari Beach, where Fort Rotterdam and PKL Centre as secondary destinations and Reclamation Losari Beach as the main destination.
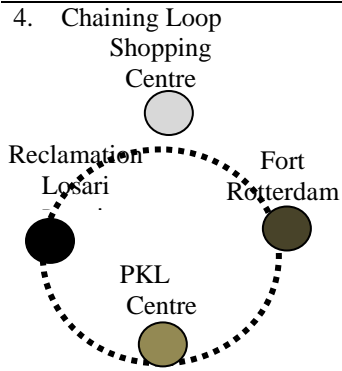
4. Chaining Loop Shopping Centre		On the movement patterns of Chaining loop with type of around like a ring that connects two or more destination point and there is no repetition route i.e. tourist movement patterns with four tourist destinations starting from Reclamation Losari beach – PKL Centre – Fort Rotterdam – Shopping Centre and after that direct tourists back to its original place

According to **Table 4 above**, is known that tourists movement patterns only two kinds are single pattern and multiple pattern. In the movement patterns of single point, dominant tourists destination to visited Reclamation Losari Beach and the next is Fort Rotterdam. In the movement patterns of base site with two tourists destination is dominated movement patterns from Reclamation Losari Beach to Fort Rotterdam and from Reclamation Losari Beach to Makassar Culinary area, which is Reclamation Losari Beach as the main destination. For a movement patterns of stopover with two or more dominated by tourist destination of movement patterns from Fort Rotterdam – PKL Centre – Reclamation Losari Beach – PKL Centre – Reclamation Losari Beach, and for the movement patterns of chaining loop with four tourist destinations dominated by movement patterns from Reclamation Losari Beach – PKL Centre – Fort Rotterdam – Shopping Centre, where tourists directly back to its original place.

IV.   CONCLUSION

Influence of exterior space to linkage and tourist movement pattern because the linkage is not optimal in connecting every tourist attraction so tourists dominant movement patterns only visited one tourist destination. Lack of motivation tourists to travel due to circulation is not yet clear, pedestrian way doesn't continuous, parking on street that hamper travel, and there is no clear route to connect each tourist attraction.

As for the local criteria exterior space that can strengthen the quality of linkage and facilitate the movement of tourists, that is.

Table 5.
Local Criteria of Exterior Space Aspect In Losari Coastal Area

Exterior Space Aspects	Criteria
1. Circulation and Parking	• Circulation that integrates every tourist attractions must support and provide a good path and interconnected, and can be accessed by all people of all ages and needs of tourists • Parking on street should be avoided, especially on the crowded corridors so that the circulation of vehicles and people are not hampered in travel.
2. Street Furniture	• Keep the availability of street furniture in each corridor in Losari Coastal Area to facilitate tourists to travel that promotes a safety and convenience of tourists]

REFERENCES

This paper is part of a post-graduate thesis ITS (Sepuluh Nopember Institute Of Technology) in Departement of Architecture. Surabaya. East Java. Indonesia
[1]   Darjosanjoto, Endang T.S "Penelitian Arsitektur Di Bidang Perumahan dan Permukiman". Itspress. Surabaya. 2012
[2]   Darjosanjoto, Endang T.S. "The Role of Riferbank Area as Community Space in Surabaya City, Case Study : Kampung Jambangan and Kampung Keputran", Great Asian Street Symposium. National University of Singapre. 2014
[3]   Gigi, Lau. McKercher, Bob. "Understanding Tourist Movement Patterns in A Destination: A Gis Approach", Hongkong.
[4]   Hakim, Rustam. Utomo, Hardi. "Arsitektur Lanskap" Bumi Aksara. Jakarta. 2008
[5]   Shirvani, Hamid. "The Urban Design Process". Van Nostrand Reinhold. New York. 1985
[6]   Trancik, Roger. "Finding Lost Spaces. Theories urban Design". Van Nostrand Reinhold Company. New York. 1986
[7]   Urban Design Toolkit, published by Ministry for the Environment, Wellington. New Zealand. 2006
[8]   Widi-Prabawasari, Veronika. Suparman, Agus. Seri Diktat Kuliah : Tata Ruang Luar 01. Gunadarma. Jakarta. 2000